VIBRATION OF MISTUNED BLADED DISC ASSEMBLIES

by

H Dare AFOLABI

a thesis submitted to the
University of London
for the degree of
Doctor of Philosophy

Department of Mechanical Engineering
Imperial College of Science & Technology
LONDON SW7

September 1982

in memory of
my father

for
my mother

"... to render as we forge ahead
service to the living, honour to the dead."

PREFACE

This thesis is condensed from notes accumulated during post-graduate studies and research on the vibration of bladed disc assemblies and related subjects. My deepest gratitude goes to Professor P. Grootenhuis for his advisory role at a critical stage in the course of the research.

Dr D. J. Ewins supervised the research programme at Imperial College and initiated contacts with Dr E. K. Armstrong, Mr C. P. Jonson, Mr J. Bennett, and Dr R. Bellamy of Rolls-Royce. I wish to thank them for many useful discussions.

I am particularly indebted to Dr Babatunde Alabi and Dr Tunde Damisah — my friends and erstwhile colleagues in the Dynamics Section — for stimulating exchange of ideas on academic matters.

The prosecution of any inquiry is usually made easier by the indirect contributions of close friends and associates. In this regard, I wish to thank Connie Allen, Jerry Antonio, Gordon Quartey, Owen Green, Sharon Romeo, Dan Obaro, Ray Johnson, John Kamalu, "DT" Etela, Arthur Ekwue, Paul Musonge, Kwaku Frimpong-Ansa, Felicité Tchibindat, John Ngundam, Joga Sidhu, Ali Hadid and many more who I cannot name for lack of space.

Ray Gunn, Technician in the Vibrations Laboratory, and George Tindall of the Reprographics Section are two of the most helpful people one could ever meet. I wish to thank them most sincerely for their support with facilities.

I am indebted to Brendan Molloy of the Communications, Microprocessors and Graphics section of the Imperial College Computer Center for answering many questions on the application of their phototypesetting utility. As the current implementation does not incoporate an automatic spelling corrector, I have had to check for spelling errors visually. Although this has been done carefully, I should be surprised if the affliction of the printer's devil has not affected my vigil. Rules governing the hyphenation of words which fall at the end of some lines in a processed text are many and various. In British English, such hyphenations take cognizance of etymological structures and phonetical conventions. On the other hand, computer procedures are based on rules that are consistent and strictly logical. The application of a logical hyphenation protocol means that certain words must be broken up at the 'wrong' places. This is regretted.

It has not been an easy task to typeset the technical scripts and equations in this thesis using a word processor designed for handling straight forward prose. Inspite of exercising great care, some of the equations have inevitably been set in an inelegant fashion. Any distraction occasioned by this is much regretted.

Finally, I wish to acknowledge financial support from Rolls-Royce Limited, the Ministry of Defence (United Kingdom), and the Federal Ministry of Education (Nigeria) at various times during the course of my post-graduate studies and research.

CONTENTS

Abstract iii
Preface iv
Notation viii

CHAPTER 1. Introduction 1

1.1 Introduction 1
1.1.1 Vibration of Bladed Disc Assemblies 2
1.1.2 Mistuning 2
1.2 Survey of Previous Studies 3
1.2.1 Tuned Assemblies 3
1.2.2 Mistuned Assemblies 4
1.3 Objectives and Scope of This Study 6

CHAPTER 2. Discretized Model 9

2.1 Introduction 16
2.2 Equations of Motion for Free Vibration 17
2.2.1 Analysis of Tuned Systems 20
2.2.2 Analysis of Mistuned Systems 21
2.3 Numerical Treatment 24
2.3.1 Modal Analysis 25
2.3.2 Forced Response Analysis 25
(*a*) Arbitrary Excitation 27
(*b*) Engine-order Excitation 30
2.4 Derivation of Model Parameters 33
2.4.1 Blade Parameters 38
2.4.2 Disc Parameters 39
2.4.3 Assemblies of Integral Construction 42
2.4.4 The Stiffness of a Clapper Ring 43
2.4.5 Practical Application (30 Bladed Disc) 44
2.5 Case Studies 44
2.5.1 Natural Frequencies and Modes Shapes of Free Vibration 45
2.5.2 Forced response Analysis 46
2.6 Concluding Remarks 48

CHAPTER 3. Statistical Analysis 53

3.1 Introduction 83
3.1.1 Measures of Central Tendency 84
3.1.2 Measures of Scatter 85
3.2 Frequency Distributions 86
3.2.1 Normal Distribution 87
3.2.2 Uniform Distribution 88
3.2.3 Skewed Distribution 88
3.3 Analysis of Blades' Dynamic Response 89
3.3.1 Introduction 89
3.3.2 Ten Bladed Disc (*Theoretical Model*) 89
3.3.3 Thirty Bladed Disc (*Theoretical Model*) 91
3.3.4 Thirty-three Bladed Disc (*Engine Test*) 93
3.4 Concluding Remarks 94

CHAPTER 4. Energy Dissipation 113
4.1 Introduction 114
4.1.1 Damped Mechanical Systems 114
4.1.2 Damping Models of Bladed Discs 115
4.2 Eigenvalue Problems of Damped Mechanical Systems 116
4.2.1 Matrix Formulations 116
4.2.2 Linearization of the Quadratic Eigenproblem 118
4.3 A Strategy for Global Convergence 120
4.3.1 Viscous Damping Model 123
4.3.2 Hysteretic Damping Model 125
4.3.3 General Case 125
4.3.4 The Algorithm 126
4.4 Application to Bladed Disc Assemblies 128
4.5 Concluding Remarks 129

CHAPTER 5. Continuum Model 136
5.1 Introduction 137
5.2 Receptances of Bladed Disc Components 139
5.2.1 Blade Receptances 139
5.2.2 Disc Receptances 140
5.3 Case Studies 144
5.3.1 Undamped Response 145
5.3.2 Response with Hysteretic Damping 147
5.4 Concluding Remarks 148

CHAPTER 6. Experimental Investigation 159
6.1 Introduction 160
6.2 Experimental Set-up and Procedure 160
6.3 Analysis of Experimental Data 163
6.4 Concluding Remarks 164

CHAPTER 7. Determination of Blade Frequencies 189
7.1 Introduction 190
7.2 Effect of Root Flexibility on the Natural Frequencies of Cantilevers 191
7.2.1 Bernoulli-Euler Model 192
7.2.2 Timoshenko Beam Model 193
7.2.3 Numerical Case Studies 194
7.3 The Frequencies of Flexibly Mounted Cantilevers 195
7.3.1 Discretized Model 195
7.3.2 Continuum Model 197
7.4 Experimental Verification 201
7.4.1 Stepped Cantilever Beam 202
7.4.2 Twisted Turbine Blade 202
7.5 Concluding Remarks 203

CHAPTER 8. Parametric Studies 210
8.1 Introduction 211
8.2 Mistune Pattern 213
8.2.1 Measure of Smoothness 213
8.2.2 'Worst' Stress 213
8.3 Disc Stiffness 214
8.3.1 Effect of Disc Stiffness on Modal Properties 214
8.3.2 Effect of Disc Stiffness on Blade Response 216
8.4 Concluding Remarks 217

CHAPTER 9. Closing Review 223
9.1 Critique of Previous Studies 224
9.1.1 Twenty-four Bladed Disc: El-Bayoumy and Srinivasan (1975) 225
9.1.2 Seventy-two Bladed Disc: Srinivasan and Frye (1976) 226
9.1.3 Twenty-three Bladed Disc: Fabunmi (1978) 227
9.1.4 Twelve Bladed Disc: Muszynska *et al* (1980) 228
9.2 A Strategy for Dealing with the Mistuning Problem 229

CHAPTER 10. Closure 237
10.1 Conclusions 238
10.2 Suggestions for Further Work 239

REFERENCES 240

Appendix 1 *Matrix forms of the equations of motion*
Appendix 2 *High frequency response of Disc 24X*
Appendix 3 *List of Figures*
Appendix 4 *List of Tables*
Appendix 5 Further details of assembly models

NOTATION

Most of the symbols are defined when referred to in the text, so that comprehension may be sustained without frequent reference to this list. The following is a list of the principal symbols; others referred to once only in the text have not been included. Matrices and vectors are, in the main, set in univers bold.

a_i $(i = 1,...,4)$	arbitrary constants
A_n ... F_n	arbitrary constants
b	frequency coefficient
D	plate flexural rigidity
E	Young's modulus
EI	flexural rigidity
h	mechanical coupling stiffness of the disc
i	index; unit imaginary number, $\sqrt{-1}$
j	unit imaginary number, $\sqrt{-1}$
J_n	Bessel's function of the first kind, of order n
k_i	stiffness of upper blade segment (ith blade)
k_{ij}	dynamic stiffness relating coordinates i and j
K_i	stiffness of lower blade segment (ith blade)
l	length
m_i	mass of upper blade segment (ith blade)
M_i	mass of lower blade segment (ith blade)
n	index
q_i	generalized displacement at the ith coordinate
r	radial coordinate
s_{ij}	dynamic stiffness relating coordinates i and j
Q	amplitude of generalzed displacement
w	plate lateral displacement
W	mass of disc sector
x_i	instantaneous blade tip displacement
X_i	amplitude of blade tip displacement
y_i	instantaneous displacement at clapper point
Y_i	amplitude of clapper point displacement
Y_n	Bessel's function of the second kind, of order n
z_i	instantaneous disc rim displacement
Z_i	amplitude of disc rim displacement

α_i	amplitude ratio
β_i	amplitude ratio
δ_{ij}	kronecker delta
λ_n	eigenvalue of the nth mode
η	loss factor
ω	circular frequency

Superscripts

^{T}	transpose of a real matrix
^{H}	hermitian transpose of a complex matrix
*	complex conjugate
$'$	partial differentiation

Matrices

$\mathbf{A}$	eigenmatrix in standard form
$\mathbf{C}$	viscous damping matrix
$\mathbf{D}(\omega)$	dynamic stiffness matrix
$\mathbf{f}$	force vector
$\mathbf{H}$	structural damping matrix
$\mathbf{H}(\omega)$	transfer function at excitation frequency ω
$\mathbf{I}$	identity matrix
$\mathbf{K}$	stiffness matrix
$\mathbf{L}$	Cholesky's factorization of the mass matrix
$\mathbf{M}$	mass matrix
$\mathbf{0}$	null vector
$\mathbf{q}$	displacement vector
$\mathbf{x}$	displacement vector
$\mathbf{Z}$	dynamic stiffness matrix
$\mathcal{I}_m\mathbf{x}$	imaginary part of $\mathbf{x}$
$\mathcal{R}_e\mathbf{x}$	real part of $\mathbf{x}$
$\mathcal{R}$	Rayleigh's functional
Λ	eigenvalue matrix
ϕ_n	eigenvector of the nth mode
ψ	eigenvector
Ψ	eigenvector matrix

Chapter 1

1.1 Introduction

1.1.1 Vibration of Bladed Disc Assemblies

The generation of electric and motive power for many important engineering activities nowadays frequently requires the use of turbomachines, important components of which are bladed disc assemblies. These machines are generally expected to operate without interruption for very long periods between overhauls or shut-down. Moreover, they are often operated under unfavourable mechanical conditions as in crude oil extraction in desert or marine environments, or in situations where exacting safety standards are required as in aircraft propulsion for civil and military purposes. The designers of such machines are therefore faced with many problems. Chief among the problems is fatigue failure of blades.

The requirements of turbomachine users, especially for aviation applications, are such that although there may be up to 2,000 blades in an aircraft engine, the failure in service of just *one* blade on the compressor or early turbine stage of such an engine could initialise a series of secondary failures leading to the destruction of the whole engine or the loss of human life. Clearly, in such instances even a low failure rate of 1 in 2,000 is not acceptable. It is, therefore, not surprising that much research effort has been expended in trying to avoid blade failure.

The majority of the studies conducted during the early days of research in this field were devoted to the analysis of a single blade cantilevered at its root. Such studies were based on the implicit assumption that each blade on the stage vibrated in isolation from the disc and from all other blades on the wheel. If this were true, then the flexibility of the disc would have no effect on the lone blade's dynamic behaviour. What is usually experienced in practice, however - and this applies even to bladed disc assemblies with considerably stiffened rims and hubs - is that the vibration characteristics of a blade when mounted on a stage are generally far more complex than those obtained when it is extracted from the wheel and grounded at its root. Moreover, a number of failures were reported in the early days of steam turbine manufacture which, as is now well-known but not fully appreciated at that time, were caused by the participation of the disc in the vibrations.

Apart from the effects of disc flexibility, there are other factors which could influence the vibrational behaviour of turbomachine blades. Among these are the effects of rotation, which leads to centrifugal stiffening of the assembly; the extrinsic excitation of the blades due to aerodynamic forces in the surrounding medium; the existence of a part-span *clapper ring*, or a *shroud band* at the blade tips, joining all or a few adjacent blades together; and the presence of minute imperfections in the disc and blades. These and other factors combine to make a 'complete' understanding of the dynamic behaviour of bladed disc assemblies an extremely difficult task.

1.1.2 Mistuning

For many years now, designers of advanced gas turbine engines have given serious thought to an irksome problem in the industry. The problem is that under certain excitation conditions, the nominally identical blades on a rotor-stage do not experience equivalent stress amplitudes. This is contrary to theoretical predictions which are based on the assumption that all the blades on a stage, having been manufactured to the same specifications, are practically identical. In practice, the small differences between the blades cause a few to vibrate vigorously while, at the same time, other blades on the stage are virtually immobile.

In order to achieve comparative levels of dynamic response, it is evidently necessary to eliminate the residual differences by 'tuning' the blades. Hence, a *tuned* bladed disc assembly is one for which all the blades are truly identical. Conversely, in a *mistuned* system the differences in blade properties have not been eliminated completely.

1.2 Survey of Previous Studies

Many research reports and papers have been issued in connection with vibrations of turbomachine components, especially of isolated cantilevered blades. No attempt will be made here to undertake a complete review of the associated literature as the task is both unwieldly and unnecessary for our immediate purposes. The interested reader is recommended to consult our comprehensive bibliography, **Afolabi** and **Ewins** (1979)†, or the excel-

†*References are given in alphabetic author sequence on pages 240 to 249 inclusive*

lent review articles by **Rao** (1973, 1977). However, a brief review of the literature that is directly pertinent to mistuned bladed disc assemblies, and other closely related matters, is necessary and is given herewith.

1.2.1 Tuned Assemblies

Studies of bladed disc assemblies have, traditionally, been based on a very crucial assumption, namely: that *all the blades on the stage are entirely identical* and are, moreover, affixed to a disc which is perfectly circularly symmetric. Vibration models previously used in the study of such idealistic rotors may be classed into three categories as follows:

(a) Unshrouded Bladed Discs

A single stage axial compressor rotor belongs in this category and may be modelled, in the first approximation, as a circumferentially-uniform wheel on to which are attached a number of identical blades. Earlier studies of unshrouded bladed discs were devoted to either the influence of the blades on the rotor disc, or to the effects of the disc on the blades. In the latter case, various theoretical models were used, one of which is due to **Ellington** and **McCallion** (1959), where the disc is assumed to be of infinite radius so that the blades may be visualized as configured in Figure 1.2.1.

The earliest and one of the most influential publications on the dynamic behaviour of bladed disc assemblies was by **Campbell** (1924). In that, and a subsequent paper, **Campbell** (1925), the effects of the blades on the vibration of the disc were examined in an attempt to prevent *disc* failure. The work was mainly experimental.

In addition to laboratory experiments, **Armstrong** (1955) carried out the first comprehensive theoretical investigation of bladed disc assemblies in which the mechanical coupling of the blades through the flexibility of the disc is admitted. He used the method of receptances. Later, Armstrong and co-workers (1960, 1965, 1966) extended his previous analysis to effect a fuller treatment of the free vibration of bladed discs. Some practical implications of their investigations for actual assemblies were also stated.

The receptance coupling method, in the general case, offers a very accurate prediction capability because of its analytic elegance, but it also suffers a major limitation for exactly the same reason since it is

very costly to implement numerically in terms of computer resources. Furthermore, it may not be easily modified to account for the influences of complex geometric shapes that are characteristic of most turbomachine blades; nor can it readily accommodate the effects due to centrifugal loading and to temperature variation. The implementation due to Armstrong, as a specific case of the receptance coupling technique, is only able to deal with rotors having a very large number of blades.

Advances in computational mechanics in the 1960's and early 1970's led to several applications of the powerful finite element method to turbomachine blading research. **Kirkhope** and **Wilson** (1971-1976) were among the earliest workers in this area, but several recent studies have been conducted in the industry as well as in academic institutes. See the reviews by Rao, *op. cit.*, for a comprehensive listing.

(*b*) Shrouded Bladed Discs

In many bladed disc assemblies, especially those commonly found in steam turbines, the blades are connected together at their tips by a welded or rivetted band known as a *shroud*. When the shroud band is circumferentially continuous, joining all the blades on the wheel together, then we have a 'shrouded bladed disc assembly'. In some other assemblies, especially in compressor stages, the blades are not connected together at their tips but at some intermediate point along the blades' length by a *clapper ring* or *snubbers*. Studies of bladed disc assemblies having shroud bands were undertaken in doctoral programmes by, for example, **Cottney** (1975), **Hall** (1968), and **Salama** (1977). Cottney used the receptance coupling technique, while Salama applied the finite element method. In each case the symmetric nature of the wheels was exploited. The receptance analysis utilized 'classical' cyclic symmetry, while the finite element implementations were based on the 'wave propagation' technique for rotationally periodic structures, which is a modification of a method originally introduced by **Brillouin** (1946) for the study of lattice structures.

(*c*) Blade Packets and Packeted Bladed Discs

Whereas in a shrouded bladed disc assembly *all* the blades are connected together, there are other instances when only a group of adjacent blades are thus inter-connected, either at their tips or along the

blade span. Such cases are known as *packeted* assemblies. Several models of the vibration of blades in packets have been considered in previous studies. The schematic illustration of Figure 1.2.2, for instance, is due to **Belek** (1977) who investigated the dynamic response characteristics of shrouded blades on a flexible disc. However, the disc is often assumed to be of infinite radius and rigidity. The blades are then effectively taken to be no more than a group of identical *cantilevers* attached together by the shroud band as illustrated in Figure 1.2.3. One of the earliest treatments is that of **Smith** (1949), while **Prohl** (1958), **Weaver** and **Prohl** (1958), **Ellington** and **McCallion** (1959), **Rieger** and **McCallion** (1965), **Thomas** and **Belek** (1977), and **Afolabi** (1978), among others, have used various theoretical and experimental devices to re-examine the same problem. The dynamic response characteristics of packeted bladed systems in which the effects of disc flexibility are accounted for have been investigated principally by **Ewins** (1980).

1.2.2 Mistuned Assemblies

As discussed in §1.1.2, *mistuning* may be regarded as the violation of circumferential uniformity of a bladed disc assembly. The introduction of mistuning to an assembly may be due to several causes, among them:

(*i*) imperfections of the disc wheel

(*ii*) random variation in blade frequencies due to manufacturing tolerance

(*iii*) non-uniform conditions prevailing at blade root from one slot to another.

It is current practice in mistuned assembly research to assume that the effects due to disc imperfections, and root fixture variations, are of secondary importance when compared with those attributable to the random scatter in blade frequencies, so that what is generally used as a measure of mistune is the cantilever frequencies of the individual blades on a stage. This is justifiable because it has been observed by engine manufacturers that the most glaring deviation from perfection is the stochastic scatter of blade-alone frequencies. Thus, although tolerance specifications may be met in manufacturing the blades on a wheel, a *random* variation of individual frequencies of up to 2 % is not uncommon, whereas it is rare to find cir-

cumferential imperfection of such magnitudes on the disc alone. Nevertheless, the dynamic characteristics of imperfect, elastic discs under static and rotating conditions which have been published by **Tobias** (1950, 1951, 1957), and with **Arnold** (1957), provide a useful insight to the vibration of mistuned bladed assemblies.

For many years now, opinion has remained divided among the leading authorities in this field as to whether or not the 'small' variations in blade frequencies that exist in practice are worth bothering about. Some researchers have dismissed the effects of mistuning as trivial while others considered them important enough to recommend a complete re-design of rotors in certain cases, or even the expensive process of blade selection in order to achieve a 'finer tune'. Nevertheless, while the arguments rage to and fro, costly failures of *rogue* blades, both during engine development and at the prototype production stage, continue to plague the industry.* Because a basic understanding of the dynamic behaviour of bladed disc assemblies is not yet attained, contemporary designs and calculations have to be based on tuned models.

Two basic approaches have been adopted by previous researchers in their theoretical investigations of mistuned assemblies, and these may be distinguished according to whether or not the interconnection of the blades is attributable to aero-elastic or purely elastic (mechanical) origins.

(a) Aero-elastic Coupling

In the first case, the influence of mechanical coupling through the elasticity of the disc or casing is ignored. However, each blade is assumed to be directly connected to its adjacent neighbours and, at the same time, to all other blades on the stage through aerodynamic forces. Such a model was put forward by **Whitehead** (1966), and it has subsequently been modified to incoporate the presence of mechanical coupling, **Whitehead** (1976). Very recently, other workers [**Kaza** and **Kielb** (1981), **Kielb** (1981), and **Srinivasan** (1980)] have adopted the Whitehead model, since it is especially suitable for studies of self-excited oscillations, or flutter.

All the previous investigators of aeroelastic effects have reported on the dual nature of the returns that accrue from the introduction of imperfections to otherwise tuned assemblies: namely, that mistuning is at one and the same time beneficial and adverse. It is favourable in the sense that certain vibration modes which would otherwise have been

* Conditions of blade failure are not always known, and other factors apart from mistuning (e.g. fatigue) play a significant part.

unstable in tuned systems become transformed to stable ones when minute variations of blade frequencies are admitted to an erstwhile tuned assembly. The unfavourable effects of mistuning are experienced when forced response levels are considered, and it is found that resonant stress levels in the mistuned assemblies are up to 300% higher than in the equivalent tuned forms. Such enormous stress increases are usually unacceptable.

(*b*) Mechanical Coupling

In the second type of physical modelling which has been applied by various workers, the disc is treated as an axisymmetric plate of uniform thickness. In some variants of the model, a degree of thickness variation in the radial direction is allowed for on the disc. To this are attached blades which differ from one another in their individual cantilever frequencies. The manner in which the blade cantilever frequencies vary around the disc rim may be displayed as a *mistune pattern*. A variety of mistune patterns has been utilized to date in several theoretical studies of bladed disc assemblies. Some of the patterns are shown schematically in Figure 1.2.4.

One of the earliest studies of the effects of mistuning on blade and disc vibrations to be reported is that by **Ewins** (1966), who applied the receptance coupling method. In addition to theoretical studies, experiments were also conducted on an assembly having five blades. Almost at the same time, **Wagner** (1967) introduced the model shown in Figure 1.2.5 through which usage he considered both mechanical coupling through the disc (modelled as a uniform ring on an elastic foundation), as well as aerodynamic damping (through the use of dashpots associated with each blade).

Another simple but representative model that was proposed by **Dye** and **Henry** in 1969 is to be found in Figure 1.2.6. In their publication, they considered almost all the various types of mistune patterns illustrated in Figure 1.2.4, with the conclusion that stress levels could be up to 200% higher than those on tuned systems, on account of mistuning. The case of only one blade mistuned was, they found, 'potentially the most dangerous'. This is also in line with the observations of **Whitehead** (1966) who employed an aeroelastic model.

Using the **Ehrich** (1956) plate model for the disc and a lumped parameter model for the blades, **El-Bayoumy** and **Srinivasan** (1975), and **Srinivasan** and **Frye** (1976), investigated the effects of the period of "systematic" (square wave) mistuning on the vibration characteristics of several assemblies. In a series of papers **Ewins** (1969-1975), and **Ewins** and **Rao** (1976), used the receptance method, accounting for both hysteretic and viscous damping. Parallel experiments were conducted on a model of a compressor rotor having 24 blades using excitation by air jets in a spin pit to simulate engine order excitations, **Ewins** (1976*b*)

In 1978, **Fabunmi** investigated the effects of random mistuning on the dynamic behaviour of a compressor rotor. He used a semi-empirical approach, in which experimentally derived data were fused with a theoretical model. Such an approach requires the recording of a 'global' set of eigenvectors, or mode-shapes, of the bladed disc. By using electronic circuits to generate a constant phase angle between excitation forces positioned at the root of each blade on a 23-bladed compressor rotor, Fabunmi was able to excite the required twenty-three linearly independent modes of vibration, some of which occured at the same resonant frequency. The mode-shapes were recorded by optical interferometry. After due processing, the holographically recorded modal properties were used to estimate the mass, stiffness and damping parameters for his theoretical model.

The damping effects produced by the environment in which bladed disc assemblies are required to operate is generally attributed to aerodynamic sources, and these are usually simulated theoretically by attaching grounded viscous dampers to blade tips. However, in a recent study, **Muszynska** *et al* (1980), it was pointed out that on account of the non-linear nature of the phenomena involved, it might be more appropriate to use material damping with dry friction. The model proposed in their paper is shown in Figure 1.2.7. It was concluded in that study that when friction was introduced between the blades, it became more dominant than other mechanical linkages furnished by the disc's flexibility.

1.3 Objectives and Scope

Although a number of workers have studied mistuned assemblies in recent

years as discussed above, the state-of-understanding of the problem is by no means settled, since the conclusions of previous workers are at variance, one with another, in many crucial areas. Moreover, many of those studies were concerned with *periodic* or "systematic" mistuning which is, although important under certain circumstances, a special case of mistuning not frequently encountered in practice. If we seek a better understanding of the behaviour of realistic rotors, it seems we cannot avoid the treatment of *random* mistuning in some considerable depth. This study is therefore perdominately based on random mistuning.

Of all the problems associated with blade failure in the turbomachine industry, one of the most intractable is the premature and peculiar failure of only a few blades while all others on the same stage are apparently stress-worthy. Those few overstressed blades which fail unexpectedly are known as *rogue blades.*

If we survey the findings of previous workers, we do not find concord among them with regard to the causes, circumstances and nature of rogue blade failure. These, for example, are some of the practical and urgent questions in response to which a united voice has not been raised to date by the authorities in this field:

(*i*) *Since variations in blade properties are usually within acceptable manufacturing tolerance, are such 'small' differences capable of giving rise to a highly uneven distribution of stresses among the blades to the extent that some could attain rogue failure conditions?*

(*ii*) *If so, what are the conditions under which rogue blade failure could occur?*

(*iii*) *Given an actual compressor rotor, say, such as could be taken straight from an engine or the production line, is it possible to predict before hand which blades are likely to turn rogue?*

(*iv*) *Given, again, a practical bladed assembly, since during an engine test one may not realistically strain gauge more than a few blades in all, how should one go about conducting the test - selecting the blades to gauge - and interpreting the results thus parochially gathered, so that one may be reasonably assured that the worst levels of stressing have not been severly underestimated?*

Before we attempt to answer these and other relevant questions, it is appropriate to re-emphasize that we are dealing here with a mechanical system the nature of which is so complex as to defy closed-form solutions. Therefore, it seems prudent to avoid the path of tedious algebraic analyses that are not likely to come to fruition, and to devise instead a strategy that yields applicable results, based on effective numerical analysis with meaningful data processing and interpretation.

A lumped parameter model was therefore used initially, as documented in Chapter 2, since such a model usually provides a rapid means of establishing relatively cheaply some fundamental patterns in the dynamic response characteristics of randomly detuned wheels. It is shown that the blades with extreme detune in cantilever frequencies are also the ones most likely to experience extreme stressing. In Chapter 3, the response data of representative mistuned assemblies are subjected to statistical scrutiny in order to investigate if bounds on response levels for an entire set of blades on a stage may be reliably estimated by strain-gauging only a few blades during industrial engine tests.

The lumped parameter treatment is extended in Chapter 4 to account for the type of damping in bladed disc assemblies normally attributed to aerodynamic forces. The introduction of damping usually doubles up the eigenmatrices of structural systems, with the effect that the problem solution immediately becomes substantially lengthened, or even impossible for large order systems. An existing algorithm for extracting the latent roots and associated vectors of damped systems - which does **NOT** double the problem size - is examined, whence it is obeserved that it only achieves local convergence if damping is not small. By modifying the original algorithm, due to **Gupta** (1974), we have usually achieved global convergence for our class of problems.

Results obtained from lumped parameter models are sometimes regarded with suspicion, and doubts may be raised on the adequacy of such a simple method for modelling the dynamic behaviour of a complex mechanical system like a bladed turbine wheel. Further studies were, therefore, carried out using finite element and receptance models to incoporate the distributed mass and elasticity of the system. This is also necessary in order to investigate if there is any basis in the oft repeated statement that the results of different workers are in conflict because they are obtained from the application of different mathematical methods. However, the finite element modelling is not documented here because the results obtained from its usage are broadly in line with those arrived at via the application of receptances, details of which are given in Chapter 5.

Some laboratory experiments were conducted, as described in Chapter 6. It is pertinent to remark, however, that the facilities normally available in university laboratories are only adequate for limited experimentation in this field, given the complex nature of *practical* bladed disc assemblies and the kinds of conditions under which they are called upon to operate. An objec-

tive common to many of the previous doctoral theses is the achievement of 'good agreement' between theoretical calculations and experimental observations. Consequently, the physical models tested in such experimental programmes tended, generally, to represent the system described by the theory much more faithfully than they represented practical bladed discs. The laboratory experiments conducted in the course of this study, on the other hand, were designed in such a way that the general principles governing the dynamic behaviour of mistuned bladed discs which were established from the theoretical studies could be verified either on academic models or on practical bladed systems.

One of the principles established from the studies in chapters 2 to 6 is that the blades with extreme detune in cantilever frequencies were those likely to experience the largest amplitudes of response. However, it is not easy to identify such blades on a stage, especially for bladed discs of integral construction, because the blades do not behave like isolated cantilevers on account of their coupling through the disc's flexibility. Chapter 7 is, therefore, devoted to the analysis of a flexibly mounted 'cantilever' blade. It is shown that the assumption of infinite rigidity at blade root, which is usually assumed in many theoretical studies, leads to an overestimation of natural frequencies. An experimental procedure is proposed for neutralising the influence of root resilience on the measured cantilever frequencies of blades affixed to flexible discs, so that the blades with extreme frequencies may be easily and accurately identified.

Parametric studies are carried out in Chapter 8, in order to investigate if certain characteristics of a given assembly which may be varied by design engineers could improve, or otherwise worsen, the vibration response of the assembly. It is shown, for example, that we do not necessarily obtain a reduction in blade vibration amplitudes by increasing the stiffness of the disc.

The penultimate chapter is devoted to an examination of the conclusions of previous workers. In light of the findings of this investigation, many of their 'contradictory' conclusions may be resolved since such deductions are actually in harmony, to the extent that they are local perceptions of a global trend. Finally, in Chapter 10 we set out some conclusions and recommendations arising out of this research.

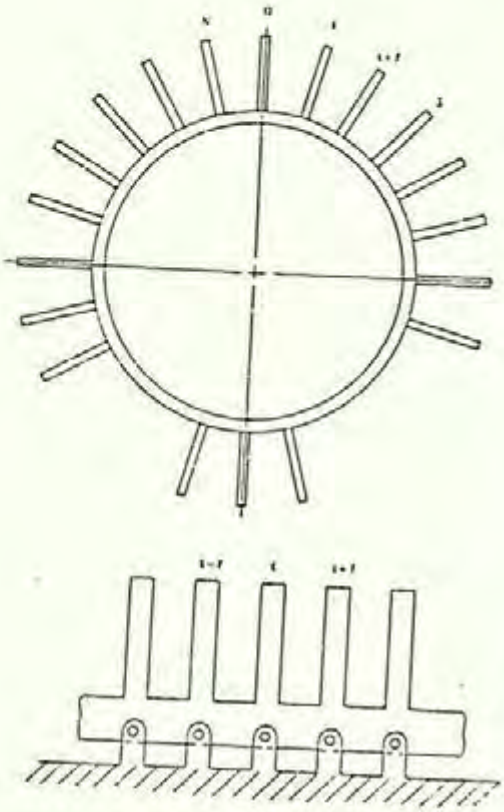

Fig. 1.2.1 *Mathematical model of a bladed disc*
Ellington & McCallion (1959)

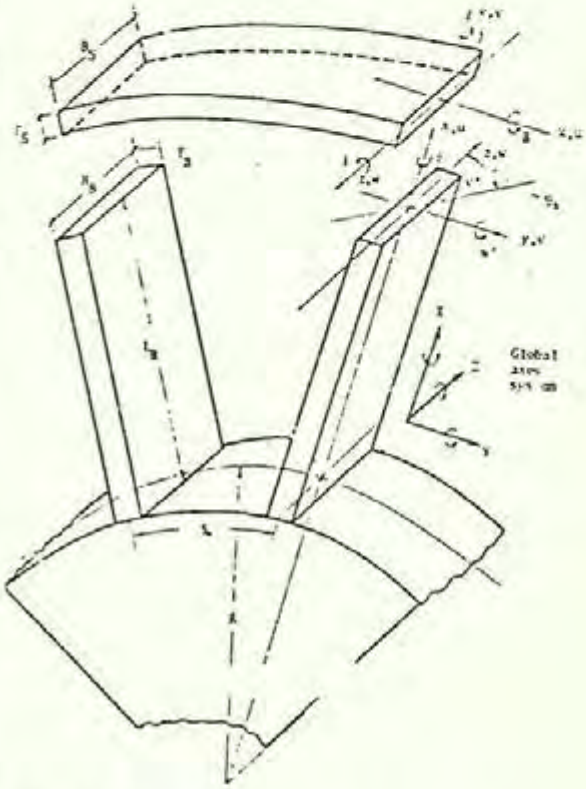

Fig. 1.2.2 *Shrouded blades on a flexible disc*
Belek (1977)

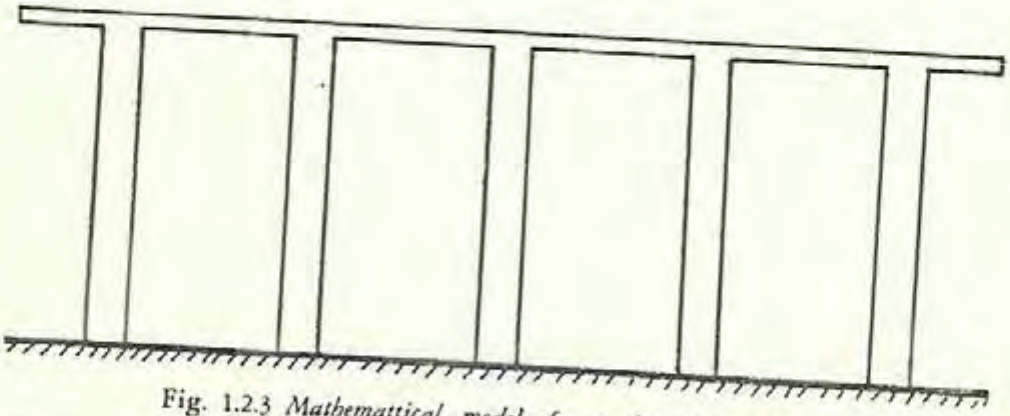

Fig. 1.2.3 *Mathemattical model of a packet of five blades*

Fig. 1.2.4 *Mistune patterns*

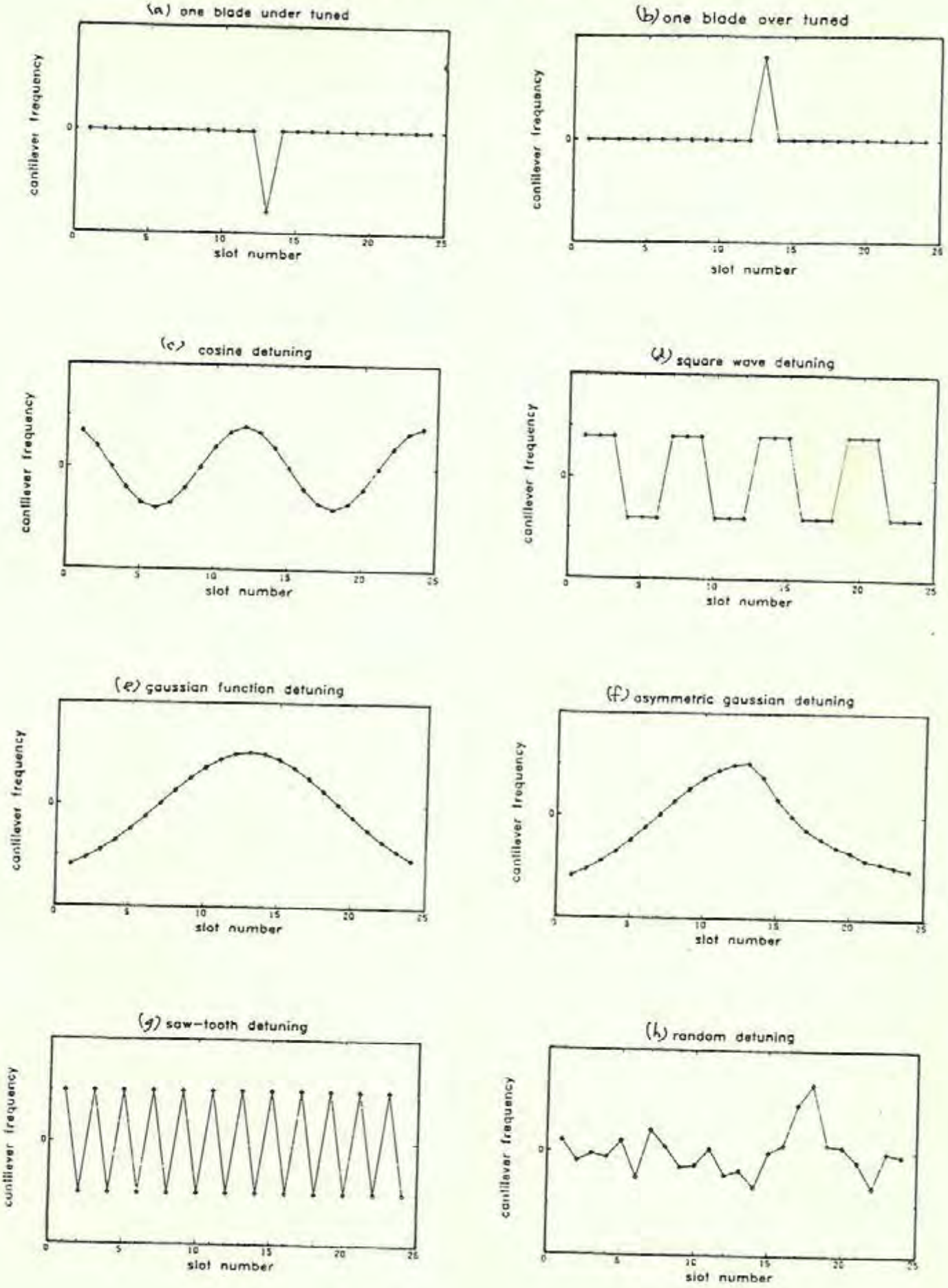

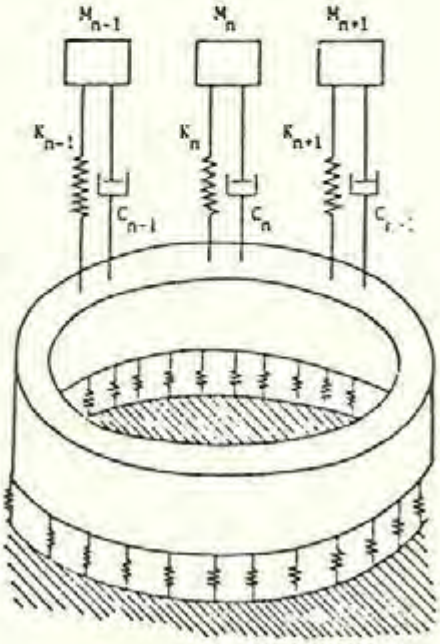

Fig. 1.2.5 *Bladed disc assembly modelled as beams on an elastic foundation*
Wagner (1967)

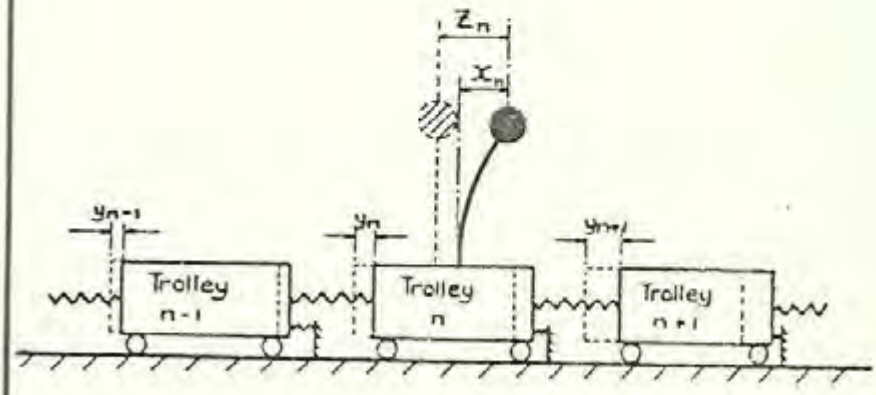

Fig. 1.2.6 *Mathematical model of a mistuned assembly*
Dye & Henry (1969)

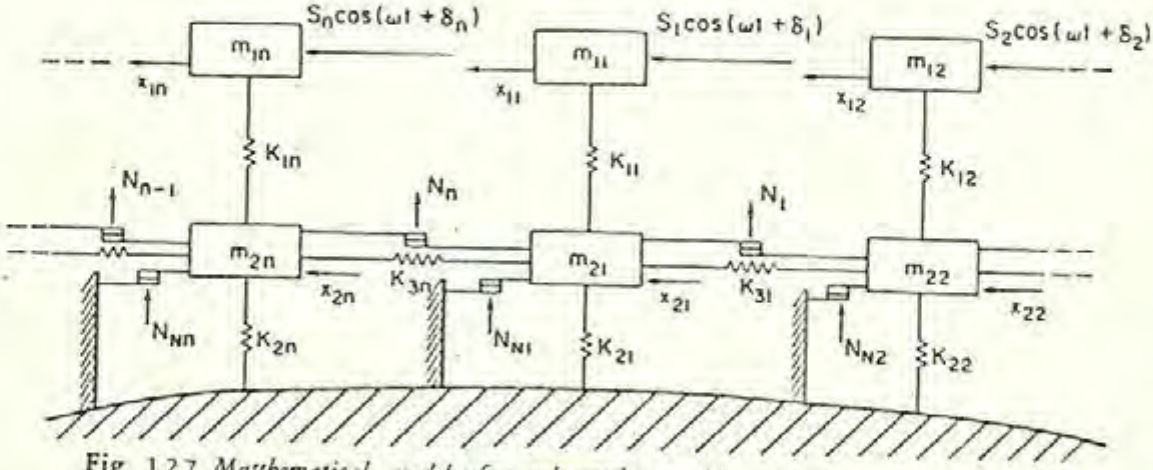

Fig. 1.2.7 *Matthematical model of a mistuned assembly with friction damping*
Muszynska *et al* (1980)

Chapter 2

2.1 INTRODUCTION

An inescapable consequence of mechanical manufacturing processes is that a certain amount of residual non-uniformity exists among nominally identical products. The resulting non-uniformity in vibration properties is, in the case of turbine blades, generally referred to as *mistuning*.

Several parameters may be used to indicate the extent of mistuning among a given batch of blades, e.g. the variation in blade mass, length, stiffness, *etc.* However, the most frequently used characteristic is the first resonant frequency a blade would have if it was clamped rigidly at its root and subjected to flapwise vibration. This is variously known in the literature as 'blade alone frequency', 'blade cantilever frequency', or 'blade 1F' - denoting the first flexural vibration mode.*

Because mistuning characteristics are engendered by the stochastic tendencies of assembly production, the blade cantilever frequency is, in general, a random function of blade slot on a practical rotor stage. Thus, out of 116 blades on the first stage of an advanced engine examined by **Srinivasan** and **Frye** (1976), a frequency scatter having a range of 90Hz about the mean value of 1343Hz was reported. For many years, engine designers ignored such small variations in blade properties - which are usually within manufacturing tolerances - in their theoretical calculations. Even now, it is still standard practice to assume that all the blades on a stage are identical when predicting the vibration response of bladed rotors. However, in addition to the basic mistune arising out of manufacturing tolerance, small differences also exist in mounting arrangements from one blade to to another.

A significant consequence of the foregoing is that certain blades, under certain excitation conditions, are liable to experience unduly high stress levels and, at times, to fracture prematurely while all other blades on the stage are still stress-worthy. This phenonmenon, as has been mentioned in the introductory chapter, is known as *rogue blade failure*.

Several investigators - notably **Dye** and **Henry** (1969), **El-Bayoumy** and **Srinivasan** (1975), **Ewins** (1966-76), **Fabunmi** (1978, 1979), **Kielb** (1981), and **Whitehead** (1966, 1976) - have at various times considered the effects of mistuning on blade and disc vibration. While they agree on certain results and observations (especially with regard to modal properties), they also disagree on many other important deductions, especially in connection

* Higher blade cantilever frequencies (e.g. 2F) may also be used as a measure of mistuning, depending on the coupled frequency of the assembly.

with forced response levels. For example, it is a crucial matter to be able to predict fairly accurately the circumstances under which rogue blade failure would occur and, moreover, to identify beforehand those few blades in the assembly that are likely to turn rogue, so that remedial measures could be taken before failure occurs. To date, no conclusive evidence has been advanced in these and other vital areas. Thus, for example, different researchers predict the blade likely to rogue variously as:

(*a*) the blade with the lowest cantilever frequency
(*b*) the blade with the worst mistune
(*c*) the blade whose cantilever frequency coincides with a resonant frequency of the whole bladed assembly
(*d*) any blade at all.

Most of the studies cited above have been based on different theoretical models in which various damping types have been used. It has, therefore, been suggested by many investigators - for instance, Srinivasan and Frye - that the different results previously attained by the different researchers may be attributed to the differences in their theoretical models. While some degree of divergence in quantitative results is to be expected, extreme variations - and even contradictions - in qualitative opinions as have been witnessed means that further work is needed to enable us understand to greater depth the consequences of these 'small' variations in blade properties on the response levels.

A notable factor that makes it difficult to obtain the 'correct' solutions to this vibration problem is the difficulty of obtaining a large enough set of representative response data. This is significant since the response levels fluctuate widely, in a mistuned assembly, from one blade to another and from one vibration environment to another. Before valid conclusions can be drawn, then, the acquisition and detailed analysis of a large amount of theoretical or experimental data is essential. Rather than study a wheel with very many blades of which we are forced to focus attention on only a few, it may be more instructive to observe a wheel with a few blades *all* of which are adequately monitored. Many previous workers have been constrained to limit their observations to a narrow frequency range (where all or most of the blades may be observed), or to only a few blades on the assembly for a wider frequency spectrum observation.

Our principal aim in this chapter is to investigate as comprehensively as possible the basic vibration characteristics of mistuned assemblies - especially in connection with their forced response properties, in which area there have been the most significant differences of expert opinions. Towards achieving this objective, we shall select a mathematical model having a few blades (between 10 and 30 on a stage) all of which may be closely observed for their response properties under various excitation conditions.

As discussed in the earlier chapter, three basic theoretical approaches have been utilized previously to investigate mistuning effects in models admitting of mechanical coupling through the disc. They are:

(*a*) lumped parameter method

(*b*) receptance methods

(*c*) influence coefficients and lumped parameter

The three approaches yield practically identical qualitative predictions of mode shapes and natural frequencies of free vibration, but the quantitative values of natural frequencies predicted are understandably different. Receptance methods are generally more accurate than lumped parameter methods, but they entail lengthy and complicated analyses and as such are not very suitable for the indepth study of various mistuning models on an economical scale. This is especially relevant since what we seek, in this chapter, are some general principles governing the dynamic behaviour of mistuned rotors and not of specific assemblies; hence the need for several case studies. The computational effort required by the lumped parameter method is, by comparison with that required by receptance techniques, almost insignificant. Moreover, it has been reported by **Fabunmi** (1978) that a lumped parameter method in which the 'parameters' are determined from an experimental modal analysis is capable of yielding very accurate predictions.

In the original lumped parameter model of a mistuned compressor rotor proposed by **Dye** and **Henry** (1968, 1969), a single lumped mass was used to represent each blade, with the sectorial mass of the disc lumped at the root of each blade. Further details are available in their 1969 paper. Their model leads to a linear algebraic eigenvalue problem of order 2N by 2N, where N is the number of blades on the rotor stage.

An improved version of their model, on which the following analyses are based, is shown in Figure 2.1.1. The blade is now modelled as two lumped masses (*cf* Figure 1.2.7), with the sectorial mass of the disc lumped, as before, at the root of each blade. Such a model leads to a 3N degree-of-

freedom problem, which means we have a bigger eigenvalue problem. However, two advantages accrue from this modification:

(*a*) the scope of observation is widened - a 3N eigenvalue spectrum provides a better view than that of 2N;

(*b*) certain assemblies are characterized by the presence of a clapper ring linking the blades at an intermediate point between blade tip and blade root. The presence of such a clapper ring or 'snubbers' may be easily incoporated in the proposed model.

It is customary in mistune investigations to assume that the deviation from the cyclically symmetric nature of the system is due to the blades only, i.e. the disc is entirely uniform around its circumference. We can therefore represent the disc mass and stiffness parameters by constant values. As for the mistuning of blades, it is of no consequence for our purposes here whether they arise out of mass non-uniformity, or they are attributable to stiffness differentials. All that matters in this formulation is that the blades have different cantilever frequencies. We shall, therefore, assume that the blades have identical masses but slightly different stiffnesses. We may furthermore assume that the system is undergoing flapwise vibration, although the analysis applies without further modification for torsional oscillations if we replace the rectilinear parameters by their rotational equivalents.

2.2 Equations of Motion for Free Vibration*

If the flexural tip deflection of the ith blade is represented by x_i, while the deflection at an intermediate point along the blade span (the point of attachment of a part-span shrouding, if one is present) is denoted by y_i, and the disc rim deflection at the root of the ith blade is z_i, then we obtain the following equations, where $\ddot{x}=\partial^2 x/\partial t^2$, *etc*:

$$m_i\ddot{x}_i + k_i(x_i-y_i) = 0 \tag{2.2.1}$$

$$M_i\ddot{y}_i + K_i(y_i-z_i) + k_i(y_i-x_i) = 0 \tag{2.2.2}$$

$$W\ddot{z}_i + K_i(z_i-y_i) + (2h+g)z_i - h(z_{i+1}+z_{i-1}) = 0 \tag{2.2.3}$$

If we assume a harmonic vibration at the frequency ω then $x_i = X_i e^{j\omega t}$ $(j=\sqrt{-1})$, *etc*; and upon removing the time dependence from equations (2.2.1) to (2.2.3), we obtain:

* See Figure 2.1.1 (page 54)

$$X_i = \alpha_i Y_i \tag{2.2.4a}$$

$$Y_i = \beta_i Z_i \tag{2.2.4b}$$

where:

$$\alpha_i = \frac{k_i}{k_i - \omega^2 m_i} \tag{2.2.5a}$$

$$\beta_i = \frac{K_i}{(K_i - \omega^2 M_i) + k_i(1-\alpha_i)} \tag{2.2.5b}$$

The equations (2.2.1) to (2.2.3) of motion may be expressed in terms of disc rim amplitudes of displacements, at the root of each blade, thus:

$$-hZ_{i+1} + [(2h+g-\omega^2 W) + K_i(1-\beta_i)]Z_i - hZ_{i-1} = 0 \tag{2.2.6}$$

2.2.1 Analysis of Tuned Systems

A study of the vibration characteristics of a perfect rotor is usually undertaken in the first instance in the course of developing procedures for analysing mistuned assemblies. This is because the vibration modes of tuned systems are circularly symmetric and are now well understood.

For an ideal rotor, equations (2.2.1) to (2.2.6) above are valid if the individual blades are made to lose their imperfections, so that their parameters become identical with the nominal value. The governing equations are then reducible to the form shown below, where Z_i is the disc-rim flapwise displacement at the root of the ith blade, as before. Thus:

$$Z_{i+1} - 2bZ_i + Z_{i-1} = 0 \tag{2.2.7}$$

with

$$b = 1 + \frac{(g-\omega^2 W) + K(1-\beta)}{2h} \tag{2.2.8a}$$

$$\beta = \frac{K}{(K-\omega^2 M) + k(1-\alpha)} \tag{2.2.8b}$$

$$\alpha = \frac{k}{K-\omega^2 m} \tag{2.2.8c}$$

and where, in equations (2.2.8), previously subscripted symbols which are now without subscripts represent the equivalent tuned parameters.

Equation (2.2.7) is a second order linear difference equation, the exact solution of which may be obtained by using the well known techniques of operational calculus. The relevant boundary conditions are as follows:

when $i=1$, $$Z_{i-1} = Z_0 = Z_N \tag{2.2.9a}$$

when $i=N$, $$Z_{i+1} = Z_{N+1} = Z_1 \tag{2.2.9b}$$

If we assume that the amplitudes vary sinusoidally around the disc rim, then

$$Z_n = Ce^{jn\theta} \tag{2.2.9c}$$

Upon substituting the boundary conditions and the assumed amplitude variation of equation (2.2.9c) into (2.2.7), we easily obtain the equations for natural frequencies and mode shapes of free vibration.

Frequency equation for the *n*th nodal diameter modes

The eigenvalues of the system may be extracted from the equation:

$$a_1\lambda^3 - a_2\lambda^2 + a_3\lambda - a_4 = 0 \tag{2.2.10}$$

where

$a_1 = mMW$

$a_2 = mM[2h(1-\cos\vartheta) + (g+K)] + k(m+M)W + KmW$

$a_3 = kK(m+W) + kM[2(1-\cos\vartheta) + (g+K)] + m(k+K)[2h(1-\cos\vartheta)+g]$

$a_4 = kK[2h(1-\cos\vartheta)+g]$

and $\vartheta = 2\pi n/N$

The roots of the cubic polynomial in λ in equation (2.2.10) are real, positive and distinct and are the three eigenvalues for the 0-, 1-, 2-circle—

n-diameter modes of vibration.

Mode shapes at the *n*th nodal diameter

The deflection amplitudes of disc rim at the points of blade attachment are of the form:

$$Z_i = A_n(\cos 2\pi ni/N + j\sin 2\pi ni/N) \tag{2.2.11}$$

where

$$j = \sqrt{-1},\ i = 1,2,3...N$$

and the limit of the series n is $\frac{1}{2}N$, for N even, and $\frac{1}{2}(N\text{-}1)$, for N odd; while A_n is an arbitrary constant for the nth mode.

For the tuned system, α_i and β_i in equations (2.2.4) are constants as given in equations (2.2.8). Hence, we may obtain the blade tip and part-span deflection mode shapes as

$$Y_i = \frac{A_n K(k - m\lambda_n)}{(k + K - M\lambda_n)(k - m\lambda_n) - k^2}\,[\cos\vartheta_i + j\sin\vartheta_i] \tag{2.2.12}$$

$$X_i = \frac{A_n kK}{(k + K - M\lambda_n)(k - m\lambda_n) - k^2}\,[\cos\vartheta_i + j\sin\vartheta_i] \tag{2.2.13}$$

where, in equations (2.1.12) and (2.2.13), λ_n is the eigenvalue of the nth mode, i.e. ω_n^2, and other symbols are as defined in equation (2.2.11).

Equations (2.2.11) to (2.2.13) reveal, on inspection, that there are two modal shapes in quadrature with each other at every mode, except when $n = 0$, for which the sine shape vanishes and all the blades on the wheel have uniform displacements (the so-called umbrella mode), and when $n = \frac{1}{2}N$, in the case of an even number of blades on the stage, the cosine form does not exist, and every blade vibrates in anti-phase with its adjacent neighbours. For the modes at which double (sine and cosine) modes co-exist, the corresponding eigenvalues are all of double multiplicity. Because the modal shapes of tuned systems can be resolved into two orthogonal circular functions as shown above, their Fourier decomposition yields 'pure nodal diameter' components.

It is to be noted that for the tuned system, the blade tip and clapper point displacements are constant multiples of each other, and of the blade root displacements.

2.2.2 Analysis of Mistuned Systems

On an actual bladed disc assembly, the perfect symmetry witnessed above in the modes of a tuned system ceases to hold. The governing equations of motion are, from equation (2.2.6),

$$Z_{i+1} - 2bZ_i + Z_{i-1} = 0 \tag{2.2.14}$$

where

$$b_i = 1 + \frac{(g-\omega^2 W) + K_i(1-\beta_i)}{2h} \tag{2.2.15a}$$

$$\beta_i = \frac{K_i}{(K_i-\omega^2 M_i) + k_i(1-\alpha_i)} \tag{2.2.15b}$$

$$\alpha_i = \frac{k_i}{K_i-\omega^2 m_i} \tag{2.2.15c}$$

Equation (2.2.14) is a second order recurrence relation with variable coefficients. An exact analytic solution of the difference equation - which is essentially a differential equation - may be accomplished through the application of integral transforms, e.g. Laplace's or Fourier's, if desired. Alternatively, we could effect its solution by the use of 'generating functions', or the method of 'reduction of order', of difference calculus.

However, the mode shapes of a mistuned system obtained from such procedures are much more complex than those of the equivalent tuned system, which were pure circular functions as given in equation (2.2.11). Thus, while the nth modal shape of the tuned system is a pure sine or cosine form of period n, the detuned mode shape is now a linear superposition of several sine and cosine wave forms of various periods. Furthermore, the deflection of blade tip and clapper point are no longer uniform multiples of each other or of the disc rim displacements. See equations (2.2.5).

2.3 Numerical Treatment

2.3.1. Modal Analysis

The eigenvalues of the mistuned system may theoretically be solved for upon substituting the boundary conditions of equations (2.2.9) into (2.2.14) and (2.2.15). It must be noted, however, that the resulting analytic expressions are rather cumbersome. Moreover, unlike in the tuned case, they do not furnish by inspection any useful insight into the system's behaviour. Attempts to construct numerical implementations directly from such analytically derived expressions are, moreover, prone to acute induced instability.

An alternative and rather more appropriate way of obtaining the required modal properties is to cast the equations of motion into matrix form and to use any of the numerous numerical routines available nowadays to effect the eigensolutions.

The required matrix equation for the basic undamped system is of the form

$$\mathbf{M}\ddot{\mathbf{q}} + \mathbf{K}\mathbf{q} = 0 \tag{2.3.1}$$

where $\mathbf{M}$ and $\mathbf{K}$ are the mass and stiffness matrices respectively, and $\mathbf{q}$ is the displacement vector of blade tip, clapper point and disc rim, i.e.

$$q_i = \{x_i, y_i, z_i\}^{\mathrm{T}}$$

Because the equations of motion are in a recursive form, the matrix $\mathbf{K}$ is very narrowly banded - i.e. its non-zero elements are very near to the leading diagonal, except for the existence of a cross-coupling term between the 1st and Nth disc rim positions. This cross-coupling term is the only non-zero element in $\mathbf{K}$ that is substantially located away from the diagonal band. This type of matrix pattern results if one numbers the blades in a natural sequence circumferentially as previous workers have usually done, i.e. if the elements of the vector $\mathbf{q}$ are ordered as

$$q_1, q_2, q_3, \ldots q_{N-1}, q_N.$$

However, by a judicious adoption of some other numbering sequence for the vector elements, it is possible to reduce the stiffness matrix into a purely band symmetric form; the mass matrix being always diagonal in this lumped parameter formulation. See Appendix I for more details. Thus, if

the vector elements are taken in the order

$$q_1,\ q_N,\ q_2,\ q_{N-1},\ q_3,\ q_{N-2}\ \cdots$$

then, the resulting **K** is band symmetric with a semi-bandwidth of 7, so that eigenproblems of size $3N$ by $3N$ consequently become reduced to those of order $3N$ by 7 (where N is the number of blades). A significant consequence of this is that we can accommodate more blades in our model for a given computer core, and obtain substantial gains in computation time.

If we let $\lambda = \omega^2$, equation (2.3.1) may be converted to the standard form of the linear eigenvalue problem:

$$\mathbf{Ax} = \lambda\mathbf{x} \tag{2.3.2}$$

by using the Cholesky factorization of the mass matrix:

$$\mathbf{M} = \mathbf{LU} = \mathbf{LL}^{\mathrm{T}} \tag{2.3.3}$$

and the similarity transformation,

$$\mathbf{x} = \mathbf{Lq} \tag{2.3.4}$$

This is possible because **M** is positive definite. It is, moreover, desirable in order to ensure that the advantageous band symmetric form cultivated above through the selection of an optimizing numbering order is preserved in **A**, where:

$$\mathbf{A} = \mathbf{L}^{\mathrm{T}}\mathbf{KL} \tag{2.3.5a}$$

since, in the alternative form for stating the eigenvalue problem,

$$\hat{\mathbf{A}} = \mathbf{M}^{-1}\mathbf{K} \tag{2.3.5b}$$

$\hat{\mathbf{A}}$ is an unsymmetric matrix which is generally neither sparseley populated nor banded.

In many instances, interest in the eigensolution is centered on a selected number of eigenvalues and their corresponding vectors; for example, in the so-called 'family' modes of vibration of bladed disc assemblies, one may be interested in, say, the second 'family' only. In such cases, it becomes uneconomical to compute the global eigensystem of **A**. It is more appropriate to use a combination of the Sturm sequence technique and the method of bisection to isolate approximations for the required latent roots, after

which we may apply a few steps of inverse iteration, which generally ensures convergence to the relevant eigenvectors. The Rayleigh's Quotient is finally used both as a test of convergence towards, and also to provide a more accurate estimate of, the required eigenvalue. The eigenvalues obtained via such a procedure are usually accurate to working precision, as shown by **Gupta** (1973) and **Wilkinson** (1965).

Because we are dealing with a mechanical system which has many repeated latent roots in the case of tuned assemblies, while the mistuned systems are characterized by several pathologically close eigenvalues, it is essential that the initial vectors selected in the inverse iteration procedure be as orthogonal as possible to all previously computed vectors, **Wilkinson** and **Reinsch** (1971). The required orthogonalization may be accomplished through the application of the well-known Gram-Schmidt process. Furthermore, the Euclidean norms of the computed vectors are constructed in such a way that all the eigenvectors are orthonormal with respect to the matrix **M**.

Other instances also arise when the complete eigensystem of **A** is required. In such cases, similarity transformation methods which compute the eigensolution directly are to be preferred to the inverse iteration procedure, so that the banded eigenmatrix **A** is first reduced to the triple diagonal form using **Wilkinson**'s (1960) implementation of the Householder transformation process. The rational QL algorithm is subsequently applied to effect the global eigensolution, **Garbow** *et al* (1977).

2.3.2 Forced Response Analysis

Much of the research effort in the vibration of turbomachinery components has been devoted mainly to the prediction of natural frequencies and mode shapes of free vibration of single blades, blades in packets, or bladed discs. This is because it is very important to be able to predict, at the design stage, the frequencies at which resonant conditions are likely to occur so that the operating speeds of the machinery may be placed at some safe distance away from such frequencies as are likely to excite any of its resonant modes. Such is the well-known principle of 'designing away from resonance'.

However, in certain installations, the machinery must necessarily operate over a wide range of speeds. In that case, it becomes impossible not to

pass through and, indeed, to dwell for a while at some of the resonant frequencies of the system. Even in the case of machines that are operated at constant speeds, it is sometimes difficult to obtain adequate safety margins between the excitation frequencies and the natural frequencies of the turbomachine components. Under such conditions, a knowledge of the natural frequencies and mode shapes alone, no matter how accurate, is not sufficient. What is of greater relevance is to be able to predetermine, fairly accurately, the probable amplitudes of displacement and stress levels *under resonant conditions*. In this way, excitation of modes which could give rise to unacceptable displacement or stress levels can be avoided so that one may yet operate under resonant conditions, provided one has ascertained beforehand that the consequences of so-doing are not likely to be severe.

In order to predict dynamic response levels reliably, it is useful to have an understanding of the nature of the exciting forces to which bladed disc assmblies are subjected in service. With regard to aero-engine turbines and compressor rotors, the more important causes of vibration are as follows:

(*a*) **Excitation Induced by Wakes**

Under normal operating conditions, blades on a rotating turbine wheel move behind a ring of nozzles through which working fluid impinges on the rotor. However, the pressure of the buffeting fluid is not generally uniform around the annulus on which the nozzles are mounted, so that each blade on the rotating wheel is subjected to excitation which varies with time during each period of revolution. The non-uniformity of the fluid pressure is caused by obstructions in the flow, such as bleed ports, stator blades, bearing supports, combustors, *etc.* Thus, the force acting on any given *i*th blade may be shown as shown in Figure 2.3.1.

(*b*) **Excitation by Partial Admission**

In the case of the excitation force depicted in Figure 2.3.1, it is taken for granted that the arc of jets through which working fluid is admitted to the turbine is circumferentially complete. However, in the early stages of some steam turbines, the fluid may be admitted through an incomplete segment of arcs, leading to what is known as *partial admission*, **Kroon** (1940). The excitation force is still of a periodic nature, but it now produces an intermittent loading on the blades, as

illustrated in Figure 2.3.2.

(*c*) **Excitation Engendered by Other Components**

It does not appear, from a perusal of the literature, that the type of excitation to be considered next had been given much thought by previous workers, although recent experience in the industry† has indicated that it could be just as frequent in practice as the type of excitation induced by wakes.

In cases (*a*) and (*b*) above, the amplitude of the exciting force, $F_p(\omega)$ is generally assumed to be invariant with respect to the speed of engine rotation, ω. In fact, the amplitude is taken to be unity throughout the speed of interest, in several theoretical treatments. However, it has been observed† that $F_p(\omega)$ attains a rapidly ascending value in the neighbourhood of some critical speeds of engine rotation as shown in Figure 2.3.3*a*. No reasons have, as yet, been advanced for such a curious variation of F_p with ω, but a possible explanation is offered here.

Suppose that some engine components, such as gearings, accesory drives, or any other devices to which the bladed disc assembly is connected - directly or indirectly - were to have a local resonance at a frequency ω_c. If damping is slight, we may represent the variation of the amplitude of the resonating component with ω as shown in Figure 2.3.3*b*. It, therefore, follows that in addition to either one of the excitation forces considered in (*a*) and (*b*) above, a third force is now present. This third force would probably have an amplitude modulating effect on, say, the excitation induced by wakes. If we devote attention to the neighbourhood of Ω_1, which is assumed to be coincident with ω_c, then the fluid pressure incident on the bladed wheel could have the pattern shown in Figure 2.3.3*c*. Such a frequency dependent excitation could pose a very serious threat, unless particular efforts were made to attenuate the secondary vibration giving cause to it.

All of the three principal types of excitation considered so far in this section are variants of what is generically known as *engine order* excitation, since they are basically related in a close manner to the speed of engine rotation. Other forms of vibration may also arise singly, or subdominantly

†Bellamy, R. A. *Private Communication*, Rolls-Royce, Derby.

in conjunction with those discussed above, on account of the following considerations: *rotating stall* - due to compressors operating below the rated speed; *turbulence* - of the working fluid, leading to random vibrations; *flutter* - due to aerodynamic forces changing with blade deflections; *etc.* These sources of vibration, while important under certain circumstances, are not of primary interest in this study. However, some non engine-ordered vibrations are considered in brief in what follows under the umbrella term 'arbitrary excitation'.

Arbitrary Excitation

In the theoretical formulation of §2.3.1, the presence of damping in the bladed system, or in the environment in which it operates, was ignored. However, bladed disc assemblies are generally assumed to operate in an environment where the effects of aerodynamic forces are not small, although the disc-blade system may itself be characterized by very small damping of a structural nature.

However, the absence of appreciable damping in the system is a convenient assumption to make in order to determine rapidly the modal properties of our assembly models, since the eigenproblem solution of *damped* structural systems is considerably more expensive in terms of computing storage and CPU time. This is principally because matrices of order N become transformed to those of order 2N. A justifiable reason for excluding damping in §2.3.1 is that many mechanical models in which damping is accounted for are based on the presence of proportional hysteretic damping. It has been shown by **Rayleigh** (1887) that when damping is proportional to either one or both of the mass and stiffness matrices, then the eigenvectors of the system are not affected by the inclusion of damping in the eigenvalue problem.

However, in this Section, we are primarily interested in response levels, so that it is advisable to incoporate some form of realistic damping into the analysis - especially in the neighbourhood of a resonant frequency - otherwise the responses would tend towards infinite values.

If the previous theory is now ammended to enable the admission of hysteretic damping into the system, such that the loss factor of every blade, and disc sector, is proportional to its corresponding stiffness parameter, then the matrix equations may be cast in the following form:

$$\mathbf{M}\ddot{\mathbf{q}} + \mathbf{K}\mathbf{q} + j\mathbf{H}\mathbf{q} = \mathbf{f} \tag{2.3.6}$$

where $j = \sqrt{-1}$, $\mathbf{H} = \eta\mathbf{K}$, and η is the loss factor, while $\mathbf{M}$, $\mathbf{K}$ and $\mathbf{H}$ are respectively the mass, stiffness and structural damping matrices; $\mathbf{q}$ the vector of displacements, and $\mathbf{f}$ is a vector of the externally applied steady state forces. If the external forces vary in both modulus and phase around the disc rim, then the elements of $\mathbf{f}$ are complex quantities, and the solution for $\mathbf{q}$ in equation (2.3.6) is therefore also complex.

Now, the eigenvalue problem represented by equation (2.3.6) when $\mathbf{f}$ is null (for free vibration), may be regarded as some perturbation of the basic eigenproblem of the undamped system given in equation (2.3.1). It has been shown elsewhere [**129**], that when elements of a matrix $\hat{\mathbf{A}}$ are small random perturbations of those of $\mathbf{A}$, i.e.

$$\hat{\mathbf{A}} = \mathbf{A} + \varepsilon$$

where ε is some perturbation matrix, and

$$\|\varepsilon\|/\|\mathbf{A}\| \to 0,$$

then, although the eigenvalues of $\mathbf{A}$ may be substantially different from those of $\hat{\mathbf{A}}$, the eigenvectors of $\hat{\mathbf{A}}$, however, are little different from those of $\mathbf{A}$. In the foregoing, $\|\ .\ \|$ denotes the matrix norm defined by

$$\|\mathbf{A}\| = max\Sigma|a_{ij}|.$$

In the particular case when $\hat{\mathbf{A}}$ is a regular perturbation of $\mathbf{A}$ i.e. $\varepsilon = \alpha\mathbf{A}$, where α is a constant, then the eigenvectors of $\hat{\mathbf{A}}$ and $\mathbf{A}$ are identical. This, of course, is another statement of the the well-known principle of vibration testing, namely: that the mode shapes of proportionally damped mechanical systems are exactly the same as those of the corresponding undamped system.

If Ψ is the global eigenvector matrix of the hysteretically damped system, orthonormalized with respect to the system mass matrix $\mathbf{M}$ as the weighting by the application of the Gram-Schmidt process, then we may construct the following transfer function of the system's frequency response:

$$\mathbf{q}(\omega)e^{j\omega t} = \Psi.\mathbf{G}(\omega).\Psi.^{H}\mathbf{f}(\omega)e^{j\omega t} \tag{2.3.7}$$

in which the superscript H denotes the Hermitian transpose, and where

$$\mathbf{G}^{-1} = \Lambda + j\Lambda - \omega^2\mathbf{I}$$

Λ being the matrix of eigenvalues of the system without damping. Consequently, $\mathbf{G}$ is a diagonal matrix, the non-zero elements of which are given by

$$g_{rr} = \frac{1}{(\lambda_r - \omega^2) + j\eta_r\lambda_r} \tag{2.3.8}$$

If Ψ is wholly real (which is the case for systems lacking any form of damping), then Ψ^H in equation (2.3.7) may be replaced by Ψ^T, where the superscript T denotes a simple matrix transpose operation, and the non-zero elements of $\mathbf{G}(\omega)$ are given by

$$g_{rr} = \frac{1}{\lambda_r - \omega^2}$$

The time dependence may be removed in equation (2.3.7), upon which we obtain the frequency response relation:

$$\mathbf{q}(\omega) = \mathbf{H}(\omega)\mathbf{f}(\omega) \tag{2.3.9}$$

where $\mathbf{H}(\omega) = \Psi\mathbf{G}(\omega)\Psi^T$ is the numerical analogue of the *transfer function* of the bladed disc assembly at the excitation frequency ω.

The vector of displacements $\mathbf{q}(\omega)$ may, after using equation (2.3.9), be separated to the blade tip, clapper point and blade root displacements: $\mathbf{x}$, $\mathbf{y}$, $\mathbf{z}$. The bending stress at the root of the ith blade may subsequently be obtained as the force per unit area transmitted by the disc to the root of the blade, by the disc, i.e.

$$\sigma_i = K_i Y_i - Z_i \tag{2.3.10a}$$

or, as

$$s_i = |X_i| \tag{2.3.10b}$$

By writing the left hand side of equation (2.3.6) in the dynamic stiffness form, the equations of motion for forced response analysis becomes, upon removing the time dependency factor:

$$\mathbf{D}(\lambda)\mathbf{q} = \mathbf{f} \tag{2.3.11}$$

where

$$\mathbf{D}(\lambda) = \mathbf{K} + j\mathbf{H} - \lambda\mathbf{M} \tag{2.3.12}$$

The solution for displacements $\mathbf{q}$ in equation (2.3.11) may also be regar-

ded as a mechanical analogue of the mathematical procedure of inverse iteration. In the inverse iteration process of the linear algebraic eigenvalue problem, we generally seek an eigenpair (λ_r, ψ_r) where $\lambda_r = \omega_r^2$, of the rth mode by evaluating the lambda matrix $\mathbf{D}(\lambda)$ at a *shift* frequency, λ_0. Now, it is well-known [see, for instance, the monograph by **Wilkinson** (1965)] that, provided the inner product of $\mathbf{f}$ and $\mathbf{q}$ does not vanish i.e.

$$\langle \mathbf{f}, \mathbf{q} \rangle \neq 0$$

then, whenever we iterate on $\mathbf{D}(\lambda_0)$ with λ_0 as a 'shift', the resulting solution for $\mathbf{q}$ in equation (2.3.11) is such that the kth iterant tends towards the required eigenvector, i.e.

$$\psi_k \Rightarrow \psi_r$$

in a rapidly converging vector sequence.

Three factors govern the rate of convergence towards a particular eigenvector, ψ_r:

(*a*) the orthogonality, or otherwise, of the eigenvector which we seek, ψ_r, with respect to the initial iterant vector which is selected; in this case, the force vector $\mathbf{f}$.

(*b*) the proximity, or otherwise, of the shift frequency λ_0 to the eigenvalue λ_r corresponding to the desired eigenvector ψ_r;

(*c*) the relative separation between the system's eigenvalues in the neighbourhood of λ_r, i.e. whether or not

$$\frac{|\lambda_r|}{|\lambda_{r-1}|} \quad \text{and} \quad \frac{|\lambda_r|}{|\lambda_{r+1}|}$$

are close to unity.

In several numerical experiments, we have observed that by and large, the dominant factor governing the rate and direction of convergence is the orthogonality condition, (*a*).

Engine Order Excitation

In bladed disc systems, one of the most commonly experienced types of

forcing is usually referred to as *engine order excitation.* This arises when the bladed wheel rotates past a pressure source which may be modelled in any one of the forms depicted in Figures 2.3.1 to 2.3.3. Under such conditions, elements of the force vector in equation (2.3.11) above may be written, for the mth order engine excitation, as:

$$f_i = B_m e^{j(2\pi mi/N)} \tag{2.3.13}$$

where B_m is an arbitrary constant for the mth order, and $f_i \equiv f_i(t)$

We can express the force vector as a function of the angular disc rim position,

$$\theta_i = 2\pi i/N$$

of the ith blade, and if we normalise such that B_m is unity, we may write

$$f_m(\theta) = \cos m\theta + j\sin m\theta \tag{2.3.14}$$

This is the 'standard' mth order *engine excitation.* Some authors, however, use special forms of equation (2.3.14) and incorrectly refer to such as 'engine order excitations'. Those special cases will be referred to in this place as

mth order *cosine* excitation,

when

$$f_m(\theta) = \cos m\theta \tag{2.3.15}$$

and

mth order *sine* excitation

for

$$f_m(\theta) = \sin m\theta \tag{2.3.16}$$

Now, an interesting observation results when we apply any of equations (2.3.14) through (2.3.16) as the *first iterant* in equation (2.3.11) for the tuned systems. We recall from equations (2.2.11) to (2.2.13) that the vector of modes at the nth nodal diameter for the tuned systems is of the form.

$$X_i = A_n(\cos 2\pi ni/N + j\sin 2\pi ni/N) \tag{2.3.17}$$

which may be further reduced to a generalized mode shape as a function of angular blade position:

$$\mathbf{q}_n(\theta) = \cos n\theta + j\sin n\theta \tag{2.3.18}$$

where $\theta = 2\pi i/N$. Now, if we liken the dynamical problem represented by equation (2.3.11) above to inverse iteration in one step, then the necessary and sufficient condition that ensures *non-convergence* towards the nth diameter modal shapes (there being two modal shapes in quadrature at all natural frequencies save those corresponding to the 'umbrella' modes) is that the vectors $\mathbf{q}_n$ and $\mathbf{f}_n$ be orthogonal to each other, i.e. that

$$\langle \mathbf{f}_m^H, \mathbf{q}_n \rangle = 0$$

For the mth order engine excitation, $\mathbf{f}_m$ is given by equation (2.3.14), and together with equation (2.3.18), we obtain the following inner product relation:

$$\begin{aligned}
\langle \mathbf{f}_m, \mathbf{q}_n \rangle &= \mathbf{f}_m^H \cdot \mathbf{q}_n \\
&= \int_0^{2\pi} \mathbf{f}_m^*(\theta) \cdot \mathbf{q}_n(\theta) d\theta \\
&= \int_0^{2\pi} (\cos m\theta - j\sin m\theta)(\cos n\theta + j\sin n\theta) d\theta \\
&= \int_0^{2\pi} \cos[(m-n)\theta] d\theta + j\int_0^{2\pi} \sin[(m-n)\theta] d\theta \\
&= \begin{cases} 2\pi & (m = n) \\ 0 & (m \pm 0) \end{cases}
\end{aligned}$$

$$\Rightarrow \mathbf{f}_m^H \cdot \mathbf{q}_n = \|C_{mn}\| \delta_{mn} \tag{2.3.19}$$

where $\|C_{mn}\|$ is some norm, and δ_{mn} is the Kronecher delta.

The physical interpretation of equation (2.3.19) is that the mth order engine excitation is *always* orthogonal to the nth order nodal diameter shapes, except when $m = n$. Thus, equation (2.3.19) may be regarded as the mathematical variant of the well-known vibration characteristic of tuned assemblies; namely, that the mth engine order force can only excite a tuned wheel to resonance at the wheel's m nodal diameter mode frequencies, and nowhere else.

With regard to the mth order *cosine* excitation, the inner product relation is given by

$$\mathbf{f}_m^H \mathbf{q}_n = \int_0^{2\pi} \cos m\theta \cos n\theta d\theta + j\int_0^{2\pi} \cos m\theta \sin n\theta d\theta \tag{2.3.20}$$

The second integral in equation (2.3.20) obviously vanishes, since the

products are orthogonal functions with respect to each other, so that equation (2.3.20) becomes

$$\mathbf{f}_{m}^{H}.\mathbf{q}_{n} = \int_{0}^{2\pi}\cos m\theta \cos n\theta d\theta = \|C_{mn}^{*}\|\delta_{mn} \qquad (2.3.21)$$

The implication of equations (2.3.20) and (2.3.21) is that the mth order *cosine* excitation is only able to excite the *cosine modal shape* of the mth nodal diameter to resonance, unlike in the 'complete' engine order case where *both* of the sine and cosine shapes may be resonanted. A similar conclusion can be drawn for the mth order *sine* excitation upon repeating the above procedure and substituting the sine expressions for the corresponding cosines. In other words, the mth order *sine* excitation, being always orthogonal to the all modal shapes except the mth diameter *sine* shape, is able to set only the latter into resonant conditions.

The distinction between sine, cosine, and engine order excitations is not very clear in the case of mistuned systems because of the multiple existence of both sine and cosine shapes *at the same frequencies* of repeated latent roots. However, when the system is slightly detuned there is a frequeny split of the previously coincident characteristic roots of the system; which is a phenomenon already well-known. But what is more important here than the split is that for low order diameter modes, such as the second or third diameters, the mode shapes are still nearly pure sine and cosine forms - almost as in the tuned case - although the corresponding natural frequencies are now slightly different from those of the equivalent tuned system. If we were to impress a cosine form of excitation upon the system during a bench test, we would not detect those resonances representing the sine modal shapes; we are, thus, only able to locate half as many modes as are actually present in the same frequency range. On the other hand, if we applied the complete 'engine order' excitation on the system, we would not be in danger of missing all those modes.

A corollary of the foregoing is that, in order to guarantee convergence to each of the two orthogonal modes which are known or suspected to be near to a 'shift frequency' λ_o, we must select our excitation source in such a way that it is *not* orthogonal to either one of the shapes. In fact, the more *linearly dependent* the excitation is on a particular modal shape close to the shift frequency, the easier it is to locate such a mode during a vibration test. Thus, if we use a 'sine' shape excitation, we must also use a 'cosine' shape excitation (e.g. by phase adjustment of the vibration ex-

citers around the disc ciremference) in order to observe both.

The preceeding discussion applies to cases in which the eigenvalues of the system are 'well separated'. The modes of a vibrating bladed disc are often clustered in certain regions of the frequency spectrum. It has been mentioned by several authors in the recent past, in connection with vibration testing, that certain modes are 'strong' and can therefore be easily excited into resonance, while some other modes are 'weak' or subdominant, and are consequently not easily resonated. We now seek to verify the truth of this through the analogous application of the theory of inverse iteration.

Let us suppose, for convenience but without loss of generality, that the matrix quantities in equation (2.3.11) are all real so that, for a stable mechanical system, the eigenpair (λ_r, ψ_r) is also real. Then, we know from the numerical characteristics of inverse iteration that if there exist some pathologically close eigenvalues in the neighbourhood of λ_r (as happens in mistuned assemblies), or if λ_r is itself an eigenvalue of twin multiplicity (which is so for the majority of tuned modes), and these eigenvalues correspond to linear elementary divisors, then the rth iterant of the vector $\mathbf{q}$ tends towards the one eigenvector in the cluster which is the *most linearly dependent* on the initial iterant vector. Components of the neighbouring eigenvectors would, of course, be present in very small quantities, according as to how much they are in turn linearly dependent upon the first iterant vector; but even these small components can usually be filtered out after a few steps of the iteration process.

The convergence or otherwise towards a particular mode in a cluster during a vibration test is obviously governed far more by the nature of the excitation, and its relationship to that particular mode, than the so-called 'strength' of that mode. For, no matter how 'strong' a mode is, we will *never* be able to observe it during a test if we apply a forcing function which is orthogonal to it, to vibrate the system. With particular regard to the case of pathologically close resonances (or, in fact, of coincident resonances) it is clearly possible to excite as many modes as exist in multiples or clusters through the selection of a sequence of different excitation patterns, since such a choice will usually lead to different modes being excited in the same subspace spanned by the multiple eigenvalues.

2.4 Derivation of Model Parameters

A good theoretical procedure should, in the final analysis, be capable of realistic predictions of the behaviour of the engineering system it seeks to model. Such predictions may be qualitative or quantitative. However, because of the complexities inherent in the operation of bladed disc assemblies - many of which complexity are not quantifiable - some degree of idealization in the theory is inevitable. A process of trading off is therefore usually involved in deciding how elegant the theory should be fashioned in order that it may yield worthwhile predictions at a reasonable cost.

In the case of the lumped parameter method as applied here to bladed assemblies, the predicted results could easily be substantially different, quantitatively, from what would be observed in practice unless careful judgement is exercised in assigning values to the lumped parameters of the model.

It is also a phenomenon well known in the theory of structures that a finite degree of freedom modelling of a continuum - such as furnished *inter alia* by the finite element, boundary integral, and lumped parameter methods - is only able to predict within acceptable accuracy for the lower modes of vibration. However, in the case of the lumped parameter method, it is possible to select the 'parameters' judiciously so as to cope adequately in any localized region of the frequency spectrum at a time (e.g. the high frequency end) provided one has some pertinent foreknowledge of the dynamic behaviour of the system being modelled. Now, the frequency spectrum of bladed disc assemblies is usually divided into 'families', with each family of modes being associated with a cantilever frequency of the blades. It is, therefore, feasible to construct a lumped parameter model which predicts very accurately for, say, the 3F family while performing less creditably for the 1T or 2F families. A different set of parameters, based again on a knowlegde *a priori* of the location of some eigenvalues associated with the 1T family, would predict satisfactorily for the 1T familiy of modes, while becoming less acceptable for all other modes. A set of parameters that would perform well globally is not generally derivable.

The main objective in this section is to lay down the procedure whereby one may arrive at the 'lumped parameters' capable of predicting for any given family of modes, with the minimum amount of prior information about the behaviour of the system in that frequency spectrum. Obviously,

the family of modes to be designed for, with respect to a given engine, depends on the nature of vibration known - or suspected to be likely - to predominate when the engine is actually in operation. These are likely to be the lower family of modes. **Armstrong** *et al* (1966), who have several years industrial experience in this area, have written:

> *"The precise nature of vibration that will occur is not known before engine testing is begun, but experience has shown that severe vibration does not usually occur in modes higher than the first four; these generally are the first and second flexural, first torsional, and first edgewise."*

2.4.1 Blade Parameters

A physical model of the blade is shown in Figure 2.4.1. The total effective mass of the blade in the family of vibration being modelled is represented by M_e, and this is further divided into three elements - being m_t, m_c and m_r - to be lumped respectively at the blade tip, clapper point and blade root. The proportion to which M_e is divided among the three locations depends on the geometry of the blade, but the division is neither difficult to achieve, nor is it very critical. One way of deriving the model parameters is to conduct an experiment on the blade over a frequency range covering the family of interest (e.g. 1T and 2T for the first torsional family, and 3F with 4F for the third flexural).

If the blade is freely suspended while an excitation is applied at its periphery (e.g. the tip or the root, but here we shall assume the root) then the following equation for the apparent mass at blade root, μ_{rr}, is easily verified:

$$\mu_{rr} = \frac{F_r(\omega)}{X_r(\omega)} = \frac{m_r(\omega^4 - A\omega^2 + B)}{\omega^4 - a\omega^2 + b} \tag{2.4.1a}$$

where

F_r = amplitude of excitation at blade root
X_r = amplitude of root response
m_r = mass to be lumped at blade root
m_c = mass to be lumped at "clapper point"
m_t = mass to be lumped at blade tip.

and

$$A = \frac{K_r}{m_r} + \frac{k_t}{m_t} + \frac{(K+k)}{m_c}$$

$$B = \frac{Kk(m_t + m_c + m_t)}{m_t m_c m_r}$$

$$a = \frac{k_t}{m_c} - \frac{(k-K)}{m_t}$$

$$b = \frac{k_t K_r}{m_c m_t}$$

The variation of the apparent mass at blade root, μ_{rr} with excitation frequency ω would therefore be as shown schematically in Figure 2.4.2, in the chosen case of interest being centred on the first flexural frequency family. The following parameters may therefore be determined from the graph of *apparent mass*, as shown in Figure 2.4.2.

(*a*) *cantilever frequencies* Since the blade is tested in a freely suspended condition, the frequencies at which it resonates are *not* the cantilever frequencies desired. However, for excitation *at the root*, the frequencies at which the free-free system becomes anti-resonant are the same ones that an equivalent system would have been resonant were it effectively cantilevered at its root. This is obvious from equation 2.4.1a, upon setting the numerator, rather than the denominator, to zero.

(*b*) *effective mass* At very low frequencies, equation (2.4.1a) becomes

$$\mu_{rr}(\omega \to 0) = m_r B/b = m_t + m_c + m_r = M_e \qquad (2.4.1b)$$

The total effective mass of the blade in vibration may, therefore, be estimated from the asymptote to the response curve at low frequencies.

(*c*) *mass to be lumped at blade root* At very high frequencies, equation (2.4.1a) takes the form:

$$\mu_{rr}(\omega \to \infty) = m_r \qquad (2.4.1c)$$

However, as $\omega \to \infty$, μ_{rr} does not behave as predicted in Figure

2.4.2 by the three degree of freedom, semi definite, lumped parameter model. Instead of an asymptotic response, several higher-order resonances are encountered, such as the 1E, 1T, 2T, *etc.* What is therefore required in such cases is an approximate 'mass line' *immediately* after the 2F resonance is passed.

(*d*) *mass at clapper point* If a clapper ring is present, then it is advisable to conduct a second test on the blade by exciting it at the point of attachment of the clapper, in order that a mass may be lumped at that point with greater accuracy. When the blade is so driven at an intermediate point along its span, then the driving point apparent mass, μ_{cc}, may be written as

$$\mu_{cc} = \frac{F_c(\omega)}{X_c(\omega)} = \frac{m_c(\omega^4 - C\omega^2 + D)}{\omega^4 - c\omega^2 + d} \tag{2.4.2}$$

where C, D, c, and d are constants. When $\omega \to \infty$, $\mu_{cc} \to m_c$, from which the mass to be lumped at the clapper point may be determined.

(*e*) *mass at blade tip* It is not usually necessary to conduct a third test in order that the mass to be lumped at blade tip may be determined. This is because it is much easier to deduce the mass from the relation

$$M_e = m_t + m_c + m_r$$

and, since the other parameters have been previously determined, m_t is easily known.

(*f*) *blade stiffness* The values of 1F, 2F, m_t, m_c, m_r may be estimated by using the procedure outlined above, or by whatever other means is best suitable for achieving it. Once the above parameters have been satisfactorily estimated, it remains to determine the stiffness of the blade.

If we denote the cantilever frequencies already determined by

$$\lambda_1 = (1F)^2 \text{ and } \lambda_2 = (2F)^2,$$

then

$$K_r = {}^1/_2 m_c(\lambda_1 + \lambda_2) \pm \sqrt{[m_c^2(\lambda_1 + \lambda_2)^2 - 4\lambda_1\lambda_2 m_c(m_t + m_c)]} \quad (2.4.3)$$

$$K_t = \frac{m_t K_r \lambda_n - m_t m_c \lambda_n^2}{K_r - \lambda_n(m_t + m_c)} \quad (2.4.4)$$

Note that in equation (2.4.3) $n = 1$ or 2, and two values are obtainable for K_r, one of which could be inadmissive.

2.4.2 Disc Parameters

As pointed out before (Section 2.2), it is customary to assume that the degree of mistuning introduced into the bladed assembly on account of the imperfections in the disc is less important than that due to the scatter in blade alone frequencies. We may, therefore, make a lumped parameter representation of the disc, after McCallion†, as in Figure 2.4.3.

It is easily shown that if there are N blades on the disc, so that the disc may itself divided into N sectors, then a portion of the mass of each sector may be lumped at the slot on the disc where a blade is normally attached; the following equation ensues:

$$\lambda_n = \omega_n^2 \frac{N}{W_D}\left[g + 2h\left(1 - \cos\frac{2\pi n}{N}\right)\right] \quad (2.4.5)$$

where

n = number of nodal diameters
N = total number of lumped masses (or, blades)
W_D = weight of the disc, less the blades
g = disc grounding stiffness
h = disc coupling stiffness

For a given mode of vibration, λ_n and n in equation (2.4.5) are known. We can, therefore, by taking some experimental measurements at two modes of vibration, obtain λ_i and λ_j, say. Assuming that the weight of the disc, W_D, is known, we may then determine h and g by using the simultaneous equations:

† McCallion, H. (1973) *Vibration of linear mechanical systems*, Longmans, London.

$$\begin{Bmatrix} \lambda_i \\ \lambda_j \end{Bmatrix} = \begin{bmatrix} 1 & 2(1 - \cos 2\pi i/N) \\ 1 & 2(1 - \cos 2\pi j/N) \end{bmatrix} \begin{Bmatrix} g \\ h \end{Bmatrix}$$

Theoretically, g and h could be determined from any pair of eigenvalues of the disc alone. In practice, however, the accuracy attainable by this process will not usually be excellent, since the behaviour of turbine discs with their peculiar characteristics may not be easily represented by the spring-mass model adopted in Figure 2.4.3. In spite of this limitation, the estimates of g and h thus obtained are practically acceptable because the vibration characteristics of the whole bladed assembly in the frequency range of interest are, generally, more dependent on the blade properties than on the disc's. We therefore find that, in fact, moderately large variations in the estimated values of W_D and g affect the natural frequencies of the system very little, although the frequencies are considerably sensitive to even small changes in h and the blade parameters.

2.4.3 Assemblies of integral construction

In deriving the blade model parameters (Section 2.4.1), it was implicitly assumed that the blade could be dismantled from the disc, in order that the former might be tested in a free-free condition.

Now, some bladed assemblies are machined in one piece, or else constructed in such a way that one may not readily sever the blade from the disc for the purposes of carrying out a free-free vibration test of the blade. In such cases, alternative means of measuring the cantliever frequencies (see Chapter 7), and of estimating the blade effective mass, must be used. Subsequently, by using equation (2.4.3) and (2.4.4), the blade siffness parameters may be determined.

Because the disc in turn may not be readily observed in free vibration, the procedure of §2.4.2 cannot be used to estimate the disc stiffness parameters. In such a case, it is preferable to observe the complete bladed assembly under vibration and to record the experimental natural frequencies of a couple of low order diameter modes in the family of interest; e.g. the 2nd and 3rd diameters for the first family (zero circle). Now, from the physics of the tuned assembly vibration, we know that as the number of nodal diameters increases the frequency curve approaches the 1F frequency asymptotically from below, in the first family region. See Figure 2.4.4. Let us denote the point corresponding to the experimentally observed 2nd and

3rd nodal diameter resonances by P and Q in Figure 2.4.4. Since we have previously estimated the blade parameters as discussed above, and we may estimate the disc mass, it only remains to set values for the disc stiffness parameters. Again, we can settle the value of g at a low magnitude and, by varying the values of h, we can obtain eigenvalues for the system. These eigenvalues would then be used to construct a resonance diagram until we obtain a diagram that passes through both P and Q, and also approaches the 1F asymptotically from below. By using such a trial and error procedure, the best set of lumped parameter values for the tuned system would be obtained.

2.4.4 The Stiffness of a Clapper Ring

It has been demonstrated by **Ewins** (1973), in studies connected with the vibration of tuned assemblies, that the resonance diagrams of a bladed disc are markedly sensitive to the presence of a shroud band. This is graphically illustrated in Figure 2.4.5, which is reproduced from the referenced work. It pertains to a 30-bladed disc. Further details of the assembly as well as the nature and extent of the changes in the natural frequencies are available in the paper.

It may be observed from Figure 2.4.5 that the vibration characteristics of the assembly in the low order diameter modes are not influenced to an extent comparable with those at higher order diameter modes by the presence of shrouding in this instance. It therefore follows that one may still use the procedures outlined above for the determination of parameters for *unshrouded* assemblies in the first approximation. Subsequently, from a knowledge of the system's behaviour at higher modes, and by adjusting the value of the shroud stiffness, one may obtain an optimum set of values.

2.4.5 Application to Practical Systems

In a previous study, **Ewins** (1972) applied the receptance coupling technique to predict the natural frequencies and mode shapes of vibration of a model compressor rotor. The assembly had 30 blades. Experiments were also performed on the model analysed by theory to verify the predictions of the latter. Good agreement between the predicted and measured frequencies were obtained for the 1F family of modes.

In order to check the applicability of the procedure described in the preceeding sub-sections, the same model compressor rotor studied by Ewins was analysed using this lumped parameter model. The eigensolution obtained for the rotor upon applying the numerical treatment of Section 2.3.1 are juxtaposed with those obtained by previous workers via the application of the receptance method, and laboratory experiment, in Table 2.4.1. It is evident from the table, and from Figure 2.4.6, that the results of the present analysis compare favourably both with experiment and with the more rigorous receptance analyses.

2.5 CASE STUDIES

The dynamic response characteristics of several bladed assemblies, under free vibration conditions and when subjected to steady state forcing, were examined in the course of this research. The lumped parameters used in modelling the assemblies were selected in such a way that the models include many of the various mistune configurations (see Figure 1.2.4) which have been used at various times by previous workers.

Preliminary results and observations of the influence of these types of mistuning on rotor vibrations, based on the lumped parameter method described in this chapter, have been communicated in previous reports [**Afolabi** (1981a, b, c; 1982a)] and will not, therefore, be duplicated in detail here. However, the mistune characteristics of two categories of models (having 10 and 30 blades) are now given in Figure 2.5.1, since they exhibit the same dynamic behavioural patterns which are typical of the other assemblies previously reported.

Models 10X and 10Y, having only one blade detuned, may be regarded as academic cases since those kinds of mistuning are hardly encountered in real aero-engines. However, because such mistuning patterns have been previously used by other workers, they have been included here for the purposes of comparison. Although perfectly tuned rotors are also not easily found in practice, models 10T and 30T are described here for two reasons. First, because conventional design calculations are based on the assumption of perfect tune in all the blades; and secondly, because designers frequently like to know the extent to which dynamic responses deteriorate in the presence of mistuning, *relative to an 'equivalent tuned system'*. Of the two models with random detuning, Model 10A has too few blades for it to

represent the great majority of realistic assemblies, but it is used nonetheless so as to enable us to obtain some fundamental understanding of assembly dynamics at a reasonable cost. Model 30A, to the extent of having as many as thirty blades in a randomly detuned formation, is typical of axial compressor rotors.

The illustrations Figure 2.5.1 depict the relationship between the first flexural frequency of the blades as a function of disc slot position, for each of the detuned model here.

2.5.1 Modal characteristics

The natural frequencies and mode-shapes of free vibration of the tuned assembly models are shown in Figures 2.5.2 and 2.5.3 for 10T and 30T respectively. This is a familiar manner of presenting the modal characteristics of perfectly tuned systems, since in the absence of imperfections, all of the modal shapes may be resolved into pure 'nodal diameter' components. When the system is mistuned, however, each mode does not usually have only one nodal diameter associated with it, and other forms of presenting the modal data become more meaningful. Such illustrations are given in Figures 2.5.4 to 2.5.9 inclusive. Each of the figures have the same format, *i.e.* there are 30 modes displayed on each page with one mode occupying a 'cell'. Within each cell, the following information is given:

(a) *the serial number of the mode in the eigenvalue spectrum, given at the top left hand corner of the cell.*

(b) *the natural frequency of vibration at this mode, displayed at the top right hand corner within the cell.*

(c) *the relative amplitude of vibration of the blades shown in the form of parallel bars. Each bar has a circular mark at one end to indicate the relative direction, or phase, of vibration of that particular blade in the mode of vibration being described. Note that, as is common in all eigensolutions of this nature, the magnitude and phase of each blade, being relative values, may only be computed to within the accuracy of an arbitrary multiplier for each mode. The slot number occupied by the blades are shown, modulo 5, at the base of the mode shapes diagram.*

(d) *the coefficients of the Fourier series decomposition of the modal shapes are shown in the form of shaded histograms. The nodal diameter having the largest component at each mode is shown in the form of a number at the lower side of the DFT (Discrete Fourier Transform) histogram.*

A study of these figures of modal characteristics confirm what previous researchers have often observed, namely: that the mode shapes of a mistuned system are, in general, 'more complex' than those of the corresponding tuned systems. This complexity of modes is usually represented by the DFT

coefficients, so that a 'pure' nodal diameter has only one shaded column in the histogram, while a highly 'impure' mode has several such non-zero DFT components.

A concept that goes further than modal 'impurity', as gauged by the DFT histograms, is that of *critical modes shapes*. A critical mode shape is distinguished from other impure shapes by a most uneven distribution of the modulus of displacement among all the blades on the stage. That is to say that at certain 'critical' modes, only one blade, and to a lesser extent a couple of blades adjacent to it on either side, has a noticeable amplitude of normalized displacements; all other blades 'vibrating' in this mode with little movement, as illustrated in Figure 2.5.10*a*. Clearly, critical mode shapes cannot occur in tuned assemblies, since such tuned systems have shapes that are of perfect sine and cosine forms. Even in the case of mistuned assemblies, critical modes are not usually found when the eigenvalues of the system are well-separated. It is only where, in some regions of the frequency spectrum of mistuned systems, the eigenvalues are clustered together within a narrow band that the modal shapes degenerate the greatest from the near perfect sines and cosines to the critical types illustrated in Figure 2.5.10*a*. Sometimes, several degenerate modes are also close together (e.g. modes 28, 29, and 30 in Figure 2.5.9) within one family, one of which would be the most degenerate, and is therefore *the* critical mode in that region. Globally, it is possible for several critical modes to exist; usually one per family of vibration (but not always so). This is apparent from Figures 2.5.4 to 2.5.9 for which the critical modes have been marked by asterisk signs in the relevant cells.

For the purpose of discussion, let us refer to the blade having the largest amplitude of displacement at a critical mode as the *critical blade*. Now, a *rogue blade* is one which, under forced vibration conditions, is subject to an unusually large stressing relative to all other blades, save those immediately next to it on either side, so that it consequently fractures prematurely. It therefore follows that a critical blade is similar to a rogue blade to the extent that both of them respond greatly, while other blades do not. The distinction between critical and rogue blades arises from the duration of the force exciting the system to resonance at the particular mode. A critical blade may be identified from free-vibration considerations, whereas a rogue blade is manifest only under forced vibration conditions. Hence, it is reasonable to suppose that some characteristics observed for critical blades would be valid also in the case of rogue blades.

Figure 2.5.10*b* shows a collection of the critical mode shapes obtained from a study of disc Models 10A, 10X, 10Y, and 30A. If we look at the scatter diagrams of each of these system (Figure 2.5.1) along with their critical mode shapes, we see immediately that there exists some form of correlation between the blades that become critical, and those that deviate most from the tuned state in the cantilever frequency scatter diagrams.

2.5.2 Forced Response Characteristics

Modal properties of bladed assemblies - which are usually obtained from free vibration analysis - are useful to the engine designer for the purpose of estimating frequency margins for safe engine operations. But of greater importance are the response characteristics of an engine's blading on resonance. As pointed out in §2.3.2, it is the engine order type of forcing that is usually encountered in turbomachine operation but which, however, is not readily simulated in a laboratory. Most laboratory bench tests are of the mechanical mobility variety, during which a sinusoidal excitation of tunable frequency is applied to some point on the structure, e.g. the tip of one blade, while the response is measured at some other, ordinarily different point, e.g. the blade root. Often, what is measured in such tests is the acceleration response relative to the excition, and when the point of measurement coincides with the point of excitation, then we have *point inertance.* A double integration of inertance with respect to time yields receptance, while a single integration yields mobility. The 'mobility' (single point) and 'engine order' (multiple points) excitations may be simulated on a digital computer.

Single Point Excitation

The data in Table 2.5.2, for instance, are of the 'mobility' type. These have been obtained theoretically by exciting each of the blades on Disc Model 30A at its tip while computing the ratio of displacement to force, in order to obtain the blade tip receptance as a function of excitation frequency. All the blades on the wheel were thus treated, one after the other. At each forcing frequency, the responses were compared to obtain:

(*i*) *the highest response* (α_{max});

(ii) *the blade with the highest modulus of response at this frequency (BHR)*

(iii) *the lowest modulus of response (α_{min});*

(iv) *the blade having the lowest response (BLR)*

It is seen from the data in Table 2.5.2 that Blade 10 suffers the maximum response at nearly all the excitation frequencies between 100Hz and 238Hz, after which range of frequencies it subsequently experiences the minimum response. Similarly, Blade 13 forms the 'lower envelope' up to the same frequency of 226Hz, after which it then forms the 'upper envelope'. Evidently, 238Hz is some sort of *cross-over frequency*, at or in the proximity of which the severly resonating and the least mobile blades alternate their positions in the response hierarchy. In fact, there are other cross over regions at higher frequencies, although the data shown in Table 2.5.2 have been limited to the first cross-over.

Now, blades 10 and 13, which respond the *greatest* and the *least*, are also the blades with the most detune, being the ones with the lowest and highest cantilever frequencies respectively. We also note from Table 2.5.2 that there are a few frequencies at which the most detuned blades do not have the limiting responses. Those frequencies are either close to, or coincide with, the eigenvalues of the mistuned system. The pattern of 'resonant peak response' will be examined in detail below. Meanwhile we may conclude that *at forcing frequencies which are sufficiently far removed from a system resonance, the blades with extreme response are also the ones with extreme detune in their cantilever frequencies.* It is, perhaps, noteworthy that previous researchers have merely computed the quantitaive values of the upper and lower envelopes, without examining the rather qualitatively significant question of *which blades* undergo the most or least stressing.

Engine Order Excitation

(I) Global Frequency Response

Figure 2.5.11 shows the response of blade 13 on Disc 30A to the third engine order excitation (3EO) super-imposed on the response of a typical blade on an equivalent tuned system. Similarly, Figures 2.5.12 to 2.5.16 inclusive show the response of various blades on Disc 10A to other EOs. The responses have been computed in terms of the bending

root stress at the root of each blade, using equations (2.3.7) and (2.3.10*a*). We observe that the upper and lower envelopes are usually very close together, i.e. the difference between the greatest and least response is very small, at nearly all the excitation frequencies except in the regions of the system's resonances and anti-resonances. The resonances may be divided into two categories in the case of excitation by engine order forces, *viz*: primary and secondary.

The concept of primary and secondary resonances is useful in discussing the frequency response patterns of mistuned assemblies. If an *N*th engine order force excites a tuned bladed wheel, the wheel would only resonate at its *N*th nodal diameter frequencies. Such frequencies are of the *primary system resonances* (PSR). A mistuned wheel likewise goes into primary resonance where the *N*th nodal diameter pattern predominates. However, because it also has other secondary diametral components than the *N*th, the mistuned assembly would resonate to a slightly lesser extent at those *secondary system resonances* (SSR). Because the mode shapes of a tuned wheel always yield pure nodal diameter patterns, secondary resonances cannot therefore occur in such system.

With reference to Figure 2.5.11, the detuned blade's response is virtually indistinguishable from that of a perfectly tuned assembly up to about 200Hz, except for the behaviour at resonances. In the neighbourhood of the 'critical' frequency of 238Hz, however, we obtain a very large increase relative to the tuned state. This frequency is styled 'critical' because it marks the region where

(*i*) the mistuned response departs the most from that of the equivalent tuned system;

(*ii*) the upper and lower envelope blades alternate position (Table 2.5.2); and

(*iii*) the maximum fluctuations of stresses among the blades are observed.

If we seek to identify where a blade is likely to turn rogue in the frequency spectrum, it seems inadvisable to overlook such a critical area.

(II) Resonant Peak Response

So far, only the 'global' frequency response patterns have been ex-

amined. Figures 2.5.17 shows the 'local' frequency response of Disc 10A, at each of its resonance in the first family. The excitation is by the 5th engine order. Similar plots are shown in Figures 2.5.18 and 2.5.19 for Disc wheels 30A and 30B respectively under a 3EO forcing. The following observations are drawn.

(*a*) The response amplitudes of blades in a mistuned assembly are usually unequal, unlike in the tuned state where all the blades attain the same level. This is true whether we measure the direct receptance of each blade when it is excited alone, or the individual response when many forces are applied to excite all blades simultaneously as in engine order excitation; or, alternatively, when a single point force is applied at the centre of the disc. However, there is always a non-uniformity associated with the dynamic response of the blades on a mistuned wheel when subjected to the same forms of excitation.

(*b*) Whenever the most uneven stressing of blades occurs, e.g. mode 10 in Figure 2.5.17 and mode 30 in Figure 2.5.19, only a few blades (typically, three or four) are subject to noticeable relative motion. Most of the other blades on the stage vibrate with less than 10% (say) of the amplitude of the most stressed blade. Such a mode is a critical mode at which the blade having the largest stressing is usually the one with extreme detune. The absolute peak stress (maximum response of the 'worst' blade) may be large or moderate depending on the linear dependence of the distribution of the excitation force with respect to the modal shape.

(*c*) The APS (absolute peak stress, i.e. the maximum stress experienced by the most highly stressed blade) is large, for example, at a 3 nodal diameter frequency if the exciting force is a 3EO (Modes 6 and 7 in Figure 2.5.19a). It is a primary resonance. In contrast, the APS at secondary resonances are not usually large except near a critical frequency. If a primary system resonance occurs at or near a critical frequency, then the combination of high APS (which is typical of primary resonances), together with the most uneven distribution of stress (which is characteristic of critical modes), can combine to produce a rogue blade condition.

(*d*) A set of blades having slightly different cantilever frequencies

was arranged on two similar discs to yield the random mistune patterns shown in Figure 2.5.20. The blade with extreme detune occupies slot 13 on Disc 30A, while it is on slot 27 for the second arrangement of Disc 30B. When both wheels are exposed to the 3rd engine order force, it is the blade with extreme detune on either wheel that vibrates the most at the respective critical resonances. Thus, although the stress magnitudes, mode shapes, and natural frequencies are different in both assemblies, the blades likely to behave in a rogue fashion at critical resonances are those with extreme detune.

(*e*) With reference to rogue blades, excessive stressing on several blades, e.g. at a PSR, does not necessarily indicate a rogue condition. If a machine is operated for any appreciable period at a PSR, then the failure of several blades may occur. Under such conditions, it is not necessarily the blades with extreme detune that experience the most stress; but then the vibration environment is already so severe that the additional effects due to mistuning are relatively insignificant; see Figure 2.5.20*b*.

(*f*) In seeking to identify which blade would become a rogue, it has been hitherto customary to devote attention to the response at a primary system resonance, whereas the responses at secondary system resonances are the more relevant for mistuned wheels, since secondary resonances and rogue blade failure cannot, by definition, occur in a tuned assembly.

Before we can attribute failure to mistuning, we must be able to establish that only a few blades from the entire batch on the same disc have failed while all others are still servicable and, all other factors remaining the same as for the mistune failure, an equivalent tuned disc would not experience any blade failure. Thus, although blade failure may occur, unless there is disproportionate stressing on only a few blades *while the other blades have low stressing*, such failure may not be attributed to mistuning. Moreover, the ratio of the maximum stress on the mistuned disc to that on a perfectly tuned system would be appreciable. Finally, the APS must be sufficiently high to cause failure.

2.6 CONCLUDING REMARKS

The blades with the largest deviation from the tuned state on a rotor stage exert a tremendous influence on the vibration characteristics of the bladed disc assembly. Their combined effect is far greater than that exercised by any other blades on the stage. It follows, therefore, that if a bench examination of the cantilever frequencies of the blades on a wheel reveals a stochastic scatter, then those blades which have the lowest and highest cantilever frequencies must be watched with particular interest during an engine test. It is not enough to devote attention to only those blade(s) with the highest cantilever frequency, or the ones with the lowest; *both* sets must be adequately monitored because of the cross-over phenomenon. The current practice of some designers to emphasize the influence of the blade with the mean ('equivalent tuned') cantilever frequency is not greatly supported by the findings in this investigation. Such a blade is not likely to become rogue at critical frequencies.

Theoretical studies designed for investigating the possibility of rogue blade failure in a given assembly should encompass the regions of secondary and critical resonant frequencies. In the past, such regions of the frequency spectrum have been overlooked, as attention was usually devoted to the primary system resonances.

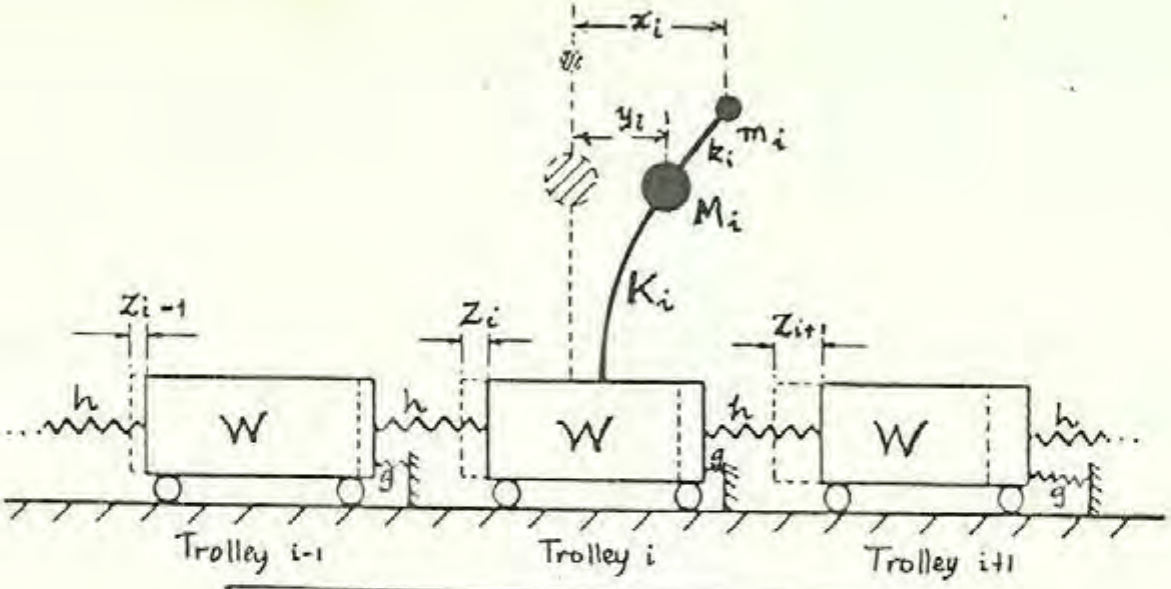

k_i = stiffness of upper blade segment
K_i = stiffness of lower blade segment
m_i = mass of blade section to be lumped at blade tip
M_i = mass of blade section b tween tip and root
W = mass of disc component
g = disc grounding stiffnes
h = stiffness due to the mechanical coupling offered by the disc
x_i = displacement at blade tip (flapwise)
y_i = displacement at blade part-span
z_i = displacement at blade root/disc rim

Fig. 2.1.1 *Mathematical model of a compressor rotor* adapted from Dye & Henry (1969)

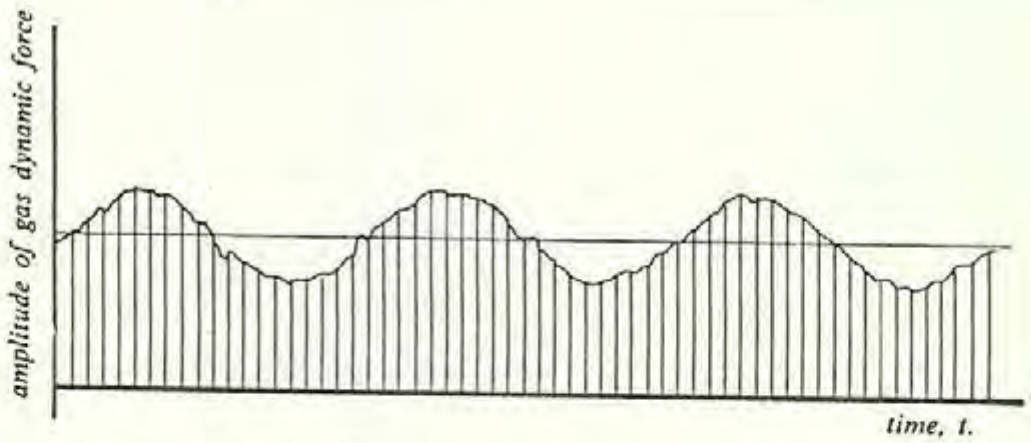

Fig. 2.3.1 *Vibration excitation force induced by wakes*

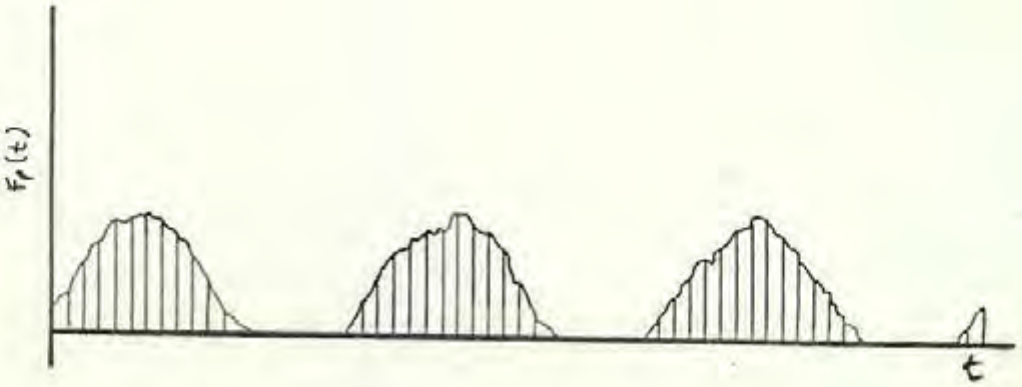

Fig. 2.3.2 *Excitation force produced by partial admission*

Fig. 2.3.3a *Actual excitation force in some engines* Bellamy (1981)

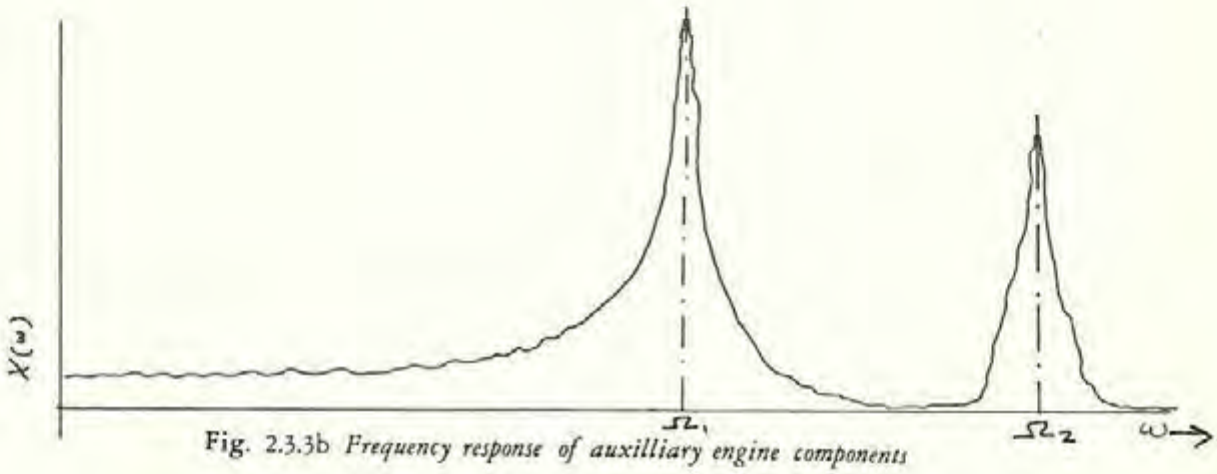

Fig. 2.3.3b *Frequency response of auxilliary engine components*

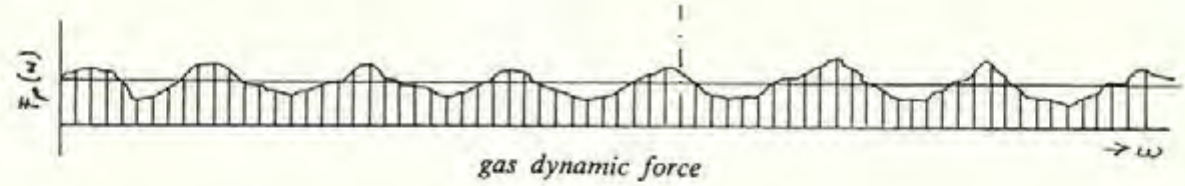

gas dynamic force

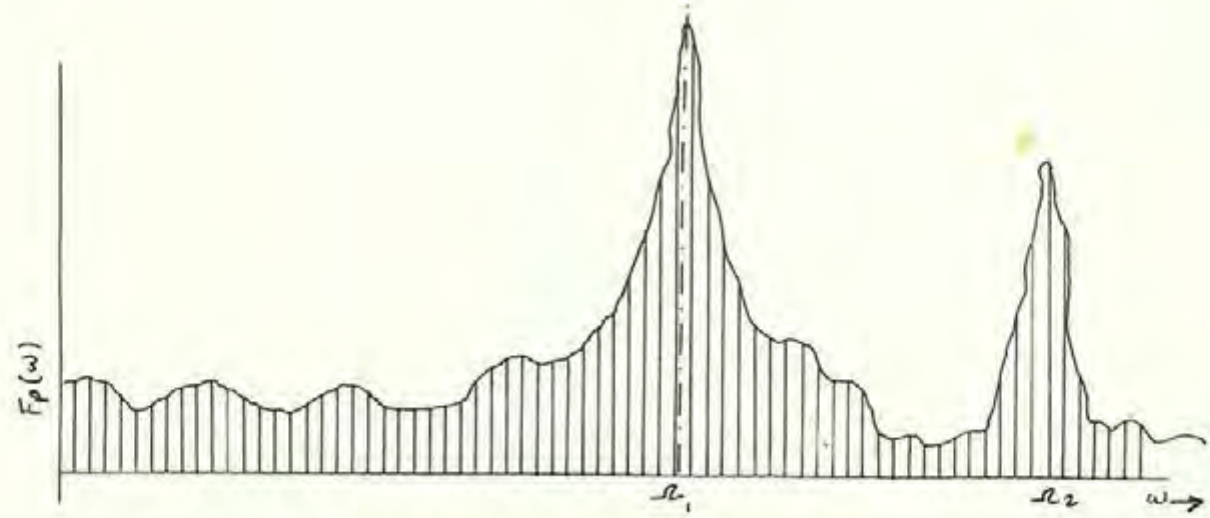

Fig. 2.3.3c *Excitation force modulated by the vibration of other engine components*

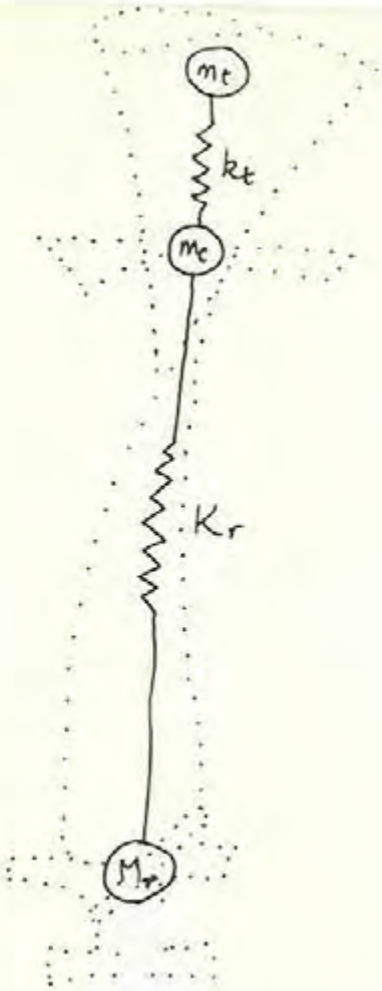

Fig. 2.4.1 *Physical model of a turbine blade*

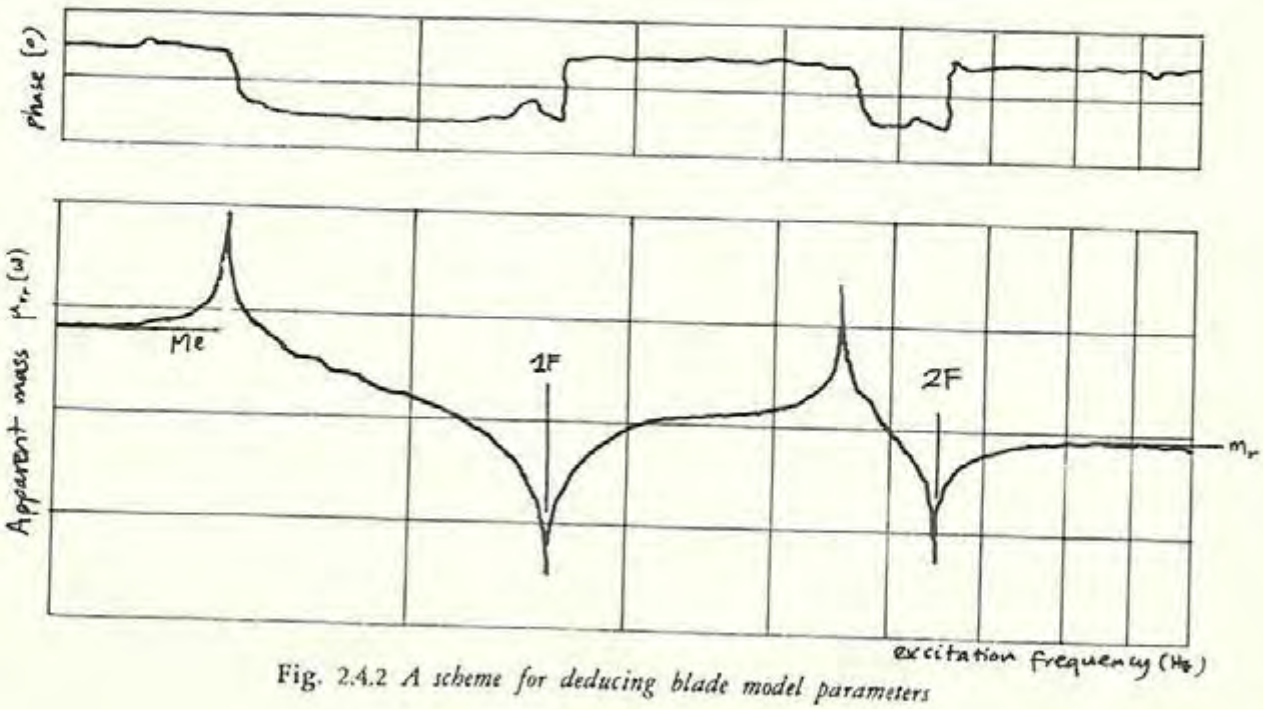

Fig. 2.4.2 *A scheme for deducing blade model parameters*

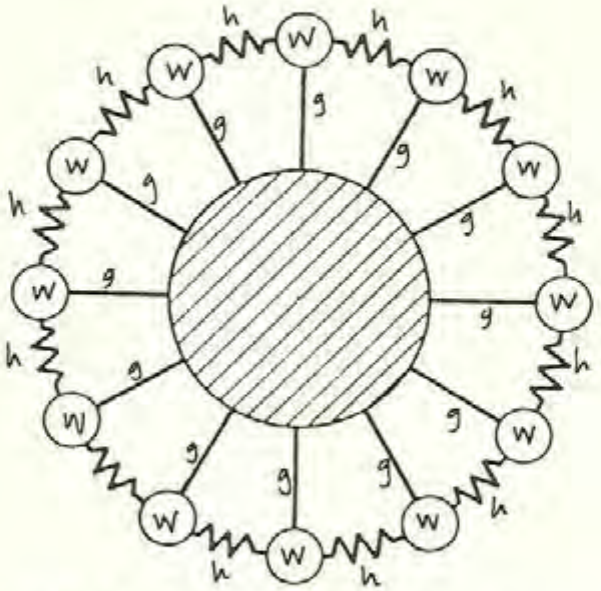

Fig. 2.4.3 *A lumped parameter model of a turbine disk*

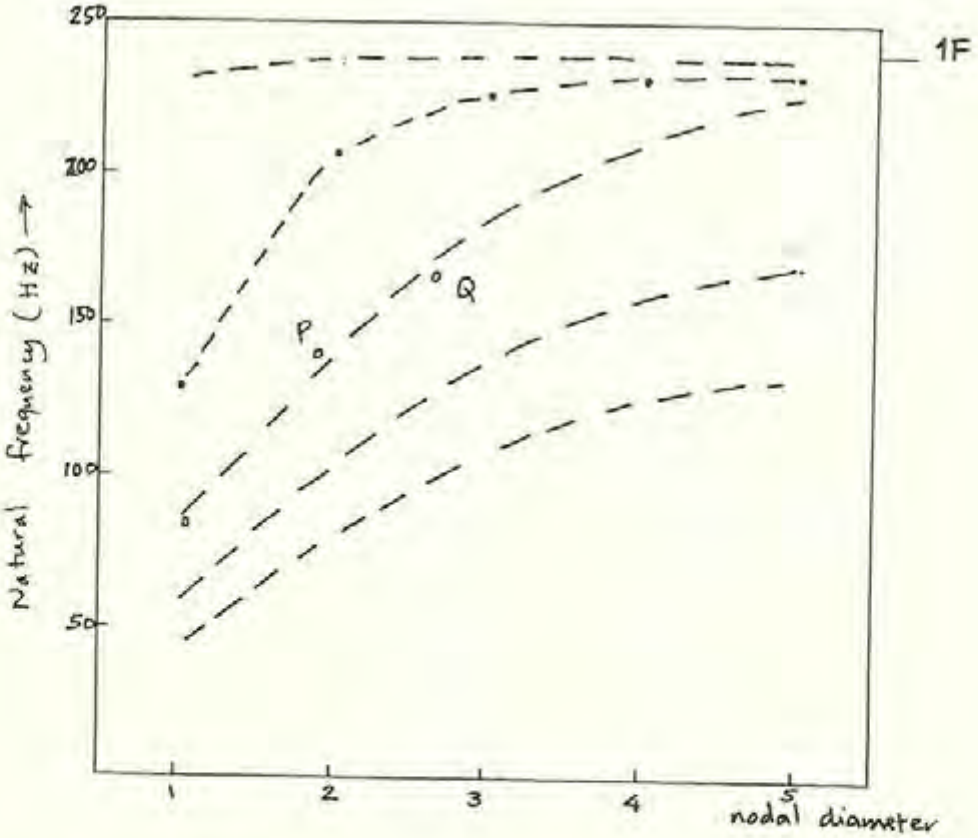

Fig. 2.4.4 *Resonance diagrams showing the influence of disc stiffness on natural frequencies*

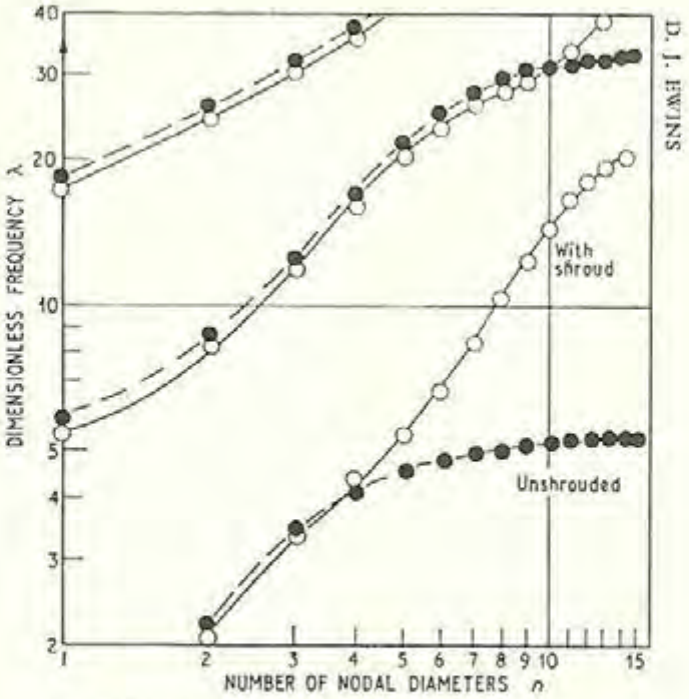

Fig. 2.4.5 *Natural frequency changes due to shrouding*

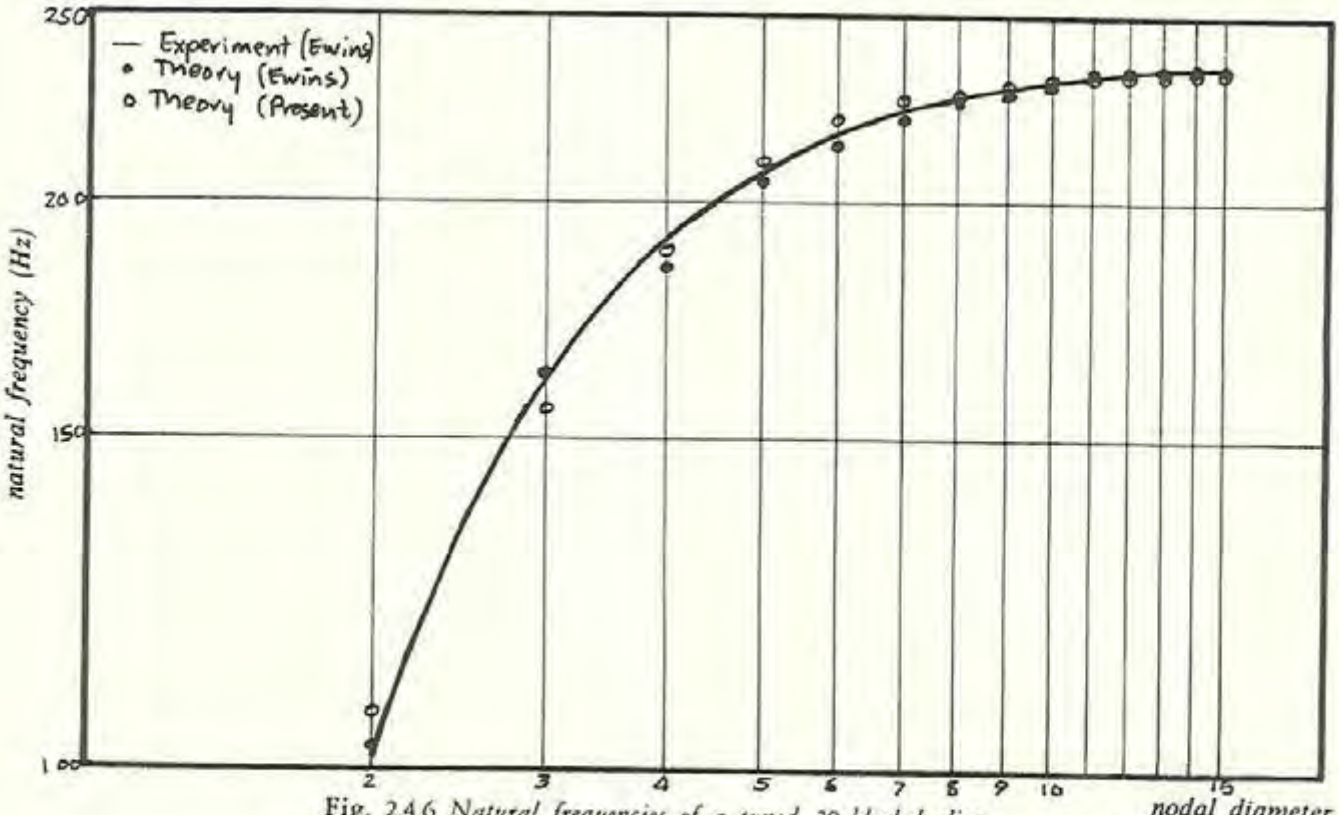

Fig. 2.4.6 *Natural frequencies of a tuned 30-bladed disc*

Fig. 2.5.1 *Scatter diagrams showing blade cantilever frequencies vs slot position*

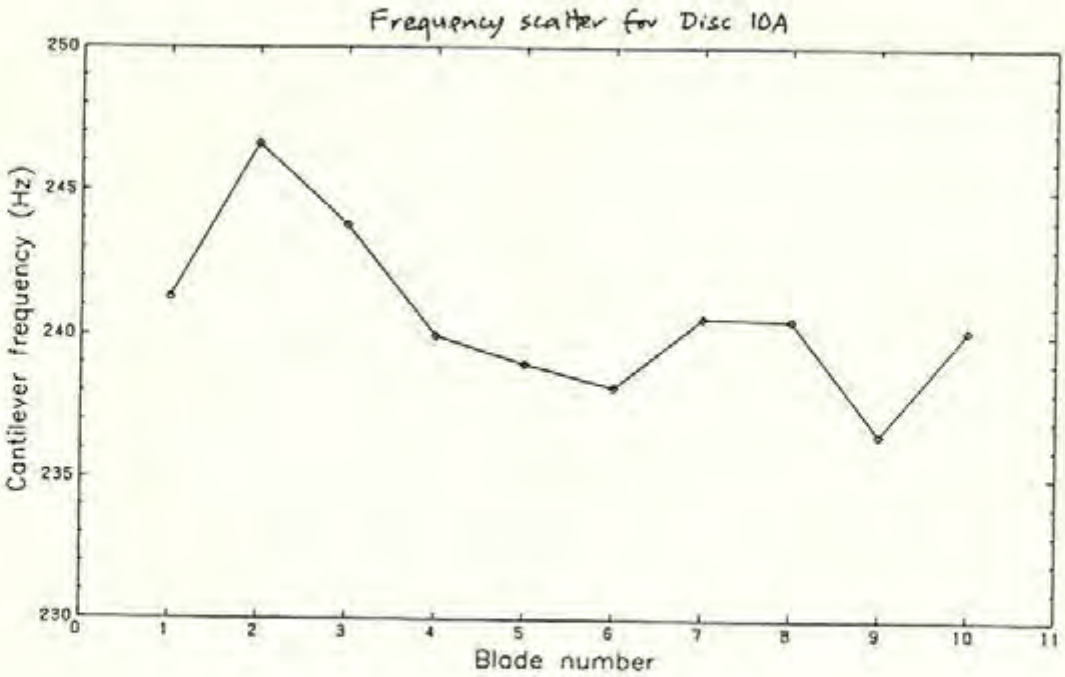

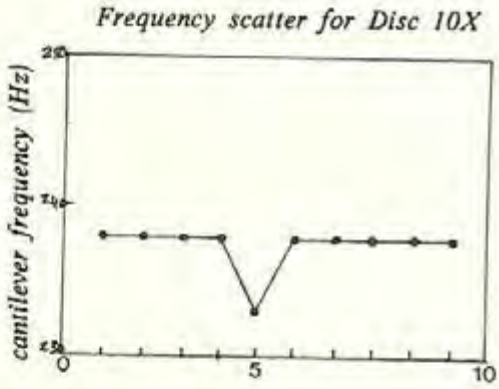

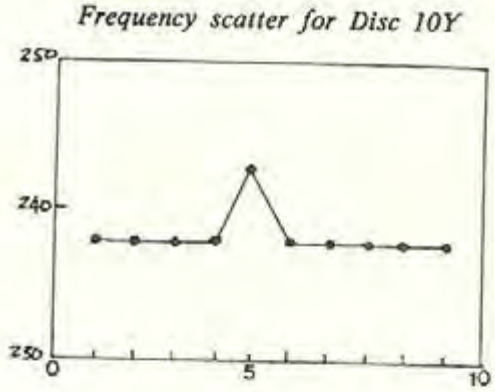

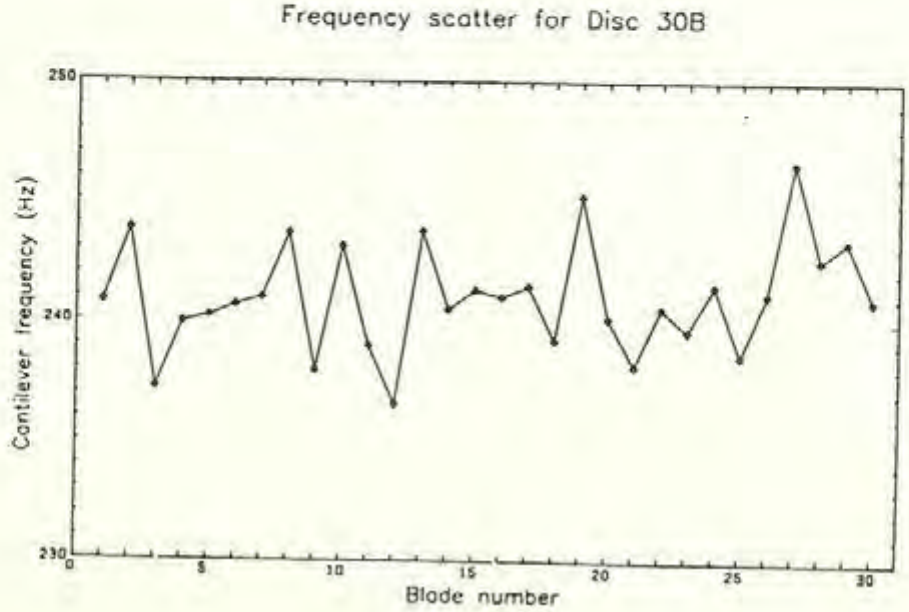

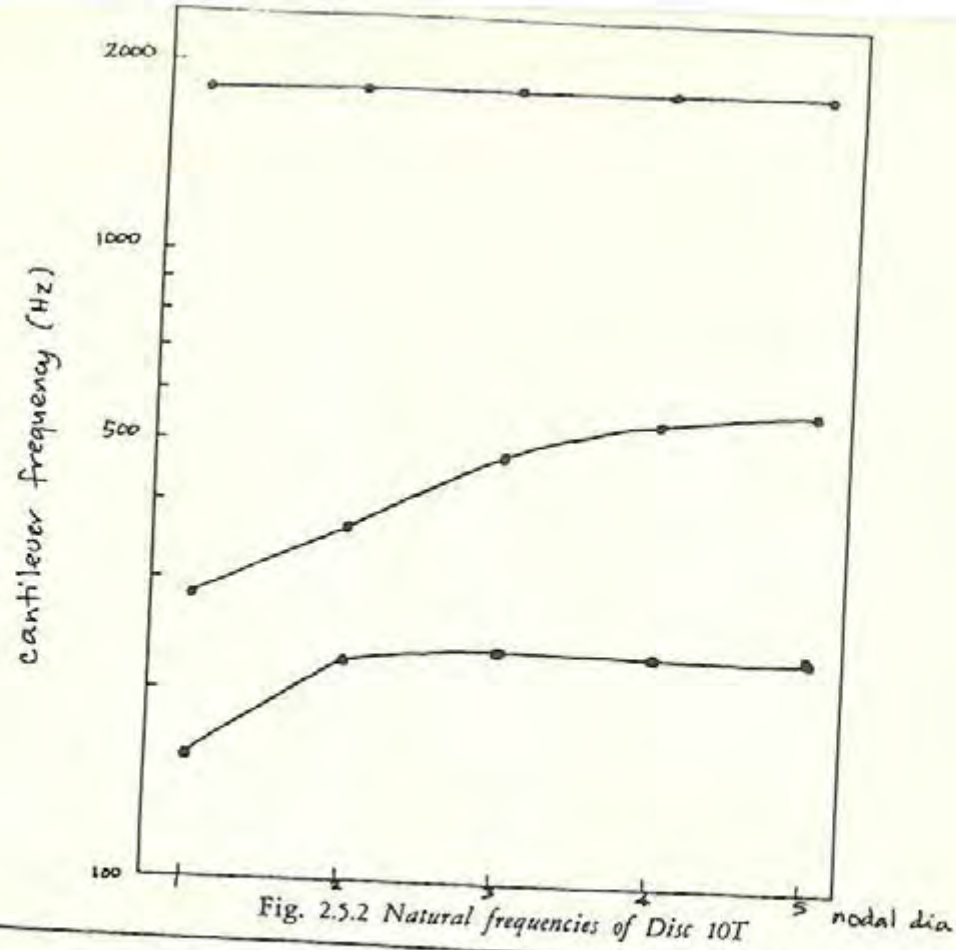

Fig. 2.5.2 *Natural frequencies of Disc 10T*

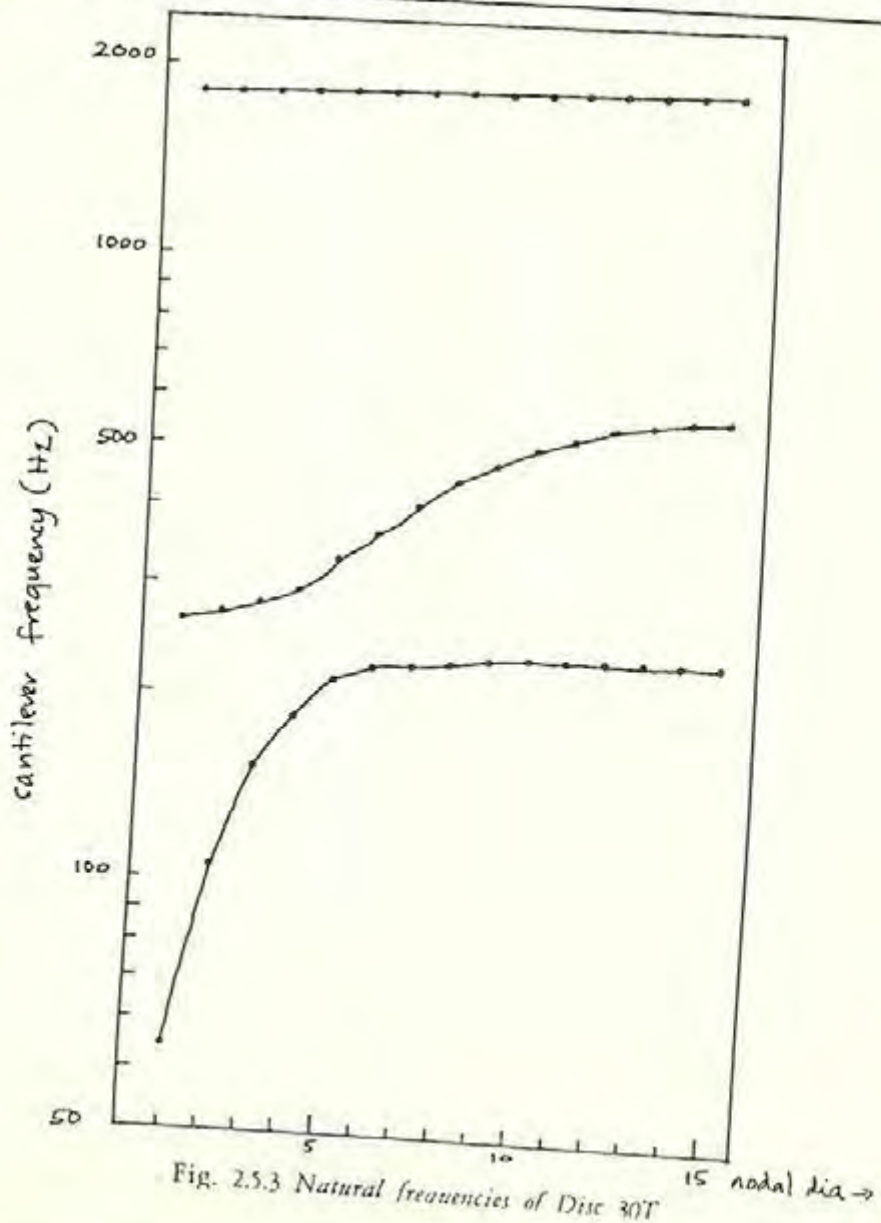

Fig. 2.5.3 *Natural frequencies of Disc 30T*

Fig. 2.5.A *Natural frequencies and mode-shapes of vibration for Disc 10T*

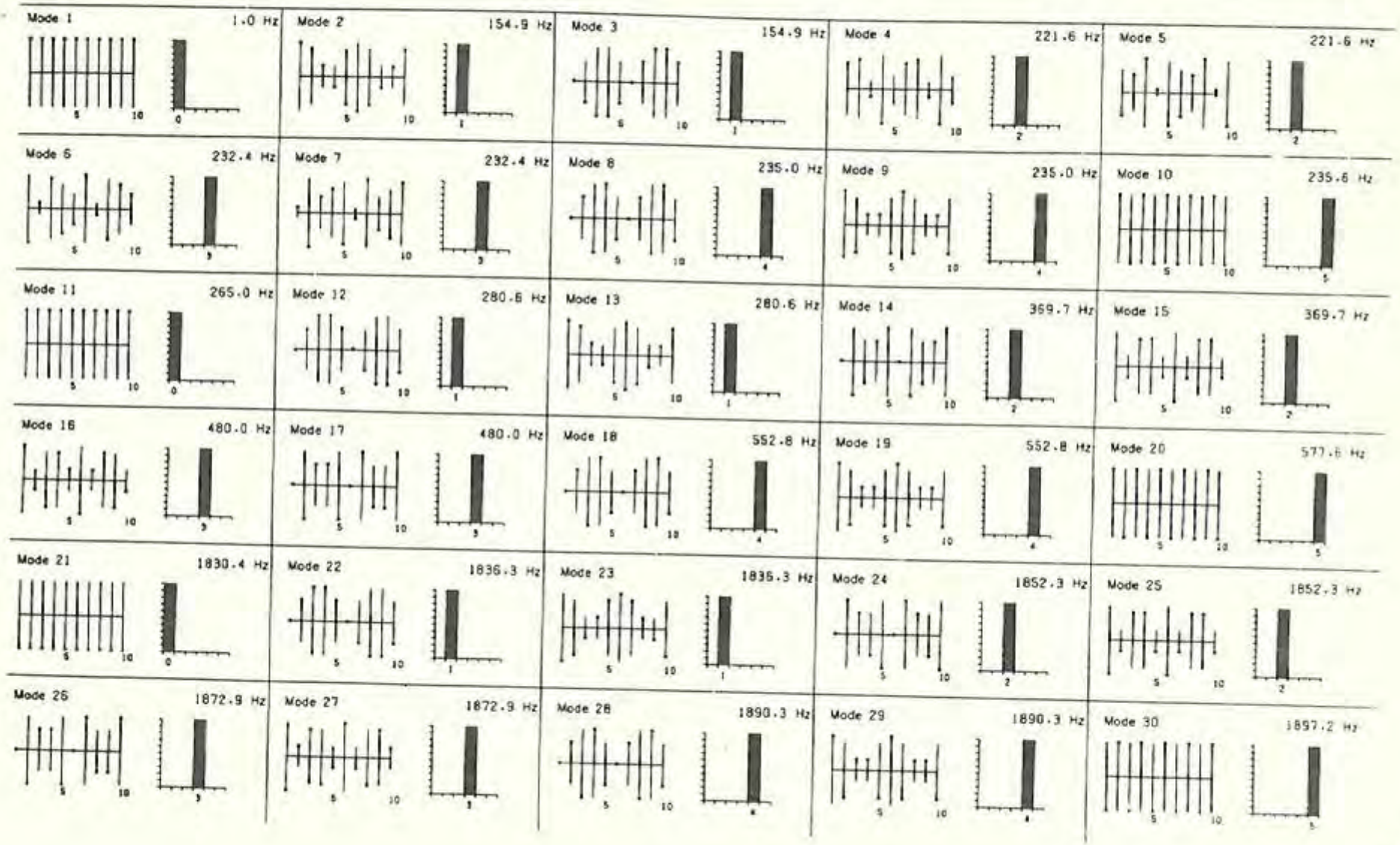

Fig. 2.5.5 *Natural frequencies and mode-shapes of vibration for Disc 10X*

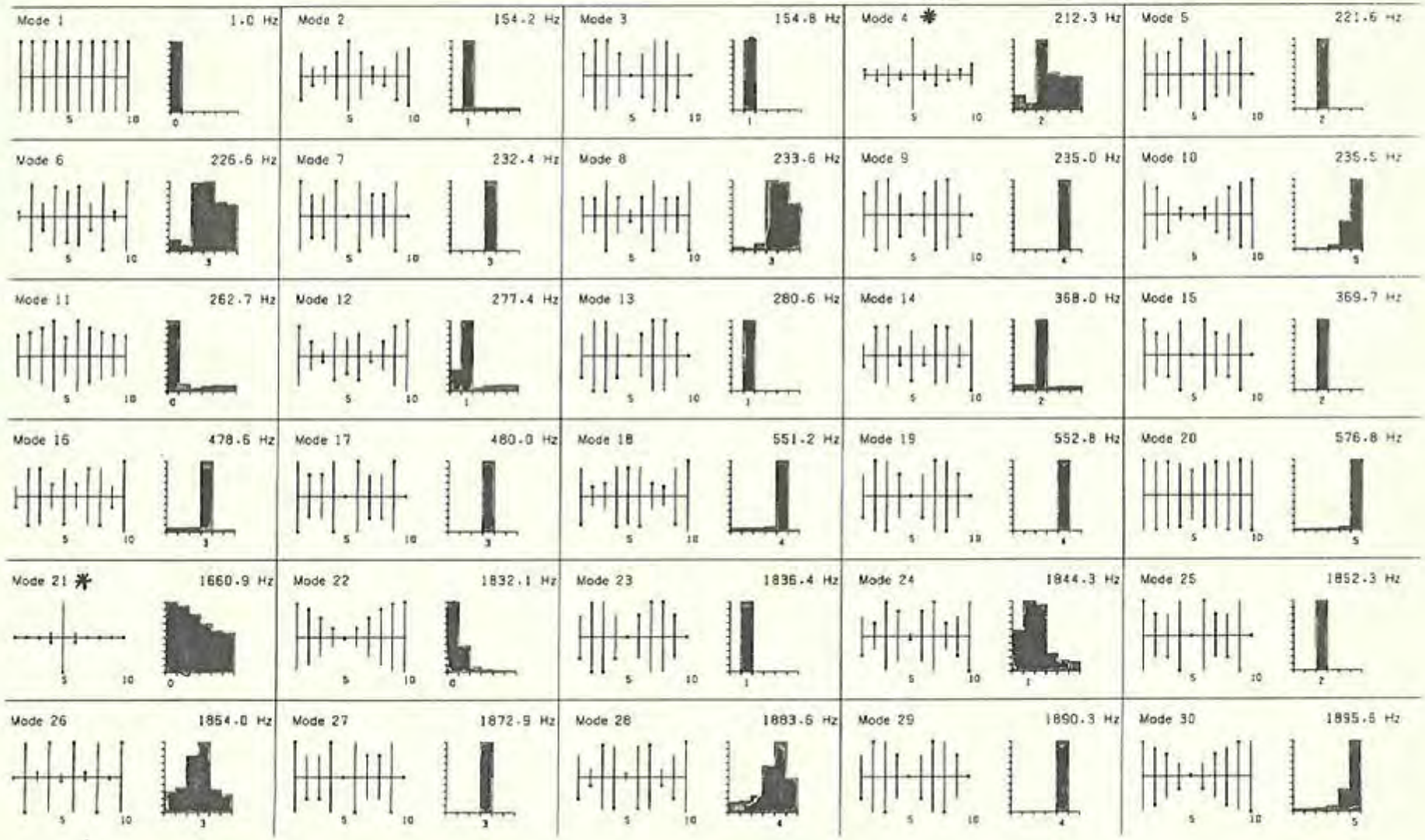

Fig. 2.5.6 *Natural frequencies and mode-shapes of vibration for Disc 10Y*

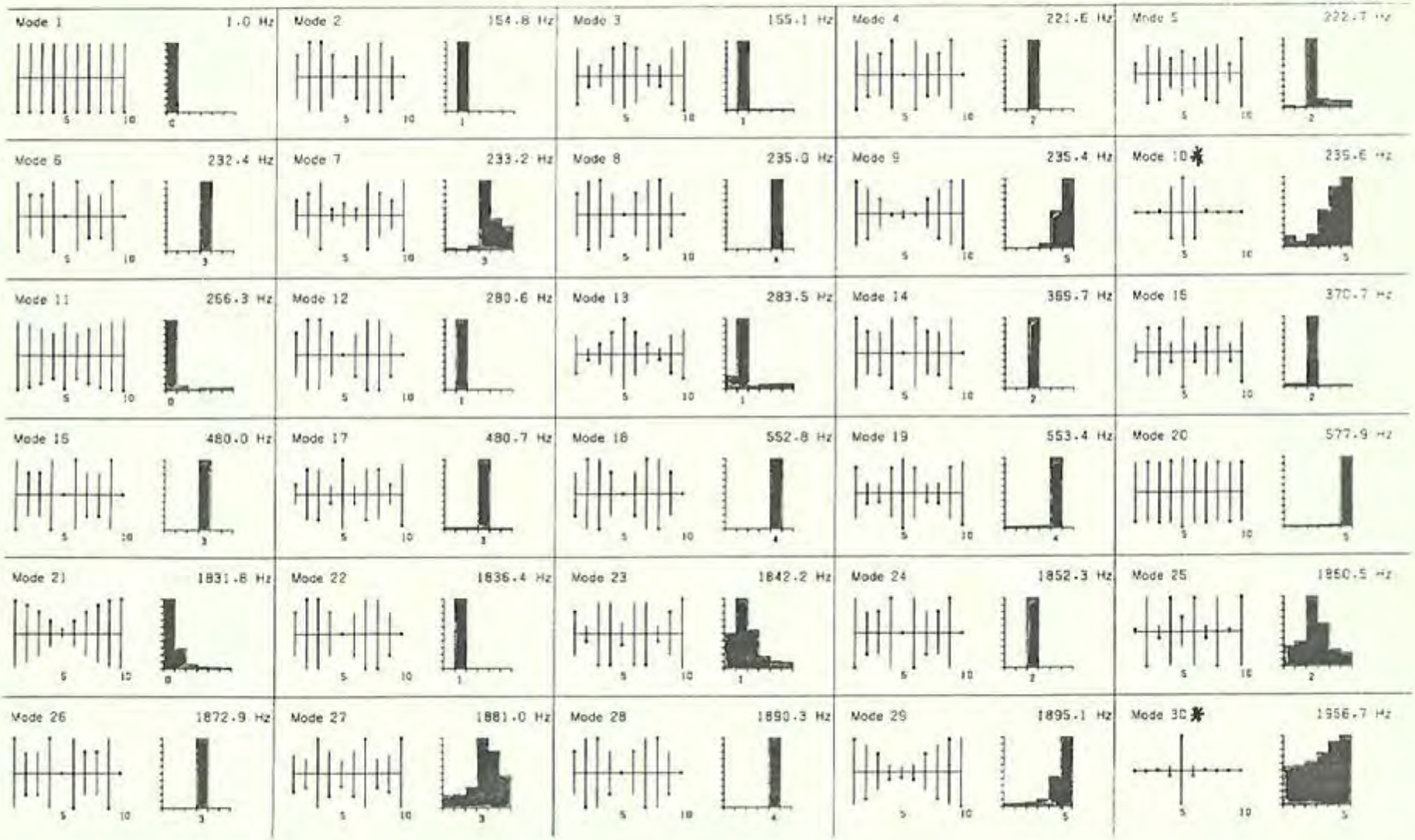

Fig. 2.5.7 *Natural frequencies and mode-shapes of vibration for Disc 10A*

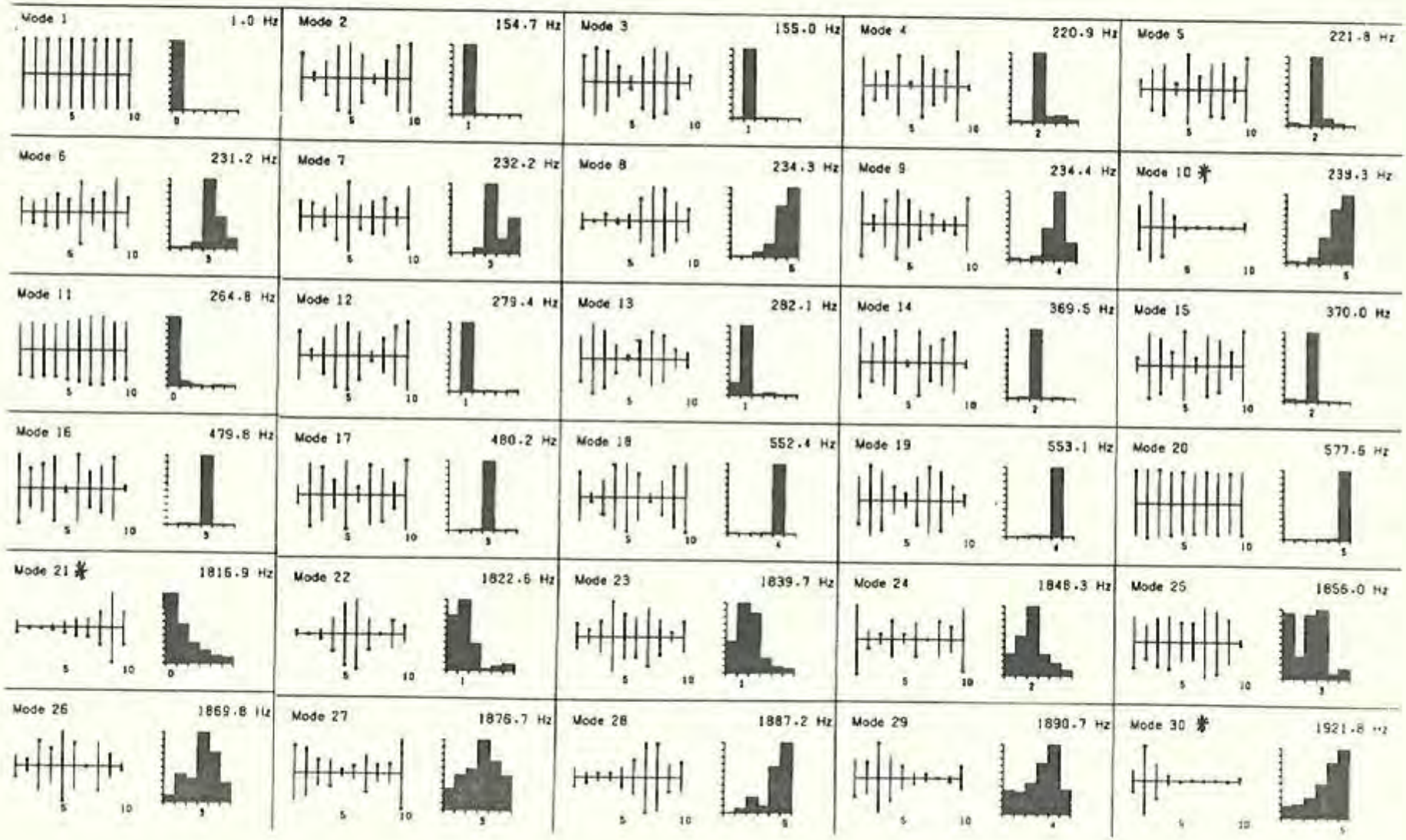

Fig. 2.5.8 *Natural frequencies and mode-shapes of vibration for Disc 30T*

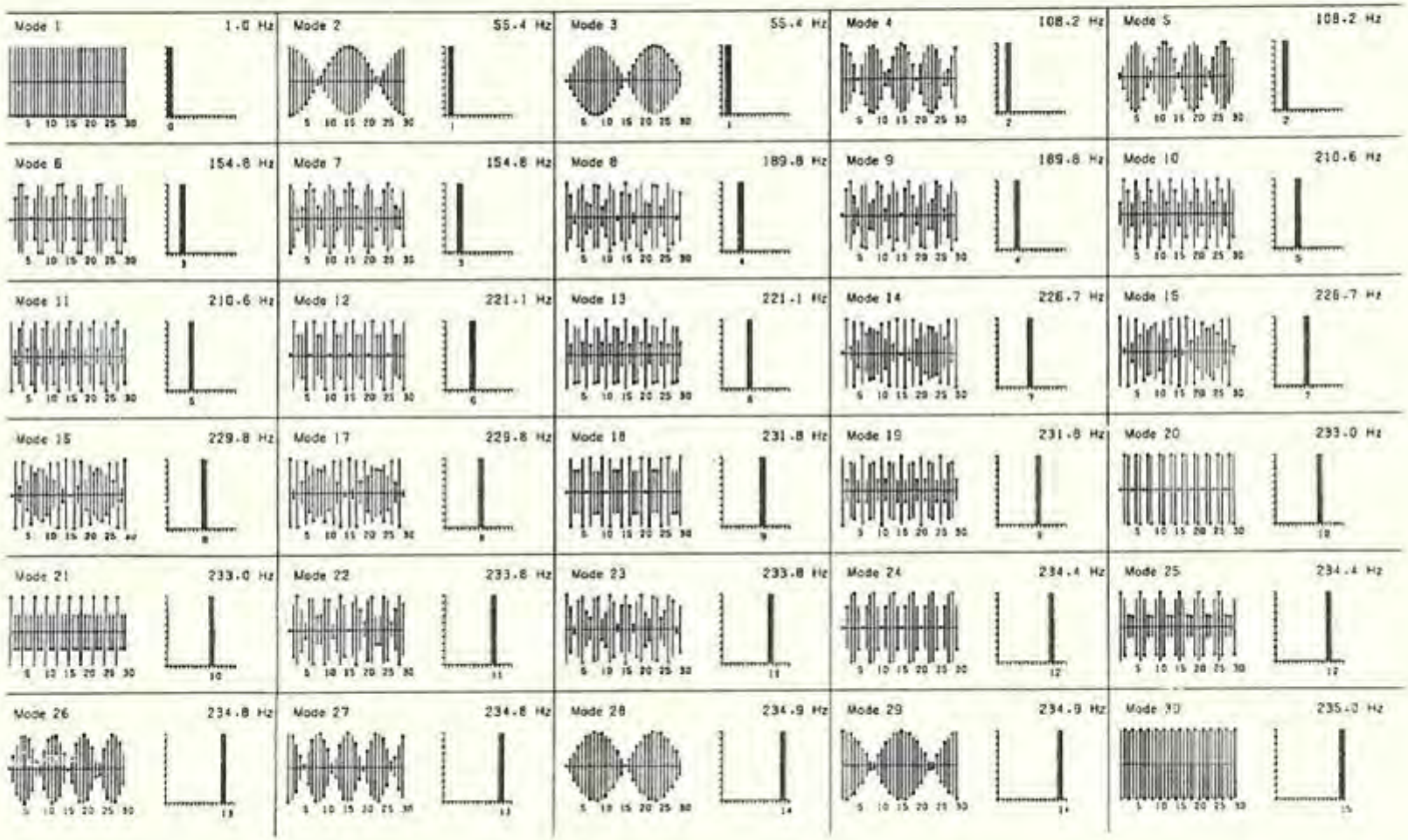

Fig. 2.5.9 *Natural frequencies and mode-shapes of vibration for Disc 30A*

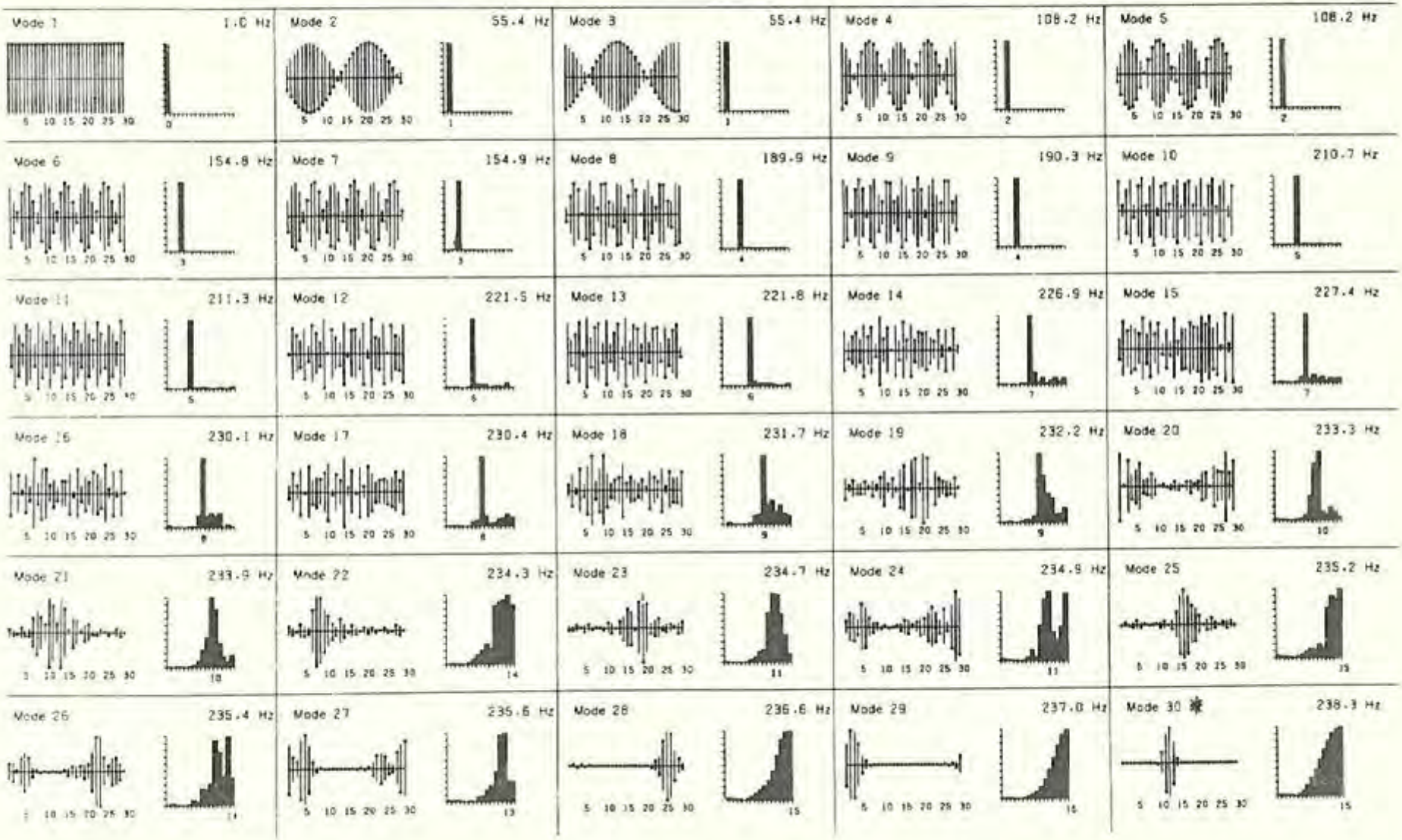

Fig. 2.5.10a *Critical and non-critical mode-shapes*

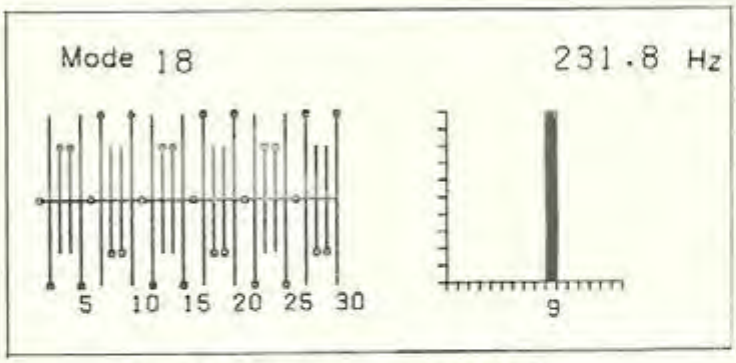

Tuned Mode-shape Non-critical

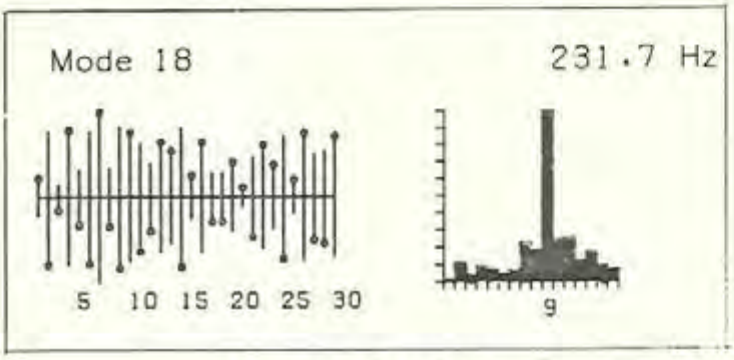

Mistuned Mode-shape
Non-critical

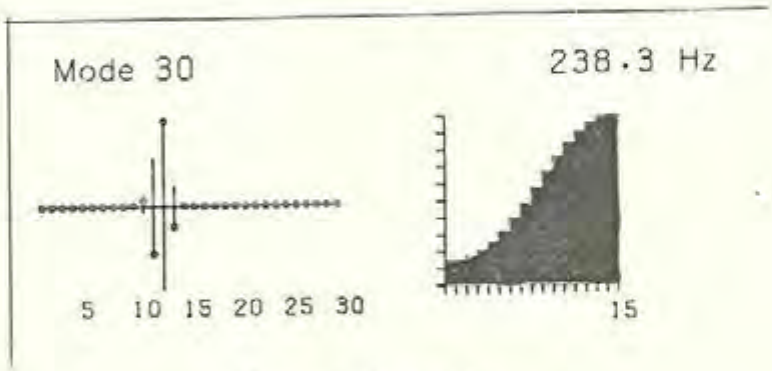

Mistuned Mode-shape
Critical

Fig. 2.5.10b *Relationship between critical blades and blades with extreme detune*

(a) Disc 10A

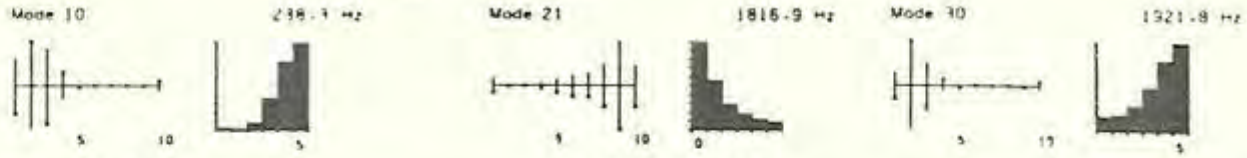

critical blade = 2 critical blade = 9 critical blade = 2

(b) Disc 10X

critical blade = 5

(c) Disc 10Y

critical blade = 5 critical blade = 5

(d) Disc 30A

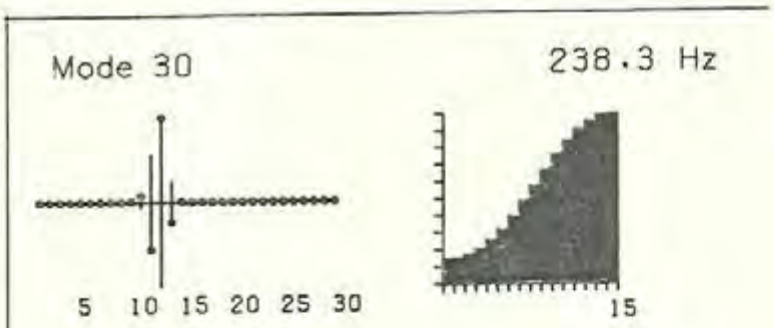

critical blade
13

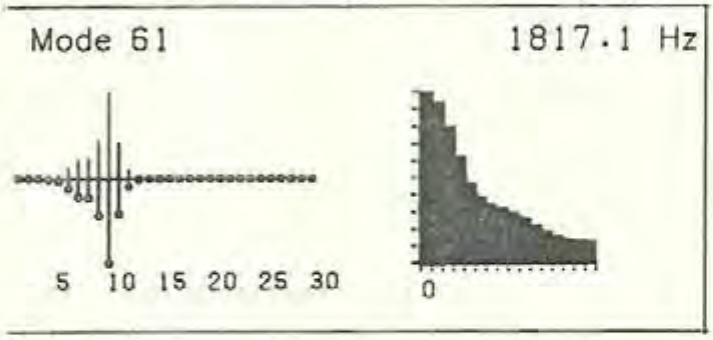

critical blade
10

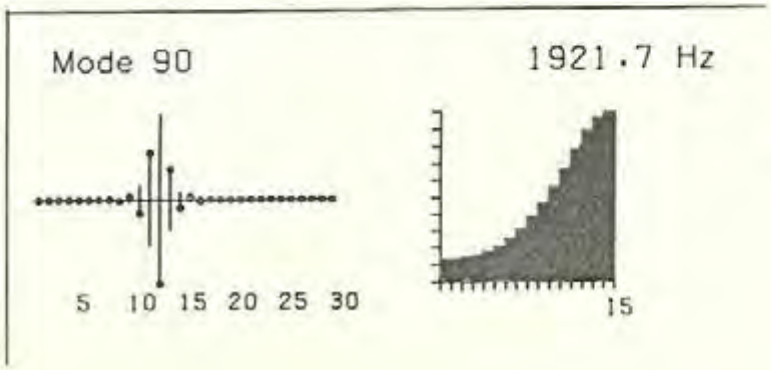

critical blade
13

Fig. 2.5.11 *Frequency response of discs 30T and 30A to 3EO excitation*

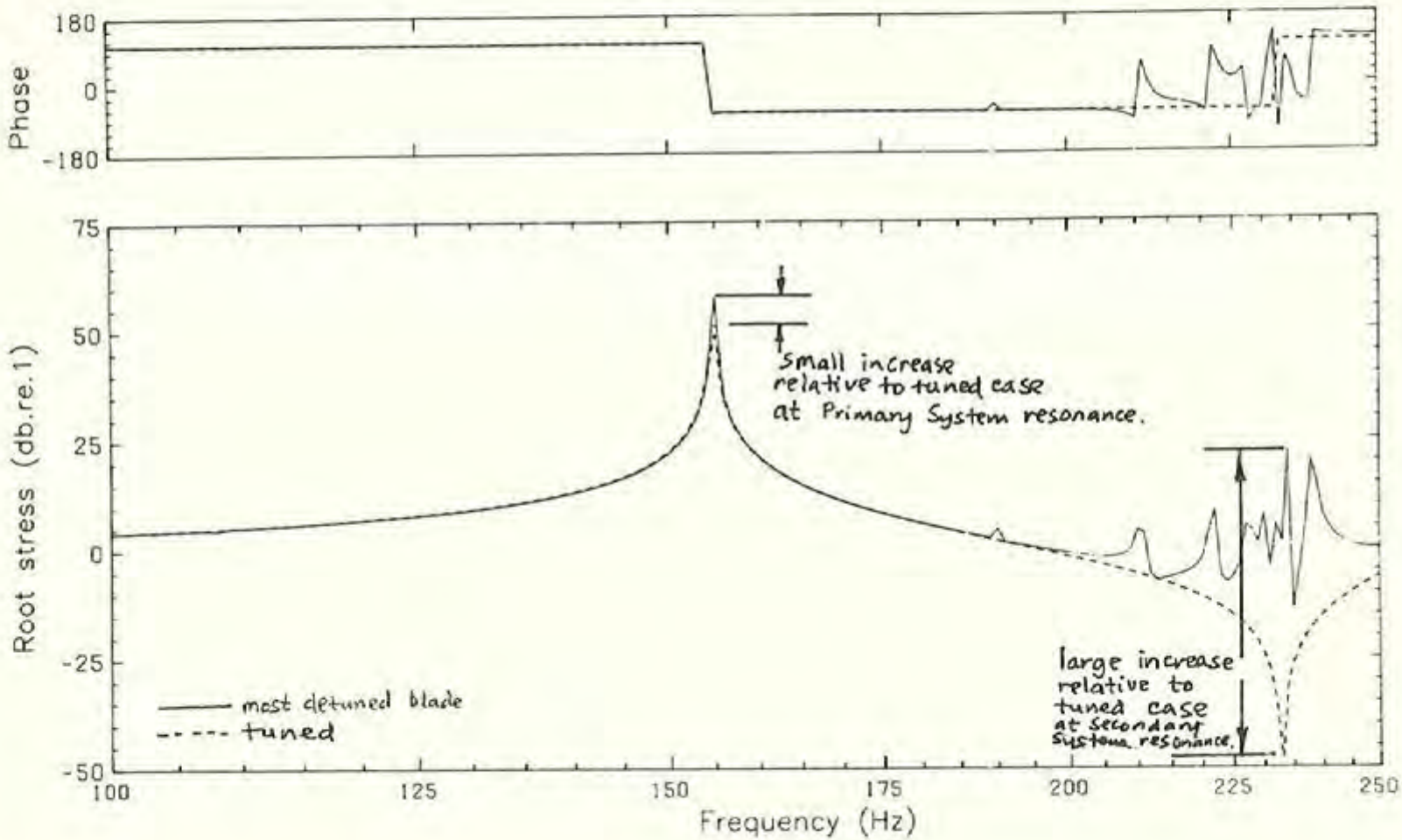

Fig. 2.5.12 *Frequency response of Disc 10A to 1EO*

(a) Q = 1000

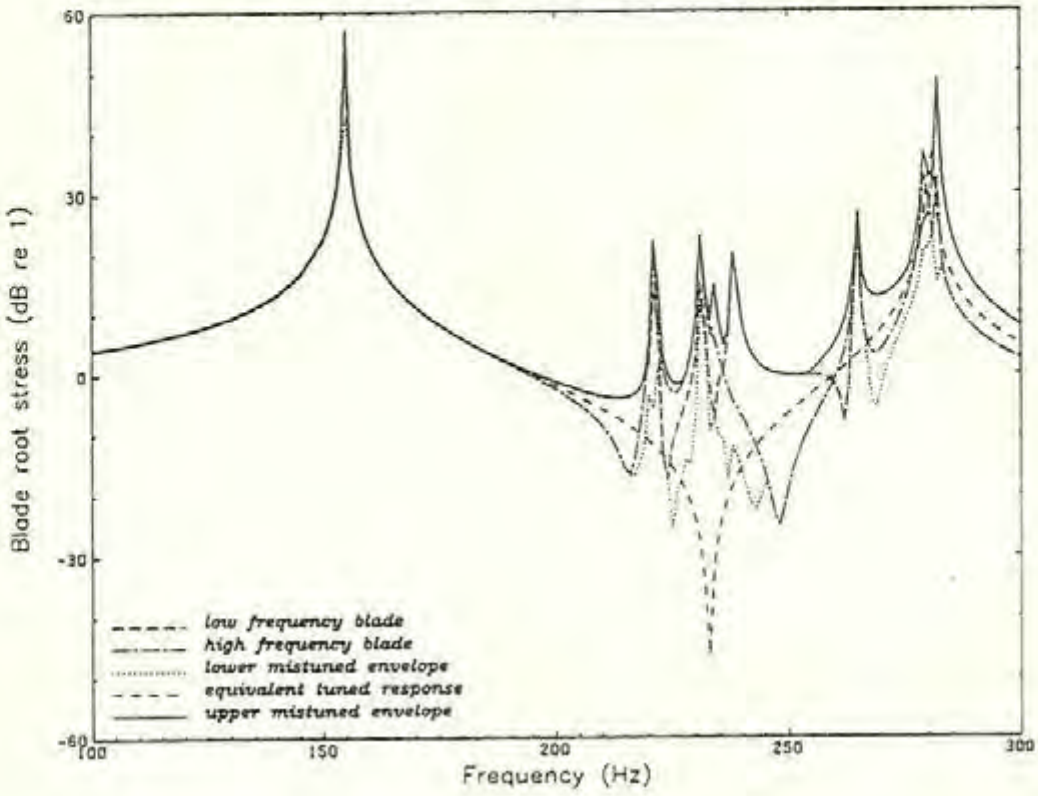

(b) Q = 50

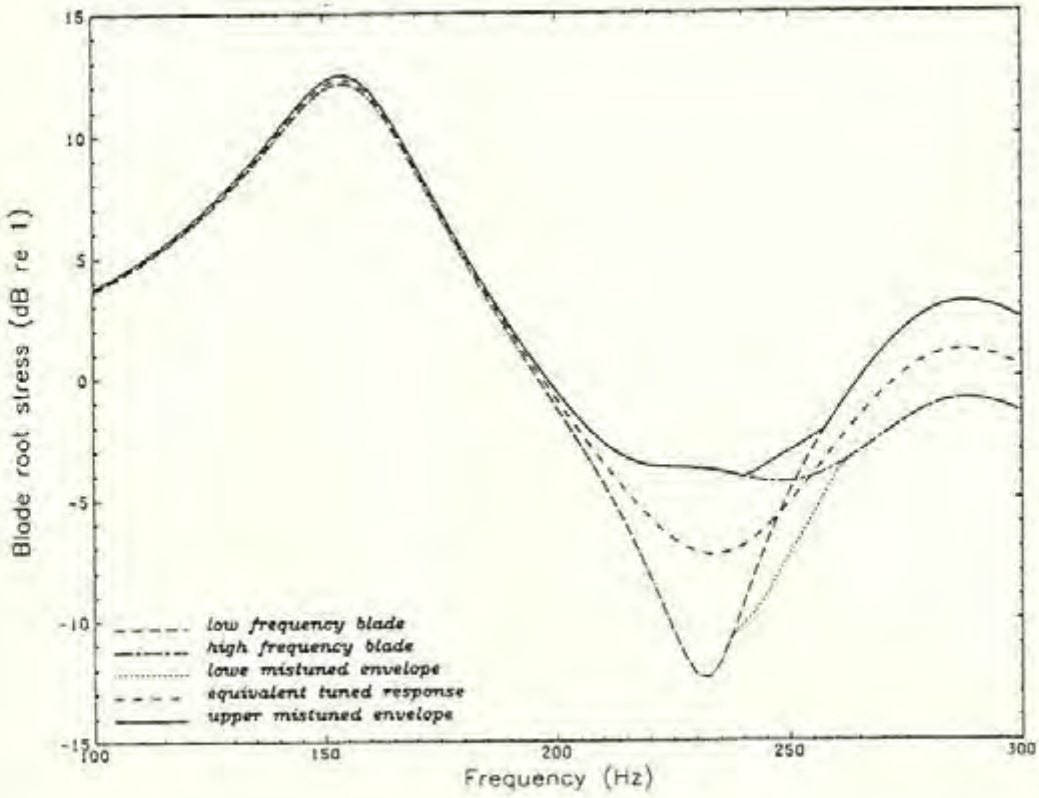

Fig. 2.5.13 *Frequency response of Disc 10A to 2EO*

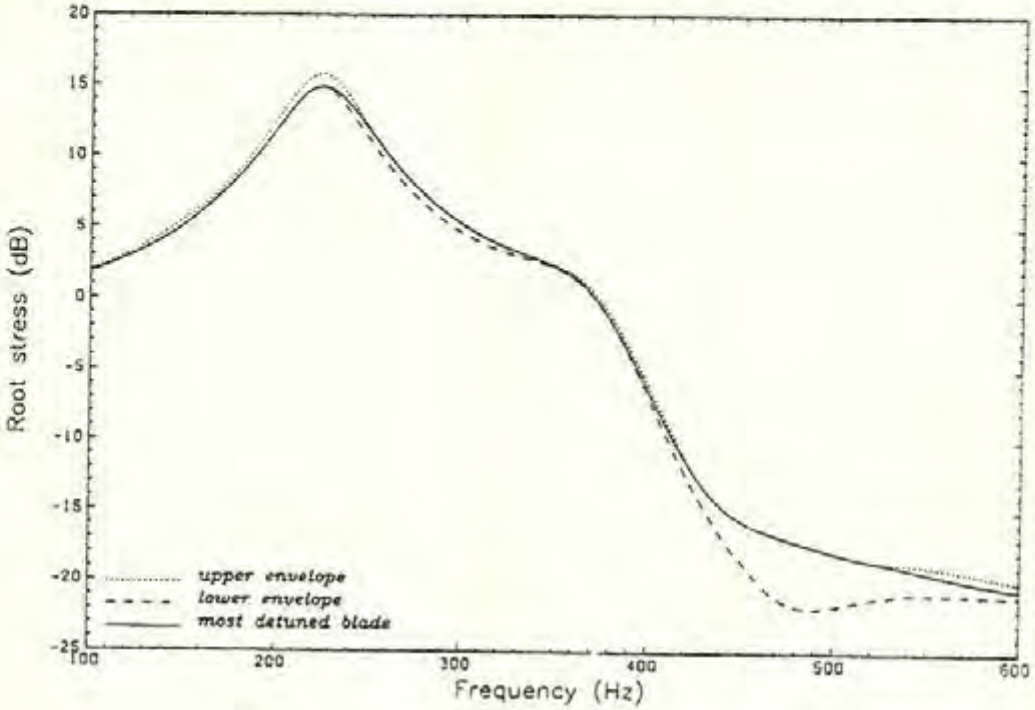

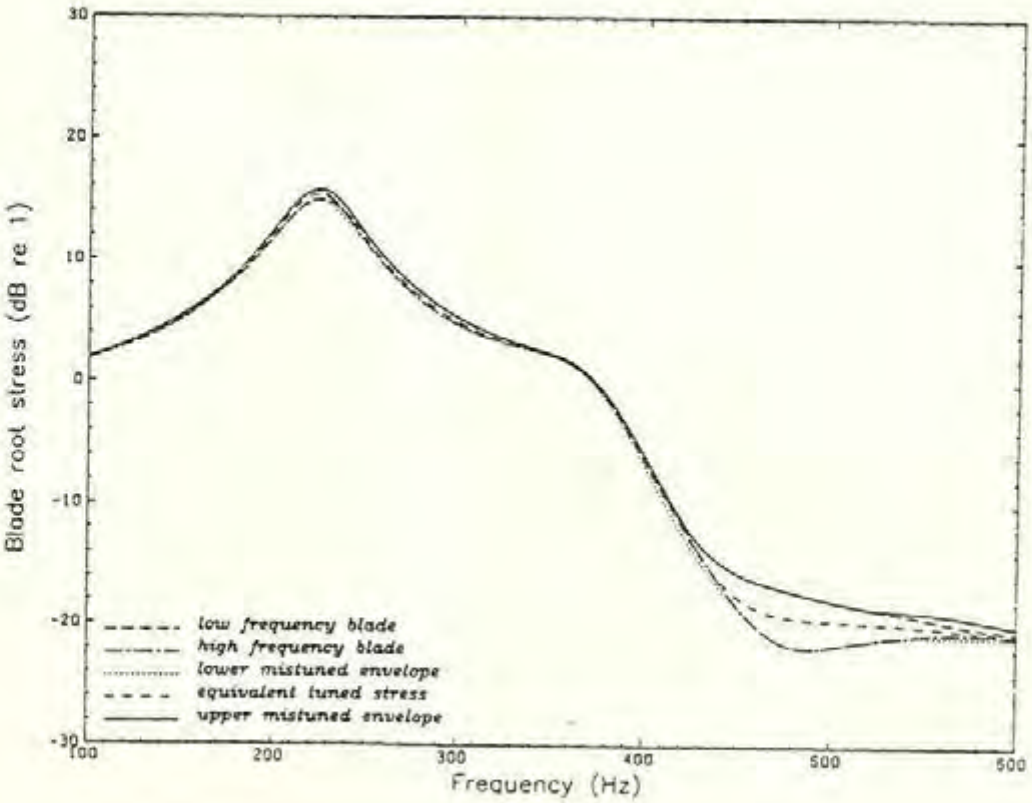

Fig. 2.5.14 *Frequency response of Disc 10A to 3EO*

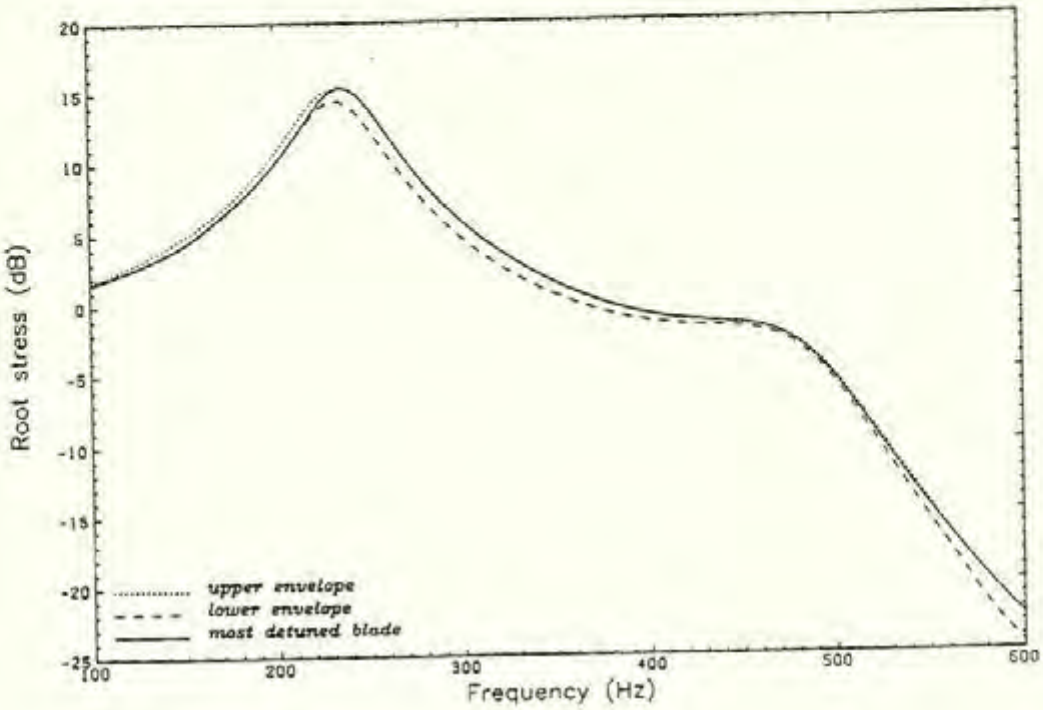

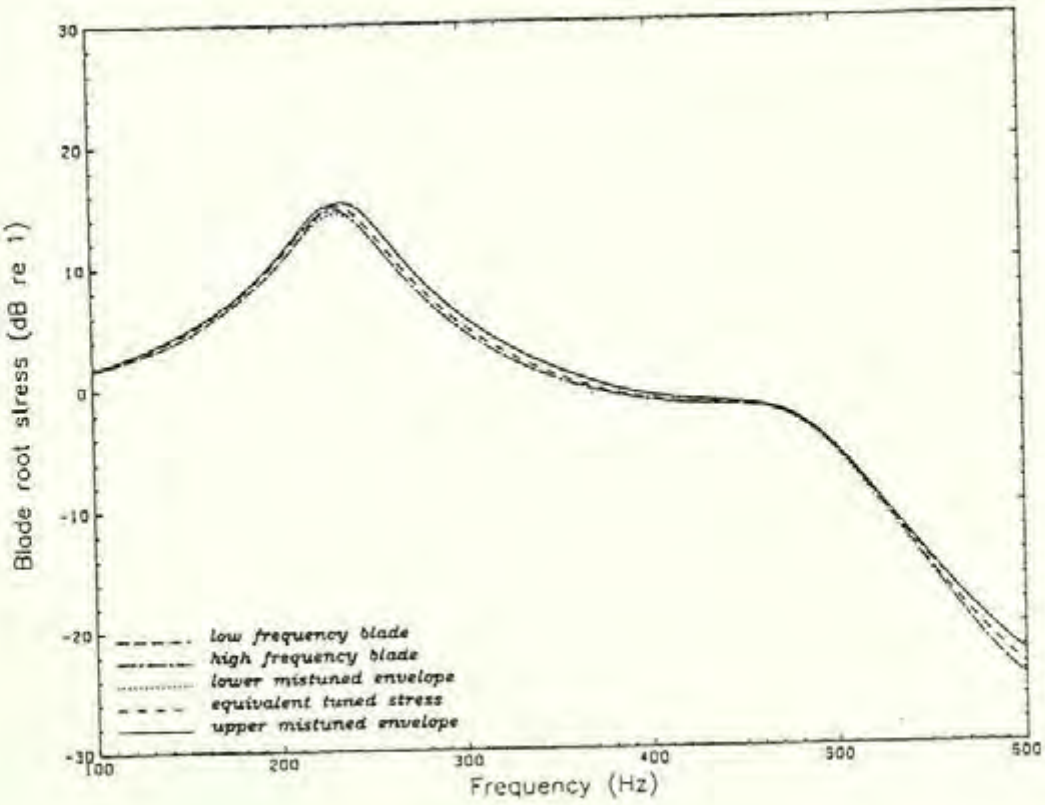

Fig. 2.5.15 *Frequency response of Disc 10A to 4EO*

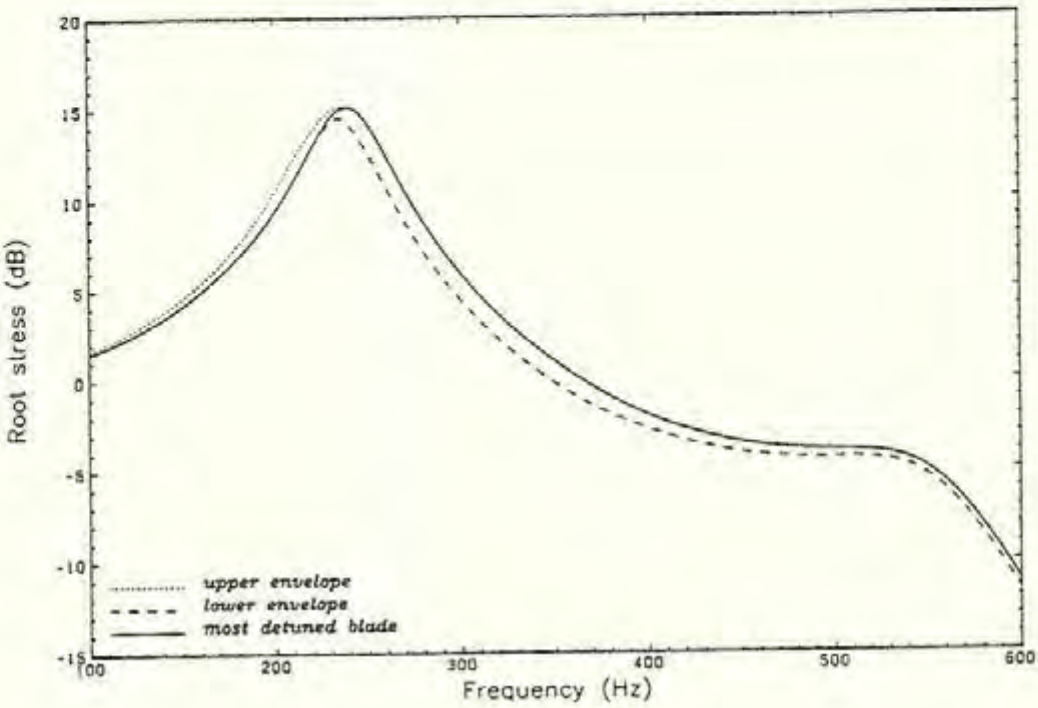

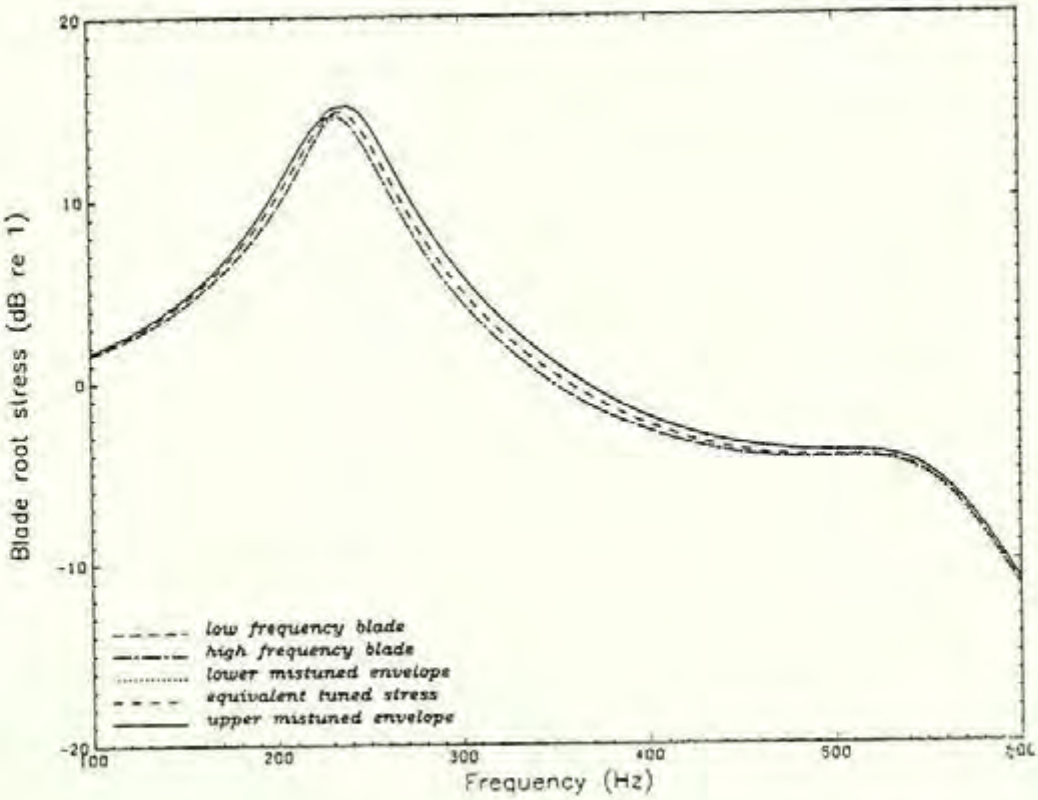

Fig. 2.5.16 *Frequency response of Disc 10A to 5EO*

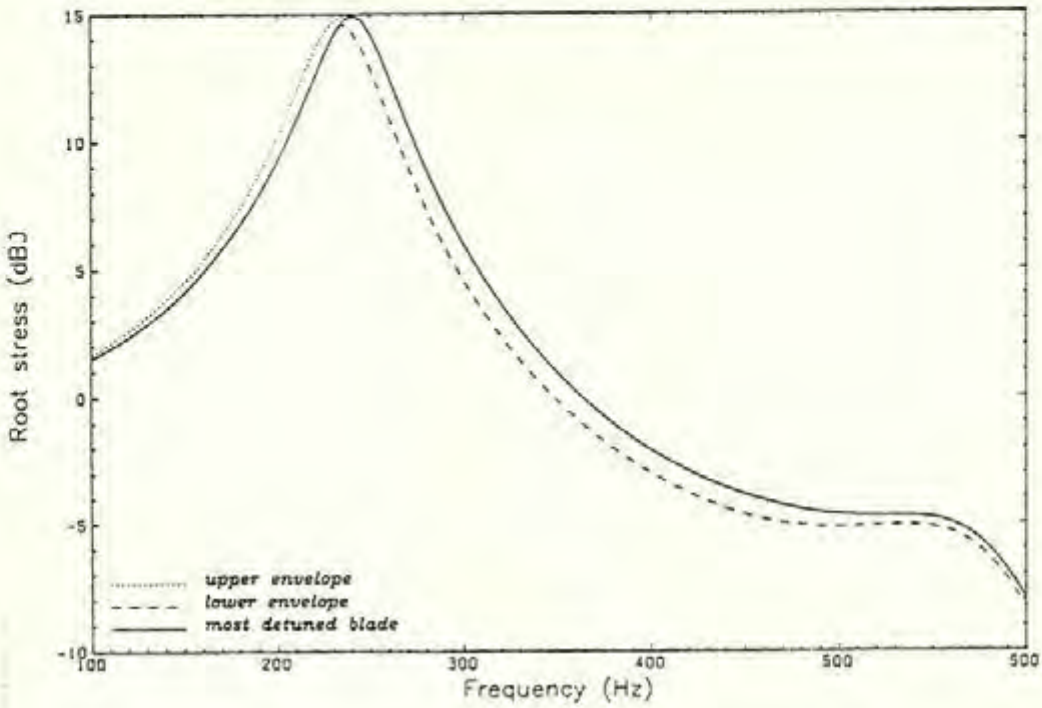

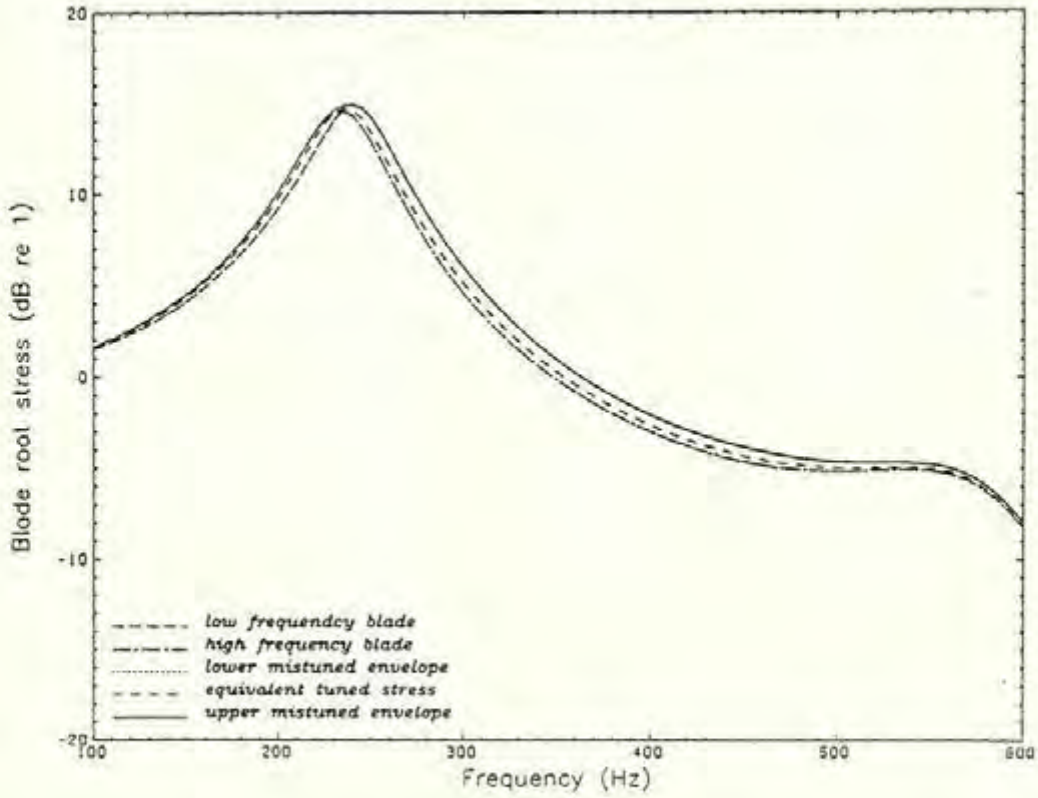

Fig. 2.5.17 *Stress amplitudes of blades on Disc 10A* ($\Omega = 1000$)

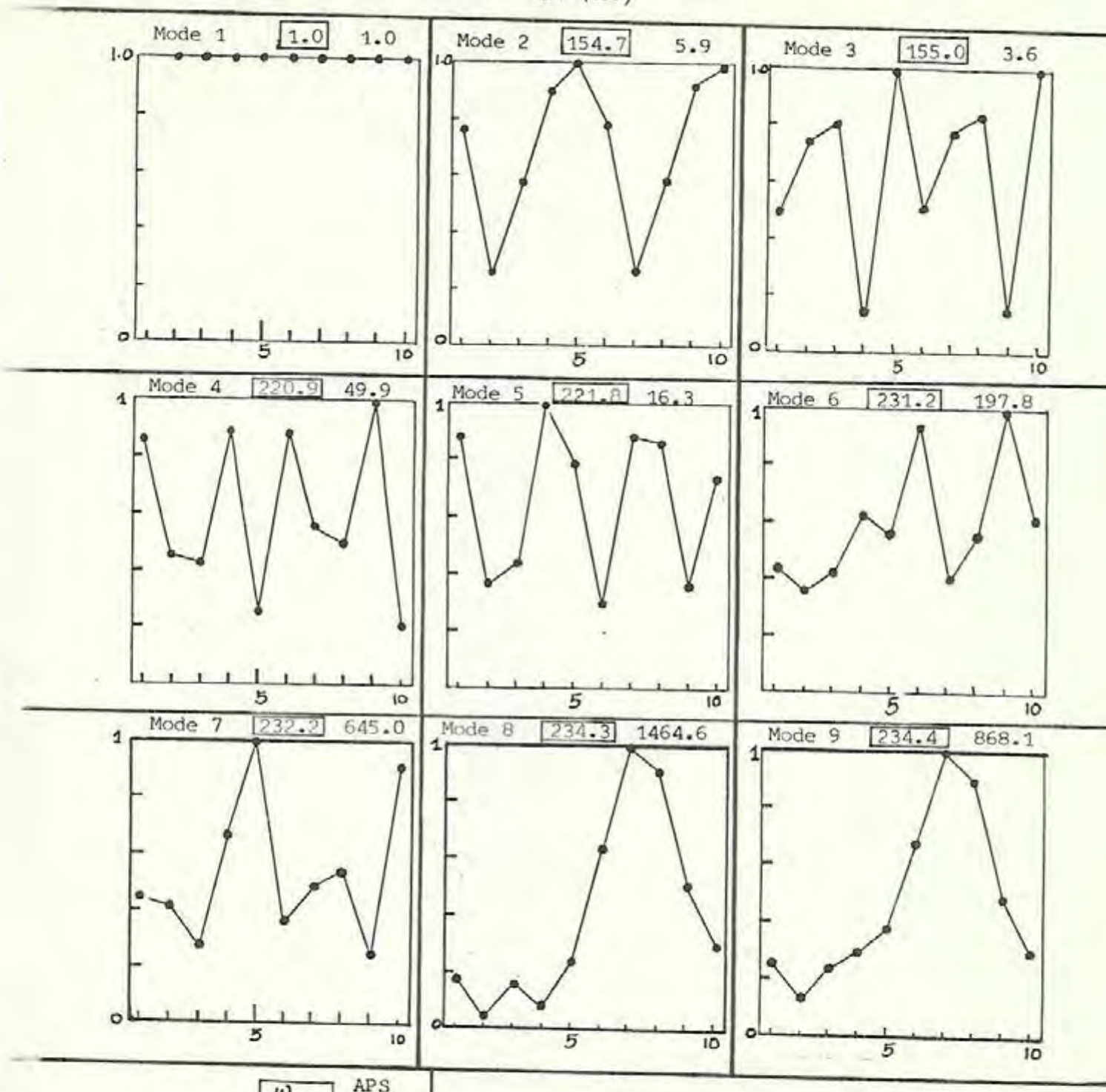

For each of the 10 graphs shown here, the following explanations apply

Horizontal axis: blade number, from 1 to 10, shown from left to right.

Vertical axis: normalized stress, from 0.0 to 1.0, shown from origin to top of graph.

ω_n: natural frequency of the mode (Hz)

APS: absolute peak stress at the mode (kN/m^2)

Fig. 2.5.18 *Response amplitudes of Disc 30A*

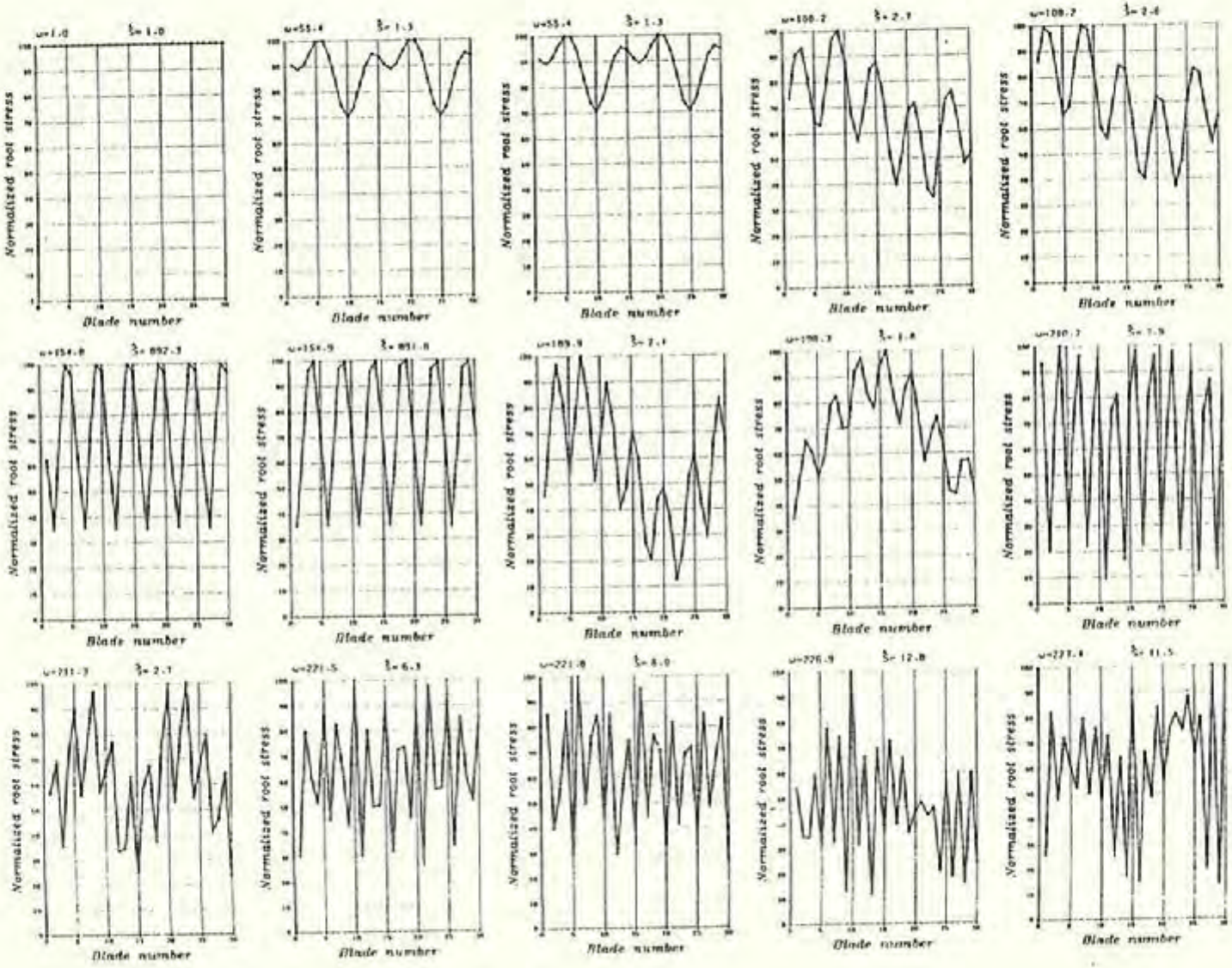

Fig 2.5.18 continued.

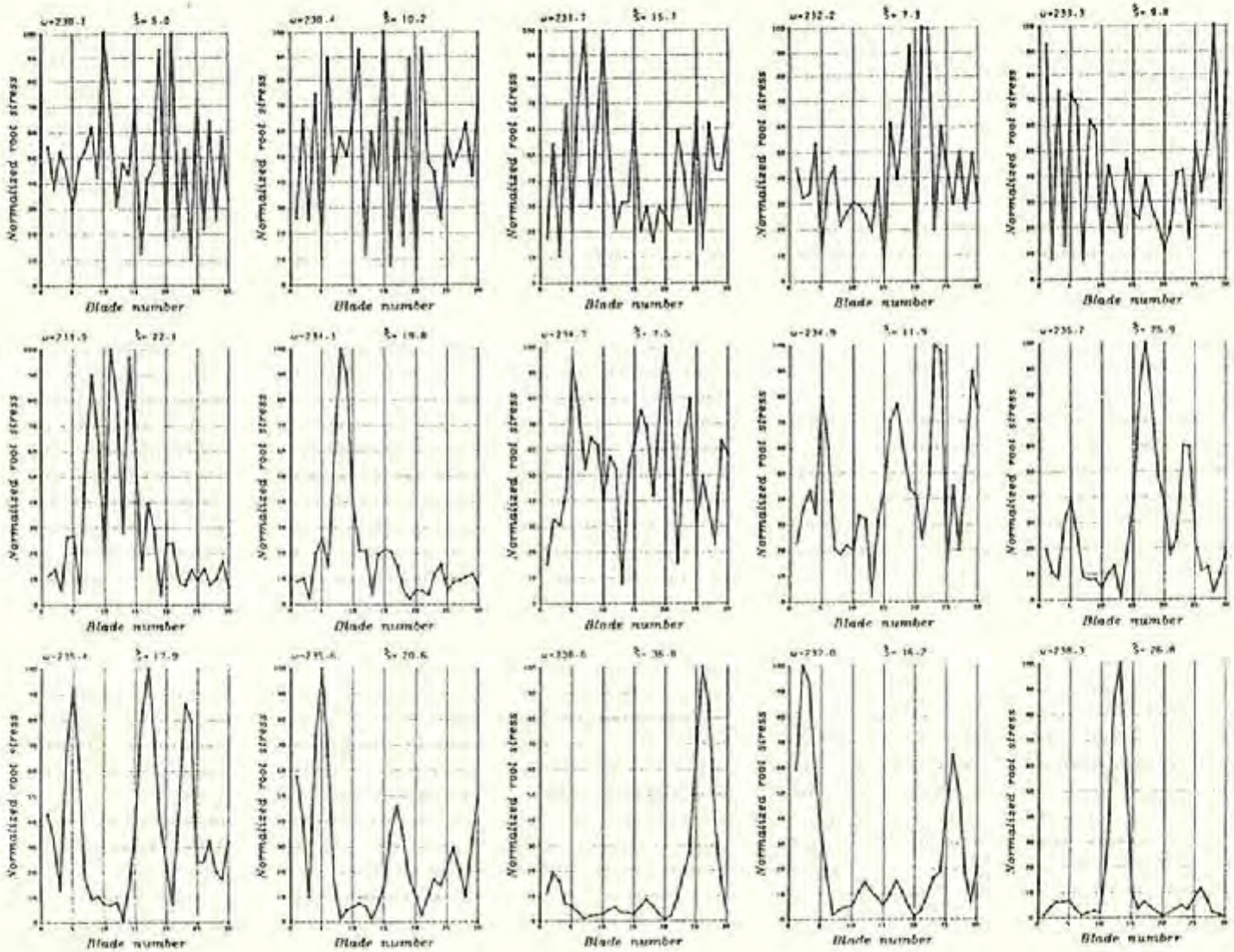

Fig. 2.5.19 *Response amplitudes of Disc 30B*

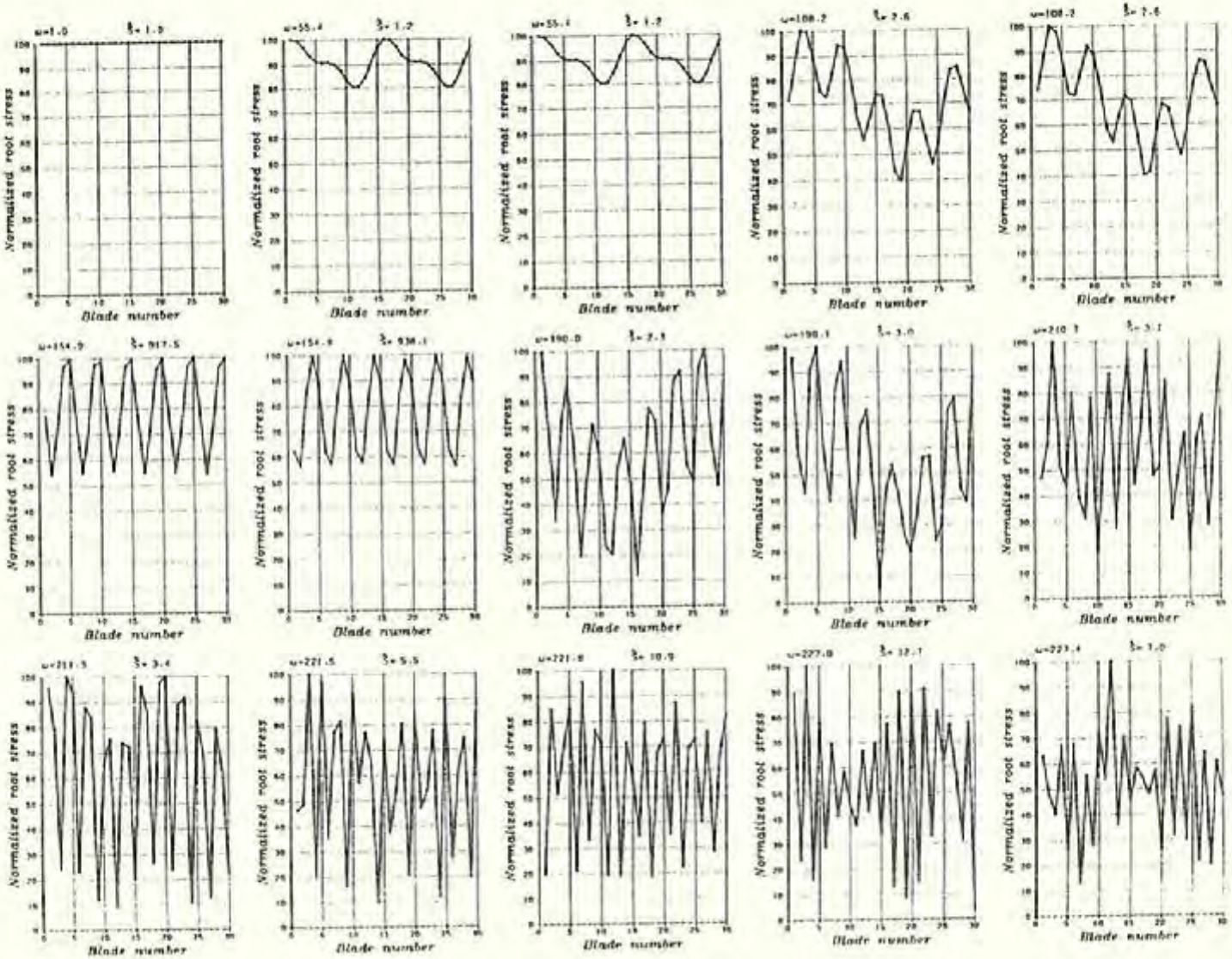

Fig 2.5.19 continued

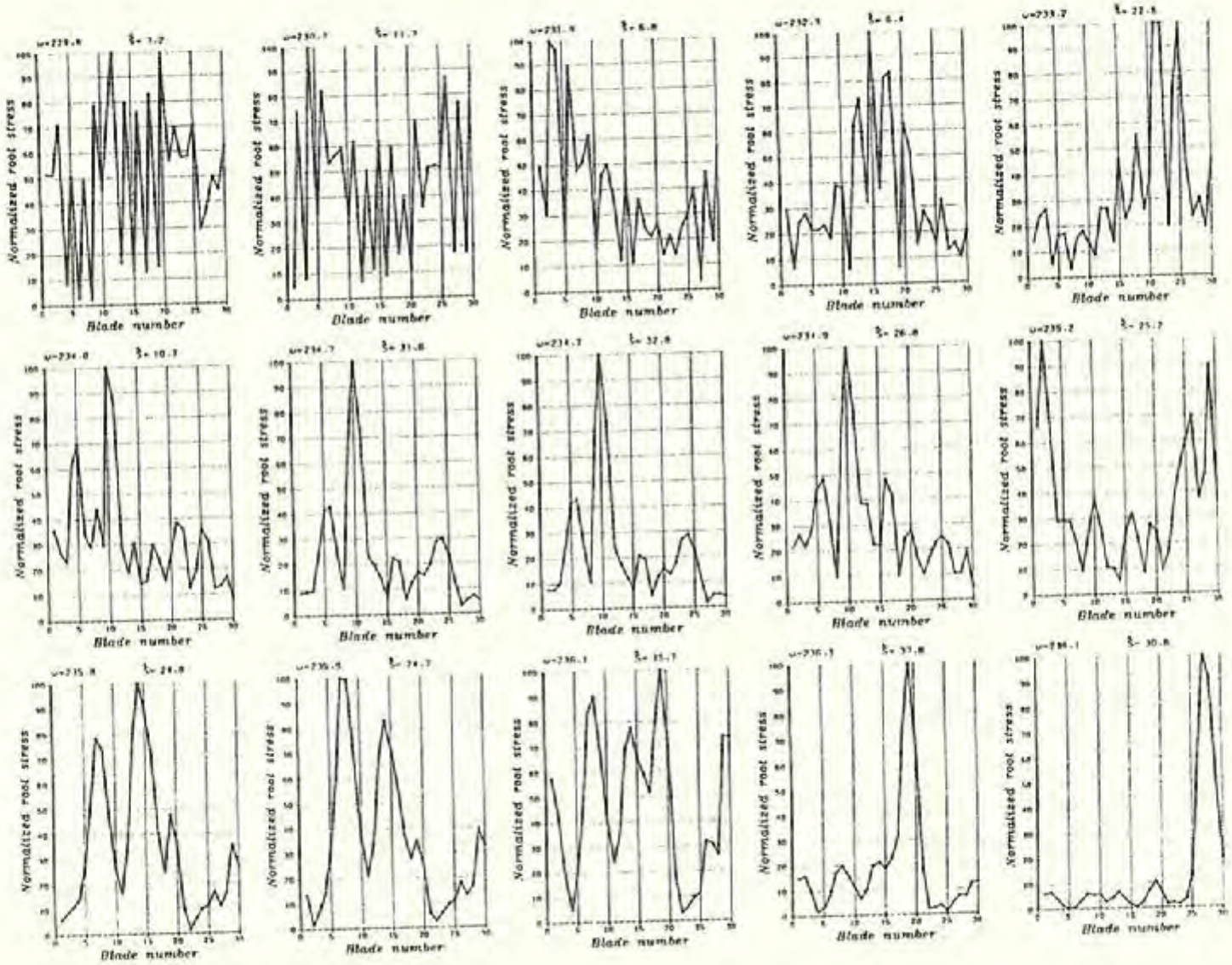

Fig. 2.5.20 *Resonant response patterns for Discs 30A and 30B*

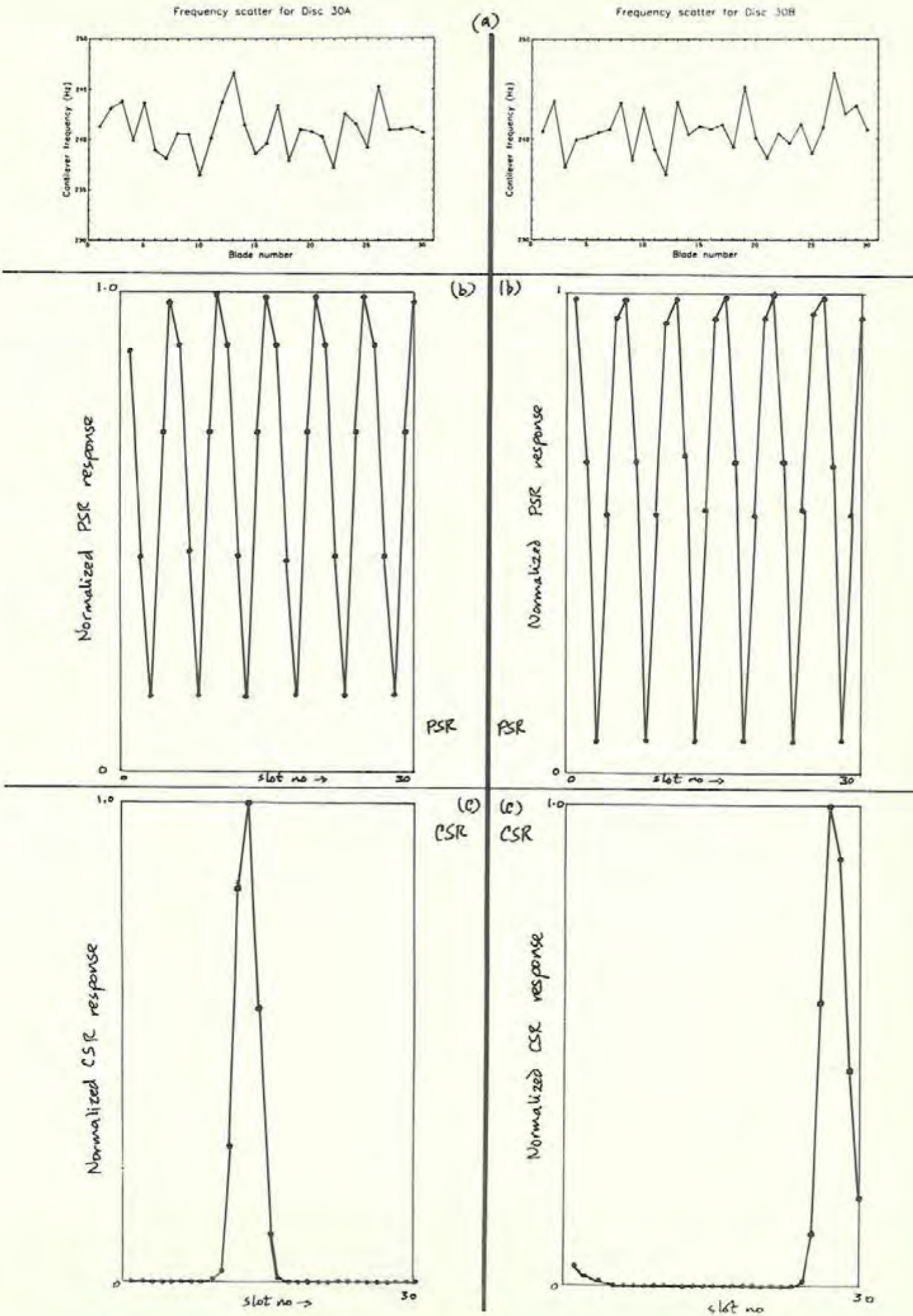

Table 2.4.1

Resonant frequencies of a tuned 30-bladed disc

Nodal dia	Theory* (Hz)	Experiment** (Hz)	Theory*** (Hz)
0	-	-	1.0
1	-	-	55.4
2	102.5	102	108.2
3	159.1	161	154.8
4	188.9	191	189.8
5	205.3	208	210.5
6	215.2	218	221.1
7	221.6	224	226.7
8	226.0	228	229.8
9	229.2	232	231.8
10	231.5	234	233.0
11	233.2	235.5	233.8
12	234.5	236.6	234.4
13	235.3	237.8	234.8
14	235.9	237.9	234.9
15	236.1	237.9	235.0

* Theory (Ewins, 1972)
** Experiment (Ewins, 1972)
*** Theory (Present study)

Table 2.5.2 *Response characteristics of Disc 30A*

(Q= 50)

(Hz) FREQUENCY	(dB) MAX. RESPONSE	BHR	(dB) MIN. RESPONSE	BLR
100.00	-101.352	10	-102.064	13
101.00	-100.942	10	-101.642	13
102.00	-100.443	10	-101.128	13
103.00	-99.814	10	-100.481	13
104.00	-98.981	10	-99.625	13
105.00	-97.801	10	-98.416	13
106.00	-95.945	10	-96.519	13
107.00	-92.384	22	-92.912	13
108.00	-78.872	15	-79.845	12
109.00	-93.724	4	-94.085	23
110.00	-105.121	26	-105.447	7
111.00	-117.125	13	-119.399	22
112.00	-119.992	10	-124.535	13
113.00	-113.014	10	-115.030	13
114.00	-110.271	10	-111.826	13
115.00	-108.707	10	-110.069	13
116.00	-107.667	10	-108.924	13
117.00	-106.910	10	-108.103	13
118.00	-106.325	10	-107.474	13
119.00	-105.852	10	-106.970	13
120.00	-105.457	10	-106.552	13
121.00	-105.116	10	-106.195	13
122.00	-104.817	10	-105.882	13
123.00	-104.548	10	-105.604	13
124.00	-104.303	10	-105.351	13
125.00	-104.076	10	-105.119	13
126.00	-103.864	10	-104.902	13
127.00	-103.663	10	-104.698	13
128.00	-103.470	10	-104.503	13
129.00	-103.284	10	-104.317	13
130.00	-103.103	10	-104.135	13
131.00	-102.926	10	-103.958	13
132.00	-102.751	10	-103.784	13
133.00	-102.577	10	-103.612	13
134.00	-102.403	10	-103.439	13
135.00	-102.227	10	-103.266	13
136.00	-102.049	10	-103.091	13
137.00	-101.868	10	-102.912	13
138.00	-101.682	10	-102.729	13
139.00	-101.489	10	-102.540	13
140.00	-101.288	10	-102.343	13
141.00	-101.076	10	-102.136	13
142.00	-100.852	10	-101.917	13
143.00	-100.611	10	-101.681	13
144.00	-100.350	10	-101.425	13
145.00	-100.063	10	-101.144	13
146.00	-99.740	10	-100.828	13
147.00	-99.372	10	-100.467	13
148.00	-98.940	10	-100.043	13
149.00	-98.416	10	-99.530	13
150.00	-97.754	10	-98.882	13
151.00	-96.867	10	-98.017	13
152.00	-95.577	10	-96.767	13
153.00	-93.424	10	-94.710	13
154.00	-88.646	10	-90.309	13
155.00	-71.116	18	-78.118	5
156.00	-97.693	18	-99.460	5
157.00	-111.956	18	-114.233	5
158.00	-116.187	10	-119.874	13
159.00	-109.149	10	-111.036	13
160.00	-106.496	10	-108.086	13
161.00	-104.993	10	-106.475	13
162.00	-103.985	10	-105.417	13
163.00	-103.239	10	-104.646	13
164.00	-102.647	10	-104.043	13
165.00	-102.155	10	-103.547	13
166.00	-101.728	10	-103.122	13
167.00	-101.348	10	-102.746	13
168.00	-101.000	10	-102.406	13
169.00	-100.675	10	-102.091	13
170.00	-100.366	10	-101.794	13
171.00	-100.069	10	-101.510	13
172.00	-99.778	10	-101.234	13
173.00	-99.491	10	-100.963	13
174.00	-99.203	10	-100.693	13
175.00	-98.913	10	-100.422	13
176.00	-98.618	10	[illegible]	[illegible]
177.00	-98.313	10	-99.865	13
178.00	-97.996	10	-99.572	13
179.00	-97.661	10	-99.264	13
180.00	-97.304	10	-98.936	13
181.00	-96.917	10	-98.582	13
182.00	-96.490	10	-98.191	13
183.00	-96.006	10	-97.750	13
184.00	-95.443	10	-97.230	13
185.00	-94.760	10	-96.619	13
186.00	-93.884	10	-95.832	13
187.00	-92.651	22	-94.750	13
188.00	-90.622	22	-93.074	13
189.00	-86.309	22	-89.804	13
190.00	-69.793	22	-97.1[illegible]	2
191.00	-91.360	16	-98.120	4
192.00	-108.456	1	-128.741	26
193.00	-107.593	7	111.494	1
194.00	-102.847	10	-105.0[illegible]	13
195.00	-100.581	10	-102.666	13
196.00	-99.169	10	-101.242	13
197.00	-98.136	10	-100.239	13
198.00	-97.297	10	-99.442	13
199.00	-96.565	10	-98.763	13
200.00	-95.893	10	-98.151	13
201.00	-95.249	10	-97.574	13
202.00	-94.609	10	-97.008	13
203.00	-93.952	10	-96.432	13
204.00	-93.256	10	-95.827	13
205.00	-92.489	10	-95.184	13
206.00	-91.608	10	-94.401	13
207.00	-90.531	10	-93.470	26
208.00	-89.082	10	-92.439	26
209.00	-86.784	10	-90.964	26
210.00	-81.444	10	-88.506	26
211.00	-78.203	20	-118.892	24
212.00	-88.753	20	-104.145	13
213.00	-102.694	28	-129.447	20
214.00	-96.604	10	-100.087	20
215.00	-93.756	10	-96.700	26
216.00	-91.824	10	-95.173	13
217.00	-90.164	10	-93.903	13
218.00	-88.492	10	-92.648	13
219.00	-86.534	10	-91.205	13
220.00	-83.706	10	-89.146	13
221.00	-76.924	10	-85.088	26
222.00	-73.348	6	-91.761	5
223.00	-96.997	5	-129.218	18
224.00	-88.799	10	-94.195	13
225.00	-84.136	10	-91.322	13
226.00	-78.508	10	-88.788	13
227.00	-64.554	10	-109.888	5
228.00	-88.398	22	-132.785	23
229.00	-80.150	7	-90.289	26
230.00	-63.392	7	-82.880	26
231.00	-85.944	10	-112.051	11
232.00	-63.926	21	-104.657	30
233.00	-68.806	28	-100.453	7
234.00	-53.656	14	-96.211	3
235.00	-52.971	29	-113.618	24
236.00	-67.156	5	-92.381	12
237.00	-38.475	2	-98.743	14
238.00	-61.211	13	-94.313	11
239.00	-68.327	13	-86.469	10
240.00	-75.866	13	-87.740	10
241.00	-79.782	13	-88.847	10
242.00	-82.466	13	-89.844	10
243.00	-84.530	13	-90.735	10
244.00	-86.225	13	-91.574	10
245.00	-87.678	13	-92.366	10
246.00	-88.965	13	-93.123	10
247.00	-90.132	13	-93.856	10
248.00	-91.214	13	-94.670	9
249.00	-92.235	13	-95.521	9
250.00	-93.217	13	-96.387	9

BLR = blade with lowest response
BHR = blade with highest response
dB = decibels relative to unity.

Chapter 3

3.1 Introduction

Aero-engine turbines and compressors are usually 'type-tested' at a certain phase in the course of developing new engines. At various other times, tests are also conducted on selected engines which have previously been in service. In the process of such engine tests, only a few of the blades on a rotor stage may be strain gauged simultaneously. If the blades were all in perfect tune, it would be of little significance which blades on the stage were monitored, since all of them would then experience identical levels of stressing at all speeds of engine operation. However, we already know from the previous chapter that the blades on a randomly detuned wheel do not exhibit the uniform response pattern which is typical of tuned assemblies. Rather, there is a fluctuation of response amplitudes from one blade to another, and the difference between the smallest and largest blade response may vary from little to quite large, depending on the frequency of the exciting force, as shown in Figure 3.1.1. It is, therefore, essential in the case of mistuned assemblies to be able to predict reliably the upper and lower bounds of response amplitudes for all the blades on the stage, from an observation of only a few of the blades. Hence, the need for some inferential statistics.

Procedures for predicting the behaviour of a *population*† from the study of a *sample* are well-established tools of statistical analysis nowadays. It matters little if the population is of finite size or otherwise. Such procedures are widely used in politics and economics, and are known by the familiar terms of *opinion polls* or *market research*. Although opinion polls may yield reliable indications of the probable behaviour of a population from a test conducted on a sample, it is well known that they may also lead to grossly erroneous inferences. An important consideration which is generally understood but nevertheless not always given due attention is that inferences are only accurate if the sample is carefully drawn and, moreover, if the relationship between the sample and its population is thoroughly understood.

If a sample is drawn from a population without prior information on the extent of variation in the properties of the individual elements, and in

† Usage of 'population' and 'sample' in this text is in accordance with statistical parlance. A *population* is the universal set of all the observable elements which generally have a random scatter in properties, whereas a *sample* is only a small subset of the population.

such a way that every element has an equal chance of being selected, then it is **random sampling**.

A biased sample may also be drawn on the basis of an 'educated choice', i.e. having known *a priori* the manner in which certain elements are likely to behave. Such a technique is known as **purposive sampling**. Random sampling is the more widely used technique of obtaining statistical samples from 'normal', or gaussian, populations, while purposive sampling is used chiefly for non-normal populations.

Statistical Terminologies

Certain terms are frequently used in the description of raw data and the statistical procedures for reducing them to more comprehensible forms. To dwell for any moment on the description of such terms would seem trivial to statisticians, although engineers may not be quite so acquainted with them. We present here, therefore, as an aid to comprehension and continuity of thought, a review of some basic terminologies which will feature in subsequent discussion in this chapter.

3.1.1 Measures of Central Tendency

Most engineering observations that are characterized by randomness have a tendency to cluster around some central value on the scale of measurement. Three parameters are customarily used to identify the centre of congregation, and these are collectively known as *measures of central tendency*, or *measures of location*.

Median If a set of measured data which is randomly ordered in its 'raw' state, hereafter referred to as the *variate*, is sorted into an ascending or descending order of magnitude, the median is that value of the variate which occurs in the middle of the ordered sequence. If there are N observations in the sorted list, the the median is easily identified as that member in the variate which occupies the $\frac{1}{2}(N+1)th$ position, when N is odd. For N even, the median is derived from the average of the elements in the $\frac{1}{2}Nth$ and $\frac{1}{2}(N+2)th$ locations. In either case, the median divides the variate into two equal halves. It is particularly useful, as a measure of dispersion, in instances when the effects of extreme elements must be eliminated from the measure of central location.

Mean The arithmetic mean is the most important measure of central tendency, both from the practical as well as from a theoretical point of view. For N observations in the variate, $x_i (i=1,...N)$, the arithmetic mean, μ, is given by

$$\mu = (\Sigma x_i)/N \tag{3.1.1}$$

Mode The element which occurs most frequently, *i.e.* the most popular, in a set of data is known as the mode. It is generally not a unique measure of central location, unlike the mean or the median. If a variate has only one mode, then it is referred to as *uni-modal*; and if two, *bi-modal*; otherwise, it is described as *multi-modal*.

3.1.2 Measures of Scatter

Although the measures of location described above are useful for identifying the 'centre' of a set of data, they are usually unable to provide any information concerning the manner of variation within the set. Two sets of data, for example, may have the same average value (or other measure of central tendency) but differing amounts of scatter, as illustrated in Figure 3.1.2.

The **standard deviation**, σ, is the most widely used measure of dispersion. If a variate consists of N discrete observations, the standard deviation is defined by the relation

$$\sigma=[\{\Sigma(x_i-\mu)^2\}/(N-1)]^{1/2} \tag{3.1.2}$$

The **coefficient of variation**, v, is a normalised form of the standard deviation. It is conveniently obtained as the ratio

$$v = \sigma/\mu \tag{3.1.3}$$

It is useful for comparing the extent of scatter in separate variates having substantially divergent arithmetic means.

In addition to the measure of scatter about a mean value, certain terms are used which may not, strictly speaking, be classed as 'measures of dispersion'. Among them is the **coefficient of skewness**, which provides a measure of how symmetric the variate is about its mean value. It is defined as

$$\frac{\sum_i (x_i - \mu)^3}{\sigma^3 - (N-1)} \tag{3.1.4}$$

and is therefore sometimes known as the *third moment*. Its value is zero for a perfectly symmetric variate. The **coefficient of kurtosis** was first used by Karl Pearson in 1906 for the purpose of measuring the peakedness or *kurtosis* of a uni-modal distribution. Like the coefficient of skewness, it is also a moment ratio, and is often known in the literature as the fourth moment. Its value may be obtained from the formula

$$\frac{\sum_i (x_i - \mu)^4}{\sigma^4 - (N-1)} \tag{3.1.5}$$

3.2 Frequency Distributions

The central issue in this chapter is essentially a practical one. It is how to solve the problem of estimating the bounds on dynamic response levels, since it is generally acknowledged that all the blades on a stage cannot be strain-gauged simultaneously during routine engine tests. The problem — which is usually addressed by several theories of random sampling — can be stated quite simply: given a sample of measured data from a population, to determine from it some or all of the properties of that population.

It has been stated above, §3.1, that inferences concerning the probable behaviour of a population cannot usually be deduced correctly from an observation of its sample unless the relationship between the two is thoroughly understood. For populations that are characteristically Gaussian, there are well established procedures for projecting the probable behaviour of the population when only small amounts of data may be sampled from it in a random manner. Now, although many engineering statistics are gaussian in nature, or are approximately so, there are exceptional cases for which the assumption of normal characteristics may not be credibly made. In such instances, it may be advisable to carry out purposive sampling, rather than random sampling. Hence, in order that the appropriate sampling technique be applied, it is mandatory to establish beforehand whether the population from which the sample is to be taken is normal or otherwise.

One of the clearest ways of knowing if a variate is normally distributed is to examine its frequency distribution by dividing the data range into only a few classes, typically between 5 and 15, which must be of equal

width. For variates exhibiting normal characteristics, the frequency distribution diagrams are approximately bell shaped. For other types of distributions, many different patterns may result. Thus, the types of distibutions depicted in Figures 3.3.1 may be observed from a statistical analysis of the dynamic response levels for turbine blades on a mistuned wheel.

3.2.1. Normal Distribution

The normal frequency distribution is usually described by the equation:

$$f(x) = \frac{1}{\sigma\sqrt{2\pi}} e^{-\frac{1}{2}\left(\frac{x-\mu}{\sigma}\right)^2} \tag{3.2.1}$$

where μ and σ are the mean and standard deviations of the variate, x. It is evident from equation (3.2.1) that only two parameters, μ and σ, are required to define a given normal distribution uniquely.

Other special features may also be noted for the normal curve. Thus:

(*i*) the mean, the median, and the mode all have practically identical numerical values

(*ii*) the curve is perfectly symmetrical about its mean, so that it has a non-existent coefficient of skewness.

(*iii*) it is uni-modal

(*iv*) if the number of observations in the sample or population from which the frequency distribution is constructed is reasonably large, then approximately 67% of all the observation lie in the interval between $\mu\text{-}\sigma \leq x \leq \mu + \sigma$; 95% in the range $\mu\text{-}2\sigma \leq x \leq \mu + 2\sigma$; and 99.7% between $\mu\text{-}3\sigma \leq x \leq \mu + 3\sigma$.

3.2.2 Uniform Distribution

In an ideal situation, a statistical examination of identical products should reveal uniform characteristics amongst all the products. This, however, hardly occurs in practice. Yet, under certain circumstances the deviation of characteristics from the centre is small, so that an assumption of uniform distribution may be justifiably made. At an 'umbrella mode' of vibration, for example, all the blades on a turbine wheel experience approximately equal dynamic response levels.

3.2.3 Skewed Distributions

Whereas the normal and uniform distributions are symmetrical about their mean values, there are other types which are not so evenly balanced, and which consequently have an appreciable coefficient of skewness. A distribution may be positively or negatively skewed, as shown in Figures 3.3.1c and 3.3.3c, depending on whether the 'tail' of the distribution is to the left or right.

3.3 Analysis of Blades' Dynamic Response

3.3.1 Introduction

According to the prevailing theories in Tests of Hypotheses — see, for instance, the treatise by **Kendall** and **Stuart** (1973) — the mean and standard deviation, μ and σ, of a population may be estimated from the corresponding values, $\bar{x}$ and s obtained from the sample. We already know that a normal population is completely describable, statistically, once its μ and σ are known. Hence, knowing $\bar{x}$ and s from a sample, one may predict for μ and σ. However, the values of $\bar{x}$ and s can vary from one sample to another, and since many possible samples can be drawn from a given population, it is evident that different impressions concerning the state of scatter within the population may be inferred from different samples. It is, therefore, necessary to provide a measure of 'confidence' in the estimated values.

Let the error incurred in estimating the population mean be given by $\varepsilon = \bar{x}-\mu$. If the sample size, n, is large, and we define the *statistic*, $v = \varepsilon\sqrt{n}/\sigma$ which is assumed to have approximately normal distribution, then we can assert with a probability of $1-\alpha$ that

$$Z_{\alpha/2}<v<Z_{\alpha/2} \tag{3.3.1}$$

where $Z_{\alpha/2}$ is a functional value such that the area under the normal curve to its right is equal to $\alpha/2$. Further details may be obtained from statistical texts, such as **Wine** (1964)

Frequently, we wish to know how large a sample should be in order that the error ε in estimating μ be less than a specified amount, e. This error gets smaller the larger the size of sample, for in the limiting case of $n=N$, when the sample is exactly as large as the population, $e=0$. The answer lies in the inequality (3.3.1) above. Hence, the following well-

established theorem:

> If $\bar{x}$ is used as an estimate of μ, we can be $100(1-\alpha)$ confident that the error will be less than a specified amount ε when the sample size is at least $n = (Z_{\alpha/2}.\sigma/\varepsilon)$

The anomally in the above theorem is at once evident. In order to know how large our *sample* should be, we must know the variance of the *population*! However, it is not always necessary to know the population variance, σ^2, beforehand. If the samples are drawn from normal populations, we are in a position to work exclusively on the sample, since by replacing σ with s, we may apply the t-distribution in lieu of the normal distribution curve to obtain

$$n=(t_{\alpha/2}.s/\varepsilon)^2 \tag{3.3.2}$$

It is the considered judgement of many statisticians that the strict application of equation (3.3.2) to determine the minimum size of sample required for accurate inferential analysis is not usually necessary. A rule of thumb has been developed which states that a random sample of size at least 30, provided it is drawn from a normal population, generally yields good practical results. Thus, the variation of the *statistic* from one sample to another can be accomodated quite easily, *once it is proven that the population is normal*, using the *'student'* (t), F, or χ distributions, or any other appropriate sampling distribution theory. On the other hand, once it is proven, or otherwise known with some certainity, that the population is **NOT** normal, an alternative means of reliably predicting a desired population statistic from that of a sample must be sought.

A designer faced with the practical problem of not being able to strain-gauge more than a few blades at a time may, therefore, make a choice of two possibilities. In one case, he can assume that the distribution of response levels within the population of all the blades on a stage is normal, so that existing sampling techniques and theories may be approximately applied to his small, randomly selected sample. However, he is likely to make grossly erroneous inferences in cases when the distribution of the responses deviate sharply from the gaussian. In the second alternative, he can carry out purposive sampling, in which case he needs to know *which* of the blades are to be sampled, and how many of them are required for the smallest tenable sample size.

The problem of which blades to strain-gauge in such instances, and how to extrapolate from those few blades to predict for the entire set on the wheel, is a crucial one which has remained unsolved for several years. Our

aim in this section is to address this basic problem. We have already observed in the previous chapter that the blades with extreme detune are also the ones most likely to experience to extreme stressing. In this section, we shall further explore this hypothesis, by examining the extent of scatter within the bounds on response which are furnished by the low and high frequency blades.

However, instead of going 'from part to whole', i.e. drawing inferences concerning the probable behaviour of a population by studying a sample thereof — which is the only way available in an experimental program — we may take advantage of working with theoretical data to examine the way in which the responses of *the whole population* of blades on a stage vary with the excitation frequency. If we are able to establish that the scatter in blade responses is at all times normal, we shall then examine the feasibility of predicting the bounds on the response levels for all the blades on a stage. If, on the other hand, we are able to show that the responses are non-gaussian in many cases, then we shall explore the possibility of devising a scheme or guide-line for conducting purposive sampling during engine tests.

3.3.2 Ten Bladed Disc

In Chapter 2, we examined the pattern of blade responses on a ten bladed wheel (Disc 10A) in the presence of various engine order excitations. It was observed (see Figures 2.5.12 to 2.5.16) that the limiting envelope on all the blades' responses at different excitation frequencies was usually experienced by a blade with extreme mistune. In this section, we shall investigate the blade response characteristics *within* the upper and lower envelope.

The dynamic stress at the interface of each blade's root and the disc rim may be calculated from equation (2.3.10*a*). For excitation by the first engine order (1EO) force, we have assumed proportional hysteretic damping with Q=1000. A frequency response diagram of the wheel under these conditions of excitation is shown in Figure 2.5.12a. Although frequency response characteristics are, generally, more easily understood when presented in graphical form, there are other instances when a tabular presentation is more istructive. For instance, it is difficult to observe from Figure 2.5.12a that between 100Hz and 150Hz:

the blade on slot number 2 has the lowest response magnitude.

the blade on slot 9 has the highest response.

the response pattern at each excitation frequency is slightly negatively skewed, and hence non-normal.

These and other features may be readily observed from Table 3.3.1a, which is a statistical summary of the blades' responses at each excitation frequency between 100Hz and 600Hz. The largest modulus of response experienced by any one blade in this frequency range occurs at 155Hz, which is a frequency of primary resonance for the 1EO excitation. It may be further observed that the coefficients of skewness and kurtosis vary considerably from one excitation frequency to another. It is clear that the response patterns are seldom gaussian, since a gaussian distribution has a coefficient of Kurtosis of approximately 3.0, and negligible skewness.

Whereas Table 3.3.1a shows the slot numbers of the two blades with the highest and lowest responses at each frequency, Table 3.3.1b reveals the ranking of the blades according to their response magnitudes, relative to another sequence which is obtained when the blades are ranked according to their cantilever frequencies. Thus, if we arrange the blades in an order of their *cantilever frequencies*, we obtain the sequence in column 3 of the table below. A similar re-arrangement of the blades according to their *response magnitudes* at 100Hz yields the sequence in column 4, while the ordering at 600Hz is given in column 5. The complete set of response rankings for each excitation frequency between 100Hz and 600Hz is given in Table 3.3.1b.

blade c.f. (Hz)	slot no.	c.f. rank	rank @ 100Hz	rank @ 600Hz
246.6	2	10	1	5
243.8	3	9	2	9
241.3	1	8	5	10
240.6	7	7	3	4
240.5	8	6	4	3
240.1	10	5	6	1
239.9	4	4	7	7
239.0	5	3	8	2
238.2	6	2	9	6
236.5	9	1	10	8

A similar presentation of the response characteristics along the lines of Tables 3.3.1a and b for the first engine order is given for the 2EO-5EO in Tables 3.3.2a-3.3.5b.

In the foregoing discussion, the 'normality' of response data was estimated from the coefficients of skewness and kurtosis. Another way of investigating

whether or not the randomness in a set of data is normal is to construct a frequency distribution histogram, which should be approximately bell-shaped for a normal distribution. Thus, the histogram of blade cantilever frequencies on a randomly mistuned wheel like Disc 10A which is shown in Figure 3.3.1a is normal. The histograms of responses at several primary resonances shown in Figures 3.3.1b-c, on the other hand, are mostly non-normal. It follows, therefore, that an inferential procedure which is based on the assumption of normality in a sampled response data may not be used with confidence for predicting the probable bounds on response magnitudes.

An alternative inferential procedure may be developed, based on the correlation between the response level of each blade and its cantilever frequency, as may be observed from Tables 3.3.1-5. One parameter that is of interest to design engineers is the 'worst' stress amplitude a given blade would experience when the wheel is operated through a resonance. For excitation of disc 10A by the 2EO force, the worst stress experienced by any blade between 100Hz and 600Hz may be displayed as shown in Figure 3.3.2a, either as a function of blade's slot position on the wheel, or of the blade's cantilever frequency. A similar presentation for 3EO to 5EO excitations is given in Figures 3.3.2*b-d*. It is evident from the figures that there exists a correlation between the 'worst' stress parameter and the cantilever frequency. On the other hand, no credible correlation exists between the worst stress and blade slot position.

3.3.3 Thirty Bladed Disc

One advantage of using a model having only 10 blades, as we have done above, is the ability to carry out several case studies at a reasonable cost. However, assemblies having only ten blades are not common in practice. By using a model with 30 blades, we can represent a compressor fan more realistically.

A scatter diagram showing the relationship between the blade 1F and slot position for Disc 30M is given in Figure 3.3.3a, with the corresponding distribution histogram in Figure 3.3.3b. Clearly, the scatter in blades' 1F is normal, as the histogram is approximately bell-shaped. When Disc 30M is exposed to the 3EO, with Q=50, the worst response on each blade around the primary resonance may be recorded. There are several ways of gauging the response of a blade. One is by measuring the stress amplitude at the root of each blade, as for Disc 10A. Another is by measuring the tip displacement of each blade using, for instance, equation (2.3.10b). The

response parameter recorded for each blade on Disc 30M is the tip displacement, in order to demonstrate that our deductions here are independent of any chosen measure of dynamic response. The scatter diagrams of the worst displacements, and the distribution histogram, are shown in Figures 3.3.3c-e. As evident from a comparison of Figures 3.3.2 and 3.3.3, much the same conclusions may be drawn for the 30 bladed disc as in the case of Disc 10A.

3.3.4 Thiry-three Bladed Disc

Whereas the preceeding results were of theoretical models, the following set of data have been recorded from a Low-Pressure compressor rotor in an aircraft engine. Each of the thirty-three blades had a strain gauge affixed to its root in order to record the stress amplitudes on *every* blade in the neighbourhood of the 1F/2D resonance. The experiment was specially conducted by researchers in the gas turbine industry, as it is not a routine matter to strain gauge all the blades on a stage during engine tests. The 1F frequencies of every blade blade were also determined, and these are shown in Figure 3.3.4a. By constructing the frequency distribution histogram of blades' 1F as shown in Figure 3.3.4b, we may observe that the randomness in blade frequencies is normal, since the histogram is symmetrically placed about the mean 1F, and approximately bell-shaped. However, if we likewise construct the histogram of response amplitudes, as in Figure 3.3.4c, we are unable to deduce gaussian characteristics.

As before, the stress amplitude of each blade may be plotted as a function of its slot position (Figure 3.3.4d) to obtain a highly scattered picture. On the other hand, if the stress amplitudes are plotted against the blades' 1F, we obtain a correlation between the two parameters. Further details of this and similar experimental results of actual bladed discs as recorded by Rolls-Royce are given by **Afolabi** (1982*c*).

3.4 Concluding Remarks

The statistical properties inherent in blade response amplitudes – such as the measures of dispersion, central tendency, symmetry, and kurtosis – vary considerably from one excitation frequency to another, even for the same bladed disc. It follows, therefore, that knowing the pattern of response at any one excitation does not indicate that a similar pattern would hold at

another frequency. In the main, however, we have observed that the blades with extreme mistune exert a greater influence on the dynamic response charaterisces of bladed discs than any other blades.

At excitation frequencies that are sufficiently far removed from resonance, the response amplitude of each blade is roughly proportional to its cantilever frequency. This relationship may be direct or inverse, depending on whether the excitation frequecy is lower or higher than the dominant resonance.

The cantilever frequencies of blades on most practical assemblies are randomly scattered about a mean value. A construction of the distribution histogram of such assemblies usually revals that the random scatter in blade frequecies is gaussian. However, a similar construction for the blade response amplitudes yields histograms that are generally non-gaussian.

There exits a correlation between the blade response amplitudes and cantilever frequencies. On account of this correlation, and appreciating that blade responses are generally non-gaussian, it does not seem a wise strategy to select the few blades to be stain-gauged during engine tests in a random manner; instead, a purposive sampling technique should be applied, such that the blades with extreme mistune *must* be selected. Additionally, one or two blades with average cantilever frequency may be selected. A regression analysis should subsequently be carried out between the amplitudes and cantilever frequencies. We may then obtain an estimate for the probable maximum stress on any blade on the stage from the limited sample, as shown in Figure 3.4.1a.If we were to carry out only a limited random sampling, however, we are in danger of grossly under estimating the worst stress, as illustrated in Figure 3.4.1b.

Fig. 3.1.1 *Frequency response of a bladed disc showing upper and lower envelopes of blade response*

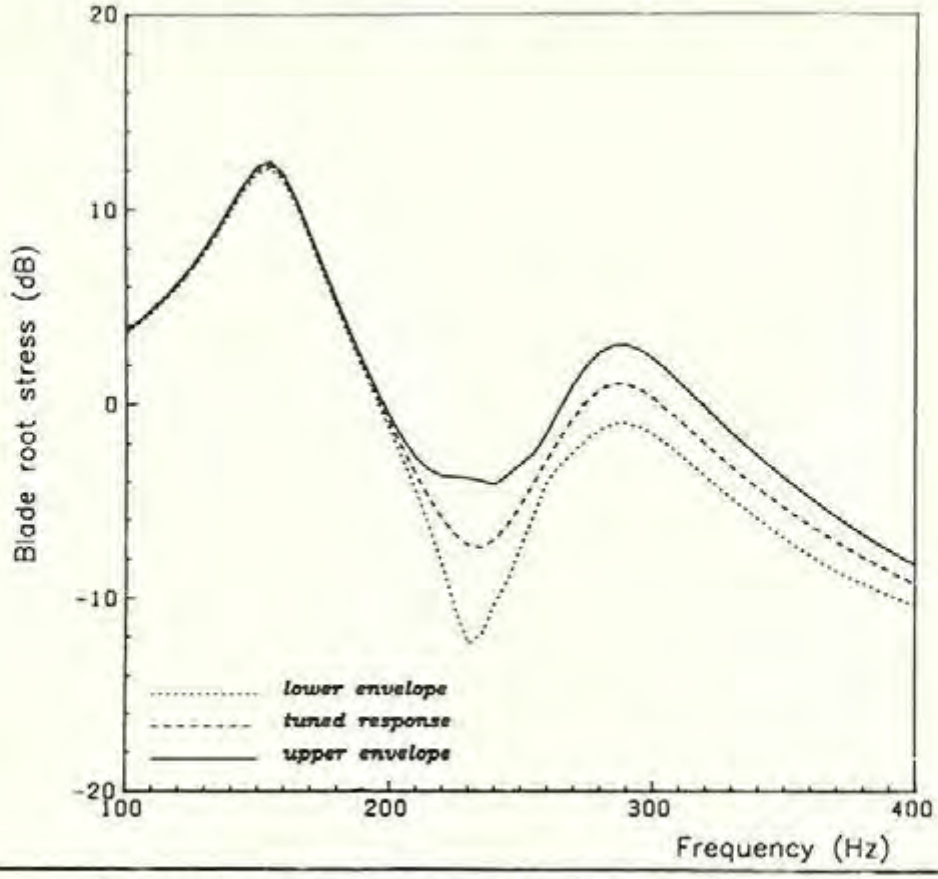

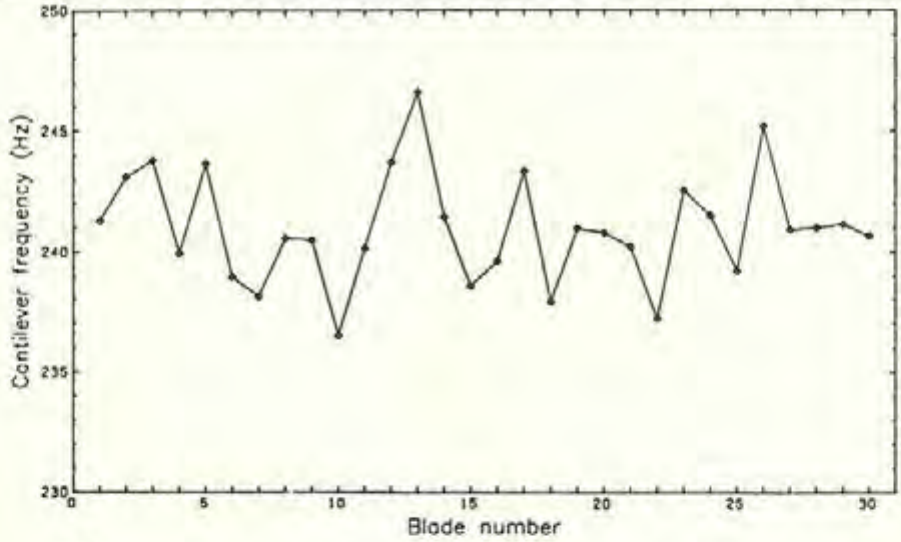

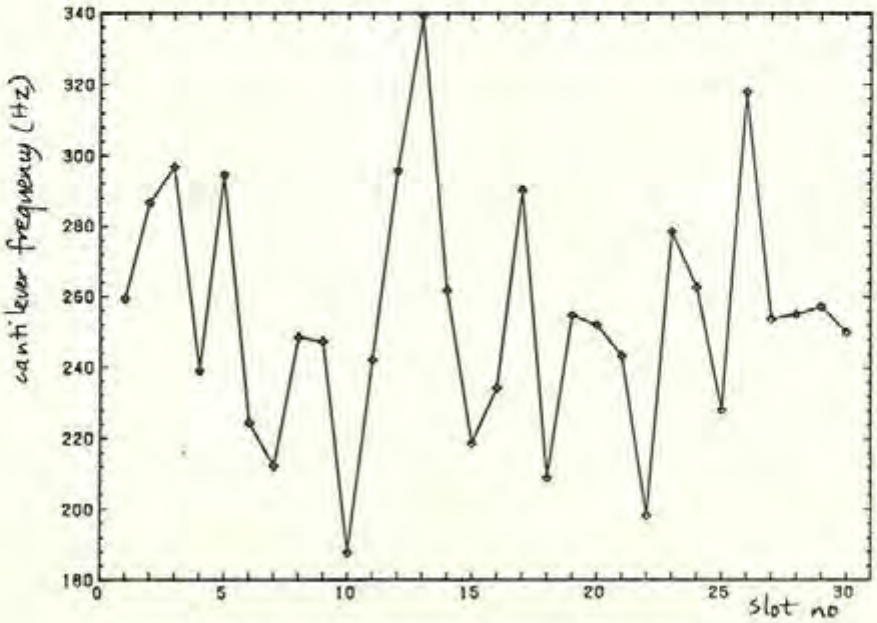

Fig. 3.1.2 *Similar mistune patterns with different scatter*

Fig. 3.3.1 *Frequency distribution histograms of a 10-bladed disc*

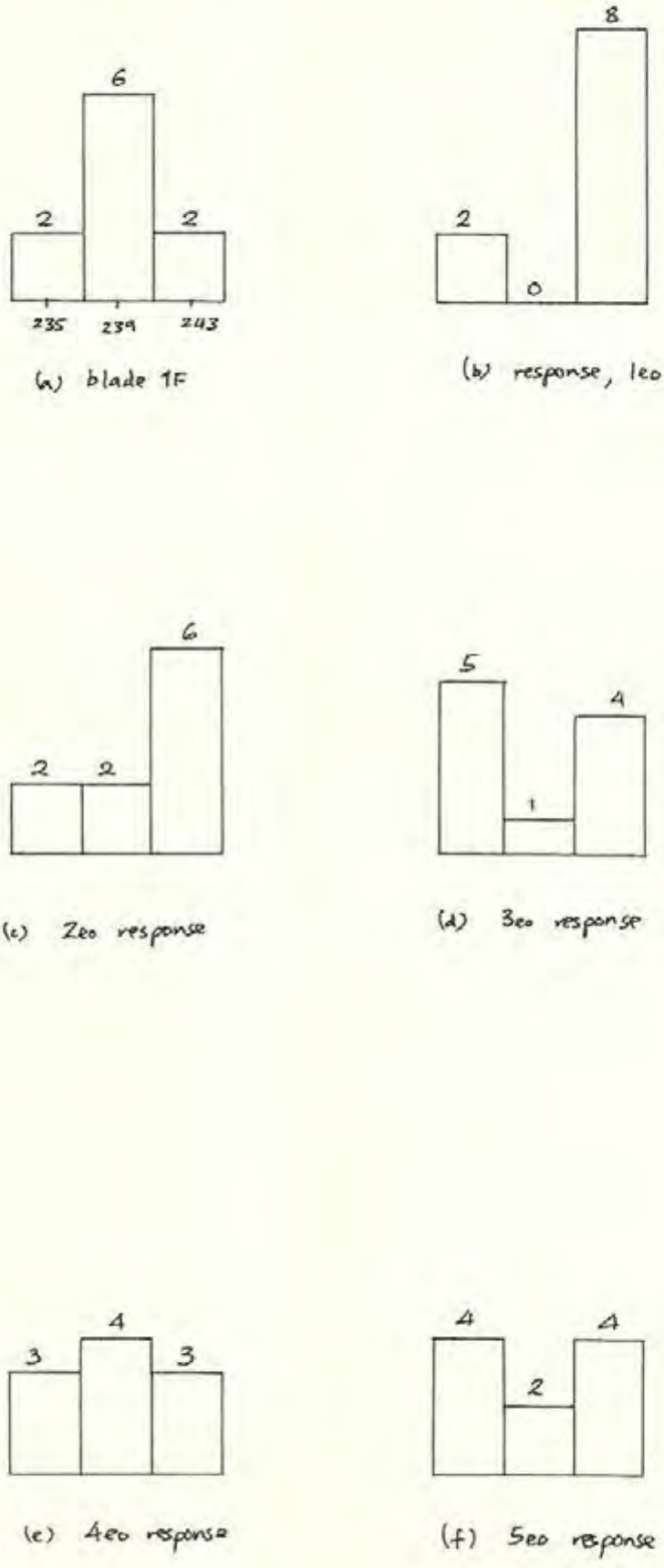

Fig. 3.3.2 *Response of Disc 10A to various EO excitations*

(a) 2EO excitation

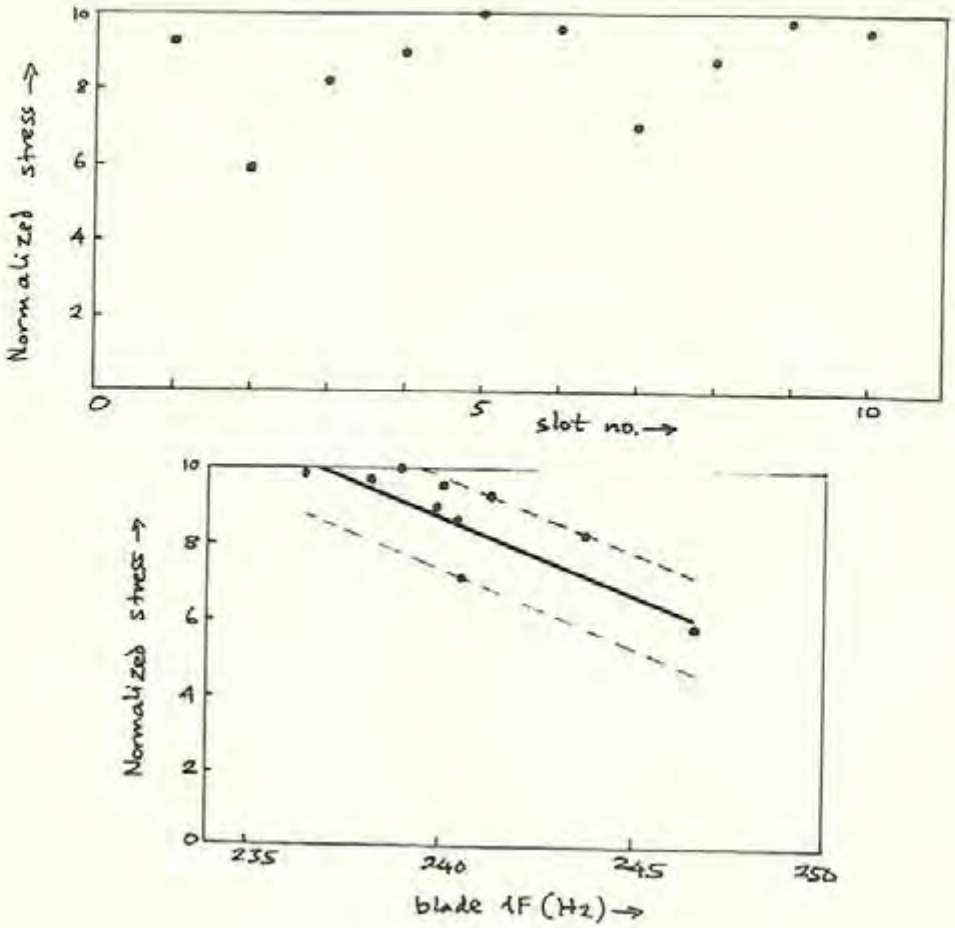

(b) 3eo excitation

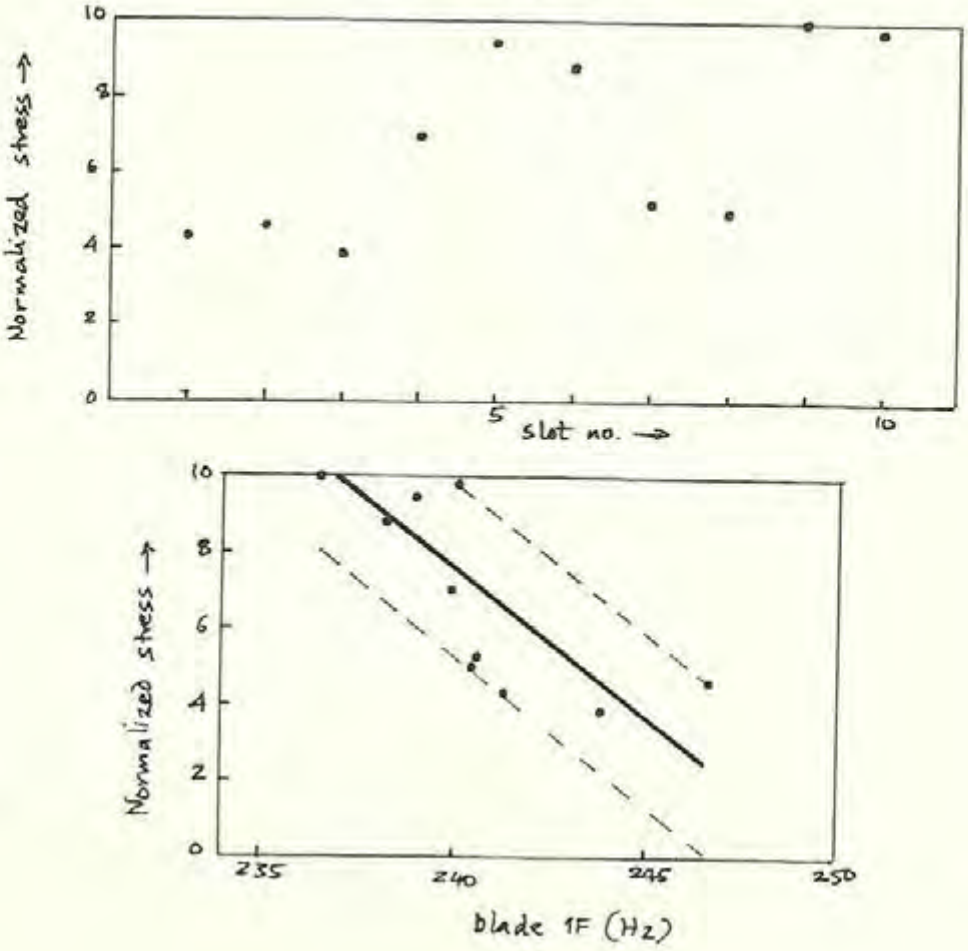

Fig. 3.3.2 *Response of Disc 10A to various EO excitations*

(c) 4EO. excitation

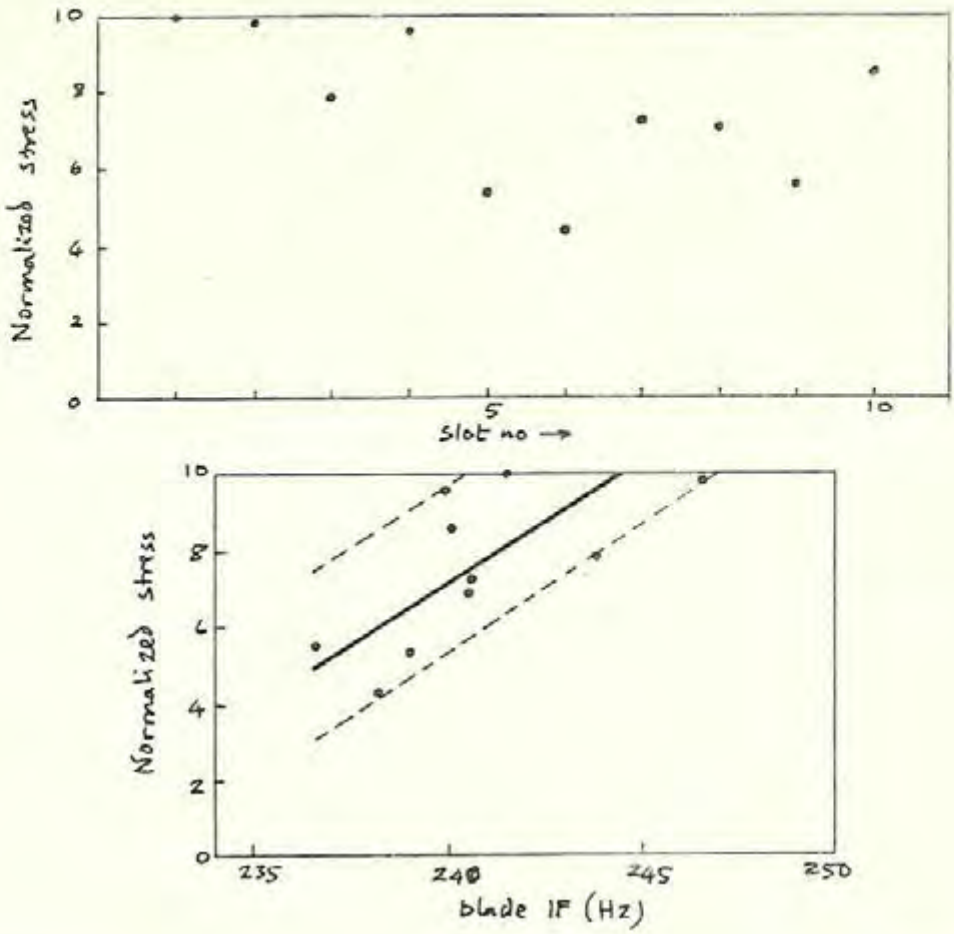

(d) 5EO excitation

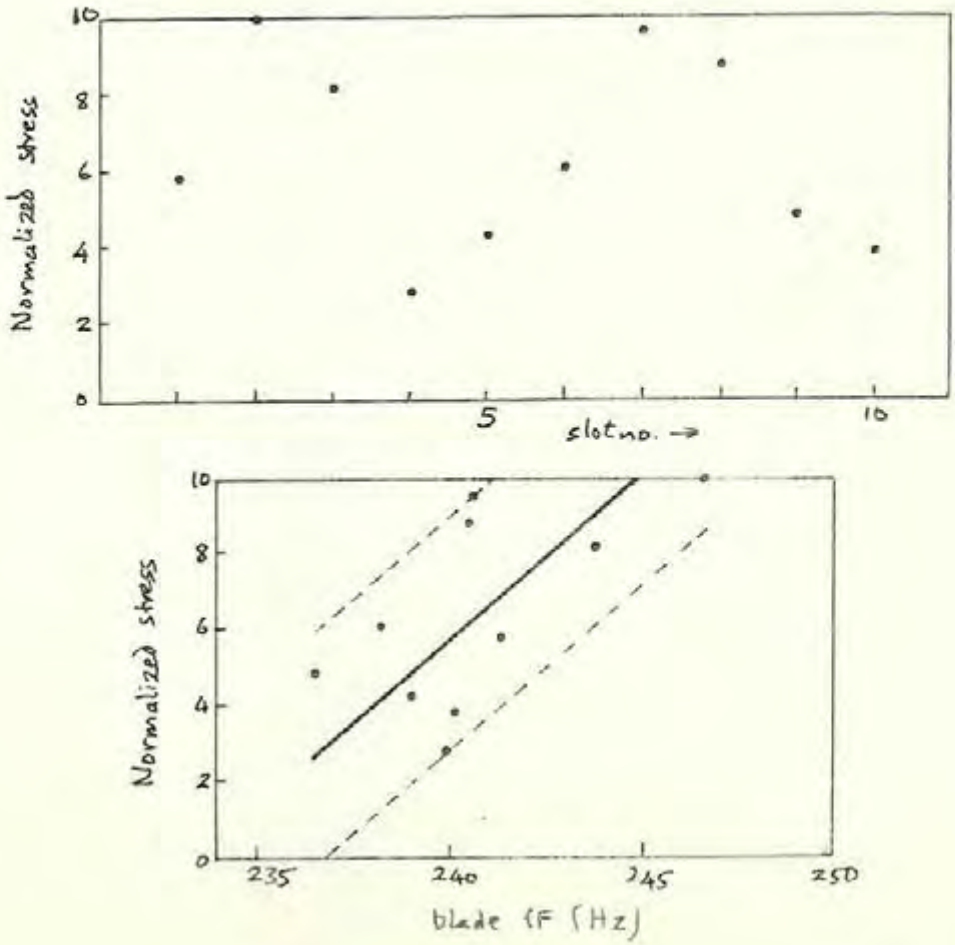

Fig. 3.3.3 *Response of Disc 30M to 3EO excitation*

(a) scatter of 1F vs slot

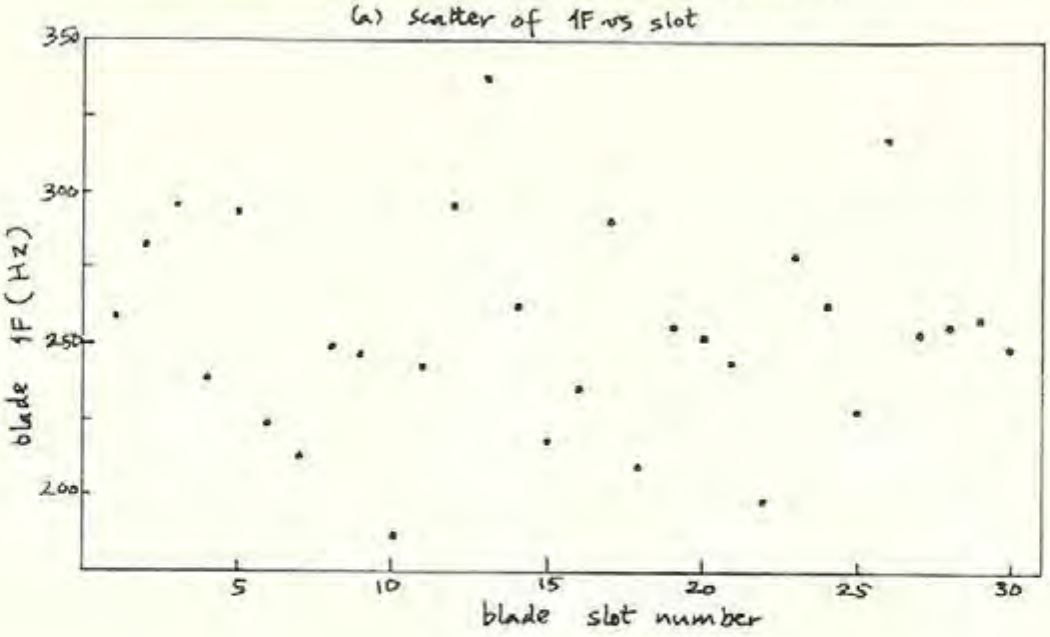

(b) Histogram of 1F distribution

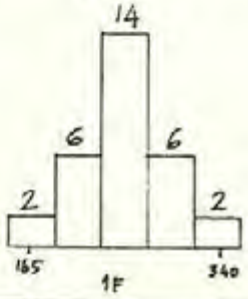

(c) Histogram of response distribution

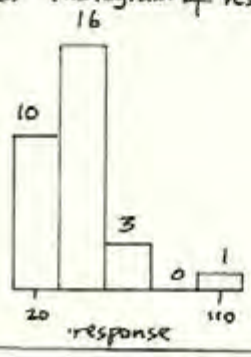

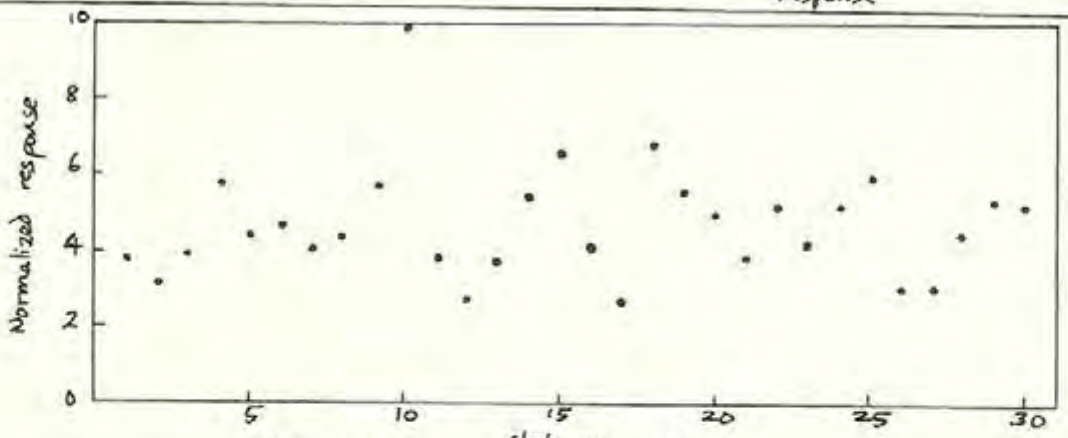

(d) response vs slot number

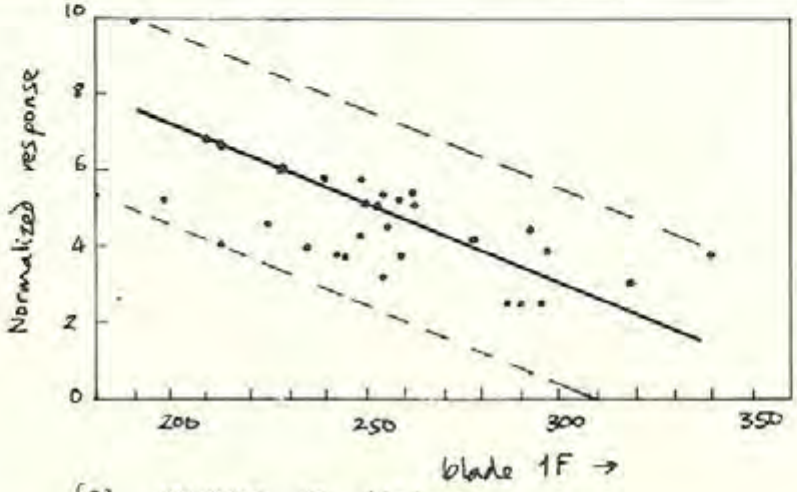

(e) response vs blade 1F

Fig. 3.3.4 *Response of Disc 33R to 2EO excitation*

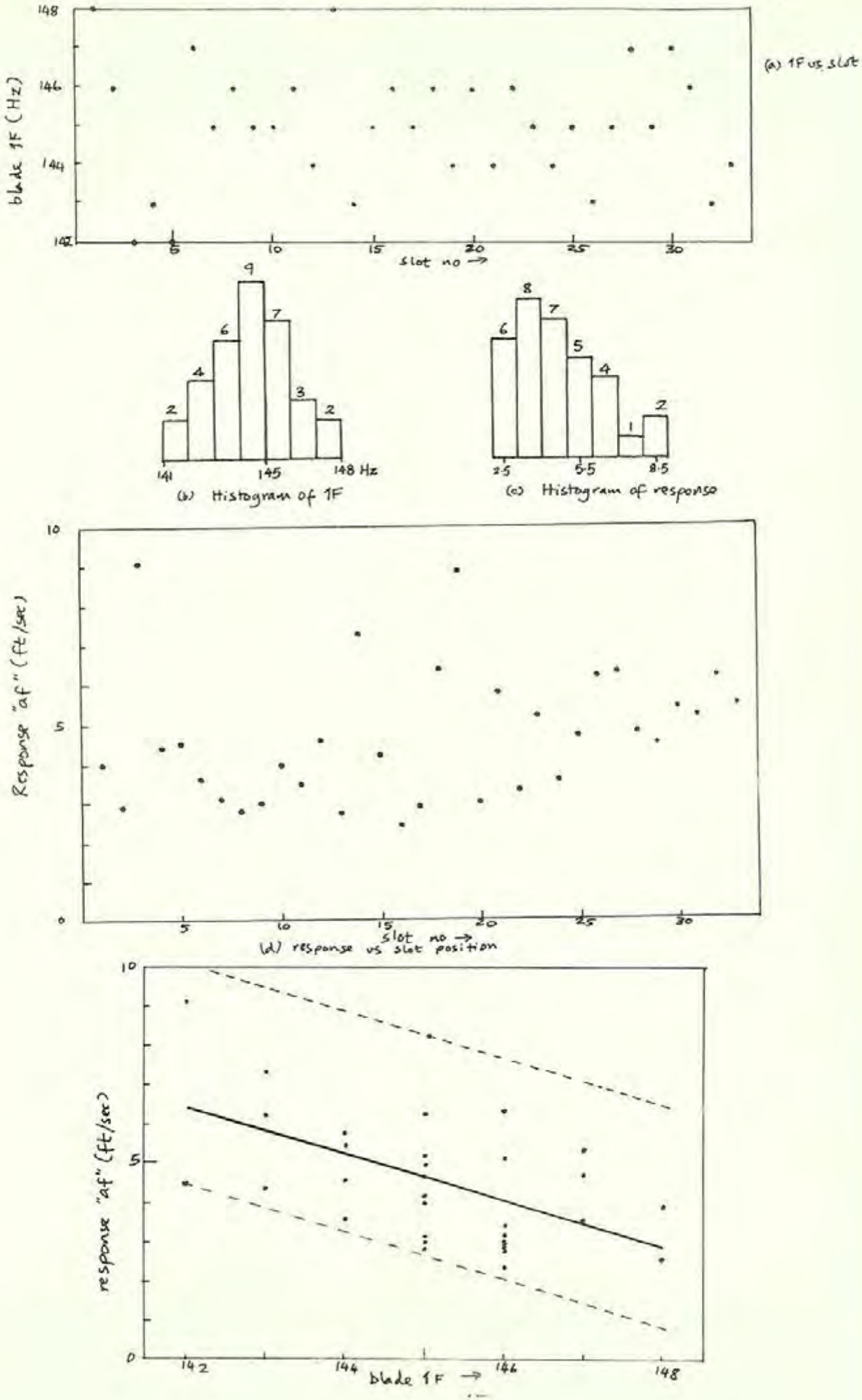

Fig 3.4.1 Purposive sampling vs. random sampling (DISC 33R)

(a) Purposive sampling

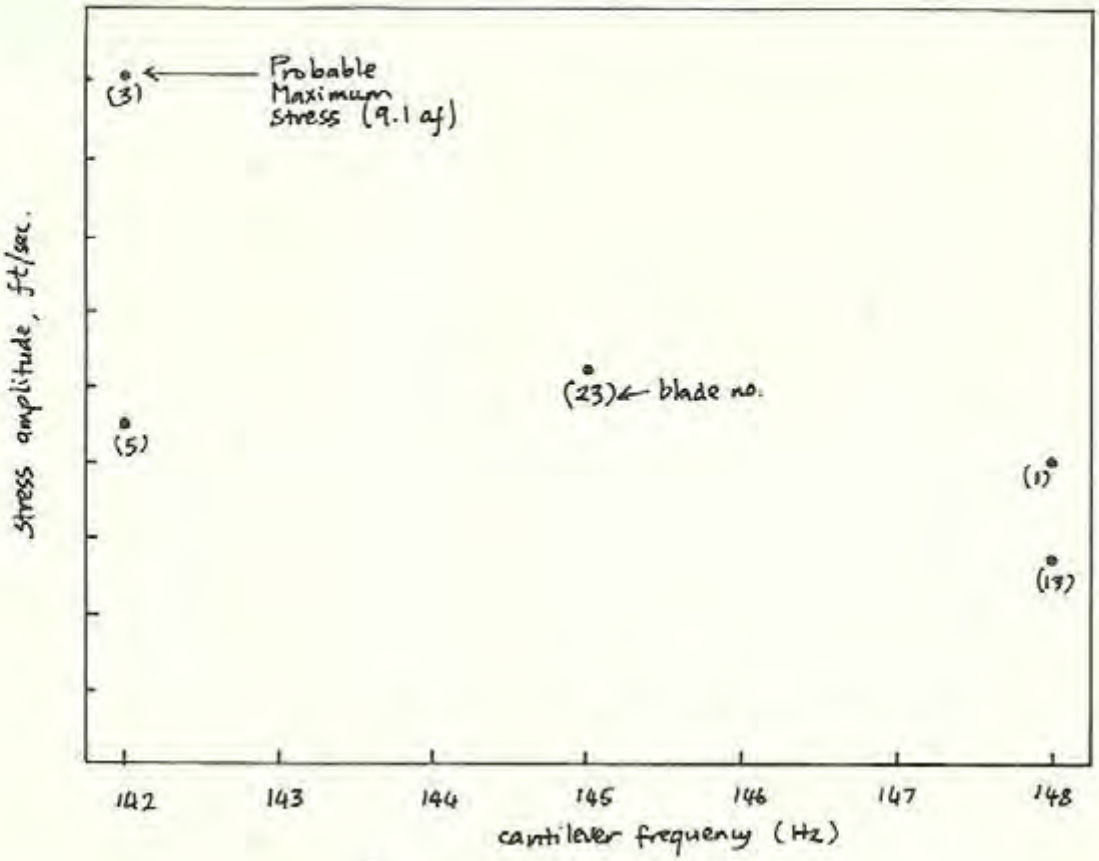

(b) Random sampling

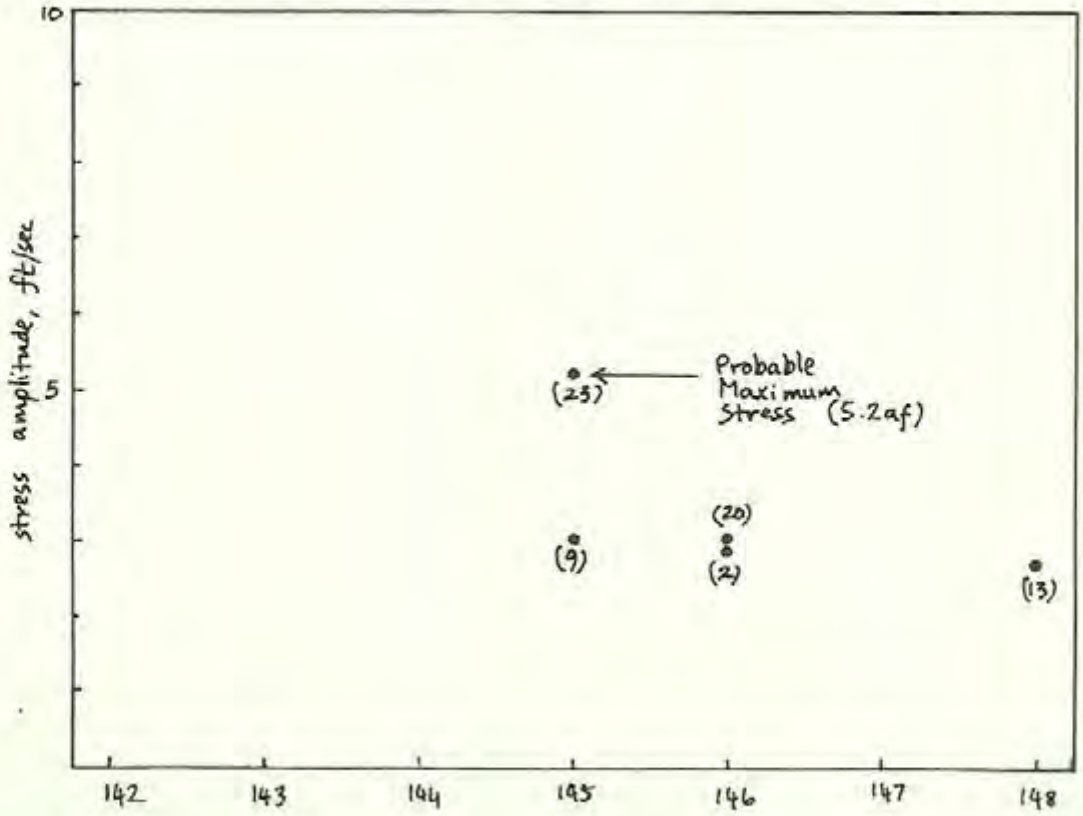

Table 3.3.1a *Response characteristics of Disc 10A to 1EO excitation*

FREQUENCY	MAX RESP	MIN RESP	RATIO	STD	SKEW	KURT	BLR	BMR
100.00	1.6178	1.5938	1.015	.418	-.547	-.344	2	9
105.00	1.7331	1.7043	1.017	.468	-.538	-.374	2	9
110.00	1.8748	1.8402	1.019	.523	-.534	-.409	2	9
115.00	2.0520	2.0107	1.021	.583	-.525	-.453	2	9
120.00	2.2825	2.2307	1.023	.651	-.515	-.508	3	9
125.00	2.5899	2.5246	1.026	.729	-.500	-.581	2	9
130.00	3.0215	2.9366	1.029	.822	-.480	-.678	2	9
135.00	3.6712	3.5553	1.033	.942	-.452	-.807	3	9
140.00	4.7603	4.5873	1.038	1.117	-.404	-.986	2	9
145.00	6.9632	6.6546	1.046	1.436	-.329	-1.228	2	9
150.00	13.7932	12.8850	1.070	2.364	-.200	-1.510	2	9
155.00	721.0162	134.1436	5.375	31.106	-.512	-1.151	10	8
160.00	11.8950	11.3857	1.045	1.383	-.191	-1.219	10	7
165.00	5.7193	5.6051	1.020	.636	.018	-1.236	10	7
170.00	3.6440	3.6034	1.011	.427	.177	-1.675	10	7
175.00	2.6013	2.5809	1.008	.272	.101	-1.435	2	9
180.00	1.9665	1.9630	1.001	.041	-.147	-1.015	2	9
185.00	1.5513	1.5333	1.012	.348	.013	-.870	9	2
190.00	1.2564	1.2137	1.035	.998	.053	-.728	9	2
195.00	1.0363	.9621	1.077	2.085	.056	-.670	9	2
200.00	.8685	.7513	1.156	3.930	.029	-.678	9	2
205.00	.7433	.5614	1.322	7.176	-.030	-.757	9	2
210.00	.6576	.3708	1.773	13.276	-.130	-.951	9	2
215.00	.6424	.1595	4.028	25.719	-.198	-1.417	9	2
220.00	1.8156	.6633	2.737	24.981	.085	-1.665	5	1
225.00	.0608	.0318	16.621	32.407	.001	-1.567	3	8
230.00	2.8111	.4378	6.421	24.824	.449	-.698	5	9
235.00	2.6417	.3125	8.455	27.754	-.276	-1.171	10	4
240.00	2.5220	.1529	16.493	30.994	1.202	.045	6	2
245.00	1.0910	.1230	8.867	25.462	.857	.292	6	2
250.00	.9741	.1153	8.451	24.425	-.187	-.461	9	2
255.00	1.0621	.3909	2.717	19.791	-.284	-.939	9	8
260.00	1.0055	.8086	2.233	20.002	.578	-1.132	2	8
265.00	21.5829	14.4884	1.490	10.037	.114	-1.071	9	2
270.00	4.3726	.7835	5.581	23.398	.086	-1.142	7	2
275.00	6.5199	2.6334	2.457	20.958	-.466	-1.429	7	2
280.00	46.9672	10.8313	4.336	24.245	-.470	-.855	7	10
285.00	14.6627	4.3266	3.389	21.492	1.014	-.059	9	2
290.00	5.4538	2.3079	2.363	16.703	1.079	.232	9	2
295.00	3.3733	1.6508	2.043	14.570	1.042	.251	9	2
300.00	2.4572	1.3113	1.874	13.222	1.000	.229	9	2
305.00	1.9421	1.0999	1.766	12.257	.964	.199	9	2
310.00	1.6119	.9536	1.690	11.530	.933	.167	9	2
315.00	1.3821	.8451	1.635	10.971	.907	.133	9	2
320.00	1.2128	.7607	1.594	10.543	.884	.095	9	2
325.00	1.0831	.6926	1.564	10.227	.863	.051	9	2
330.00	.9807	.6360	1.542	10.016	.842	-.002	9	2
335.00	.8981	.5878	1.528	9.914	.819	-.069	9	2
340.00	.8307	.5459	1.522	9.941	.792	-.160	9	2
345.00	.7757	.5087	1.525	10.144	.756	-.287	9	2
350.00	.7318	.4745	1.542	10.626	.703	-.471	9	2
355.00	.6997	.4416	1.584	11.632	.613	-.740	9	2
360.00	.6860	.4066	1.687	13.878	.454	-1.123	6	3
365.00	.7292	.3216	2.268	20.416	.150	-1.579	7	2
370.00	4.6404	.6634	6.995	27.239	-.302	-1.164	9	5
375.00	.5923	.3369	1.758	14.763	.333	-1.319	1	7
380.00	.4942	.3620	1.367	8.546	.559	-.870	1	7
385.00	.4505	.3605	1.250	6.738	.433	-1.144	1	7
390.00	.4209	.3523	1.195	6.176	.321	-1.457	1	7
395.00	.3990	.3353	1.190	6.015	.291	-1.503	9	2
400.00	.3866	.3201	1.208	5.917	.300	-1.414	9	2
405.00	.3743	.3064	1.221	5.915	.320	-1.297	9	2
410.00	.3623	.2940	1.232	5.966	.340	-1.194	9	2
415.00	.3500	.2824	1.242	6.053	.357	-1.116	9	2
420.00	.3400	.2717	1.252	6.173	.369	-1.061	9	2
425.00	.3299	.2615	1.262	6.326	.377	-1.027	9	2
430.00	.3205	.2518	1.273	6.518	.381	-1.013	9	2
435.00	.3118	.2426	1.285	6.762	.383	-1.015	9	2
440.00	.3040	.2336	1.301	7.073	.383	-1.033	9	2
445.00	.2970	.2248	1.321	7.477	.381	-1.065	9	2
450.00	.2911	.2160	1.348	8.017	.377	-1.112	9	2
455.00	.2866	.2069	1.385	8.762	.373	-1.172	9	2
460.00	.2842	.1971	1.442	9.847	.371	-1.245	9	2
465.00	.2856	.1858	1.537	11.543	.373	-1.330	9	2
470.00	.2958	.1714	1.726	14.491	.390	-1.425	9	2
475.00	.3407	.1592	2.141	20.153	.472	-1.520	9	2
480.00	2.5504	.5139	4.962	32.175	-.064	-1.705	8	9
485.00	.3001	.1085	2.767	22.216	-.321	-1.428	7	4
490.00	.2422	.1523	1.590	11.976	-.355	-1.277	7	4
495.00	.2210	.1640	1.348	7.741	-.407	-.915	7	4
500.00	.2086	.1675	1.246	5.603	-.460	-.408	7	4
505.00	.1997	.1677	1.191	4.467	-.470	-.070	7	4
510.00	.1927	.1664	1.158	3.917	-.395	-.218	7	4
515.00	.1871	.1642	1.139	3.743	-.251	-.724	7	10
520.00	.1830	.1615	1.133	3.826	-.101	-1.186	7	10
525.00	.1794	.1584	1.132	4.128	.007	-1.446	7	10
530.00	.1774	.1549	1.145	4.632	.065	-1.549	7	2
535.00	.1761	.1501	1.174	5.458	.081	-1.614	9	2
540.00	.1761	.1432	1.230	6.918	.068	-1.699	9	2
545.00	.1794	.1328	1.351	10.110	.036	-1.826	9	2
550.00	.2039	.0984	2.073	22.511	.002	-1.968	9	8
555.00	.2239	.0753	2.974	24.960	-.010	-1.709	8	3
560.00	.1702	.1234	1.378	10.394	-.083	-1.587	6	3
565.00	.1618	.1228	1.317	8.396	-.164	-1.407	6	5
570.00	.1650	.1155	1.429	10.468	-.150	-1.601	6	5
575.00	.2002	.0871	2.299	21.970	-.176	-1.761	6	5
580.00	.2017	.0756	2.668	22.714	-.247	-1.528	10	1
585.00	.1557	.1117	1.393	9.566	-.106	-1.459	10	1
590.00	.1448	.1177	1.230	6.076	-.069	-1.331	10	1
595.00	.1387	.1191	1.165	4.507	-.039	-1.252	10	1
600.00	.1344	.1189	1.130	3.634	-.005	-1.186	10	1

Table 3.3.2a *Response characteristics of Disc 10A to 2EO excitation*

FREQUENCY	MAX RESP	MIN RESP	RATIO	STD	SKEW	KURT	BLK	BRK
100.00	1.2571	1.2381	1.015	.447	-.394	-.439	2	9
105.00	1.2933	1.2714	1.017	.502	-.387	-.471	2	9
110.00	1.3334	1.3081	1.019	.574	-.579	.509	2	9
115.00	1.3777	1.3485	1.022	.649	-.569	-.533	2	9
120.00	1.4260	1.3931	1.024	.735	-.555	-.607	2	9
125.00	1.4822	1.4424	1.028	.831	-.532	-.673	2	6
130.00	1.5445	1.4972	1.032	.942	-.499	-.754	2	6
135.00	1.6147	1.5583	1.036	1.068	-.447	-.852	2	6
140.00	1.6940	1.6270	1.041	1.207	-.362	-.966	2	6
145.00	1.7834	1.7053	1.046	1.346	-.229	-1.093	2	6
150.00	1.8826	1.7968	1.048	1.448	-.040	-1.217	2	6
155.00	1.9903	1.9050	1.045	1.460	.150	-1.336	2	6
160.00	2.1106	2.0300	1.040	1.372	.187	-1.470	2	5
165.00	2.2466	2.1697	1.035	1.272	-.003	-1.605	2	5
170.00	2.4063	2.3263	1.034	1.247	-.240	-1.633	2	4
175.00	2.6022	2.5051	1.039	1.309	-.352	-1.472	2	9
180.00	2.8397	2.7126	1.047	1.435	.368	-1.223	2	9
185.00	3.1195	2.9555	1.055	1.606	-.352	1.011	2	9
190.00	3.4500	3.2409	1.065	1.810	-.334	-.877	2	9
195.00	3.8396	3.5754	1.074	2.041	-.319	-.820	2	9
200.00	4.2922	3.9621	1.083	2.295	-.306	.037	2	9
205.00	4.7986	4.3944	1.092	2.563	-.289	-.920	2	9
210.00	5.3205	4.8439	1.099	2.836	-.254	-1.104	2	9
215.00	5.7720	5.2481	1.100	3.098	-.169	-1.349	2	9
220.00	6.0747	5.5146	1.102	3.314	.013	-1.528	3	10
225.00	6.1518	5.5643	1.106	3.466	.293	-1.366	3	10
230.00	5.9254	5.2761	1.123	3.578	.565	-.846	4	10
235.00	5.4772	4.8406	1.130	3.624	.705	-.510	4	10
240.00	4.9295	4.3901	1.123	3.561	.717	-.717	4	10
245.00	4.3824	3.9580	1.107	3.373	.699	-1.135	4	10
250.00	3.8893	3.5742	1.088	3.095	.698	-1.299	4	10
255.00	3.4895	3.2138	1.086	2.786	.680	-1.097	6	2
260.00	3.1651	2.9076	1.089	2.531	.613	-.714	6	2
265.00	2.8807	2.6540	1.088	2.382	.540	-.414	6	2
270.00	2.6554	2.4437	1.087	2.313	.523	-.298	6	2
275.00	2.4583	2.2683	1.084	2.280	.558	-.277	6	2
280.00	2.2907	2.1167	1.082	2.246	.609	-.249	9	2
285.00	2.1471	1.9851	1.082	2.195	.663	-.183	9	2
290.00	2.0231	1.8738	1.080	2.118	.712	-.093	9	2
295.00	1.9153	1.7796	1.076	2.016	.753	-.009	9	2
300.00	1.8212	1.6995	1.072	1.889	.782	.063	9	2
305.00	1.7389	1.6313	1.066	1.744	.799	.112	9	2
310.00	1.6671	1.5732	1.060	1.587	.804	.138	9	2
315.00	1.6044	1.5235	1.053	1.424	.798	.133	9	2
320.00	1.5496	1.4811	1.046	1.259	.778	.085	9	2
325.00	1.5015	1.4445	1.039	1.095	.739	-.037	9	2
330.00	1.4586	1.4127	1.032	.939	.673	-.276	9	2
335.00	1.4194	1.3840	1.026	.798	.570	-.673	9	2
340.00	1.3818	1.3534	1.021	.686	.441	-1.093	4	2
345.00	1.3476	1.3264	1.021	.623	.365	-.999	4	10
350.00	1.3130	1.2832	1.023	.630	.381	-.326	4	10
355.00	1.2712	1.2385	1.026	.711	.366	-.092	4	10
360.00	1.2184	1.1827	1.030	.850	.279	-.341	4	10
365.00	1.1521	1.1124	1.036	1.026	.177	-.614	3	10
370.00	1.0713	1.0272	1.043	1.228	.097	-.779	3	10
375.00	.9781	.9305	1.051	1.450	.040	-.854	3	10
380.00	.8771	.8272	1.060	1.686	-.003	-.869	3	10
385.00	.7740	.7232	1.070	1.936	-.038	-.843	3	10
390.00	.6746	.6240	1.081	2.198	-.067	-.794	3	10
395.00	.5828	.5334	1.093	2.471	-.092	-.740	3	10
400.00	.5010	.4536	1.104	2.753	-.111	-.713	3	10
405.00	.4299	.3850	1.117	3.049	-.119	-.754	3	10
410.00	.3692	.3273	1.128	3.367	-.107	-.906	3	10
415.00	.3180	.2795	1.138	3.726	-.052	-1.178	3	10
420.00	.2754	.2406	1.145	4.165	.078	-1.477	3	10
425.00	.2402	.2095	1.147	4.722	.296	-1.587	3	10
430.00	.2162	.1851	1.168	5.317	.576	-1.332	3	2
435.00	.1980	.1628	1.216	6.018	.850	-.779	5	2
440.00	.1839	.1444	1.274	6.806	1.055	-.180	5	2
445.00	.1732	.1304	1.329	7.628	1.167	.258	5	2
450.00	.1650	.1200	1.374	8.424	1.193	.406	5	2
455.00	.1586	.1090	1.454	9.138	1.149	.553	9	2
460.00	.1534	.0999	1.537	9.735	1.053	.531	9	2
465.00	.1491	.0928	1.608	10.194	.920	.472	9	2
470.00	.1454	.0875	1.661	10.507	.764	.400	9	2
475.00	.1419	.0839	1.692	10.678	.608	.316	9	2
480.00	.1386	.0817	1.697	10.715	.441	.210	9	2
485.00	.1354	.0807	1.678	10.638	.299	.070	9	2
490.00	.1324	.0806	1.642	10.471	.184	-.108	9	2
495.00	.1296	.0812	1.595	10.244	.099	-.315	9	2
500.00	.1270	.0822	1.544	9.985	.045	-.537	9	2
505.00	.1246	.0835	1.493	9.718	.023	-.758	9	2
510.00	.1224	.0847	1.445	9.458	.026	-.966	9	2
515.00	.1204	.0860	1.401	9.215	.049	-1.151	9	2
520.00	.1186	.0871	1.361	8.989	.086	-1.304	9	2
525.00	.1172	.0882	1.329	8.742	.134	-1.421	9	3
530.00	.1167	.0891	1.309	8.444	.188	-1.495	9	3
535.00	.1161	.0900	1.290	8.148	.247	-1.524	9	3
540.00	.1155	.0906	1.274	7.847	.309	-1.507	10	3
545.00	.1147	.0906	1.266	7.534	.374	-1.448	10	3
550.00	.1137	.0906	1.256	7.205	.440	-1.356	10	3
555.00	.1127	.0905	1.244	6.860	.506	-1.243	10	3
560.00	.1114	.0905	1.231	6.499	.568	-1.123	10	3
565.00	.1101	.0904	1.217	6.129	.625	-1.010	10	3
570.00	.1086	.0903	1.203	5.755	.675	-.912	10	3
575.00	.1071	.0901	1.188	5.383	.716	-.832	10	3
580.00	.1055	.0898	1.175	5.022	.749	-.768	6	3
585.00	.1039	.0894	1.162	4.677	.774	-.716	6	3
590.00	.1024	.0890	1.151	4.351	.794	-.672	6	3
595.00	.1009	.0885	1.140	4.051	.811	-.632	6	3
600.00	.0994	.0880	1.130	3.776	.824	.595	6	3

Table 3.3.3a *Response characteristics of Disc 10A to 3EO excitation*

FREQUENCY	MAX DISP	MIN DISP	RATIO	SIG	[illegible]	[illegible]	[illegible]	[illegible]
100.00	1.2944	1.2523	1.033	.367	-.[illegible]	-.[illegible]	?	?
105.00	1.2589	1.2249	1.031	.368	-.[illegible]	-.247	?	?
110.00	1.2274	1.2001	1.024	.345	-.[illegible]	-.[illegible]	?	?
115.00	1.2296	1.2430	1.027	.731	-.[illegible]	.021	?	?
120.00	1.3708	1.3240	1.031	.928	-.[illegible]	.086	?	?
125.00	1.4178	1.3882	1.035	.931	-.[illegible]	.127	?	?
130.00	1.4496	1.4111	1.041	1.084	-.[illegible]	.202	?	?
135.00	1.4774	1.4579	1.048	1.308	-.7[illegible]	.280	?	?
140.00	1.5219	1.5095	1.055	1.396	-.723	.353	?	?
145.00	1.5530	1.5072	1.061	1.531	-.724	.330	?	?
150.00	1.7400	1.6346	1.064	1.657	-.671	.11[illegible]	?	?
155.00	1.8313	1.7163	1.064	1.5[illegible]	-.307	-.242	?	?
160.00	1.8703	1.8132	1.059	1.929	-.338	-.555	?	?
165.00	1.9248	1.9211	1.054	1.952	-.479	-.429	?	?
170.00	2.1403	2.0384	1.050	1.587	-.[illegible]	-1.225	?	?
175.00	2.3337	2.1678	1.055	1.087	-.256	-1.[illegible]	?	?
180.00	2.4519	2.3137	1.059	1.355	-.2[illegible]	-1.334	?	?
185.00	2.6452	2.4507	1.066	2.039	-.271	-1.574	?	?
190.00	2.8717	2.6738	1.074	2.346	-.[illegible]	-1.559	?	?
195.00	3.1365	2.8904	1.082	2.523	-.2[illegible]	-1.394	?	?
200.00	3.4453	3.1649	1.090	2.499	-.221	-1.361	?	?
205.00	3.8326	3.4794	1.099	3.132	-.102	-1.377	?	?
210.00	4.2595	3.8531	1.103	3.273	-.071	-1.396	?	?
215.00	4.7177	4.2635	1.105	3.266	.064	-1.373	?	?
220.00	5.1703	4.6713	1.107	3.112	-.27	-1.1[illegible]	?	?
225.00	5.5535	5.0359	1.104	3.301	-.213	-.402	?	?
230.00	5.7383	5.2552	1.090	3.207	-.[illegible]	-.[illegible]	?	?
235.00	5.8578	5.2266	1.121	3.311	-.2[illegible]	-1.347	?	?
240.00	5.7720	5.0230	1.149	3.306	.[illegible]	-1.[illegible]	?	?
245.00	5.4556	4.6785	1.166	3.760	.[illegible]	-.9[illegible]	?	?
250.00	5.0707	4.2249	1.182	3.394	.[illegible]	-.557	?	?
255.00	4.5533	3.7900	1.1[illegible]	3.790	.[illegible]	-.34[illegible]	?	?
260.00	4.0257	3.3573	1.165	3.557	.272	-.273	?	?
265.00	3.5709	3.0573	1.178	3.481	.[illegible]	-.29[illegible]	?	?
270.00	3.2334	2.7061	1.194	3.313	.7[illegible]	-.37[illegible]	?	?
275.00	3.0224	2.5171	1.161	3.172	.7[illegible]	-.3[illegible]	?	?
280.00	2.5511	2.3033	1.155	3.069	.7[illegible]	-.327	?	?
285.00	2.4608	2.1204	1.15[illegible]	3.447	.72[illegible]	-.3[illegible]	?	?
290.00	2.2534	1.9622	1.149	3.928	.7[illegible]	-.304	?	?
295.00	2.0324	1.8254	1.14[illegible]	3.651	.727	-.449	?	?
300.00	1.8520	1.7069	1.144	3.775	.77[illegible]	-.384	?	?
305.00	1.8285	1.6028	1.141	3.590	.7[illegible]	-.330	?	?
310.00	1.7194	1.5113	1.137	3.397	.821	-.2[illegible]	?	?
315.00	1.6324	1.4335	1.138	3.903	.821	-.250	?	?
320.00	1.5365	1.3604	1.12[illegible]	3.411	.8[illegible]	-.3[illegible]	?	?
325.00	1.4506	1.2972	1.12[illegible]	3.323	.829	-.4[illegible]	?	?
330.00	1.3911	1.2409	1.121	3.238	.829	-.2[illegible]	?	?
335.00	1.3235	1.1935	1.117	3.195	.7[illegible]	-.27[illegible]	?	?
340.00	1.2740	1.1436	1.112	3.073	.7[illegible]	-.33[illegible]	?	?
345.00	1.2340	1.1055	1.107	2.947	.6[illegible]	-.3[illegible]	?	?
350.00	1.1737	1.0496	1.102	2.905	.797	-.2[illegible]	?	?
355.00	1.1375	1.0362	1.098	2.812	.77[illegible]	-.4[illegible]	?	?
360.00	1.0930	1.0052	1.094	2.709	.7[illegible]	-.48[illegible]	?	?
365.00	1.0454	.9775	1.090	2.289	.7[illegible]	-.5[illegible]	?	?
370.00	1.0344	.9529	1.085	2.930	.677	-.5[illegible]	?	?
375.00	1.0241	.9313	1.08[illegible]	2.305	.5[illegible]	-.[illegible]	?	?
380.00	.9994	.9123	1.07[illegible]	2.122	.5[illegible]	-.7[illegible]	?	?
385.00	.9570	.8956	1.070	2.014	.574	-.5[illegible]	?	?
390.00	.9333	.8810	1.06[illegible]	1.870	.[illegible]	-.[illegible]	?	?
395.00	.9204	.8684	1.06[illegible]	1.790	.[illegible]	-.[illegible]	?	?
400.00	.9158	.8574	1.05[illegible]	1.447	.5[illegible]	-.[illegible]77	?	?
405.00	.9020	.8481	1.05[illegible]	1.049	.[illegible]	-.[illegible]	?	?
410.00	.8919	.8403	1.04[illegible]	1.482	.5[illegible]	-.[illegible]	?	?
415.00	.8797	.8339	1.047	1.3[illegible]	.5[illegible]	-.[illegible]	?	?
420.00	.8550	.8286	1.04[illegible]	1.31[illegible]	.574	-.[illegible]	?	?
425.00	.8[illegible]	.8244	1.04[illegible]	1.2[illegible]	.5[illegible]	-.[illegible]	?	?
430.00	.8[illegible]	.8210	1.03[illegible]	1.1[illegible]	.[illegible]	-.[illegible]	?	?
435.00	.8592	.8180	1.037	1.124	.574	-.3[illegible]	?	?
440.00	.8636	.8151	1.033	1.072	.5[illegible]	-.755	?	?
445.00	.8593	.8115	1.033	1.027	.[illegible]	-.631	?	?
450.00	.8317	.8066	1.031	.969	.[illegible]	-.4[illegible]	?	?
455.00	.8090	.7990	1.030	.967	.5[illegible]	-1.07[illegible]	?	?
460.00	.8105	.7872	1.029	.9[illegible]	.475	-1.[illegible]	?	?
465.00	.7930	.7720	1.028	.9[illegible]	.4[illegible]	-1.3[illegible]	?	?
470.00	.7717	.7507	1.027	.9[illegible]	.4[illegible]	-1.[illegible]	?	?
475.00	.7459	.7266	1.031	1.012	.4[illegible]	-1.[illegible]	?	?
480.00	.7134	.6962	1.034	1.072	.4[illegible]	-1.[illegible]	?	?
485.00	.6741	.6494	1.03[illegible]	1.1[illegible]	.4[illegible]	-1.[illegible]24	?	?
490.00	.6304	.6050	1.04[illegible]	1.2[illegible]	.4[illegible]	-.4[illegible]	?	?
495.00	.5840	.5570	1.047	1.377	.4[illegible]	-.[illegible]	?	?
500.00	.5358	.5040	1.053	1.910	.4[illegible]	-.[illegible]	?	?
505.00	.4870	.4639	1.05[illegible]	1.9[illegible]	.4[illegible]	-.[illegible]	?	?
510.00	.4414	.4148	1.06[illegible]	1.[illegible]	.4[illegible]	-.[illegible]	?	?
515.00	.3979	.3714	1.071	2.367	.[illegible]	-.5[illegible]	?	?
520.00	.3574	.3315	1.07[illegible]	2.2[illegible]	.5[illegible]	-.[illegible]	?	?
525.00	.3272	.2953	1.0[illegible]	2.231	.5[illegible]	-.4[illegible]	?	?
530.00	.3075	.2627	1.049	2.751	.6[illegible]	-.4[illegible]	?	?
535.00	.2939	.2336	1.10[illegible]	3.343	.6[illegible]	-.4[illegible]	?	?
540.00	.2921	.2079	1.110	3.316	.6[illegible]	-.4[illegible]	?	?
545.00	.2937	.1852	1.127	3.598	.5[illegible]	-1.613	?	?
550.00	.1977	.1653	1.13[illegible]	3.3[illegible]	.5[illegible]	-1.4[illegible]	?	?
555.00	.1488	.1479	1.143	4.142	.6[illegible]	-1.07[illegible]	?	?
560.00	.1520	.1326	1.146	4.3[illegible]	.[illegible]7	-1.[illegible]	?	?
565.00	.1349	.1185	1.154	4.342	.1[illegible]	-1.1[illegible]	?	?
570.00	.1247	.1055	1.179	5.159	.6[illegible]	-1.2[illegible]	?	?
575.00	.1134	.0942	1.204	5.495	.5[illegible]	-1.[illegible]	?	?
580.00	.1037	.0845	1.226	5.793	.5[illegible]	-1.[illegible]	?	?
585.00	.0951	.0765	1.244	6.1[illegible]	.5[illegible]	-1.[illegible]	?	?
590.00	.0875	.0697	1.255	6.4[illegible]	.[illegible]	-.[illegible]	?	?
595.00	.0807	.0641	1.259	6.7[illegible]	.4[illegible]	-.[illegible]	?	?
600.00	.0755	.0[illegible]	1.2[illegible]	7.1[illegible]	.4[illegible]	-.[illegible]	?	?

Table 3.3.4a *Response characteristics of Disc 10A to 4EO excitation*

FREQUENCY	MAX RESP	MIN RESP	RATIO	STD	SKEW	KURT	[illegible]	[illegible]
100.00	1.2138	1.1937	1.017	.467	-.607	-.257	?	?
105.00	1.2436	1.2203	1.019	.526	-.593	-.253	?	?
110.00	1.2763	1.2494	1.022	.590	-.579	-.247	?	?
115.00	1.3123	1.2812	1.024	.661	-.562	-.243	?	?
120.00	1.3519	1.3160	1.027	.738	-.542	-.239	?	?
125.00	1.3956	1.3542	1.031	.823	-.518	-.236	?	?
130.00	1.4440	1.3962	1.034	.917	-.490	-.239	?	?
135.00	1.4976	1.4425	1.038	1.019	-.454	-.257	?	?
140.00	1.5571	1.4938	1.042	1.128	-.416	-.300	?	?
145.00	1.6230	1.5510	1.046	1.242	-.387	-.398	?	?
150.00	1.6954	1.6156	1.049	1.359	-.397	-.589	?	?
155.00	1.7748	1.6885	1.051	1.491	-.467	-.855	?	?
160.00	1.8635	1.7696	1.053	1.657	-.546	-1.049	?	?
165.00	1.9653	1.8589	1.057	1.846	-.588	-1.114	?	?
170.00	2.0832	1.9582	1.064	2.047	-.603	-1.112	?	?
175.00	2.2197	2.0700	1.072	2.263	-.602	-1.085	?	?
180.00	2.3779	2.1973	1.082	2.500	-.589	-1.056	?	?
185.00	2.5619	2.3432	1.093	2.760	-.567	-1.034	?	?
190.00	2.7768	2.5119	1.105	3.043	-.536	-1.022	?	?
195.00	3.0287	2.7083	1.118	3.339	-.495	-1.024	?	?
200.00	3.3239	2.9390	1.131	3.633	-.446	-1.040	?	?
205.00	3.6666	3.2125	1.141	3.889	-.394	-1.075	?	?
210.00	4.0545	3.5389	1.146	4.046	-.354	-1.133	?	?
215.00	4.4703	3.9271	1.138	4.004	-.348	-1.226	?	?
220.00	4.8730	4.3730	1.114	3.643	-.376	-1.357	1	?
225.00	5.2393	4.8087	1.090	2.860	-.256	-1.355	1	7
230.00	5.5866	5.2065	1.073	1.870	.959	.709	3	7
235.00	5.7044	5.3467	1.067	1.955	.954	-.423	0	7
240.00	5.7250	5.1171	1.119	3.211	.490	-.916	0	?
245.00	5.5479	4.7402	1.170	4.397	.581	-.815	0	?
250.00	5.1671	4.2962	1.203	5.177	.631	-.861	0	?
255.00	4.6901	3.8507	1.218	5.574	.644	-.921	0	?
260.00	4.2057	3.4408	1.222	5.707	.641	-.956	0	?
265.00	3.7606	3.0807	1.221	5.684	.632	-.956	0	?
270.00	3.3728	2.7719	1.217	5.576	.626	-.922	0	?
275.00	3.0417	2.5096	1.212	5.425	.627	-.862	0	?
280.00	2.7603	2.2868	1.207	5.257	.637	-.785	0	?
285.00	2.5202	2.0966	1.202	5.084	.653	-.698	0	?
290.00	2.3138	1.9331	1.197	4.918	.672	-.612	0	?
295.00	2.1352	1.7916	1.192	4.762	.689	-.536	0	?
300.00	1.9794	1.6681	1.187	4.616	.701	-.476	0	?
305.00	1.8429	1.5596	1.182	4.483	.707	-.434	0	?
310.00	1.7226	1.4638	1.177	4.361	.706	-.407	0	?
315.00	1.6163	1.3787	1.172	4.251	.700	-.392	0	?
320.00	1.5218	1.3026	1.168	4.151	.698	-.386	0	?
325.00	1.4376	1.2342	1.165	4.060	.671	-.387	0	?
330.00	1.3620	1.1726	1.162	3.978	.648	-.394	0	?
335.00	1.2940	1.1169	1.159	3.902	.618	-.405	0	?
340.00	1.2325	1.0663	1.156	3.830	.582	-.421	0	?
345.00	1.1767	1.0204	1.153	3.759	.540	-.439	0	?
350.00	1.1257	.9787	1.150	3.685	.492	-.462	0	?
355.00	1.0789	.9409	1.147	3.603	.441	-.490	0	?
360.00	1.0358	.9068	1.142	3.510	.393	-.525	0	?
365.00	.9960	.8762	1.137	3.401	.355	-.568	0	?
370.00	.9594	.8489	1.130	3.277	.334	-.620	0	?
375.00	.9257	.8244	1.123	3.142	.335	-.680	0	?
380.00	.8949	.8023	1.115	3.003	.357	-.744	0	?
385.00	.8669	.7822	1.108	2.869	.393	-.807	0	?
390.00	.8415	.7638	1.102	2.747	.438	-.861	0	?
395.00	.8185	.7467	1.096	2.641	.485	-.905	0	?
400.00	.7975	.7308	1.091	2.551	.530	-.938	0	?
405.00	.7785	.7160	1.087	2.476	.571	-.962	0	?
410.00	.7612	.7023	1.084	2.413	.607	-.977	0	?
415.00	.7455	.6897	1.081	2.360	.639	-.987	0	?
420.00	.7312	.6781	1.078	2.314	.666	-.993	0	?
425.00	.7182	.6676	1.076	2.273	.689	-.997	0	?
430.00	.7064	.6580	1.074	2.237	.708	-1.000	0	?
435.00	.6958	.6494	1.072	2.202	.724	-1.002	0	?
440.00	.6863	.6418	1.069	2.169	.737	-1.005	0	?
445.00	.6778	.6351	1.067	2.136	.747	-1.009	0	?
450.00	.6703	.6293	1.065	2.101	.753	-1.012	0	?
455.00	.6637	.6245	1.063	2.063	.756	-1.016	0	?
460.00	.6579	.6204	1.060	2.022	.756	-1.021	5	?
465.00	.6530	.6164	1.059	1.976	.751	-1.027	5	?
470.00	.6488	.6133	1.058	1.925	.741	-1.033	5	?
475.00	.6454	.6110	1.056	1.868	.728	-1.039	5	?
480.00	.6426	.6092	1.055	1.807	.711	-1.047	5	?
485.00	.6405	.6079	1.054	1.742	.692	-1.052	5	?
490.00	.6389	.6073	1.052	1.676	.673	-1.057	5	?
495.00	.6377	.6071	1.050	1.613	.653	-1.061	5	?
500.00	.6369	.6073	1.049	1.553	.635	-1.065	5	?
505.00	.6362	.6075	1.047	1.501	.619	-1.068	5	?
510.00	.6353	.6074	1.046	1.457	.603	-1.071	5	?
515.00	.6340	.6067	1.045	1.422	.587	-1.076	5	?
520.00	.6317	.6050	1.044	1.399	.572	-1.079	5	?
525.00	.6280	.6017	1.044	1.386	.555	-1.081	5	?
530.00	.6223	.5962	1.044	1.386	.536	-1.083	5	?
535.00	.6140	.5881	1.044	1.397	.515	-1.083	5	?
540.00	.6025	.5767	1.045	1.420	.493	-1.083	5	?
545.00	.5874	.5616	1.046	1.454	.471	-1.082	5	?
550.00	.5685	.5428	1.047	1.497	.450	-1.083	5	?
555.00	.5458	.5202	1.049	1.549	.430	-1.088	5	?
560.00	.5196	.4943	1.051	1.606	.417	-1.098	5	?
565.00	.4907	.4659	1.053	1.666	.409	-1.113	5	?
570.00	.4598	.4357	1.055	1.728	.408	-1.134	5	?
575.00	.4278	.4047	1.057	1.787	.414	-1.161	5	?
580.00	.3957	.3738	1.059	1.842	.426	-1.192	5	?
585.00	.3641	.3436	1.060	1.892	.442	-1.227	5	?
590.00	.3337	.3147	1.061	1.933	.460	-1.264	5	?
595.00	.3049	.2875	1.061	1.967	.479	-1.302	5	?
600.00	.2778	.2621	1.060	1.992	.498	-1.339	5	?

Table 3.3.5a *Response characteristics of Disc 10A to 5EO excitation*

OLD-ES-
.1 MH

FREQUENCY	MAX RESP	MIN RESP	RATIO	STD	SKEW	KURT	DLE	BWD
100.00	1.2114	1.1912	1.017	.481	.560	.399	2	9
105.00	1.2400	1.2175	1.019	.543	-.545	.403	2	9
110.00	1.2731	1.2461	1.022	.612	-.529	-.405	2	9
115.00	1.3086	1.2775	1.024	.687	-.510	-.412	2	9
120.00	1.3470	1.3110	1.027	.771	-.488	-.421	2	9
125.00	1.3909	1.3492	1.031	.865	-.465	.431	2	9
130.00	1.4386	1.3905	1.035	.967	.443	-.443	2	9
135.00	1.4914	1.4350	1.039	1.078	-.427	-.453	2	9
140.00	1.5496	1.4859	1.043	1.199	-.431	-.453	2	9
145.00	1.6134	1.5418	1.046	1.283	-.488	-.436	2	9
150.00	1.6824	1.6050	1.048	1.347	-.610	-.485	2	9
155.00	1.7567	1.6770	1.048	1.432	-.841	.027	2	9
160.00	1.8467	1.7578	1.051	1.608	-.434	-1.196	2	5
165.00	1.9534	1.8468	1.058	1.819	-.282	-1.302	2	5
170.00	2.0704	1.9453	1.064	2.016	-.264	-1.313	2	5
175.00	2.2015	2.0538	1.071	2.211	-.306	-1.297	2	5
180.00	2.3511	2.1809	1.078	2.422	-.361	-1.266	2	5
185.00	2.5237	2.3239	1.086	2.657	-.410	-1.228	2	5
190.00	2.7240	2.4882	1.095	2.917	-.451	-1.189	2	5
195.00	2.9577	2.6780	1.104	3.198	-.486	-1.147	2	5
200.00	3.2308	2.8982	1.115	3.488	-.523	-1.101	2	5
205.00	3.5486	3.1541	1.125	3.762	-.569	-1.041	2	5
210.00	3.9133	3.4516	1.134	3.974	-.639	-.955	2	5
215.00	4.3189	3.7953	1.130	4.044	-.741	-.829	2	5
220.00	4.7412	4.1880	1.132	3.851	-.872	.667	2	5
225.00	5.1272	4.6229	1.109	3.227	-.995	-.514	2	5
230.00	5.4094	5.0639	1.068	2.054	.891	-.521	2	5
235.00	5.5692	5.3826	1.035	1.030	1.023	.107	9	2
240.00	5.5800	5.2069	1.072	2.402	.210	-1.501	9	2
245.00	5.4754	4.0536	1.128	3.963	.533	-1.232	9	2
250.00	5.1491	4.4119	1.167	5.007	.648	1.115	9	2
255.00	4.7060	3.9505	1.189	5.551	.697	-1.063	9	2
260.00	4.2386	3.5367	1.198	5.744	.722	-1.010	9	2
265.00	3.8003	3.1634	1.201	5.722	.739	-.960	9	2
270.00	3.4119	2.8410	1.201	5.602	.756	-.883	9	2
275.00	3.0761	2.5654	1.199	5.431	.776	-.787	9	2
280.00	2.7883	2.3306	1.196	5.247	.800	-.680	9	2
285.00	2.5418	2.1303	1.193	5.067	.825	-.576	9	2
290.00	2.3296	1.9509	1.189	4.897	.847	-.472	9	2
295.00	2.1450	1.8114	1.185	4.737	.864	-.395	9	2
300.00	1.9857	1.6836	1.179	4.587	.874	-.342	9	2
305.00	1.8454	1.5720	1.174	4.445	.880	-.309	9	2
310.00	1.7220	1.4730	1.168	4.312	.881	-.292	9	2
315.00	1.6131	1.3869	1.163	4.188	.880	-.286	9	2
320.00	1.5164	1.3095	1.158	4.072	.878	-.287	9	2
325.00	1.4302	1.2403	1.153	3.966	.875	.293	9	2
330.00	1.3531	1.1780	1.149	3.867	.871	.301	9	2
335.00	1.2830	1.1217	1.145	3.776	.866	.311	9	2
340.00	1.2214	1.0707	1.141	3.692	.862	-.323	9	2
345.00	1.1640	1.0244	1.137	3.615	.857	-.336	9	2
350.00	1.1135	.9821	1.134	3.544	.851	.351	9	2
355.00	1.0667	.9434	1.131	3.478	.846	-.368	9	2
360.00	1.0240	.9080	1.128	3.416	.839	.387	9	2
365.00	.9849	.8754	1.125	3.360	.832	-.408	9	2
370.00	.9490	.8455	1.122	3.307	.824	-.431	9	2
375.00	.9160	.8179	1.120	3.258	.815	-.456	9	2
380.00	.8857	.7924	1.118	3.214	.806	-.480	9	2
385.00	.8578	.7689	1.116	3.173	.797	.503	9	2
390.00	.8321	.7472	1.114	3.136	.788	-.525	9	2
395.00	.8084	.7271	1.112	3.101	.780	-.544	9	2
400.00	.7866	.7085	1.110	3.069	.773	-.561	9	2
405.00	.7665	.6912	1.109	3.039	.766	-.577	9	2
410.00	.7479	.6753	1.107	3.011	.759	-.593	9	2
415.00	.7308	.6606	1.106	2.984	.753	-.607	9	2
420.00	.7149	.6471	1.105	2.958	.747	-.621	9	2
425.00	.7004	.6346	1.104	2.932	.741	-.634	9	2
430.00	.6869	.6232	1.102	2.905	.736	-.646	9	2
435.00	.6746	.6127	1.101	2.878	.731	-.658	9	2
440.00	.6632	.6032	1.100	2.843	.728	-.668	9	2
445.00	.6528	.5946	1.098	2.806	.727	-.675	9	2
450.00	.6433	.5869	1.096	2.760	.728	-.680	9	2
455.00	.6345	.5801	1.094	2.704	.733	-.682	9	2
460.00	.6265	.5742	1.091	2.636	.741	-.679	9	2
465.00	.6191	.5691	1.088	2.555	.754	-.673	9	2
470.00	.6125	.5648	1.084	2.461	.770	-.667	9	2
475.00	.6065	.5613	1.080	2.356	.788	-.664	9	2
480.00	.6011	.5586	1.076	2.245	.805	-.671	9	2
485.00	.5965	.5566	1.072	2.135	.815	-.694	9	2
490.00	.5925	.5552	1.067	2.031	.815	-.739	9	2
495.00	.5893	.5544	1.063	1.939	.800	-.807	9	2
500.00	.5869	.5540	1.059	1.861	.772	-.889	9	2
505.00	.5851	.5541	1.056	1.797	.735	-.972	9	2
510.00	.5840	.5545	1.053	1.746	.694	-1.062	9	2
515.00	.5835	.5553	1.051	1.706	.654	-1.137	9	2
520.00	.5833	.5562	1.049	1.674	.617	-1.202	9	2
525.00	.5834	.5571	1.047	1.649	.587	-1.255	9	2
530.00	.5836	.5580	1.046	1.630	.561	-1.300	9	2
535.00	.5834	.5584	1.045	1.615	.540	-1.337	9	2
540.00	.5827	.5582	1.044	1.604	.523	-1.368	6	2
545.00	.5810	.5568	1.043	1.596	.509	-1.396	8	2
550.00	.5770	.5539	1.043	1.591	.496	-1.422	8	2
555.00	.5728	.5491	1.043	1.588	.484	-1.446	8	2
560.00	.5653	.5420	1.043	1.585	.473	-1.468	8	2
565.00	.5549	.5322	1.043	1.582	.463	-1.489	8	2
570.00	.5414	.5192	1.043	1.579	.452	-1.508	8	2
575.00	.5245	.5031	1.042	1.575	.442	1.527	8	2
580.00	.5042	.4838	1.042	1.569	.432	1.545	8	2
585.00	.4810	.4617	1.042	1.562	.420	1.562	8	2
590.00	.4554	.4372	1.042	1.553	.409	-1.578	8	2
595.00	.4281	.4111	1.041	1.542	.396	-1.594	8	2
600.00	.3992	.3841	1.041	1.531	.383	-1.607	8	2

Table 3.3.1b *Response characteristics of Disc 10A to 1EO excitation*

excitation frequency	LOWEST RESPONSE			Blade numbers, by ranks						LARGEST RESPONSE
100.0	1	2	5	3	4	6	7	8	9	10
105.0	1	2	5	3	4	6	7	8	9	10
110.0	1	2	5	3	4	6	7	9	8	10
115.0	1	2	5	3	4	6	7	9	8	10
120.0	1	2	5	3	4	6	7	9	8	10
125.0	1	2	5	3	4	6	7	9	8	10
130.0	1	2	5	3	4	6	7	9	8	10
135.0	1	2	5	3	4	8	7	9	6	10
140.0	1	2	5	3	4	8	7	9	6	10
145.0	1	2	5	3	4	8	7	9	6	10
150.0	1	3	5	2	4	8	7	9	6	10
155.0	7	9	3	8	10	1	5	2	4	6
160.0	8	6	5	10	9	1	3	2	7	4
165.0	4	5	6	10	8	1	3	2	9	7
170.0	2	5	6	10	7	1	4	3	9	8
175.0	1	3	6	8	7	2	5	4	9	10
180.0	1	3	4	8	7	2	6	5	9	10
185.0	10	9	6	3	4	8	7	5	2	1
190.0	10	9	7	3	4	8	6	5	2	1
195.0	10	9	7	3	4	8	6	5	2	1
200.0	10	9	7	3	4	8	6	5	2	1
205.0	10	9	8	3	4	7	6	5	2	1
210.0	10	9	8	3	4	6	7	5	2	1
215.0	10	9	8	3	4	6	7	5	2	1
220.0	5	6	10	4	2	3	9	1	7	8
225.0	3	1	4	8	10	2	5	6	9	7
230.0	6	2	3	5	8	4	7	1	9	10
235.0	2	7	6	8	9	1	10	3	4	5
240.0	10	9	8	6	7	4	2	3	1	5
245.0	10	9	5	7	8	6	4	3	1	2
250.0	10	6	4	8	9	7	3	5	2	1
255.0	8	5	3	9	10	7	4	6	2	1
260.0	1	2	4	9	10	8	5	7	6	3
265.0	10	7	2	9	8	3	4	6	5	1
270.0	10	9	7	1	2	8	6	5	4	3
275.0	10	8	5	1	4	9	7	6	3	2
280.0	2	7	6	1	4	10	9	8	3	5
285.0	10	9	7	8	6	4	5	2	3	1
290.0	10	9	8	7	6	4	5	3	2	1
295.0	10	9	8	7	6	5	4	3	2	1
300.0	10	9	8	7	6	5	4	3	2	1
305.0	10	9	8	5	7	6	4	3	2	1
310.0	10	9	8	5	6	7	4	3	2	1
315.0	10	9	8	5	6	7	4	3	2	1
320.0	10	9	8	4	6	7	5	3	2	1
325.0	10	9	8	4	5	7	6	3	2	1
330.0	10	9	8	4	5	7	6	3	2	1
335.0	10	9	8	4	5	7	6	3	2	1
340.0	10	9	8	3	5	7	6	4	2	1
345.0	10	9	8	3	5	6	7	4	2	1
350.0	10	9	8	3	4	6	7	5	2	1
355.0	10	9	8	3	4	6	7	5	2	1
360.0	10	9	8	3	4	6	7	5	1	2
365.0	10	9	8	1	3	6	7	5	2	4
370.0	5	7	3	6	9	8	2	10	4	1
375.0	3	2	1	10	9	5	4	6	8	7
380.0	7	3	1	10	9	6	2	5	8	4
385.0	8	5	1	10	9	6	2	4	7	3
390.0	8	7	1	10	9	5	2	4	6	3
395.0	10	7	3	9	8	6	2	4	5	1
400.0	10	7	3	9	8	6	2	4	5	1
405.0	10	7	3	9	8	6	2	4	5	1
410.0	10	7	3	9	8	6	2	4	5	1
415.0	10	7	3	9	8	6	2	4	5	1
420.0	10	7	3	9	8	6	2	4	5	1
425.0	10	7	3	9	8	6	2	4	5	1
430.0	10	7	3	9	8	6	2	5	4	1
435.0	10	7	3	9	8	6	2	5	4	1
440.0	10	7	4	9	8	6	2	5	3	1
445.0	10	7	5	9	8	6	2	4	3	1
450.0	10	7	5	9	8	6	2	4	3	1
455.0	10	7	5	9	8	6	2	3	4	1
460.0	10	7	5	9	8	6	2	3	4	1
465.0	10	7	5	9	8	6	2	3	4	1
470.0	10	7	6	9	3	5	2	3	4	1
475.0	10	7	5	9	8	4	2	3	6	1
480.0	7	2	5	8	1	4	9	3	6	10
485.0	2	3	6	1	4	8	10	5	7	9
490.0	2	3	5	1	4	8	10	7	6	9
495.0	2	3	5	1	4	9	10	7	6	8
500.0	4	2	5	1	3	9	10	8	6	7
505.0	4	2	5	1	3	9	10	8	7	6
510.0	8	2	5	1	4	9	10	7	6	3
515.0	8	2	4	1	6	10	9	7	5	3
520.0	8	3	4	1	7	10	9	6	5	2
525.0	9	3	4	1	7	10	8	6	5	2
530.0	10	4	3	1	7	9	8	6	5	2
535.0	10	4	3	2	7	9	8	5	6	1
540.0	10	4	3	2	8	9	7	5	6	1
545.0	10	3	4	2	8	9	7	5	6	1
550.0	9	2	4	3	10	7	8	5	6	1
555.0	3	10	6	9	1	5	2	7	4	8
560.0	4	10	6	9	2	5	3	8	1	7
565.0	6	9	4	8	3	7	2	10	1	5
570.0	6	7	3	8	5	9	2	10	1	4
575.0	8	6	2	7	5	9	3	10	1	4
580.0	3	6	10	4	5	1	7	2	9	8
585.0	3	6	10	4	5	1	7	2	9	8
590.0	5	6	10	4	3	1	7	2	8	9
595.0	5	9	10	4	3	1	7	2	6	8
600.0	5	9	10	4	3	1	7	2	6	8

Table 3.3.2b *Response characteristics of Disc 10A to 2EO excitation*

100.0	1	2	3	5	4	7	6	8	9	10
105.0	1	2	3	5	4	7	6	9	8	10
110.0	1	2	3	5	4	7	6	9	8	10
115.0	1	2	3	5	4	7	6	9	8	10
120.0	1	2	3	5	4	7	6	9	8	10
125.0	1	2	3	6	4	7	5	9	8	10
130.0	1	2	3	6	4	7	5	9	8	10
135.0	1	2	3	6	4	7	5	9	8	10
140.0	1	2	3	5	4	7	6	9	8	10
145.0	1	2	3	5	4	7	6	9	8	10
150.0	1	2	3	4	5	6	7	9	8	10
155.0	1	2	3	4	5	6	7	8	9	10
160.0	1	2	3	4	5	6	7	8	9	10
165.0	1	2	3	4	5	6	8	7	9	10
170.0	1	2	3	4	5	6	8	7	9	10
175.0	1	2	3	4	5	6	8	7	9	10
180.0	1	2	3	4	5	6	8	7	9	10
185.0	1	2	3	4	5	6	8	7	9	10
190.0	1	2	3	4	5	6	8	7	9	10
195.0	1	2	3	4	5	6	9	7	8	10
200.0	1	2	3	4	5	6	9	7	8	10
205.0	1	2	3	4	5	6	9	7	8	10
210.0	1	2	3	5	4	6	9	7	8	10
215.0	1	3	2	8	4	5	9	6	7	10
220.0	2	3	1	9	5	4	8	6	7	10
225.0	3	2	1	10	6	4	8	5	7	9
230.0	4	1	2	10	6	3	9	5	8	7
235.0	9	5	8	10	4	3	6	2	7	1
240.0	10	7	9	8	4	3	5	2	6	1
245.0	10	8	9	7	6	3	4	2	5	1
250.0	10	8	9	7	6	4	5	2	3	1
255.0	10	9	8	7	6	4	5	2	3	1
260.0	10	9	8	7	6	5	4	2	3	1
265.0	10	9	8	7	6	5	4	2	3	1
270.0	10	9	8	7	6	5	4	3	2	1
275.0	10	9	8	7	6	5	4	3	2	1
280.0	10	9	8	7	6	5	4	3	2	1
285.0	10	9	8	7	6	5	4	3	2	1
290.0	10	9	8	7	6	5	4	3	2	1
295.0	10	9	8	7	6	5	4	3	2	1
300.0	10	9	8	7	6	5	4	3	2	1
305.0	10	9	8	7	6	5	4	3	2	1
310.0	10	9	8	7	6	5	4	3	2	1
315.0	10	9	8	7	6	5	4	3	2	1
320.0	10	9	8	7	6	5	4	3	2	1
325.0	10	9	8	7	6	5	4	3	2	1
330.0	10	9	8	7	6	5	4	3	2	1
335.0	10	9	8	7	6	5	3	4	2	1
340.0	10	9	8	7	6	5	3	4	2	1
345.0	10	9	8	7	6	5	2	4	3	1
350.0	10	9	8	7	5	6	2	4	3	1
355.0	10	9	8	7	5	6	2	3	4	1
360.0	10	9	8	7	5	6	2	3	4	1
365.0	10	9	8	7	5	6	2	3	4	1
370.0	10	9	8	6	4	7	2	3	5	1
375.0	10	8	9	6	3	7	2	4	5	1
380.0	10	8	9	5	3	7	2	4	6	1
385.0	10	8	9	4	3	7	2	5	6	1
390.0	10	8	9	4	2	7	3	5	6	1
395.0	10	8	9	3	2	7	4	5	6	1
400.0	10	8	9	2	3	7	6	5	4	1
405.0	10	8	9	2	3	7	6	5	4	1
410.0	10	8	9	2	3	7	6	5	4	1
415.0	10	8	9	2	4	7	6	5	3	1
420.0	10	9	8	2	4	7	6	5	3	1
425.0	10	9	8	3	4	7	6	5	2	1
430.0	10	9	8	3	5	7	6	4	2	1
435.0	10	9	8	3	5	7	6	4	2	1
440.0	10	9	8	3	5	7	6	4	2	1
445.0	10	9	8	4	5	7	6	3	2	1
450.0	10	8	9	4	5	7	6	3	2	1
455.0	10	8	9	4	5	7	6	3	2	1
460.0	10	8	9	4	5	7	6	3	1	2
465.0	10	8	9	4	5	7	6	3	1	2
470.0	10	8	9	4	6	7	5	2	1	3
475.0	10	8	9	4	6	7	5	2	1	3
500.0	10	9	3	8	6	2	7	5	4	1
505.0	10	9	3	8	7	2	6	5	4	1
510.0	10	9	3	8	7	2	6	5	4	1
515.0	10	9	3	8	7	2	6	5	4	1
520.0	10	9	3	8	7	2	5	6	4	1
525.0	9	10	3	7	8	2	5	6	4	1
530.0	9	10	3	7	8	2	5	6	4	1
535.0	9	10	3	7	8	2	6	5	4	1
540.0	9	10	3	7	8	1	6	5	4	2
545.0	9	10	3	7	8	1	6	5	4	2
550.0	8	10	2	7	9	1	6	5	4	3
555.0	8	10	2	7	9	1	6	5	3	4
560.0	8	10	2	7	9	1	6	5	3	4
565.0	8	10	2	6	9	1	7	5	3	4
570.0	8	10	3	6	9	1	7	5	2	4
575.0	8	10	3	5	9	1	7	6	2	4
580.0	8	10	3	5	9	2	7	6	1	4
585.0	8	10	3	4	9	2	7	6	1	5
590.0	8	10	3	4	9	2	7	6	1	5
595.0	8	10	3	4	9	2	7	6	1	5
600.0	8	10	3	4	9	2	7	6	1	5

Table 3.3.3b *Response characteristics of Disc 10A to 3EO excitation*

100.0	1	2	3	7	6	4	5	8	9	10
105.0	1	2	3	7	6	4	5	8	9	10
110.0	1	2	3	7	6	4	5	8	9	10
115.0	1	2	3	7	6	4	5	8	9	10
120.0	1	2	3	7	6	4	5	8	9	10
125.0	1	2	3	7	6	4	5	8	10	9
130.0	1	2	3	7	6	4	5	8	10	9
135.0	1	2	3	7	5	4	6	8	10	9
140.0	1	2	3	7	5	4	6	8	10	9
145.0	1	2	4	6	5	3	7	9	10	8
150.0	1	4	3	6	5	2	8	9	10	7
155.0	1	5	4	6	3	2	8	9	10	7
160.0	1	5	6	4	3	2	8	10	9	7
165.0	1	5	6	4	2	3	9	10	8	7
170.0	1	5	6	3	2	4	10	9	8	7
175.0	1	4	6	3	2	5	8	7	9	10
180.0	1	4	8	3	2	5	7	6	9	10
185.0	1	2	9	4	3	5	7	6	8	10
190.0	1	2	9	4	3	5	6	7	8	10
195.0	1	2	9	3	4	7	5	6	8	10
200.0	1	2	9	3	4	7	5	6	8	10
205.0	1	2	9	3	4	7	5	6	8	10
210.0	1	2	9	3	5	7	4	6	8	10
215.0	1	2	9	4	5	8	3	6	7	10
220.0	1	2	9	4	5	10	3	6	7	9
225.0	2	1	9	5	4	10	3	6	7	8
230.0	3	2	9	5	4	10	1	6	7	8
235.0	7	2	9	6	3	10	1	4	5	8
240.0	8	2	9	7	3	10	1	5	4	6
245.0	8	2	9	7	5	10	1	6	3	4
250.0	9	4	8	7	6	10	1	5	2	3
255.0	10	5	8	7	6	9	3	4	1	2
260.0	10	5	8	6	7	9	3	4	1	2
265.0	10	7	6	5	8	9	4	3	1	2
270.0	10	8	5	6	7	9	4	3	1	2
275.0	10	9	5	6	8	7	4	3	1	2
280.0	10	9	5	7	8	6	4	3	2	1
285.0	10	9	5	7	8	6	4	3	2	1
290.0	10	9	5	7	8	6	4	3	2	1
295.0	10	9	5	7	8	6	4	3	2	1
300.0	10	9	5	8	7	6	4	3	2	1
305.0	10	9	5	8	6	7	4	3	2	1
310.0	10	9	5	7	6	8	4	3	2	1
315.0	10	9	6	7	5	8	4	3	2	1
320.0	10	9	7	6	5	8	4	3	2	1
325.0	10	9	7	6	5	8	3	4	2	1
330.0	10	8	7	6	5	9	3	4	2	1
335.0	10	7	8	6	5	9	3	4	2	1
340.0	10	5	8	7	6	9	1	4	2	3
345.0	9	4	8	7	6	10	1	5	2	3
350.0	8	2	9	7	6	10	1	5	3	4
355.0	5	2	9	7	4	10	1	6	3	8
360.0	3	2	9	6	5	10	1	7	4	8
365.0	3	1	8	6	5	10	2	7	4	9
370.0	3	1	8	6	5	10	2	7	4	9
375.0	3	1	8	6	4	10	2	7	5	9
380.0	3	1	8	6	4	10	2	7	5	9
385.0	3	1	8	7	4	10	2	6	5	9
390.0	3	1	8	7	4	10	2	6	5	9
395.0	4	1	8	7	3	10	2	6	5	9
400.0	4	1	8	7	3	10	2	6	5	9
405.0	6	1	8	7	3	10	2	5	4	9
410.0	6	1	8	7	3	10	2	5	4	9
415.0	7	1	8	6	3	10	2	4	5	9
420.0	9	1	8	6	3	10	2	4	5	7
425.0	9	1	8	6	2	10	3	4	5	7
430.0	10	1	8	6	3	9	5	2	4	7
435.0	10	4	8	6	2	9	5	1	3	7
440.0	10	6	8	7	2	9	4	1	3	5
445.0	10	7	8	5	2	9	6	1	3	4
450.0	10	7	9	5	3	8	6	1	4	2
455.0	10	7	9	5	3	8	6	2	4	1
460.0	10	9	8	5	3	7	6	2	4	1
465.0	10	9	8	5	3	6	7	2	4	1
470.0	10	9	7	5	2	6	8	4	3	1
475.0	10	9	7	6	2	5	8	4	3	1
480.0	10	9	6	7	3	2	8	5	4	1
485.0	10	9	6	7	4	2	8	5	3	1
490.0	10	9	4	7	5	2	8	6	3	1
495.0	10	9	3	8	5	2	7	6	4	1
500.0	10	8	9	5	6	7	3	1	2	4
505.0	10	8	9	5	6	7	3	1	2	4
510.0	10	8	9	5	6	7	3	1	2	4
515.0	10	8	9	5	6	7	2	1	3	4
520.0	10	8	9	5	6	7	2	1	3	4
525.0	10	8	9	5	6	7	2	1	3	4
530.0	10	8	9	5	6	7	2	1	3	4
535.0	10	8	9	5	6	7	2	1	3	4
540.0	10	8	9	5	6	7	2	1	3	4
545.0	10	8	9	5	6	7	2	1	3	4
550.0	10	8	9	5	6	7	2	1	3	4
555.0	10	8	9	5	6	7	2	1	3	4
560.0	10	8	9	5	6	7	2	1	3	4
565.0	10	8	9	5	6	7	2	1	3	4
570.0	10	8	9	4	6	7	2	1	3	5
575.0	10	8	9	4	6	7	3	1	2	5
580.0	10	8	9	4	5	7	3	1	2	6
585.0	10	8	9	4	5	7	3	1	2	6
590.0	10	8	9	4	5	7	3	1	2	6
595.0	10	8	9	3	5	7	4	1	2	6
600.0	10	8	9	3	4	7	5	1	2	6

Table 3.3.4b *Response characteristics of Disc 10A to 4EO excitation*

100.0	1	2	3	4	5	6	7	8	9	10
105.0	1	2	3	4	5	6	7	8	9	10
110.0	1	2	3	4	5	6	7	8	9	10
115.0	1	2	3	4	5	6	7	8	9	10
120.0	1	2	3	4	6	5	7	8	9	10
125.0	1	2	4	3	6	5	7	8	9	10
130.0	1	2	4	3	6	5	7	8	9	10
135.0	1	2	4	3	6	5	8	7	9	10
140.0	1	2	4	3	8	5	9	6	7	10
145.0	1	4	2	3	9	5	8	7	6	10
150.0	1	5	2	3	9	4	8	7	6	10
155.0	1	8	2	4	9	3	7	6	5	10
160.0	1	7	2	8	10	3	4	6	5	9
165.0	1	5	2	8	10	3	4	6	7	9
170.0	1	5	2	9	10	4	3	6	7	8
175.0	1	4	2	10	8	5	3	6	7	9
180.0	1	3	2	10	7	5	4	6	8	9
185.0	1	2	3	10	6	5	4	7	8	9
190.0	1	2	3	10	6	5	4	7	9	8
195.0	1	2	3	10	6	5	4	7	9	8
200.0	1	2	3	9	6	4	5	7	10	8
205.0	1	2	3	9	6	4	5	8	10	7
210.0	1	2	3	9	4	5	6	8	10	7
215.0	2	1	4	9	3	5	6	8	10	7
220.0	3	1	4	9	2	5	7	8	10	6
225.0	4	1	5	9	2	7	6	8	10	3
230.0	7	2	8	6	1	9	4	5	10	3
235.0	10	2	9	6	1	8	5	4	7	3
240.0	10	3	9	7	1	8	5	4	6	2
245.0	10	4	9	7	1	8	6	3	5	2
250.0	10	7	9	5	2	8	6	3	4	1
255.0	10	7	9	5	2	8	6	4	3	1
260.0	10	8	9	5	2	7	6	4	3	1
265.0	10	8	9	5	3	7	6	4	2	1
270.0	10	8	9	4	5	7	6	3	2	1
275.0	10	9	8	4	5	7	6	3	2	1
280.0	10	9	8	4	5	7	6	3	2	1
285.0	10	9	8	4	5	7	6	3	2	1
290.0	10	9	8	4	5	7	6	3	2	1
295.0	10	9	8	4	5	7	6	3	2	1
300.0	10	9	8	4	5	7	6	3	2	1
305.0	10	9	8	4	5	7	6	3	2	1
310.0	10	9	8	4	5	7	6	3	2	1
315.0	10	9	8	4	5	7	6	3	2	1
320.0	10	9	8	4	5	7	6	3	2	1
325.0	10	9	8	4	5	7	6	3	2	1
330.0	10	9	8	4	5	7	6	3	2	1
335.0	10	9	8	4	5	7	6	3	2	1
340.0	10	9	8	4	5	7	6	3	2	1
345.0	10	9	8	4	6	7	5	3	2	1
350.0	10	9	8	4	6	7	5	3	2	1
355.0	10	9	8	4	6	7	5	3	1	2
360.0	10	9	8	4	6	7	5	3	1	2
365.0	10	9	8	5	6	7	4	2	1	3
370.0	10	9	8	5	6	7	4	2	1	3
375.0	10	9	8	5	6	7	4	2	1	3
380.0	10	9	8	5	6	7	4	2	1	3
385.0	10	8	9	5	6	7	4	2	1	3
390.0	10	8	9	5	6	7	3	2	1	4
395.0	10	8	9	5	6	7	3	2	1	4
400.0	10	8	9	5	6	7	3	2	1	4
405.0	10	8	9	5	6	7	3	2	1	4
410.0	10	8	9	6	5	7	2	3	1	4
415.0	10	8	9	6	5	7	2	3	1	4
420.0	10	8	9	6	5	7	2	4	1	3
425.0	10	8	9	6	5	7	2	4	1	3
430.0	10	8	9	6	5	7	2	4	1	3
435.0	10	7	9	6	5	8	2	4	1	3
440.0	10	7	9	6	5	8	2	4	1	3
445.0	10	7	9	6	5	8	2	4	1	3
450.0	10	7	8	6	5	9	2	3	1	4
455.0	10	6	8	7	5	9	1	3	2	4
460.0	10	6	8	7	5	9	1	3	2	4
465.0	10	6	8	7	5	9	1	3	2	4
470.0	10	4	8	7	5	9	1	3	2	6
475.0	9	3	8	7	5	10	1	4	2	6
480.0	9	3	8	7	5	10	1	4	2	6
485.0	8	2	9	7	4	10	1	5	3	6
490.0	8	2	9	7	4	10	1	5	3	6
495.0	8	2	9	7	4	10	1	5	3	6
500.0	8	2	9	6	4	10	1	5	3	7
505.0	8	2	9	6	4	10	1	5	3	7
510.0	8	2	9	6	4	10	1	5	3	7
515.0	8	2	9	6	3	10	1	5	4	7
520.0	8	2	9	6	3	10	1	4	5	7
525.0	8	2	9	6	3	10	1	4	5	7
530.0	8	2	10	6	3	9	1	4	5	7
535.0	8	3	10	6	2	9	1	4	5	7
540.0	8	4	10	6	2	9	1	3	5	7
545.0	8	7	10	5	2	9	1	3	6	4
550.0	9	7	10	5	2	8	1	3	6	4
555.0	9	7	10	5	3	8	1	4	6	2
560.0	9	7	10	5	3	8	1	4	6	2
565.0	9	8	10	6	3	7	2	4	5	1
570.0	10	8	9	6	4	7	2	3	5	1
575.0	10	8	9	7	4	6	2	3	5	1
580.0	10	9	8	7	5	4	3	2	6	1
585.0	10	9	8	7	6	2	4	3	5	1
590.0	10	9	8	7	6	2	5	3	4	1
595.0	10	9	8	7	6	2	5	3	4	1
600.0	9	10	7	6	8	2	5	3	4	1

Table 3.3.5b *Response characteristics of Disc 10A to 5EO excitation*

100.0	1	2	3	6	7	5	4	8	9	10
105.0	1	2	3	6	7	5	4	8	9	10
110.0	1	2	3	6	7	5	4	8	9	10
115.0	1	2	3	6	7	5	4	8	9	10
120.0	1	2	3	6	7	5	4	8	9	10
125.0	1	2	3	6	7	5	4	8	9	10
130.0	1	2	3	6	7	5	4	8	9	10
135.0	1	2	3	6	7	5	4	8	9	10
140.0	1	2	3	6	7	5	4	8	9	10
145.0	1	2	3	6	7	5	4	8	9	10
150.0	1	2	3	4	5	6	7	8	9	10
155.0	1	4	5	2	3	6	9	8	7	10
160.0	3	5	8	1	2	6	10	7	4	9
165.0	3	5	9	1	2	7	10	6	4	8
170.0	3	5	9	1	2	7	10	6	4	8
175.0	3	5	9	1	2	6	10	7	4	8
180.0	3	5	8	1	2	6	10	7	4	9
185.0	3	5	8	1	2	6	10	7	4	9
190.0	3	5	8	1	2	6	9	7	4	10
195.0	3	4	8	1	2	6	9	7	5	10
200.0	3	4	8	1	2	6	9	7	5	10
205.0	3	4	8	1	2	6	9	7	5	10
210.0	3	4	8	1	2	6	9	7	5	10
215.0	2	5	9	3	1	4	8	6	7	10
220.0	3	7	10	5	1	2	8	4	6	9
225.0	7	9	10	8	3	1	4	2	6	5
230.0	8	9	7	10	6	2	4	1	5	3
235.0	9	7	6	10	8	2	4	1	5	3
240.0	9	7	6	10	8	3	4	2	5	1
245.0	10	7	6	9	8	4	2	3	5	1
250.0	10	7	6	9	8	4	2	3	5	1
255.0	10	7	4	9	8	5	2	3	6	1
260.0	10	7	4	9	8	6	2	3	5	1
265.0	10	7	4	9	8	6	2	3	5	1
270.0	10	7	4	9	8	6	2	3	5	1
275.0	10	7	4	9	8	6	2	3	5	1
280.0	10	7	5	9	8	6	2	3	4	1
285.0	10	7	5	9	8	6	2	3	4	1
290.0	10	8	6	9	7	5	2	3	4	1
295.0	10	9	6	8	7	5	2	3	4	1
300.0	10	9	6	8	7	5	3	2	4	1
305.0	10	9	6	8	7	5	4	2	3	1
310.0	10	9	6	8	7	5	4	2	3	1
315.0	10	9	6	8	7	5	4	2	3	1
320.0	10	9	6	8	7	5	4	2	3	1
325.0	10	9	6	8	7	5	4	2	3	1
330.0	10	9	6	8	7	5	3	2	4	1
335.0	10	9	6	8	7	5	3	2	4	1
340.0	10	9	6	8	7	5	3	2	4	1
345.0	10	9	6	8	7	5	3	2	4	1
350.0	10	9	6	8	7	5	4	2	3	1
355.0	10	9	6	8	7	5	4	2	3	1
360.0	10	9	6	8	7	5	4	3	2	1
365.0	10	9	6	8	7	5	4	3	2	1
370.0	10	9	5	7	8	6	3	4	2	1
375.0	10	9	5	7	8	6	3	4	2	1
380.0	10	9	4	6	7	8	3	5	2	1
385.0	10	9	3	5	7	8	4	6	2	1
390.0	10	8	3	4	6	9	5	7	2	1
395.0	10	8	4	3	6	9	5	7	2	1
400.0	10	8	4	3	6	9	5	7	2	1
405.0	10	8	4	3	5	9	6	7	2	1
410.0	10	7	4	3	5	9	6	8	2	1
415.0	10	7	4	3	5	9	6	8	2	1
420.0	10	7	4	3	5	9	6	8	2	1
425.0	10	7	4	3	6	9	5	8	2	1
430.0	10	7	4	3	6	9	5	8	2	1
435.0	10	7	4	3	6	9	5	8	2	1
440.0	10	7	4	3	6	9	5	8	2	1
445.0	10	7	4	3	6	9	5	8	2	1
450.0	10	7	4	3	6	9	5	8	2	1
455.0	10	7	3	4	6	9	5	8	2	1
460.0	10	7	3	4	6	9	5	8	2	1
465.0	10	8	3	4	6	9	5	7	2	1
470.0	10	8	3	4	6	9	5	7	2	1
475.0	10	8	3	4	6	9	5	7	2	1
480.0	10	8	3	4	6	9	5	7	2	1
485.0	10	8	3	4	6	9	5	7	2	1
490.0	10	8	3	4	6	9	5	7	2	1
495.0	10	8	3	4	6	9	5	7	2	1
500.0	10	8	3	5	6	9	4	7	2	1
505.0	10	8	3	5	6	9	4	7	2	1
510.0	10	8	3	5	6	9	4	7	2	1
515.0	10	8	3	5	6	9	4	7	2	1
520.0	10	8	3	5	6	9	4	7	2	1
525.0	10	8	3	5	6	9	4	7	2	1
530.0	10	8	3	5	6	9	4	7	2	1
535.0	10	8	3	4	7	9	5	6	2	1
540.0	10	8	3	4	7	9	5	6	2	1
545.0	10	8	3	4	7	9	6	5	2	1
550.0	10	8	3	4	7	9	6	5	2	1
555.0	10	9	4	3	6	8	7	5	2	1
560.0	10	9	5	4	6	8	7	3	2	1
565.0	10	9	5	4	6	8	7	3	2	1
570.0	10	9	6	4	5	8	7	2	3	1
575.0	10	9	7	4	5	6	8	2	3	1
580.0	10	9	8	3	5	6	7	2	4	1
585.0	10	9	8	3	5	6	7	2	4	1
590.0	10	9	8	3	5	6	7	2	4	1
595.0	10	9	8	4	5	6	7	2	3	1
600.0	10	9	8	5	6	4	7	1	3	2

Chapter 4

4.1 Introduction

4.1.1 Damped Mechanical Systems

Engineering systems are generally non-conservative. That is to say whenever energy is impressed upon a physical structure, some of the energy is lost during the course of its transfer from one location to another within the system. The precise nature of this energy dissipation is not properly understood as yet, although a considerable amount of effort has been devoted to its discussion for a very long time now. Lord **Rayleigh** addressed himself to the problem in his celebrated treatise of 1887, and from that time until the present several publications have been issued on the nature of damping and the mechanics of energy dissipation in non-conservative mechanical systems.

The equations describing the motion of an engineering structure are usually cast in matrix form, after which they must be solved for forced response values. This solution may be achieved directly by transforming the equations to the dynamic stiffness format, i.e. $\mathbf{K}(\omega)\mathbf{x}=\mathbf{f}$, where $\mathbf{K}$ is the dynamic stiffness matrix of the system, $\mathbf{f}$ is the force vector impressed on the system, and $\mathbf{x}$ is the response vector. Alternatively, the eigenvalues and eigenvectors of the system are obtained initially from free vibration considerations, and a subsequent application of 'modal superposition' usually yields the desired response values. The latter method is generally more economical to apply. This, therefore, requires the calculation of the eigenvalues and corresponding vectors of the system.

However, procedures for extracting the latent roots and vectors of large order matrices, for systems in which damping is not 'proportional', are not well established at present. The problem of solving for the eigensystems of structures with arbitrary damping is re-examined in this chapter. An existing scheme for the solution of such non-linear eigenvalue problems is modified in order to improve its convergence capability. It is shown that when a bladed disc assembly has arbitrary damping, then the real components of the eigenvectors of the damped system are little different from the mode shapes of the corresponding undamped system, provided the damping is 'smoothly' distributed within the system. When this condition is not satisfied, then some vectors of the damped system are very much unlike the corresponding vectors of the undamped system.

4.1.2 Damping Models of Bladed Discs

A bladed disc assembly, as a component of an aircraft engine, is a non-conservative mechanical system, since it is subjected to at least three kinds of damping whenever the engine is operated. The first type of damping experienced by the assembly is intrinsic, in as much as the dissipation of mechanical energy is due to the materials used in the manufacture of the blades and disc. It is, therefore, usually known as *material damping*. Blades on the vast majority of turbomachine rotors are, however, manufactured separately from the disc, with the two components sebsequently assembled together. Now, some frictional forces come into play at the interface of the blade root and disc rim when such assemblies are exposed to vibration; and that is the origin of *frictional damping*. The third kind is external to the bladed disc assembly, since it arises mainly from aerodynamic forces impinging on the blades from without. It is sometimes known as *aerodynamic damping*.

Material Damping Model

The dissipation of vibrational energy in the material of blades and discs is usually modelled by the introduction of hysteretic dampers; see, for instance, **Ewins** (1975), or **Fabunmi** (1978). A general theory of hysteretic damping in mechanical systems has been presented by **Bishop** (1956), among others. This type of damping is relatively easy to model, both analytically and numerically, and has been applied in Chapter 2 to account for damping in bladed disc assemblies.

Friction Damping Model

Another category of damping models is based on the influence of frictional forces, which operate at the point of attachmnent of blades to the disc. This is especially true, for example, of blades having serrated or 'fir-tree' roots. The vibration of blade-like structures with damping at their roots has been studied extensivelly by **Jones** (1969, 1978). Generally speaking, the mathematical analysis of vibrating systems which embody frictional dissipative forces gives rise to non-linear differential equations. In a recent report by **Muszynska** *et al* (1980), a lumped parameter method incoporating this form of damping was applied to model mistuned bladed discs.

Aerodynamic Damping Model

With regard to aerodynamic damping, neither is its nature properly understood at present, nor the mechanics by which it influences the dynamic behaviour of bladed disc assemblies. Several theories have, in fact, been published in the last two decades. In *cascade* theory, the mechanical coupling among the blades is assumed to be weak, which is true if the stiffness of the disc is very large so that the blades may be considered as a cascade of aerofoils oscillating in incompressible (**Whitehead**, 1965), subsonic (**Srinivasan**, 1980), or supersonic (**Kielb**, 1981) flow of fluids.

The flexibility offered by the disc provides some form of mechanical linkages of all the blades, and when the cascade theory is modified to take cognizance of this, an *aeroelastic* theory results. See, for instance, the paper by **Whitehead** (1976). The cascade and aeroelastic theories both require the derivation of aerodynamic coefficients.

Another type of modelling is based purely on the structural properties of the disc and blades, with a grounded viscous damper attached at the tip of each blade to simulate aerodynamic damping. This type of modelling will be referred to in this text as the *aerodynamic* model, for want of a more suitable term. Such an aerodynamic model has been utilised by **Ewins** (1976), among others, in various previous studies. (This is not the same as the *aeroelastic* model).

The categorization above, of the various types of 'aerodynamic' damping models, is not the standard - there is, in fact, no standard - but is introduced here for the purposes of discussion in this thesis, and for the avoidance of confusion. The model used in this study is in the same category of aerodynamic damping as that of Ewins (1976). The difference between this model and the previous studies is that the structural elements here are based on the lumped mass formulation, whereas distributed receptances were used by Ewins.

4.2 Eigenvalue Problems of Damped Mechanical Systems

4.2.1 Matrix Formulations

The equations of motion of a mechanical system lacking any form of damping, under free vibration, may be written in matrix notation as:

$$\lambda^2 \mathbf{M}\mathbf{x} + \mathbf{K}\mathbf{x} = \mathbf{0} \qquad (4.2.1)$$

where the symbols have their customary meanings.

When material or hysteretic damping is not negligible, the relevant equation is

$$\lambda^2 \mathbf{Mx} + i\mathbf{Hx} + \mathbf{Kx} = \mathbf{0} \tag{4.2.2}$$

If, in addition to the hysteretic damping, there exist some other dissipating forces, the corresponding lambda matrix equation is

$$\lambda^2 \mathbf{Mx} + \lambda \mathbf{Vx} + i\mathbf{Hx} + \mathbf{Kx} = \mathbf{0} \tag{4.2.3a}$$

where $\mathbf{V}$ represents the matrix of the coefficients of additional damping. In most structural analysis problems, the matrix $\mathbf{V}$ is replaceable by the viscous damping matrix, $\mathbf{C}$, so that equation (4.2.2) becomes

$$\lambda^2 \mathbf{Mx} + \lambda \mathbf{Cx} + i\mathbf{Hx} + \mathbf{Kx} = \mathbf{0} \tag{4.2.3b}$$

The structural matrices above are usually symmetric for formulations based on lumped parameter modelling, finite elements and receptance methods. They are also sometimes banded, and positive definite. In the boundary integral formulation method of structural analysis, however, the matrices are, usually, neither symmetric nor banded. See, for instance, the thesis by **Damisah** (1981).

If $\mathbf{C}$ is merely non-positive definite, then several unstable modes of vibration will arise, while for negative definite $\mathbf{C}$, all modes are unstable. Further details are given in the monograph on lambda matrices and vibrating systems by **Lancaster** (1966).

In systems where self-excited oscillations could occur, $\mathbf{C}$ and $\mathbf{K}$ may be replaced by the flutter matrices:

$$\begin{aligned} \mathfrak{C} &= \mathbf{C}_s + \rho V \mathbf{C}_a \\ \mathfrak{K} &= \mathbf{K}_s + \rho V^2 \mathbf{K}_a \end{aligned} \tag{4.2.3c}$$

where $\mathbf{C}_s$ and $\mathbf{K}_s$ are the structural damping and stiffness matrices respectively and $\mathbf{C}_a$, $\mathbf{K}_a$ are the aerodynamic damping and stiffness matrices, while ρ is the air density, and V the air speed.

The analysis of a conservative, holonomic mechanical system in terms of coordinates which are defined relative to a moving frame of reference gives rise to equations of motion which are rather more complicated than (4.2.1). Thus, for spinning structures, substantial gyroscopic effects may come into play, resulting in a Hermitian matrix eigenvalue problem:

$$\lambda^2 \mathbf{Mx} + \lambda \mathbf{C}_c \mathbf{x} + \mathbf{Kx} = \mathbf{0}$$

where **M** is real, symmetric and positive definite; $\mathbf{C}_c$ is Hermitian, and sometimes known as the *Corioli's matrix*; while **K** is the non-negative definite, real symmertic stiffness matrix. Further details are given by **Whittaker** (1952), **Gupta** (1974) and **Lancaster** (1966).

If we set aside aeroelastic considerations, and concentrate on the dynamics of a bladed disc assembly purely as a stable mechanical structure whose motion is, however, retarded by damping forces that are proportional to the wheel's velocity, then equation (4.2.3b) ensues. This quadratic lambda-matrix equation is a special form of what is generically known as the 'non-linear eigenvalue problem', **Ruhe** (1973), in contra-distinction to equation (4.2.1) which is linear.

The vast majority of eigenproblems are linear, for which several algorithms have been devised by Wilkinson and others. These have been implemented on digital computers by various software houses, for example - the *Numerical Algorithms Group* (NAG) of Great Britain.

4.2.2 Linearization of the Quadratic Eigenproblem

Duncan and **Collar** (1935) were probably the first to solve the quadratic eigenvalue problem, by transforming it to a linear form. Later, **Lancaster** (1966) presented an extensive exposition of the generalized lambda-matrix problem. Recently, Axel **Ruhe** (1973) published some algorithms for solving certain kinds of problems which cannot be linearized by Duncan and Collar's augmentation procedure.

The linearization strategy proposed by Duncan and Collar has remained basically the same for several years, and is now a standard feature of many vibration texts in which the eigensolution of viscously damped systems is discussed. The essence of the linearization procedure consists of tranforming the square matrices of order N into a $2N$-dimensional space, as follows:

$$\mathbf{A}\mathbf{y} = \lambda\mathbf{B}\mathbf{y} \tag{4.2.4a}$$

$$\mathbf{A} = \begin{bmatrix} \mathbf{M} & \mathbf{0} \\ \mathbf{0} & -\mathbf{K} \end{bmatrix} \begin{Bmatrix} \lambda\mathbf{x} \\ \mathbf{x} \end{Bmatrix} \tag{4.2.4b}$$

$$\mathbf{B} = \begin{bmatrix} \mathbf{0} & \mathbf{M} \\ \mathbf{M} & -\mathbf{C} \end{bmatrix} \begin{Bmatrix} \lambda \mathbf{x} \\ \mathbf{x} \end{Bmatrix} \tag{4.2.4c}$$

which can then be solved directly by applying the QZ algorithm. Alternatively, we may further reduce it to the 'standard' form:

$$\mathbf{Gz} = \lambda \mathbf{z} \tag{4.2.5a}$$

where **G** is the generalized matrix of the standard eigenvalue problem, and is given by

$$\mathbf{G} = \begin{bmatrix} -\mathbf{M}^{-1}\mathbf{C} & -\mathbf{M}^{-1}\mathbf{K} \\ \mathbf{0} & -\mathbf{I} \end{bmatrix} \begin{Bmatrix} \lambda \mathbf{x} \\ \mathbf{x} \end{Bmatrix} \tag{4.2.5b}$$

It is to be noted that this linearization process, by transforming an N-dimensional problem to that of $2N$, is very inefficient to implement numerically for large order systems, in terms of computer resources. In fact, for the type of huge matrices characteristic of aerospace structures, it may be impossible to find the required computation resources even on many 'main-frames'.

Duncan and Collar's usage of **M** to augment the matrix as in equation (4.2.4) above may be modified in a small but signifant way. We have observed, in several numerical experiments, that we may replace **M** by any arbitrary, non-singular matrix, $\mathbf{S}$. This is advantageous if, for instance, we want to use the QZ algorithm directly on the generalized form of the eigenproblem, as given in equation (4.2.4a). Thus, we may write:

$$\mathbf{A} = \begin{bmatrix} \mathbf{S} & \mathbf{0} \\ \mathbf{0} & -\mathbf{K} \end{bmatrix} \begin{Bmatrix} \lambda \mathbf{x} \\ \mathbf{x} \end{Bmatrix} \tag{4.2.6a}$$

$$\mathbf{B} = \begin{bmatrix} \mathbf{0} & \mathbf{S} \\ \mathbf{M} & -\mathbf{K} \end{bmatrix} \begin{Bmatrix} \lambda \mathbf{x} \\ \mathbf{x} \end{Bmatrix} \tag{4.2.6b}$$

and set $\mathbf{S}$ to the identity matrix **I** which is diagonal, rather than the mass matrix as in equations (4.2.4) which is banded in many 'consistent mass' finite element formulations.

An alternative to the matrix augmentation procedure - which is very difficult to implement for large order systems on commonly existing computers - is that proposed by **Gupta** (1974) for the eigensolutions of banded matrices. The strategy adopted in Gupta's scheme is to separate the solution steps into two divisions. In the first level, the damping present in the system is ignored, while a combination of the method of bisection and the Sturm sequence technique is used to locate selected roots of the undamped

system, **Gupta** (1973). The system's damping is introduced at the second stage, when the inverse iteration technique is applied to steer convergence towards one pair of complex eigenvalues and associated vectors at a time, starting from the real eigenvalue of the corresponding undamped system as a 'shift'. While Gupta's scheme is undoubtedly of great aid in the solution of *lightly damped structures*, convergence is not always towards the desired eigenpair in the complex plane which corresponds to the selected undamped root, in the presence of appreciable damping, as illustrated in Figure 4.2.1. This point is further high-lighted with respect to the generalized non-linear eigenvalue problem by **Ruhe** (1973).

4.3 A Strategy for Global Convergence

When the damping in a mechanical system is negligible, or its eigenproblem is constructed in such a way that the damping matrices are omitted, it is easy to obtain all - or, as many as may be desired - of the latent roots and vectors of the system. Thus, a global convergence scheme for undamped systems may be established; based, for example, on the method of inverse iterartion, together with the Gram-Schmidt orthogonalization procedure and the Rayleigh Quotient. For the more difficult case of the non-linear eigenvalue problem, one may not readily devise that type of strategy which would locate all the roots, when dealing with the size of matrices typical of practical structures. In order to preserve and exploit the banded nature of the eigenmatrices of such structures, some convergence strategies have been published, for instance, by Gupta and Ruhe, *op cit*. These are based on local convergence. This means that if we know *a priori* the approximate point in the complex plane where a particular root is located, we can place the 'shift' of iteration anywhere in that region and commence an iterative search in order to converge on that root. Unlike in the undamped case, however, we cannot employ orthogonalizations of the Gram-Schmidt type to 'deflate' or 'purify' the initial iterant vectors. Hence, successful convergence on one eigenpair does not offer us any advantage in the subsequent search for the other eigenvalues in the subspace spanned by the eigensystem. However, it has been possible for us to steer convergence away from previously computed vectors by using a pseudo orthogonalization procedure. The scheme requires the application of Gram-Schmidt procedure to make the *real parts* of the complex vectors already computed orthogonal

to the undamped mode shape corresponding to the complex mode which we seek. An elegant mathematical proof that such an empirical scheme works, and the conditions under which it does not, has not yet been found. Numerical analysts and other mathematicians† are currently active in this area of research.

The engineering problem with which we are faced in this chapter is how to model, and solve with limited computer resources, the effect of energy dissipation through aerodynamic damping on the modal properties of bladed disc assemblies. Using the lumped parameter method, and the 3 degree-of-freedom per blade model as discussed in Chapter 2 for a 30-bladed disc, we immediately have a very huge quadratic eigenproblem. Since, in this particular case, our matrices are already in a band symmetric form, Gupta's algorithm may appear to suit the problem. However, we are dealing with systems in which the damping is not slight (e.g. $Q=50$) and where several roots are pathologically close together. It does not appear as if that type of problem may be adequately solved by Gupta's (1974) algorithm.

If the damping in the system is *proportional* to either the mass or the stiffness, the task of computing the eigensolution becomes very much simplified. That is, however, a special case. Generally, the damping in the system is neither proportional nor slight. Hence, we have to devise a workable algorithm that converges to all the roots of this type of dynamic system. Most of the algorithms for computing the eigenvalues of the non-linear problem are based on inverse iteration.

The effectiveness of any inverse iteration strategy depends on the selection of appropriate initial iterants. Before deciding on the selection of iterants for this quadratic problem, we carried out several empirical studies on the relationship between the eigenpairs of damped systems and their corresponding undamped systems.

The following observations are pertinent, the first of which is very well known.

1. The eigenvectors of *proportionally damped* systems, ϕ_r^* are identical to those of the corresponding undamped system, ϕ_r. The eigenvalues of both systems are, however, different.

2. When the damping is slight, albeit non-proportional, then the eigensolutions of the

† **Adeyeye, J. O.** (1979). The calculation of eigenvalues for Laplace's operator using boundary integral equations. *MSc Thesis*, Imperial College, Department of Mathematics.

damped and undamped systems are almost the same:

$$\lambda_r^* = \mu_r + i\nu_r \simeq \lambda_r;\ \nu_r \to 0$$
$$\phi_r^* = \chi_r + i\phi_r \simeq \phi_r;\ \phi_r \to 0$$

3. If the damping in the system is approximately *not concentrated in only a few coordinates* in the system, then the real components of the eigenvectors in the damped and undamped systems differ only slightly, although the eigenvalues, and the imaginary components of the eigenvectors may be substantially different in the two systems.

It is evident from the foregoing that the damped 'mode shapes' (*ie* real components of the eigenvectors) of many systems resemble the corresponding modes of the equivalent undamped system. It seems judicious, therefore, to select ϕ_r as the initial iterant vector, i.e.

$$\mathcal{R}_e\phi_0^* = \phi_n$$
$$\mathcal{I}_m\phi_0^* = 0$$

rather than any other arbitrary vector. This contrasts with Gupta's scheme, for which elements of $\mathcal{R}_e\phi_0^*$ are all unity, while $\mathcal{I}_m\phi_0^* = 0$.

Choice of initial eigenvalue

Whereas all the latent roots of an undamped mechanical system may be found on a *line* - the imaginary axis - on the complex plane, it requires the entire *plane* to contain those of the damped system, since in the latter case each root has both real and imaginary components, i.e. $\lambda_r^* = \mu_r + j\nu_r$, where μ_r is the decay part, and ν_r is the oscillatory part of the rth eigenvalue. Thus, we may plot the eigenvalue of the rth mode schematically as shown in Figure 4.3.1.

If we are dealing with a stable structural system for which damping is slight, and the latent roots of the system are well-separated, then the shifts of iteration for each of the complex eigenvalue may be placed at those points on the imaginary axis which represent the eigenvalues of the system when damping is removed, i.e. $\lambda_0^* = j\omega_r^2 = \lambda_r$. That is the central part of the strategy adopted by Gupta (1974).

However, if damping is not slight, it is necessary to accelerate convergence towards the required complex root by shifting the origin of iteration to a location in the complex plane, to be determined by the amount of damping actually present in the model, as discussed presently.

4.3.1 Viscous Damping Model

Using this model, the equations of motion for a body under free vibration conditions may be cast in matrix form:

$$\mathbf{M}\ddot{\mathbf{x}} + \mathbf{C}\dot{\mathbf{x}} + \mathbf{K}\mathbf{x} = \mathbf{0} \tag{4.3.1}$$

where **M**, **C**, and **K** are real and square matrices, and the solution for the displacement is assumed to be in the form:

$$\mathbf{x} = \mathbf{X}e^{\lambda t} \tag{4.3.2}$$

which, if λ and **X** are complex quantities, satisfies equation (4.3.1) exactly. However, we may assume *as an approximate solution* that the imaginary components of λ and **X** are small, so that $\mathbf{x}=\mathbf{X}_o e^{\lambda_o t}$, where both λ_o and $\mathbf{X}_o$ have only real components.

If we neglect damping in equation (4.3.1), then the eigenproblem becomes:

$$\mathbf{K}\mathbf{X} = \lambda^2\mathbf{M}\mathbf{X} \tag{4.3.3}$$

leading to an eigenvalue, λ_r^2 and eigenvector $\mathbf{X}_r$, for the rth mode.

Since we do not yet know the exact eigenpair (λ_r^*, $\mathbf{X}_r^*$) for the damped system, it is reasonable to suppose - as a first approximation - that the roots and vectors of equation (4.3.3) are 'close' to those of (4.3.1). Hence, by making use of equations (4.3.1) and (4.3.2), and assuming that

$$|\lambda_o - \lambda_r| \Rightarrow 0,$$
$$|\mathbf{X}_o|_2 - |\mathbf{X}_r|_2 \Rightarrow 0,$$

we obtain:

$$\lambda_o^2\mathbf{X}_o^T\mathbf{M}\mathbf{X}_o + \lambda_o\mathbf{X}_o^T\mathbf{C}\mathbf{X}_o + \mathbf{X}_o^T\mathbf{K}\mathbf{X}_o = \varepsilon \tag{4.3.4}$$

where λ_o and $\mathbf{X}_o$ are approximate solutions to equation (4.3.1), and ε is a residual quantity which does not actually vanish due to the fact that λ_o and $\mathbf{X}_o$ do not satisfy equation (4.3.1) exactly.

Now, since **M**, **C**, and **K** are all real, while the imaginary component of $\mathbf{X}_o$ is assumed to be non-existent for the mean while, we have, from equation (4.3.4):

$$\lambda_o^2 m_r + \lambda_o c_r + k_r = 0 \tag{4.3.5}$$

where

$$m_r = \mathbf{X}_o^T\mathbf{M}\mathbf{X}_o$$

$$c_r = \mathbf{X}_o^T \mathbf{C} \mathbf{X}_o$$
$$k_r = \mathbf{X}_o^T \mathbf{K} \mathbf{X}_o$$

are all *real scalars*. Equation (4.3.5) is a quadratic algebraic equation in λ_o, with the solution:

$$\lambda_o = \frac{-c_r}{2m_r} \pm j\sqrt{\frac{k_r}{m_r} - \frac{c_r^2}{4m_r^2}} \tag{4.3.6}$$

If ω_r denotes the natural frequency of oscillation for the undamped system at its rth mode, then an approximation to the complex eigenvalue of the rth damped mode is, from equation (4.3.6),

$$\lambda_o = \beta_r\omega_r \pm j\omega_r\sqrt{1-\beta_r^2} \tag{4.3.7}$$

where $\omega_r = \sqrt{k_r/m_r}$ and $\beta_r = c_r/2m_r\omega_r$, which may be used as a shift frequency in an iteration procedure. It may be noted that in Gupta's scheme, the shift frequency is always set at the undamped natural frequency of an equivalent structural system, i.e. $\beta_r=0$, since c_r is not calculated.

The following observations may be made concerning the foregoing.

1. If the imaginary components of the eigenvector of the rth mode are small, and if in addition the undamped mode shapes are very similar to those of the damped system at this rth mode, then equation (4.3.7) is a very good approximation to the complex root λ_r^* which we seek.

2. In the special case of proportionally damped systems, the analysis becomes greatly simplified. This is because

$$\mathbf{X}_r^* \equiv \mathbf{X}_o \equiv \mathbf{X}_r,$$

hence, λ_o is the required eigenvector of the damped system, so that no iteration need be carried out at all. For each mode, therefore, once the undamped eigenpair λ_r and $\mathbf{X}_r$ are known, the damped eigenvalue, λ_r^* is easily obtained from the computation of m_r, k_r and c_r (which is not so costly, since the matrices are usually banded) and the application of equation (4.3.7). The dependence of the eigenvalue components - real and imaginary - upon the level of damping present in the system model as represented by β_r is shown in Figure 4.3.2a, for a four degree-of-freedom model.

3. A further simplification in the relationship between the damped and undamped eigenvalues ensues if the damping within the system is known or assumed to be proportional to the *mass* only. This is shown in figure 4.3.2b, from which it is seen that the modal damping, β_r is actually invariant with the mode, unlike in the previous case.

4. If the mode shapes are orthonormalized with respect to the mass matrix, then $m_r=1$, $k_r=\omega_r^2$, and the task of calculating λ_o is even more simplified.

4.3.2 Hysteretic Damping Model

Under free vibration conditions, the familiar equaions of motion for a hysteretically damped system is, in matrix form,

$$\mathbf{M}\ddot{\mathbf{x}} + \mathbf{K}\mathbf{x} + j\mathbf{H}\mathbf{x} = \mathbf{0} \tag{4.3.8}$$

Upon applying the same reasoning as before, we obtain an analogous equation to equation (4.3.4), thus:

$$\lambda_o^2\mathbf{X}_o^T\mathbf{M}\mathbf{X}_o + j\mathbf{X}_o^T\mathbf{H}\mathbf{X}_o + \mathbf{X}_o^T\mathbf{K}\mathbf{X}_o = \varepsilon \tag{4.3.9}$$

which yields

$$\lambda_o^2 m_r + k_r + jh_r \tag{4.3.10}$$

where $j=\sqrt{-1}$, $h_r=\mathbf{X}_o^T\mathbf{H}\mathbf{X}_o$ while m_r and k_r are as defined in equation (4.3.5).

The shift frequency is subsequently obtained as:

$$\frac{h_r}{\sqrt{2m_r[(k_r^2+h_r^2)^{1/2} + k_r]}} + i\,\frac{(k_r^2+h_r^2)^{1/2} + k_r}{2m_r} \tag{4.3.11}$$

When, as is customary, the mode-shapes are normalised so that $\|\mathbf{X}_o\|_2 = 1$, and $m_r = 1$, then the equation above may be further reduced to

$$\lambda_o = -h_r/\delta_r + i\delta_r/2 \tag{4.3.12}$$

where $\delta_r = \sqrt{2[\sqrt{(k_r^2+h_r^2)} + k_r]}$

4.3.3. General Case

In the generalized case of the damped mechanical system, the matrix equation of motion is:

$$\mathbf{M}\ddot{\mathbf{x}} + \mathbf{C}\dot{\mathbf{x}} + \mathbf{K}\mathbf{x} + i\mathbf{H}\mathbf{x} = \mathbf{0} \tag{4.3.13}$$

which, upon pre- and post-multiplication by $\mathbf{X}_o^T$ and $\mathbf{X}_o$ respectively, and proceeding as before, becomes:

$$\lambda_o^2\mathbf{X}_o^T\mathbf{M}\mathbf{X}_o + \lambda_o\mathbf{X}_o^T\mathbf{C}\mathbf{X}_o + \mathbf{X}_o^T\mathbf{K}\mathbf{X}_o + i\mathbf{X}_o^T\mathbf{H}\mathbf{X}_o = \varepsilon \tag{4.3.14}$$

We may simplify this to yield a quadratic equation in λ_o,

$$\lambda_o^2 m_r + \lambda_o c_r + k_r + jh_r = 0 \tag{4.3.15a}$$

the solution of which is

$$\lambda_o = -(c_r/2m_r + h_r p_r m_r) + p_r/2 \tag{4.3.15b}$$

where

$$p_r = \left[2\left\{\left(\frac{k_r}{m_r} - \frac{c_r^2}{4m_r^2}\right) + \sqrt{\left(\frac{k_r}{m_r} - \frac{c_r^2}{4m_r^2}\right)^2 + \left(\frac{h_r}{m_r}\right)^2}\right\}\right]^{1/2}$$

and the modal properties m_r, h_r, k_r and c_r are as previously defined.

4.3.4. The algorithm

Equation (4.2.5) may be expanded to yield two simultaneous equations, from which we may obtain an iterative procedure. Thus we may write:

$$(\lambda^2\mathbf{I} + \lambda\mathbf{C} + \mathbf{K})\mathbf{y}_{i+1} = \mathbf{K}\mathbf{x}_i - \lambda\mathbf{I}\mathbf{y}_i$$
$$\mathbf{K}\mathbf{x}_{i+1} = (\mathbf{C} + \lambda\mathbf{I})\mathbf{y}_{i+1} - \mathbf{I}\mathbf{y}_i \tag{4.3.16}$$

(N.B. The identity matrix **I** may be replaced by the mass matrix, **M**). An alternative pair of iterative equations may be formed, again from an expansion of equation (4.2.5), as follows:

$$(\lambda^2\mathbf{I} + \lambda\mathbf{C} + \mathbf{K})\mathbf{x}_{i+1} = (\lambda\mathbf{I} + \mathbf{C})\mathbf{x}_i + \mathbf{I}\mathbf{y}_i$$
$$\mathbf{I}\mathbf{y}_{i+1} = \lambda\mathbf{I}\mathbf{x}_{i+1} - \mathbf{I}\mathbf{x}_i \tag{4.3.17}$$

However, although the following pair of equations is algebraically correct, it is surprising, as **Wilkinson** (1965) has noted, that using them for inverse iteration does **NOT** work!

$$(\lambda^2\mathbf{I} + \lambda\mathbf{C} + \mathbf{K})\mathbf{x}_{i+1} = (\lambda\mathbf{I} + \mathbf{C})\mathbf{x}_i + \mathbf{I}\mathbf{y}_i$$
$$(\lambda^2\mathbf{I} + \lambda\mathbf{C} + \mathbf{K})\mathbf{y}_{i+1} = \mathbf{K}\mathbf{x}_i - \lambda\mathbf{I}\mathbf{y}_i \tag{4.3.18}$$

The algorithmic steps are now given. It may be noted that although the algorithm is essentially a strategy for *local* convergence, the algorithm is nevertheless constructed in such a way that all the eigenvalues may be converged upon automatically. Hence, it is effectively a strategy for *global* convergence.

1. solve for the rth mode eigen-pair, (ω_r, ϕ_r), by neglecting all forms of damping within the system

2. calculate the *shift frequency*, λ_o, using the procedure described in §4.3.1 to §4.3.3; and set $\mathbf{x}_o = \phi_r$, $\mathbf{y}_o = \lambda_o \mathbf{x}_o$; and normalise such that

$$\mathbf{x}'_o = \mathbf{x}_o/|\mathbf{x}_o|_\infty; \quad \mathbf{y}'_o = \mathbf{y}_o/|\mathbf{y}_o|_\infty$$

3. set up the dynamic stiffness matrix,

$$\mathbf{D}_o = \mathbf{D}(\lambda_o) = \lambda^2\mathbf{M} + \lambda\mathbf{C} + \mathbf{K}$$

4. decompose $\mathbf{D}_o$ into the the LU factorizations.

5. set up the iteration vector for the ith step

$$\mathbf{q}_i = (\lambda_o\mathbf{M} + \mathbf{C})\mathbf{x}'_i + \mathbf{M}\mathbf{y}_i$$

6. solve for $\mathbf{x}_{i+1}$, $\mathbf{y}_{i+1}$, λ_o in:

$$\mathbf{D}_o\mathbf{x}_{i+1} = \mathbf{q}_i$$

$$\mathbf{y}_{i+1} = \lambda_o\mathbf{x}_{i+1} - \mathbf{x}'_i$$

$$\lambda_{i+1} = y'_{i+1}/x'_{i+1}$$

7. test for convergence
   (a) if $|(\mu_{i+1} - \mu_i)/\mu_{i+1}| < \epsilon$ then EXIT; ELSE increment iteration step and go to step 5.
   (b) if not yet convergence after a pre-determined number of iteration steps, say 10, but convergence is otherwise proceeding in the right direction, then

$$\mathbf{x}_o = \mathbf{x}'_i$$

$$\mathbf{y}_o = \mathbf{y}'_i$$

$$\lambda_o = \lambda_i$$

go to step 3.

   (c) if no convergence after N iterations, EXIT with a failure flag.

The algorithm outlined above differs from the due to by Gupta (1974) in the following principal respects.

(a) in lieu of Gupta's equation (16), we use in our step 6, the expression

$$\mathbf{y}_{i+1} = \lambda_o\mathbf{x}_{i+1} - \mathbf{x}'_i$$

(b) the estimate of the eigenvalue obtained at the ith iteration was ob-

tained from the application of the 'Rayleigh Quotient' in Gupta's equation (17), which is different from the generalized Rayleigh Quotient introduced by **Lancaster** (1966, *p*72) for the non-linear eigenvalue problem as defined, with notation to suit the problem at hand, as

$$R(\mathbf{x}_i,\lambda_o) = \mathbf{x}_i^H \mathbf{D}_o \mathbf{x}_i \;/\; \mathbf{x}_i^H \mathbf{D}_o' \mathbf{x}_i$$

where the symbol $'$ denotes partial differetiation of the matrix with respect to λ_o, and ^{H} denotes a Hermitian vector transposition.

According to **Ruhe** (1973), the existence of the Rayleigh's functional $R(\mathbf{x},\lambda)$ is not always certain for the non-linear eigenproblem, so that Gupta's definition - and application - of the 'Rayleigh Quotient' for this class of problem may probably be non-existent or inapplicable. In view of the foregoing, therefore, the estimate of λ_i - after the *i*th iteration - are obtained in the present algorithm without the use of Rayleigh's functional, but simply by taking the ratio of corresponding elements of $\mathbf{x}_i$ and $\mathbf{y}_i$.

Elements of the initial iterant vector, $\mathbf{x}_o$ are usually selected arbitrarily; in Gupta's implementation, for example, they were all assigned unit values. In the present algorithm, however, the initial vector is set identical to the undamped mode shape, i.e. $Re\mathbf{x}_o = \phi_r$.

(d) Finally, instead of setting $\lambda_o = j\omega_r$ in all cases, we have used the procedures of section 4.3 to provide estimates for the complex shift frequency at each stage.

It is believed that the ammendments of Gupta's algorithm, as described above, further enhances the capability of an already useful numerical tool for extracting the eigen-solutions of damped structural systems.

4.4. Application to Bladed Disc Assemblies

The algorithm described above for the extraction of the latent roots and vectors of systems exhibiting non-proportional damping was implemented on a digital computer (CDC 6600) in order to investigate the dependence of the eigensolution of a mistuned assembly upon the nature and distribution of damping within the system. The assembly has 10 blades whose cantilever frequencies are randomly scattered as previously described in Chapter 2, when damping was not taken into account in formulating the equations of motion. The lumped parameter method is used here, as in the earlier chapter.

Figure 4.4.1 shows a modification of the basic lumped parameter model previously used in §2.1. Unlike in figure 2.1.1, however, each blade is now connected to ground at its tip by a dash-pot to simulate aerodynamic damping. Material damping in the blades is accounted for by placing hysteretic elements in each blade. The damping present in the disc itself is assumed to be relatively unimportant compared to blade damping, but may be accounted for in full, if desired. Extra dashpots are placed in the blades, in parallel with the hysteretic dampers, as shown in the figure.

The eigensolution of this model as obtained from the digital computer implementation of our algorithm is presented in Table 4.4.1.

4.5 Concluding Remarks

A lumped parameter model, based on Disc 10A, has been used to obtain the natural frequencies and mode-shapes of free vibration of a damped bladed disc. The following observations may be drawn.

(*a*) When damping is light, (e.g. $Q \approx 1000$) the frequencies and mode shapes are little affected by the nature of the damping; i.e. whether it is proportional or otherwise.

(*b*) As damping levels are increased, ($Q \approx 100$) the real parts of the eigenvalues (which are negative for stable modes) are usually found to increase, indicating increasing modal damping, while the imaginary parts of the of eigenvalues (which represent oscillatory motion) retain almost the same values as for the corresponding undamped modes.

(*c*) When the distribution of damping elements within the system is 'smooth', even if random, then the real components of the eigenvectors of then the real components of the damped system are almost linearly dependent upon the mode shapes of the undamped system. Two extreme cases of 'smoothnes' may be cited. In the one case, damping is wholly proportional to the stiffness, so that we have a 'uniform' type of smoothness, and the eigenvectors of the damped and undamped systems - when normalized to within an arbitrary multiplier - are entirely identical. At the other extreme, when all the damping in the system may be as med to be lumped at only one coordinate within the system, the damped eigenvectors are very different from the undamped mode shapes. **Kirshenboim** (1981) has recently investigated in detail the extent to which the eigenvectors of damped systems deviate

from those of the corresponding undamped system, as the damping is varied from 'extremely smooth' to 'localised'.

Fig. 4.2.1 *Typical convergence paths in inverse iteration for damped eigenvalues*

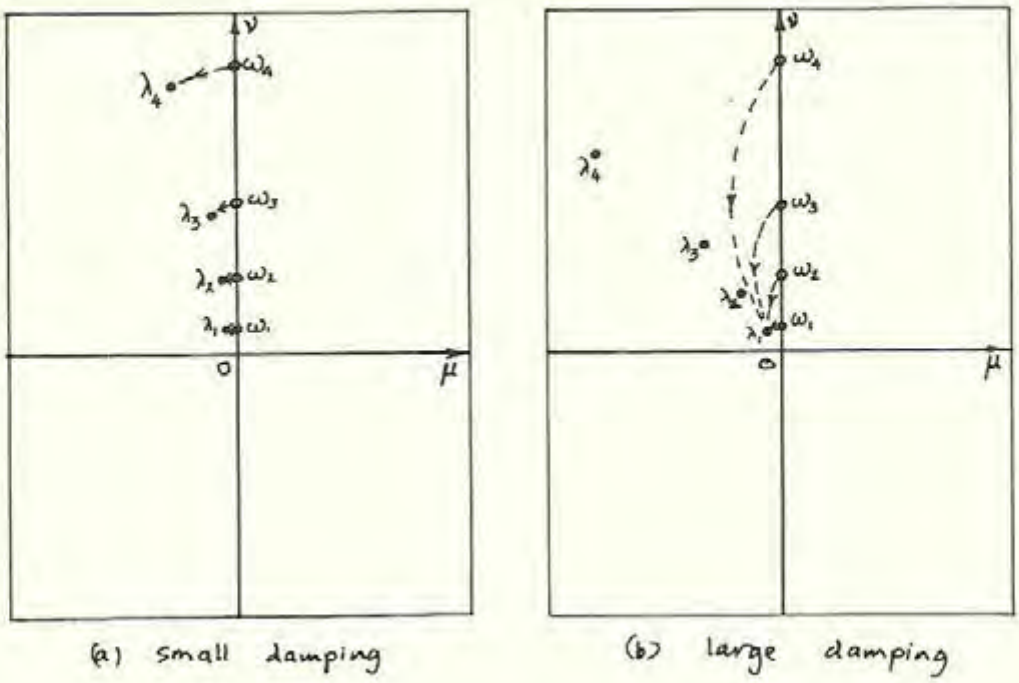

Fig. 4.3.1 *Eigensystems and characteristic motions of damped and undamped systems*

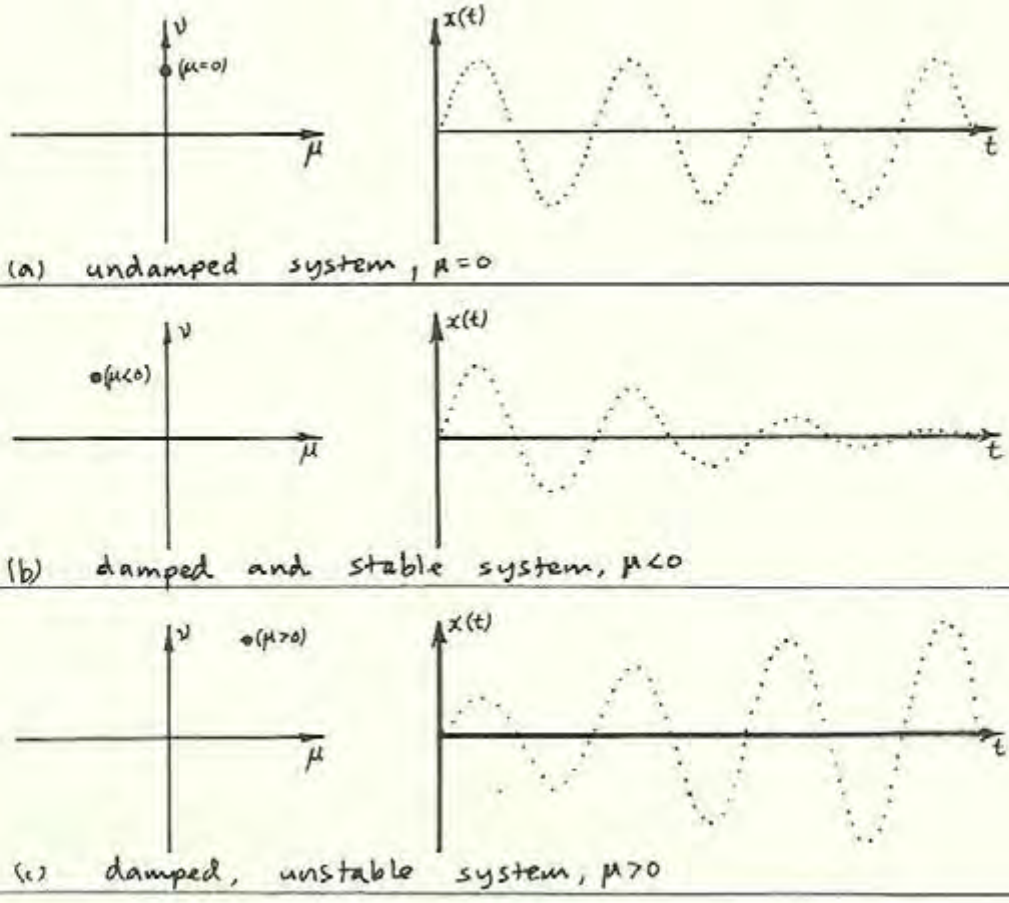

Fig. 4.3.2 *Variation of complex latent root with damping*

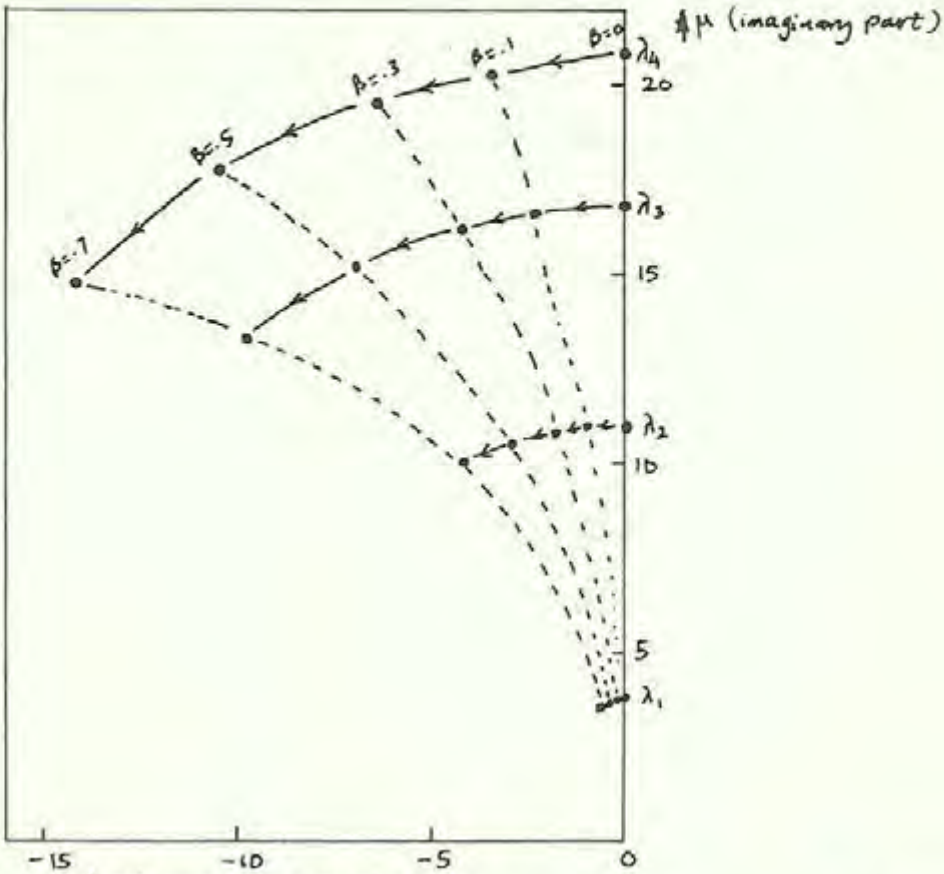

(a) viscous damping matrix ∝ stiffness matrix : $[C] = \beta[K]$

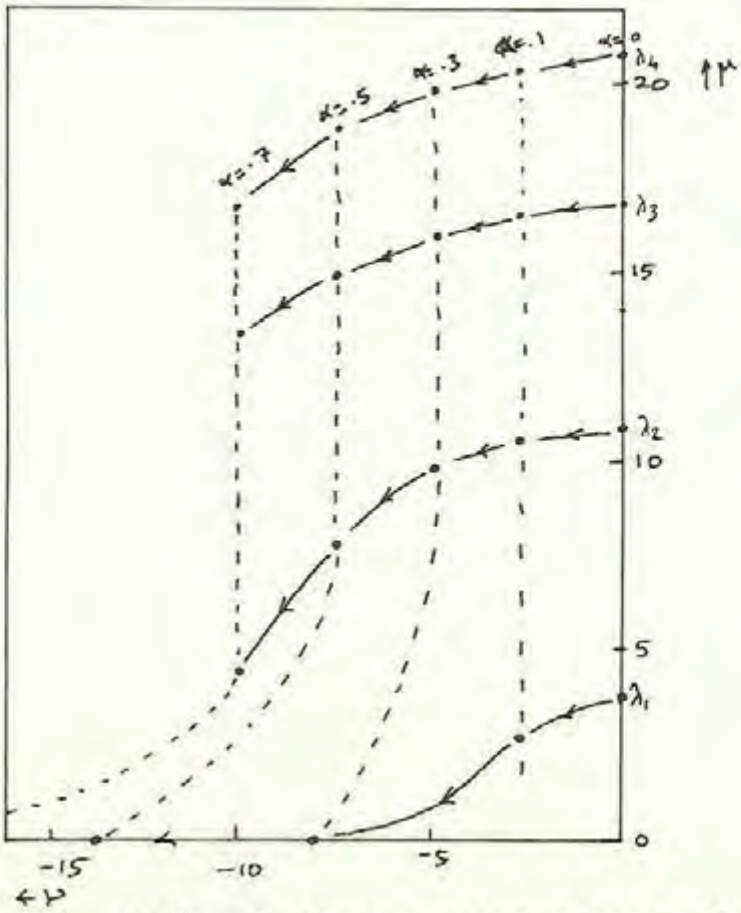

(b) Viscous damping matrix ∝ mass matrix : $[C] = \alpha[M]$

Fig. 4.4.1 *Mathematical model of a bladed disc with aerodynamic damping*

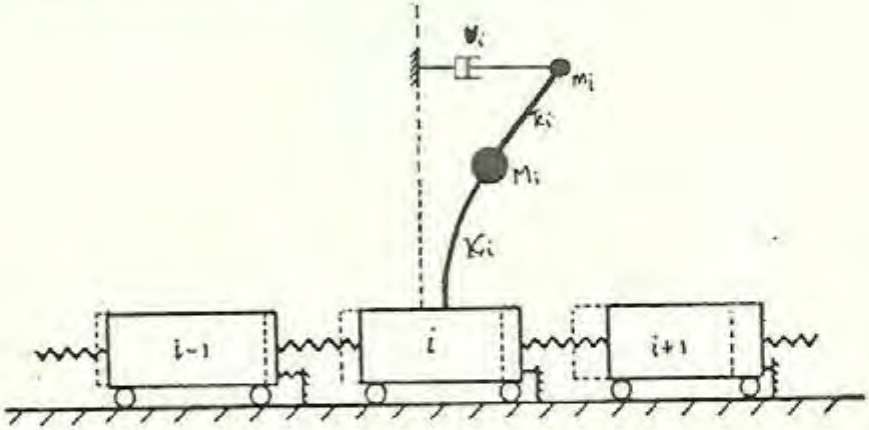

$$K_i = K_i + jH_i + wC_i$$

$$k_i = k_i + jh_i + wc_i$$

i	m_i	M_i	k_i	K_i			v_i
1	.08948	.17896	2.08779596E+05	1.41841852E+07	0	0	
2	.08948	.17896	2.18078159E+05	1.48159162E+07	0	0	
3	.08948	.17896	2.13137060E+05	1.44802251E+07	0	0	
4	.08948	.17896	2.06448412E+05	1.40258080E+07	0	0	
5	.08948	.17896	2.04781221E+05	1.39125414E+07	0	0	
6	.08948	.17896	2.03388321E+05	1.38179098E+07	0	0	
7	.08948	.17896	2.07527843E+05	1.40991429E+07	0	0	
8	.08948	.17896	2.07403165E+05	1.40906725E+07	0	0	
9	.08948	.17896	2.00609239E+05	1.36291030E+07	0	0	
10	.08948	.17896	2.06806009E+05	1.40501026E+07	0	0	
[H] 1	0	0	350	10000			
2			420	12000			
3			410	9000.			
4			390	11000			
5			400	10000			
6			450	12000			
7			380	18000			
8			390	15000			
9			405	12000			
10			375	11000			
[C] 1	0	0	.5325	4.635			25.
2			.5325	4.635			22.
3			.5325	4.635			18.
4			.5325	4.635			23.7
5			.5325	4.635			20.1
6			.5325	4.635			21.5
7			.5325	4.635			22.
8			.5325	4.635			19.
9			.5325	4.635			18.
10			.5325	4.635			21.7

Table 4.4.1 *Eigensolutions of a damped bladed disc*

EIGENVALUES IN ASCENDING ORDER

1.	-1.0298 + J(-.16819156E-05)	.000 HZ
2.	-46.6148 + J(-.97488953E+03)	155.150 HZ
3.	-43.1151 + J(-.97504225E+03)	155.183 HZ
4.	-116.0722 + J(-.13853678E+04)	220.488 HZ
5.	-108.7025 + J(-.13910216E+04)	221.388 HZ
6.	-126.8727 + J(-.14488355E+04)	230.740 HZ
7.	-131.8782 + J(-.14532253E+04)	231.288 HZ
8.	-135.8348 + J(-.14637673E+04)	232.966 HZ
9.	-143.0715 + J(-.14691846E+04)	233.828 HZ
10.	-135.5537 + J(-.14859322E+04)	236.494 HZ
11.	-99.1943 + J(-.16580308E+04)	263.884 HZ
12.	-77.8376 + J(-.17484565E+04)	278.275 HZ
13.	-77.7979 + J(-.17639937E+04)	280.748 HZ
14.	-16.0078 + J(-.23194103E+04)	369.146 HZ
15.	-15.8594 + J(-.23225842E+04)	369.651 HZ
16.	-7.5292 + J(-.30145446E+04)	479.780 HZ
17.	-7.5552 + J(-.30165890E+04)	480.107 HZ
18.	-7.5209 + J(-.34706476E+04)	552.371 HZ
19.	-7.4910 + J(-.34749187E+04)	553.050 HZ
20.	-7.8232 + J(-.36289447E+04)	577.584 HZ
21.	-18.0257 + J(-.11415756E+05)	1816.874 HZ
22.	-18.5657 + J(-.11451847E+05)	1822.618 HZ
23.	-18.9852 + J(-.11598894E+05)	1839.671 HZ
24.	-19.9283 + J(-.11613113E+05)	1848.284 HZ
25.	-19.8326 + J(-.11661460E+05)	1855.979 HZ
26.	-22.5613 + J(-.11748065E+05)	1869.763 HZ
27.	-21.5172 + J(-.11791429E+05)	1876.684 HZ
28.	-22.1817 + J(-.11857542E+05)	1887.186 HZ
29.	-23.0717 + J(-.11870431E+05)	1889.670 HZ
30.	-22.8382 + J(-.12074885E+05)	1921.778 HZ

MODE 1 -1.030 +J(-.0000) .000 HZ

BLADE	REAL	IMAGINARY	MODULUS	PHASE	DIA	DFT	COSINE	SINE	EIGENVALUE CHECK
1	1.000 +J(	0)	1.000	0	0	100.0	-100.0	-.0	-1.030 + J(-.0000)
2	1.000 +J(	.0000)	1.000	.00	1	0	.0	-.0	-1.030 + J(-.0000)
3	1.000 +J(	.0000)	1.000	.00	2	.0	.0	.0	-1.030 + J(-.0000)
4	1.000 +J(	-.0000)	1.000	-.00	3	.0	-.0	.0	-1.030 + J(-.0000)
5	1.000 +J(	-.0000)	1.000	-.00	4	.0	-.0	-.0	-1.030 + J(-.0000)
6	1.000 +J(	.0000)	1.000	.00	5	.0	.0	.0	-1.030 + J(-.0000)
7	1.000 +J(	.0000)	1.000	.00					-1.030 + J(-.0000)
8	1.000 +J(	.0000)	1.000	.00					-1.030 + J(-.0000)
9	1.000 +J(	-.0000)	1.000	-.00					-1.030 + J(-.0000)
10	1.000 +J(	-.0000)	1.000	-.00					-1.030 + J(-.0000)

MODE 2 -46.615 +J(-974.8895) 155.150 HZ

BLADE	REAL	IMAGINARY	MODULUS	PHASE	DIA	DFT	COSINE	SINE	EIGENVALUE CHECK
1	-.979 +J(	-.0283)	.979	-178.34	0	.8	-.3	.8	-46.615 + J(-974.8897)
2	-.671 +J(	-.1177)	.681	-170.05	1	100.0	-18.9	-100.0	-46.615 + J(-974.8890)
3	-.142 +J(	-.1933)	.240	-126.23	2	1.4	1.1	.9	-46.615 + J(-974.8910)
4	.478 +J(	-.1868)	.517	-22.37	3	.7	.7	.3	-46.615 + J(-974.8894)
5	.911 +J(	-.1390)	.921	-8.68	4	.8	.2	-.8	-46.615 + J(-974.8895)
6	1.000 +J(	0)	1.000	0	5	1.3	.7	-1.1	-46.615 + J(-974.8897)
7	.691 +J(	.1251)	.702	10.27					-46.615 + J(-974.8901)
8	.137 +J(	.2035)	.245	56.08					-46.616 + J(-974.8908)
9	-.486 +J(	.2270)	.536	154.97					-46.615 + J(-974.8903)
10	-.907 +J(	.1285)	.916	171.94					-46.614 + J(-974.8896)

MODE 3 -43.115 +J(-975.0423) 155.183 HZ

BLADE	REAL	IMAGINARY	MODULUS	PHASE	DIA	DFT	COSINE	SINE	EIGENVALUE CHECK
1	-.208 +J(	.1928)	.283	137.11	0	1.2	.2	1.2	-43.116 + J(-975.0422)
2	-.718 +J(	.1172)	.727	170.73	1	100.0	100.0	-10.8	-43.114 + J(-975.0425)
3	-.984 +J(	.0213)	.984	178.76	2	2.1	-.7	-2.0	-43.116 + J(-975.0423)
4	-.876 +J(	-.1608)	.890	-169.59	3	.8	.8	-.5	-43.115 + J(-975.0422)
5	-.426 +J(	-.2110)	.475	-153.65	4	1.2	-.3	1.1	-43.115 + J(-975.0421)
6	.202 +J(	-.2008)	.285	-44.67	5	1.4	-1.4	-.1	-43.115 + J(-975.0416)
7	.739 +J(	-.1075)	.747	-8.28					-43.115 + J(-975.0416)
8	1.000 +J(	.0000)	1.000	.00					-43.115 + J(-975.0417)
9	.902 +J(	.1278)	.911	8.07					-43.116 + J(-975.0418)
10	.415 +J(	.2127)	.467	27.12					-43.113 + J(-975.0424)

MODE 4 -116.072 +J(-1385.3678) 220.488 HZ

BLADE	REAL	IMAGINARY	MODULUS	PHASE	DIA	DFT	COSINE	SINE	EIGENVALUE CHECK
1	-.769 +J(	-.1476)	.783	-169.14	0	2.8	2.5	2.3	-116.072 + J(-1385.3674)
2	-.432 +J(	-.0113)	.432	-178.50	1	.8	1.0	.3	-116.073 + J(-1385.3682)
3	.348 +J(	-.0540)	.349	-8.88	2	100.0	85.1	-100.0	-116.072 + J(-1385.3692)
4	.834 +J(	.1629)	.850	11.05	3	14.2	-16.7	2.8	-116.072 + J(-1385.3677)
5	.157 +J(	-.0186)	.158	-7.10	4	6.2	-3.6	-6.5	-116.073 + J(-1385.3681)
6	-.841 +J(	-.1151)	.849	-172.20	5	10.7	9.7	8.4	-116.073 + J(-1385.3677)
7	-.560 +J(	-.0133)	.560	-178.64					-116.074 + J(-1385.3680)
8	.401 +J(	.0241)	.402	3.43					-116.070 + J(-1385.3680)
9	1.000 +J(	0)	1.000	0					-116.072 + J(-1385.3674)
10	-.081 +J(	.0771)	.089	128.55					-116.076 + J(-1385.3669)

MODE 5 -109.702 +J(-1391.0216) 221.388 HZ

BLADE	REAL	IMAGINARY	MODULUS	PHASE	DIA	DFT	COSINE	SINE	EIGENVALUE CHECK
1	.288 +J(	.0065)	.289	1.29	0	4.6	-1.5	5.1	-109.703 + J(-1391.0248)
2	-.551 +J(	-.0684)	.556	-172.93	1	1.2	-1.2	.6	-109.703 + J(-1391.0229)
3	-.748 +J(	.0732)	.752	174.42	2	100.0	100.0	55.1	-109.702 + J(-1391.0208)
4	.125 +J(	-.0334)	.129	-15.01	3	7.7	-4.8	-7.3	-109.704 + J(-1391.0193)
5	1.000 +J(	.0000)	1.000	.00	4	5.2	-5.0	3.3	-109.703 + J(-1391.0215)
6	.410 +J(	.0638)	.415	8.82	5	3.4	3.3	2.0	-109.702 + J(-1391.0224)
7	-.710 +J(	-.0735)	.714	-174.09					-109.704 + J(-1391.0211)
8	-.831 +J(	.0604)	.833	175.84					-109.703 + J(-1391.0214)
9	.310 +J(	-.0539)	.314	-9.88					-109.702 + J(-1391.0190)
10	.917 +J(	.0696)	.919	4.34					-109.703 + J(-1391.0220)

MODE 6 -126.873 +J(-1449.8359) 230.748 HZ

BLADE	REAL	IMAGINARY	MODULUS	PHASE	DIA	DFT	COSINE	SINE	EIGENVALUE CHECK
1	-.388 +J(	-.0213)	.389	-176.85	0	2.7	2.2	1.7	-126.874 + J(-1449.8352)
2	.262 +J(	.2221)	.343	40.33	1	2.7	2.3	-1.4	-126.873 + J(-1449.8358)
3	.373 +J(	-.1098)	.389	-16.42	2	3.7	-3.2	1.9	-126.873 + J(-1449.8360)
4	-.367 +J(	-.2171)	.426	-149.38	3	100.0	.0	-100.0	-126.873 + J(-1449.8391)
5	-.499 +J(	.2648)	.565	152.06	4	51.8	-39.0	34.1	-126.873 + J(-1449.8398)
6	.935 +J(	.1128)	.942	6.88	5	17.4	13.2	11.4	-126.873 + J(-1449.8353)
7	-.179 +J(	-.5641)	.592	-107.59					-126.873 + J(-1449.8367)
8	-.741 +J(	.4473)	.865	148.87					-126.872 + J(-1449.8353)
9	1.000 +J(	.0000)	1.000	.00					-126.873 + J(-1449.8357)
10	-.318 +J(	-.2561)	.408	-141.15					-126.873 + J(-1449.8381)

MODE 7 -131.878 +J(-1453.2253) 231.288 HZ

BLADE	REAL	IMAGINARY	MODULUS	PHASE	DIA	DFT	COSINE	SINE	EIGENVALUE CHECK
1	.332 +J(	.1648)	.371	26.38	0	2.0	1.0	-1.8	-131.880 + J(-1453.2269)
2	.394 +J(	-.4336)	.586	-47.71	1	1.6	-1.5	-.8	-131.878 + J(-1453.2256)
3	-.190 +J(	.0172)	.191	174.82	2	6.5	.4	6.9	-131.880 + J(-1453.2266)
4	-.730 +J(	.3789)	.823	152.58	3	100.0	-100.0	37.5	-131.878 + J(-1453.2250)
5	1.000 +J(	.0000)	1.000	.00	4	36.8	38.0	10.1	-131.878 + J(-1453.2254)
6	-.261 +J(	-.5724)	.629	-114.49	5	22.4	-11.4	21.0	-131.879 + J(-1453.2255)
7	-.708 +J(	.4674)	.848	146.56					-131.877 + J(-1453.2262)
8	.742 +J(	-.0196)	.742	-1.50					-131.878 + J(-1453.2240)
9	.119 +J(	-.4098)	.427	-73.85					-131.878 + J(-1453.2262)
10	-.805 +J(	.3627)	.883	155.75					-131.878 + J(-1453.2258)

MODE 8 -135.835 +J(-1463.7673) 232.966 HZ

BLADE	REAL	IMAGINARY	MODULUS	PHASE	DIA	DFT	COSINE	SINE	EIGENVALUE CHECK
1	.227 +J(	-.1001)	.248	-23.82	0	1.5	-1.3	.8	-135.835 + J(-1463.7672)
2	-.007 +J(	-.1490)	.149	-92.67	1	1.5	.7	1.4	-135.835 + J(-1463.7674)
3	-.056 +J(	.2037)	.211	105.40	2	11.2	-4.4	10.4	-135.835 + J(-1463.7674)
4	-.155 +J(	-.0086)	.156	-176.85	3	44.6	29.6	33.8	-135.835 + J(-1463.7675)
5	.479 +J(	-.2097)	.523	-23.64	4	66.1	-40.7	-52.7	-135.835 + J(-1463.7673)
6	-.837 +J(	.2690)	.878	162.19	5	100.0	-11.8	100.0	-135.835 + J(-1463.7673)
7	1.000 +J(	.0000)	1.000	.00					-135.835 + J(-1463.7674)
8	-.744 +J(	-.2679)	.791	-160.20					-135.835 + J(-1463.7672)
9	.387 +J(	.1787)	.426	24.92					-135.835 + J(-1463.7672)
10	-.258 +J(	.1309)	.287	152.91					-135.835 + J(-1463.7672)

MODE 9 -143.071 +J(-1469.1845) 233.828 HZ

BLADE	REAL	IMAGINARY	MODULUS	PHASE	DIA	DFT	COSINE	SINE	EIGENVALUE CHECK
1	1.000 +J(	.0000)	1.000	.00	0	5.8	-3.2	5.9	-143.072 + J(-1469.1846)
2	-.359 +J(	-.3255)	.485	-137.82	1	2.5	-2.4	1.5	-143.072 + J(-1469.1846)
3	-.373 +J(	.4401)	.583	129.74	2	13.7	8.0	13.6	-143.072 + J(-1469.1844)
4	.613 +J(	-.2583)	.666	-22.84	3	59.8	2.9	68.8	-143.072 + J(-1469.1844)
5	-.287 +J(	.1117)	.308	158.72	4	100.0	-57.4	100.0	-143.071 + J(-1469.1844)
6	.123 +J(	-.0311)	.126	-14.34	5	38.0	-34.1	23.8	-143.071 + J(-1469.1847)
7	-.054 +J(	.0215)	.058	158.45					-143.075 + J(-1469.1852)
8	.010 +J(	-.0302)	.032	-71.69					-143.067 + J(-1469.1789)
9	.256 +J(	-.0214)	.257	-4.78					-143.071 + J(-1469.1842)
10	-.728 +J(	.1704)	.747	166.82					-143.072 + J(-1469.1844)

MODE10 -135.554 +J(-1485.9327) 236.484 HZ

BLADE	REAL	IMAGINARY	MODULUS	PHASE	DIA	DFT	COSINE	SINE	EIGENVALUE CHECK
1	-.518 +J(	.4425)	.679	139.37	0	5.2	-4.3	-3.8	-135.554 + J(-1485.9326)
2	1.000 +J(	0)	1.000	0	1	3.8	-1.0	-4.1	-135.554 + J(-1485.9327)
3	-.940 +J(	-.2005)	.981	-163.38	2	20.0	-21.7	6.1	-135.554 + J(-1485.9328)
4	.423 +J(	.1696)	.455	21.87	3	82.7	-68.9	-15.8	-135.554 + J(-1485.9328)
5	-.104 +J(	.0706)	.126	146.86	4	100.0	-82.4	-77.0	-135.554 + J(-1485.9328)
6	.013 +J(	-.0235)	.027	-60.12	5	88.0	-7.9	-100.0	-135.550 + J(-1485.9330)
7	.014 +J(	.0075)	.016	28.31					-135.561 + J(-1485.9100)
8	-.015 +J(	-.0038)	.016	-169.78					-135.545 + J(-1485.9449)
9	.039 +J(	.0702)	.087	63.55					-135.555 + J(-1485.9327)
10	-.010 +J(	-.3242)	.325	-93.17					-135.554 + J(-1485.9327)

Chapter 5

5.1 Introduction

The application of a lumped parameter model to formulate the dynamic behaviour of a structural system rests upon a fundamental assumption, namely: that the elastic, damping and inertia parameters of the system are concentrated only at certain locations which are discretely dispersed within the system. Thus, the *springs* are assumed to be weightless and devoid of any form of damping, while the *masses* are represented by elements lacking elasticity and damping.

In reality, this type of representation is not strictly valid since the elastic, geometric, and other structural properties are distributed in a piece-wise continuous manner, rather than being lumped at only a few 'coordinates', within the system. Some errors are, therefore, inevitably incurred whenever the lumped parameter method is used to model a structural continuum.

The magnitude of error due to an assumption of lumped properties, in lieu of distributed parameters, is generally the greatest for eigenvalues of the largest modulus. Consequently, the accuracy of results computed from lumped formulations may be improved by using a larger number of degrees of freedom than is actually desired. In the limit, when the number of 'elements' tends to the infinite, we arrive at the 'exact' solution.

The finite element method, the method of influence coeficients, *etc*, advance the problem formulation from the 'elementary' basis offered by lumped parameter modelling, since they recognise to varying degrees, the continuum nature of the structure. All these methods, including the lumped parameter approach, have been used in the past by other investigators to study the dynamic response characteristics of mistuned bladed disc assemblies.

The method of receptances, for example, was first applied to structural problems in a monograph by Duncan†, in which he drew an analogy between the 'receptance' of mechanical systems, and the admittance of electrical networks. But by far the most influential publication on the theory and application of receptances is the book by **Bishop** and **Johnson** (1960). The term *receptance* was therein defined by the authors as describing the relationship between harmonic response and excitation in a mechanical system such that

†**Duncan, W. J.** (1944) *Mechanical Admittances and their Application to Oscillation Problems* Her Majesty's Stationery Office, London.

$$\alpha_{ij} = x_i/f_j \tag{5.1.1}$$

where α_{ij} is the *cross receptance*, being the ratio of the response x_i at the ith coordinate of the structure when a single point loading, f_j is applied at coordinate j, while no other excitation is impressed upon the system.

Receptances of multi-degree of freedom systems are usually expressed in matrix form, so that equation (5.1.1) becomes modified as

$$\mathbf{x} = \mathbf{A}\mathbf{f} \tag{5.1.2}$$

where $\mathbf{A}$ is the receptance matrix (often written as $[\alpha_{ij}]$), $\mathbf{x}$ the response vector, and $\mathbf{f}$ the force vector.

Receptance matrices were initially applied to the solution of dynamical problems in the aerospace industry. The method has since then been extensively developed, so that it is now a formidable tool of structural analysis which is widely used in other industries, as well as for teaching and research purposes. The receptance coupling technique is essentially the enforcement of dynamic equilibrium and compatibility conditions in a system, at each coordinate which is shared by two or more sub-systems. Any engineering structure, no matter how complex, may be analysed - at least qualitatively - for its dynamic response characteristics by using the receptance coupling technique and the *building block approach*. The procedure entails a decomposition of the complex structure to its basic components, or 'elements', each of which may be separately analysed by using theoretical or experimental sub-procedures. Upon obtaining the receptance matrices of the individual components, the dynamical equations of the entire system may be set up by applying standard procedures for assembling sub-structure matrices, as given, for instance, by **Zienkiewicz** and **Cheung** (1967).

Armstrong (1955) was one of the earliest to utilise the concept of receptance coupling to the solution of the blade and disc vibration problem. His analysis was subsequently improved upon by several researchers, among them **Ewins** (1966) and **Cottney** (1975).

If we examine Figure 5.1.1, which shows a four 'bladed disc' that has been decomposed into its five components - the disc, D, together with the four blades, B_1, B_2, B_3, and B_4 - we can apply the matrix assembly procedure to obtain the receptance matrix of the entire structure once the sub-matrices of the disc and blades have been separately calculated or experimentally derived. The first step in the procedure for applying the receptance coupling technique to a structure, therefore, is the collection of the receptance data of the components.

5.2 Receptances of Bladed Disc Components

Turbomachine blades are generally characterised by complex geometric profiles and, as such, are not easily ammenable to 'exact' theoretical treatments. They are, therefore, usually represented by uniform prismatic beams of circular or rectangular cross-section. Similarly, the receptance analyses of turbine discs are frequently based on a greatly simplified model of the disc. These are generally assumed to be of small and uniform thickness, so that the model adopted is typically a flat, circular plate.

The receptance matrices of flat circular plates and uniform prismatic beams are usually obtained from a vibration analysis of these components when a specified amount of excitation is applied to them in their freely suspended state. Such receptance expressions have been derived by **Bishop** and **Johnson** (1960) for uniform prismatic beams, and **McLeod** and **Bishop** (1965) in the case of thin, flat circular plates. The following analysis is summarised from the two publications cited above and the study of **Ewins** (1966). It is given here in a brief form in order to sustain continuity.

5.2.1. Blade Receptance

Twelve coordinates are required for the complete description of the motion of a uniform prismatic beam freely suspended in space - three translational and three rotational at either end of the beam element. These coordinates are identified in Figure 5.2.1. The Bernoulli-Euler equation of beam vibration is assumed to govern the dynamics of the beam's flexure, although the Timoshenko equation must be substituted when the effects of shear deformation and rotatory inertia are not small. This is especially true for blades exposed to high frequency oscillations.

The in-plane vibration of blades which are modelled as uniform, untwisted beams may often be considered uncoupled with out-of-plane motion, since movements in the two planes are mutually orthogonal. A coupling of the vibration in the two planes occurs, for instance, when the blades are mounted on a disc at a *stagger angle*. Excepting this instance, which may be corrected for at the matrix assembly stage by applying appropriate transformation matrices, the receptance matrices of in-plane and out-of-plane vibrations may be separately deduced.

For in-plane vibration, the receptance matrix is obtained by enforcing the boundary conditions prevailing at the ends of a free-free beam that is loaded by excitation forces and moments as shown in Figure 5.2.1 to yield:

$$\mathbf{x} = \mathbf{A}\mathbf{f} \tag{5.2.1}$$

where A is a symmetric 6x6 matrix.

5.2.2. Disc Receptance

As in the case of uniform prismatic bars, the receptance expressions for a flat circular plate are usually derived from a consideration of the motion of the plate when freely suspended. The dynamics of such a plate were investigated as long ago as 1910 by **Airey**, whose publication forms an important platform upon which subsequent workers based their research. In 1921, **Lamb** published an influential paper on the motion of spinning discs, accounting for the influence of gyration on the vibration of such elastic bodies as turbine wheels which, under normal operating conditions, are subject to rotation.

Between the early days and the present, a very large amount of technical reports and other publications have been issued on the vibration of plates of diverse geometric profiles and manifold edge conditions. Two excellent reviews of the publications have been given by **Leissa** (1969, 1978). Most of the studies covered in the survey by Leissa are based on the thin-plate theory, in which the 'secondary' effects of shear deformation and rotatory inertia are not taken into account. More advanced theories have subsequently emerged, with the works of **Mindlin** (1951), **Reissner** (1945), and **Snowdown** (1971) being the most influential in this respect. It is, perhaps, important to remark that almost all the studies covered in Leissa's reviews were concerned with the determination of natural frequencies and mode shapes of free vibration, and not the derivation of receptance matrices. The monograph by McLeod and Bishop, however, contains a com-

prehensive treatment of the motion of flat circular plates, based on the thin-plate theory, with the derivation of receptance expressions for a variety of discs having different boundary conditions. Although the receptances published by McLeod and Bishop are adequate for the analysis of many bladed disc assemblies, it has been observed by **Cottney** (1975) that a more accurate representation of discs - especially those with radial thickness variations - is obtained if each disc is modelled as a series of concentric rings of successively varying thicknesses. This refinement in receptance modelling leads, naturally, to a more complex solution procedure. Although Cottney's treatment is undoubtedly justifiable for certain categories of problems, it is not economical to apply it here, since what we seek is some basic understanding of the effects of mistuning on assembly dynamics, and not of specific wheels. It is therefore sufficient to use the uniform, thin-plate theory, after **Ewins** (1966), to model the disc.

If we define the Laplacian operator in polar coordinates as

$$\nabla^2=\frac{\partial^2}{\partial r^2}+\frac{1}{r}\frac{\partial}{\partial r}+\frac{1}{r^2}\frac{\partial^2}{\partial\theta^2} \tag{5.2.3}$$

then, the well-known equation of motion of the thin, uniform, isotropic, flat circular plate may be written as:

$$\nabla^4 w - k^4 w = 0 \tag{5.2.4}$$

where

$$k^4=\frac{\rho w^2 h}{D}$$

$$D=\frac{Eh^3}{12(1-\nu^2)}$$

and

r = distance along the radius, measured from plate's central axis
θ = angular position
h = plate thickness
ρ = material density
w = transverse deflection of plates neutral axis
ω = frequency of vibration
D = plate's flexural rigidity

with E and ν being the Young's modulus and Poisson's ratio respectively.

The general solution of equation (5.2.4) is

$$w(r,\theta) = \sum[A_nJ_n(kr) + B_nJ_n(jkr) + C_nY_n(kr) + D_nY_n(jkr)]E_n\cos(n\theta) \quad (5.2.5)$$

where J_n and Y_n are the nth integral order Bessel's functions of the first and second kinds respectively, and A_n, B_n, *etc* are arbitrary constants, the values of which are to be determined from the boundary conditions.

When the boundary conditions appropriate to the free-free plate are applied, it is found that at $r=0$, $Y_n(jkr)\to\infty$ and $Y_n(kr)\to\infty$. These make the value of w locally infinite at the centre of the disc. Infinite displacements are, however, inadmissive at the centre of a solid plate. Hence, the coefficients of the Bessels functions which would otherwise be infinite must vanish, i.e.

$$C_n = D_n = 0 \quad (5.2.6)$$

The remaining boundary conditions are satisfied at the periphery of the plate, ie.

at $r=a$, $$M_r=0,\ V=0 \quad (5.2.7)$$

where

$$Q_r=-D\frac{\partial}{\partial r}(\nabla^2 w)$$

$$V_r=Q_r+\frac{1}{r}\frac{\partial M_{r\theta}}{\partial\theta}$$

$$M_r=-D\left[\frac{\partial^2 w}{\partial r^2}+\nu\left(\frac{1}{r}\frac{\partial w}{\partial r}+\frac{1}{r^2}\frac{\partial^2 w}{\partial\theta^2}\right)\right]$$

$$M_\theta=-D\left[\frac{1}{r}\frac{\partial w}{\partial r}+\frac{1}{r^2}\frac{\partial^2 w}{\partial\theta^2}+\nu\frac{\partial^2 w}{\partial r^2}\right]$$

$$M_{r\theta}=-D(1-\nu)\frac{\partial}{\partial r}\left(\frac{1}{r}\frac{\partial w}{\partial\theta}\right)$$

In order to obtain the desired receptance expressions, it is necessary to apply external loading at a selected point on the disc which is deemed appropriate for the type of receptance required. For turbine disc wheels which are here being modelled as plates, the principal excitations impressed on them are due to the blades. Receptances may therefore be derived by applying excitations to the plate rim, being the interface of blade root with the disc. Details of the algebra required for the derivation of receptances in this instance are lengthy; the interested reader may consult **Ewins** (1966), from where it may be verified that the receptance between two points i and j on the disc periphery are given by

$$\alpha_{ij} = \frac{1}{\pi}\left\{\frac{1}{2}\alpha(0) + \sum_n \alpha(n)\cos[n(\theta_i-\theta_j)]\right\} \quad (5.2.8)$$

$$\alpha'_{ij} = \frac{1}{\pi}\left\{\frac{1}{2}\alpha'(0) + \sum_n \alpha'(n)\cos[n(\theta_i-\theta_j)]\right\}$$

$$\alpha''_{ij} = \frac{1}{\pi}\left\{\frac{1}{2}\alpha''(0) + \sum_{n} \alpha''(n) \cos[(\theta_i - \theta_j)]\right\}$$

where the summations range from 1 to ∞, and other symbols have their usual meanings.

As pointed out in an earlier section, the application of receptance ccoupling procedures is, in essence, the enforcement of the structural requirements of compatibility and dynamic equilibrium at the interface of two or more connected substructures. If there are N blades mounted on a stage, and we define for the ith blade the following parameters:

x_i, s_i = displacement and slope, respectively, at *blade root*;
X_i, S_i = displacement and slope at the corresponding point on *disc rim*
f_i, m_i = applied force and moment, measured at blade root
F_i, M_i = force and moment at disc rim

then receptance equations may be written for the dynamic displacements at the blade root and disc rim respectively, as follows.

$$x_j = \beta_i f_i + \beta'_i m_i \tag{5.2.9}$$

$$X_i = \alpha_{ij} f_j + \alpha'_{ij} M_j \tag{5.2.10}$$

Similarly, the expressions for the slopes are

$$s_j = \beta_i f_i + \beta'_i m_i \tag{5.2.11}$$

$$S_i = \alpha'_{ij} f_j + \alpha''_{ij} M_j \tag{5.2.10}$$

The conditions of equilibrium require that

$$F_i + f_i = 0 \text{ and } M_i + m_i = 0 \tag{5.2.13}$$

and for compatibility,

$$X_i + x_i = 0 \text{ and } S_i + s_i = 0 \tag{5.2.14}$$

where, in equations (5.2.9) to (5.2.14), the indices i and j range from 1 to N inclusive.

These equations may be collected together to form the system's dynamical matrix,

$$\mathbf{D}(\lambda)\mathbf{q} = \mathbf{p} \tag{5.2.15}$$

where $\lambda = \omega^2$, and $\mathbf{p}$ is the vector of externally applied excitations which becomes null for free vibration, and elements of $\mathbf{D}$ are transcendentally dependent upon the kernel, λ.

Equation (5.2.15) with $\mathbf{p} = \mathbf{0}$ is a non-linear eigenvalue problem which cannot, however, be solved by the procedures described in Chapter 4 for quadratic problems. The eigenvalues of $\mathbf{D}(\lambda)$ may nevertheless be extracted,

in a locally convergent sequence, by using the determinant search technique, i.e. locating the zeros of the determinant polynomial in

$$|\mathbf{D}(\lambda)| = 0 \tag{5.2.16}$$

The roots of equation (5.2.16), being the eigenvalues of equation (5.2.15), are the natural frequencies of the bladed disc assembly. Upon locating a root, λ_k, of equation (5.2.16), the corresponding mode shape, ϕ_k, may be obtained, to within an arbitrary multiplier, by applying inverse iteration on

$$\mathbf{D}(\lambda_k)\mathbf{u}_{r+1} = \mathbf{u}_r,$$

where $\mathbf{u}_r$ is the rth iterant vector, and $\mathbf{u}_r \to \phi_k$ as $r \to \infty$.

The response of each blade in the assembly may be computed in the form of stresses at blade root, or displacements at blade tip, at any excitation frequency ω in at least two ways. In the more popular method, several matrix inversions are carried out by operating on equation (5.2.15) to yield

$$\mathbf{q}(\omega) = \mathbf{D}(\omega)^{-1}\mathbf{p}(\omega) \tag{5.2.17}$$

which is a lengthy and costly process. An alternative way is to operate on equation (5.2.15) directly, and solve for the response $\mathbf{q}$, using Gauss decomposition on $\mathbf{D}$, and backward substitution with $\mathbf{p}$. A considerable amount of computation resources may be saved in this way, as estimated by **Westlake** (1968), since every inversion of a matrix of order N is equivalent to the solution of N simultaneous equations, N number of times. Furthermore, the manner of calculating $\mathbf{q}$ in equation (5.2.17) entails several unnecessary multiplications, which could lead to the accumulation of round off errors unless additional precision were used, **Wilkinson** (1963).

5.3 Case Studies

In a previous study, **Ewins** and **Rao** (1976) applied the method of receptances to investigate the influence of mistuning on the vibration response of a mistuned assembly having 24 blades. The principal conclusions reached in that study were that

(a) *"mistuning is seen to cause a worsening in the incidence of resonance"*

(b) *the receptance coupling technique predicts natural frequencies reliably, as verified by experiment; and*

(c) *that the escalation of stress levels as a result of mistuning is "seldom more than about 25% higher than it would be on tuned systems".*

5.3.1 Undamped Response

As we have demonstrated in Chapter 2, it is possible to show that mistuning may cause certain *rogue* blades to experience relatively large stresses at certain 'critical' frequencies of excitation. This observation was made from samples drawn from lumped parameter modelling. In this section, we shall apply the computer program for receptance analysis of bladed discs previously used by Ewins and Rao to study the same 24 bladed wheel employed in that study in order to verify the validity of the deductions arrived at in Chapter 2 via the application of the simpler theoretical modelling.

The 24 bladed model is designated as *Disc 24J* in this text. The variation of blades' cantilever frequencies (1F) with the slot position on the disc is as shown in Figure 5.3.1. The disc and blades have the following geometric and material properties:

Disc Properties

radius =	127.00mm
thickness =	5.59mm
elastic modulus =	206.84GN/m^2
density =	7833.4kg/m^3
poisson's ratio =	0.287

Blade Properties

number of blades =	24
blade stagger anlge =	45°
blade length =	80.26mm
blade width =	10.78mm
blade thickness =	3.05mm
elastic modulus =	206.84GN/m^2
density =	7833.4kg/m^3.

The vibration characteristics of the assembly in the presence of excitation by the first engine order was calculated using Ewins' program *BLD*. The responses were obtained for each blade at every excitation frequency. These have beeen analysed statistically as in §3.3.2, the summaries of which are given in the form of

(*i*) blade tip displacement (Tables 5.3.1)

(*ii*) root stress on the narrow blade face (Tables 5.3.2)

(*iii*) root stress on the wider face (Tables 5.3.3)

It is evident from the tables that the inferences drawn from the lumped parameter data analysis are also upheld here for all the three types of responses. Because of the similarity in the statistics of these responses, only one set of data will be discussed here. These are the data in Tables 5.3.2a

and 5.3.2b.

The parameter usually used to describe steady state response of mistuned assemblies is the stress at the root of the blades on their wider face, as reported by **Ewins** (1976), since that is the location frequently used for strain gauge measurement during vibration testing. If we restrict attention to this response as a function of exctiation frequencies in the range $10 \leq \omega \leq 500$Hz, we may observe from Table 5.3.2a that the pattern of stress distibution among the blades fluctuates widely from one excitation frequency to another. The accompanying data in Table 5.3.2b is an alternative presentation of the root stress response pattern. The presentation format shows a row-wise ranking of the blades in ascending order of response magnitude. Each blade is identified by the slot number it occupies on the disc. Thus, if we examine the stress response at the excitation frequency of 10Hz, we notice that the blade with the lowest response is the one on slot number 18, followed by blades 17, 7, 1, *etc*, until we arrive at blade number 14, which has the largest response at this frequency (10Hz).

If we study the response sequence at the low frequencies, $10\text{Hz} \leq \omega \leq 100\text{Hz}$, we notice that the blades' stress amplitudes are in *inverse* proportion to their cantilever frequencies. Thus, blade 18 - which is the one with the highest 1F - has the lowest reponse; while blade 14, being among the blades with the lowest 1F, suffers the greatest stressing. Other blades are correspondingly placed in the response hierachy, in accordance with their ratings in the 1F league.

It is evident from the foregoing that the scatter characteristics of the bladed disc assembly are transmitted to influence, in some inverse proportion, the blades' dynamic response at *low frequencies*. This observation may be readily confirmed by carrying out a Discrete Fourier Transform (DFT) of the blades' frequency scatter, and comparing the result with that of the DFT of the blades' responses at low frequencies. They will be found to be mirror images of each other.*

Apart from the region of low excitation frequencies, which is close to static conditions, and some regions in the frequency spectrum which are 'far' away from system resonances, the statistical properties inherent in a particular arrangement of blades around the disc do not appear to be related in any straight forward manner to those in the blades' responses. Therefore, one may not generally predict with confidence for the pattern to be expected in responses at each and every excitation frequency, from a cursory examination of the scatter in blade alone frequencies.

* See, for instance, Afolabi (1981b)

In the neighbourhood of system's resonances, rogue conditions may or may not occur, as discussed in Chapter 2. When rogue conditions occur, it is usually a blade with extreme detune in cantilever frequency that becomes rogue. The data in Tables 5.3.1 to 5.3.3 do not, however, tell us much about the onset of rogue conditions as they stand. If we plot the relative stress experienced by each blade as a function of the slot number occupied by that blade, a better picture emerges. Thus we obtain the illustrations of Figures 5.3.2. Each of the graphs has been selected on the signifance, from a statistical point of view, of the manner of stress amplitude variation among the blades. Thus,

Figure	Frequency	Response characteristic
5.3.2a	135	minimum coefficient of variation in response
5.3.2b	145	minimum negative coefficient of kurtosis
5.3.2c	351	maximum coefficient of variation
5.3.2d	353	minimum coefficient of skewness
5.3.2e	371	maximum negative kurtosis
5.3.2f	398	maximum positive kurtosis
5.3.2g	400	maximum global stress amplitude
5.3.2h	495	minimum positive kurtosis

5.3.2 Response with Damping

One way of representing the damping inherent in the components of bladed disc assemblies is to use a complex modulus of elasticity, i.e. $E^* = E(1+j\eta)$ where η is the hysteretic loss factor of blade material in direct strain, and j is the unit imaginary number. This type of damping was imposed on Ewins' 24 bladed wheel previously considered without damping in this chapter, §5.3.1. Different levels of damping, ranging from 'light', through 'medium', to 'heavy' were used. It is sufficient for our purpose here to present only the response of the wheel in the presence of 'medium' damping, i.e. $Q=100$, approximately. Figure 5.3.3a is reproduced from **Ewins** and **Rao** (1976), and it shows the upper and lower envelope of mistuned response, as well as the equivalent tuned response, for excitation by the sixth engine order force. Nine resonant frequencies were covered in the frequency range surveyed. The results as presented by the original workers do not reveal the extent of scatter in the response at these resonances, since only the upper and lower bounds were highlighted. A re-examination of their data has therefore been carried out and the results are presented in Figure 5.3.3b.

Each of the identified resonances in Figure 5.3.3a are designated by letters in the range A to I. At each of these resonances, the stress on the

blades are normalised and plotted as a function of blade slot number. It is immediately obvious from the graphs that mode I is a critical mode, since at this reonance, nearly all the blades on the stage experience less than 20% of the peak stress on the worst blade. In contrast, modes E and F are easily identified as primary resonances, since the stress peaks are the highest, and the blade responses are clustered near the mean value. A closer examination of mode I shows that the blade with rogue characteristics is that on slot number 18, which is one of extreme detune in 1F.

5.4 Concluding Remarks

For many years, different researchers have presented various results on the steady state response of mistuned bladed disc assemblies, which differ greatly in both quantitative and qualitative dteails. This divergence of results has brought conflicting implications in its wakes, and is usually attributed to differences in the mathematical modelling employed by different analysts.

In chapters 2 and 3, a lumped parameter method was used to establish some vibration characteristics for Disc 10A and other mistuned assemblies. In this chapter, the receptance method has been used to study disc 24J. We have, therefore, applied two different techniques to study different wheels with diverse mistune conditions. Yet, in all cases, we have found that the influence exercised by the blades with extreme detune in cantilever frequencies is very profound. Furthermore, it has been possible to identify certain rogue blades based on the information extracted from the relative position of such blades in the cantilever frequency rankings.

Since concurrence of results has been achieved in this study by using *different methods* to analyse *different assemblies*, we are not in a position to support the view held by other investigators that the calculated responses of mistuned assemblies are heavily dependent upon the method of analysis employed. While recognizing that minor influences may be exerted by different modelling techniques, the divergences in the conclusions published by other workers could probably have been resolved by a judicious interpretation of their data.

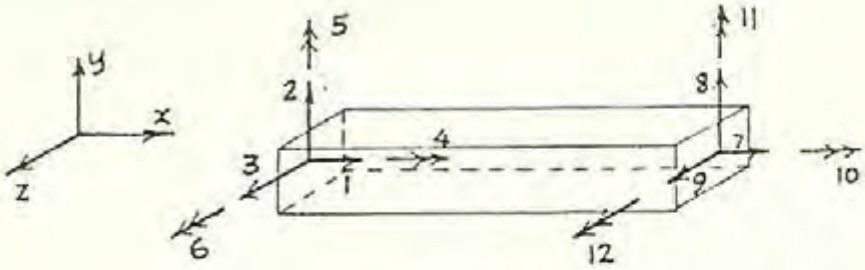

Fig. 5.2.1 *Coordinates associated with the spatial motions of a beam*

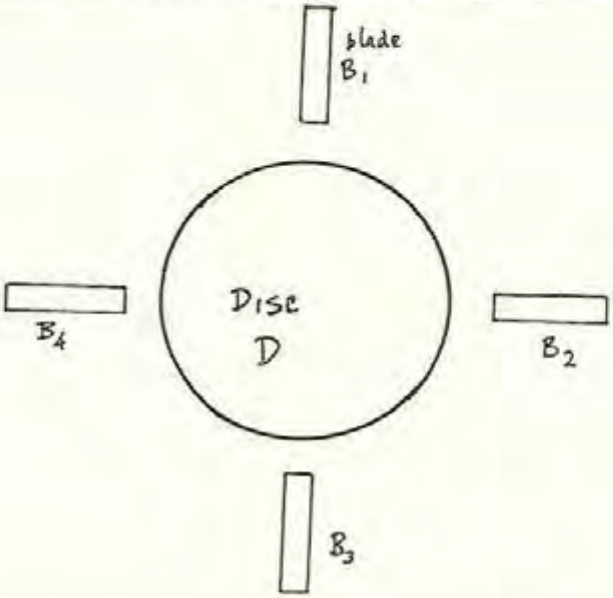

Fig. 5.2.1 *Building blocks of a 4-bladed disc assembly*

Fig. 5.3.1 *Frequency scatter of Disc 24J*

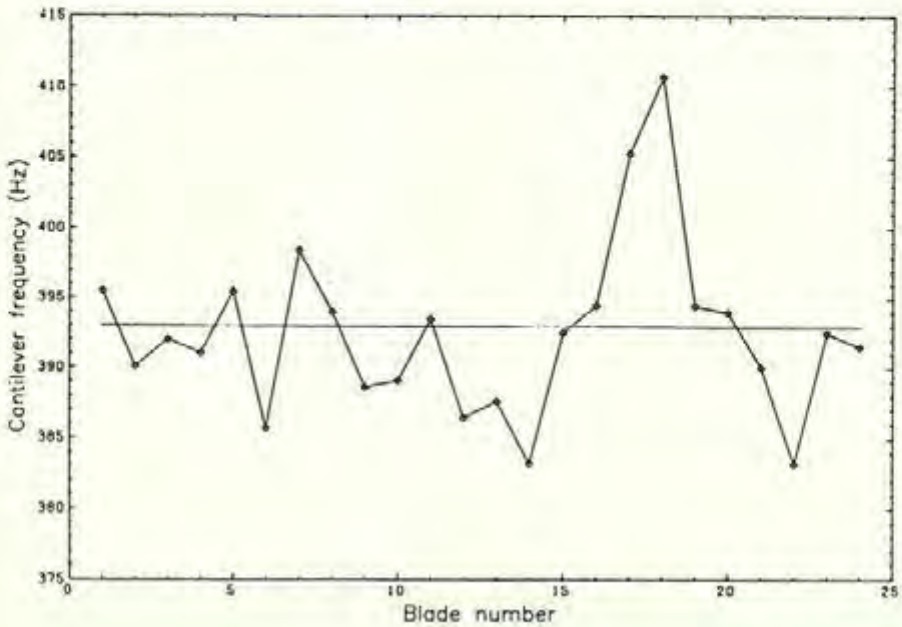

Fig. 5.3.2 *Response of disc 24J to 1eo at selected frequencies*

ω = excitation frequency (Hz)
α = blade with LOWEST response
β = blade with LARGEST response

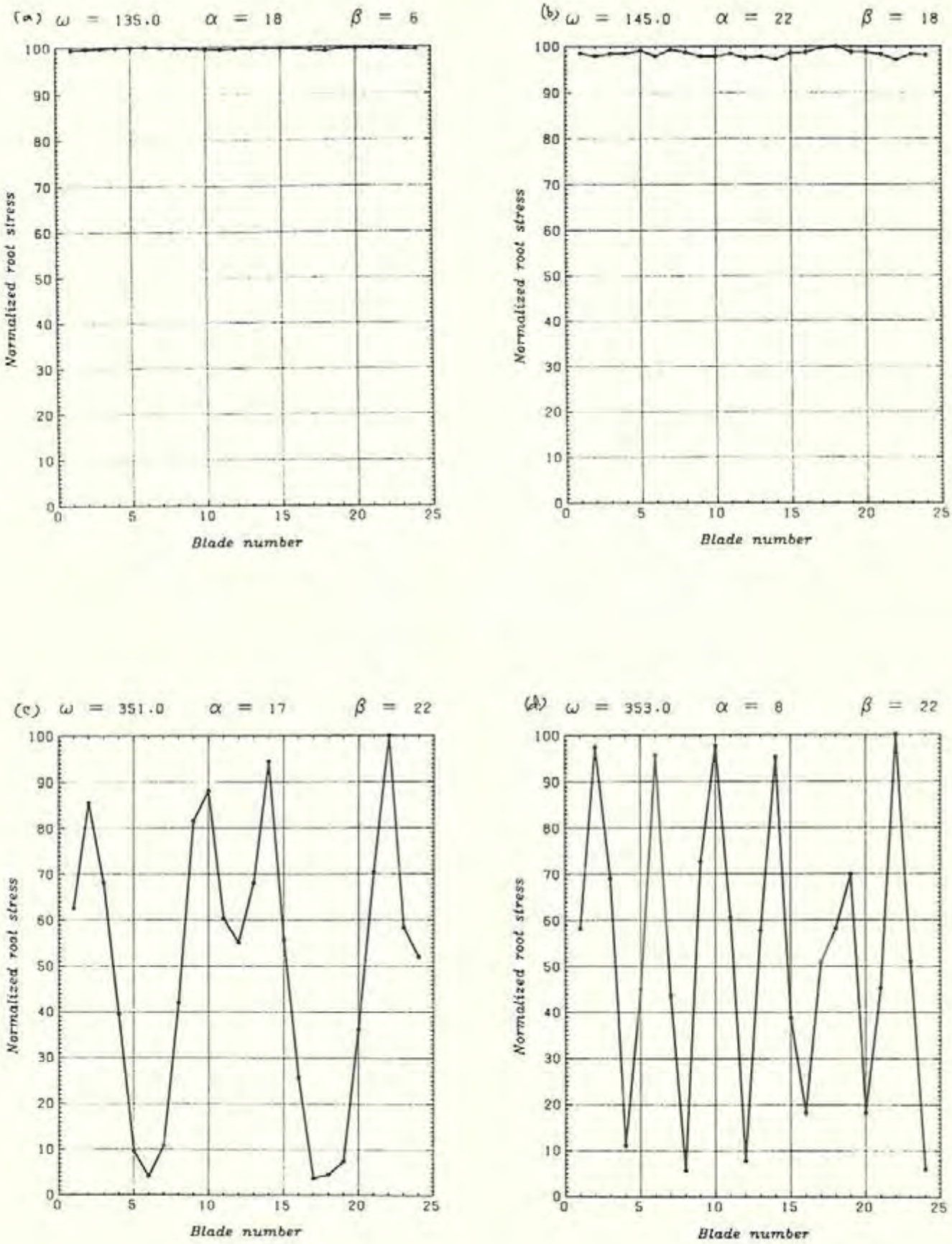

(e) ω = 371.0 α = 2 β = 22

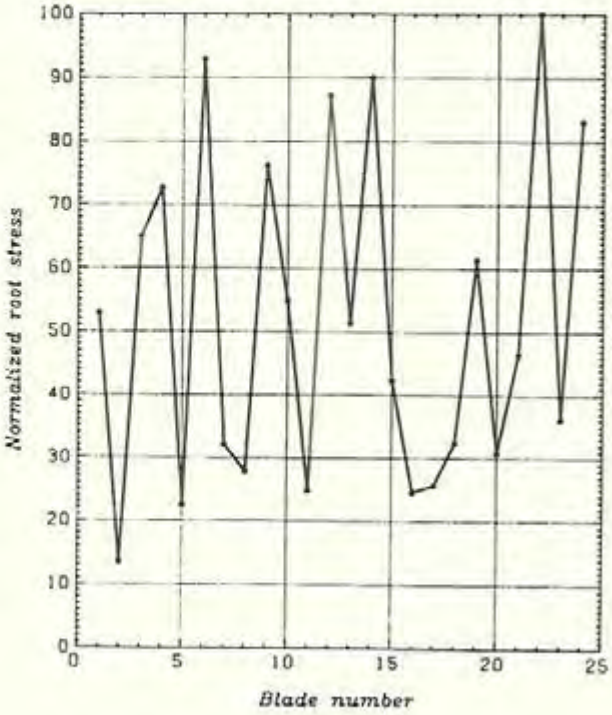

(f) ω = 398.0 α = 6 β = 17

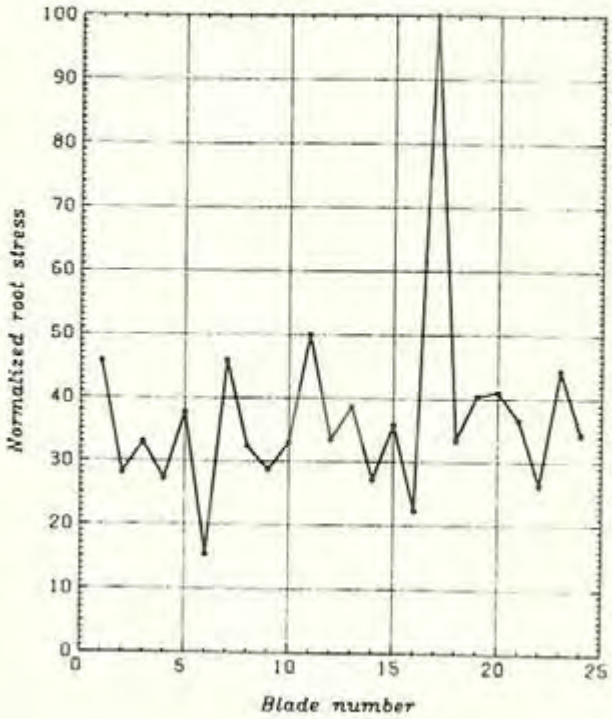

(g) ω = 400.0 α = 1 β = 18

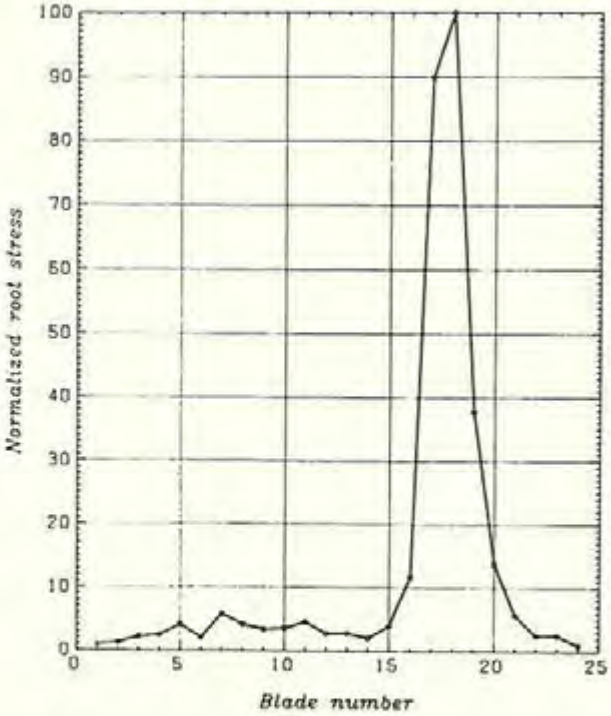

(h) ω = 495.0 α = 17 β = 22

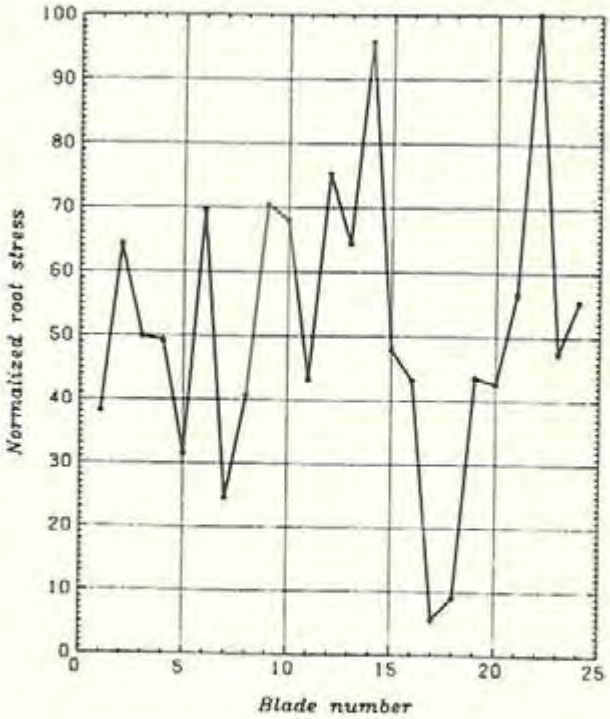

Fig. 5.3.3 *Frequency response of Disc 24J (with damping)*

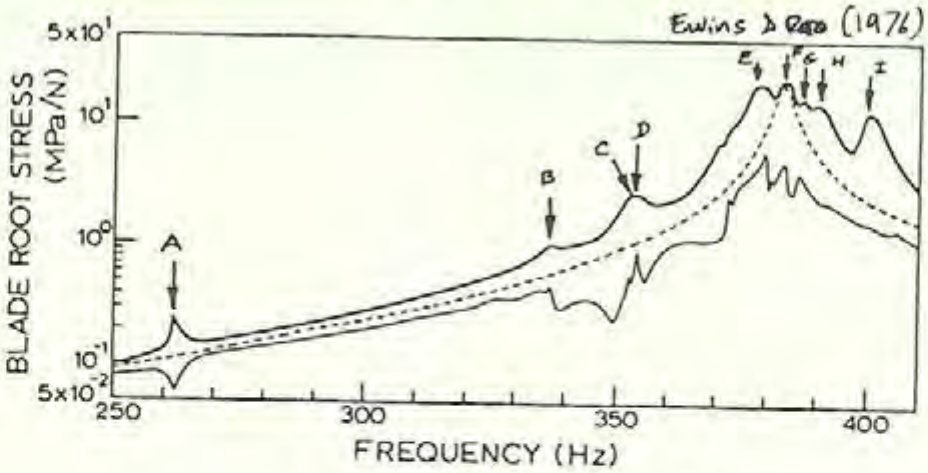

Damped 6 EO Response: 24-Bladed Disc
Type I Damping η_{st} =0.01
(—— upper envelope mistuned; —— lower envelope mistuned; - - - tuned)

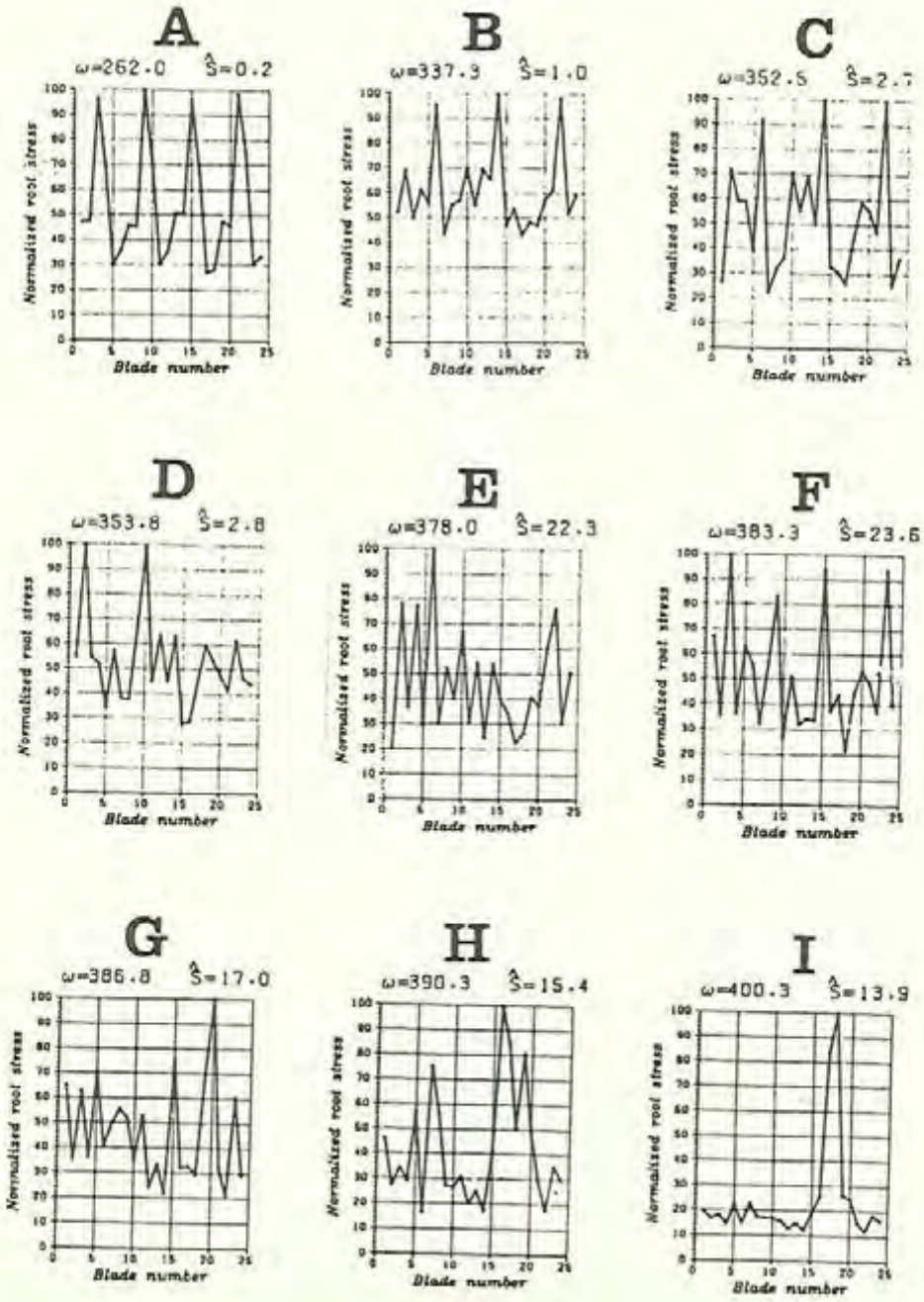

Table 5.3.1a *Response characteristics of Disc 24J (tip displacement)*

FREQUENCY	MAX RESP	MIN RESP	STD	SKEW	KURT	BLR	BHR
10.00	.000347	.000338	.564	-.914	1.340	18	14
15.00	.000348	.000339	.565	-.913	1.338	18	14
20.00	.000348	.000339	.568	-.913	1.338	18	14
25.00	.000348	.000339	.572	-.913	1.338	18	14
30.00	.000349	.000340	.576	-.913	1.337	18	14
35.00	.000349	.000340	.581	-.913	1.337	18	14
40.00	.000350	.000341	.587	-.913	1.337	18	14
45.00	.000351	.000342	.593	-.913	1.338	18	14
50.00	.000352	.000342	.601	-.912	1.337	18	14
55.00	.000353	.000343	.609	-.912	1.337	18	14
60.00	.000354	.000344	.618	-.912	1.337	18	14
65.00	.000355	.000345	.629	-.912	1.337	18	14
70.00	.000357	.000346	.640	-.912	1.337	18	14
75.00	.000358	.000347	.652	-.912	1.336	18	14
80.00	.000360	.000349	.665	-.912	1.336	18	14
85.00	.000361	.000350	.679	-.911	1.335	18	14
90.00	.000363	.000352	.694	-.911	1.334	18	14
95.00	.000365	.000353	.710	-.911	1.333	18	14
100.00	.000367	.000355	.728	-.910	1.331	18	14
105.00	.000369	.000357	.746	-.910	1.330	18	14
110.00	.000372	.000359	.766	-.909	1.328	18	14
115.00	.000374	.000361	.787	-.908	1.326	18	14
120.00	.000377	.000363	.810	-.907	1.323	18	14
125.00	.000380	.000365	.834	-.906	1.320	18	14
130.00	.000383	.000368	.860	-.905	1.317	18	14
135.00	.000386	.000370	.888	-.904	1.313	18	14
140.00	.000389	.000373	.917	-.903	1.309	18	14
145.00	.000393	.000376	.949	-.901	1.304	18	14
150.00	.000396	.000379	.982	-.900	1.299	18	14
155.00	.000400	.000382	1.018	-.898	1.293	18	14
160.00	.000405	.000386	1.056	-.896	1.287	18	14
165.00	.000409	.000389	1.096	-.894	1.279	18	14
170.00	.000414	.000393	1.140	-.892	1.271	18	14
175.00	.000419	.000397	1.187	-.889	1.261	18	22
180.00	.000424	.000401	1.237	-.886	1.250	18	22
185.00	.000430	.000405	1.292	-.883	1.238	18	22
190.00	.000436	.000410	1.350	-.880	1.223	18	22
195.00	.000443	.000415	1.414	-.877	1.206	18	22
200.00	.000450	.000420	1.483	-.873	1.186	18	22
205.00	.000457	.000425	1.559	-.868	1.161	18	22
210.00	.000465	.000431	1.644	-.863	1.131	18	22
215.00	.000473	.000437	1.738	-.856	1.092	18	22
220.00	.000482	.000443	1.844	-.847	1.042	18	22
225.00	.000492	.000450	1.967	-.836	.976	18	22
230.00	.000503	.000456	2.112	-.820	.884	18	22
235.00	.000515	.000463	2.293	-.795	.752	18	22
240.00	.000527	.000470	2.530	-.756	.556	18	22
245.00	.000542	.000477	2.877	-.687	.254	18	22
250.00	.000559	.000483	3.473	-.562	-.209	18	22
255.00	.000582	.000485	4.857	-.350	-.844	18	22
260.00	.000677	.000445	11.161	.106	-1.316	17	9
265.00	.000704	.000469	11.646	.408	-1.338	15	6
270.00	.000643	.000547	4.543	.437	-1.075	15	6
275.00	.000652	.000574	3.536	.471	-1.109	18	6
280.00	.000670	.000585	3.380	.358	-.900	18	6
285.00	.000693	.000599	3.478	.236	-.607	18	6
290.00	.000721	.000615	3.688	.153	-.362	18	6
295.00	.000756	.000633	3.951	.110	-.185	18	14
300.00	.000797	.000654	4.275	.100	-.065	18	14
305.00	.000844	.000677	4.661	.171	.014	18	14
310.00	.000899	.000703	5.122	.171	.063	18	14
315.00	.000966	.000732	5.679	.256	.095	18	14
320.00	.001049	.000766	6.375	.388	.123	18	14
325.00	.001157	.000805	7.306	.592	.175	18	14
330.00	.001315	.000859	8.802	.907	.309	18	14
335.00	.001683	.000843	13.912	.993	.188	16	14
340.00	.001809	.000621	14.653	-.356	.193	18	12
345.00	.001886	.000700	14.896	-.559	.120	18	12
350.00	.002994	.000339	22.779	-.145	-.251	18	14
355.00	.004292	.000494	28.344	-.106	-1.388	14	2
360.00	.003420	.001428	15.225	.653	-.247	6	10
365.00	.004359	.001714	18.689	.234	-1.080	18	12
370.00	.017300	.001940	25.141	.614	-.575	18	12
375.00	.019141	.004522	18.759	1.391	1.493	18	6
380.00	1.685238	.011740	25.359	2.066	3.318	17	13
385.00	.041602	.002229	28.714	.533	-1.113	22	15
390.00	.488387	.002051	29.859	1.862	1.847	22	16
395.00	.008062	.001820	21.953	1.245	.414	14	17
400.00	1.042839	.003066	25.859	2.699	5.729	24	18
405.00	.005848	.001059	19.186	2.422	5.025	22	18
410.00	.002865	.000796	19.177	.826	.234	11	17
415.00	.002822	.000331	24.622	.038	-1.112	22	5
420.00	.002545	.000434	17.657	1.652	2.988	6	18
425.00	.001656	.000541	13.926	1.931	4.073	6	18
430.00	.001287	.000517	12.508	1.891	3.949	6	18
435.00	.001056	.000473	11.677	1.792	3.627	6	18
440.00	.000891	.000428	11.108	1.682	3.287	6	18
445.00	.000765	.000385	10.696	1.568	2.952	6	18
450.00	.000664	.000346	10.395	1.446	2.613	6	18
455.00	.000582	.000310	10.185	1.306	2.246	6	18
460.00	.000513	.000278	10.062	1.132	1.809	6	18
465.00	.000452	.000247	10.053	.892	1.232	6	18
470.00	.000398	.000219	10.278	.528	.404	6	18
475.00	.000345	.000189	11.332	.008	-.702	6	18
480.00	.000322	.000154	16.171	-.026	-1.210	6	15
485.00	.000592	.000110	26.293	.078	-1.246	21	7
490.00	.000422	.000117	19.290	1.150	.526	9	18
495.00	.000307	.000118	14.600	1.477	1.966	22	18
500.00	.000262	.000108	13.498	1.586	2.460	22	18

Table 5.3.1b *Response characteristics of Disc 24J (tip displacement)*

10.0	18	17	7	1	5	11	16	19	8	20	23	15	24	3	4	2	21	10	9	13	12	6	22	14
15.0	18	17	7	1	5	11	16	19	8	20	23	15	24	3	4	2	21	10	9	13	12	6	22	14
20.0	18	17	7	1	5	11	16	19	8	20	23	15	24	3	4	2	21	10	9	13	12	6	22	14
25.0	18	17	7	1	5	11	16	19	8	20	23	15	24	3	4	2	21	10	9	13	12	6	22	14
30.0	18	17	7	1	5	11	16	19	8	20	23	15	24	3	4	2	21	10	9	13	12	6	22	14
35.0	18	17	7	1	5	11	16	19	8	20	23	15	24	3	4	2	21	10	9	13	12	6	22	14
40.0	18	17	7	1	5	11	16	19	8	20	23	15	24	3	4	2	21	10	9	13	12	6	22	14
45.0	18	17	7	1	5	11	16	19	8	20	23	15	24	3	4	2	21	10	9	13	12	6	22	14
50.0	18	17	7	1	5	11	16	19	8	20	23	15	24	3	4	2	21	10	9	13	12	6	22	14
55.0	18	17	7	1	5	11	16	19	8	20	23	15	24	3	4	2	21	10	9	13	12	6	22	14
60.0	18	17	7	1	5	11	16	19	8	20	23	15	24	3	4	2	21	10	9	13	12	6	22	14
65.0	18	17	7	1	5	11	16	19	8	20	23	15	24	3	4	2	21	10	9	13	12	6	22	14
70.0	18	17	7	1	5	11	16	19	8	20	23	15	24	3	4	2	21	10	9	13	12	6	22	14
75.0	18	17	7	1	5	11	16	19	8	20	23	24	15	3	4	2	21	10	9	13	12	6	22	14
80.0	18	17	7	1	5	11	16	19	8	20	23	24	15	3	4	2	21	10	9	13	12	6	22	14
85.0	18	17	7	1	5	11	16	19	8	20	23	24	15	3	4	2	21	10	9	13	12	6	22	14
90.0	18	17	7	1	5	11	16	19	8	20	23	24	15	3	2	4	21	10	9	13	12	6	22	14
95.0	18	17	7	1	5	11	16	19	8	20	23	24	15	3	2	4	21	10	9	13	12	6	22	14
100.0	18	17	7	1	11	5	16	19	8	20	23	24	15	3	2	4	21	10	9	13	12	6	22	14
105.0	18	17	7	1	11	5	16	19	8	20	23	24	15	3	2	4	10	21	9	13	12	6	22	14
110.0	18	17	7	1	11	5	16	19	8	23	20	24	15	3	2	4	10	21	9	13	12	6	22	14
115.0	18	17	7	1	11	16	5	19	23	8	20	24	15	3	2	10	4	21	9	13	12	6	22	14
120.0	18	17	1	7	11	23	16	19	24	6	5	20	15	3	2	10	21	4	9	13	12	22	6	14
125.0	18	17	1	7	11	23	24	16	19	8	20	5	15	3	2	10	21	9	4	13	12	22	14	6
130.0	18	17	1	11	24	23	7	16	19	8	2	10	20	3	15	5	9	12	13	21	4	22	14	8
135.0	18	1	24	17	11	23	10	2	12	9	22	13	16	3	14	19	8	15	21	20	7	4	5	6
140.0	22	14	12	10	24	13	2	9	23	11	1	21	6	3	15	16	4	8	19	20	17	18	5	[illegible]
145.0	22	14	12	13	10	9	8	2	24	21	23	11	3	1	4	15	8	16	20	19	5	7	17	18
150.0	22	14	12	6	13	10	9	2	24	21	23	4	3	11	15	1	8	20	16	19	5	7	17	18
155.0	22	14	12	6	13	9	10	2	21	24	4	23	3	15	11	8	20	1	16	19	5	7	17	18
160.0	22	14	12	6	13	9	10	2	21	24	4	3	23	15	11	20	8	16	19	1	5	7	17	18
165.0	22	14	6	12	13	9	10	2	21	24	4	3	23	15	11	20	8	19	16	1	5	7	17	18
170.0	22	14	6	12	13	9	10	2	21	24	4	3	23	15	11	20	8	19	16	1	5	7	17	18
175.0	22	14	6	12	13	9	10	2	21	4	24	3	23	15	11	20	8	19	16	1	5	7	17	18
180.0	22	14	6	12	13	9	10	2	21	4	24	3	23	15	11	20	8	19	16	1	5	7	17	18
185.0	23	15	3	24	11	4	20	8	19	18	21	2	1	5	10	9	13	7	12	6	14	22	17	18
190.0	18	17	7	1	5	16	19	8	20	11	23	15	3	24	4	2	21	10	9	13	12	6	22	14
195.0	18	17	7	1	5	16	19	8	20	11	23	15	3	24	4	2	21	10	9	13	12	6	22	14
200.0	18	17	7	1	5	19	16	8	20	11	23	15	3	24	4	2	21	10	9	13	12	6	22	14
205.0	18	17	7	1	5	19	16	8	20	11	23	15	3	24	4	2	21	10	9	13	12	6	22	14
210.0	18	17	7	1	5	19	16	20	8	11	23	15	3	24	4	2	21	10	9	13	12	6	22	14
215.0	18	17	7	1	5	19	16	20	8	11	23	15	3	24	4	2	21	10	9	13	12	6	22	14
220.0	18	17	7	1	19	16	5	20	8	11	23	15	24	3	4	2	21	10	9	13	12	6	22	14
225.0	18	17	7	1	19	16	5	20	8	11	23	15	24	3	2	4	10	21	9	13	12	6	22	14
230.0	18	17	7	1	19	16	5	20	8	11	23	15	24	3	2	4	10	21	9	13	12	6	22	14
235.0	18	17	7	1	19	16	20	5	8	11	23	24	15	3	2	4	10	21	9	13	12	6	22	14
240.0	18	17	1	7	19	16	20	8	11	5	24	23	15	3	2	10	4	9	21	13	12	6	22	14
245.0	18	17	1	7	19	16	20	11	8	24	23	5	3	15	2	10	9	4	21	13	12	6	22	14
250.0	18	17	1	19	16	7	20	11	8	24	2	23	3	15	5	10	9	4	21	12	13	22	6	14
255.0	18	17	1	19	16	2	24	20	7	11	8	5	10	23	15	9	5	21	4	12	13	22	14	6
260.0	18	17	1	2	16	19	10	9	24	3	8	11	20	15	23	7	21	4	5	12	22	13	14	6
265.0	5	6	7	4	13	14	21	8	15	12	22	3	20	11	23	18	9	10	17	19	7	1	19	23
270.0	5	7	18	4	6	17	13	8	21	10	20	11	23	3	12	14	16	1	19	22	24	10	[illegible]	[illegible]
275.0	18	7	5	17	4	8	20	11	15	23	13	6	21	5	3	16	19	12	24	14	19	7	5	[illegible]
280.0	18	7	17	5	5	20	4	11	23	15	1	16	21	19	3	13	6	24	19	13	[illegible]	9	[illegible]	[illegible]
285.0	18	17	7	5	8	20	11	4	23	1	15	16	19	21	3	13	24	6	12	2	10	9	14	22
290.0	18	17	7	5	8	20	11	1	23	4	16	19	15	3	21	24	13	6	12	2	10	9	14	22
295.0	18	17	7	5	20	8	11	1	19	16	23	15	4	3	21	24	13	6	2	12	10	9	14	22
300.0	18	17	7	5	20	8	1	11	19	16	23	15	4	3	21	24	13	6	2	12	10	9	14	22
305.0	18	17	7	5	20	1	8	19	11	16	23	15	4	3	21	24	13	2	6	12	10	9	14	22
310.0	18	17	7	5	20	19	1	16	8	11	23	15	4	3	24	21	13	2	6	12	10	9	14	22
315.0	18	17	7	5	20	19	16	1	8	11	23	15	4	3	24	21	13	2	6	12	10	9	22	14
320.0	18	17	7	5	19	20	16	1	23	8	11	15	4	24	21	3	13	2	6	12	10	9	22	14
325.0	18	17	7	5	19	20	16	1	23	8	11	15	4	21	24	3	13	2	6	12	10	9	22	14
330.0	18	17	7	19	5	20	16	23	1	15	21	11	8	24	4	3	13	2	6	12	10	9	22	14
335.0	18	17	19	20	16	21	23	15	1	7	24	5	22	11	3	4	8	13	2	12	14	6	10	9
340.0	7	5	18	8	6	17	11	4	9	3	10	1	12	16	19	13	15	24	2	23	20	21	14	22
345.0	18	17	7	5	6	19	8	16	4	11	20	1	15	3	24	23	12	13	9	10	2	21	14	22
350.0	18	17	6	5	7	19	16	20	4	8	24	15	11	23	12	1	3	13	21	9	2	10	14	22
355.0	11	24	23	12	1	13	8	21	3	10	15	20	7	7	22	14	9	18	4	17	5	16	19	6
360.0	11	1	24	8	18	10	23	7	3	17	9	2	12	15	13	21	20	4	5	16	19	14	22	6
365.0	18	11	1	17	10	8	24	7	23	3	9	2	15	16	5	4	20	12	13	21	19	14	22	6
370.0	17	18	10	2	1	8	16	19	11	9	23	5	20	7	15	4	3	24	13	21	12	14	22	6
375.0	13	23	24	7	18	5	8	21	17	20	15	6	4	22	12	11	1	3	19	14	16	9	10	2
380.0	17	18	20	5	22	1	24	15	3	23	2	19	16	9	4	11	21	7	8	6	10	14	12	13
385.0	22	20	18	1	7	5	6	14	17	9	19	13	21	3	23	15	24	12	2	8	16	10	4	[illegible]

Table 5.3.2a *Response characteristics of Disc 24J (root stress A)*

FREQUENCY	MAX RESP	MIN RESP	STD	SKEW	KURT	BLR	BHR
10.00	.000010	.000010	1.984	-.984	1.426	18	14
15.00	.000023	.000021	1.980	-.983	1.426	18	14
20.00	.000042	.000038	1.976	-.983	1.426	18	14
25.00	.000065	.000059	1.969	-.984	1.427	18	14
30.00	.000092	.000084	1.961	-.984	1.428	18	14
35.00	.000125	.000114	1.952	-.984	1.429	18	14
40.00	.000162	.000148	1.940	-.985	1.430	18	14
45.00	.000203	.000186	1.927	-.985	1.432	18	14
50.00	.000248	.000227	1.911	-.986	1.434	18	14
55.00	.000297	.000272	1.893	-.987	1.437	18	14
60.00	.000348	.000319	1.872	-.988	1.440	18	14
65.00	.000403	.000370	1.848	-.989	1.443	18	14
70.00	.000460	.000422	1.821	-.991	1.448	18	14
75.00	.000518	.000477	1.790	-.993	1.453	18	14
80.00	.000578	.000532	1.754	-.996	1.459	18	14
85.00	.000638	.000589	1.714	-.999	1.467	18	14
90.00	.000698	.000646	1.667	-1.002	1.476	18	14
95.00	.000757	.000703	1.613	-1.007	1.488	18	14
100.00	.000815	.000758	1.551	-1.013	1.503	18	14
105.00	.000869	.000812	1.479	-1.021	1.522	18	14
110.00	.000921	.000863	1.395	-1.031	1.547	18	14
115.00	.000967	.000911	1.296	-1.045	1.580	18	14
120.00	.001008	.000954	1.180	-1.064	1.628	18	14
125.00	.001041	.000992	1.042	-1.093	1.697	18	14
130.00	.001066	.001023	.876	-1.139	1.808	18	14
135.00	.001080	.001047	.676	-1.218	2.004	18	14
140.00	.001083	.001062	.432	-1.376	2.397	18	14
145.00	.001074	.001066	.163	-.817	1.113	18	21
150.00	.001058	.001044	.336	-.089	-.679	6	18
155.00	.001036	.001001	.831	.428	.236	22	18
160.00	.000999	.000936	1.492	.599	.590	22	18
165.00	.000944	.000847	2.382	.678	.760	22	18
170.00	.000869	.000733	3.626	.721	.856	14	18
175.00	.000772	.000589	5.465	.748	.917	14	18
180.00	.000651	.000412	8.420	.766	.958	14	18
185.00	.000501	.000197	13.870	.778	.985	14	18
190.00	.000321	.000005	22.859	1.539	2.342	12	18
195.00	.000361	.000029	22.948	.249	-.383	17	22
200.00	.000717	.000146	18.160	-.755	1.027	18	22
205.00	.001131	.000440	13.907	-.797	1.033	18	22
210.00	.001611	.000781	11.716	-.799	1.035	18	22
215.00	.002166	.001174	10.407	-.799	1.035	18	22
220.00	.002804	.001623	9.558	-.799	1.032	18	22
225.00	.003536	.002136	8.984	-.799	1.025	18	22
230.00	.004376	.002717	8.593	-.798	1.015	18	22
235.00	.005338	.003373	8.339	-.797	.997	18	22
240.00	.006441	.004110	8.200	-.796	.966	18	22
245.00	.007712	.004931	8.189	-.791	.901	18	22
250.00	.009192	.005829	8.383	-.770	.748	18	22
255.00	.010986	.006752	9.188	-.674	.292	18	22
260.00	.014058	.007242	14.628	-.123	-1.086	18	9
265.00	.017015	.010029	12.538	.669	-.853	15	6
270.00	.017245	.012011	7.638	.252	-.655	18	6
275.00	.019546	.013552	7.450	-.085	-.087	18	6
280.00	.022589	.015459	7.516	-.219	.192	18	14
285.00	.026219	.017667	7.635	-.272	.322	18	14
290.00	.030416	.020188	7.803	-.285	.382	18	14
295.00	.035302	.023056	8.010	-.273	.404	18	14
300.00	.041035	.026316	8.258	-.244	.402	18	14
305.00	.047823	.030028	8.554	-.197	.385	18	14
310.00	.055958	.034264	8.908	-.131	.355	18	14
315.00	.065860	.039119	9.339	-.040	.317	18	14
320.00	.078187	.044723	9.879	.090	.275	18	14
325.00	.094117	.051303	10.597	.285	.240	18	14
330.00	.116446	.059546	11.726	.615	.257	18	14
335.00	.161519	.074261	15.506	1.098	.337	16	14
340.00	.182526	.051926	14.829	-.461	.788	18	12
345.00	.209602	.062271	16.841	-.286	.065	18	14
350.00	.372837	.031844	23.237	.152	-.219	18	14
355.00	.545135	.078013	27.636	.028	-1.291	14	10
360.00	.468519	.197555	16.073	.639	-.338	6	10
365.00	.655425	.210948	19.879	.192	-1.108	18	12
370.00	2.806828	.263627	25.763	.649	-.576	18	12
375.00	3.353731	.650798	19.129	1.383	1.618	18	6
380.00	313.234974	1.823059	25.550	2.061	3.251	17	13
385.00	7.932596	.473064	28.869	.505	-1.149	22	15
390.00	97.560041	.410490	29.104	1.921	2.152	22	16
395.00	1.633438	.437034	21.203	1.318	.620	14	19
400.00	210.061496	.583652	26.360	2.633	5.376	24	18
405.00	1.264817	.295385	18.214	2.369	4.764	22	18
410.00	.683532	.227993	17.521	.617	-.202	11	17
415.00	.723201	.131565	23.684	.028	-1.114	22	5
420.00	.646988	.157110	16.260	1.439	2.221	6	18
425.00	.454308	.194330	11.869	1.746	3.422	6	18
430.00	.377412	.192831	10.254	1.702	3.314	6	18
435.00	.329637	.184564	9.382	1.573	2.926	6	18
440.00	.295402	.174441	8.887	1.420	2.484	6	18
445.00	.268910	.163599	8.663	1.257	2.043	6	18
450.00	.247273	.152238	8.681	1.088	1.621	6	18
455.00	.228795	.140237	8.949	.912	1.226	6	18
460.00	.212343	.126158	9.511	.729	.868	14	18
465.00	.197001	.109051	10.446	.536	.556	14	18
470.00	.181951	.089347	11.901	.322	.303	14	18
475.00	.165924	.065571	14.134	.064	.142	22	18
480.00	.145461	.036400	17.312	-.258	.139	22	18
485.00	.158472	.030704	19.600	.745	.382	13	17
490.00	.177472	.024091	18.946	2.168	4.829	24	18
495.00	.136304	.003759	27.311	.947	-.339	21	18
500.00	.201698	.005858	28.965	1.095	-.081	20	14

Table 5.3.2 *Response characteristics of Disc 24J (root stress A)*

10.0	18	17	7	1	5	11	16	19	8	20	23	15	24	3	4	2	21	10	9	13	12	6	22	14
15.0	18	17	7	1	5	11	16	19	8	20	23	15	24	3	4	2	21	10	9	13	12	6	22	14
20.0	18	17	7	1	5	11	16	19	8	20	23	15	24	3	4	2	21	10	9	13	12	6	22	14
25.0	18	17	7	1	5	11	16	19	8	20	23	15	24	3	4	2	21	10	9	13	12	6	22	14
30.0	18	17	7	1	5	11	16	19	8	20	23	15	24	3	4	2	21	10	9	13	12	6	22	14
35.0	18	17	7	1	5	11	16	19	8	20	23	15	24	3	4	2	21	10	9	13	12	6	22	14
40.0	18	17	7	1	5	11	16	19	8	20	23	15	24	3	4	2	21	10	9	13	12	6	22	14
45.0	18	17	7	1	5	11	16	19	8	20	23	15	24	3	4	2	21	10	9	13	12	6	22	14
50.0	18	17	7	1	5	11	16	19	8	20	23	15	24	3	4	2	21	10	9	13	12	6	22	14
55.0	18	17	7	1	5	11	16	19	8	20	23	15	24	3	4	2	21	10	9	13	12	6	22	14
60.0	18	17	7	1	5	11	16	19	8	20	23	15	24	3	4	2	21	10	9	13	12	6	22	14
65.0	18	17	7	1	5	16	11	19	8	20	23	15	24	3	4	2	21	10	9	13	12	6	22	14
70.0	18	17	7	1	5	16	11	19	8	20	23	15	24	3	4	2	21	10	9	13	12	6	22	14
75.0	18	17	7	1	5	16	11	19	8	20	23	15	24	3	4	2	21	10	9	13	12	6	22	14
80.0	18	17	7	1	5	16	11	19	8	20	23	15	24	3	4	2	21	10	9	13	12	6	22	14
85.0	18	17	7	1	5	16	11	19	8	20	23	15	24	3	4	2	21	10	9	13	12	6	22	14
90.0	18	17	7	1	5	16	19	11	8	20	23	15	24	3	4	2	21	10	9	13	12	6	22	14
95.0	18	17	7	1	5	16	19	11	8	20	23	15	24	3	4	2	21	10	9	13	12	6	22	14
100.0	18	17	7	1	5	16	19	11	8	20	23	15	24	3	4	2	21	10	9	13	12	6	22	14
105.0	18	17	7	1	5	16	19	11	8	20	23	15	24	3	4	2	21	10	9	13	12	6	22	14
110.0	18	17	7	1	5	16	19	11	8	20	23	15	24	3	4	2	21	10	9	13	12	6	22	14
115.0	18	17	7	1	5	16	19	11	8	20	23	15	24	3	4	2	21	10	9	13	12	6	22	14
120.0	18	17	7	1	5	16	19	11	8	20	23	15	24	3	4	2	21	10	9	13	12	6	22	14
125.0	18	17	7	1	5	16	19	11	8	20	23	15	24	3	4	2	21	10	9	13	12	6	22	14
130.0	18	17	7	1	5	16	19	11	8	20	23	15	24	3	4	2	21	10	9	13	12	6	22	14
135.0	18	17	7	1	5	16	19	11	8	20	23	15	24	3	4	2	21	10	9	13	12	6	22	14
140.0	18	17	7	1	5	16	19	11	8	20	23	15	24	3	4	2	21	10	9	13	12	6	22	14
145.0	18	17	7	1	5	16	19	11	8	20	23	15	24	3	4	2	21	10	9	13	12	6	22	14
150.0	18	17	7	1	5	16	19	11	8	20	23	15	24	3	4	2	21	10	9	13	12	6	22	14
155.0	18	17	7	1	5	16	19	11	8	20	23	15	24	3	4	2	21	10	9	13	12	6	22	14
160.0	18	17	7	1	5	16	19	11	8	20	23	15	24	3	4	2	21	10	9	13	12	6	22	14
165.0	18	17	7	1	5	16	19	11	8	20	23	15	24	3	2	4	21	10	9	13	12	6	22	14
170.0	18	17	7	1	16	5	19	11	8	20	23	15	24	3	2	4	21	10	9	13	12	6	22	14
175.0	18	17	7	1	16	19	5	11	8	20	23	15	24	3	2	4	21	10	9	13	12	6	22	14
180.0	18	17	7	1	16	19	5	11	8	20	23	15	24	3	2	4	21	10	9	13	13	6	22	14
185.0	18	17	7	1	19	16	5	11	20	8	23	24	15	3	2	4	21	10	9	13	12	6	22	14
190.0	18	17	7	1	19	16	5	11	20	8	23	24	15	3	2	4	21	10	9	13	12	6	22	14
195.0	18	17	7	1	19	16	5	11	20	8	23	24	15	3	2	4	21	10	9	13	12	6	22	14
200.0	18	17	7	1	19	16	5	11	20	8	23	24	15	3	2	4	10	21	9	13	12	6	22	14
205.0	18	17	7	1	19	16	5	11	20	8	23	24	15	3	2	4	10	21	9	13	12	6	22	14
210.0	18	17	7	1	19	16	11	20	5	8	23	24	15	3	2	4	10	21	9	13	12	6	22	14
215.0	18	17	7	1	19	16	11	20	8	5	23	24	15	3	2	4	10	21	9	13	12	6	22	14
220.0	18	17	1	7	19	16	11	20	8	5	23	24	15	3	2	10	4	21	9	13	12	6	22	14
225.0	18	17	1	7	19	16	11	20	8	5	24	23	15	3	2	10	4	9	21	13	12	6	22	14
230.0	18	17	1	7	19	16	11	20	8	24	23	5	15	3	2	10	4	9	21	13	12	6	22	14
235.0	18	17	1	19	7	16	11	20	8	24	23	5	3	15	2	10	9	4	21	13	12	6	22	14
240.0	18	17	1	19	16	7	20	11	24	8	23	2	3	15	5	10	9	4	21	12	13	22	6	14
245.0	18	17	1	19	16	7	24	20	11	8	2	23	3	15	10	9	5	21	4	12	13	22	6	14
250.0	18	17	1	19	16	24	2	20	11	7	8	5	23	10	15	9	5	21	4	12	13	22	14	6
255.0	18	17	1	19	16	2	24	10	20	11	8	9	3	23	15	7	21	4	5	12	13	22	14	6
260.0	18	17	1	2	16	19	9	10	24	3	8	11	20	15	23	7	21	4	12	22	5	13	14	6
265.0	5	6	7	4	13	14	21	8	12	22	15	3	20	11	23	9	10	16	18	2	24	17	1	19
270.0	5	7	8	4	13	18	21	8	15	12	11	20	14	23	17	3	22	16	19	1	24	9	10	2
275.0	5	7	18	17	4	6	13	8	21	20	11	15	23	3	12	16	1	19	14	24	22	10	9	2
280.0	18	7	5	17	4	8	20	11	23	15	13	6	21	3	16	1	19	12	24	14	10	2	9	22
285.0	18	7	6	17	8	4	20	11	23	15	21	1	13	16	19	3	6	24	12	10	2	9	14	22
290.0	18	17	7	5	8	20	11	4	23	15	1	16	19	21	3	13	6	24	12	2	10	9	14	22
295.0	18	17	7	5	20	8	11	23	4	1	15	19	16	21	3	13	24	6	12	2	10	9	14	22
300.0	18	17	7	5	20	8	11	23	19	1	16	4	15	21	3	24	13	6	12	2	10	9	14	22
305.0	18	17	7	5	20	8	19	11	1	16	23	15	4	21	3	24	13	6	12	2	10	9	14	22
310.0	18	17	7	5	20	19	16	8	1	11	23	15	4	21	3	24	13	6	12	2	10	9	14	22
315.0	18	17	7	5	20	19	16	1	8	23	11	15	4	21	24	3	13	6	2	12	10	9	22	14
320.0	18	17	7	5	19	20	16	1	23	8	11	15	4	21	24	3	13	6	2	12	10	9	22	14
325.0	18	17	7	5	19	20	16	23	1	15	8	11	21	4	24	3	13	6	2	12	10	9	22	14
330.0	18	17	7	19	20	5	16	23	1	15	21	24	11	8	4	3	13	2	6	12	10	22	9	14
335.0	18	17	19	20	21	16	23	15	1	24	7	5	22	11	3	4	8	13	2	12	14	6	10	9
340.0	7	5	6	18	8	17	11	4	9	10	3	12	1	16	13	19	15	24	2	23	20	21	14	22
345.0	18	17	7	5	6	19	8	18	4	11	20	1	15	3	24	23	12	13	9	10	2	21	14	22
350.0	18	17	6	5	7	19	16	20	4	8	24	15	11	12	23	1	3	13	21	9	2	10	14	22
355.0	11	24	12	23	1	13	8	21	3	10	15	20	7	2	22	14	9	18	4	17	5	16	19	6
360.0	11	1	24	10	6	23	18	3	9	7	2	17	12	15	13	21	4	20	5	16	14	19	22	6
365.0	11	1	18	17	10	8	24	7	23	9	3	2	15	16	5	4	12	20	13	21	19	14	22	6
370.0	17	18	10	2	1	8	16	19	11	9	23	5	20	7	15	4	3	24	13	21	12	14	22	6
375.0	13	23	24	7	18	5	8	21	20	17	15	6	4	22	12	11	3	1	19	14	16	9	10	2
380.0	17	20	18	5	22	1	24	15	3	23	2	19	16	9	4	11	21	7	6	6	10	14	12	13
385.0	22	20	18	1	7	5	6	14	17	9	13	19	21	3	23	15	24	12	2	8	16	10	4	11
400.0	1	24	2	14	6	5	4	22	23	12	13	9	10	15	5	8	11	21	7	16	20	19	17	18
405.0	19	6	16	4	17	22	9	20	8	5	14	2	3	7	21	10	15	12	24	13	23	1	11	18
410.0	6	19	5	7	17	18	4	16	8	20	9	22	3	14	21	2	15	10	12	13	24	23	1	11
415.0	12	24	22	11	14	10	13	1	23	2	9	19	21	16	15	6	3	20	4	8	17	5	7	18
420.0	12	24	11	22	10	1	13	14	23	2	9	21	19	16	15	3	6	20	4	8	17	5	7	18
425.0	12	22	24	14	10	2	13	1	11	9	23	19	21	16	6	15	3	20	4	8	17	5	7	18
430.0	22	14	12	24	10	2	9	13	1	23	19	11	6	21	16	15	3	20	4	8	17	5	7	18
435.0	22	14	12	10	24	2	9	13	6	19	1	23	21	16	11	15	3	20	4	8	17	5	7	18
440.0	22	14	12	10	2	9	24	13	6	19	21	16	1	23	11	3	15	20	4	8	17	5	7	18
445.0	22	14	12	10	9	2	24	6	13	19	21	16	23	1	3	11	15	20	4	8	17	5	7	18
450.0	22	14	12	10	8	2	6	24	13	19	21	16	23	1	3	15	11	20	4	8	17	5	7	18
455.0	22	14	12	9	10	5	2	13	24	19	21	16	3	23	1	15	4	11	20	8	17	5	7	18
460.0	22	14	12	6	9	10	2	13	24	21	19	16	3	23	15	1	4	11	20	8	17	5	7	18
465.0	22	14	6	12	9	10	2	13	24	21	19	16	3	15	4	23	1	20	11	8	17	5	7	18
470.0	6	12	14	9	22	10	2	13	24	21	3	19	16	4	15	23	1	20	11	8	17	5	7	18
475.0	21	2	13	10	9	24	3	4	16	19	15	1	12	23	20	11	8	6	17	14	22	5	7	18
480.0	20	8	15	1	16	4	19	17	3	23	11	21	24	5	2	18	10	9	13	7	12	6	22	14
485.0	8	5	11	15	3	16	23	20	1	24	4	21	19	7	2	10	17	9	13	18	22	12	14	6
490.0	7	1	5	17	6	16	19	11	20	4	23	15	3	6	21	24	13	18	2	10	9	12	14	22
495.0	17	18	7	5	1	8	20	16	19	11	23	15	4	3	24	21	2	13	10	9	6	12	14	22
500.0	18	17	7	5	1	8	20	16	19	11	23	15	3	4	24	21	2	10	13	9	6	12	14	22

Table 5.3.3a *Response characteristics of Disc 24J (root stress B)*

FREQUENCY	MAX RESP	MIN. RESP	STD	SKEW	KURT	BLR	BHK
10.00	.000037	.000034	1.992	-.983	1.425	18	14
15.00	.000064	.000076	1.998	-.982	1.424	18	14
20.00	.000150	.000136	2.007	-.982	1.422	18	14
25.00	.000236	.000214	2.018	-.981	1.420	18	14
30.00	.000342	.000311	2.031	-.980	1.419	18	14
35.00	.000470	.000427	2.047	-.979	1.416	18	14
40.00	.000620	.000563	2.066	-.978	1.414	18	14
45.00	.000794	.000720	2.086	-.977	1.411	18	14
50.00	.000994	.000900	2.109	-.975	1.408	18	14
55.00	.001220	.001104	2.134	-.974	1.405	18	14
60.00	.001476	.001334	2.161	-.972	1.401	18	14
65.00	.001762	.001590	2.191	-.970	1.397	18	14
70.00	.002082	.001876	2.222	-.968	1.393	18	14
75.00	.002437	.002183	2.255	-.966	1.389	18	14
80.00	.002831	.002543	2.290	-.964	1.385	18	14
85.00	.003267	.002929	2.327	-.962	1.380	18	14
90.00	.003749	.003354	2.366	-.960	1.375	18	14
95.00	.004279	.003821	2.406	-.957	1.370	18	14
100.00	.004863	.004333	2.449	-.955	1.365	18	14
105.00	.005504	.004894	2.493	-.952	1.360	18	14
110.00	.006208	.005507	2.539	-.950	1.354	18	14
115.00	.006979	.006177	2.586	-.947	1.348	18	14
120.00	.007825	.006908	2.635	-.944	1.343	18	14
125.00	.008750	.007705	2.686	-.941	1.336	18	14
130.00	.009763	.008575	2.739	-.938	1.330	18	14
135.00	.010870	.009521	2.794	-.935	1.324	18	14
140.00	.012081	.010551	2.850	-.932	1.317	18	14
145.00	.013404	.011672	2.909	-.929	1.310	18	14
150.00	.014849	.012891	2.969	-.925	1.303	18	14
155.00	.016427	.014216	3.032	-.922	1.296	18	14
160.00	.018151	.015656	3.097	-.918	1.288	18	14
165.00	.020033	.017220	3.165	-.915	1.280	18	14
170.00	.022089	.018918	3.235	-.911	1.272	18	14
175.00	.024334	.020763	3.308	-.907	1.264	18	14
180.00	.026788	.022768	3.384	-.903	1.255	18	22
185.00	.029470	.024941	3.463	-.899	1.245	18	22
190.00	.032402	.027302	3.547	-.895	1.235	18	22
195.00	.035609	.029866	3.635	-.891	1.224	18	22
200.00	.039120	.032648	3.727	-.886	1.212	18	22
205.00	.042966	.035670	3.826	-.882	1.200	18	22
210.00	.047183	.038950	3.931	-.878	1.185	18	22
215.00	.051813	.042510	4.045	-.873	1.169	18	22
220.00	.056902	.046375	4.169	-.869	1.149	18	22
225.00	.062507	.050567	4.306	-.864	1.124	18	22
230.00	.068694	.055110	4.461	-.858	1.090	18	22
235.00	.075546	.060024	4.644	-.851	1.041	18	22
240.00	.083170	.065316	4.872	-.840	.962	18	22
245.00	.091728	.070959	5.165	-.817	.821	18	22
250.00	.101514	.076818	5.699	-.759	.533	18	22
255.00	.113380	.082297	6.889	-.585	-.120	18	22
260.00	.139325	.081819	12.934	-.015	-1.240	17	9
265.00	.157026	.097739	12.076	.536	-1.064	15	6
270.00	.151903	.119447	5.951	.470	-.982	18	6
275.00	.164171	.127727	5.526	.148	-.520	18	6
280.00	.180131	.138558	5.643	-.047	-.125	18	6
285.00	.200108	.151102	5.846	-.143	.100	18	14
290.00	.223273	.165281	6.097	-.182	.223	18	14
295.00	.249859	.181201	6.391	-.188	.285	18	14
300.00	.280658	.199062	6.725	-.169	.311	18	14
305.00	.316724	.219130	7.106	-.129	.313	18	14
310.00	.359518	.241748	7.545	-.065	.298	18	14
315.00	.411182	.267371	8.063	.026	.272	18	14
320.00	.475102	.296658	8.694	.158	.241	18	14
325.00	.557435	.330860	9.515	.358	.221	18	14
330.00	.673205	.373987	10.782	.693	.265	18	14
335.00	.913182	.432276	14.946	1.091	.313	16	14
340.00	1.019233	.308851	14.679	-.434	.644	18	12
345.00	1.133145	.363502	16.374	-.361	.074	18	12
350.00	1.973533	.182644	23.106	.072	-.237	18	14
355.00	2.875209	.360500	27.853	-.013	-1.321	14	10
360.00	2.428089	1.018709	15.815	.656	-.308	6	10
365.00	3.319726	1.131621	19.558	.203	-1.106	18	12
370.00	13.978577	1.383027	25.597	.639	-.581	18	12
375.00	16.417999	3.364824	19.031	1.386	1.584	18	6
380.00	1516.012128	9.214938	25.500	2.063	3.272	17	13
385.00	38.254780	2.228192	28.828	.513	-1.140	22	15
390.00	466.191555	1.937674	29.301	1.904	2.064	22	16
395.00	7.701432	2.008371	21.661	1.293	.550	14	19
400.00	1008.849404	2.778098	26.226	2.651	5.469	24	18
405.00	5.990442	1.322105	18.439	2.389	4.857	22	18
410.00	3.167794	1.022591	17.837	.693	-.092	11	17
415.00	3.280686	.562840	23.831	.028	-1.113	22	5
420.00	2.965840	.676396	16.497	1.515	2.484	6	18
425.00	2.055548	.835245	12.307	1.809	3.639	6	18
430.00	1.688282	.822791	10.756	1.758	3.498	6	18
435.00	1.458951	.781340	9.904	1.633	3.110	6	18
440.00	1.294309	.732866	9.405	1.488	2.681	6	18
445.00	1.166992	.682445	9.156	1.335	2.256	6	18
450.00	1.063358	.631012	9.130	1.175	1.845	6	18
455.00	.975409	.578122	9.332	1.008	1.450	6	18
460.00	.897861	.521035	9.798	.830	1.074	14	18
465.00	.826518	.451203	10.600	.637	.723	14	18
470.00	.757703	.372979	11.864	.420	.408	14	18
475.00	.685875	.281258	13.821	.151	.149	14	18
480.00	.596057	.164826	16.809	-.237	.041	22	18
485.00	.691762	.084690	19.902	.715	.440	13	7
490.00	.738083	.079450	19.290	2.178	4.572	14	18
495.00	.582498	.018910	24.367	1.138	.731	9	18
500.00	.700126	.017331	30.631	1.055	-.782	20	14

Table 5.3.3 *Response characteristics of Disc 24J (root stress B)*

10.0	18	17	1	11	7	23	24	8	5	20	10	16	3	15	2	19	13	12	21	9	4	22	14	6
15.0	18	17	1	11	7	23	24	8	5	20	16	10	3	15	2	19	13	12	21	9	4	22	14	6
20.0	18	17	1	11	7	23	24	8	5	20	16	3	15	10	2	19	13	12	21	9	4	22	14	6
25.0	18	17	1	11	7	23	24	8	5	20	16	3	15	10	2	19	13	12	21	9	4	22	14	6
30.0	18	17	1	11	7	23	24	8	5	20	16	15	3	10	2	19	13	12	21	9	4	22	14	6
35.0	18	17	1	11	7	23	24	8	5	20	16	15	3	10	2	19	13	12	21	9	4	22	14	6
40.0	18	17	1	11	7	23	24	8	5	20	16	15	3	10	2	19	13	12	21	9	4	22	14	6
45.0	18	17	1	11	7	23	24	8	5	20	16	15	3	10	2	19	13	21	12	9	4	22	14	6
50.0	18	17	1	11	7	23	24	8	5	16	20	15	3	2	10	19	13	21	12	9	4	22	14	6
55.0	18	17	1	11	7	23	24	8	5	16	20	15	3	19	2	10	13	21	12	9	4	22	14	6
60.0	18	17	1	11	7	23	24	8	5	16	20	15	3	19	2	10	13	21	12	9	4	22	14	6
65.0	18	17	1	11	7	23	24	8	16	5	20	19	15	3	2	10	21	13	12	9	4	22	14	6
70.0	18	17	1	11	7	23	24	8	16	5	20	19	15	3	2	10	21	13	12	9	4	22	14	6
75.0	18	17	1	11	7	23	24	8	16	5	20	19	15	3	2	10	21	13	9	12	4	22	14	6
80.0	18	17	1	11	7	23	24	8	16	5	20	19	15	3	2	10	21	13	9	4	12	22	14	6
85.0	18	17	1	11	7	23	24	8	16	20	5	19	15	3	2	10	21	13	9	4	12	22	14	6
90.0	18	17	1	11	7	23	24	8	16	20	5	19	15	3	2	10	21	9	13	4	12	22	14	6
95.0	18	17	1	7	11	23	24	8	16	19	20	5	15	3	2	10	21	9	4	13	12	22	14	6
100.0	18	17	1	7	11	23	24	16	8	19	20	5	15	3	2	10	21	9	4	13	12	22	14	6
105.0	18	17	1	7	11	23	24	16	8	19	20	5	15	3	2	10	21	9	4	13	12	22	14	6
110.0	18	17	1	7	11	23	24	16	8	19	20	5	15	3	2	10	21	9	4	13	12	22	14	6
115.0	18	17	1	7	11	23	24	16	8	19	20	5	15	3	2	10	21	9	4	13	12	22	14	6
120.0	18	17	1	7	11	23	24	16	19	8	20	5	15	3	2	10	21	9	4	13	12	22	14	6
125.0	18	17	1	7	11	23	24	16	19	8	20	5	15	3	2	10	21	9	4	13	12	22	14	6
130.0	18	17	1	7	11	23	24	16	19	8	20	5	15	3	2	10	21	9	4	13	12	22	14	6
135.0	18	17	1	7	11	23	24	16	19	8	20	5	15	3	2	10	21	9	4	13	12	22	14	6
140.0	18	17	1	7	11	23	24	16	19	8	20	5	15	3	2	10	21	9	4	13	12	22	14	6
145.0	18	17	1	7	11	16	24	23	19	8	20	5	15	3	2	10	21	9	4	13	12	22	14	6
150.0	18	17	1	7	11	16	19	24	23	8	20	5	15	3	2	10	21	9	4	13	12	22	14	6
155.0	18	17	1	7	11	16	19	24	23	8	20	5	15	3	2	10	21	9	4	13	12	22	6	14
160.0	18	17	1	7	11	16	19	24	23	8	20	5	15	3	2	10	9	21	4	13	12	22	6	14
165.0	18	17	1	7	11	16	19	24	23	20	8	5	15	3	2	10	9	21	4	13	12	22	6	14
170.0	18	17	1	7	11	16	19	24	23	20	8	5	15	3	2	10	9	21	4	13	12	22	6	14
175.0	18	17	1	7	19	16	11	24	23	20	8	5	15	3	2	10	9	21	4	13	12	22	6	14
180.0	18	17	1	7	19	16	11	24	23	20	8	2	15	3	5	10	9	21	4	12	13	22	6	14
185.0	18	17	1	7	19	16	11	24	23	20	8	2	15	3	5	10	9	21	4	12	13	22	6	14
190.0	18	17	1	7	19	16	11	24	23	20	8	2	3	15	5	10	9	21	4	12	13	22	6	14
200.0	18	17	1	19	16	7	11	24	20	23	8	2	3	15	5	10	9	21	4	12	13	22	6	14
205.0	18	17	1	19	16	7	11	24	20	23	8	2	3	15	10	5	9	21	4	12	13	22	6	14
210.0	18	17	1	19	16	7	24	11	20	23	8	2	3	15	10	5	9	21	4	12	13	22	14	6
215.0	18	17	1	19	16	24	7	11	20	23	8	2	3	15	10	5	9	21	4	12	13	22	14	6
220.0	18	17	1	19	16	24	11	7	20	23	2	8	3	15	10	9	5	21	4	12	13	22	14	6
225.0	18	17	1	19	16	24	11	7	20	2	23	8	3	15	10	9	5	21	4	12	13	22	14	6
230.0	18	17	1	19	16	24	11	2	20	7	23	8	3	10	15	9	5	21	4	12	13	22	14	6
235.0	18	17	1	19	16	24	2	11	20	23	8	7	10	3	15	9	21	5	4	12	13	22	14	6
240.0	18	17	1	19	16	24	2	11	20	8	10	23	3	7	9	15	21	5	4	12	13	22	14	6
245.0	18	17	1	19	16	24	2	11	20	10	8	9	3	23	15	7	21	4	5	12	13	22	14	6
250.0	18	17	1	19	16	2	24	10	9	11	20	3	8	23	15	7	21	4	12	5	22	13	14	6
255.0	18	17	1	19	16	2	24	10	9	3	11	20	8	23	15	7	21	4	12	22	5	13	14	6
260.0	18	17	1	2	16	19	9	10	24	3	8	11	20	15	23	21	7	4	12	22	14	13	5	6
265.0	5	6	4	7	13	14	21	22	12	8	15	3	20	11	23	9	10	2	16	24	19	1	18	17
270.0	5	6	7	13	4	14	21	12	8	22	15	23	11	20	3	18	9	10	16	24	17	19	1	2
275.0	5	7	6	13	4	21	12	8	14	15	23	11	20	18	22	3	17	16	24	19	1	10	9	2
280.0	5	7	6	4	13	18	21	8	23	15	20	11	12	17	14	3	22	16	19	24	1	10	9	2
285.0	5	7	18	4	6	17	13	8	21	20	23	11	15	12	3	16	19	14	1	24	22	10	9	2
290.0	5	7	18	17	4	6	13	20	8	23	11	21	15	12	3	19	16	1	24	14	22	10	2	9
295.0	18	5	7	17	4	20	23	8	11	13	15	6	21	19	16	1	3	12	24	14	22	10	2	9
300.0	18	7	5	17	20	4	23	8	11	15	21	19	13	16	6	1	3	24	12	14	2	10	22	9
305.0	18	17	7	5	20	23	4	8	11	19	15	16	21	1	13	6	3	24	12	2	10	14	22	9
310.0	18	17	7	5	20	19	23	16	4	8	11	15	21	1	13	24	6	3	12	2	10	14	22	9
315.0	18	17	7	5	20	19	23	16	15	11	8	4	1	21	24	13	3	6	12	2	10	22	9	14
320.0	18	17	7	5	20	19	16	23	15	1	11	8	21	4	24	13	3	6	12	2	10	22	9	14
325.0	18	17	7	5	19	20	16	23	15	21	1	11	4	8	24	3	13	6	12	2	22	10	14	9
330.0	18	17	19	20	7	5	18	23	21	15	1	24	4	11	8	3	13	6	22	12	2	14	10	9
335.0	18	17	19	20	21	16	23	15	24	22	1	5	7	13	4	3	11	2	8	14	12	6	10	9
340.0	7	5	6	8	18	11	4	17	9	10	12	3	1	13	16	19	2	24	15	23	20	14	21	22
345.0	18	7	5	17	6	19	8	4	16	11	20	1	12	15	3	24	23	13	9	10	2	21	14	22
350.0	18	17	6	5	7	19	16	4	20	8	24	12	15	11	23	1	13	3	21	9	2	10	14	22
355.0	11	12	24	23	1	13	8	21	3	10	15	20	22	14	7	2	9	4	18	5	17	16	19	6
360.0	11	1	10	24	8	23	9	3	12	2	7	13	18	15	21	17	4	20	5	16	14	22	19	6
365.0	11	1	18	10	17	8	24	7	23	9	2	3	15	16	12	4	5	13	20	21	19	14	22	6
370.0	17	16	10	2	8	16	1	19	11	9	23	5	20	7	15	4	3	24	13	21	12	14	22	8
375.0	13	23	24	7	18	8	5	21	20	6	15	17	22	4	12	3	11	1	19	14	9	16	10	2
380.0	17	20	18	5	22	1	15	24	3	23	2	19	16	9	4	11	21	7	6	8	10	14	12	13
385.0	22	20	18	1	14	7	5	6	17	9	13	19	3	21	23	15	24	12	2	8	10	16	4	11
400.0	1	24	2	14	6	3	4	22	23	12	13	9	10	15	5	8	11	21	7	16	20	19	17	18
405.0	19	6	16	4	17	22	9	20	8	5	14	2	7	3	21	10	15	12	24	13	23	1	11	18
410.0	6	19	5	7	17	18	4	16	8	20	9	22	3	14	2	21	15	10	12	24	13	23	1	11
415.0	12	24	22	11	10	14	13	1	23	2	9	19	21	16	10	6	3	20	4	8	17	5	7	18
420.0	12	24	11	22	1	10	13	14	23	2	9	21	19	16	15	3	6	20	4	8	17	5	7	18
425.0	12	22	24	14	10	2	13	1	11	9	23	19	21	16	6	15	3	20	4	8	17	5	7	18
430.0	22	14	12	24	10	2	9	13	1	23	19	11	6	16	21	15	3	20	4	8	17	5	7	18
435.0	22	14	12	10	24	2	9	13	6	19	1	23	16	21	11	15	3	20	4	8	17	5	7	18
440.0	22	14	12	10	2	9	24	6	13	18	16	21	1	23	11	3	15	20	4	8	17	5	7	18
445.0	22	14	12	10	9	2	24	6	13	19	21	16	1	23	3	15	11	20	4	8	17	5	7	18
450.0	22	14	12	9	10	2	6	24	13	19	21	16	23	1	3	15	11	20	4	8	17	5	7	18
455.0	22	14	12	6	9	10	2	13	24	21	19	16	3	23	1	15	4	11	20	8	17	5	7	18
460.0	22	14	12	6	9	10	2	13	24	21	19	16	3	15	23	4	1	11	20	8	17	5	7	18
465.0	14	22	6	12	9	10	2	13	24	21	19	3	16	4	15	23	1	20	11	8	5	17	7	18
470.0	9	10	13	2	6	12	21	24	3	4	19	14	16	15	22	23	1	20	11	8	5	17	7	18
475.0	4	3	15	16	21	19	1	20	24	23	8	11	2	10	13	9	12	5	17	6	7	18	14	22
480.0	17	5	20	8	1	16	11	15	19	23	3	18	4	7	24	21	2	10	9	13	12	6	22	14
485.0	5	8	7	11	1	16	15	20	23	19	24	3	21	17	2	4	18	10	9	13	22	12	14	6
490.0	17	7	5	1	8	11	20	16	19	4	18	23	15	3	8	21	13	24	2	10	9	12	14	22
495.0	17	18	7	5	1	8	20	16	11	19	23	15	4	3	24	21	2	13	10	6	9	12	14	22
500.0	18	17	7	5	1	8	20	16	19	11	23	15	3	4	24	21	2	13	10	9	6	12	14	22

Chapter 6

6.1 Introduction

It has been shown in the preceeding chapters that an in-depth analysis of computed response data reveals certain characteristics concerning the dynamic behaviour of mistuned assemblies. Such basic characteristics are invariant with the theoretical methods employed in calculating the data.

In the present chapter, our aim is to explore further whether or not the qualitative features which were observed from the lumped parameter and receptance modelling would be experimentally verifiable. The type of comparison, between theory and experiment, which we seek in this place is not the usual verification of 'accuracy' in the prediction of natural frequencies and mode shapes. Whilst the prediction of these modal properties is of great significance, no theoretical methods exist, to our knowledge, for accurately predicting the response levels of individual blades in actual engines under typical operating conditions. Yet, a knowledge of response levels is ultimately of greater interest than the calculation of frequencies and mode shapes. Engine designers, for example, are especially interested in knowing how to identify the particular blade(s), if any, which are likely to turn rogue, so that remedial measures may be taken before failure occurs. The theoretical treatments in the earlier chapters have revealed that it is possible to identify, fairly accurately, those few blades on a stage that could turn rogue should the engine be operated at critical speeds. The experiments conducted in the course of this research are, therefore, intermediate between rapid theoretical procedures and costly full-scale engine tests.

6.2 Apparatus

(*a*) *The Test Piece.* The test-piece employed for this experimental programme is a scaled down model of a 24 bladed turbine wheel. The model, designated in this text as Disc 24X, was first used by **Ewins** (1973, 1976). It was initially designed for verifying the predictions of receptance methods. Hence, the blades are of uniform cross-section, while the disc is thin, in accordance with the requirements of the thin-plate theory used in the receptance formulations. A significant feature of Disc 24X is the ability to delibrately detune each of its blades by small amounts, simply by attaching nuts, bolts, and washers to the tip of each blade.

Although precision manufacturing techniques were employed in the fabrication of the test-piece to ensure that all the blades were initially in

perfect tune, significant residual non-uniformity nevertheless existed, as reported by Ewins (1976). In addition, the nuts, bolts, and washers are themselves subject to 'mistuning', since stochastic deviations from nominal values are characteristic of most batch products. Nevertheless, it is possible to deduce the approximate state of tune of the individual blades by weighing the 'detuning washers' affixed to each blade.

(*b*) *Instrumentation.*

The experimental set up shown schematically in Figure 6.2.1, is an automated facility for measuring the mobility of engineering structures as currently configured in the Dynamics Laborartory at Imperial College. The system is built around a *Digital Equipment* PDP 11/34 mini-computer, which is interfaced with several peripheral devices, and coupled to a *Solatron* analogue scanner. The scanner is connected via separate channels (only 10 channels are available in the current configuration) to transducers attached to the test-piece for the measurement of excitation and response data. Excitation, at a level specified by the computer operator, is applied from the oscillator through the power amplifier and shaker unto the disc. The measurement of mobility data is under the control of MOB3 - an, in-house software due to **Kirshenboim** (1980). The program is in turn controlled by the BASAC operating system (version 4), issued by Solatron Instrumentation Group, which is a variant of *Digital Equipment*'s 'single job' operating system, **RT-11**.

The mobility data acquired in the course of an experiment may be 'saved' on any of the storage devices interfaced to the PDP bus; floppy diskettes (DX0, DX1) or paper tapes (PP0) are the most commonly used.

(*c*) *Experimental Procedure.* Two procedures for simulating engine order excitations have been described by **Ewins** (1976) and **Fabunmi** (1978). In the former case, the bladed disc assembly is rotated in an evacuated chamber, while k equispaced air jets are positioned to excite the spining wheel near the blade root and disc rim interface, to induce the kth order engine excitation. In Fabunmi's method, a piezo-electric exciter is placed at the root of each blade while the assembly is freely suspended. These exciters are then driven by a single oscillator whose output is multiplexed into N signals, for an N bladed wheel. The output signals from the N channels are, after amplification, electronically phase shifted relative to one another, before being passed to the exciter to produce the desired engine order excitation.

In either procedure, at least 24 channels are required for the testing of a 24 bladed rotor. However, only 10 channels are available on the current set-up of the mobility system available at Imperial College. Therefore, instead of using 24 exciters, only a single point force was applied - at the center of the disc. Now, if the disc is isotropic, waves emanating from the centrally applied force would arrive with equal intensity at the root of each blade. This type of excitation of the blades would induce the zeroth order engine vibration in the bladed wheel. Since no relative temporal difference may be introduced deliberately into the wave motion, excitations arriving at the roots of the blades cannot be phase shifted relative to one another, so that the scope for varying the order of excitation is severely limited in this method.

By applying the single point force at the centre of the disc, the response of the assembly at the root of any one blade may be measured. In this way, only two channels are required for the measurements. However, the data acquisition routine consequently becomes laboriously lengthened and, moreover, the data are themselves liable to a certain amount of inconsistency, since transducers have to be changed from one blade to another between test-runs – a procedure attendant with inevitable alterations in the suspension of the bladed disc. Obviously, it is far more desirable to have the capability of monitoring all the blades simultaneously during such tests as these, which are geared towards clarifying a situation which is generally acknowledged as 'confusing' by most experts in this field.

The above limitations notwithstanding, two sets of experiments were performed; one in a 'low frequency' range ($60\text{Hz} \leq \omega \leq 700\text{Hz}$), and the other in a 'high frequency' range ($1.2\text{kHz} \leq \omega \leq 1.5\text{kHz}$). Before each test was commenced, a simultaneous calibration of the force and acceleration channels was carried out. This requires the application of a regulated force to a freely suspended block of known mass in order to obtain the *inertance* of the block as a function of excitation frequency. A calibration chart ensues from such tests from which a scale factor may be deduced.

After calibration, the vibrator is connected to the center of the freely suspended disc through the previously calibrated force gauge, while the accelerometer is attached to the root of the ith blade. The modulus and phase of the response of that blade are then measured relative to those of the centrally applied force to yield inertance, as the excitation frequency is slowly swept from one end of the desired spectrum to the other. At the

end of the sweep, the accelerometer is detached, taking care not to alter in any appreciable manner the free suspension characteristics of the system (an extremely difficult task). The accelerometer is then affixed at the root of the next blade, and the measurement procedure repeated, until all the blades have been tested.

6.3 Data Analysis

After the inertance of the system has been measured at the root of every blade, it is necessary to subject the test data to further processing in order to extract meaningful interpretations from them. The numerical precision and graphics capability attainable from the Computer Centre's CDC Cyber 174 and associated peripherals are far superior to those available on the PDP 11 configuration in the Dynamics Laboratory. It was therefore necessary to transfer the raw data from the mini-computer to the mainframe for post-measurement processing. The usual practice is to output the measured data to paper tapes via the puching machine interfaced with the PDP-11. The tapes are subsequently carried to the CDC. It is, however, a very slow and tedious procedure which is, moreover, wasteful of paper tapes, especially if several files have to be thus transferred. It was therefore necessary for us to devise a way of rapidly effecting the data transfer in order to devote greater time to the more important task of post-processing and interpretation.

Our scheme consists essentially of setting up a protocol, controlled by software, for the asynchronous transmission of information between the two computers. This is because the modem link to the CDC cannot handle parallel data transmission, and is moreover limited to a fixed serial data traffic rate of 300 baud; while the PDP bus operates at 9.6kbps, and the other slow speed peripherals interfaced with it are all hard-wired for parallel data handling.

Upon arrival at the CDC mainframe, the data are captured and 'saved' on disk packs. Statistical and graphical routines are subsequently invoked to process and display the results.

The frequency response of each blade is shown in Figures 6.3.1 to 6.3.24. The relative response of *all* the blades at selected frequencies in the low frequency range are depicted in the 'cells' of Figure 6.3.25. Each cell contains information pertaining to the excitation frequency, the magnitude of the largest response suffered by the blades at this frequency, and verti-

cal bars to show, sequentially from left to right, the relative response levels of blades 1 to 24. A statistical analysis of the response data is shown in Table 6.3.1, where the notations are as defined in Chapter 3. Similar results for the 'high frequency' range are given in Appendix II.

6.4 Concluding Remarks

At low excitation frequencies, each of the graphs in Figures 6.3.1 to 6.3.24 are characterised by well-defined *mass lines*. Thus, between $60\text{Hz} \leq \omega \leq 200\text{Hz}$, the receptance at the root of each blade decreases uniformly with excitation frequency. Now, blades 6 and 7 are the high frequency blades, while blades 19 and 20 have relatively lower cantilever frequencies. An examination of the relative response of the blades in this frequency range shows that blades 19 and 20 have the largest moduli of response, while blades 6 and 7 are at the low end of the response level ratings. This is in accordance with the predictions of our theoretical model, as described in Chapter 2.

Again, the relative response levels of the blades at the resonant frequenices of the system reveal (Table 6.3.1) that certain blades are likely to suffer extreme responses; this is qualitatively in line with the theoretical predictions of earlier chapters. Specifically, blade 7 which is one with extreme detune, suffers the largest global response at the 'worst' resonance (307 Hz) as shown below.

response magnitude	excitation frequency	blade with lowest response	blade with highest response
22.283	307	17	7
18.686	615	6	17
00.850	511	17	7

Results in the high frequency range are also in agreement with these observations. However, they are clouded by the proximity of the resonances. Owing to the poor frequency resolution of the measurement system, frequency sweeps cannot be made finer than four digits. Thus, although several resonances occur between 1268Hz and 1280Hz, the excitation frequency could not be incremented during the test by steps finer than 1Hz.

It is evident from the foregoing that a static bench test can be of value in identifying those blades that are likely to experience the largest dynamic response on a stage. It is therefore recommended that whenever a full-scale

engine test cannot be conduted on a rotating rig, a combination of the theoretical procedure of Chapter 2, and a static bench test should be substituted. In this way, one could gain valuable insight into the probable dynamic behaviour of a mistuned bladed disc assembly.

Fig. 6.2.1 *Schematic diagram of experimental set-up*

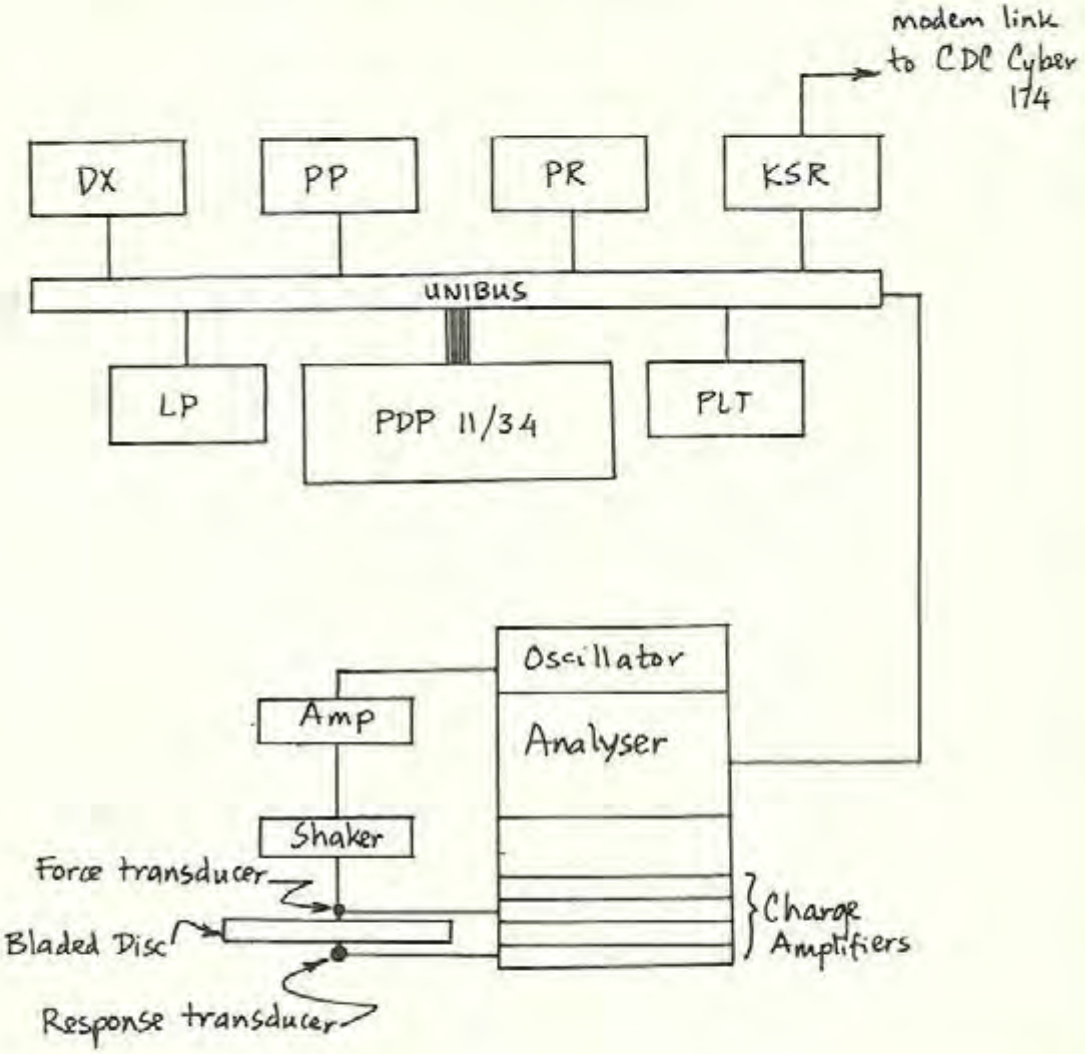

Key to mnemonics

DX	Floppy Disk Drives
PP	Paper-tape punch
PR	Paper-tape High-speed reader
KSR	Keyboard-Send-Receive terminal
LP	Receive-only printing terminal
PLT	Plotter

Fig. 6.3.1—6.3.24 *Frequency response of blades on Disc 24X*

Fig 6.3.1
Blade 1

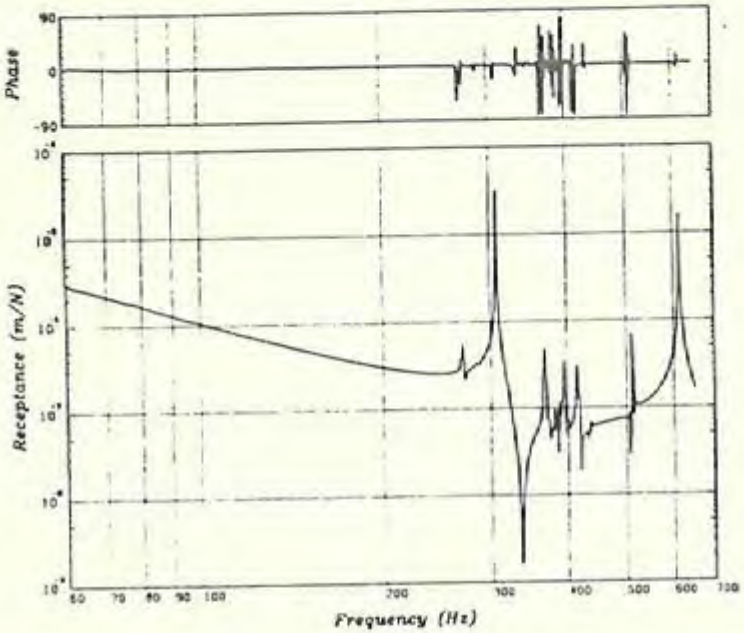

Fig 6.3.2
Blade 2

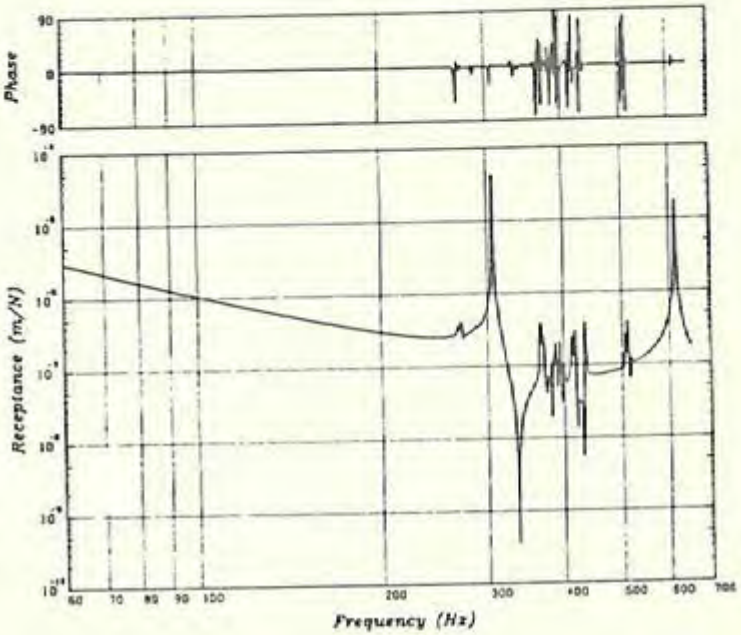

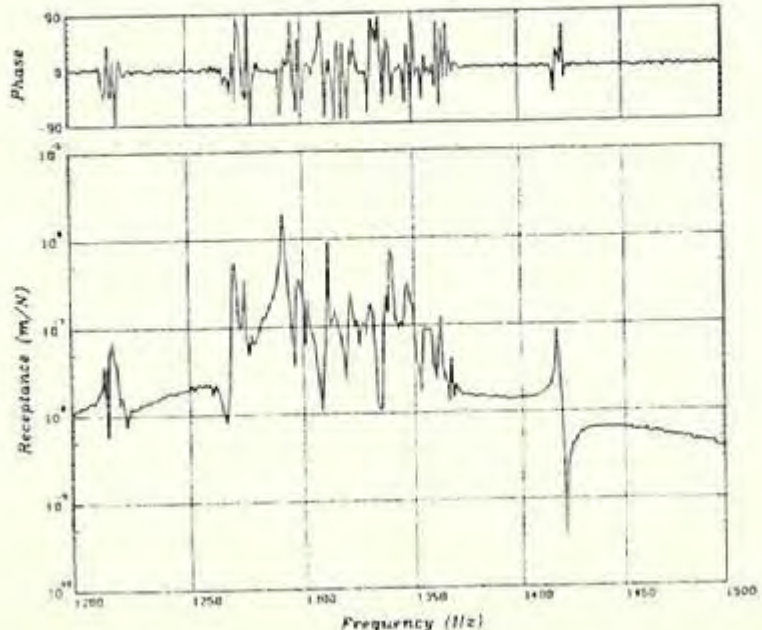

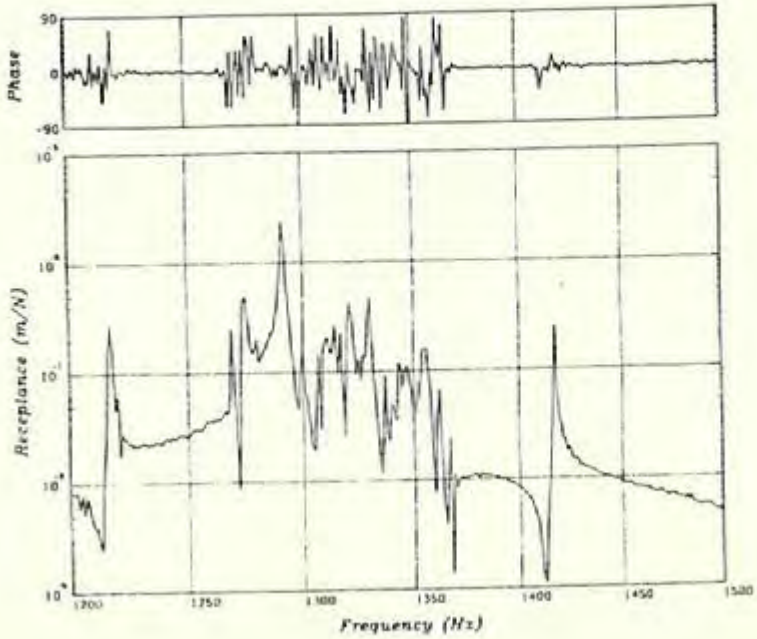

Blade 3

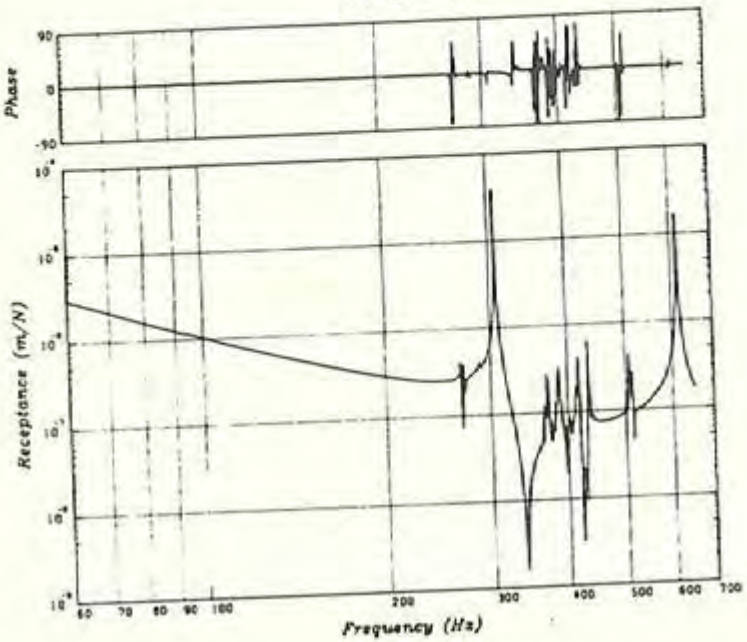

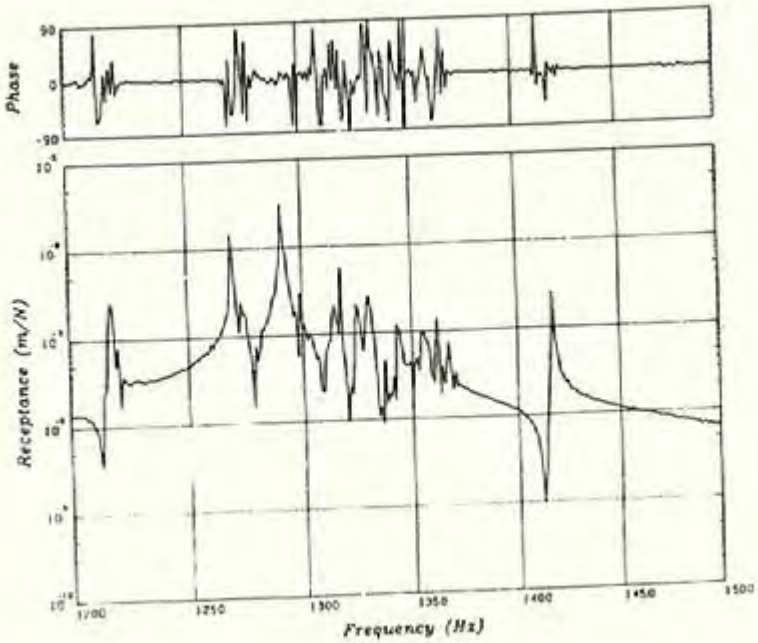

Blade 4

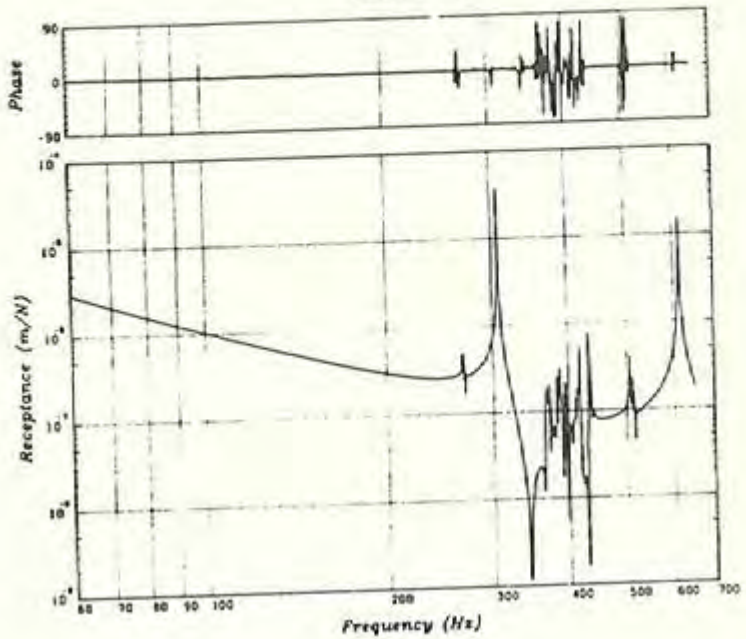

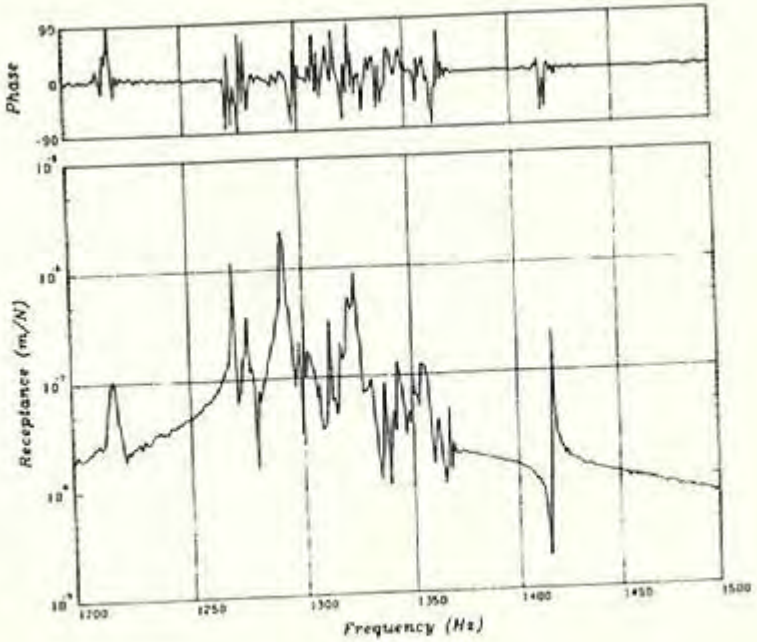

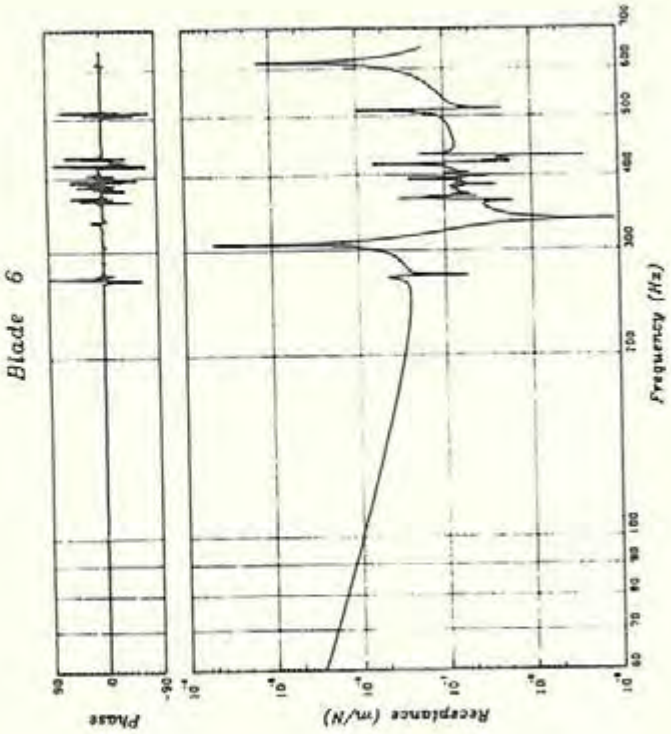
Blade 6
Phase
Receptance (m/N)
Frequency (Hz)

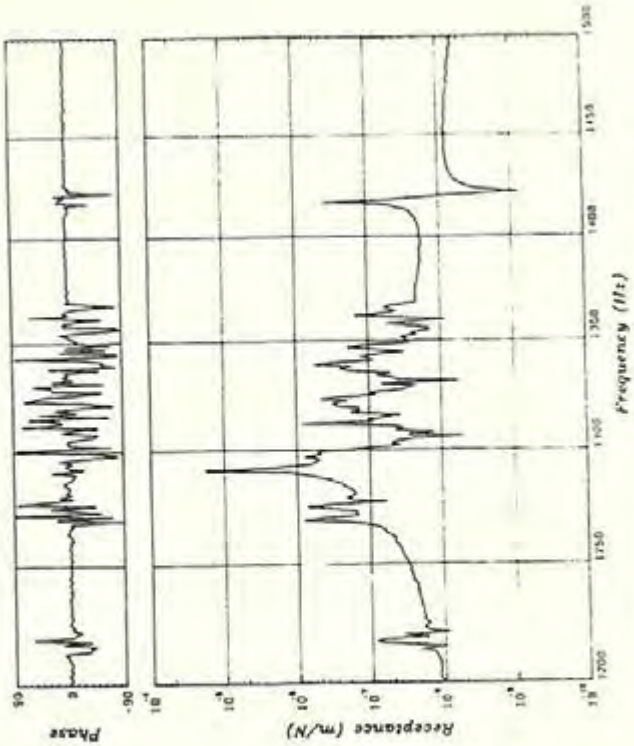
Phase
Receptance (m/N)
Frequency (Hz)

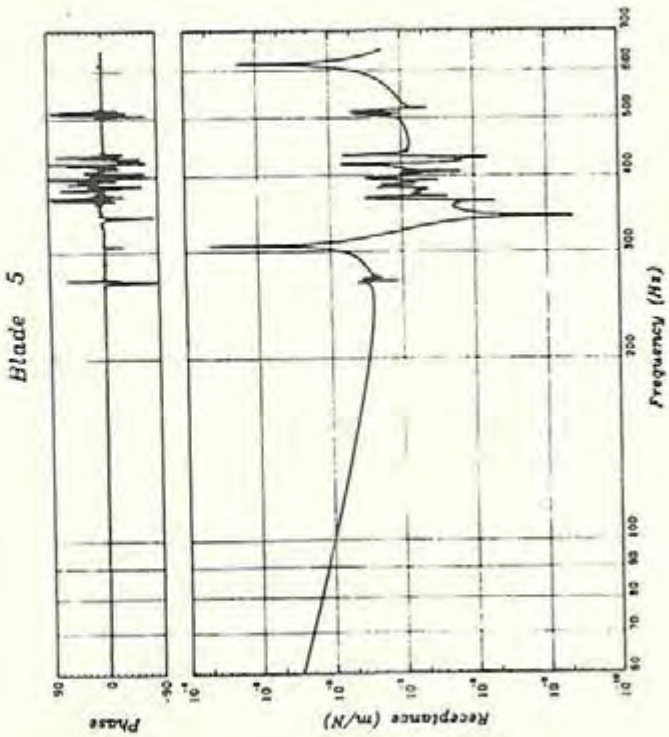
Blade 5
Phase
Receptance (m/N)
Frequency (Hz)

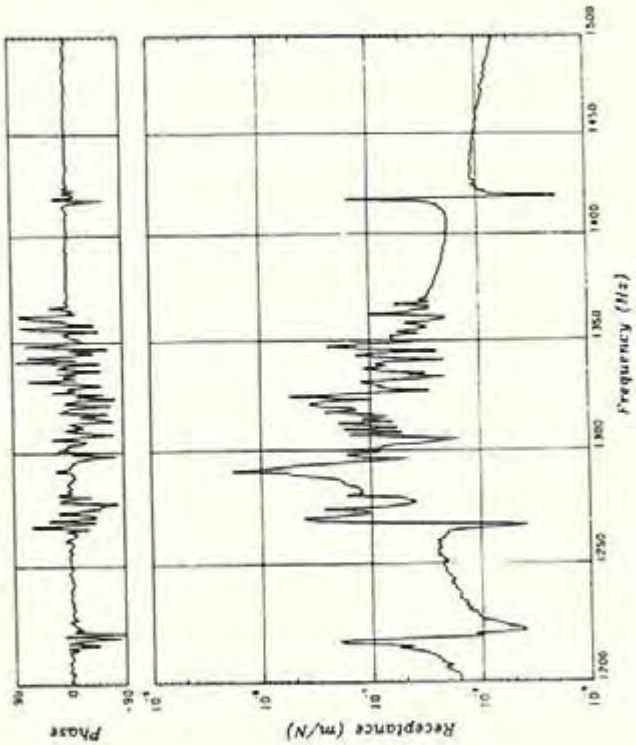
Phase
Receptance (m/N)
Frequency (Hz)

Blade 7

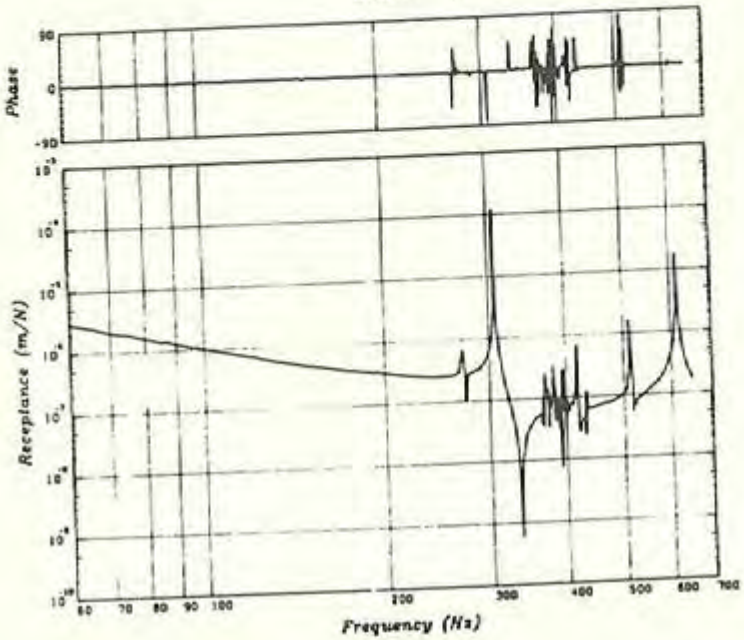

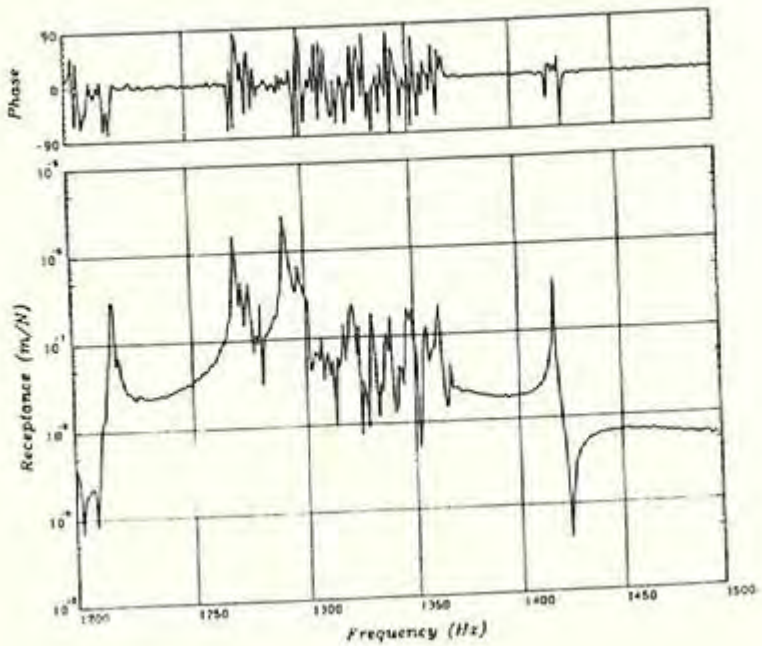

Blade 8

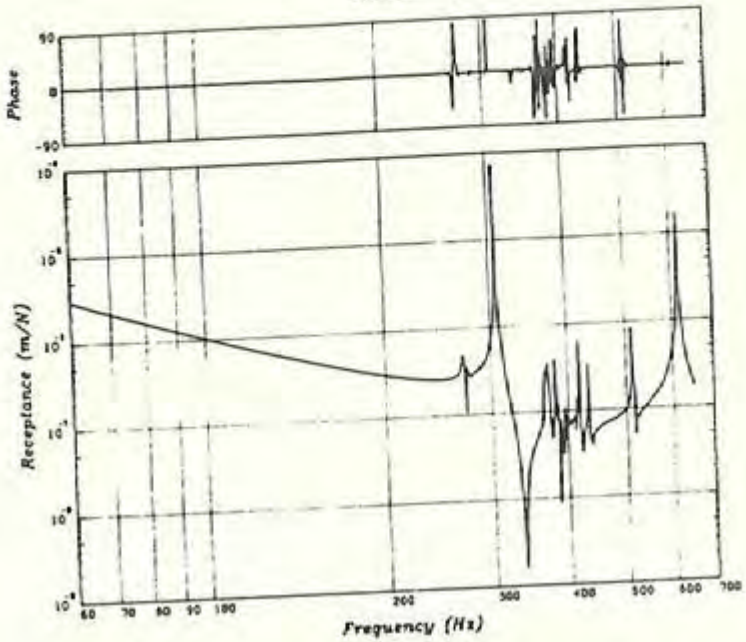

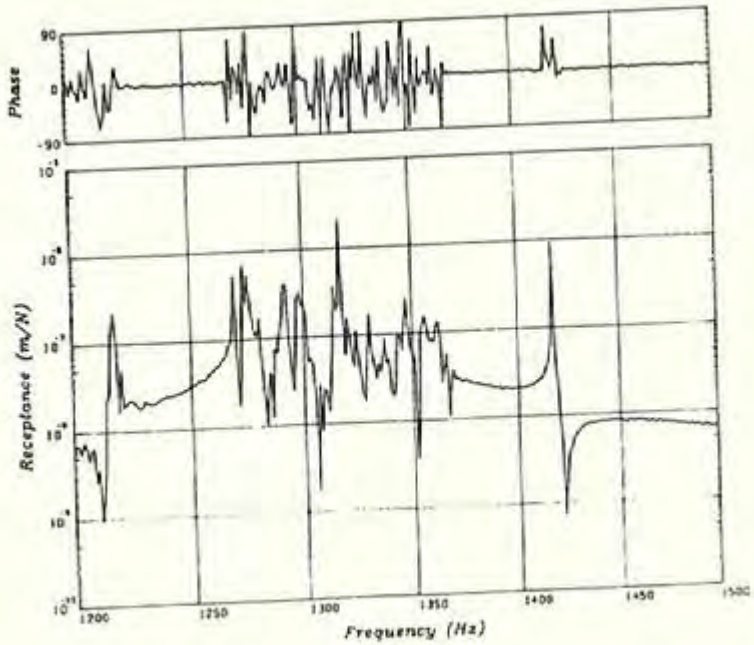

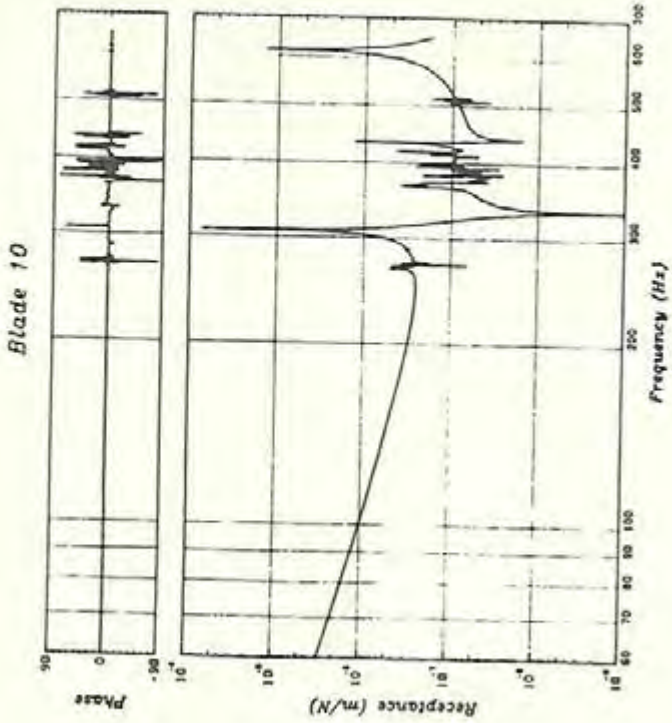
Blade 10
Phase
Receptance (m/N)
Frequency (Hz)

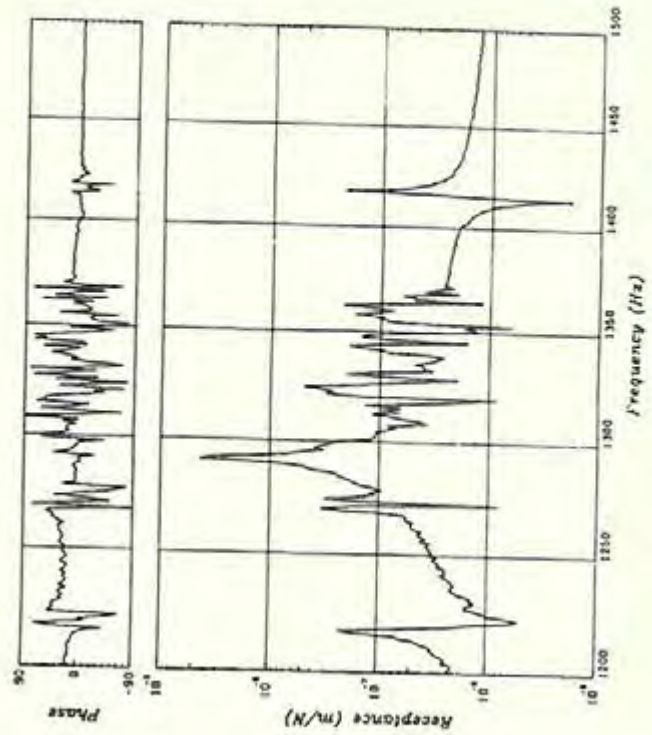
Phase
Receptance (m/N)
Frequency (Hz)

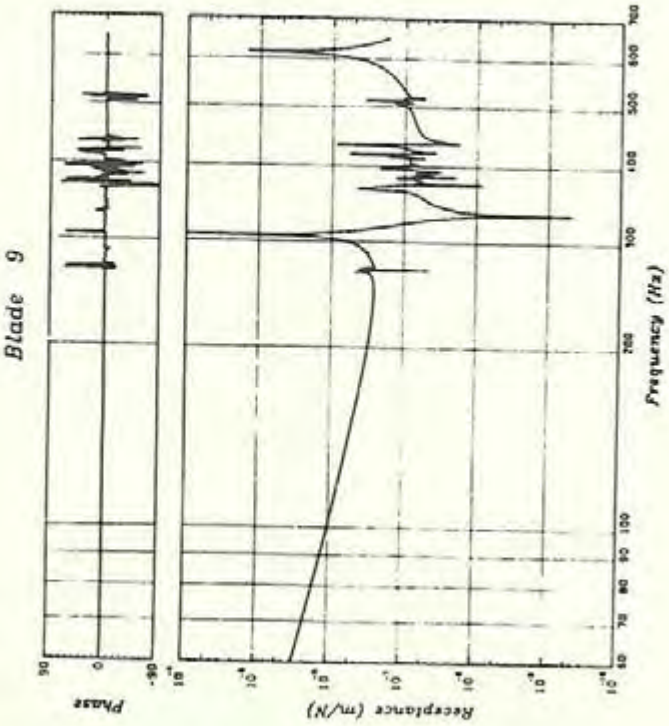
Blade 9
Phase
Receptance (m/N)
Frequency (Hz)

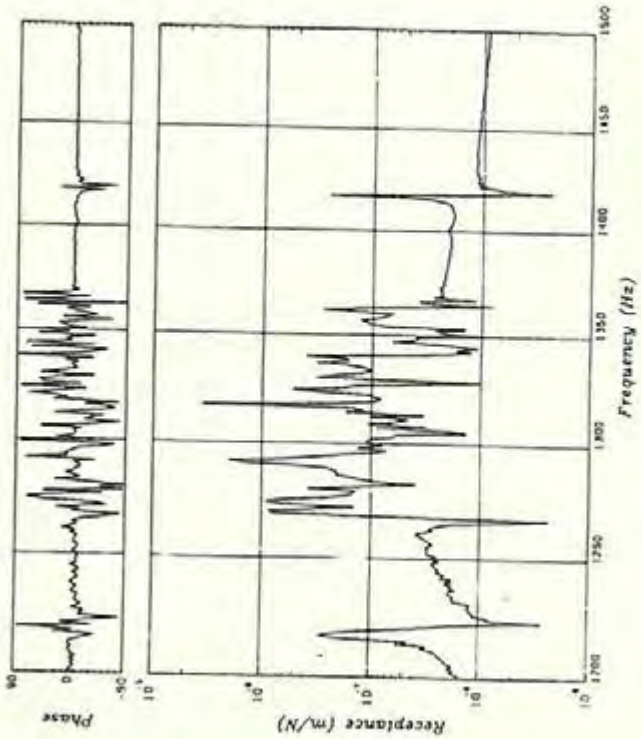
Phase
Receptance (m/N)
Frequency (Hz)

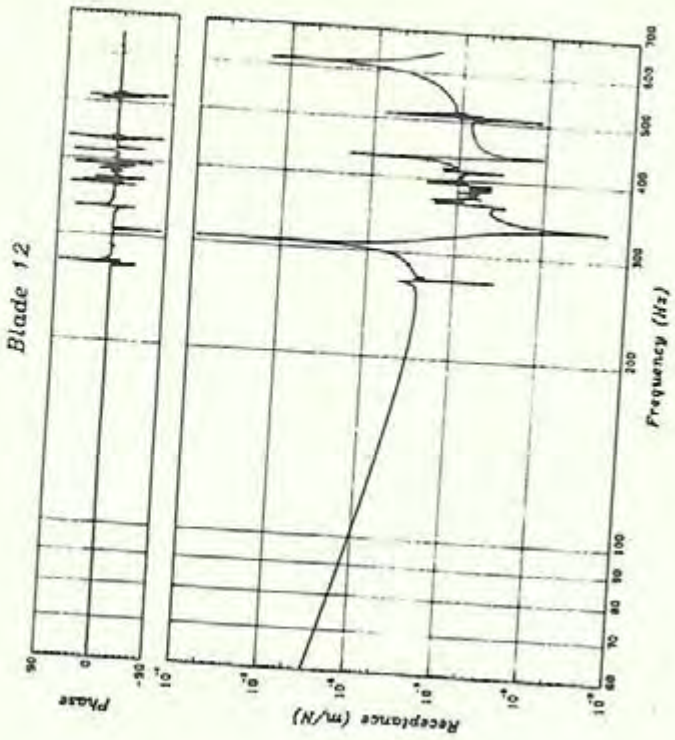
Blade 12
Phase
Receptance (m/N)
Frequency (Hz)

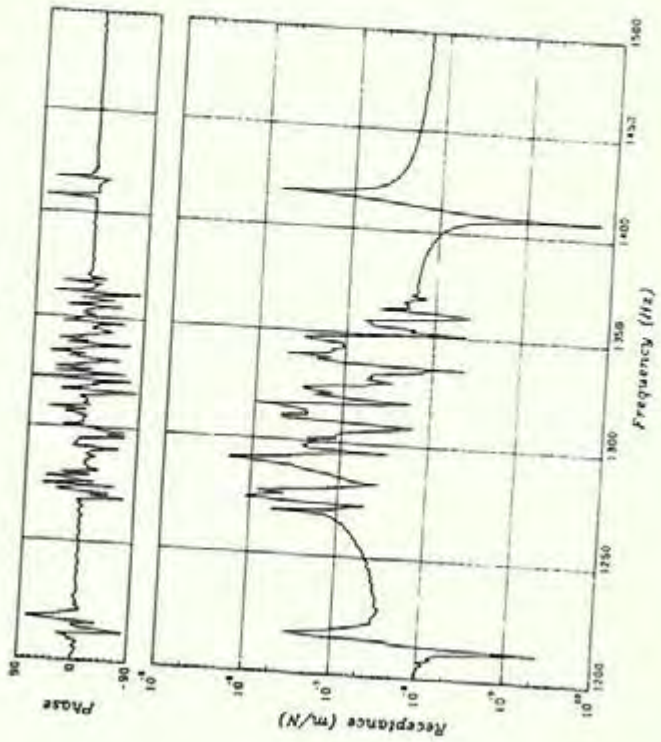
Phase
Receptance (m/N)
Frequency (Hz)

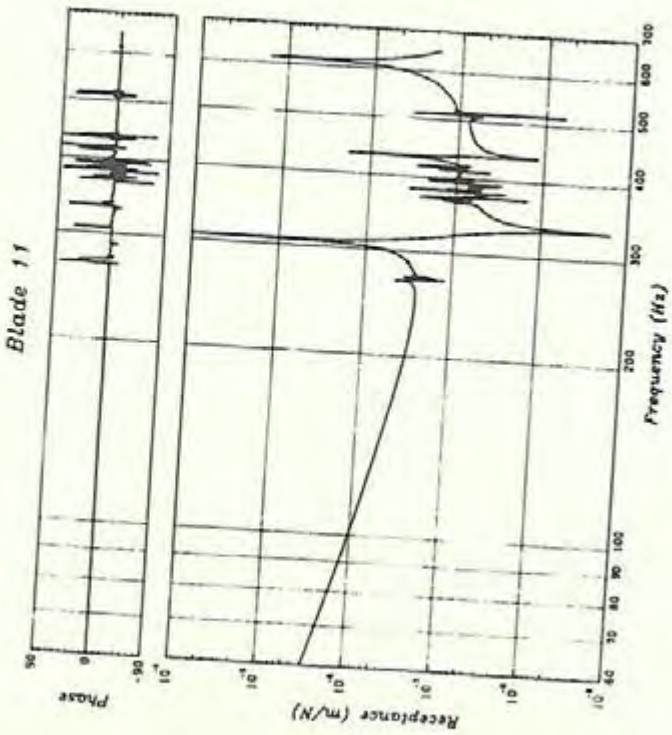
Blade 11
Phase
Receptance (m/N)
Frequency (Hz)

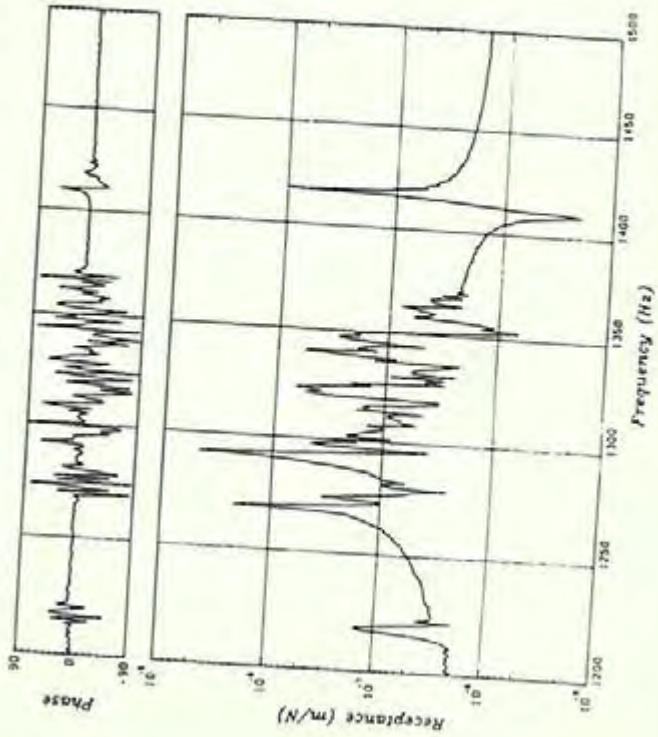
Phase
Receptance (m/N)
Frequency (Hz)

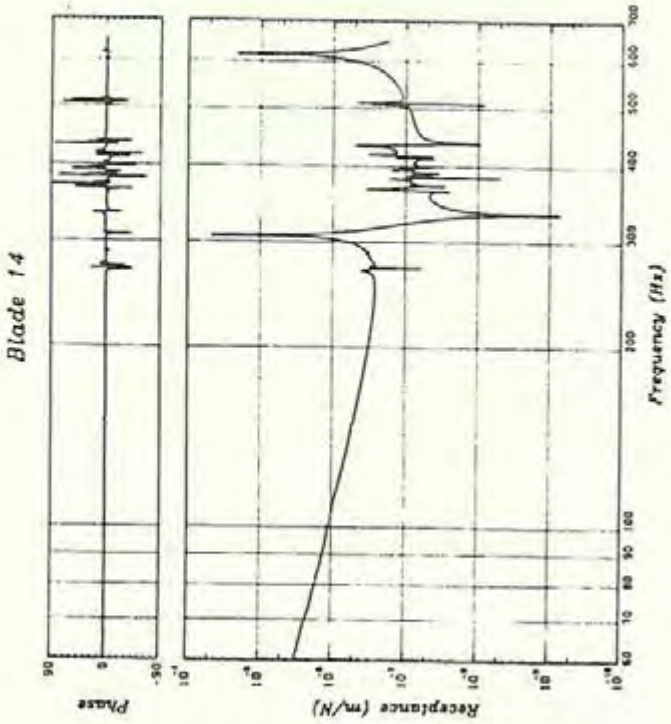
Blade 14
Phase
Receptance (m/N)
Frequency (Hz)

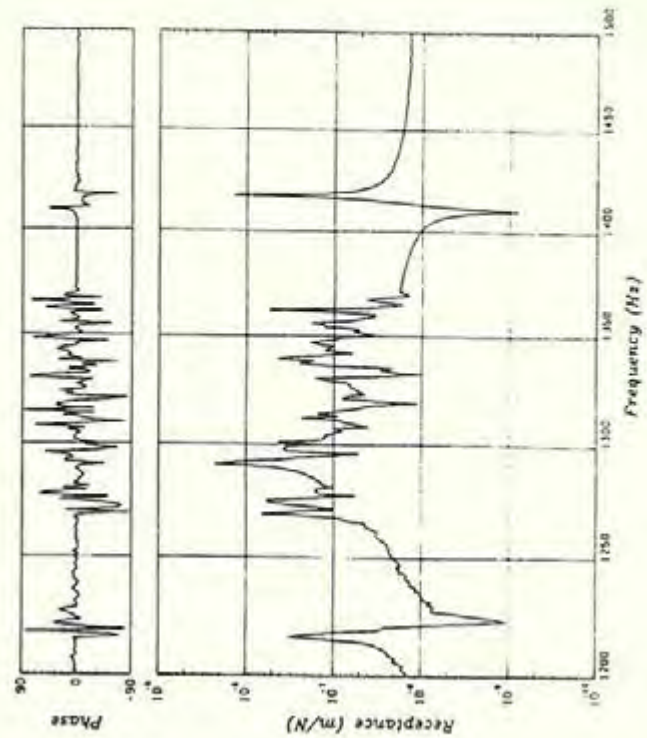
Phase
Receptance (m/N)
Frequency (Hz)

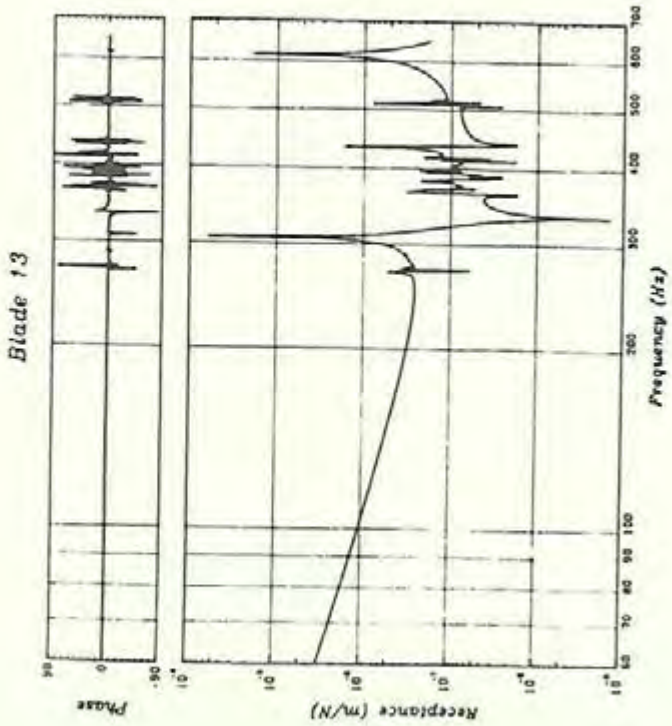
Blade 13
Phase
Receptance (m/N)
Frequency (Hz)

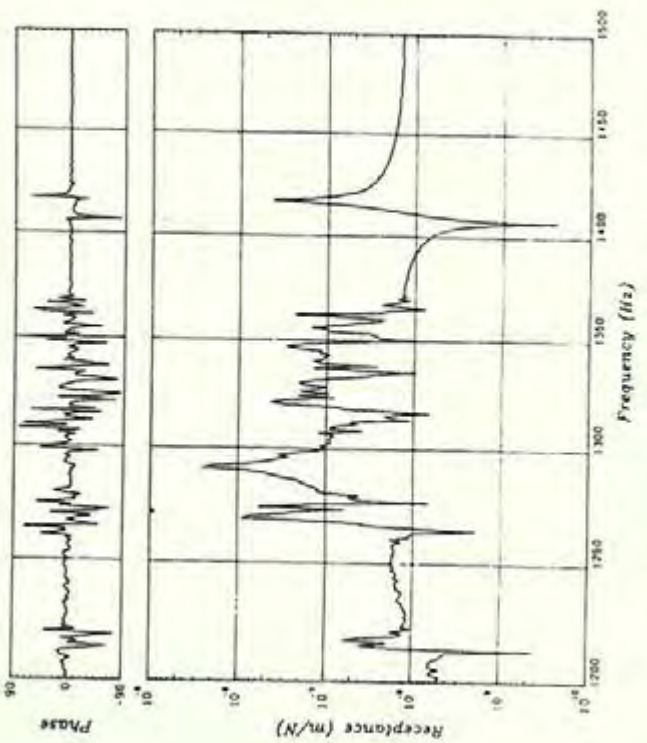
Phase
Receptance (m/N)
Frequency (Hz)

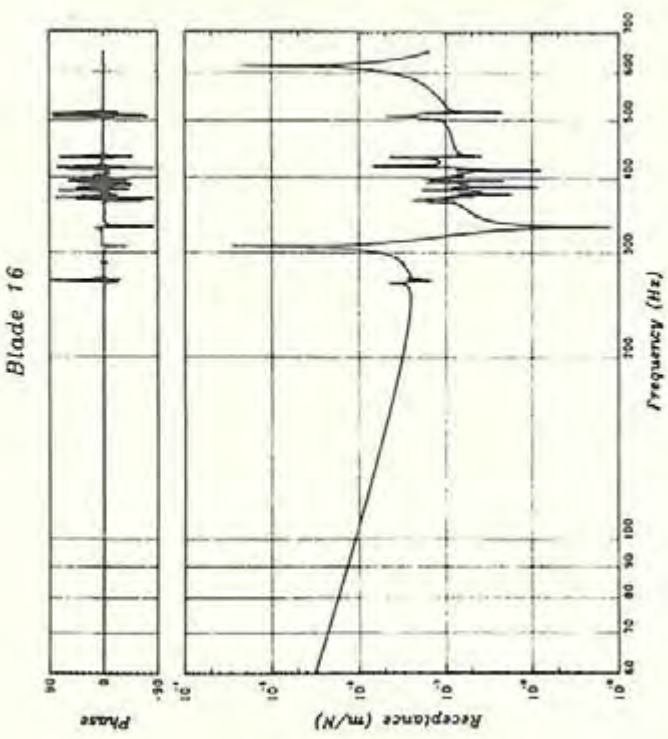
Blade 16
Phase
Receptance (m/N)
Frequency (Hz)

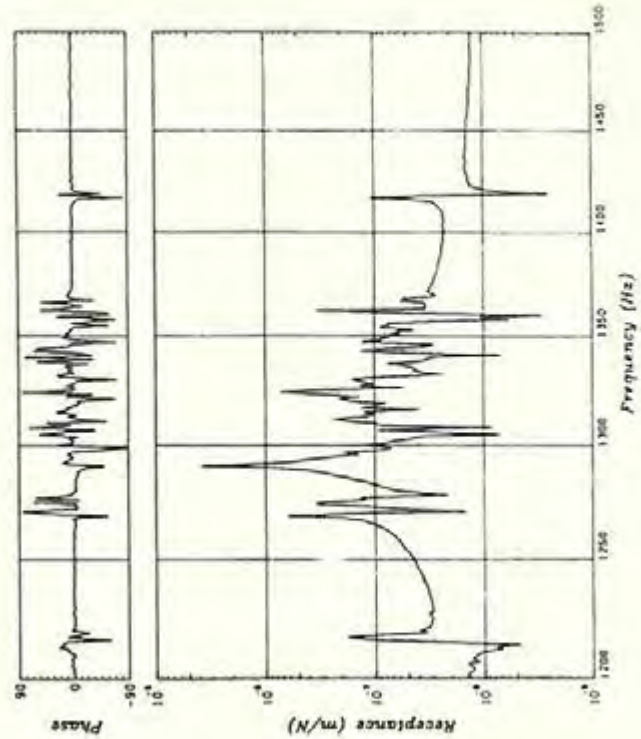
Phase
Receptance (m/N)
Frequency (Hz)

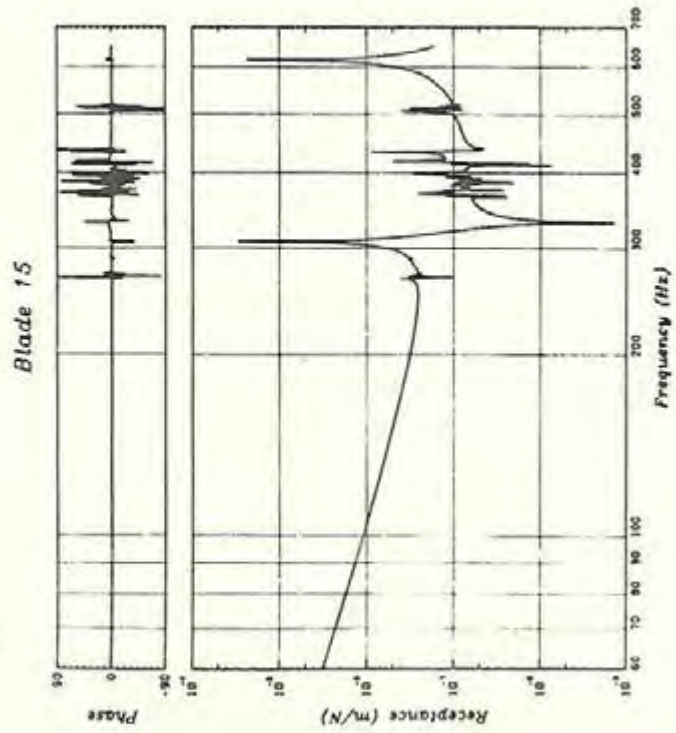
Blade 15
Phase
Receptance (m/N)
Frequency (Hz)

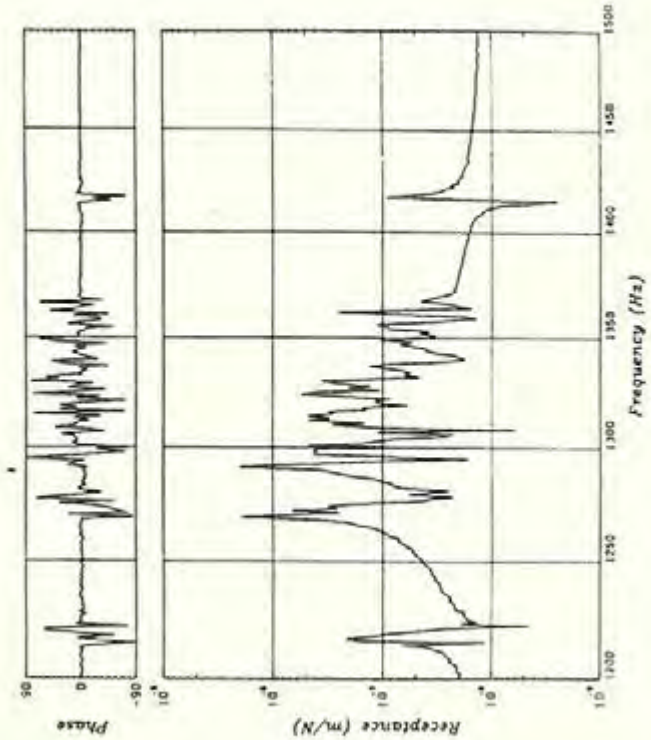
Phase
Receptance (m/N)
Frequency (Hz)

Blade 17

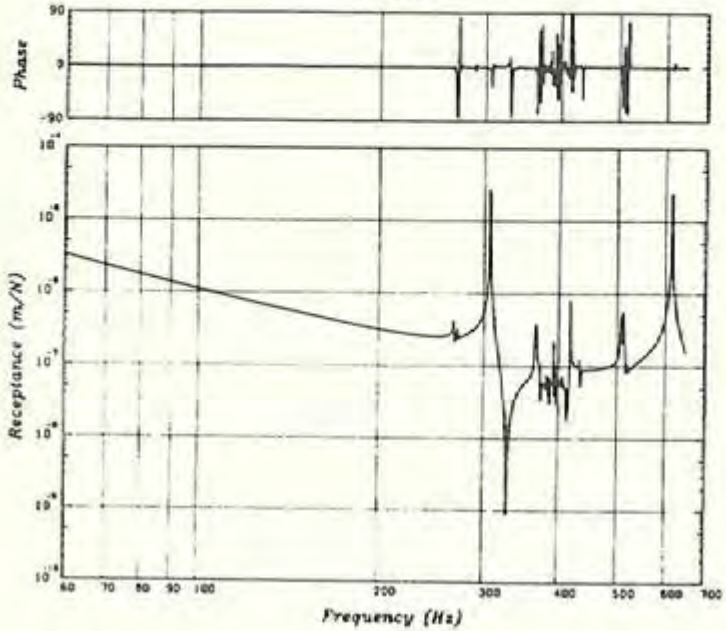

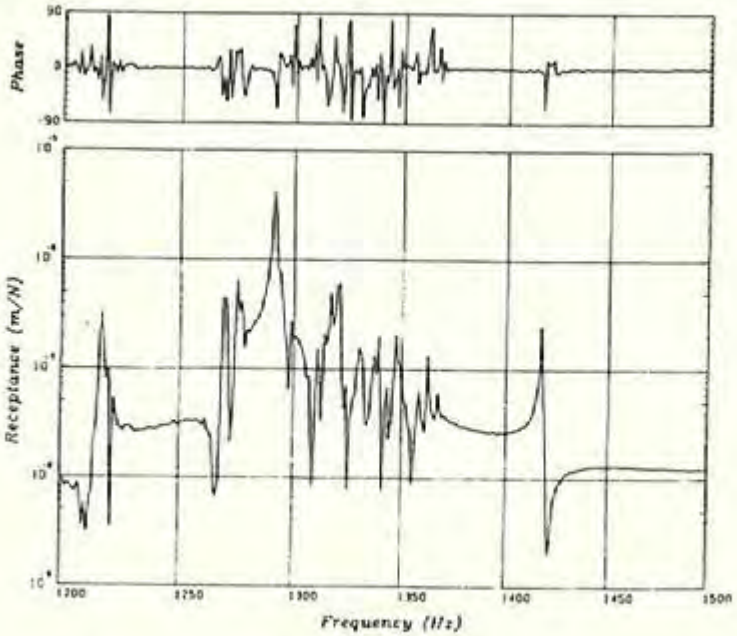

Blade 18

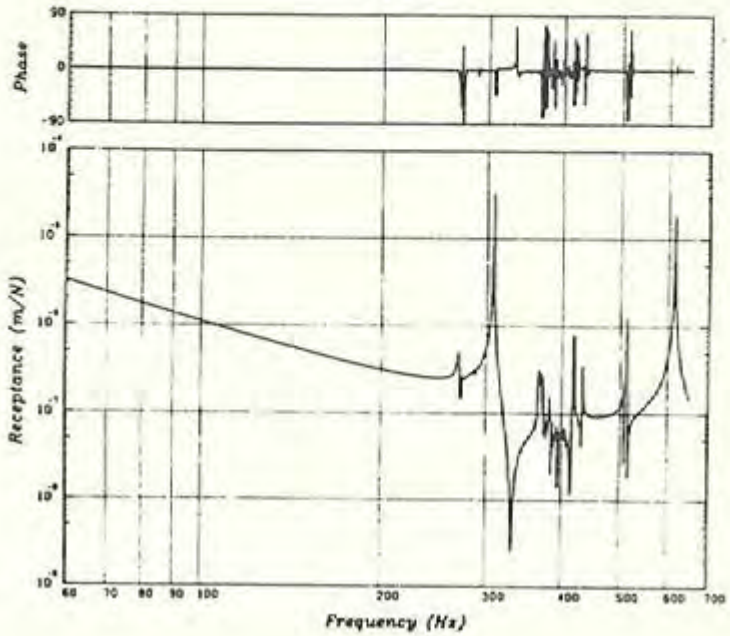

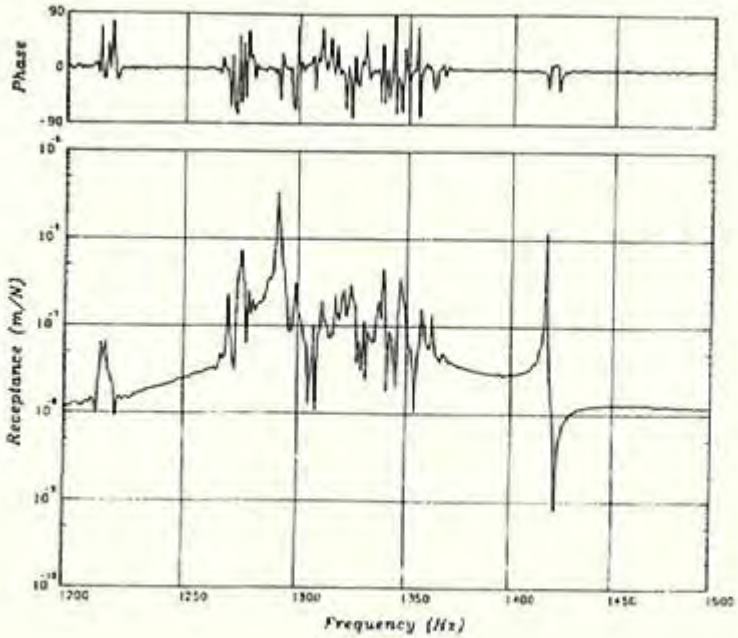

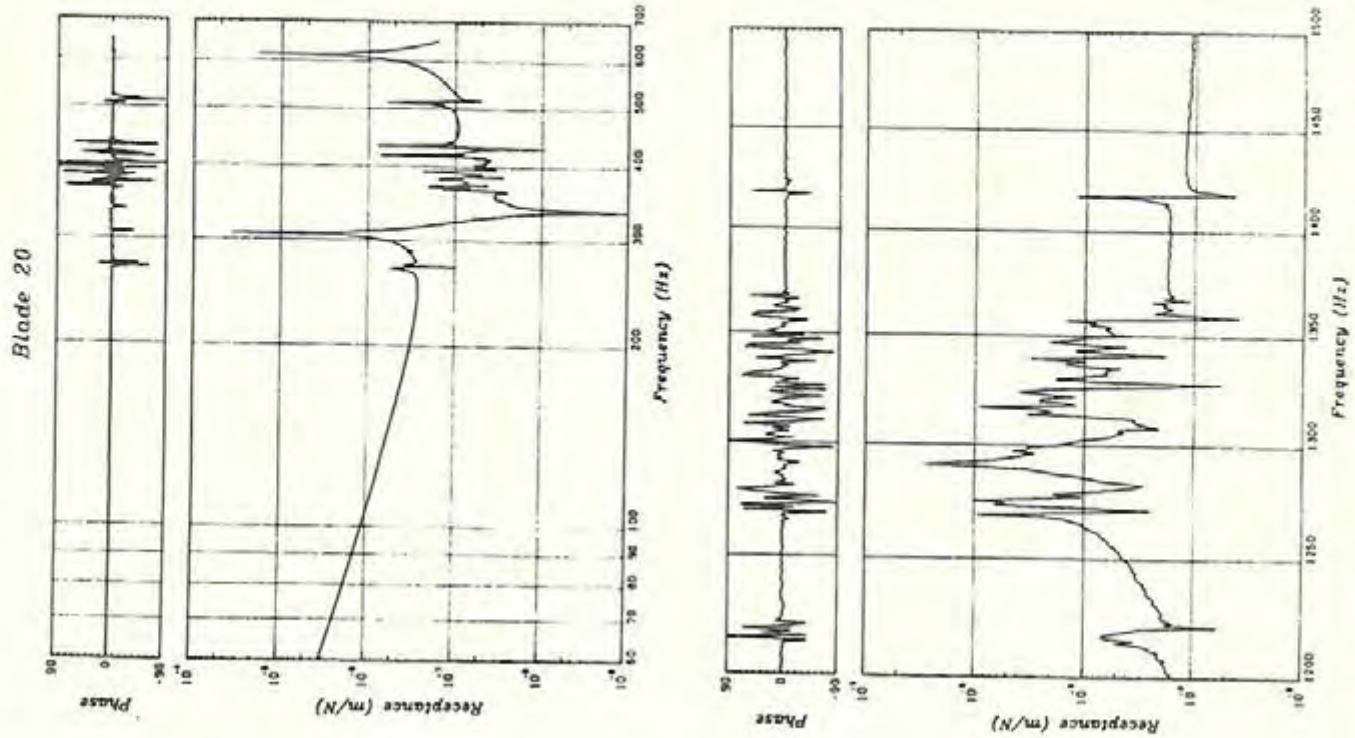
Blade 20
Phase
Receptance (m/N)
Frequency (Hz)

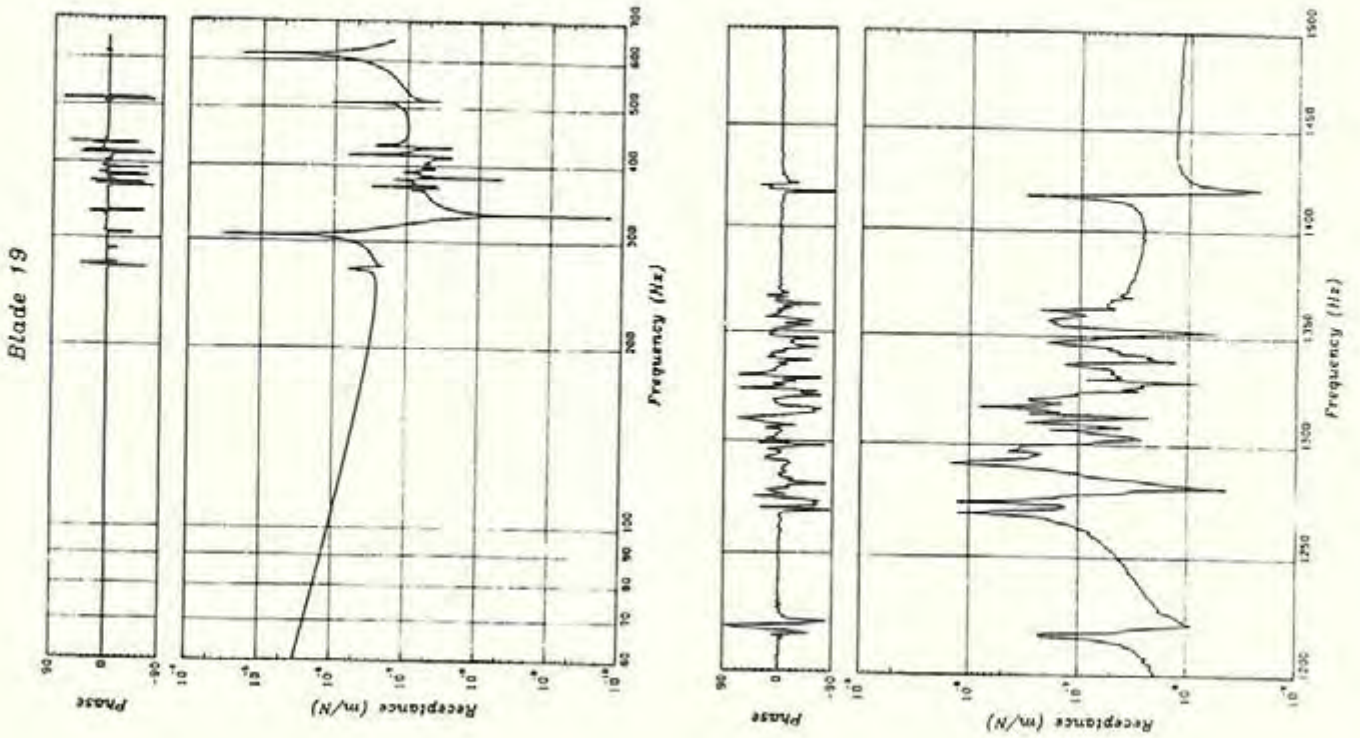
Blade 19
Phase
Receptance (m/N)
Frequency (Hz)

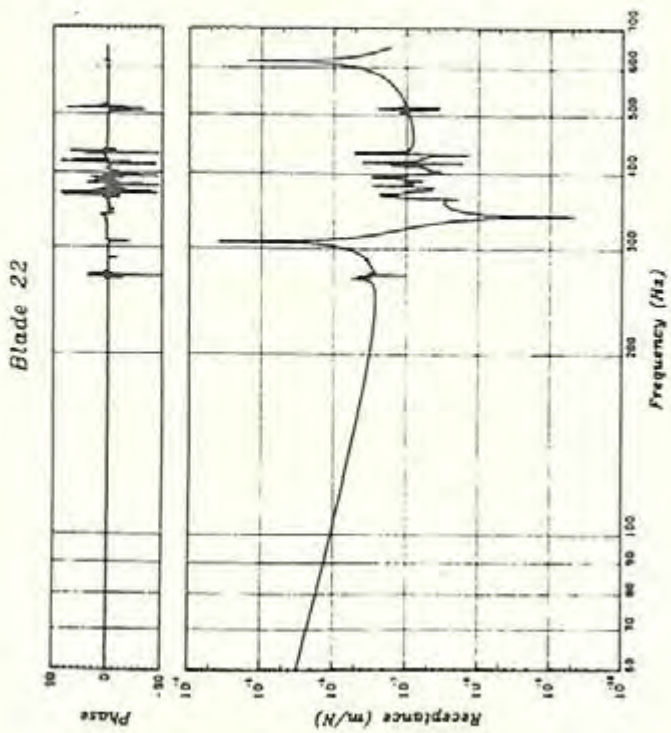
Blade 22
Phase
Receptance (m/N)
Frequency (Hz)

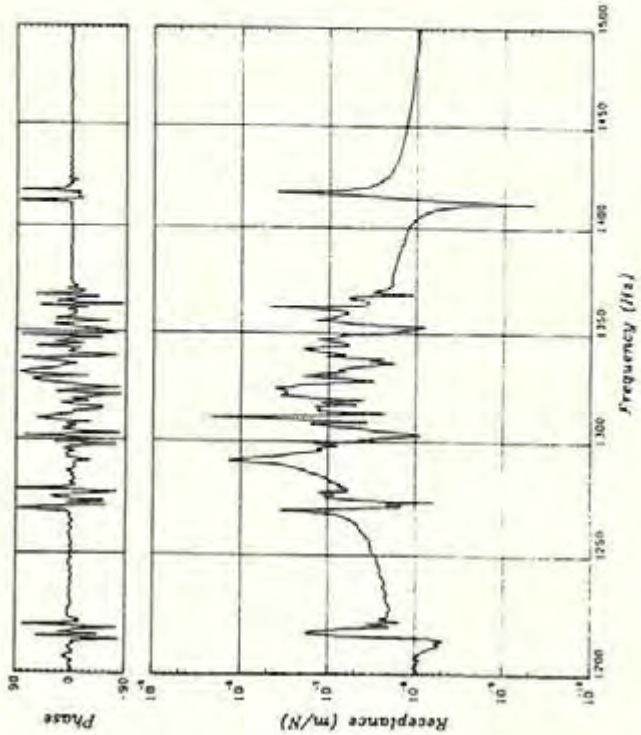
Phase
Receptance (m/N)
Frequency (Hz)

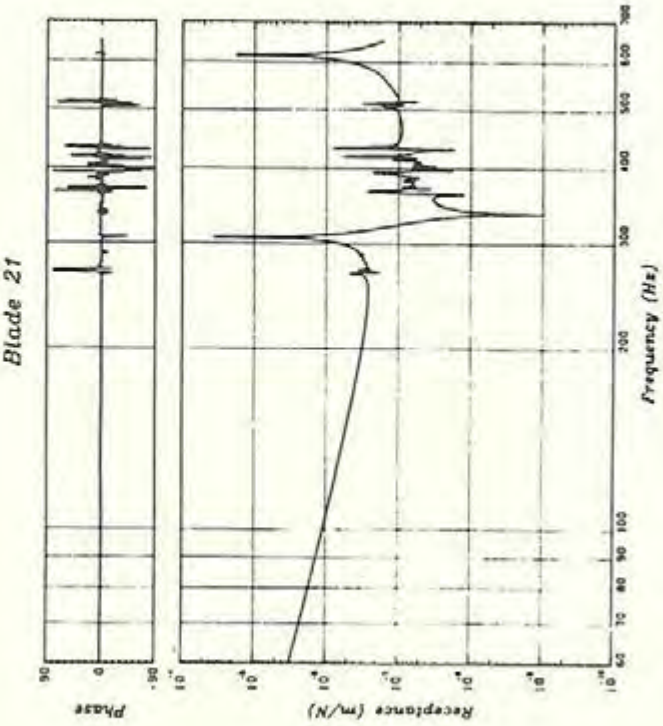
Blade 21
Phase
Receptance (m/N)
Frequency (Hz)

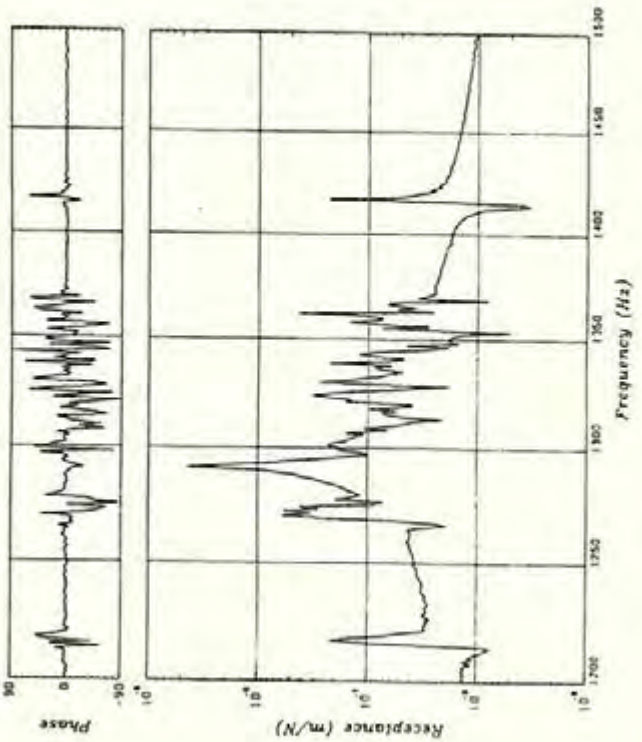
Phase
Receptance (m/N)
Frequency (Hz)

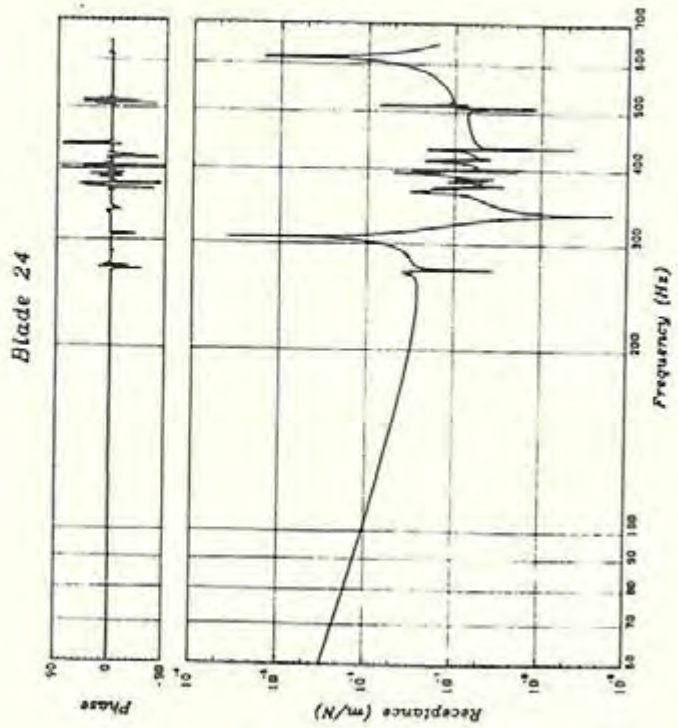
Blade 24
Phase
Receptance (m/N)
Frequency (Hz)

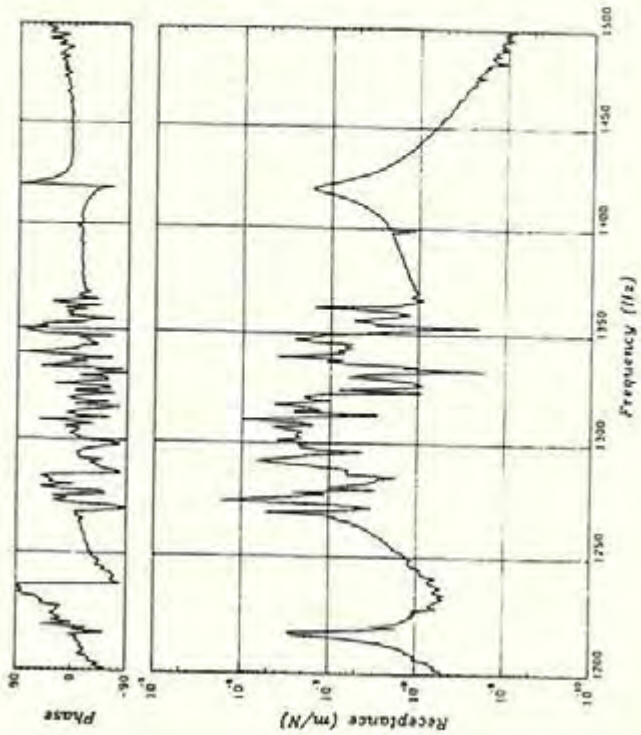
Phase
Receptance (m/N)
Frequency (Hz)

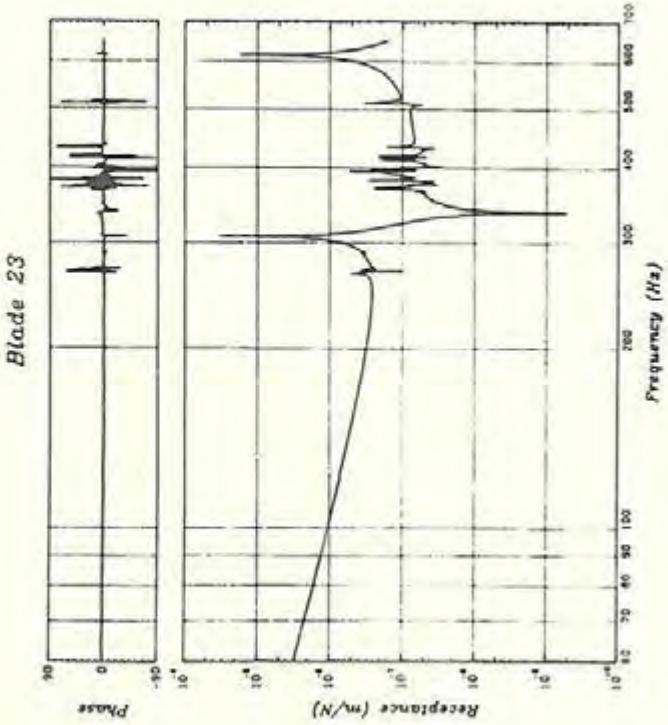
Blade 23
Phase
Receptance (m/N)
Frequency (Hz)

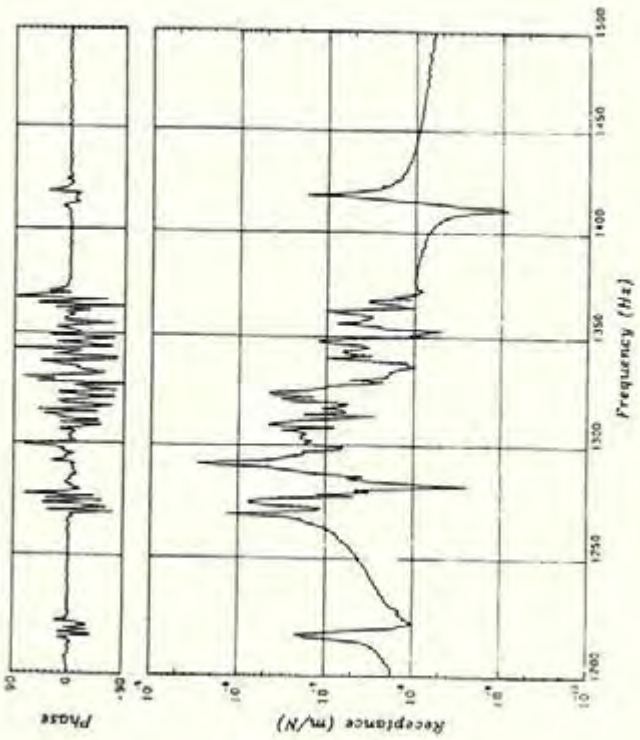
Phase
Receptance (m/N)
Frequency (Hz)

Fig. 6.3.25 *Relative blade amplitudes at selected frequencies*

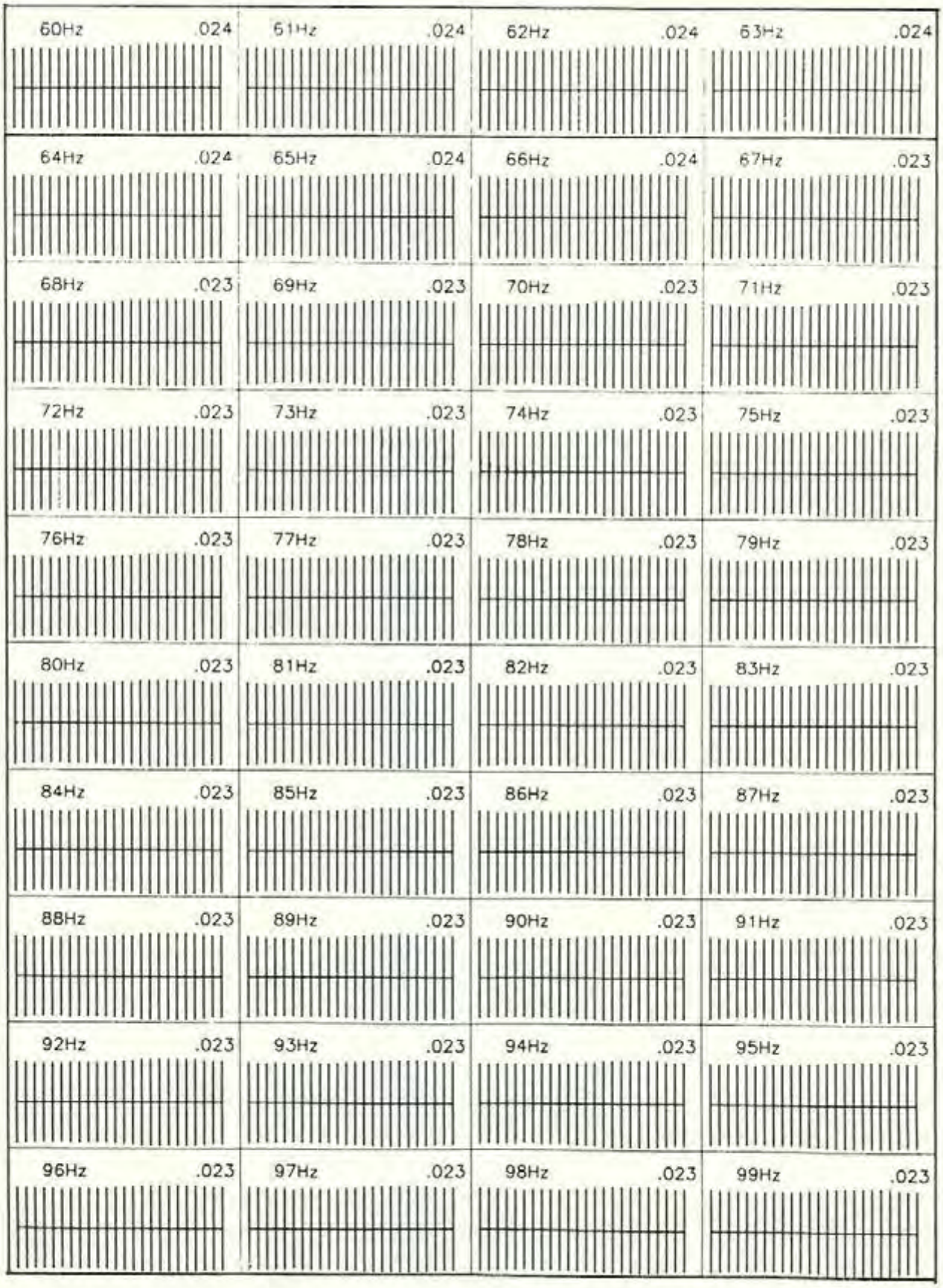

Fig 6.3.25 contd.

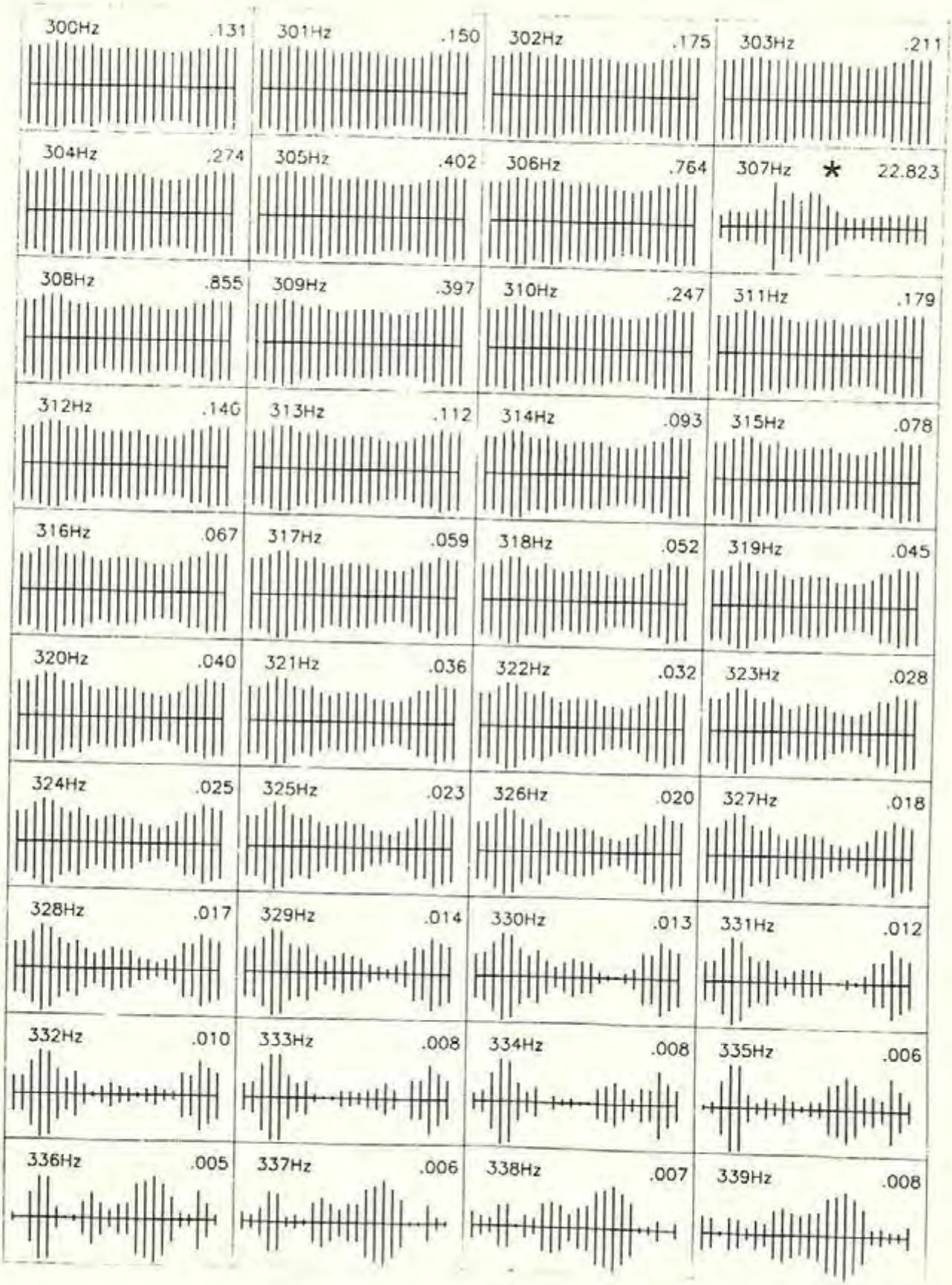

Fig 6.3.25 contd.

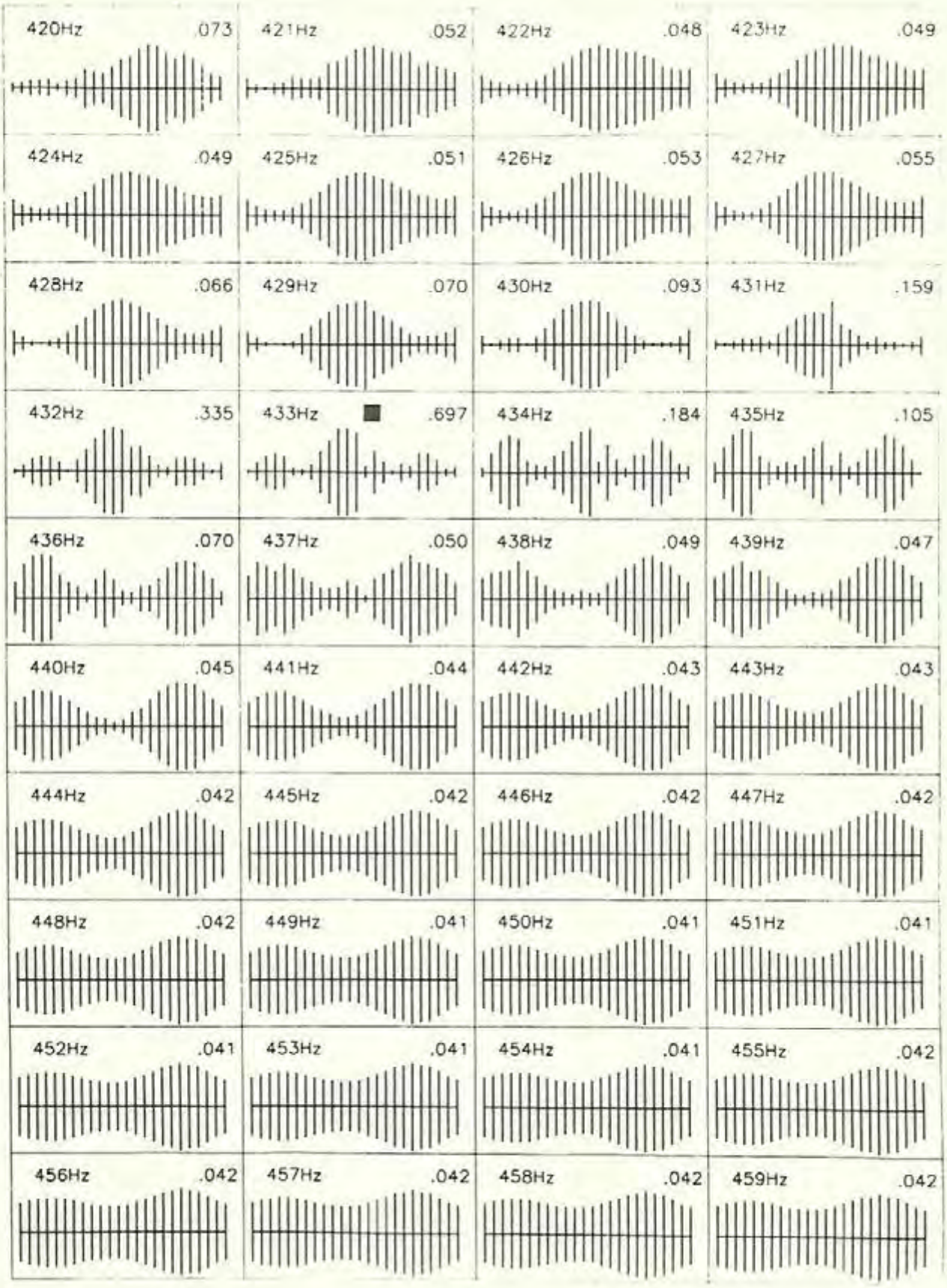

Fig 6.3.25 contd.

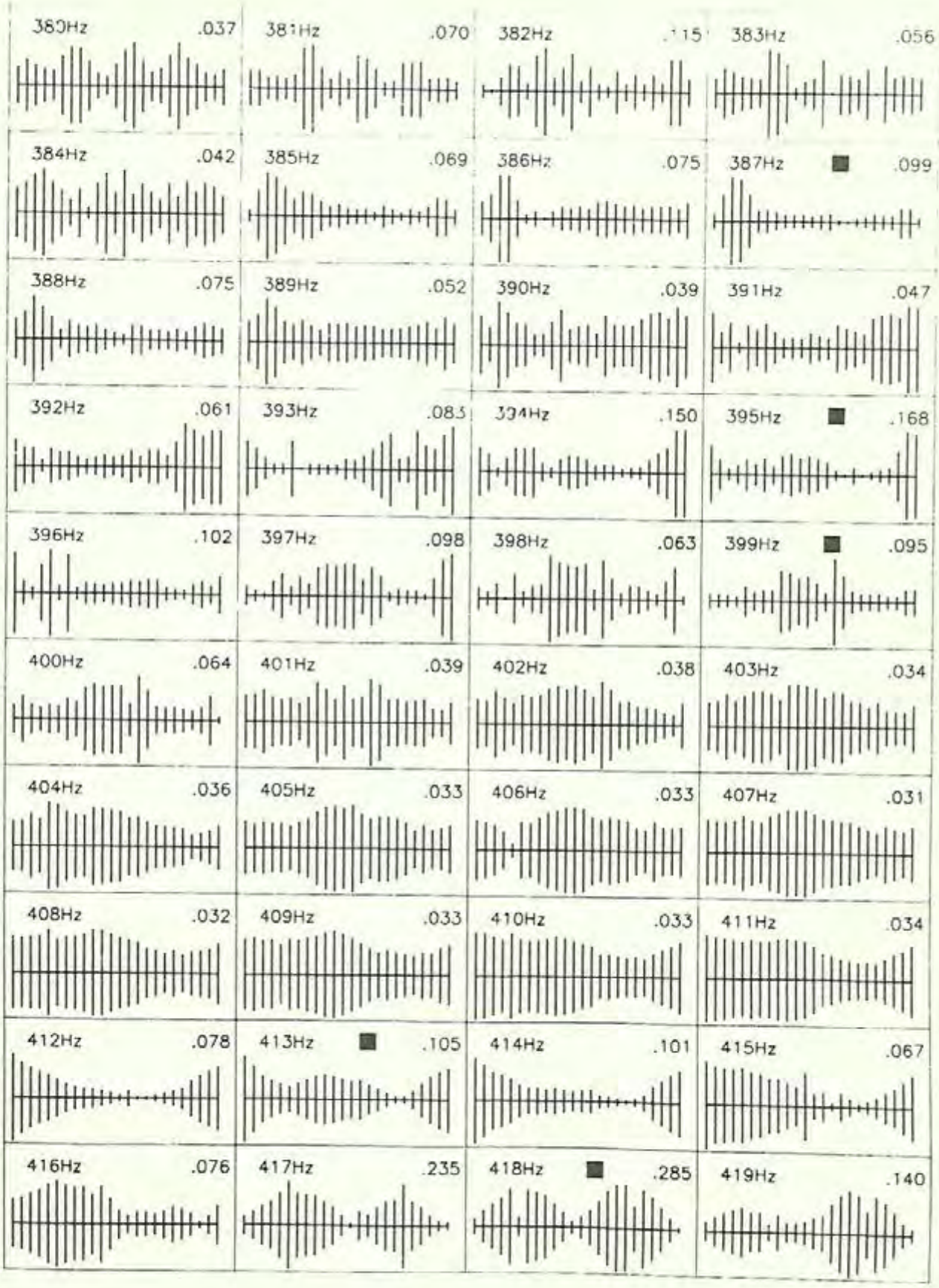

Fig 6.3.25 contd.

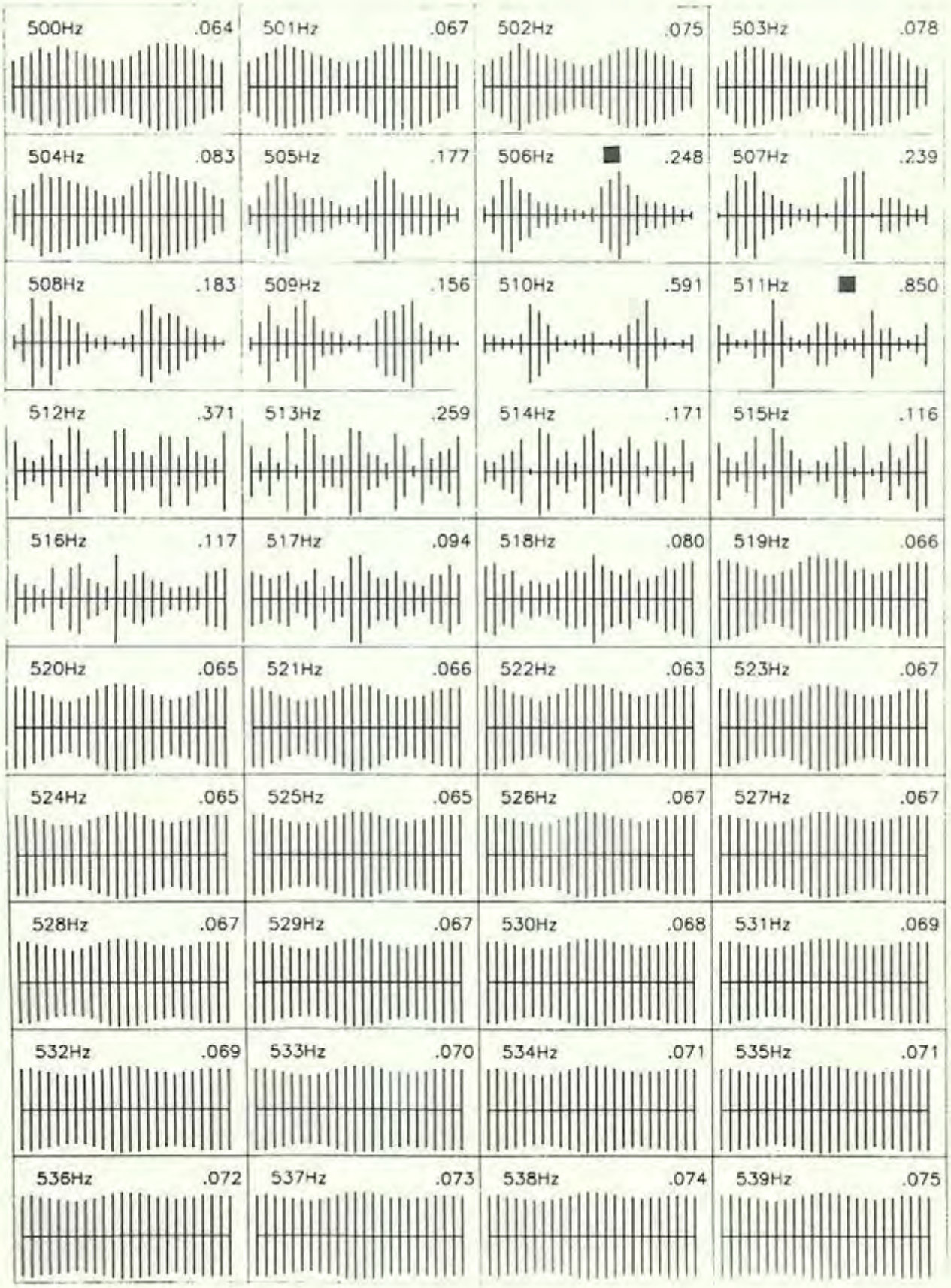

Fig 6.3.25 concluded.

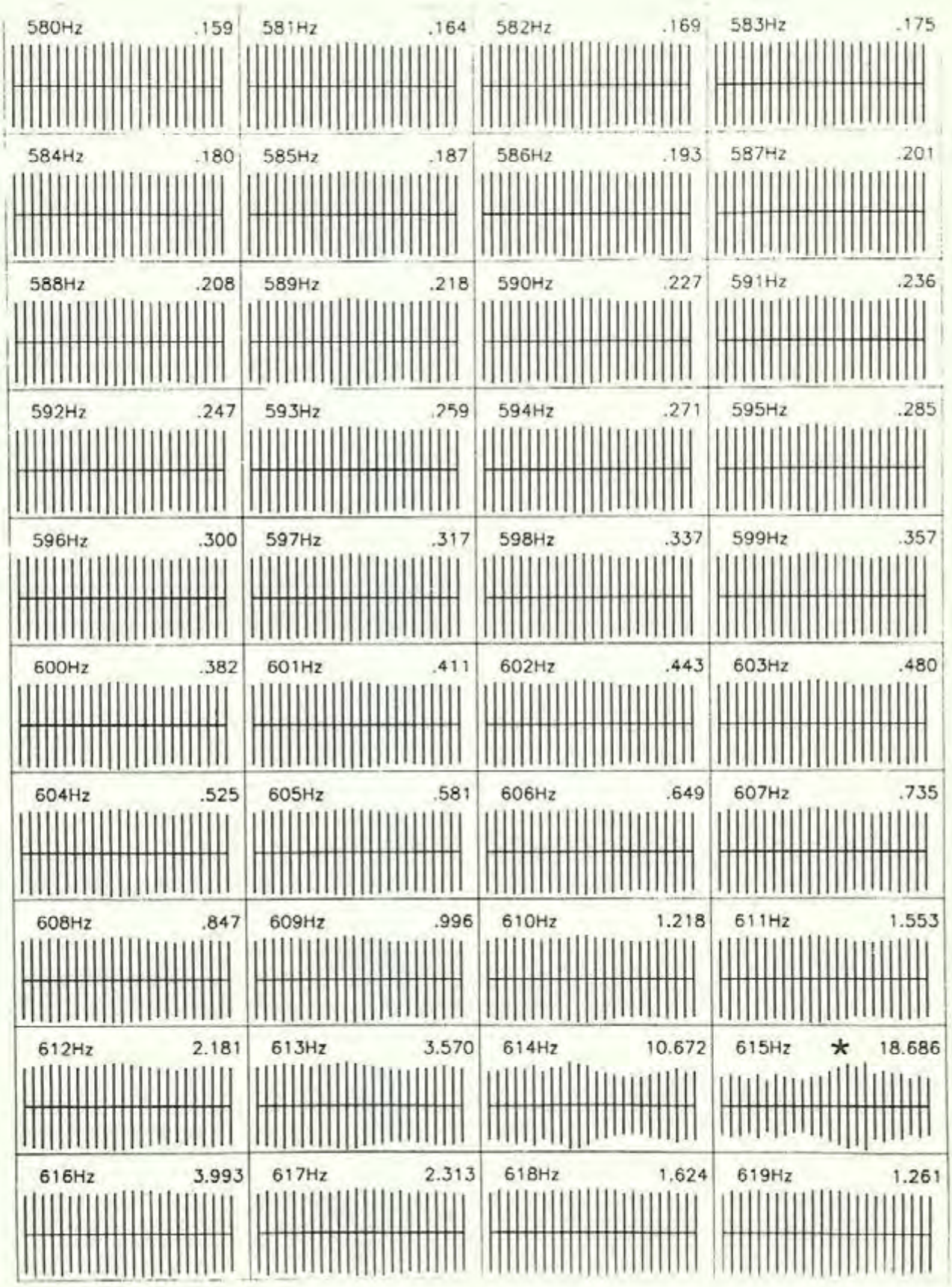

Table 6.3.1. Response characteristics of Disc 24X.

FREQUENCY	MAX RESP	MIN RESP	STD	SKEW	KURT	BLR	BHR
60.00	.023989	.021281	3.742	.112	-1.500	6	17
61.00	.023941	.021200	3.719	.176	-1.519	6	20
62.00	.023787	.021164	3.658	.139	-1.511	6	20
63.00	.023695	.021062	3.504	.115	-1.464	6	20
64.00	.023675	.021050	3.664	.112	-1.549	6	20
65.00	.023639	.020992	3.397	.096	-1.438	6	20
66.00	.023536	.021006	3.488	.156	-1.546	6	20
67.00	.023418	.020976	3.619	.039	-1.598	6	20
68.00	.023331	.020943	3.577	.071	-1.637	6	20
69.00	.023289	.020421	3.751	-.126	-1.31	7	19
70.00	.023269	.020492	3.714	-.037	-1.402	7	19
71.00	.023209	.020568	3.599	.064	-1.396	7	19
72.00	.023183	.020710	3.491	.099	-1.412	7	19
73.00	.023126	.020750	3.501	.224	-1.460	6	19
74.00	.023135	.020726	3.353	.269	-1.391	6	19
75.00	.023082	.020713	3.363	.231	-1.399	6	19
76.00	.023039	.020674	3.387	.176	-1.395	6	19
77.00	.023004	.020673	3.456	.161	-1.450	6	19
78.00	.022974	.020613	3.543	.126	-1.487	6	19
79.00	.022945	.020565	3.519	.176	-1.451	6	19
80.00	.022937	.020581	3.434	.250	-1.388	6	19
81.00	.022930	.020607	3.432	.272	-1.410	6	19
82.00	.022904	.020627	3.456	.177	-1.480	6	19
83.00	.022864	.020626	3.402	.195	-1.475	6	19
84.00	.022844	.020321	3.530	.141	-1.368	7	19
85.00	.022820	.020541	3.487	.222	-1.445	7	19
86.00	.022819	.020575	3.339	.264	-1.378	6	19
87.00	.022796	.020566	3.327	.191	-1.384	6	19
88.00	.022774	.020535	3.337	.231	-1.364	6	20
89.00	.022780	.020518	3.424	.196	-1.467	6	20
90.00	.022744	.020526	3.401	.254	-1.437	6	19
91.00	.022742	.020490	3.450	.190	-1.419	6	19
92.00	.022715	.020446	3.509	.184	-1.462	4	20
93.00	.022731	.020391	3.395	.244	-1.436	6	20
94.00	.022695	.020343	3.381	.227	-1.397	6	19
95.00	.022683	.020352	3.365	.197	-1.451	6	19
96.00	.022689	.020292	3.273	.125	-1.338	6	19
97.00	.022678	.020261	3.213	.134	-1.303	6	19
98.00	.022672	.020509	3.089	.235	-1.438	6	20
99.00	.022695	.020615	3.232	.229	-1.532	7	20
100.00	.022911	.020716	3.116	.286	-1.453	6	14
101.00	.022769	.020342	3.265	.095	-1.368	7	14
102.00	.022655	.020735	3.064	.309	-1.466	7	20
103.00	.022645	.020749	3.075	.285	-1.525	7	19
104.00	.022670	.020804	3.109	.270	-1.602	6	20
105.00	.022667	.020456	3.239	.127	-1.503	7	20
106.00	.022818	.020764	3.133	.237	-1.568	6	14
107.00	.022843	.020737	3.097	.189	-1.525	6	14
108.00	.023223	.020739	3.237	.291	-1.332	6	14
109.00	.023304	.020709	3.304	.300	-1.277	6	14
110.00	.023443	.020723	3.453	.369	-1.202	6	14
111.00	.023220	.020712	3.349	.283	-1.368	6	14
112.00	.023365	.020732	3.345	.334	-1.265	6	14
113.00	.023150	.020714	3.240	.275	-1.421	6	14
114.00	.023148	.020699	3.291	.283	-1.443	6	14

FREQUENCY	MAX. RESP.	MIN. RESP.	STD	SKEW	KURT	BLR	BHR
115.00	.023200	.020719	3.258	.307	.374	6	14
116.00	.022793	.020743	3.106	.143	.586	6	14
117.00	.022922	.020763	3.122	.140	.529	6	14
118.00	.023057	.020882	2.991	.267	-1.457	6	14
119.00	.022952	.020793	3.103	.205	-1.499	7	19
120.00	.023002	.020963	3.042	.298	-1.498	5	14
121.00	.022954	.020972	2.940	.210	-1.516	5	19
122.00	.022977	.020980	2.950	.254	-1.491	5	19
123.00	.022963	.021043	2.994	.123	-1.579	5	19
124.00	.023015	.021089	3.079	-.003	-1.669	5	14
125.00	.023019	.020468	3.310	-.230	-1.295	7	19
126.00	.023023	.020812	3.157	-.102	-1.546	7	19
127.00	.023143	.020692	3.220	-.114	-1.424	7	20
128.00	.023158	.020629	3.229	-.149	-1.329	7	20
129.00	.023158	.020793	3.166	-.097	-1.446	7	20
130.00	.023262	.020491	3.363	-.233	-1.178	7	20
131.00	.023311	.020504	3.364	-.223	-1.156	8	20
132.00	.023326	.020425	3.376	-.293	-.992	7	20
133.00	.023383	.020601	3.285	-.187	-1.169	8	20
134.00	.023388	.020792	3.223	-.130	-1.345	7	20
135.00	.023386	.021036	3.112	-.059	-1.501	8	20
136.00	.023384	.020813	3.155	-.171	-1.272	7	20
137.00	.023397	.020973	3.052	-.094	-1.377	7	20
138.00	.023448	.020857	3.076	-.184	-1.175	8	20
139.00	.023477	.021063	2.944	-.071	-1.309	7	20
140.00	.023496	.020921	3.055	-.189	-1.115	7	20
141.00	.023583	.020790	3.120	-.300	-.820	7	20
142.00	.023595	.021038	3.014	-.186	-1.166	7	20
143.00	.023621	.021140	2.969	-.157	-1.226	7	20
144.00	.023668	.021072	2.976	-.228	-1.034	7	20
145.00	.023728	.021066	3.026	-.229	-.994	7	20
146.00	.023744	.021299	2.961	-.115	-1.288	7	20
147.00	.023738	.021148	2.989	-.215	-1.068	7	20
148.00	.024145	.020947	3.237	.186	-.677	7	14
149.00	.023702	.020594	3.239	-.714	.359	7	20
150.00	.023650	.021958	2.620	.072	1.620	6	19
151.00	.023991	.021659	2.720	.137	-1.243	7	20
152.00	.024001	.021757	2.770	.046	-1.435	7	20
153.00	.023881	.021604	2.760	-.064	-1.286	7	20
154.00	.023953	.021693	2.734	-.013	-1.343	7	20
155.00	.023913	.021638	2.746	-.086	-1.255	7	20
156.00	.023967	.021987	2.604	.065	-1.480	7	20
157.00	.023990	.021784	2.678	-.057	-1.308	7	20
158.00	.024066	.022258	2.515	.093	-1.533	6	20
159.00	.024088	.022177	2.522	.073	-1.516	7	20
160.00	.024072	.022053	2.549	-.023	-1.436	7	20
161.00	.024153	.022073	2.545	.072	-1.408	7	20
162.00	.024172	.022179	2.483	.051	-1.439	7	20
163.00	.024265	.022486	2.438	.026	-1.593	7	20
164.00	.024288	.022430	2.443	-.049	-1.567	7	20
165.00	.024325	.022262	2.486	.127	-1.403	7	20
166.00	.024375	.022395	2.439	.085	-1.475	7	20
167.00	.024398	.022417	2.445	-.106	-1.482	7	20

168.00	.024497	.022624	2.384	-.022	-1.530	7	20
169.00	.024469	.022642	2.384	-.048	-1.570	7	20
170.00	.024573	.022672	2.398	-.032	-1.539	7	20
171.00	.024572	.022734	2.368	-.048	-1.548	7	20
172.00	.024566	.022816	2.338	.046	-1.586	7	20
173.00	.024674	.022746	2.340	-.074	-1.457	7	20
174.00	.024702	.023018	2.268	.030	-1.610	6	20
175.00	.024753	.023004	2.267	.007	-1.539	7	20
176.00	.024780	.023137	2.223	.035	-1.599	6	20
177.00	.024850	.023086	2.215	.035	-1.553	6	20
178.00	.024895	.023204	2.192	.035	-1.565	6	20
179.00	.024929	.023257	2.171	.042	-1.585	6	20
180.00	.024995	.023341	2.115	.052	-1.569	6	20
181.00	.025037	.023360	2.099	.059	-1.564	6	20
182.00	.025092	.023493	2.061	.091	-1.607	6	20
183.00	.025198	.023522	2.027	.108	-1.488	6	20
184.00	.025228	.023642	1.947	.092	-1.506	6	20
185.00	.025294	.023723	1.958	.068	-1.527	6	20
186.00	.025350	.023803	1.916	.041	-1.487	6	20
187.00	.025401	.023882	1.871	.009	-1.502	6	20
188.00	.025451	.023921	1.906	-.020	-1.525	6	20
189.00	.025525	.024025	1.878	-.048	-1.531	6	20
190.00	.025631	.024056	1.888	-.008	-1.495	6	20
191.00	.025644	.024171	1.867	-.074	-1.545	6	20
192.00	.025779	.024161	1.899	-.155	-1.476	6	20
193.00	.025804	.024296	1.872	-.143	-1.536	6	20
194.00	.025955	.024336	1.930	-.137	-1.511	6	20
195.00	.025995	.024426	1.850	-.145	-1.499	6	20
196.00	.026027	.024506	1.861	-.159	-1.522	6	20
197.00	.026088	.024490	1.909	-.230	-1.491	6	20
198.00	.026333	.024556	1.968	-.037	-1.354	6	7
199.00	.026299	.024694	1.793	-.158	-1.410	6	20
200.00	.026346	.024700	1.827	-.139	-1.408	6	20
201.00	.026526	.024885	1.804	-.054	-1.348	6	20
202.00	.026497	.024967	1.753	-.166	-1.424	6	20
203.00	.026581	.024982	1.789	-.157	-1.416	6	20
204.00	.026650	.025061	1.713	-.188	-1.322	6	20
205.00	.026755	.025169	1.700	-.149	-1.321	6	20
206.00	.026850	.025282	1.709	-.152	-1.394	6	20
207.00	.026913	.025363	1.645	-.129	-1.334	6	20
208.00	.027028	.025419	1.679	-.155	-1.280	6	20
209.00	.027082	.025632	1.617	-.125	-1.390	6	20
210.00	.027183	.025736	1.557	-.109	-1.276	6	20
211.00	.027278	.025831	1.569	-.096	-1.292	6	20
212.00	.027423	.025906	1.583	-.052	-1.195	6	20
213.00	.027472	.026072	1.523	-.017	-1.246	6	20
214.00	.027632	.026184	1.525	.048	-1.160	6	20
215.00	.027704	.026235	1.513	.029	-1.154	6	20
216.00	.027819	.026363	1.507	.035	-1.132	10	20
217.00	.027872	.026466	1.473	-.061	-1.155	10	20
218.00	.027990	.026574	1.491	-.008	-1.128	10	20
219.00	.028192	.026726	1.461	.104	-1.021	10	20
220.00	.028321	.026817	1.484	.068	-.990	6	20
221.00	.028392	.026932	1.468	.054	-.958	10	20
222.00	.028558	.027086	1.485	.173	-.967	10	20
223.00	.028678	.027165	1.474	.147	-.908	10	20
224.00	.028888	.027300	1.490	.263	-.698	10	20
225.00	.028959	.027437	1.457	.253	-.768	10	20
226.00	.029075	.027591	1.450	.174	-.861	10	20
227.00	.029191	.027732	1.447	.267	-.891	10	20
228.00	.029356	.027825	1.431	.319	-.716	10	20
229.00	.029525	.027963	1.427	.285	-.684	10	20
230.00	.029646	.028123	1.407	.312	-.646	10	20
231.00	.029787	.028235	1.419	.295	-.720	10	20
232.00	.029970	.028449	1.373	.384	-.607	10	22
233.00	.030126	.028585	1.402	.382	-.638	10	22
234.00	.030309	.028769	1.362	.513	-.515	10	20
235.00	.030465	.028930	1.359	.466	-.585	10	22
236.00	.030642	.029092	1.375	.495	-.629	10	22
237.00	.030858	.029271	1.380	.460	-.641	10	22
238.00	.030969	.029405	1.350	.414	-.637	10	22
239.00	.031189	.029609	1.361	.519	-.613	10	22
240.00	.031446	.029818	1.382	.546	-.590	10	22
241.00	.031635	.030037	1.393	.601	-.658	10	22
242.00	.031888	.030157	1.417	.561	-.523	10	22
243.00	.032097	.030389	1.443	.538	-.635	10	22
244.00	.032347	.030494	1.452	.468	-.451	10	22
245.00	.032628	.030776	1.480	.569	-.459	10	22
246.00	.032868	.031008	1.526	.581	-.591	10	22
247.00	.033138	.031205	1.536	.504	-.659	10	22
248.00	.033377	.031428	1.532	.370	-.741	10	22
249.00	.033729	.031768	1.601	.589	-.739	10	22
250.00	.034082	.032036	1.633	.543	-.740	10	22
251.00	.034452	.032250	1.719	.637	-.720	10	22
252.00	.034648	.032536	1.599	.435	-.874	10	22
253.00	.034963	.032844	1.573	.425	-.882	10	22
254.00	.035239	.033214	1.529	.530	-.864	10	22
255.00	.035655	.033542	1.550	.552	-.783	10	22
256.00	.036053	.033913	1.577	.588	-.814	10	22
257.00	.036638	.034353	1.634	.706	-.574	10	22
258.00	.037130	.034732	1.711	.676	-.677	10	22
259.00	.037614	.035240	1.754	.651	-.807	10	22
260.00	.038326	.035677	1.803	.703	-.591	10	22
261.00	.039368	.036457	1.986	.878	-.181	11	22
262.00	.039459	.037029	1.945	.694	-.934	13	22
263.00	.041388	.037623	2.301	.710	-.412	13	22
264.00	.042790	.038129	2.546	.889	.363	13	22
265.00	.045237	.039160	3.479	.423	-.742	13	23
266.00	.052573	.040836	5.763	.869	.928	13	22
267.00	.082702	.041442	13.239	.906	-.782	13	22
268.00	.070847	.032120	15.155	.344	-.652	3	7
269.00	.080220	.006661	28.014	-.238	-1.397	9	20
270.00	.098086	.025131	17.762	.262	-.240	4	7
271.00	.076937	.005034	26.998	.009	-1.117	12	7
272.00	.069660	.008486	20.261	-.172	.244	6	7
273.00	.057268	.015753	17.868	-.008	-.250	7	20
274.00	.050747	.025097	9.670	-.554	2.244	7	13
275.00	.047550	.034674	5.934	.357	.257	7	8
276.00	.044927	.039150	3.764	-.015	-1.214	18	7
277.00	.045437	.040120	3.462	.263	-1.075	18	24
278.00	.046306	.041040	3.323	.067	-1.092	18	24
279.00	.047819	.041911	3.430	.045	-1.027	18	4
280.00	.048479	.043038	3.501	-.038	-1.198	18	4
281.00	.050307	.044243	3.485	-.383	-.837	18	22
282.00	.051729	.045283	3.666	-.123	-1.147	18	24
283.00	.053490	.046105	3.953	-.020	-1.050	17	3

284.00	.054497	.048279	3.350	-.317	-.957	18	24
285.00	.057251	.049227	3.838	-.039	-.967	17	3
286.00	.058981	.048266	4.551	.439	-.318	18	3
287.00	.068617	.053729	4.819	1.106	1.782	17	3
288.00	.062221	.047059	6.206	-.122	-.779	18	4
289.00	.062096	.050543	5.190	-.153	-1.113	15	4
290.00	.065992	.055787	4.452	-.136	-.911	17	4
291.00	.068765	.058659	4.382	-.165	-.988	17	4
292.00	.071308	.059927	4.568	-.166	-.930	18	4
293.00	.074822	.062676	4.781	-.181	-.983	17	4
294.00	.078940	.065872	4.957	-.093	-1.098	17	4
295.00	.085388	.069560	5.092	.026	-.930	17	4
296.00	.091147	.073636	5.343	-.025	-.916	17	4
297.00	.098297	.078917	5.548	-.044	-.956	17	4
298.00	.106614	.084911	5.695	-.097	-.926	17	4
299.00	.117265	.093750	5.777	-.047	-.953	17	4
300.00	.131391	.103560	5.987	-.133	-.887	17	4
301.00	.150401	.116435	6.314	-.198	-.822	17	4
302.00	.175494	.135015	6.560	-.221	-.832	17	4
303.00	.211360	.162821	6.724	-.323	-.832	17	4
304.00	.274117	.206840	6.872	-.328	-.708	17	4
305.00	.401745	.296465	7.451	-.336	-.714	17	4
306.00	.763526	.542868	7.858	-.469	-.564	17	4
307.00	22.822541	5.077773	21.681	1.228	.236	17	7
308.00	.855429	.590978	9.505	.400	-1.109	10	4
309.00	.396890	.274851	8.827	.186	-1.074	17	4
310.00	.246702	.173995	8.693	.059	-1.125	17	4
311.00	.179045	.121989	9.160	.021	-1.018	17	4
312.00	.139561	.092331	9.597	.055	-.946	17	4
313.00	.111554	.072309	9.962	.003	-.983	17	4
314.00	.092577	.059186	10.382	.058	-.925	17	4
315.00	.078257	.048534	10.831	.022	-.922	17	4
316.00	.067033	.040580	11.245	.083	-.861	17	4
317.00	.058788	.033687	11.977	.120	-.824	17	4
318.00	.051606	.028562	12.418	.112	-.891	17	4
319.00	.045340	.024127	13.271	.075	-.917	17	4
320.00	.039848	.020072	13.841	.058	-.898	17	4
321.00	.035521	.017242	14.418	.094	-.861	17	4
322.00	.031683	.014121	15.246	.069	-.849	17	4
323.00	.028356	.011393	16.452	.076	-.903	17	4
324.00	.025180	.009172	17.492	.029	-.873	17	4
325.00	.022786	.007271	18.549	.067	-.876	17	4
326.00	.020171	.005764	19.719	.094	-.868	17	4
327.00	.018446	.004350	20.736	.121	-.825	17	4
328.00	.016626	.002603	22.277	.158	-.771	17	4
329.00	.014463	.001482	24.522	.163	-.808	17	4
330.00	.012759	.000198	27.261	.103	-.817	17	4
331.00	.011675	.000278	27.541	.374	-.722	16	4
332.00	.009893	.000588	27.925	.631	-.685	15	4
333.00	.008420	.000033	28.506	.797	-.234	19	4
334.00	.007681	.000110	27.060	.865	.059	9	4
335.00	.006426	.000373	27.925	.782	-.531	1	4
336.00	.005412	.000082	32.664	.335	-1.300	2	17
337.00	.006489	.000217	28.879	.383	-1.012	21	17
338.00	.007094	.000125	28.384	.450	-.871	23	17
339.00	.007997	.000370	27.190	.514	-.760	3	17
340.00	.008436	.000109	27.402	.312	-.977	22	17
341.00	.009171	.000541	26.887	.185	-.949	22	17
342.00	.009552	.000374	27.264	-.056	-.839	4	17
343.00	.010304	.000103	26.096	-.262	-.584	5	17
344.00	.010727	.000426	25.351	-.361	-.406	4	17
345.00	.011449	.000964	23.543	-.348	-.468	5	17
346.00	.011938	.001278	22.665	-.379	-.359	5	17
347.00	.012216	.002129	22.178	-.430	-.437	4	17
348.00	.012333	.002424	21.993	-.467	-.606	5	17
349.00	.013621	.003038	20.111	-.305	-.587	5	17
350.00	.013238	.003324	20.519	-.437	-.664	5	17
351.00	.014381	.003619	19.081	-.413	-.459	5	17
352.00	.014521	.004092	19.411	-.450	-.642	5	17
353.00	.015235	.004329	18.436	-.460	-.504	5	17
354.00	.015720	.004663	18.758	-.454	-.654	5	17
355.00	.015793	.004967	18.660	-.478	-.668	5	17
356.00	.016704	.005049	18.769	-.478	-.682	5	17
357.00	.017183	.005154	19.307	-.446	-.852	5	17
358.00	.017902	.005193	19.786	-.379	-.941	5	17
359.00	.018440	.005052	20.496	-.360	-1.002	5	17
360.00	.019412	.004405	22.801	-.283	-1.138	5	17
361.00	.020238	.004551	23.968	-.213	-1.307	5	17
362.00	.021513	.003651	25.681	-.226	-1.313	5	9
363.00	.028612	.001384	31.251	.002	-1.537	5	9
364.00	.025635	.001576	28.308	-.101	-1.353	5	9
365.00	.072884	.006580	27.702	.284	-1.245	15	1
366.00	.108990	.017937	25.531	-.082	-1.365	23	9
367.00	.130296	.006902	27.752	.125	-1.097	15	1
368.00	.108353	.009980	25.544	.179	-1.199	19	1
369.00	.082504	.017802	20.418	.137	-.597	11	8
370.00	.099294	.011868	24.812	-.306	-.985	6	8
371.00	.079591	.006523	26.099	-.110	-1.065	5	18
372.00	.063560	.010699	24.260	.313	-1.032	10	18
373.00	.041002	.004240	23.340	.106	-.614	11	7
374.00	.037747	.002351	20.898	.146	.193	9	15
375.00	.029857	.004996	21.040	-.690	-.162	16	18
376.00	.024494	.007853	18.612	-.253	-.853	24	12
377.00	.025244	.010665	15.759	.114	-.888	16	13
378.00	.025334	.013416	13.623	.451	-.589	16	13
379.00	.027761	.012292	16.021	.344	-.911	11	14
380.00	.036810	.007810	22.851	.485	.924	11	19
381.00	.070403	.011439	23.994	.934	-.263	16	8
382.00	.115212	.005862	26.715	.545	-.887	2	8
383.00	.056281	.001450	24.052	.504	.150	19	7
384.00	.041726	.005905	21.579	.056	-.476	9	4
385.00	.069213	.006108	24.463	1.197	.579	18	3
386.00	.075287	.002698	22.607	1.805	3.084	8	3
387.00	.099489	.002602	25.715	1.806	2.118	16	3
388.00	.074962	.007857	19.840	1.650	2.618	13	3
389.00	.052040	.015452	16.120	1.873	3.277	9	3
390.00	.038772	.009476	20.492	.202	-.821	7	3
391.00	.047398	.005464	24.858	.451	-.947	4	23
392.00	.061014	.008357	24.940	.888	-.504	4	20
393.00	.083124	.002387	28.806	.550	-.978	7	24
394.00	.150475	.012538	25.336	1.084	.600	17	24
395.00	.168406	.004543	25.340	1.179	.898	18	23
396.00	.101999	.010741	25.846	1.590	1.149	20	5
397.00	.097806	.005896	28.052	.343	-1.164	21	24
398.00	.062643	.001749	29.183	.524	-1.170	4	9
399.00	.095129	.011003	23.045	1.292	.807	4	15

284.00	.054497	.048279	3.350	-.317	-.957	18	24
285.00	.057251	.049227	3.838	-.039	-.967	17	3
286.00	.058981	.048266	4.551	.439	-.318	18	3
287.00	.068617	.053729	4.819	1.106	1.782	17	5
288.00	.062221	.047059	6.206	-.122	-.779	18	4
289.00	.062096	.050543	5.190	-.153	-1.113	15	4
290.00	.065992	.055787	4.452	-.136	-.911	17	4
291.00	.068765	.058659	4.382	-.165	-.988	17	4
292.00	.071308	.059927	4.568	-.166	-.930	18	4
293.00	.074822	.062676	4.781	-.181	-.983	17	4
294.00	.078940	.065872	4.957	-.093	-1.098	17	4
295.00	.085388	.069560	5.092	.026	-.930	17	4
296.00	.091147	.073636	5.343	-.025	-.916	17	4
297.00	.098297	.078917	5.548	-.044	-.956	17	4
298.00	.106614	.084911	5.695	-.097	-.926	17	4
299.00	.117265	.093750	5.777	-.047	-.953	17	4
300.00	.131391	.103560	5.987	-.133	-.887	17	4
301.00	.150401	.116435	6.314	-.198	-.822	17	4
302.00	.175494	.135015	6.560	-.221	-.832	17	4
303.00	.211360	.162821	6.724	-.323	-.832	17	4
304.00	.274117	.206840	6.872	-.328	-.708	17	4
305.00	.401745	.296465	7.451	-.336	-.714	17	4
306.00	.763526	.542868	7.858	-.469	-.564	17	4
307.00	22.822641	5.077773	21.681	1.228	.236	17	7
308.00	.855429	.590978	9.505	.400	-1.109	10	4
309.00	.396890	.274851	8.827	.186	-1.074	17	4
310.00	.246702	.173995	8.693	.059	-1.125	17	4
311.00	.179045	.121989	9.160	.021	-1.018	17	4
312.00	.139561	.092331	9.597	.055	-.946	17	4
313.00	.111554	.072309	9.962	.003	-.983	17	4
314.00	.092577	.059186	10.382	.058	-.925	17	4
315.00	.078257	.048534	10.831	.022	-.922	17	4
316.00	.067033	.040580	11.245	.083	-.861	17	4
317.00	.058788	.033687	11.977	.120	-.824	17	4
318.00	.051606	.028562	12.418	.112	-.891	17	4
319.00	.045340	.024127	13.271	.075	-.917	17	4
320.00	.039848	.020072	13.841	.058	-.898	17	4
321.00	.035521	.017242	14.418	.094	-.861	17	4
322.00	.031683	.014121	15.246	.069	-.849	17	4
323.00	.028356	.011393	16.452	.076	-.903	17	4
324.00	.025180	.009172	17.492	.029	-.873	17	4
325.00	.022786	.007271	18.549	.067	-.876	17	4
326.00	.020171	.005764	19.719	.094	-.868	17	4
327.00	.018446	.004350	20.738	.121	-.825	17	4
328.00	.016626	.002603	22.277	.158	-.771	17	4
329.00	.014463	.001482	24.522	.163	-.808	17	4
330.00	.012759	.000198	27.261	.103	-.817	17	4
331.00	.011675	.000278	27.541	.374	-.722	16	4
332.00	.009893	.000588	27.925	.631	-.685	15	4
333.00	.008420	.000033	28.506	.797	-.234	19	4
334.00	.007681	.000110	27.060	.865	.059	9	4
335.00	.006426	.000373	27.925	.782	-.531	1	4
336.00	.005412	.000082	32.664	.335	-1.300	2	17
337.00	.006489	.000217	28.879	.383	-1.012	21	17
338.00	.007094	.000125	28.384	.450	-.871	23	17
339.00	.007997	.000370	27.190	.514	-.760	3	17
340.00	.008436	.000109	27.402	.312	-.977	22	17
341.00	.009171	.000541	26.887	.185	-.949	22	17
342.00	.009552	.000374	27.264	-.056	-.839	4	17
343.00	.010304	.000103	26.096	-.262	-.584	5	17
344.00	.010727	.000426	25.351	-.361	-.406	4	17
345.00	.011449	.000964	23.543	-.348	-.468	5	17
346.00	.011938	.001278	22.665	-.379	-.359	5	17
347.00	.012216	.002129	22.178	-.430	-.432	4	17
348.00	.012333	.002424	21.993	-.467	-.606	5	17
349.00	.013621	.003038	20.111	-.305	-.587	5	17
350.00	.013238	.003324	20.519	-.437	-.664	5	17
351.00	.014381	.003619	19.081	-.413	-.459	5	17
352.00	.014521	.004092	19.411	-.450	-.642	5	17
353.00	.015235	.004329	18.436	-.460	-.504	5	17
354.00	.015720	.004663	18.758	-.454	-.654	5	17
355.00	.015793	.004967	18.660	-.478	-.668	5	17
356.00	.016704	.005049	18.769	-.478	-.682	5	17
357.00	.017183	.005154	19.307	-.446	-.852	5	17
358.00	.017902	.005193	19.786	-.379	-.941	5	17
359.00	.018440	.005052	20.496	-.360	-1.002	5	17
360.00	.019412	.004405	22.801	-.283	-1.138	5	17
361.00	.020238	.004551	23.968	-.213	-1.307	5	17
362.00	.021513	.003651	25.681	-.226	-1.313	5	9
363.00	.028612	.001384	31.251	.002	-1.537	5	9
364.00	.025635	.001576	28.308	-.101	-1.353	5	9
365.00	.072884	.006580	27.702	.284	-1.245	15	1
366.00	.108990	.017937	25.531	-.082	-1.365	23	9
367.00	.130296	.006902	27.752	.125	-1.097	15	1
368.00	.108353	.009980	25.544	.179	-1.199	19	1
369.00	.082504	.017602	20.418	.137	-.597	11	8
370.00	.099294	.011868	24.812	-.306	-.985	6	8
371.00	.079591	.006523	26.099	-.110	-1.065	5	18
372.00	.063560	.010699	24.260	.313	-1.032	10	18
373.00	.041002	.004240	23.340	.106	-.614	11	7
374.00	.037747	.002351	20.898	.146	.193	9	15
375.00	.029857	.004996	21.040	-.690	-.162	16	18
376.00	.024494	.007853	18.612	-.253	-.853	24	12
377.00	.025244	.010665	15.759	.114	-.888	16	13
378.00	.025334	.013416	13.623	.451	-.589	16	13
379.00	.027761	.012292	16.021	.344	-.911	11	14
380.00	.036810	.007810	22.851	.485	-.924	11	19
381.00	.070403	.011439	23.994	.934	-.263	16	8
382.00	.115212	.005862	26.715	.545	-.887	2	8
383.00	.056281	.001450	24.052	.504	.150	19	7
384.00	.041726	.005905	21.579	.056	-.476	9	4
385.00	.069213	.006108	24.463	1.197	.579	18	3
386.00	.075287	.002698	22.607	1.805	3.084	8	3
387.00	.099489	.002602	25.715	1.806	2.118	16	3
388.00	.074962	.007857	19.840	1.650	2.618	13	3
389.00	.052040	.015452	16.120	1.873	3.277	9	3
390.00	.038772	.009476	20.492	.202	-.821	7	3
391.00	.047398	.005464	24.858	.451	-.947	4	23
392.00	.061014	.008357	24.940	.888	-.504	4	20
393.00	.083124	.002387	28.806	.550	-.978	7	24
394.00	.150475	.012538	25.336	1.084	.600	17	24
395.00	.168406	.004543	25.340	1.179	.898	18	23
396.00	.101999	.010741	25.846	1.590	1.149	20	5
397.00	.097806	.005896	28.052	.343	-1.164	21	24
398.00	.062643	.001749	29.183	.524	-1.170	4	9
399.00	.095129	.011003	23.045	1.292	.807	4	15

400.00	.063592	.005248	23.914	.574	-.846	24	15
401.00	.038874	.011941	17.566	.648	-.195	23	15
402.00	.037511	.009165	19.979	-.080	-.864	23	15
403.00	.033862	.012545	18.498	.002	-.992	23	11
404.00	.035591	.009828	19.973	-.012	-.981	21	5
405.00	.033306	.014430	16.822	.597	-.817	20	13
406.00	.032770	.005173	19.140	-.414	.477	5	12
407.00	.031468	.015453	14.435	.163	-.814	20	12
408.00	.031715	.013616	17.768	-.271	-1.279	20	10
409.00	.032532	.014461	16.697	-.086	-1.287	20	11
410.00	.033241	.014118	19.205	-.362	-1.355	20	1
411.00	.033800	.013543	20.823	-.425	-1.481	20	1
412.00	.078344	.002590	27.380	.659	-.718	15	1
413.00	.104977	.008247	21.816	.392	.131	18	1
414.00	.100628	.004095	25.877	.746	-.422	18	1
415.00	.066946	.004684	28.101	-.080	-1.318	15	1
416.00	.075869	.005909	27.976	.161	-1.425	22	6
417.00	.235373	.012507	25.859	.269	-.687	13	6
418.00	.285218	.014082	28.598	-.064	-1.262	24	17
419.00	.139531	.020185	25.083	.613	-.761	24	17
420.00	.073313	.006287	29.952	.315	-1.323	6	16
421.00	.051607	.001161	31.590	.042	-1.443	3	15
422.00	.047859	.005329	29.730	-.005	-1.486	4	14
423.00	.048670	.005254	30.240	-.021	-1.402	4	14
424.00	.048729	.006435	28.593	.098	-1.344	4	14
425.00	.050680	.006124	28.858	.151	-1.291	5	13
426.00	.053369	.005398	29.274	.268	-1.259	4	14
427.00	.055424	.004780	30.288	.307	-1.243	5	13
428.00	.065592	.001747	31.604	.433	-1.226	4	13
429.00	.070145	.000609	31.958	.486	-1.158	4	14
430.00	.093242	.000925	34.538	.659	-1.147	6	13
431.00	.158554	.005204	27.082	1.116	.025	22	14
432.00	.334711	.009333	28.882	.947	-.201	7	12
433.00	.696507	.021416	29.380	1.032	-.036	1	12
434.00	.184310	.019063	28.026	.248	-1.290	1	13
435.00	.104939	.001618	28.859	.337	-1.147	24	4
436.00	.070357	.006798	28.629	.181	-1.277	9	4
437.00	.049872	.003724	23.747	-.185	-.941	14	19
438.00	.049445	.005809	27.973	-.019	-1.255	11	20
439.00	.047483	.004613	28.365	-.126	-1.221	11	20
440.00	.044878	.004234	27.775	-.223	-1.169	12	19
441.00	.044104	.009574	24.309	-.133	-1.172	12	19
442.00	.043266	.011957	22.399	-.064	-1.139	12	19
443.00	.042811	.013695	20.830	-.003	-1.124	12	19
444.00	.042358	.014946	19.713	.017	-1.107	11	19
445.00	.042018	.016822	18.312	.084	-1.091	11	19
446.00	.041795	.017556	17.508	.114	-1.088	12	19
447.00	.041628	.018809	16.530	.170	-1.086	11	19
448.00	.041513	.019816	15.784	.211	-1.057	12	19
449.00	.041423	.020760	15.049	.245	-1.045	11	19
450.00	.041390	.021393	14.465	.293	-1.029	11	19
451.00	.041361	.022083	13.981	.318	-1.025	11	19
452.00	.041408	.022722	13.460	.342	-.938	11	19
453.00	.041414	.023217	13.050	.353	-1.000	11	19
454.00	.041486	.023793	12.574	.367	-.969	11	19
455.00	.041551	.024310	12.288	.382	-.999	11	19
456.00	.041658	.025052	11.978	.419	-.976	11	19
457.00	.041753	.025497	11.641	.437	-.965	11	19
458.00	.041917	.025956	11.431	.439	-.980	11	19
459.00	.042052	.026398	11.180	.443	-.981	11	19
460.00	.042203	.026972	10.948	.471	-.962	11	19
461.00	.042375	.027415	10.693	.485	-.958	11	19
462.00	.042553	.027748	10.559	.474	-.980	11	19
463.00	.042721	.028270	10.360	.497	-.963	11	19
464.00	.042926	.028630	10.103	.521	-.921	11	19
465.00	.043142	.029038	9.948	.512	-.921	12	19
466.00	.043391	.029304	9.862	.531	-.928	11	19
467.00	.043584	.029686	9.736	.533	-.918	24	19
468.00	.043839	.030063	9.668	.535	-.929	11	19
469.00	.044115	.030263	9.565	.519	-.932	11	19
470.00	.044382	.030471	9.439	.526	-.930	24	19
471.00	.044693	.030804	9.406	.516	-.964	24	19
472.00	.044941	.031115	9.301	.507	-.968	24	19
473.00	.045259	.031367	9.250	.502	-.967	24	19
474.00	.045586	.031541	9.226	.491	-.973	24	19
475.00	.045911	.031842	9.116	.497	-.969	24	19
476.00	.046220	.032073	9.060	.476	-.974	24	19
477.00	.046618	.032174	9.058	.482	-.958	24	19
478.00	.047003	.032495	9.043	.470	-.978	24	19
479.00	.047352	.032664	9.079	.446	-.990	24	19
480.00	.047782	.033030	9.046	.448	-.988	24	19
481.00	.048177	.033148	9.048	.421	-.997	24	19
482.00	.048569	.033430	9.090	.402	-1.019	24	19
483.00	.048997	.033685	9.128	.379	-1.036	24	19
484.00	.049484	.033821	9.186	.355	-1.036	24	19
485.00	.049940	.034088	9.279	.336	-1.051	24	19
486.00	.050431	.034318	9.386	.325	-1.066	24	19
487.00	.050904	.034534	9.479	.287	-1.101	24	19
488.00	.051495	.034630	9.676	.263	-1.125	24	19
489.00	.052049	.034906	9.832	.237	-1.147	24	19
490.00	.052693	.035139	9.953	.209	-1.169	24	19
491.00	.053324	.035316	10.172	.196	-1.180	24	19
492.00	.054019	.035485	10.401	.156	-1.210	24	19
493.00	.054774	.035525	10.694	.125	-1.238	24	19
494.00	.055598	.035756	10.983	.099	-1.254	24	19
495.00	.056491	.035739	11.328	.065	-1.281	24	19
496.00	.057443	.035710	11.761	.029	-1.297	24	19
497.00	.058528	.035665	12.238	-.018	-1.341	24	19
498.00	.059715	.035585	12.936	-.038	-1.373	24	19
499.00	.061342	.035410	13.440	-.067	-1.368	24	17
500.00	.063730	.035036	13.857	-.018	-1.283	24	17
501.00	.066675	.034588	15.464	-.119	-1.421	24	17
502.00	.075146	.034100	15.908	.029	-1.230	24	5
503.00	.078110	.032912	18.249	-.142	-1.359	24	17
504.00	.083449	.030687	19.638	-.168	-1.271	24	16
505.00	.177042	.028349	25.191	.679	-.760	24	16
506.00	.248447	.021709	27.386	.740	-.794	24	16
507.00	.238788	.013670	32.079	.629	-1.013	13	17
508.00	.183273	.006297	29.327	.425	-1.028	12	3
509.00	.156017	.004386	31.426	.386	-1.234	14	7
510.00	.590736	.012097	26.724	1.422	.985	14	19
511.00	.849824	.067593	22.692	1.293	1.502	10	7
512.00	.370920	.047232	27.123	.276	-1.448	10	7
513.00	.258728	.033278	28.572	.247	-1.346	19	7
514.00	.170521	.011497	28.275	.164	-1.213	6	7
515.00	.115892	.003219	28.447	.142	-1.271	11	7

Chapter 7

7.1 Introduction

Turbine blades mounted on a rotor, in common with many other engineering structures and components, are usually modelled as cantilever beams vibrating in flexure. It is, therefore, assumed in such theoretical modelling that the effects of root flexibility on the natural frequencies and mode shapes of vibration are negligible, so that the blades may be considered as being attached to the disc with infinite rigidity.

In reality, however, the stiffness conditions prevailing at the roots of a 'cantilevered' blade do not always tend to the infinite since many bladed disc assemblies are characterized by very complex end-fixing conditions at the roots of the blades. Thus, for example, we have *fir-tree* and *pin-jointed* mountings, which admit of substantial resilience at the blade-root and disc-rim interface. It is, therefore, to be expected that the correctness of cantilever frequencies measured for any given blade depends to a great extent upon the flexibility prevailing at the root during the measurement.

The influence of a flexible support on the natural frequencies of cantilevers has been the subject of several theoretical and experimental studies. In both cases, there is agreement that the dynamic properties of bars with non-rigid roots deviate sharply from those of the equivalent *en castré* forms. Isolated cantilever blades such as those studied by **Rissone** and **Williams** (1965) are seldom encountered in practical engineering systems. Usually, several blades are attached to a rotor with the result that all the blades are mechanically coupled to one another, and to the rotor, through the elasticity of the disc. Both **Ewins** (1976) and **Fabunmi** (1978) have reported the experimental difficulties encountered in their efforts to measure the individual frequencies of blades affixed to actual compressors or models of turbine rotors.

The construction of many bladed disc assemblies is such that the severance of an individual blade from the rest of the assembly may be achieved relatively easily, so that one may undertake to measure its 'cantilever' frequency more readily by applying some considerable restraint at the root of the isolated blade. However, even in such cases, it has been reported, **Gleeson** (1979), that not only is the measured blade-alone frequency sensitive to the degree and type of clamping, it is also much dependent on the nature and location of the exciting force. Hence, different frequencies were obtained according as whether the force was applied at

the root, tip, or elsewhere along the axis of the blade.

An even more difficult problem is presented to the turbine designer who requires a fairly accurate estimate of the blade alone frequencies of mistuned assemblies that are of integral construction. In such systems, the blades and disc are machined together from the solid and, moreover, there exists minute but significant variations in the individual blades' cantilever frequencies. A popular method of neutralising the influence of the disc flexibility in such instances is to cast heavy alloys on the rotor **Fabunmi** (1978), or else machine some heavy steel plates to suit the disc **Ewins** (1972), so as to achieve a greater measure of rigidity at the blade root. Nevertheless, the motion of any one blade on such 'weighted discs' may still be coupled to those of all other blades on the stage by the residual flexibility of the weighted disc. In such a case, plasticine has been used to good effect, **Ewins** (1972), in damping out the residual coupling.

From the foregoing, it is evident that there is general awareness in the industry of the influence of the flexible joint on the dynamic behaviour of blades, and there thus appears to be a need to devise a simple and more effective way of defeating the problems arising out of root resilience.

7.2 Effect of Root Flexibility on the Natural Frequencies

The theoretical treatment of the dynamic behaviour of a resiliently mounted cantilever has been studied by several authors, for example: **Belagumkar** *et al* (1962), **Chun** (1972), **McBain** and **Genin** (1973). Recently, **Justine** and **Krishnan** (1980) used a matrix iteration procedure to study the same problem. Their analysis was based on a discretized beam model in which the cantilever was divided into sixteen finite elements. They obtained dimensionless frequency parameters and mode shapes for a variety of root stiffness parameters. Along with the previous researchers, they concluded that the fundamental frequency which is obtained for a 'cantilever' when flexibility is accounted for is lower than that obtained from a model of infinite rigidity at the cantilevered end.

Although the fundamental frequency is nearly always required, there are other instances when a knowledge of the second, third, and even higher resonant frequencies is also of interest. In the analysis of higher modes of vibration, approximate techniques based on a finite degree of modelling, as in many finite element schemes, is known to be inaccurate. In what fol-

lows, the Bernoulli-Euler and Timoshenko theories of beam vibration are utilized to obtain general fequency equations for the in-plane vibration of flexibly mounted prismatic bars of uniform cross-section.

7.2.1. Bernoulli-Euler Theory

Consider the in-plane vibration of a uniform prismatic beam with linear and rotational restraining springs K_L and K_R respectively at one end as depicted in Figure 7.2.1.

Subject to the limitations inherent in the Bernoulli-Euler theory, the governing equation of motion for the beam may be written, given that $y=y(x,t)$, as follows:

$$EI \frac{\partial^4 y}{\partial x^4} + \rho A \frac{\partial^2 y}{\partial t^2} = 0 \tag{7.2.1}$$

in which:

EI = flexural rigidity
ρA = mass per unit length
y = transverse displacement
x = co-ordinate along beam axis, measured from the sprung end

The general solution of equation (7.2.1) is, in terms of the nth principal mode of vibration,

$$Y_n(x) = C_{1n}\cos(\lambda_n x) + C_{2n}\sin(\lambda_n x) + C_{3n}\cosh(\lambda_n x) + C_{4n}\sinh(\lambda_n x) \tag{7.2.2}$$

where:

$$\lambda_n^4 = \rho A \omega_n^2 / \mathrm{EI}$$

ω_n is the circular frequency of vibration at the nth mode, and $C_{jn}(j=1,4)$ are arbitrary constants, the values of which depend on the boundary conditions. The frequency equation is obtained when the boundary conditions at $x = 0$ and $x = l$ are substituted into equations (7.2.1) and 7.2.2), and the frequency equation is obtained from (7.2.1) to (7.2.2), and is given by:

$$\begin{aligned} &Z_L Z_R(\cos\theta_n\cosh\theta_n + 1) + Z_L\theta_n(\cos\theta_n\sinh\theta_n - \sin\theta_n\cosh\theta_n) \\ &-Z_R\theta_n^3(\cos\theta_n\sinh\theta_n + \sin\theta_n\cosh\theta_n) - \theta_n^4(\cos\theta_n\cosh\theta_n - 1) = 0 \end{aligned} \tag{7.2.3}$$

where $\theta_n = \lambda_n l$, and $Z_L = K_L l/EI$, $Z_R = K_R l/EI$ are the dimensionless linear and rotational stiffness parameters respectively. We observe that

as $K_L \to \infty$, equation (7.2.3) becomes

$$Z_R(\cos\theta_n\cosh\theta_n + 1) + \theta_n(\cos\theta_n\sinh\theta_n - \sin\theta_n\cosh\theta_n) = 0 \quad (7.2.4)$$

which is the frequency equation for a spring-hinged beam, **Chun** (1972).

For a clamped-free beam, the familiar equation of a cantilevered beam is

$$\cos\lambda_n\cosh\lambda_n + 1 = 0 \quad (7.2.5)$$

which is the form equation (7.2.3) takes as K_L and K_R both tend to infinity, and on replacing θ_n by $\lambda_n l$

Finally, if $K_L = K_R = 0$, we obtain the frequency equation

$$\cos\lambda_n\cosh\lambda_n - 1 = 0 \quad (7.2.6)$$

7.2.2 Timoshenko Theory

Components like turbine blades operating in high frequency environments are more accurately modelled if the effects of shear deformation and rotatory inertia are taken into consideration. For stubby blades in particular, it is appropriate to use the Timoshenko theory, even for low frequency oscillations.

The equation for the transverse vibrations of a uniform prismatic beam is, as given by **Timoshenko** (1921),

$$EI\frac{\partial^4 y}{\partial x^4} + \rho A\frac{\partial^2 y}{\partial t^2} - \rho I\left(1 + \frac{E}{kG}\right)\frac{\partial^4 y}{\partial x^2\,\partial t^2} + \frac{\rho^2 I}{kG}\frac{\partial^4 y}{\partial t^4} = 0 \quad (7.2.7)$$

where, $y = y(x,t)$ and

k = shear coefficient dependent on the shape of the beam section

G = modulus of rigidity in shear

I = second moment of area of beam section

and other symbols have their usual meanings. If we let

$$\begin{aligned} p_n &= \rho\omega_n^2/2kg \\ r_n &= \rho\omega_n^2/2E \\ \lambda_n^4 &= \rho\omega_n^2 A/EI \end{aligned} \quad (7.2.8)$$

then the general solution of equation (7.2.7) is

$$Y_n(x) = A_{1n}\cos\lambda\alpha_n x + A_{2n}\sin\lambda\alpha_n x + A_{3n}\cosh\lambda\alpha_n x + A_{4n}\sinh\lambda\alpha_n x \quad (7.2.9)$$

where

$$\begin{aligned} \alpha_n^2 &= p_n + r_n + \sqrt{[\lambda_n^4 + (p_n - r_n)^2]} \\ \beta_n^2 &= -p_n + r_n + \sqrt{[\lambda_n^4 + (p_n - r_n)^2]} \end{aligned} \quad (7.2.10)$$

and $A_{jn}(j=1,4)$ are arbitrary constants as before.

By following the procedure of §7.2.1, or else by using the concept of receptance coupling, we obtain after some algebra the following frequency equation:

$$Z_L Z_R(\phi_1\phi_2+\phi_3^2) + Z_L\theta\phi_1 - Z_R\tau\theta^3\phi_2 - \tau^2\theta^4 = 0 \qquad (7.2.11)$$

where, in addition to symbols previously defined in equations (7.2.3), (7.2.8) and (7.2.10), we have, upon dropping the subscript n,

$$\begin{aligned}
\phi_1 &= (\alpha^2+\beta^2)(\beta\lambda c_1 s_2/\gamma - \alpha\lambda s_1 c_2/\gamma_2)/\lambda^2 \\
\phi_2 &= (\alpha^2+\beta^2)(\gamma_1 c_1 s_2/\beta + \gamma_2 s_1 c_2/\alpha)/\lambda^3 \\
\phi_3 &= (\gamma_1-\gamma_2)(c_1c_2-1)/\lambda^2 + s_1 s_2(\alpha\gamma_1/\beta\lambda^2+\beta\gamma_2/\alpha\lambda^2) \\
\tau &= 2(c_1c_2-1) + s_1 s_2(\beta\gamma_2/\alpha\gamma_1 - \alpha\gamma_1/\beta\gamma_2) \\
\gamma_1 &= a^2 - 2p \\
\gamma_2 &= \beta^2 + 2p \\
\theta &= \lambda l
\end{aligned}$$

and $c_1=\cos\alpha$, $c_2=\cosh\beta$, $s_1=\sin\alpha$, $s_2=\sinh\beta$.

If the shear strain at the centroid of the beam is assumed negligible, then $K\Rightarrow\infty$; If rotatory inertia effects are negligible in addition, then $\alpha = \beta = \lambda = \sqrt{\gamma_1} = \sqrt{\gamma_2}$, and equation (7.2.11) reduces to (7.2.3)

7.2.3 Numerical Case Study

The roots of the frequency equation (7.2.3) and (7.2.4) were evaluated on the CDC Cyber 174 Computer and the results are presented in Table 7.2.1 for the three lowest modes, and in the surface plot of Figure 7.2.2, showing the variation of the frequency parameter $\lambda n_l = [\rho A\omega_n^2/EI]^{1/4}$ as a function of non-dimensional root stiffness $K_L l^3/EI$ and $K_R l/EI$ for the fundamental mode.

It is evident that on account of the consideration of shear and rotatory inertia, the roots of equation (7.2.11) are dependent on the length-to-depth ratio and the cross-sectional shape of the beam, so that $\lambda_n l$ becomes a function of several dimensionless parameters such as Z_L, Z_R, Z_S, l/h, E/kG. The results in Tables 7.2.1 and 7.2.2 pertain to a square sectioned beam having the following characteristics:

$b = h = 1$; $k = 2/3$; $\rho = 1$; $l/h = 5$; $\rho A/EI = 1$; $E/kG = 4$.

For a specific example, we consider a uniform cantilever beam previously studied by **Rissone** and **Williams** (1965), and **McBain** and **Genin**

(1973). The beam is of hot-rolled stainless steel *EN56A* with the following material properties as given by Rissone and Williams followed in each case by the SI equivalents used in this numerical investigation in parenthesis.

E	$3.05\text{x}10^7 lbf/in^2$	(210.29GN/m^2)
G	$11.9\text{x}10^6 lbf/in^2$	(82.051GN/m^2)
ρ	$0.279 lbm/in^3$	(7722.5kg/m^3)
l	$6.0 in$	(0.1524m)
h	$1.0 in$	(0.0254m)
b	$0.183 in$	(0.004682m)
k	0.851	(dimensionless)

An estimate for Z_R for such a beam was given by MacBain and Genin as $2.267l/h$, in which reference it was also pointed out that Z_S (and hence Z_L) could empirically be taken as an integral multiple of Z_R, the limits of the multiplier being unity and infinity. They furthermore observed that for many practical systems, Z_S would be sufficiently large for its effects to be ignored. In the absence of any analytically derived estimates for Z_L, we have taken $Z_L \to \infty$ in the numerical case study. It is evident from the results in Table (7.2.3) that equation (7.2.11) yields the most accurate theoretical prediction of the natural frequencies.

7.3 The Natural Frequencies of Systems with Resilient Roots

7.3.1 Lumped Parameter Model

It was pointed out in Section 7.2 that several theoretical studies have been conducted on the effect of support resilience on the natural frequencies and mode-shapes of 'cantilevered' structures. In the previously published approximate results of other workers, as well as in the 'exact' treatment of the preceeding Section, a fundamental assumption is that one could, reasonably accurately, estimate the root stiffness parameters K_R and K_L for a given system so that by taking those estimated values into account in either of equations (7.2.3) or (7.2.11) we may attain a more acccurate value for the desired resonant frequency.

In many bladed disc assemblies, however, it is not an easy matter to derive values for the stiffness parameters K_R and K_L. In this Section, a new procedure is developed whereby the 'true' cantilever frequencies of each individual blade may be determined without the need for estimating the disc stiffness parameter.

Physical Model of a Compressor Rotor

Figure 7.3.1 shows a simple but representative model of a single stage axial compressor rotor. Each blade is modelled as two lumped masses interconnected by springs - the springs representing the flexural rigidity of the blades. The flexibility of the disc is similarly represented by a series of springs arranged in a closed circuit, as discussed in Chapter 2.

Consider an arbitrarily selected ith blade from the rotor stage. Let us assume that the rotor is set in motion by either a force momentarily applied, so that the system undergoes free vibration, or is otherwise subject to steady-state forcing applied at the root of the blade under observation or, if desired, at any other location on the rotor *except* anywhere along the free length of the blade whose natural cantilever frequency is desired.

In view of the foregoing asumptions, we may write the following equation of motion for the ith blade:

$$m_i\ddot{x}_i + k_i(x_i - y_i) = 0 \tag{7.3.1}$$

$$M_i\ddot{y}_i + k_i(y_i - x_i) + K_i(y_i - z_i) = 0 \tag{7.3.2}$$

From equations (7.3.1) and (7.3.2), we obtain (assuming sinusoidal oscillations at a circular frequency ω,

$$x_i = X_i e^{j\omega t}$$
$$y_i = Y_i e^{j\omega t}$$
$$z_i = Z_i e^{j\omega t}$$

$$(k_i - \omega^2 m_i)X_i = k_i Y_i \tag{7.3.3}$$

$$(k_i + K_i - \omega^2 M_i) = k_i X_i + K_i Z_i \tag{7.3.4}$$

Eliminating Y_i from (7.3.3) and (7.3.4) yields:

$$X_i[(k_i - \omega^2 m_i)(k_i + K_i - \omega^2 M_i - k_i^2] = k_i K_i Z_i \tag{7.3.5}$$

Let μ_i represent the ratio of the ith blade tip displacement relative to its root displacement

$$\mu_i = X_i/Z_i \tag{7.3.6}$$

Thus, we may write (7.3.5) and (7.3.6) as

$$\mu_i(\omega) = \frac{k_i K_i}{(k_i - \omega^2 m_i)(k_i + K_i - \omega^2 M_i) - k_i} \tag{7.3.7}$$

If we observe the variation of $|\mu_i|$ in equation (7.3.7) with the excitation frequency, ω, $|\mu_i|$ reaches an infinte peak when the denominator of equation (7.3.7) goes to zero, since $k_i K_i$ is a constant and cannot tend to the infinite due to a variation in the value of ω. Thus, the condition that $|\mu_i|$ attain a large local peak value is given by

$$(k_i - \omega^2 m_i)(k_i + K_i - \omega^2 M_i) - k_i = 0 \tag{7.3.8}$$

which is the frequency equation of a two-degree-of-freedom model of a cantilever as shown below, upon dropping the subscript i in equation (7.3.7)

By taking the ratio $|\mu_i|$, therefore, we have obtained the frequency equation whose elements are parameters of the ith blade only, and are *independent* of the values of M_D, K_D, K_G (which are the disc properties) or the parameters of all other blades on the stage.

7.3.2 Receptance Model

A more accurate theoretical representation of a mistuned compressor rotor than the lumped parameter model employed in §7.3.1 is shown in Figure 7.3.2. In this latter model, the disc is represented by a circularly profiled plate, while the blades are modelled as uniform prismatic beams of rectangular cross section.

Free-body Dynamic Analysis of the Blade

Since the dynamic behaviour of the *blades* is of primary interest here, an elaborate mathematical treatment of the disc is not necessary in this context. It is sufficient here that the interaction which occurs between the blade root and the disc rim is accounted for through linear and rotational restraining springs, in the manner previously depicted (Figure 7.2.1); the figure represents an arbitrarily selected blade mounted on the rotor.

Consider the in-plane vibration of the blade as shown in Figure 7.2.1. We shall apply the principles of receptance coupling. The coordinates associated with the blades are 1, 2, 3, 4 (see Figure 7.3.2), while the disc coordinates, in so far as the disc interacts with the ith blade's root, are 3, 4. Let the receptance of the blade subsystem be represented by α, while β denotes the receptance of the remainder of the whole system external to the blade under consideration, i.e. the disc and all the other blades. We may, therefore, write the following matrices, elements of which will remain undefined for the time being.

$$[\alpha] = \begin{bmatrix} \alpha_{11} & \alpha_{12} & \alpha_{13} & \alpha_{14} \\ & \alpha_{22} & \alpha_{23} & \alpha_{24} \\ & & \alpha_{33} & \alpha_{34} \\ \text{symmetric} & & & \alpha_{44} \end{bmatrix} \qquad [\beta] = \begin{bmatrix} \beta_{33} & \beta_{34} \\ & \beta_{44} \end{bmatrix} \tag{7.3.12}$$

In order that we may apply the receptance coupling procedure, it is required to invert α and β, so as to yield the dynamic stiffness matrices of

the two sub-systems, thus:

$$[k] = [\alpha]^{-1} = \begin{bmatrix} k_{11} & k_{12} & k_{13} & k_{14} \\ & k_{22} & k_{23} & k_{24} \\ & & k_{33} & k_{34} \\ & & & k_{44} \end{bmatrix} \qquad [s] = [\beta]^{-1} = \begin{bmatrix} s_{33} & s_{34} \\ & s_{44} \end{bmatrix} \tag{7.3.13}$$

where, as we know from the principles of reciprocity, the receptance and dynamic stiffness matrices in equations 7.3.12 and 7.3.13 are symmetric.

The combined dynamic stiffness equation of the bladed rotor, with respect to the ith blade under consideration here, is given by

$$\mathbf{f} = \mathbf{Zx} \tag{7.3.14}$$

$$\begin{Bmatrix} f_1 \\ f_2 \\ f_3 \\ f_4 \end{Bmatrix} = \begin{bmatrix} k_{11} & k_{12} & k_{13} & k_{14} \\ & k_{22} & k_{23} & k_{24} \\ & & k_{33}+s_{33} & k_{34}+s_{34} \\ & & & k_{44}+s_{44} \end{bmatrix} \begin{Bmatrix} x_1 \\ x_2 \\ x_3 \\ x_4 \end{Bmatrix} \tag{7.3.15}$$

Boundary Conditions

Equations (7.3.15) define the motions of the ith blade when it is coupled to the disc, along with all other blades. If the bladed disc system as a whole is subjected to free vibration, or else set into motion in such a way that the ith blade, whose dynamic behaviour is under investigation, is not subjected to any steady state forcing along its length, then the forces f_1 and f_2 must be made to vanish in equation (7.3.15) Furthermore, if the wheel is built in such a way that it has a thickened rim, or is otherwise additionally stiffened at the rim, then s_{44} in such a system is, generally, very large, so that x_{44} may be assumed to be negligible.

Taking cognizance of the foregoing assumptions, we may re-write equation (7.3.15) as follows:

$$\begin{Bmatrix} 0 \\ 0 \\ f_3 \\ f_4 \end{Bmatrix} = \begin{bmatrix} k_{11} & k_{12} & k_{13} & 0 \\ k_{21} & k_{22} & k_{23} & 0 \\ k_{31} & k_{32} & k_{33}+s_{33} & 0 \\ 0 & 0 & 0 & s_{44} \end{bmatrix} \begin{Bmatrix} X_1 \\ X_2 \\ X_3 \\ 0 \end{Bmatrix} \tag{7.3.16}$$

where s_{44} is assumed to be so large that elements in column 4 and row 4 of **Z** are relatively negligible.

Expanding equation (7.3.16) and using the following amplitude ratio symbols,

$$\mu = X_1/X_3 \tag{7.3.17}$$

$$\gamma = X_2/X_3 \tag{7.3.18}$$

we obtain

$$\mu k_{11} + \gamma k_{12} = -k_{13} \tag{7.3.19}$$

$$\mu k_{21} + \gamma k_{22} = -k_{23} \tag{7.3.20}$$

$$\mu k_{31} + \gamma k_{32} = F_3/X_3 - (k_{33}+s_{33}) \tag{7.3.21}$$

Eliminating γ from equations (7.3.19) and (7.3.20), we get

$$\mu = \frac{X_1}{X_3} = \frac{k_{12}k_{23} - k_{13}k_{22}}{k_{11}k_{22} - k_{12}k_{21}} \tag{7.3.22}$$

and we notice, in equation (7.3.22) that all the dynamic properties relating to the disc and all other blades have vanished. The amplitude ratio, μ, is now a function of the dynamic stiffness properties relating to the ith blade only, and is *independent* of all other subsystems externally coupled to it. However, if we were to solve for X_1, X_2, or X_3 individually in equations (7.3.19) and (7.3.20) the solution will necessarily, incoporate s_{33} from equation (7.3.21), which is a property of the whole system - the disc and all other blades. In other words, if we solve for the three unknowns individually, we must use all the three equations (7.3.19) to (7.3.21), whereas if we solve for the amplitude ratios we need use only *two* of these equations. Hence, using two of the equations, we obtain a result which is *independent* of s_{33}.

Frequency Equation

A consideration of the way in which μ varies, in equation (7.3.22), with the excitation frequency, ω, reveals that the amplitude ratio reaches an infinite value when the denominator vanishes, i.e. when

$$k_{11}k_{22} - k_{12}k_{21} \tag{7.3.23}$$

On account of the symmetric nature of the dynamic stiffness matrix,

$k_{ij} = k_{ji}$, and equation (7.3.23) may be written as

$$k_{12}k_{22} - k_{12}^2 = 0 \tag{7.3.24}$$

Elements of the dynamic stiffness matrices for the flexural vibrations of unform beams of rectangular cross-section are available in many texts. For the Bernoulli-Euler analysis, the relevant expressions are

$$\begin{aligned} k_{11} &= -EI\lambda^3 F_6/F_3 \\ k_{12} &= EI\lambda^2 F_1/F_3 \\ k_{22} &= EI\lambda F_5/F_3 \\ k_{13} &= EI\lambda^3 F_7/F_3 \\ k_{23} &= -EI\lambda^2 F_{10}/F_3 \end{aligned} \tag{7.3.25}$$

where, in equations (7.3.25), $F_i(i=1,3,5,6,7,10)$ are the frequency functions tabulated by **Bishop** and **Johnson** (1960):

$$\begin{aligned} F_1 &= \sin\lambda l \sinh\lambda \\ F_3 &= \cos\lambda l \cosh l\lambda l - 1 \\ F_5 &= \cos\lambda l \sinh\lambda l - \sin\lambda l \cosh\lambda l \\ F_6 &= \cos\lambda l \sinh\lambda l + \sin\lambda l \cosh\lambda l \\ F_7 &= \sin\lambda l + \sinh\lambda l \\ F_{10} &= \cos\lambda l - \cosh\lambda l \end{aligned} \tag{7.3.26}$$

After some algebra, equation (7.3.22) simplifies to

$$\mu = \frac{\cos\lambda l + \cosh\lambda l}{\cos\lambda l \cosh\lambda l + 1} \tag{7.3.26}$$

and the condition that the amplitude ratio, μ tends to the infinite is, therefore, given by

$$\cos\lambda l \cos\lambda l + 1 = 0 \tag{7.3.28}$$

which is the well-known frequency equation of an *encastré* beam.

Numerical Implementation

In order to verify the foregoing, the dynamic response of a flexibly mounted cantilever beam shown in Figure 7.2.1 was investigated numerically on a CDC Cyber 174 computer. The values of the linear and rotational root springs used in the computation are as follows.

Test #	value of K_L (N/m)	value of K_R
1	0	∞
2	10^3	∞
3	10^6	∞
4	10^9	∞

The blade itself, treated as a Timoshenko beam, has the following characteristics

material = stainless steel
length = 0.6096mm (24") (½" x ½")
area of cross section = $1.6129 \times 10^{-4} m^2$
second moment of area = $5.4197 \times 10^{-10} m^4$
density = $7811 kg/m^3$
elastic modulus = $1.5306 \times 10^{11} N/m^2$
shear modulus = $5.887 \times 10^9 N/m^2$

length = 24"
breadth = ½"
depth = ½"

Results of the computer studies are summarised in Figure 7.3.3, which shows the responses of the beam when the linear restraining springs are set at

$$K_L=0,\ K_L=10^6,\ \text{and}\ K_L=10^9.$$

It may be observed from the figure that whereas the tip displacement, X_t traces out a different curve each time a new value is used for K_L (as shown by the three dotted curves), the amplitude ratio μ on the other hand follows the same pattern of variation with ω (the solid curve), no matter the value assigned to K_L, in the range $0 \leq K_L \leq \infty$. Thus, provided that the rotational coordinate at blade root is effectively grounded, μ always reaches a peak at the true cantilever frequencies, whereas under the same conditions, the tip displacement by itself does not indicate the true resonances.

7.4 Experiment

Two sets of experiment were conducted in order to verify the practical validity of the preceeding theoretical considerations. In the first test, a cantilever beam of uniform, rectangular cross-section was used, whilst the second test was carried out on a more realistic model of a turbine blade,havinga tapered aerofoil section and pre-twisted profile. Results from both tests show that a better estimate of cantilever frequencies is obtained by measuring the ratio of the tip and root displacements, rather than from either parameter considered alone.

7.4.1 Stepped Cantilever Beam

Figure 7.4.1. shows a two-stage stepped cantilever beam. Either segment of the beam is of uniform rectangular cross section. This type of stepped beam is one way of modelling a blade (the upper segment of the stepped beam) which is connected to other components, represented by the lower segment. Evidently, there is some coupling of the motion between the lower and upper segments of the beam. For descriptive purposes, it is convenient to refer to the upper, slender part of the beam as the 'blade section', while the lower segment will be termed the 'root section'.

During the experiment, a sinusoidal excitation was applied at a point on the root section, while the frequency of excitation was slowly swept through the range $10\text{Hz} \leq \omega \leq 1\text{kHz}$. The displacements X_t, X_r were measured relative to the impressed force, at each frequency. Certain parts of the clamping device employed in securing an adequately stiffened root were seen to resonate vigorously at several excitation frequencies during the test. This is reflected in the response curve, shown in Figure 7.4.2, where it is seen that the signals picked up by transducers mounted at blade tip and root indicate many 'resonances'. However, the ratio of tip and root displacement amplitudes reveals only two resonant peaks, one near 60Hz and the other at about 380Hz. From the elementary theory of transverse beam vibration, the two lowest cantilever frequencies of the 'blade section' of the stepped beam are 63.25Hz and 395.5Hz. Clearly, a better estimate of the actual cantilever frequencies of the 'blade section' has been obtained in this test from the ratio curve, in contrast to the separate response curves which lead us to deduce quite a few other resonances, most of which are due to the vibration of the table and clamping devices and not of the 'blade section'.

7.4.2 Twisted Turbine Blade

For the second test, a twisted steam turbine blade of aerofoil section and pre-twisted contour was rested on a soft foam - to simulate free suspension. In order to ensure the mandatory conditions of small rotational displacements at root as required in the theory, a heavy block of steel was glued to the base of the turbine blade, as shown in Figure 7.4.3. Excitation was applied outside the length of the blade proper, at a point on the block affixed to the root. Tip and root response X_t and X_r, were measured by

accelerometers located as shown in the illustration. The respective acceleration signals are displayed, after conversion to the *cross receptance* format, as a function of the forcing frequency in Figure 7.4.4 and 7.4.5. More results, processed to yield the tip and root displacements as well as their ratio, are shown in Figures 7.4.6, where all the three parameters are plotted on the same graphs. It is seen from Figure 7.4.6a that whereas the individual responses indicate that a resonance occurs around 645Hz, the predicted frequency from the ratio curve is, in fact, at 703Hz - which is an anti-resonace in the root displacement curve.

In figure 7.4.6b, the peak of the ratio curve is at 762Hz, which is also the value observable on the tip displacement curve. However, the only peak in the root trace within the frequency range depicted is at 772Hz. It may be noted that the amplitude ratio attains a peak value at

(*i*) some *anti-resonant* frequencies of the *root* response, when the denominator of the ratio tends towards zero, as at 703Hz in Figure 7.4.6a.

(*ii*) some *resonant* frequencies of the *tip* response, e.g at 760Hz in figure 7.4.6b, when the numerator becomes extremely large.

It may be fallaciously deduced from the foregoing that true cantilever frequencies could be obtained merely by locating the anti-resonances of the root response, or the resonaces in the tip response curve, without the calculation of any ratio. That such an approach is prone to error may be verified from Figure 7.4.6c; anti-resonances occur *simultaneously* on the separate response curves, so that their ratio does not become infinite, at about 816Hz. Similarly, at 820Hz, both the tip and root responses attain a local maximum, and hence the amplitude ratio is not very large. Unless the amplitude ratio is computed and displayed as a function of the excitation frequency, we cannot derive the correct frequencies from the observation of resonances or anti-resonances in only one displacement curve.

7.5 Concluding Remarks

Turbomachine blades mounted on a rotor stage, especially those with complex root fixures have substantial flexibility at their root. The natural frequencies of such flexibly mounted cantilever systems are very much influenced by the resilience at the blade root. The resonant frequencies usually perceived from conventional tests are based on the observation of peaks in the displacement response, measured at an arbitrary location along

the blade span, are not those actually desired. A method has been proposed for defeating the influence exercised by subsytems external to the blade, upon that blade's resonant frequencies. The method is based on the calculation of the amplitude ratio of tip and root displacements. Theoretical modelling as well experimental results have been given, and these support the opinion advanced here that the frequencies deduced from amplitude ratios are usually closer to the desired cantilever frequencies than those obtained from a single displacement curve. Accuracy is generally improved if the root is restrained against *rotational* movement during the test.

Fig. 7.2.1 *Mathematical model of a cantilever with restraining root springs*

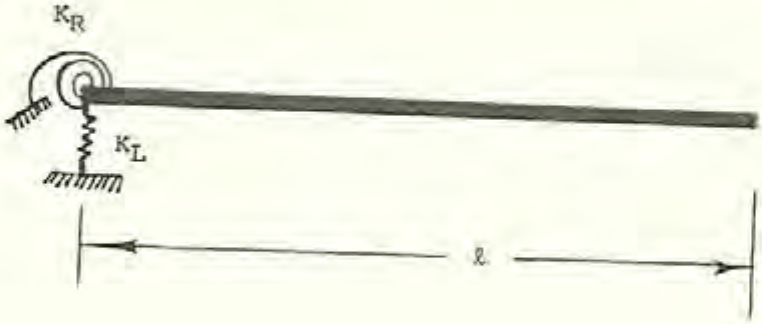

Fig. 7.2.2 *Variation of dimensioless frequency with root resilence*

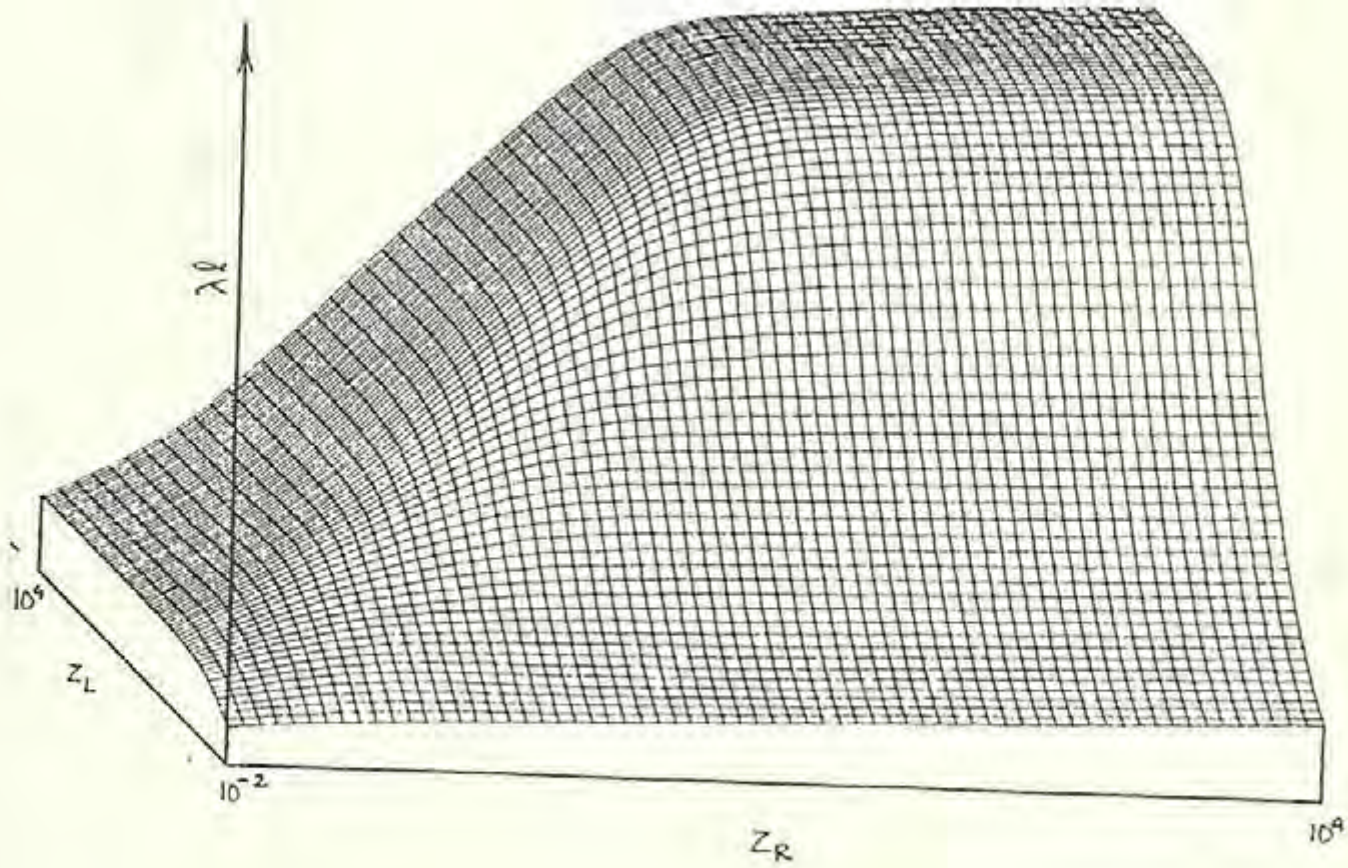

Fig. 7.3.1 *Physical model of a compressor rotor* (lumped parameter analysis)

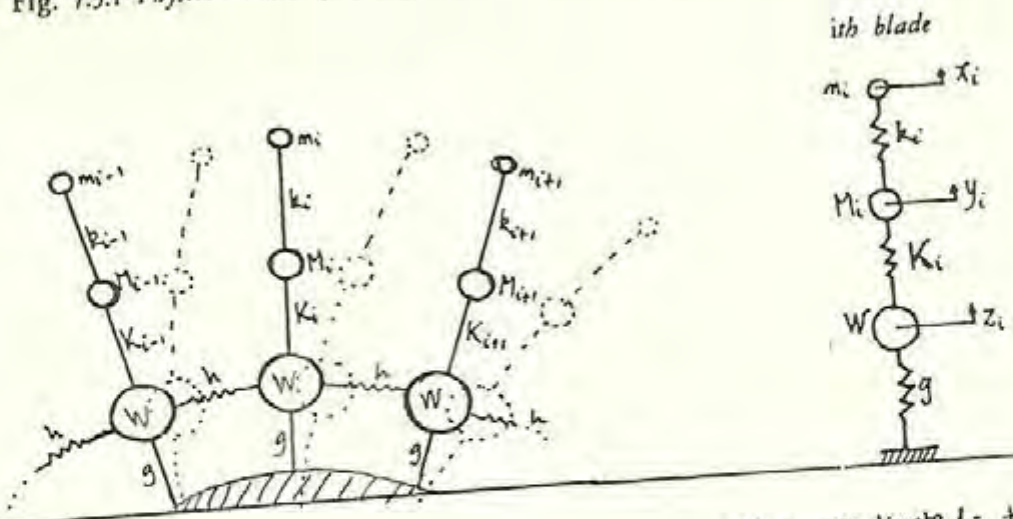

X_t : coordinate 1 = transverse tip displ.
θ_t : coordinate 2 = rotational tip "
X_r : coordinate 3 = transverse root "
θ_r : coordinate 4 = rotational root "

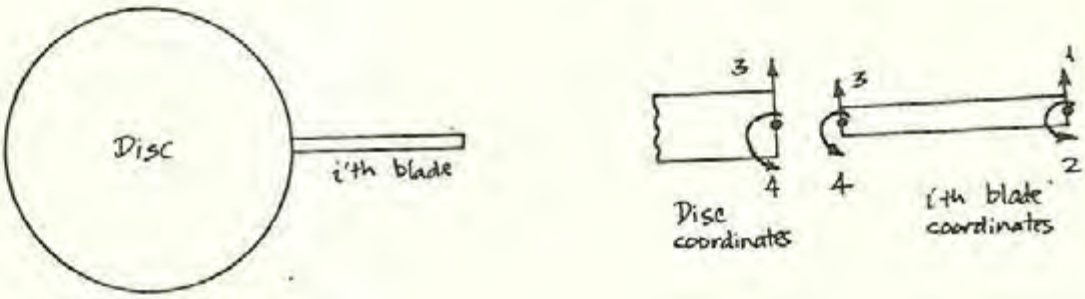

Fig 7.3.2 Physical model of a compressor rotor (Continuum Analysis)

Fig. 7.3.3 *Frequency response of a flexibly mounted cantilever beam*

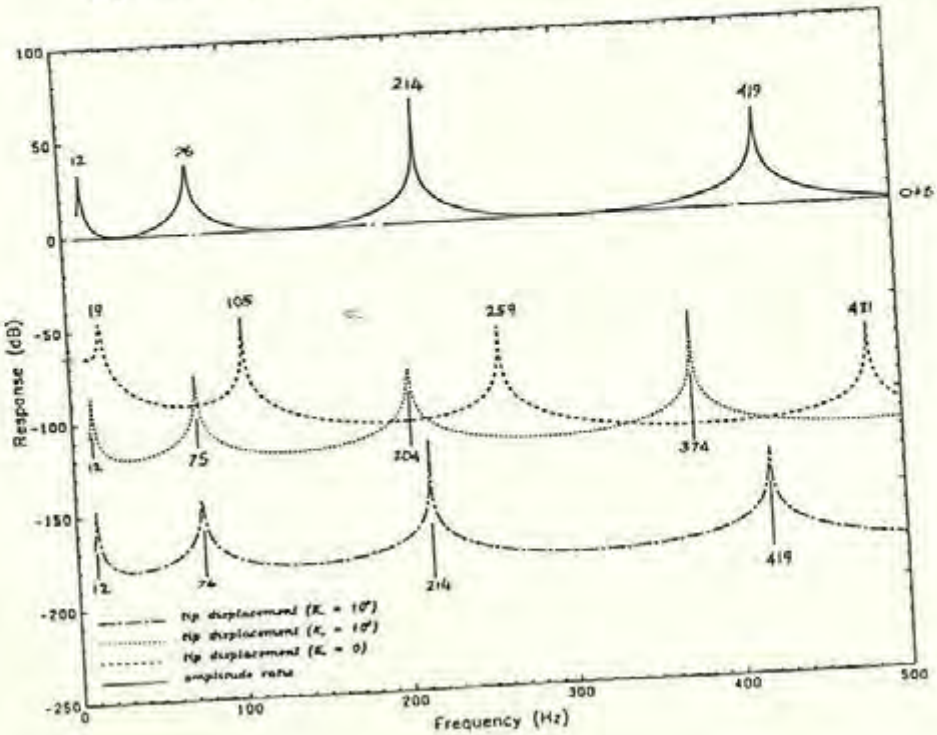

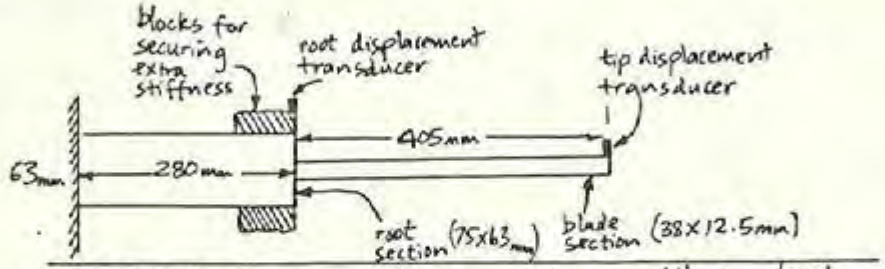

Fig 7.4.1 Experimental set-up for cantilever test

Fig. 7.4.2 *Frequency response of a stepped cantilever beam with stiffened joint*

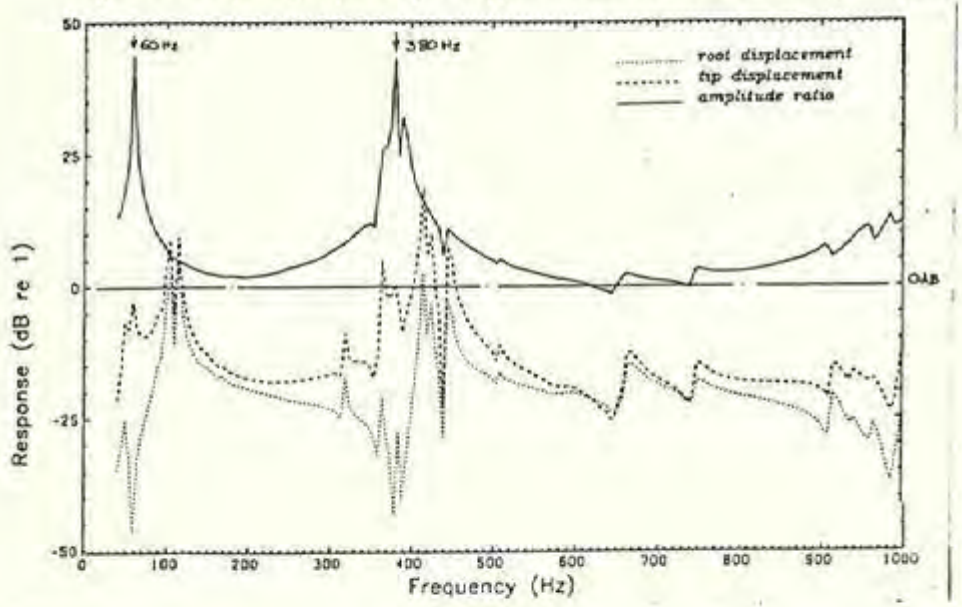

Fig. 7.4.3 *Schematic illustration of experimetal layout*

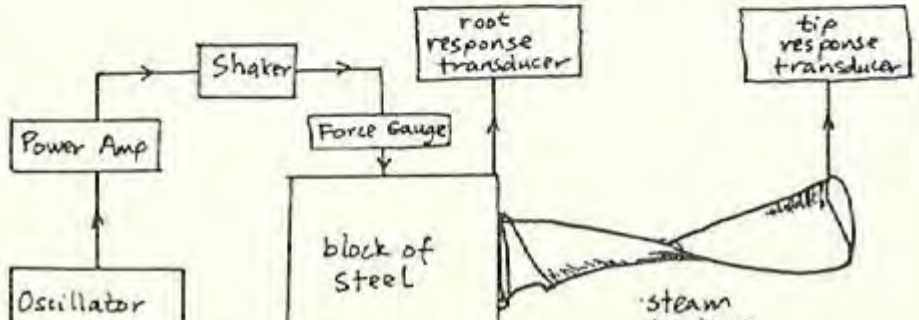

Fig. 7.4.4 *Tip response of a steam turbine blade*

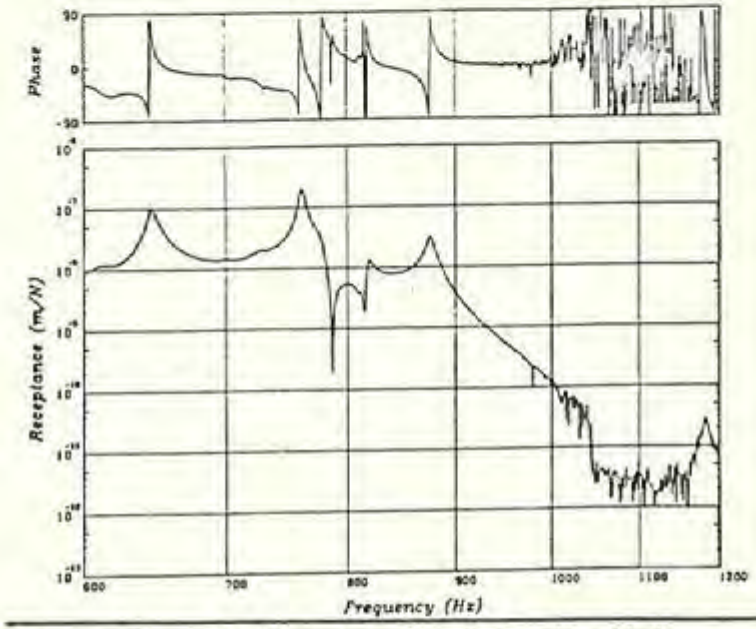

Fig. 7.4.5 *Root respose of a steam turbine blade*

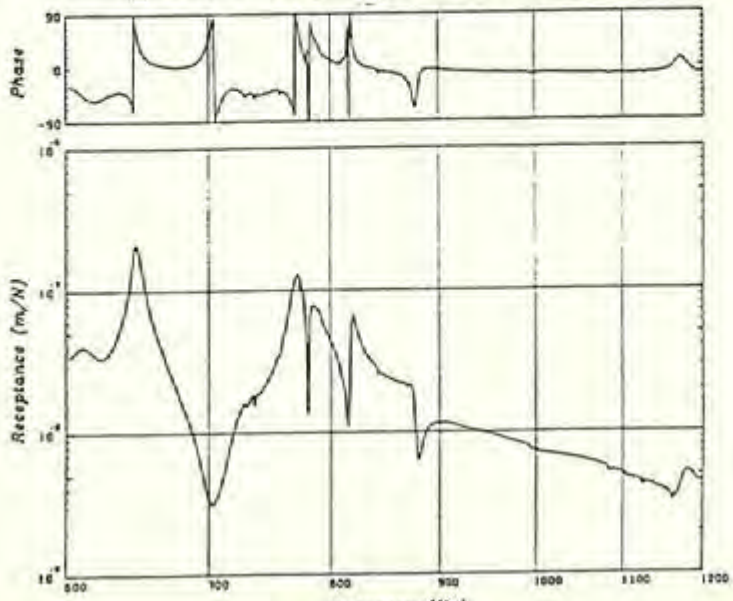

Fig. 7.4.6 *Amplitude ratio of a steam turbine blade*

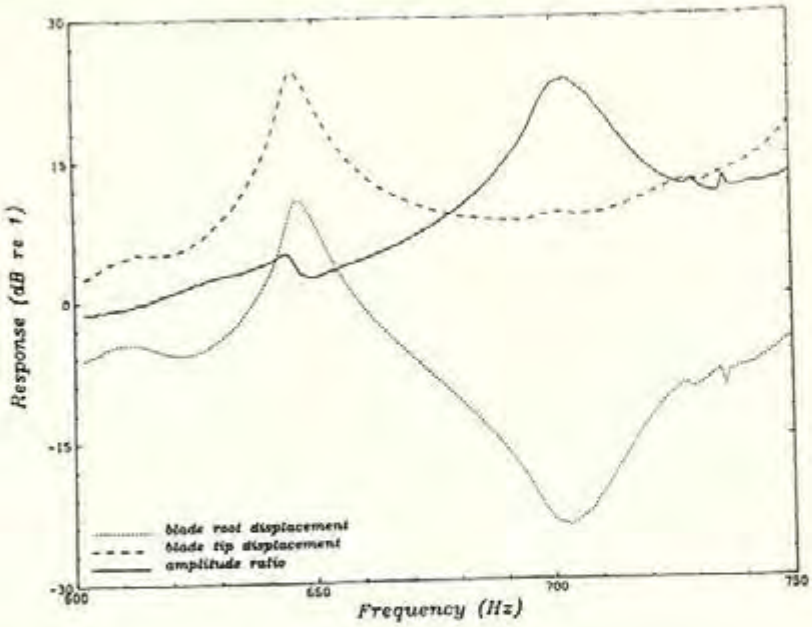

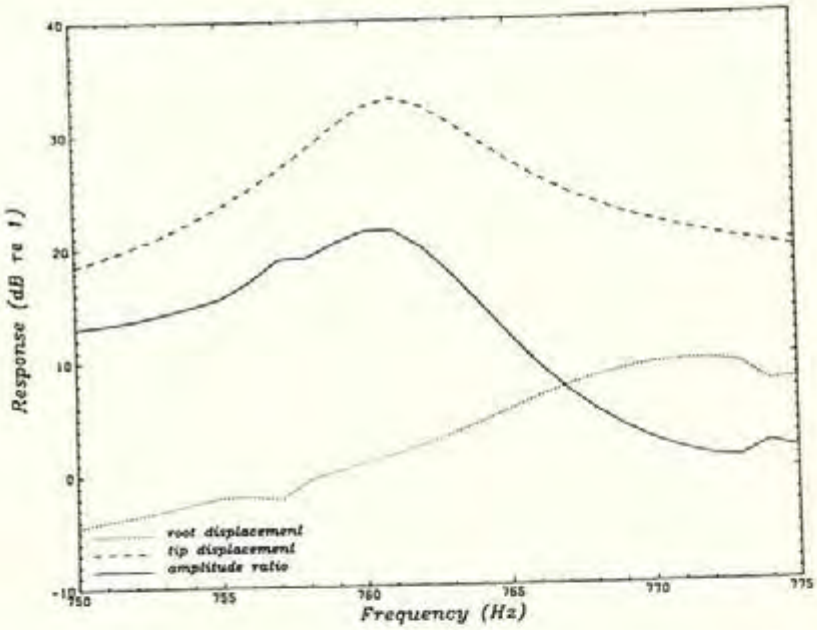

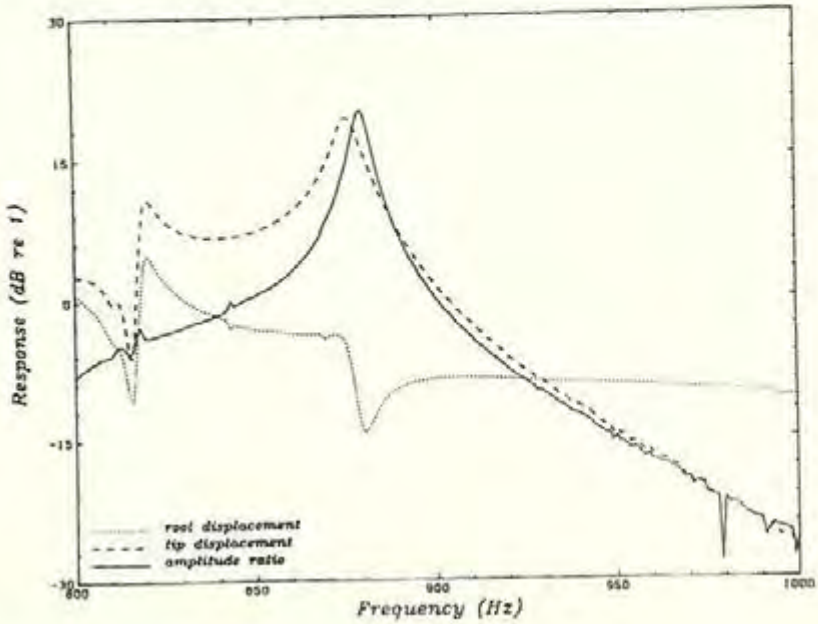

Table 7.2.1 *Variation of λ with Z_R and Z_L for a classical beam*

MODE 1

Z_L \ Z_R	0	0.01	0.1	1	10	100	1000	10000	∞
0	0	0	0	0	0	0	0	0	0
0.01	0	.297992	.314227	.315991	.316168	.316186	.316188	.316188	.316188
0.1	0	.394250	.529359	.558157	.561288	.561603	.561635	.561638	.561638
1.0	0	.413616	.698245	.931611	.981460	.986917	.987467	.987522	.987528
10	0	.415701	.731779	1.195670	1.507035	1.569480	1.576304	1.576994	1.577071
100	0	.415911	.735379	1.242448	1.698027	1.832736	1.837922	1.839475	1.839648
1000	0	.415932	.735743	1.247368	1.720254	1.853372	1.869694	1.871365	1.871551
10000	0	.415934	.735778	1.247862	1.722493	1.854445	1.872880	1.874561	1.874749
∞	0	.415934	.735782	1.247917	1.722742	1.856787	1.873233	1.874917	1.875104

MODE 2

Z_L \ Z_R	0	0.01	0.1	1	10	100	1000	10000	∞
0	0	.508021	1.037125	1.718881	2.234921	2.350326	2.363531	2.364871	2.365020
0.01	.447203	.623990	1.043705	1.720136	2.235315	2.350617	2.363812	2.365151	2.365300
0.1	.795081	.838528	1.101487	1.731420	2.238864	2.353239	2.366339	2.367668	2.367816
1.0	1.410844	1.418276	1.481058	1.841351	2.274598	2.379709	2.391062	2.393096	2.393234
10	2.454761	2.455427	2.461235	2.505060	2.606356	2.643005	2.647710	2.648185	2.648238
100	3.606129	3.606525	3.610015	3.638625	3.728452	3.774507	3.781057	3.781740	3.781816
1000	3.894379	3.895485	3.905285	3.990078	4.321452	4.544126	4.579567	4.583319	4.583739
10000	3.923399	3.924592	3.935167	4.027051	4.391768	4.639302	4.678700	4.682859	4.683324
∞	3.926602	3.927805	3.938466	4.031139	4.399523	4.649726	4.689424	4.693622	4.694091

MODE 3

Z_L \ Z_R	0	0.01	0.1	1	10	100	1000	10000	∞
0	4.730041	4.732076	4.749948	4.892770	5.294379	5.471498	5.495096	5.497532	5.497804
0.01	4.730135	4.732171	4.750041	4.892851	5.294425	5.471530	5.495126	5.497563	5.497834
0.1	4.730906	4.733020	4.750878	4.893579	5.294841	5.471821	5.495402	5.497837	5.498108
1.0	4.739521	4.741540	4.759266	4.900873	5.299003	5.474737	5.498163	5.500582	5.500852
10	4.827158	4.829012	4.845284	4.975098	5.341051	5.504244	5.526115	5.528375	5.528627
100	5.620752	5.629164	5.632794	5.663001	5.763221	5.817799	5.825731	5.826561	5.826653
1000	6.877299	6.877715	6.881421	6.915229	7.086500	7.254936	7.287519	7.291081	7.291480
10000	7.050790	7.051469	7.057537	7.113627	7.416630	7.735002	7.797396	7.804196	7.804959
∞	7.068503	7.069291	7.075616	7.134132	7.451057	7.782671	7.846972	7.853973	7.854757

Table 7.2.2 *Variation of λ with Z_R and Z_L for a Timoshenko beam*

Z_L \ Z_R	0	0.01	0.1	1	10	100	1000	10000
0	0	0	0	0	0	0	0	0
0.01	0	.297980	.314226	.315990	.316168	.316185	.316187	.316187
0.1	0	.394088	.529326	.558141	.561272	.561588	.561619	.561623
1.0	0	.413365	.697904	.931344	.981171	.986645	.987195	.987250
10	0	.415439	.731269	1.194295	1.504894	1.566072	1.572841	1.573525
100	0	.415647	.734848	1.240672	1.692232	1.814891	1.829790	1.831313
1000	0	.415668	.735208	1.245546	1.714054	1.844863	1.860960	1.862497
10000	0	.415670	.735244	1.246035	1.716251	1.847869	1.863975	1.865623
∞	0	.415670	.735248	1.246089	1.716495	1.848204	1.864321	1.865970

Table 7.2.3 *Natural frequencies of a cantilever with root flexibilty*

	Experimental natural frequency Ω Hz [Ref 104]	Theoretical Prediction, ω Hz ($Z_L = \infty$)		
		[Ref 104] ($Z_R = \infty$)	[Ref 90] ($Z_R = 13.602$)	[Present study] ($Z_R = 13.602$)
Mode 1	803	926	810	796
% error: $\left\lvert \frac{\omega - \Omega}{\Omega} \right\rvert$	–	(15.3%)	(0.9%)	(0.9%)
Mode 2	4598	5818	5200	4675
% error	–	(26.5%)	(13.1%)	1.7%

Chapter 8

8.1 Introduction

Efforts have been devoted in the earlier parts of this thesis, in chapters 2 to 6 inclusive, to seeking a better understanding of the vibration characteristics of bladed disc assemblies. It was found, as reported in detail in those chapters, that the frequency spectrum of a vibrating bladed wheel could be divided into critical and non-critical zones, and that certain blades were likely to become *rogue* at the critical resonances. Such rogue blades were usually those with extreme detune in their cantilever frequencies.

However it is not always an easy or straightforward matter to identify the blades with extreme detune from an entire batch of blades in an assembly. This is because of the influence usually exerted by the flexibility of the disc upon the measurement of blade alone frequencies, especially in assemblies of integral construction where the blades cannot be separated from the assembly for isolated testing. Therefore, in chapter 7, a procedure was developed for measuring blade cantilever frequencies more accurately than is possible with conventional testing procedures.

In the present chapter, some studies are undertaken in order to investigate if certain engine parameters which may be varied by design engineers - such as the stiffness of the disc, or the manner of arranging a given set of blades on a wheel to yield different mistuning patterns - are likely to improve, or otherwise worsen, the vibration response of the assembly. Previous investigators have reported that certain parameters of the assembly, if assigned some specially selected values, are likely to reduce the harmful influence of mistuning. For example, **Whitehead** (1966) has suggested that a smooth variation of blade cantilever frequencies around the disc is beneficial while, on the other hand, **El-Bayoumy** and **Srinivasan** (1975) have written that "smooth mistune distributions do not necessarily imply lower vibration stresses" - a dichotomy of opinion characteristic of findings on the mistuning problem.

The objective of most parametric studies is to investigate the relationship between a *parameter* and its *dependent variable* as the former is changed by several small *incrementals* in order to produce a chart or other means of demonstrating the parametric dependence. With reference to the parametric studies of bladed discs, two types of dependent variables are usually of interest to the engine designer. These are:

(*i*) the relative separation of the eigenvalues of the assembly -

usually known as *frequency splits* - since the repeated roots of tuned systems become 'split' into two distinct eigenvalues when the system is detuned;

(*ii*) the maximum stress experienced by the most highly stressed blade on the stage at the most 'dominant' system resonance, sometimes known as the *worst stress*.

Whereas it is relatively easy to define the modulus of a dependent variable in terms of stresses or eigenvalues, the specification of the magnitude of *parameters* is not always so clear-cut. Thus, although the investigator may want to examine the dependence of frequency split on the smoothness of mistuning, it is not usually easy to quantify this measure of 'smoothness' in an unambiguous manner.

Another obstacle to the implementation of an in-depth parametric study is the computation cost, since several discrete incrementals in a parameter are required, along with the computed corresponding values of dependent variables, to provide a parametric curve. One way of reducing costs is to use a simple model. Hence, although one is at liberty to use a variety of theoretical methods (receptances, lumped parameters, *etc*), it is evidently advantageous to employ the least costly - the lumped parameter method in this instance. Even so, the computational resources consumed in the course of producing a single dependent variable, using the 'simple' method, is still considerable.

Using a 30 bladed model, for example, over 2000 seconds of the Central Processor Unit (CPU) on a CDC Cyber 174 are spent in calculating the stresses on all the blades, for a given engine excitation, from which the 'worst case' is selected to produce *one* dependent variable. This amounts to approximately 30 computation 'units', as charged by the Imperial College Computer Centre. By using an optimizing compiler (FTN5), and saving the object code (LGO) to avoid subsequent compilations, it is possible to reduce the computing costs by approximately 50%. Further economy has been achieved by working at weekends, when computer units are offered at a cheaper rate, and by using a model with 10 blades, rather than 30, for some of the studies.

In view of such constraints as mentioned above, it has not been possible to carry out 'full scale' parametric studies. However, the foundations have been laid here, and these should form the basis of some future research.

8.2 Mistune Pattern

Figures 8.2.1 and 8.2.2 show two different patterns of arranging the same set of mistuned blades on wheels 30A and 30B respectively. The stress response of either wheel when vibrated by a third engine order excitation, has been calculated using the procedures described in Chapter 2. Our aim in this section is to investigate the relationship between the 'worst stress' in each case and the smoothness of the mistune pattern.

8.2.1 Measure of Smoothness

One way of measuring the smoothness of a discretely defined function is to decompose the function into its Dicrete Fourier Transform (DFT) components. Thus, if the blade cantilever frequencies, f_i, are given as a function of the angular position of the blades on the disc, θ_i, we can obtain the coefficients shown in Tables 8.2.1 and 8.2.2 for Discs 30A and 30B respectively upon applying the formula:

$$f_i = a_0 + \sum \left(a_i \cos \theta_i + b_i \sin \theta_i \right) \qquad (8.2.1)$$

The first component of the DFT, a_0, usually represents the mean value of the function, or the *dc component*, after electrical engineering usage; whilst the higher components, a_i, b_i $(i=1,N/2)$, indicate the presence or ortherwise of sharp edges in the defined function. For a perfectly tuned rotor, which represents an extremely smooth distribution, these higher coefficients are all zero, but the zero'th component, a_0, still indicates the magnitude of the mean value as before.

If we let c_i represent the modulus of the DFT coefficients, i.e.

$$c_i = \sqrt{(a_i^2 + b_i^2)}/a_0 \qquad (8.2.2)$$

then we may define a *coefficient of smoothness*, c_s, based on a summation of the moduli c_i, the standard deviation, and some appropriate weighting function.

8.2.2. Worst Stress

When the primary system resonances are well-removed from the critical ones, the largest levels of stressing are most likely to occur at the primary resonances. However, it is not always clear which of the resonances are likely to be the 'worst' for engine excitations which bring about a spectrum in which the primary resonancess are very close to the

secondary resonances.

The largest stress level which is observed through out the frequency response spectrum, on any blade, is known as the *worst stress*. Table 8.3.3 shows the relationship between the worst stress and the coefficient of smoothness for discs 30A and 30B, with that of the tuned state, 30T, as the datum of comparison for excitation by a 3Eo forcing function. Based on the information referred to above, it does not appear as if a direct link exists between the 'smoothness' of mistune, as defined in this chapter, and the 'worst stress'. This is in agreement with the conclusions reached by **Srinivasan** and **Frye**, although other workers have suggested that smoother mistuning are likely to reduce the stress levels.

8.3 Disc Stiffness

It does not appear, from a search of published research findings, that the effects of disc stiffness on the vibration of mistuned assemblies have been investigated in detail by previous workers. Previous researches on the vibration of bladed disc assemblies may be classified into three categories, as follows:

(*a*) studies in which the effects of mechanical coupling are entirely ignored, such as the earlier works of **Whitehaed** (1966). In such treatments, the coupling of the blades is attributed to purely aerodynamic forces, although each blade is assumed to possess its individual mechanical (usually, torsional stiffness) properties.

(*b*) those in which blade coupling is assumed to be due only to mechanical, i.e. purely elastic, stiffness of the disc such as the receptance models of **Ewins** (1973), or the lumped parameter methods of **Dye** and **Henry** (1969), or the influence coefficients modelling of **Srinivasan** and **Frye** (1976). Aerodynamic *damping* may be accounted for in such cases, but not aerodynamic *coupling*, through the introduction of viscous dampers at the tip of each blade.

(*c*) the third type of modelling was recently introduced by **Kielb** (1981). he considers both aeodynamic and mechanical coupling.

Only a few workers have noted, in passing, that the magnitude of stiffness coupling could have a significant influence on the vibration of mistuned bladed discs. There thus appears to be a need for carrying out some parametric studies on the probable influence of disc flexibility upon the vibration of bladed disc assemblies.

8.3.1 Effect of Disc Stiffness on Modal Properties

The eigenvalue spectrum of vibrating bladed discs is frequently of major interest to designers, in addition to the worst stress levels. For example, it may be desirable to split neighbouring eigenvalues by specified amounts, or to shape the eigenvalue spectrum in such a way as to obtain adequate safety

margins in the neighbourhood of critical speeds. One way of significantly affecting the spectrum is to alter the degree of mechanical coupling of the blades provided by the disc flexibility.

Figures 8.3.1 to 8.3.3 show the parametric dependence of spectral characteristics (*i.e.* the natural frequencies and mode shapes of free vibration) on the mechanical coupling stiffness of the disc. Three models of bladed assemblies were made. The discs have, respectively, weak, average and strong mechanical coupling stiffnesses linking the same set of blades, arranged in the same sequence, to give identical mistune patterns. The three assemblies have the following characteristics:

Figure	Disk Model #	Coupling Stiffness
8.3.1	10KB	$1.5 kN/m^2$
8.3.2	10KM	$575 kN/m^2$
8.3.3	10KY	$1.5 GN/m^2$

An examination of the spectrum of Disc 10KB, as illustrated in Figure 8.3.1, shows that all the modes in the first family are very 'pure'. Also, the eigenvalues are well separated, except for the case of repeated roots, when two are coincident as in tuned assemblies.

The eigenvalues of the second family (modes 11 to 20) are, however, severely clustered together. All modes in this region are 'critical' in that only one blade resonates at such modes while the other blades are stationary. It may be noted that the resonating blades at each of modes 11 to 20 are, respectively, blades 9, 6, 5, 4, 10, 8, 7, 1, 3, 2, which is the sequence obtained when the blades are arranged in an ascending order of their cantilever frequencies. The dominant diameter order, in the DFT histograms, is in every case the zeroth or the fifth. The foregoing observations also hold for the third family of modes.

For the assembly of moderate mechanical coupling, Disc 10KM, only one critical mode is observed in the first family; that is mode 10. The eigenvalues are well separated in the lower frequencies, while they are clustered at the upper end of the first family, and throughout the third family.

Figure 8.3.3 shows the spectrum of Disc 10KY which is an assembly with extremely stiff disc. All the modes in the first and second families are 'critical', and the system resonances are very close to the individual cantilever frequencies of the blades. Therefore, whenever a system resonance occurs, it is the blade with a cantilever frequency close to the system's frequency that resonates the greatest. With such a strong disc stiffness, each

blade vibrates more or less as an isolated cantilever, and consequently resonates whenever the excitation frequency is close to its own resonant frequency, irrespective of the motion of all other blades. Whereas the eigenvalues are very close in the first and second families, and the mode shapes are degenerate, the third family resonances have pure modes and widely spaced eigenvalues.

8.3.2 Effect of Disc Stiffness on Blade Response

The parametric study in this instance is concerned with investigating the dependence of the 'worst stress' experienced by any blade in the assembly on the mechanical stiffness coupling all the blades on the stage together. The 'worst stress' parameter is as defined in §8.2.2, while the stiffness variable is the value of h in equation (2.2.3). Thus, by keeping all other factors constant from one case to another, we can vary the value of h in order to obtain a corresponding worst stress, σ_w.

Figure 8.3.4 is a parametric curve showing the variation of σ_w with h for a 10-bladed disc which is excited by a 5EO forcing function. It may be observed from the graph that the absolutely worst case for this model occurs when the coupling stiffness is approximately $h=5\text{x}10^5\text{N/m}$. (Although it is possible to express h and σ_w in dimensionless form, it is not particularly important for our objective here to do so. We are primarily interested in finding out if, *in principle*, a variation in disc stiffness has an effect on blade response levels.) Furthermore, the parametric curve apporoaches an asymptote at its either end which means that if the disc stiffness is *too strong* or *too weak*, a small change in the stiffness does not produce any significant change in the respnose level of the worst stressed blade. In their 1976 paper, **Srinivasan** and **Frye** reported that

> *"...effects of mistuning in a rotor assembly may be reduced if the disk flexibility can be decreased"*

Clearly, the observation of Srinivasan and Frye seems to have been overgeneralized beyond their specific case, for which their report is obviously valid. It would therefore be misleading if their interpretation were to be applied to our 10-bladed disc, since an effect exactly opposite to that desired can be induced if the disc flexibility is decreased from $h=5\text{x}10^8\text{N/m}$, say, to $h=5\text{x}10^5\text{N/m}$. In fact, a reduction in the unfavourable effect of mistuning can be achieved either by decreasing or increasing the stiffness away from the worst condition of $h=5\text{x}10^5\text{N/m}$.

8.4 Concluding Remarks

By arranging a given set of thirty blades in two different random orders on identical discs, we have not been able to establish a relationship between the smoothness of mistune pattern and the level of largest global stresses. However, we have demonstrated that, in either case, it is the blade with extreme detune that experineces the largest stress at critical resonances, when other blades are generally immobile. Thus, blade 10 on Disc 30A, which becomes blade 21 in the re-arranged formation on Disc 30B, is the blade with the lowest cantilever frequency, and the largest stress at CSR as shown in Table 8.2.1.

When the mechanical stiffness of the disc is *extremely strong*, the blades are likely to behave as individual cantilevers, each of which vibrates and resonates more on its own, and less as part of an assembly. Interestingly, this also happens when the mechanical coupling through the disc is *extremely weak*. Under such conditions, the blade that is likely to become rogue is not necessarily the one with extreme detune, but the one whose cantilever frequency coincides with a system resonant frequency. This is a clarification of an observation previously made as a general case for mistuned bladed discs by other workers. For moderately stiff discs, however, it is invariably the blade with extreme detune that becomes rogue at critical frequencies.

We have observed that the spectra of wheels with very weak, or very strong, mechanical coupling have pure and well spaced modes at one end, and highly degenerate modes at the other. We also know already that when the modes are pure and well separated, stresses are generally evenly distributed amongst the blades, as in tuned systems. Hence, if we want to operate a machine in an environment where the predominant excitation is of low frequency, one could reduce the disc stiffness so as to achieve uniform stressing of the blades. Conversely, in order to avoid rogue blade failure during high frequency excitations, the stiffness of the disc should be significantly increased.

Fig. 8.2.1 *Mistune pattern for Disc 30A*

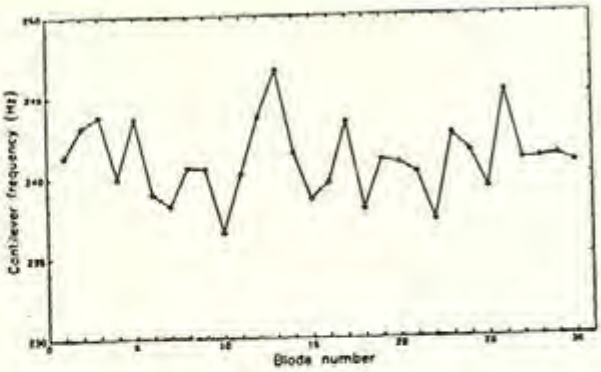

Fig. 8.2.2 *Mistune pattern for Disc 30B*

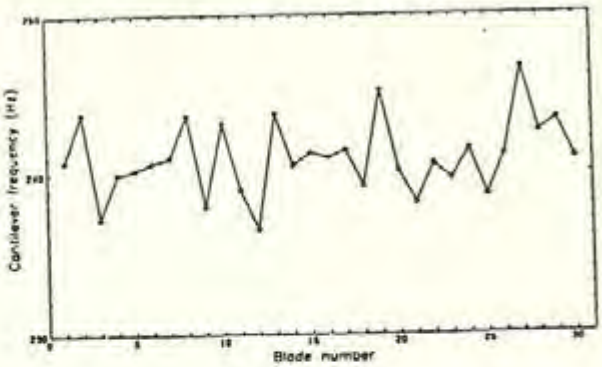

Table 8.2.1: Disc 30A Fourier Coefficients

blade number	cantilever frequency	DFT index	cosine component	sine component	normalised modulus
1	241.287	0	240.975	0	100.000
2	243.103	1	.204	-.041	.086
3	243.792	2	.355	-.320	.198
4	239.936	3	.015	.535	.227
5	243.640	4	-.394	.193	.182
6	238.966	5	.382	.043	.159
7	238.151	6	-.244	.359	.150
8	240.563	7	-.062	-.397	.167
9	240.490	8	.511	.256	.237
10	236.519	9	-.408	-.108	.175
11	240.144	10	-.461	.438	.264
12	243.712	11	-.055	.034	.027
13	246.602	12	.208	-.082	.093
14	241.455	13	.126	-.395	.172
15	238.586	14	-.236	-.193	.127
16	239.619	15	.430	.000	.178
17	243.350				
18	237.933				
19	240.979				
20	240.791				
21	240.214				
22	237.217				
23	242.558				
24	241.505				
25	239.209				
26	245.192				
27	240.914				
28	241.001				
29	241.155				
30	240.664				

Table 8.2.2 : Disc 30B Fourier Coeffi

blade number	cantilever frequency	DFT index	cosine component	sine component	normalised modulus
1	240.791	0	240.975	0	100.000
2	243.792	1	.200	-.195	.116
3	237.217	2	.240	-.284	.154
4	239.936	3	-.277	-.538	.251
5	240.214	4	-.063	-.183	.080
6	240.664	5	.124	.231	.109
7	240.979	6	-.217	.131	.105
8	243.640	7	.366	.417	.230
9	237.933	8	.239	.022	.100
10	243.103	9	-.113	-.204	.097
11	238.966	10	.334	.370	.207
12	236.519	11	-.753	.219	.325
13	243.712	12	-.210	.189	.117
14	240.490	13	.420	.275	.208
15	241.287	14	-.363	.261	.186
16	241.001	15	-.038	-.000	.016
17	241.455				
18	239.209				
19	245.192				
20	240.144				
21	238.151				
22	240.563				
23	239.619				
24	241.505				
25	238.586				
26	241.155				
27	246.602				
28	242.558				
29	243.350				
30	240.914				

Table 8.3.3. Variation of 'worst' stress amplitude with mistune smoothness, C_s.

Disc Model	C_s, coefficient of smoothness	Worst stress (GN/m^2) at Primary Resonance	Worst Stress (GN/m^2) at Secondary Resonance
30A	6.38	1.529	1.205
30B	6.19	1.496	1.401
30T	0	1.528	–

Fig. 8.3.1 *Natural frequencies and mode-shapes of vibration for Disc 10KB*

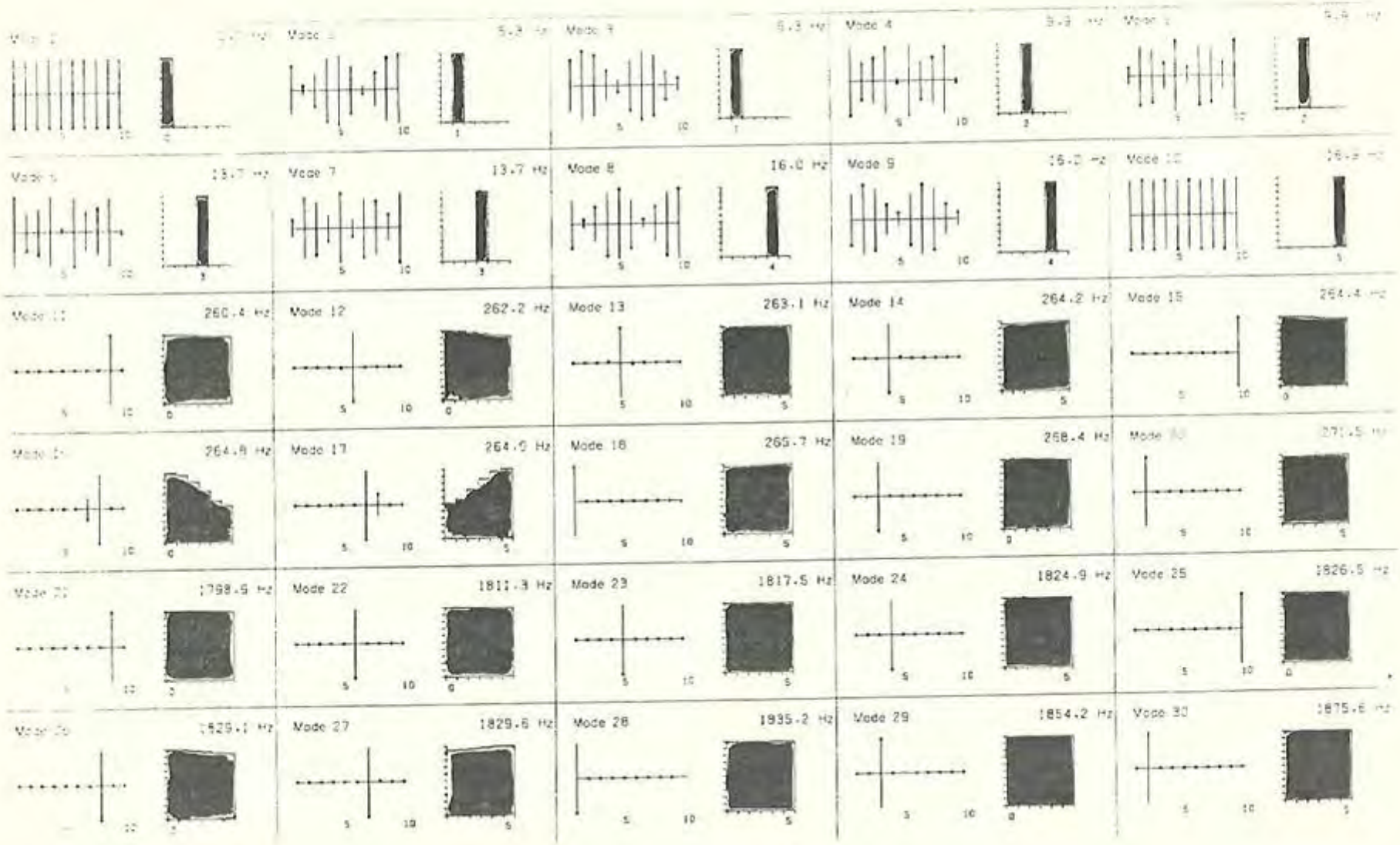

Fig. 8.3.2 *Natural frequencies and mode-shapes of vibration for Disc 10KM*

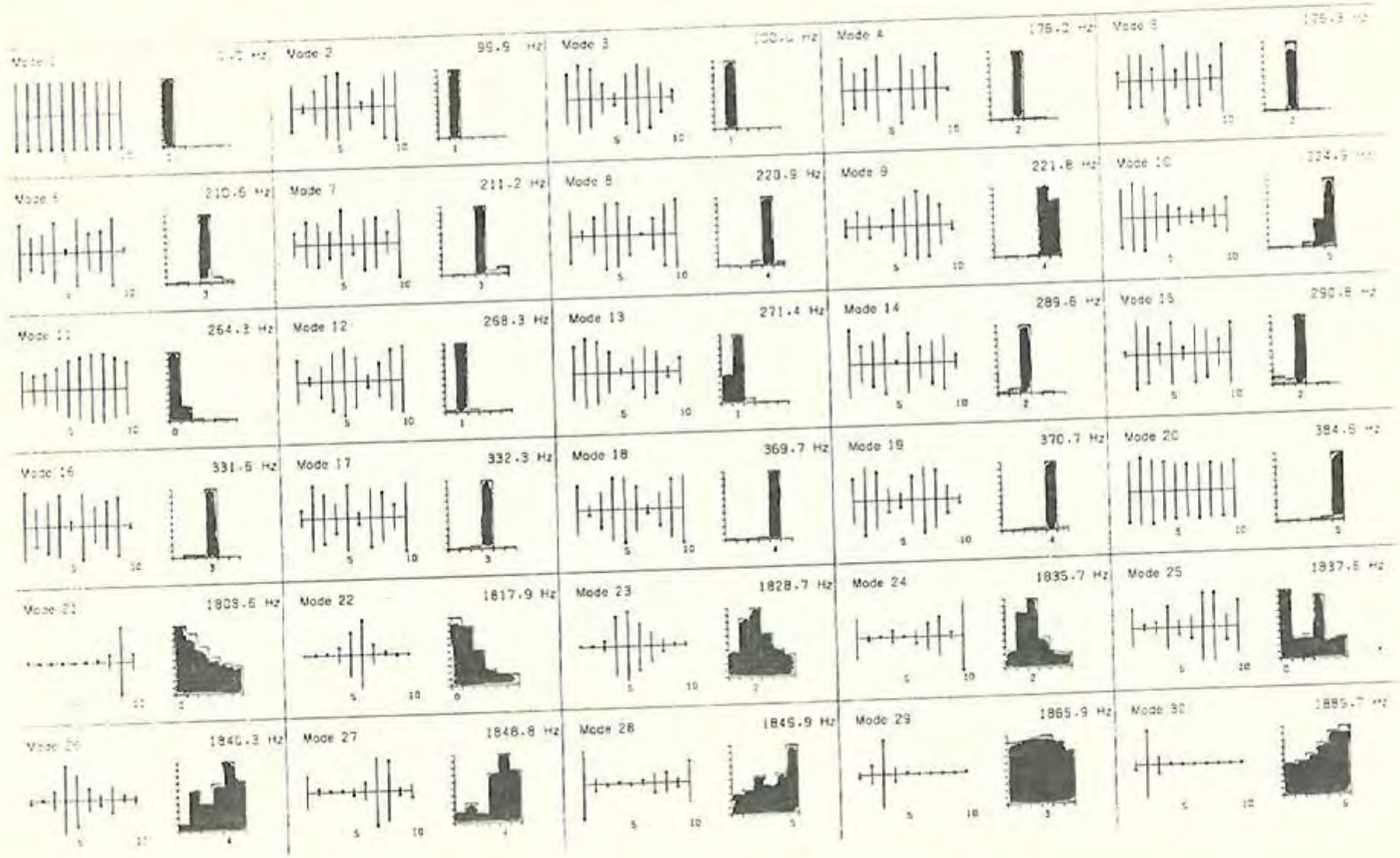

Fig. 8.3.3 *Natural frequencies and mode-shapes of vibration for Disc 10KY*

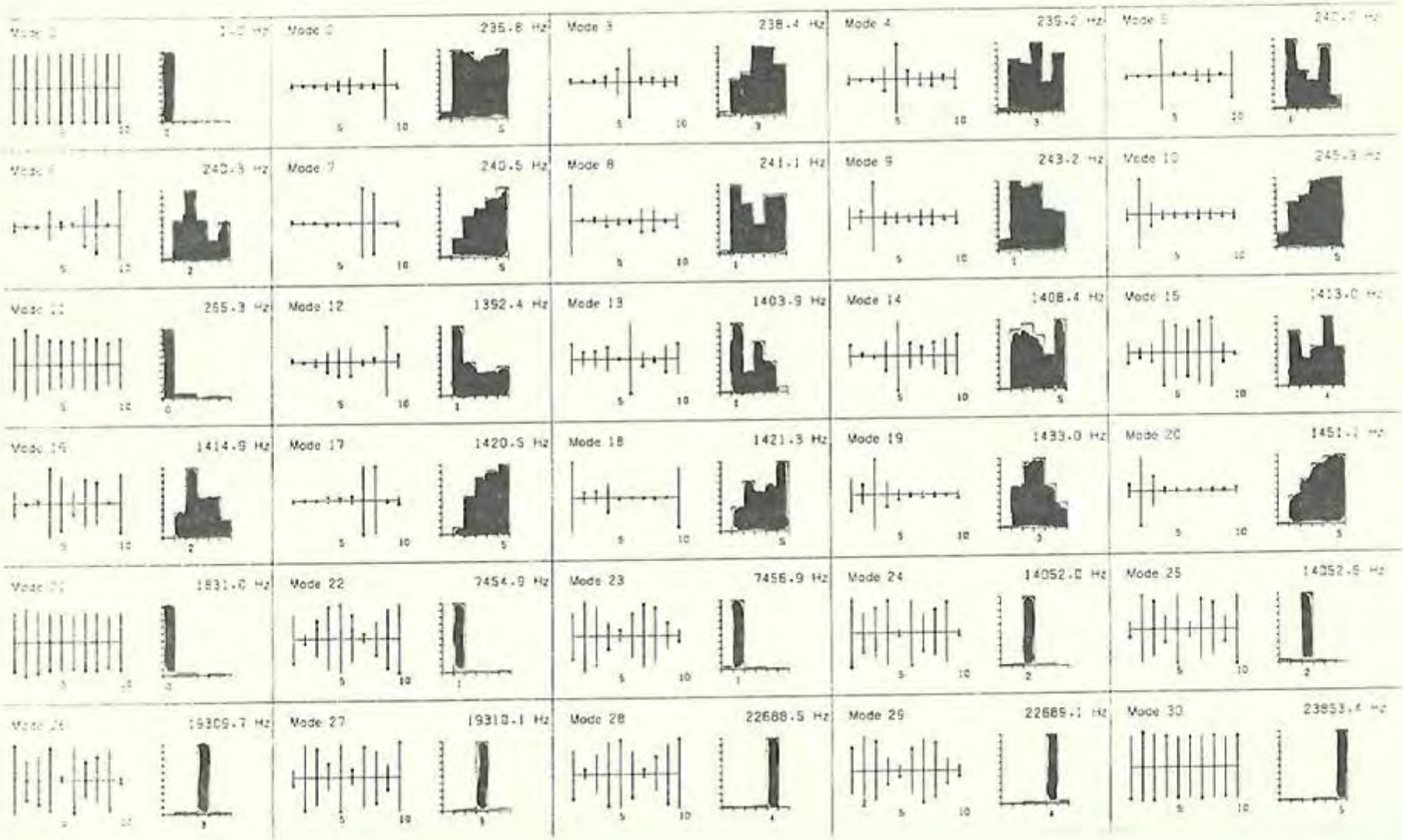

Fig. 8.3.4 *Parametric dependence of 'worst stress' on disc stiffnes*

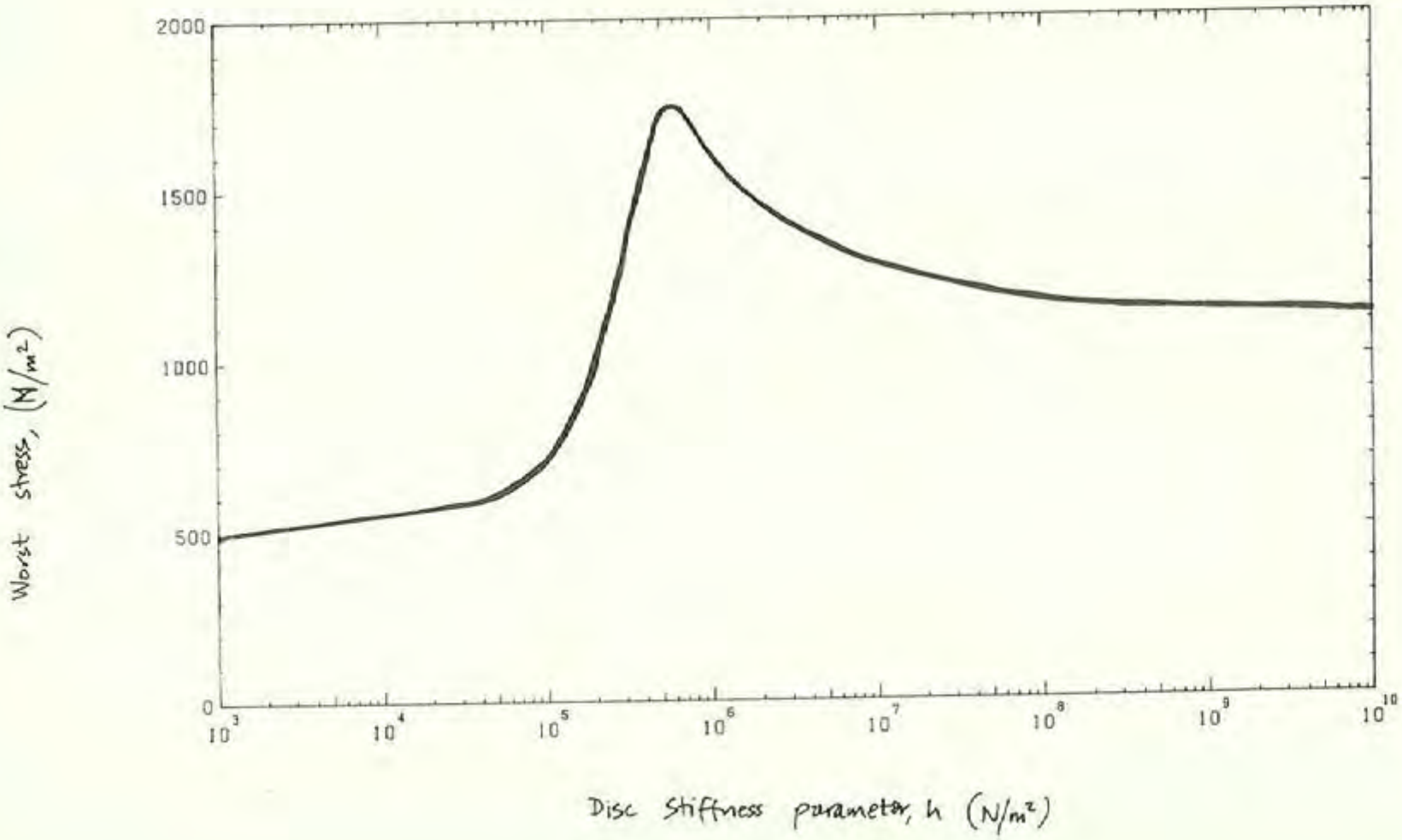

Chapter 9

9.1. Critique of Previous Studies

Many researchers have investigated the vibration of bladed disc assemblies in the past, as reviewed in §1.2. Different models were employed in the investigations. These were mainly theoretical, since it is very difficult to carry out meaningful experimental tests in this field. The conclusions and recommendations put forward in those studies were generally at variance with one another. Such discrepancies are usually attributed to the differences in theoretical modelling methods.

However, we have examined various models of mistuned assemblies using a lumped parameter method in Chapter 2, and the receptance coupling technique in Chapter 5, and have obtained broadly similar results in all the cases considered. Moreover, the conclusions drawn from a statistical analysis of theoretical data, §3.3.2, agree with those obtained when the same procedures were applied to experimental data recorded from actual bladed discs during engine tests, §3.3.4. It seems, therefore, that the application of a procedure of accurate data analysis, followed by judicious interpretation of the results, would lead us to the correct deductions irrespective of the theoretical model applied in the initial problem formulation.

We have drawn attention in the preceeding chapters to some basic characteristics of the vibration response of mistuned bladed discs. Such characteristics are qualitative, and generally invariant with the mathematical method of system modelling, or the assumed mistuning pattern, or the number of blades on a stage. Our objective in this chapter is two-fold:

(*i*) to reconcile, where possible, apparent differences in the findings of previous workers

(*ii*) to establish a strategy for dealing with practical vibration problems which are caused or aided by the mistuning phenomenon.

One way of reconciling the 'conflicting' findings of previous workers is to point out the manner in which certain aspects of their work are in harmony with our own findings, and to explain how they all are local perceptions of a much bigger picture. In the following sections, §9.1.1 to §9.1.5, we shall examine in chronological order a selection of results from previous publications. The aim of this exercise is not to find fault with the scholarship of previous workers, since it is easy to be 'wiser' with hindsight, but rather to make a searching and objective review of the mistuning problem in order to draw out the 'truth' of the matter.

9.1.1 Twenty-four Bladed Disc

In their 1975 paper, **El-Bayoumy** and **Srinivasan** published an account of a theoretical investigation into the vibration of a 24-bladed wheel. They used the method of *influence coefficients*. Physical characteristics of their assembly were based on an experimental model previously used by **Ewins** (1972). The assembly was of integral construction - the disc and 24 blades all machined together from the solid. The blades on the wheel were deliberately detuned to give a

random scatter in blades' cantilever frequencies. The mode shapes were holographically recorded, as illustrated in Figure 9.1.1*a*

Figure 9.1.1*b* shows some of the natural frequencies and mode shapes of vibration observed by Ewins during the experiment. The corresponding parameters calculated by El-Bayoumy and Srinivasan are depicted in Figure 9.1.1*c*. It may be noted that the mode shapes obtained in the course of both studies are in good qualitative agreement. However, the qantitative values of resonant frequencies calculated from the theoretical procedure are not as close to the exprimental values. Thus, it is clear that the modeshape observed at 2478Hz during the experiment is a 'critical' one, as defined earlier on in Chapter 2, and is almost identical to the theoretical mode shape at 2568Hz.

Although both studies have yielded slightly different results in some respects, it may be pointed out that a particular prediction resulting from our analysis of Chapter 2 holds good for both theory and experiment. Thus, a critical mode may be clearly identified at 2568Hz and 2478Hz respectively; at such a mode, the blade with a rogue-like behaviour is blade 18 in either case. This blade is one with extreme detune in cantilever frequency, asis evident from the system's frequency scatter diagram which is shown in the bottom right-hand corner of Figure 9.1.1*c*.

Again, as pointed out in chapter 2, the blades with extreme detune such as blades 18 and 14 on the twenty-four bladed disc under consideration are most likely to have the smallest or largest amplitude relative to all other blades on the wheel, in addition to standing out conspicuously in a critical mode-shape diagram. Although this principle is clearly illuminated by the data of El-Bayoumy and Srinivasan, it appears they did not recognise it as such. Thus, in discussing Figure 9.1.1*d* (their Fig 5) they state in their paper:

"Blade 4, which has a bench frequency equal to the mean blade frequency suffers a maximum stress level near the tuned system frequency. The tuned absorber behaviour is well-illustrated in Fig 5, i.e. while blade 14 may be resonating, blade 18 is almost stationary"

In fact, blade 14 is not just 'resonating' as such, because it had all along been subject to the *largest* response since the commencement of their data analysis (at about 2050Hz) up to the first cross-over frequency at around 2450Hz. At the same time, blade 18 had been virtually immobile, responding with the *lowest* response magnitude compared to all other blades. The simple fact is that blade 14, being the blade with the lowest cantilever frequency, suffers the highest response while the blade with the highest cantilever frequency, blade 18, suffers the smallest response at frequencies below the cross-over point. After the cross-over, these two blades alternate their positions in the response sequence. There does not appear to be a cause and effect relationship between the *tuned* system's resonant frequency and the response of blades on the *mistuned* assembly. Focusing attention on the response of blade 4, which has the average frequency, merely diverts attention from the much more importatant information offered by the blades with extreme mistune.

As for the tuned absorber phenomenon, its linkage with the mistuning problem as they have done seems to be due to an unfortunate coincidence - namely, the proximity of blade 14's cantilever frequency, which is fixed, to a resonant frequency of the assembly, which is dependent on the order of engine excitation. If the authors had considered the response of the assembly to different excitation patterns in addition to the 6EO, they probably would have drawn a different conclusion.

9.1.2 Seventy-two Bladed Disc

An investigation into the effects of random mistuning on the vibration of turbomachine blades was carried out by **Srinivasan** and **Frye**, a report of which was given in their 1976 paper. They used a variant of the influence coefficient method referred to in §9.1.1 above to study the forced response characteristics of two bladed disc assemblies. One of the assemblies has 116 blades while the other has 72.

Figure 9.1.2*a* (their Fig 5) shows the random scatter in blade-alone frequencies as a function of slot position for the 72 bladed wheel. The worst

stress experienced by each blade when the the wheel is excited by the 5th engine order force is shown against the blade slot number in Figure 9.1.2*b* (their Fig 9). The stress peak of each blade is also depicted as a function of the blade's cantilever frequency in Figure 9.1.2*c* (their Fig 15). It may be noted that the cantilever frequency axis in Figure 9.1.2*c* has been normalized relative to the tuned (or mean-value) case.

We recall from Chapter 3 that a completely random picture is obtained, with no credible correlation, if we plot resonant stress against blade slot position as in Figure 9.1.2*b*. On the other hand, a graph such as Figure 9.1.2*c* showing stress magnitudes against cantilever frequency usually reveals a linear correlation between the two parameters. The conclusion drawn by Srinivasan and Frye from Figure 9.1.2*c*, is given in the following extract from their paper:

> *"Note that, in general, blades with blade alone frequencies close to the nominal predicted coupled mode frequency experience the highest response. This is the well-known characteristic of a tuned absorber."*

A different interpretation of their results is given in Figure 9.1.2*d*, which is based on the same set of data used in Figure 9.1.2*c*. Evidently, a case can be made for a correlation between the stress magnitude of each blade and its cantilever frequency.

9.1.3 Twenty-three Bladed Disc

Figure 9.1.3*a* shows the frequency response of the three blades strain-gauged during an experimental test conducted by **Fabunmi** (1978) on a single stage axial compressor rotor. There were 23 blades on the rotor but, as usual in experiments on the mistuning problem, only a few of the blades were instrumented with strain-gauges. The three blades were selected using a random sampling procedure. Incidentally, the blade on slot number 1, which has the lowest cantilever frequency, was included in the sample. The other two blades are on slots 22 and 23. Unfortunately, blade 5 which has the highest cantilever frequency (see Figure 9.1.3*b*) was not strain-gauged during the test.

It is interesting to note in Figure 9.1.3*a* that blade 1 has the largest peak response, at about 391Hz, which is substantially bigger than the amplitude of any other blade. The frequency range between 370Hz and 390Hz seems to be a cross-over band, since the response of blade 1 has alternated from the lower extreme position in the response hierarchy to the

upper after the cross-over. In view of the findings reported earlier on in Chapters 2 and 3 of this thesis, it would have been more instructive had a purposive sampling procedure been applied for blade selection in a parallel test. In that case, the response of the blade having the lowest cantilever frequency (blade 5) would have been available for comparison. Ideally, all blades on the stage should have been strain-gauged but this is usually very difficult to achieve in practice.

9.1.4 Twelve Bladed Disc

Most of the theoretical studies conducted by various workers have been built on two primary models. In one case, the blades are assumed to be mechanically coupled together through the flexibility of the disc; in the second basic model, all the blades on a stage are assumed to be aerodynamically connected through the viscosity of the surrounding fluid medium. In a recent study by **Muszynska** *et al* (1980), the effects of friction damping at the root of each blade were accounted for through the application of a model shown in Figure 9.1.4*a*.

In the past, it has been reported in the literature by other investigators that the application of different models of mechanical coupling representation (*e.g.*: receptances on the one hand and influence coefficients on the other) had led to their divergent conclusions. Now, since this new friction model introduced by Muszynska *et al* represents an even more complex variation of the mechanical coupling modelling, it would be expected that the conclusions drawn from its application should be divergent from those of other models. However, this is not the case. Figure 9.1.4*b* shows the mistuning pattern for one of the bladed disc assemblies considered in their paper. The pattern is a half-period sine variation of blade cantilever frequencies with slot position. Of the eleven blades on the stage, blades 6 and 7 both have the highest cantilever frequency, while the lowest frequency blade is on slot number 1. The responses of all the blades in the assembly when it is exposed to steady state forcing are shown, plotted on the same axes, in Figure 9.1.4*c*. It may be observed that the response magnitude of each blade is approximately linearly related to its cantilever frequency. Further, the blades with the largest amplitudes throughout the frequency range surveyed are blades 1 and 11 at about 150Hz, and blades 6 and 7 at approximately 120Hz. These are blades with extreme cantilever

frequencies. The cross-over phenomenon could be detected in Figure 9.1.4*c*, although this may be difficult to appreciate on account of the crowded appearance of the graphs.

Evidently, the results of this non-linear, frictional damping model are not in conflict with those obtained when the lumped parameter model was applied in Chapter 2, or the receptance analysis of Chapter 5.

9.2 A strategy for Dealing with Mistuning

We have seen from the reviews above, as well as in the earlier chapters of this thesis, that mistuning usually leads to a deterioration in the vibration response of bladed disc assemblies. In other words, the blades on a mistuned wheel do not experience comparative response magnitudes at all speeds of engine operation, unlike in the tuned case. Moreover, it is not easy to predict the onset of all the resonant conditions within the range of engine speeds since many secondary resonances are likely to arise, unlike in tuned systems. The overall effect of mistuning on an assembly for which mechanical coupling conditions are dominant is that blade amplitudes may be severely unequal under certain excitation conditions, to the extent that a few blades may exhibit the rogue behaviour by failing prematurely. Under such conditions, it is unrealistic to ignore the differences in blade properties as is the case in current design procedures where tuned conditions are almost invariably assumed.

In designing a strategy for defeating the problems posed by mistuning, the overiding aim must be to prevent the failure of any blade in service. This may be achieved by predicting the blade(s) that are likely to be subject to excessive and disproportionate stressing, or of specifying a procedure for estimating the upper bounds on the response amplitude of any blade on the stage, so that in either case remedial measures may be taken before actual failure occurs.

Whereas it is feasible to adopt an experimental approach based along the lines of conventional engine tests, it is evidently cheaper and faster to employ a representative theoretical model in the first instance. By selecting the mass, stiffness and damping coefficients in a judicious manner as discused in Chapter 2, it is possible to utilise a lumped parameter model for predicting the vibration properties of a practical bladed disc. Alternatively, one could apply the receptance coupling procedure developed by **Ewins**

(1973). If suitable facilities are accesible, it would be very convenient to employ the elaborate scheme designed by **Fabunmi** (1978) in which holographic techniques are used to determine the actual modal properties of a bladed disc, while a lumped parameter model is used to obtain the forced response magnitudes. Upon selecting a theoretical modelling technique adjudged most suitable for the problem at hand, the design engineer can then proceed to calculate the response amplitude of *every blade* on the stage under various excitation conditions. In this way, it is possible to identify in an unambiguous manner the blades which are likely to experience unusually large stress and, moreover, to simulate the behaviour of the rotor stage under anticipated operating conditions without the danger of causing actual damage to any rogue blades. It is this 'non-destructive testing' feature of being able to observe *every blade* on the stage under resonant conditions that makes a carefully designed theoretical procedure much more attractive than costly engine tests, especially since blade failure can occur during the testing programme, before meaningful use may be made of the measured data.

However, it must be recognized that when modelling the dynamic behaviour of such a complex engineeering system as a vibrating bladed disc, theoretical procedures cannot be a substitute for engine tests. For even if the theoretical technique adopted was perfect, certain inputs to the calculation process are bound to be only approximate. For instance, the mistuning pattern presented to a computer program may have been obtained by testing each blade in isolation, under static (i.e. non-rotating conditions), whereas additional mistuning may be in operation in the complete assembly due differences in root fixure conditions. It is, therefore, desirable to conduct engine tests in parallel with, and verification of, the theoreticalcalculations.

Whenever an engine test is conducted in such a way that only a handful of blades may be strain-gauged, purposive sampling should be applied in the blade selection process so that blades with extreme mistune in cantilever frequencies are included in the sample. Additionally, one or two blades with average frequency could be strain-gauged. On the conclusion of the measurement process, the statistical procedures described in Chapter 3 may be applied to estimate the probable maximum stress.

By designing a representative theoretical model of a practical rotor stage in the first instance, it is possible to identify the conditions under which the worst vibration amplitudes may occur, and those blades in the

assembly that are likely to be most affected. Subsequently, engine tests should be conducted, guided by the deductions and observations of the theoretical model. In this way, a strategy based on a combination of theory and experiment may be fashioned for dealing with the vibration problems due to mistuning conditions.

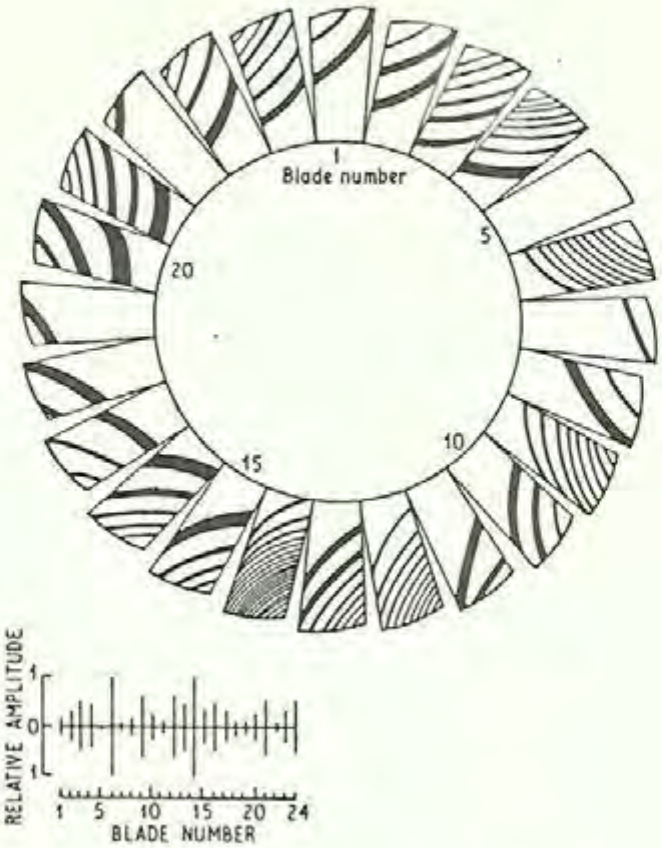

Fig. 9.1.1a *Holographic mode-shapes of a bladed disc*

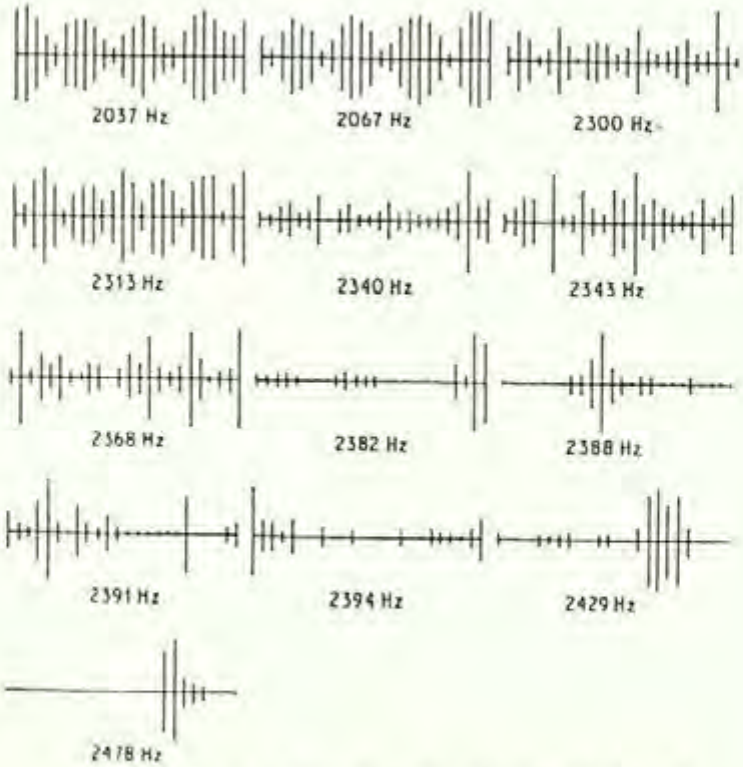

Fig. 9.1.1b *Measured modes of a 24-bladed disc*

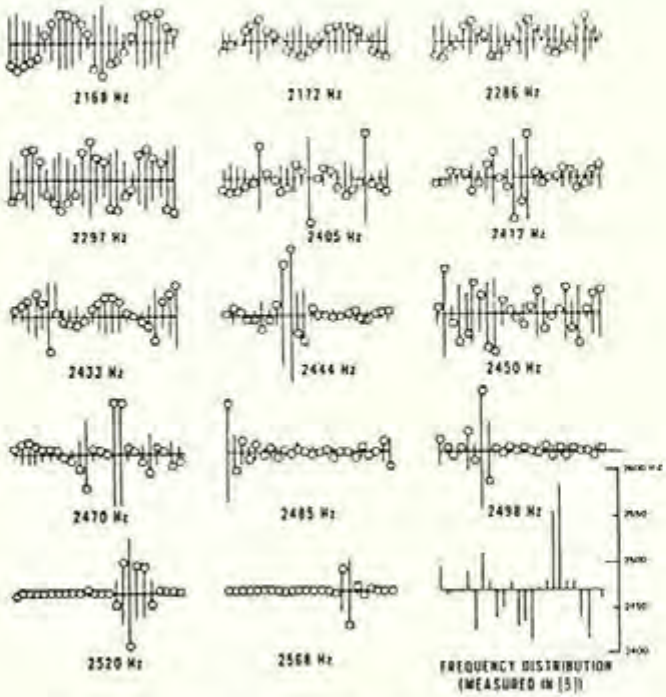

Fig. 9.1.1c *Computed modes of a 24-bladed disc*

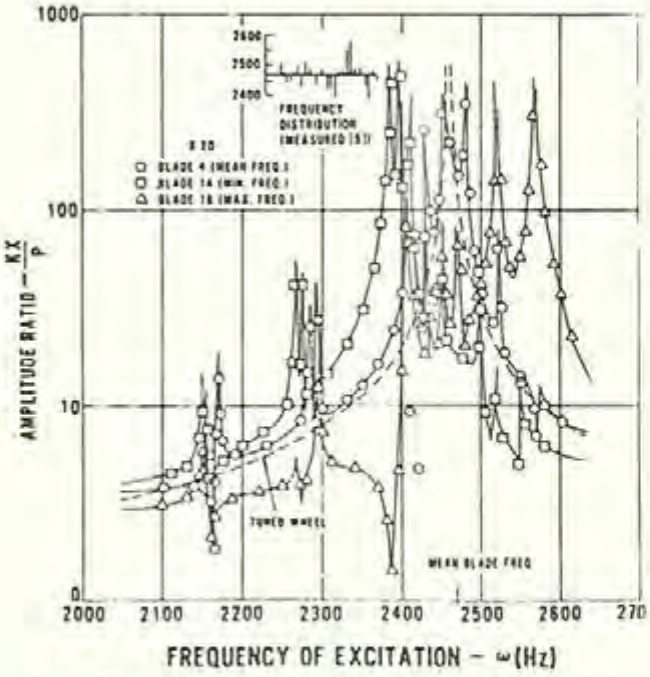

Fig. 9.1.1d *Frequency response of a 24-bladed disc*

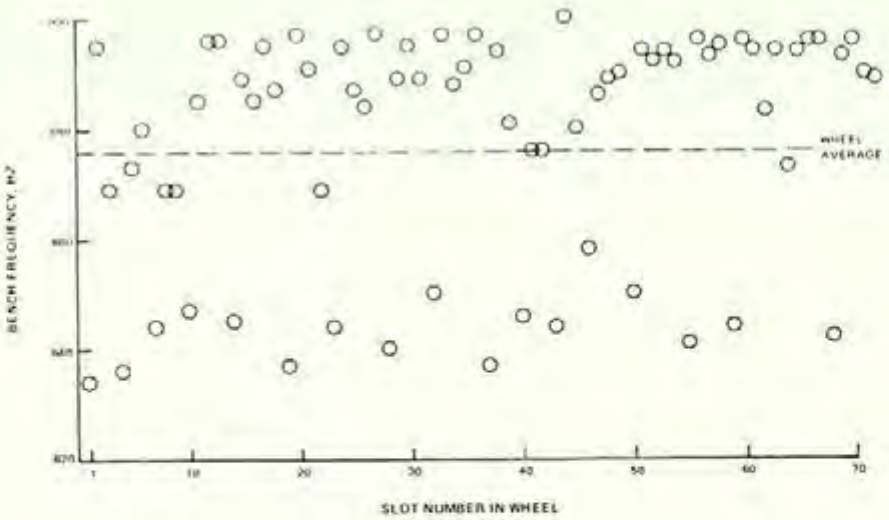

Fig. 9.1.2a *Frequency scatter for a 72-bladed disc*

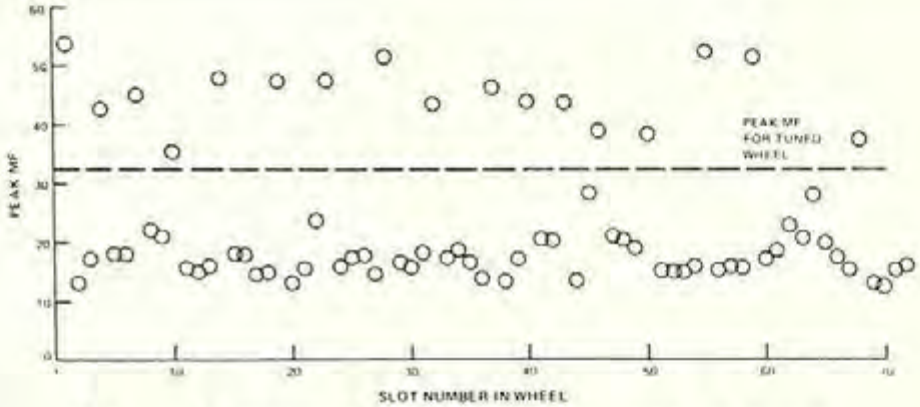

Fig. 9.1.2b *Variation of stress amplitude with blade slot position*

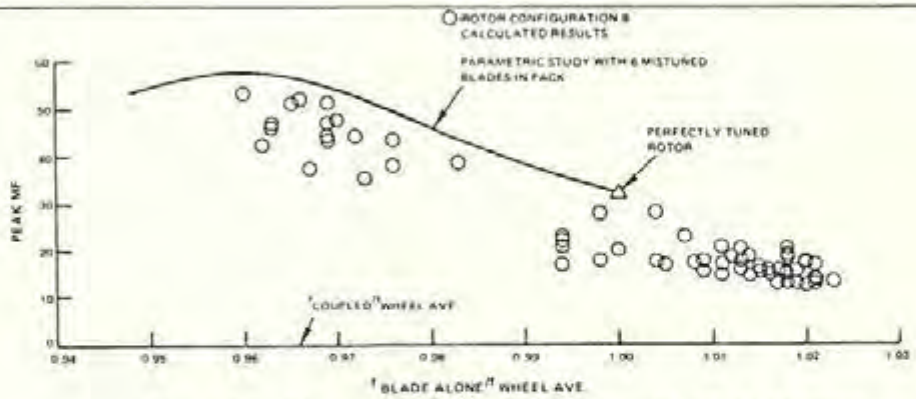

Fig. 9.1.2c *Variation of stress amplitude with blade frequency*

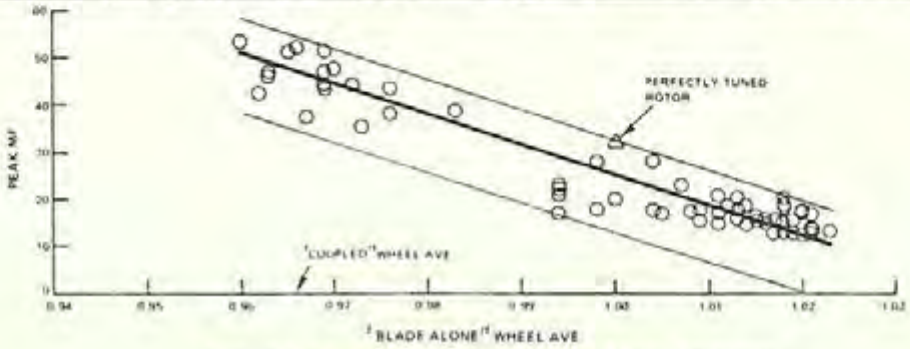

Fig. 9.1.2d *Regression of stress on blade frequency*

Fig. 9.1.3a *Frequency response of a 23-bladed disc*

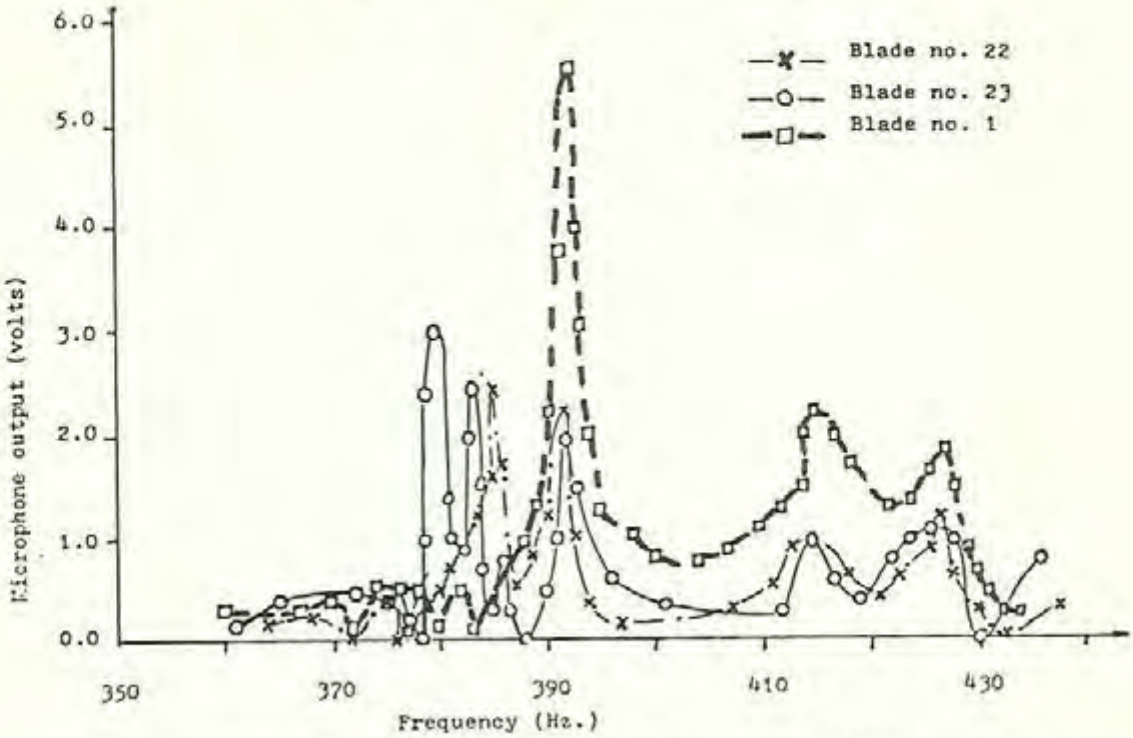

Responses from three blades.(All blades are driven @ 300 volts(PTP) with phase shift $\theta = 2\pi/23$. The disc was freely supported.

Fig. 9.1.3b *Frequency scatter of a 23-bladed disc*

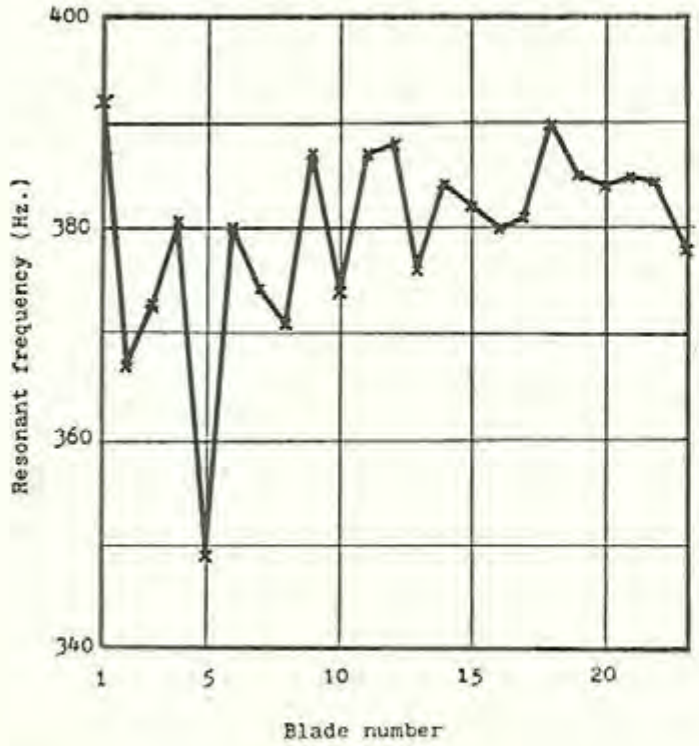

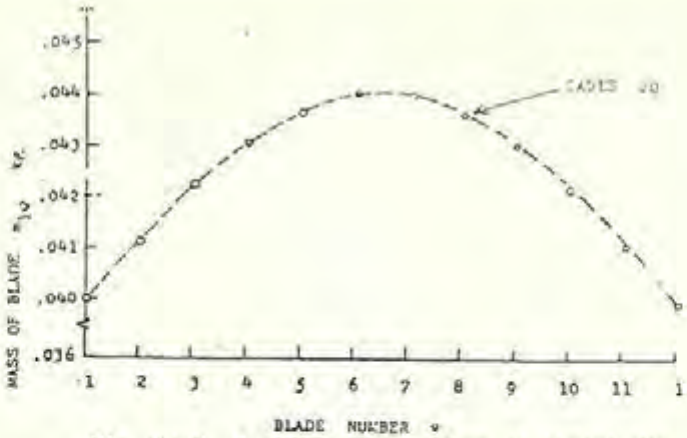

Fig. 9.1.4b *Frequency scatter of an 11-bladed disc*

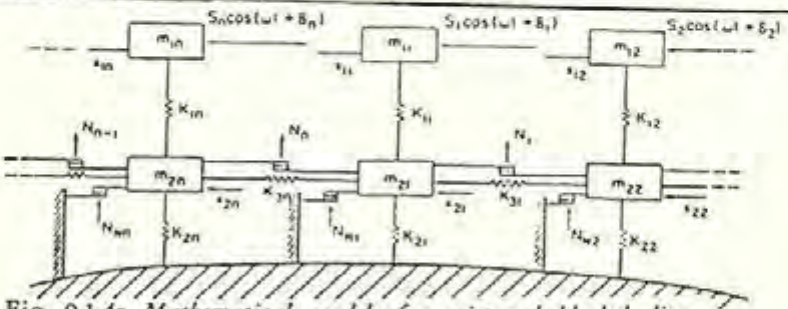

Fig. 9.1.4a *Mathematical model of a mistuned bladed disc*

Fig. 9.1.4c *Frequency response of an 11-bladed disc*

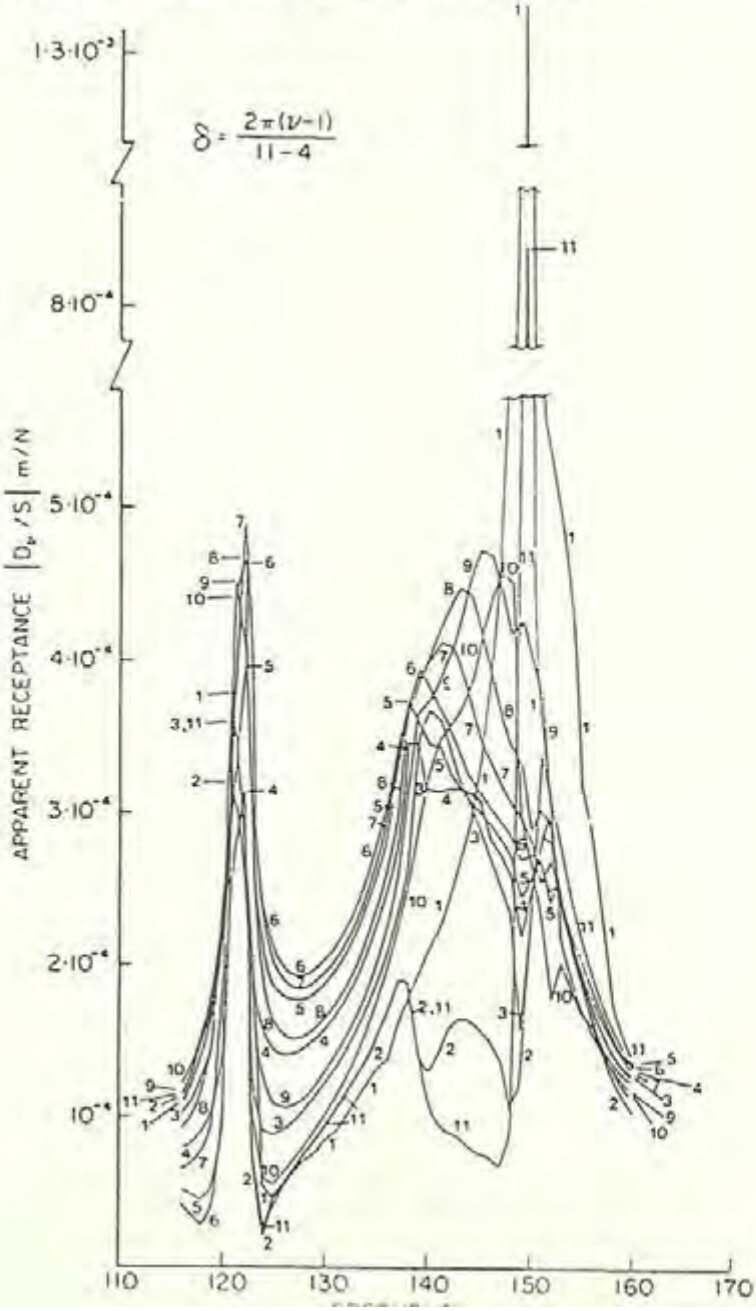

Chapter 10

10.1 Conclusions

For many years, researchers and engine designers have devoted attention to the phenomenon of rogue blade failure. Some workers have postulated that the small differences between the nominally identical blades on each stage of a turbomachine could give rise to a very uneven distribution of vibration amplitudes amongst the blades and, by implication, to rogue blade failure. Thus, they have considered the effects of mistuning to be so serious as to warrant a complete re-design of rotors in certain cases.

Such conclusions are not, however, universally held. Indeed, many important questions surrounding the vibration response characteristics of blades in a mistuned assembly have usually been met by widely divergent conclusions. It is believed that some 'conflicting' results of previous workers may be reconciled in light of the findings in this thesis, and that the understanding of mistuning has been advanced in some measure as a result of this investigation.

The theoretical and experimental results obtained in the course of this research have already been discussed and concluding remarks given at end of each chapter. Further details of some points may be obtained from our previous reports, **Afolabi** (1979-82). A brief summary of these conclusions is now given.

Modal characteristics A discrete fourier analysis of the eigenvectors of tuned systems reveals that the vectors are pure circular convolutions. However, when mistuning is admitted into an erstwhile tuned system, only a few of the eigenvectors are still 'pure', while most of them become highly 'impure'. In general, at least one eigenvector may be identified as a *critical mode shape* in a given family of modes. The corresponding eigenvalue for such a mode is a 'critical resonance', at which the conspicuously vibrating blade is usually the one with extreme mistune.

Forced response characteristics For a tuned system, there are two orthogonal (sine and cosine) mode-shapes at each resonant frequency, except when 'umbrella' modes occur and *all* the blades have equal amplitudes of displacement. It has been shown earlier that the modes of tuned systems are orthogonal to engine order forcing functions, so that only primary system resonances (PSR) can occur in tuned systems.

The chief difference between the frequency response characteristics of tuned and mistuned assemblies is the presence of secondary system resonances (SSR) in the latter. Several SSRs may arise at different frequencies in a mistuned assembly out of which one may be identified as a 'critical' resonance. It is at such a critical excitation frequency that a rogue behaviour may be identified.

The upper and lower limits on blade response amplitudes at a given excitation frequency are most likely to be experienced by blades with extreme detune. Furthermore, at excitation frequencies sufficiently far removed from resonance, the response of each blade is proportional to its measure of deviation from the tuned state.

The response spectra of a mistuned assembly are characterized by *cross-over bands* where the high and low frequency blades alternate their positions in the response hierarchy. As a result of this 'cross-over', a rogue blade which is subject to the *largest* amplitude of vibration at one critical frequency would most probably suffer the *least* vibration at the next critical resonance.

Statistical characteristics It is well-known that the random variation in the properties of nominally identical products is statistically 'normal'. Thus, the differences in blade cantilever frequencies conform to statistical normality. However, the variation in blade response amplitudes is **not** usually normal. Hence, an inferential procedure which is based on random sampling and the assumption of normal characteristics may not be used to predict with meaningful accuracy the probable limits on blade response amplitudes.

There is usually a linear correlation between the resonant response of of each blade and its cantilever frequency. This correlation may be positive or negative. Consequently, it is pos-

sible to estimate the *probable maximum response* amplitude for a set of blades on a rotor stage, using a purposive sampling technique to select the blade to strain-gauge, followed by a regression analysis of the data.

Modelling techniques The application of different mathematical procedures does not necessarily lead to widely divergent conclusions. A lumped parameter model and a continuum receptance techinque have been used to equally good effect in this work. Provided a theoretical method is well-formulated, or experiment carefully conducted, any convenient procedure may be used to model the behaviour of a mistuned assembly. The overiding factor seems to be, from the results of this research, a judicious interpretation of data and not the method of data acquisition.

In predicting the response of a mistuned asembly, a simple but representative theoretical model should be applied in the first instance to establish a basic understanding of the assembly. Upon carrying out detailed analysis using the simple model, guide lines for the allocation of strain-gauges should be established since it is not possible to strain gauge all the blades during an engine test. Thus, a combination of theoretical modelling and engine tests may be used to good advantage.

Cantilever frequencies The resonant frequencies usually observed of flexibly mounted blades are not the actual cantilever frequencies desired. This is because of the influence exercised by root resilience on natural frequencies. A procedure has been outlined for measuring the cantilever frequencies of blades, especially on wheels of integral construction. The procedure is based on the computation of tip and root displacement ratio at each excitation frequency.

Parametric studies It has been suggested by some previous investigators that the stress amplitude of blades may be reduced if the stiffness of the disc is increased. It has been shown in this study that this is only partially correct. In certain instances, increasing the disc stiffness could lead to *higher* vibration amplitudes.

10.2 Suggestions for Further Work

Several theoretical treatments have been undertaken in the past by various workers. Experiments have also been conducted using models of bladed discs. Although it is recognised that the conduction of full scale engine tests using actual bladed discs under opertaing conditions is difficult and costly, there is a need for such tests. In the first place, it is necessary to clarify once and for all certain important points that have that have been held in dispute by many workers. Secondly, such tests should not be as inconclusive as in the past in view of the findings in this thesis. Thus, when conducting engine tests in future, allowance must be made for monitoring the response of *all* the blades on a stage simultaneously, perhaps by selecting a rotor with a few blades. Futher, the range of excitation speed must be wide enough to permit the observation of critical resonances, and the cross-over phenomenon. Finally, a means of varying the 'order' of engine order excitation should be provided. Subsequent to the experiment, statistical analysis of the acquired data should be done along the lines suggested earlier.

Once the basic issues have been clarified, it should be possible to carry out in-depth parametric studies. This is desirable in order to establish some qualitative relationship between vibration characteristics and the physical parameters of an assembly.

1. **Afolabi, H. D. (1978)**
The vibration of turbine blade packets *MSc Thesis*, University of London (Imperial College). *Report No 78007*, Mechanical Engineering Department, Dynamics Section, Imperial College, London.

2. **Afolabi, H. D. & Ewins, D. J. (1979)**
A bibliography of blade and disc vibration *Report No 7919*, Mechanical Engineering Department, Dynamics Section, Imperial College, London.

3. **Afolabi, H. D. (1981a)**
Vibration of mistuned bladed assemblies *Contract Report No 8106*, Mechanical Engineering Department, Dynamics Section, Imperial College, London.

4. **Afolabi, H. D. (1981b)**
Vibration of mistuned bladed assemblies *Contract Report No 8117*, Mechanical Engineering Department, Dynamics Section, Imperial College, London.

5. **Afolabi, H. D. (1981c)**
A strategy for dealing with blade vibration problems due to mistuining *Seminar Presentation*, Rolls-Royce Derby, November 5.

6. **Afolabi, H. D. (1982a)**
Effects of random detuning on the vibration of coupled turbomachine blades *Contract Report No 8201*, Mechanical Engineering Department, Dynamics Section, Imperial College, London.

7. **Afolabi, H. D. (1982b)**
The application of a lumped parameter model to predict some vibration characteristics of an aeroengine compressor fan *Contract Report No 8202*, Mechanical Engineering Department, Dynamics Section, Imperial College, London.

8. **Afolabi, H. D. (1982c)**
A statistical interpretation of dynamic response data of bladed-disc assemblies *Contract Report No (82)*, Mechanical Engineering Department, Dynamics Section, Imperial College, London.

9. **Agbasiere, J. A. (1965)**
Flexural vibration of multi-layer beams with visco-elastic damping *PhD Thesis*, University of London (Imperial College).

10. **Airey, J. R. (1910)**
The vibrations of circular plates and their relation to Bessel functions *Proc Phys Soc London*, series A, vol 23, pp225–232.

11. **Alabi, B. (1979)**
A conformal mapping solution to elastodynamic boundary value problems *PhD Thesis*, University of London (Imperial College).

12. **Armstrong, E. K. (1955)**
An investigation into the coupling between blade and disc vibration *PhD Thesis*, Cambridge University.

13. **Armstrong, E. K. & Stevenson, R. E. (1960)**
Some practical aspects of compressor blade vibration *Journal of the Royal Aeronautical Society*, 64(591), pp117–130.

14. **Armstrong, E. K.; Christie, P. I. & Hague, W. (1965)**
Natural frequencies of bladed discs *Proceedings of the Institution of Mechanical Engineers*, vol 180, Part 3.I, pp110–123.

15. **Armstrong, E. K.; Crowcroft, R. S. & Hunt, T. M. (1966)**
Fatigue life of compressor blading *Proceedings of the Institution of Mechanical Engineers*, vol 180, Part 3.I.

16. **Armstrong, E. K. (1967)**
Recent blade vibration technique *Journal of Engineering for Power, Trans ASME*, pp437–444.

17. **Ashmore, S. C. F. (1976)**
Use of point forces to simulate vibration in turbine wheels caused by the vibration environment *MSc Thesis*, University of London (Imperial College).

18. **Bauman, K. (1921)**
Some recent developments in large scale turbine practise *J. Inst of Elec Engrs*, vol 59, pp565–663.

19. **Beglinger, V.; Bolleter, U. & Locher, W. E. (1976)**
Effects of shear deformation, rotatory inertia and elasticity of the support on the resonance frequencies of short cantilever beams *Journal of Engineering for Power, Trans ASME*, 98, 79–87.

20. **Belagumkar, B. M.; Laksminarayana, K. & Nakra, B. C. (1962)**
Vibration characteristics of axial flow compressor blades *Journal of Science and Educational Research*, 6(2), pp153–168.

21. **Belek, H. T. (1977)**
The vibration characteristics of shrouded blades on rigid and flexible disk *PhD Thesis*, University of Surrey.

22. **Bishop, R. E. D. (1956)**
A general theory of hysteretic damping *Aeronautical Quaterly*, 7, 60–70.

23. **Bishop, R. E. D. & Johnson, D. C. (1960)**
The Mechanics of Vibration Cambridge University Press.

24. **Boole, G. (1880)**
A Treatise on the Calculus of Finite Differences MacMillan and Co., New York.

25. **Brillouin, L. (1946)**
Wave Propagation in Periodic Structures Dover Publications, New York.

26. **Campbell, W. (1924)**
The protection of steam turbine disc wheels from axial vibration *Trans ASME*, vol 46, pp31–160.

27. **Campbell, W. (1925)**
Tangential vibrations of steam turbine buckets *Trans ASME*, vol 47, pp643*ff*.

28. **Capriz, G. (1967)**
Interaction between disk and blades during vibrations of a thick bladed turbine disk *ASME Paper 67–Vibr–52*.

29. **Chun, K. R. (1972)**
Free vibration of a beam with one end spring-hinged and the other free *Journal of Applied Mechanics, Trans ASME*, 39(4), 1154–1155.

30. **Cottney, D. J. (1971)**
Natural frequency changes due to shrouding a bladed disc *MSc Thesis*, University of London (Imperial College).

31. **Cottney, D. J. & Ewins, D. J. (1974)**
Towards the efficeint vibration analysis of shrouded bladed disc assemblies *Journal of Engineering for Industry, Trans ASME*, 96, 1054–1959.

32. **Cottney, D. J. (1975)**
The receptance analysis of disc, blade and shroud vibration *PhD Thesis*, University of London (Imperial College).

33. **Damisah, F. O. (1981)**
The application of the boundary integral equation method to foundation dynamics *PhD Thesis*, University of London (Imperial College)

34. **Dimitriadis, E. K. (1979)**
The vibration of packeted bladed discs *MSc Thesis*, University of London (Imperial College).

35. **Duncan, W. J. & Collar, A. R. (1935)**
Matrices applied to the motions of damped systems *Philosophical Magazine*, Series 7, 19, 197–219.

36. **Dye, R. C. F. & Henry, T. A. (1968)**
Effects of frequency scatter on the resonant amplitudes of compressor blades *Symposium Mech Reliability Turbo Mach Blading*, Derby.

37. **Dye, R. C. F. & Henry, T. A. (1969)**
Vibration amplitudes of compressor blades resulting from scatter in natural frequencies *J. Eng For Power, Trans ASME*, vol 91, pp182–188.

38. **Ehrich, F. F. (1956)**
A matrix solution for the vibration modes of non-uniform discs *Journal of Applied Mechanics*, ASME, vol 23, pp109–115.

39. **Ellington, J. P. & McCallion, H. (1957)**
The vibration of laced turbine blades *Journal of the Royal Aeronautical Society*, 61, 563–.

40. **Ellington, J. P. & McCallion, H. (1959)**
Blade frequency of turbines—effect of disc elasticity *Engineering*, 887, 645.

41. **El-Bayoumy, L. E. & Srinivasan, A. V. (1975)**
Influence of mistuning on rotor blade vibration *AIAA Journal*, 13(4), 460–464.

42. **Erf, R. K. (1974)**
Holographic non-destructive testing Academic Press, London.

43. **Ewins, D. J. (1966)**
The vibration of bladed discs *PhD Thesis*, Cambridge University.

44. **Ewins, D. J. (1969)**
The effects of detuning upon the forced vibration of bladed disks *Journal of Sound and Vibration*, vol 9, pp65–79.

45. **Ewins, D. J. (1970)**
A study of resonance coincidence in bladed discs *Journal of Mechanical Enginering Science*, vol 12, pp305–312.

46. **Ewins, D. J. (1972)**
A study of the vibration modes of a bladed turbine wheel *Proc IMechE Conference On Vibrations In Rotating Systems*, pp170–184.

47. **Ewins, D. J. (1973)**
Vibration characteristics of bladed disc assemblies *Journal of Mechanical Engineering Science*, 15(3), 165–186.

48. **Ewins, D. J. (1975)**
Vibration modes of mistuned bladed discs ASME Paper 75–GT–114, March.

49. **Ewins, D. J. (1976a)**
Studies to gain insight into the complexities of blade vibration phenomena *Proc IMechE Conf Vibr Rotating Mach*, Paper C184/76.

50. **Ewins, D. J. (1976b)**
An experimental investigation of the forced vibration of bladed discs due to aerodynamic excitation *Structural Dynamic Aspects of Bladed Disks*, ASME, pp15–28.

51. **Ewins, D. J. & Sadasiva Rao, Y. V. K. (1976)**
A theoretical study of the forced vibration response of bladed discs *Ibid.*, pp29–44.

52. **Ewins D. J. (1980)**
Bladed Disc Vibration – A Review of techniques and characteristics *Proceedings of the ISVR Conference*, Southampton, July, 1980.

53. **Fabunmi, J. A. (1978)**
Forced vibrations of a single stage axial compressor rotor *PhD Thesis*, MIT, Cambridge, Massachussettss, USA.

54. **Fabunmi, J. A. (1979)**
Forced vibrations of a single stage axial compressor rotor *ASME Paper 79–GT–108*.

55. **Fawzy, I. & Bishop, R. E. D. (1976)**
On the dynamics of linear, non-conservative systems *Proceedings of the Royal Society London*, A352, 25–40.

56. **Garbow, B. S.** *et al* **(1977)**
Eigensystems Subroutine Package, EISPACK Guide Extension. Lecture Notes in Computer Science, Number 51. Springer–Verlag, Berlin.

57. **Gleeson, P. T. (1979)**
Identification of spatial models for the vibration analysis of lightly damped structures *PhD Thesis*, University of London (Imperial College).

58. **Grinstead, B. (1952)**
Nodal pattern analysis *Proceedings of the Institution of Mechanical Engineers*, vol 166, pp309.

59. **Gupta, K. K. (1973)**
Eigenproblem solution by a combined Sturm sequence and inverse iteration technique *International Journal for Numerical Methods in Engineering*, 7, 17–42.

60. **Gupta, K. K. (1974)**
Eigenproblem solution of damped structural systems *International Journal for Numerical Methods in Engineering*, 8, 877–911.

61. **Hall, R. M. (1968)**
The effect of mid-span shroud constraint on the vibration of compressor blade systems *PhD Thesis*, University of Surrey.

62. **Hazell, C. R. (1981)**
Recording receptances of flat plates by holographic interferomotery *Journal of Sound and Vibration*, 75(2), 275–283

63. **Hockley, B. S.; Ford, R. A. & Foord, C.A. (1978)**
Measurement of fan vibration using double pulse holography *ASME Paper 78–GT–111*.

64. **Huang, T. C. (1961)**
Effect of rotatory inertia and the shear deformation on the frequency and normal mode equations of uniform beams with simple end conditions *Journal of Applied Mechanics, Trans ASME*, 28, 579–583.

65. **Jacobsen, L. S. & Ayre, R. S. (1958)**
Engineering Vibrations McGraw-Hill Book Company, New York.

66. **Jones, D. I. G. & Nashif, A. D. (1969)**
Damping of blade like structures *Shock and Vibration Bulletin*, vol 39, No 4, pp19–29.

67. **Jones, D. I. G. & Muszynska, A. (1978)**
Vibrations of a compressor blade with slip at the root *Shock and Vibration Bulletin*, vol 48, Pt 2, pp5361–.

68. **Justine, T. & Krishnan, A. (1980)**
Effects of support flexibility on the fundamental frequency of beams *Journal of Sound and Vibration*, 68(2), 310–312.

69. **Kaza, K. R. V. & Kielb, R. E. (1981)**
Effects of mistuning on bending-torsion flutter and response of a cascade in incompressible flow *NASA Technical Memorandum*, TM-81674.

70. **Kendall, M. G. & Stuart, A. (1973)**
The Advanced Theory of Statistics, volume 2: Inference and Relationship Griffin & Co, London.

71. **Kielb, R. E. (1981)**
Aeroelastic characteristics of a mistuned bladed-disc assembly *PhD Thesis*, Ohio State University, USA.

72. **Kirkhope, J. (1971)**
Vibrations of systems of elastically coupled concentric rings *Journal of the Acoustical Society of America*, 47(3), 371–373.

73. **Kirkhope, J. & Wilson, G. J. (1971)**
Analysis of coupled blade-disc vibration in axial flow turbines *AIAA Paper No 71-375*, AIAA–ASME Conference, April.

74. **Kirkhope, J. & Wilson, G. J. (1972)**
Vibration of circular and annular plates using finite elements *International Journal for Numerical Methods in Engineering*, vol 4, pp49–65.

75. **Kirkhope, J. & Wilson, G. J. (1975)**
Vibration anlysis of axial flow turbine disks using finite elements *ASME Paper 75-DET-80*.

76. **Kirkhope, J. & Wilson, G. J. (1976a)**
A finite element analysis for the vibration modes of a bladed disk *Journal of Sound and Vibration*, vol 49, No 4, pp469–482.

77. **Kirkhope, J. & Wilson, G. J. (1976b)**
Vibration and stress analysis of thin rotating discs using annular finite elements *Journal of Sound and Vibration*, 44(4), 461–474.

78. **Kirshenboim, J. (1980)**
Users' Guide for the mobility measurement and analysis programs on the 1191 computer *Report No 80007*, Mechanical Engineering Department, Dynamics Section, Imperial Colege, London.

79. **Kirshenboim, J. (1981)**
Theory and practise of modal identification applied to helicopter structures *PhD Thesis*, University of London, Imperial College.

80. **Kolb, R. P. (1967)**
Measured vibratory motions of turbine blades *ASME Paper 67-Vibr-66*.

81. **Kroon, R. P. (1940)**
Turbine blade vibration due to partial admission *Trans ASME*, 62, A161–A165.

82. **Lamb, H. & Southwell, R. V. (1921)**
The vibrations of a spinning disc *Proceedings of the Royal Society, A99, 272–280*.

83. **Lancaster, P. (1966)**
Lambda Matrices and Vibrating Systems Pergamon Press, London.

84. **Leissa, A. W. (1969)**
Vibration of plates *NASA SP-160.*

85. **Leissa, A. W. (1978)**
Recent researches in plate vibration *Shock and Vibration Digest*, 10, 21–35.

86. **Luck, G. A. & Kell, R. C. (1956)**
Measuring turbine blade vibrations *Engineering*, August 31.

87. **Luck, G. A. (1962)**
Blade vibration measurement on rotating turbine wheels *GEC Journal of Science & Technology*, 29(2), 86–91.

88. **Luck, G. A. (1963)**
Role of blade vibration failures in improving steam turbine reliability *The Engineer*, pp674-678.

89. **Mac Bain, J. C. & Genin, J. (1973a)**
Effect of support flexibility on the fundamental frequency of vibrating beams *Journal of the Franklin Institute*, vol 296, pp259–273.

90. **Mac Bain, J. C. & Genin, J. (1973b)**
Natural frequencies of a beam considering support characteristics *Journal of Sound and Vibration*, 27(2), 197–206.

91. **Mac Bain, J. C. (1978)**
Displacement and strain of vibrating structures using time-averaged holography *Experimental Mechanics*, 18, 361–372.

92. **McLeod, A. J. & Bishop, R. E. D. (1965)**
The forced vibration of circular flat plates *Mechanical Engineering Science Monograph*, Number 1.

93. **Mindlin, R. D. (1951)**
Influence of rotary inertia and shear on flexural motions of isotropic elastic plates *Journal of Applied Mechanics*, Trans ASME, vol 18, pp31–38.

94. **Muszynska, A. *et al* (1980)**
On the non-linear response of multiple blade systems *Report No AFSC 80-1211* Air Force Systems Command, Office of Public Affairs, Wright Patterson Air Force Base, Ohio, USA.

95. **Peter, A. F. (1969)**
Practical holographic mode shapes on turbine blades *ASME Paper 69-Vibr-32*

96. **Peters, G. & Wilkinson, J. H. (1 969)**
Eigenvalues of $Ax=\lambda Bx$ with band symmetric A and B *Computer Journal*, 12, 398–404.

97. **Prohl, M. A. (1958)**
A method of calculating vibration frequencies and stresses of banded groups of turbine buckets *Trans ASME*, vol 80, pp169–180.

98. **Rao, J. S. (1973)**
Natural frequencies of turbomachine blading : a survey *Shock and Vibration Digest*, 5(10), 3–16.

99. **Rao, J. S. (1977)**
Turbine blading excitation and vibration *Shock and Vibration Digest*, 9(3), 15–22.

100. **Rayleigh, Lord *a.k.a* J. W. Strutt (1887)**
The Theory of Sound Dover Publications, New York (*reprinted*, 1945).

101. **Reismann, N. (1959)**
Forced vibrations of a circular plate *Journal of Applied Mechanics*, ASME, vol 26, pp526–527.

102. **Reisner, E. (1945)**
The effect of transverse shear deformation on the bending of elastic plates *Journal of Applied Mechanics*, Trans ASME, vol 12, pp69–77.

103. **Rieger, N. F. & McCallion, H. (1965)**
The natural frequencies of portal frames (Parts 1 and 2)
International Journal of Mechanical Sciences, vol 7, pp263–271.

104. **Rissone, R. F. & Williams, J. J. (1965)**
Vibration of non-uniform cantilever blades *The Engineer*, 217, 220.

105. **Ruhe, A. (1973)**
Algorithms for the nonlinear eigenvalue problem *SIAM Journal of Numerical Analysis*, 10(4), 674–689.

106. **Sadighi, B. (1977)**
An analysis of root flexibility effects on turbine blade vibration characteristics *MSc Thesis*, University of London, (Imperial College).

107. **Salama, A. M. (1977)**
Finite element dynamic analysis of blade packets and bladed discs *PhD Thesis*, University Of Southampton.

108. **Sezewa, K. (1933)**
Vibrations of turbine blades with shrouding *Philosophical Magazine*, pp164–174.

109. **Smith, D. M. (1949)**
Vibration of turbine blades in packets *Proc 7th International Congress of Applied Mechanics*, London.

110. **Snowdon, J. C. (1971)**
Forced vibrations of internally damped circular and annular plates with clamped boundaries *Journal of the Acoustical Society of America*, 50(3), 846–858.

111. **Southwell, R. V. (1922)**
On the free transverse vibrations of a uniform circular disc clamped at its centre and on the effect of rotation *Proc Roy Soc London*, A101, 133–153.

112. **Srinivasan, A. V. & Frye, H. M. (1976)**
Effects of mistuning on the resonant stresses of turbine blades *Structural Dynamic Aspects of Bladed Disks*, ASME, pp57–72.

113. **Srinivasan, A. V. (1980)**
Influence of mistuning on blade torsional flutter NASA Contract Report, CR–165131.

114. **Stathoyannopolous, A. (1978)**
Using a mathematical model to investigate the vibration characteristics of packeted bladed disc assemblies *MSc Thesis*, Imperial College, University Of London.

115. **Stetson, K. A. (1974)**
Fringe interpretation for hologram interferometry of rigid body motions and homogeneous deformation *Journal of the Acoustical Society of America*, 64(1), 1–10.

116. **Thomas, J. & Belek, H. T. (1977)**
Free vibration of blade packets *Journal of Mechanical Engineering Science*, 19(1), 13–21.

117. **Timoshenko, S. P. (1921)**
On the correction for shear of the differential equation for transverse vibration of prismatic bars *Philosophical Magazine*, series 6, vol 41, pp744–.

118. **Tobias, S. A. (1950)**
Vibrations of elastic bodies of revolution containing imperfections *PhD Thesis*, Edinburgh University.

119. **Tobias, S. A. (1951)**
A theory of imperfections for the vibration of elastic bodies of revolution *Engineering*, 172, 409–.

120. **Tobias, S. A. (1957)**
Free undamped non–linear vibrations of imperfect circular discs *Proceedings of the Institution of Mechanical Engineers*, vol 171, pp691–701.

121. **Tobias, S. A. & Arnold, R. N. (1957)**
The influence of dynamical imperfections on the vibration of rotating discs *Proceedings of the Institution of Mechanical Engineers*, vol 171, pp669–690.

122. **Wagner, J. T. (1967)**
Coupling of turbomachine blade vibrations through the rotor *Journal of Engineering for Power, Trans ASME*, 89(4), 502–513.

123. **Weaver, F. L. & Prohl, M. A. (1958)**
High frequency vibrations of steam turbine buckets *Trans ASME*, 80, 181–194.

124. **Westlake, J. R. (1968)**
A Handbook of Numerical Matrix Inversions and Solutions of Linear Equations John Wiley and Sons, New York.

125. **Whittaker, E. T. (1952)**
Analytical Dynamics Cambridge University Press.

126. **Whitehead, D. S. (1965)**
Aerodynamic aspects of blade vibration *Proceedings of the Applied Mechanics Convention*, IMechE, Paper No 19.

127. **Whitehead, D. S. (1966)**
Effects of mistuning on the vibration of turbomachine blades induced by wakes *Journal of Mech Engg Sci*, 8(1), 15–21.

128. **Whitehead, D. S. (1976)**
Effect of mistuning on the forced vibration of blades with mechanical coupling *Journal of Mechanical Enginering Science*, vol 18, pp306–307.

129. **Wilkinson, J. H. (1960)**
Householder's method for the solution of the algebraic eigenproblems *Computer Journal*, 3(1),

130. **Wilkinson, J. H. (1963)**
Rounding Errors in Algebraic Processes Notes on Applied Science, No 2. Her Majesty's Stationery Office, London.

131. **Wilkinson, J. H. (1965)**
The Algebraic Eigenvalue Problem Clarendon Press, Oxford.

132. **Wilkinson, J. H. & Reinsch, C. (1971)**
Handbook for Automatic Computation Springer–Verlag, Berlin.

133. **Wilson, G. J & Kirkhope, J. (1974)**
Vibration of a bladed disc *Trans Canadian Aero Space Inst*, vol 7, pp41–48.

134. **Wine, R. L. (1964)**
Statistics for Scientists and Engineers Prentice–Hall, Inc., Englewood Cliffs, USA.

135. **Zarek, J. H. B. & Gibbs, B. M. (1981)**
The derivation of eigenvalues and mode shapes for the bending motion of a damped beam with general end conditions. *Journal of Sound and Vibration* 78(2), 185–196.

136. **Zienkiewicz, O. C. & Cheung, Y. K. (1967)**
The Finite Element Method in Structural and Continuum Mechanics McGraw–Hill, London.

APPENDIX I

Matrix Forms of the Equations of Motion.

(A) Sequential Formation: Matrix is 'fully' populated.

$$
\left[\begin{array}{cccc|cccc|cccc}
\alpha_1 & & & & -k_1 & & & & & & & \\
 & \alpha_2 & & & & -k_2 & & & & & & \\
 & & \ddots\ \alpha_i & & & & \ddots\ -k_i & & & & \bigcirc & \\
 & & & \alpha_{N-1} & & & & -k_{N-1} & & & & \\
 & & & \alpha_N & & & & -k_N & & & & \\
\hline
-k_1 & & & & \beta_1 & & & & -K_1 & & & \\
 & -k_2 & & & & \beta_2 & & & & -K_2 & & \\
 & & \ddots\ -k_i & & & & \ddots\ \beta_i & & & & \ddots\ -K_i & \\
 & & & -k_{N-1} & & & & \beta_{N-1} & & & & -K_{N-1} \\
 & & & -k_N & & & & \beta_N & & & & -K_N \\
\hline
 & & & & -K_1 & & & & \gamma_1 & & & -h \\
 & & & & & -K_2 & & & & \gamma_2 & & \\
 & & \bigcirc & & & & \ddots\ -K_i & & & & \ddots\ \gamma_i & \\
 & & & & & & & -K_{N-1} & & & & \gamma_{N-1} \\
 & & & & & & & -K_N & -h & & & \gamma_N
\end{array}\right]
\left\{\begin{array}{c}
x_1 \\ x_2 \\ \vdots \\ x_i \\ \vdots \\ x_{N-1} \\ x_N \\
\hline
y_1 \\ y_2 \\ \vdots \\ y_i \\ \vdots \\ y_{N-1} \\ y_N \\
\hline
z_1 \\ z_2 \\ \vdots \\ z_i \\ \vdots \\ z_{N-1} \\ z_N
\end{array}\right\}
$$

where: α, β, γ are functions of mass and frequency, ω.

(B) <u>Nearly Banded Formation: Matrix is 'sparsely' populated.</u>

$$
\begin{bmatrix}
\alpha_1 & -k_1 & 0 & 0 & & & & & & & & & & & 0 & 0 & 0 \\
-k_1 & \beta_1 & -K_1 & 0 & 0 & & & & & & & & & & 0 & 0 & 0 \\
0 & -K_1 & \gamma_1 & 0 & 0 & -h & & & & & & & & & 0 & 0 & -h \\
0 & 0 & 0 & \alpha_2 & -k_2 & 0 & 0 & & & & & & & & & & \\
 & 0 & 0 & -k_2 & \beta_2 & 0 & 0 & 0 & & & & & & & & & \\
 & & -h & 0 & -K_2 & \gamma_2 & 0 & 0 & -h & & & & & & & & \\
 & & & & 0 & 0 & 0 & \alpha_i & -k_i & 0 & 0 & & & & & & \\
 & & & & & 0 & 0 & -k_i & \beta_i & -K_i & 0 & 0 & & & & & \\
 & & & & & & 0 & 0 & -K_i & \gamma_i & 0 & 0 & -h & & & & \\
 & & & & & & & & 0 & 0 & 0 & \alpha_{N-1} & 0 & 0 & 0 & & \\
 & & & & & & & & & 0 & 0 & -k_{N-1} & \beta_{N-1} & -K_{N-1} & 0 & 0 & \\
 & & & & & & & & & & 0 & 0 & -K_{N-1} & \gamma_{N-1} & 0 & 0 & -h \\
 & & & & & & & & & & & 0 & 0 & 0 & \alpha_N & 0 & 0 \\
 & & & & & & & & & & & & 0 & 0 & -k_N & \beta_N & 0 \\
 & & & & & & & & & & & & & 0 & 0 & -K_N & \gamma_N \\
0 & 0 & 0 & & & & & & & & & & & & & & \\
0 & 0 & 0 & & & & & & & & & & & & & & \\
0 & 0 & -h & & & & & & & & & & & & & &
\end{bmatrix}
\begin{Bmatrix}
x_1 \\ y_1 \\ z_1 \\ x_2 \\ y_2 \\ z_2 \\ \vdots \\ x_i \\ y_i \\ z_i \\ \vdots \\ x_{N-1} \\ y_{N-1} \\ z_{N-1} \\ x_N \\ y_N \\ z_N
\end{Bmatrix}
$$

(c) Band Symmetric Formation

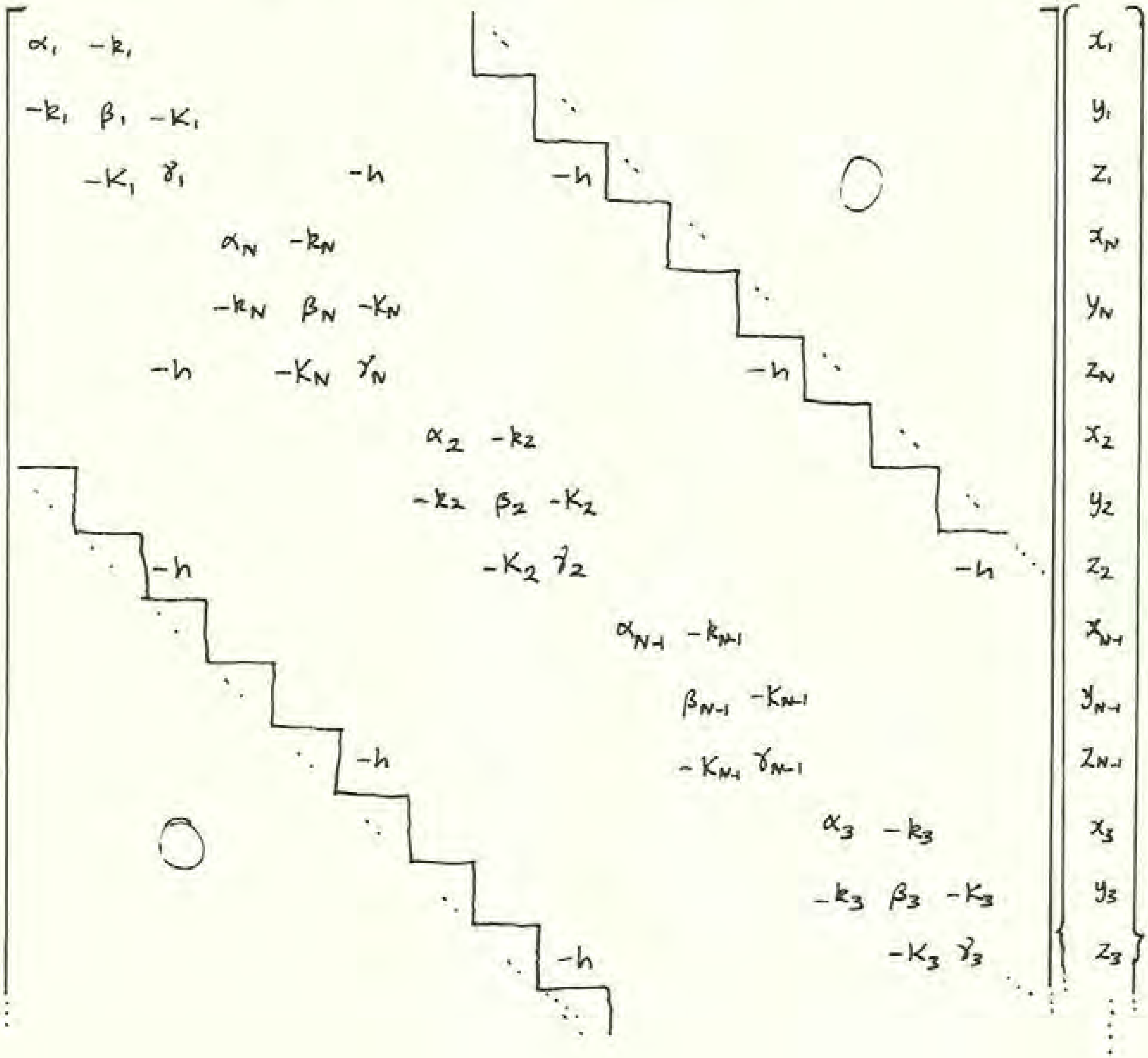

APPENDIX 2

'High Frequency' Response of Disc 24X

FREQUENCY	MAX RESP	MIN RESP	STD	SKEW	KURT	BLR	BHR
1200.00	.061439	.003006	25.742	-.344	-.772	7	10
1201.00	.066535	.011171	22.797	-.046	-.943	7	10
1202.00	.065148	.008024	25.124	-.143	-1.071	7	4
1203.00	.063964	.002076	26.036	-.291	-.780	7	19
1204.00	.074789	.005026	23.348	-.054	-.873	7	10
1205.00	.069730	.005644	26.203	-.094	-1.157	7	10
1206.00	.074676	.006198	27.641	-.080	-1.310	7	19
1207.00	.083986	.006818	24.135	.244	-1.025	7	10
1208.00	.088828	.006399	25.570	.135	-1.209	7	10
1209.00	.097347	.002395	27.935	.126	-1.246	7	10
1210.00	.094171	.008765	29.116	.168	-1.442	7	10
1211.00	.111224	.002871	28.910	.187	-1.328	8	10
1212.00	.128371	.001240	30.225	.249	-1.332	12	10
1213.00	.137312	.001259	31.034	.251	-1.417	13	10
1214.00	.200212	.014168	28.444	.196	-1.222	22	15
1215.00	.380596	.017425	22.404	.969	.922	1	14
1216.00	.952711	.058508	26.011	.430	-.567	13	14
1217.00	1.028622	.184920	25.319	-.238	-1.102	13	12
1218.00	.749815	.094918	24.076	.780	-.373	18	9
1219.00	.380237	.030513	24.911	.825	-.299	5	9
1220.00	.303634	.034945	23.052	.880	.179	5	17
1221.00	.156635	.010744	23.126	.799	.222	17	12
1222.00	.163723	.006798	24.474	.762	-.122	14	17
1223.00	.115425	.003308	28.389	-.009	-1.212	14	17
1224.00	.108520	.004370	25.961	.093	-1.116	14	12
1225.00	.102326	.007797	25.841	.026	-1.173	14	12
1226.00	.101050	.012510	24.098	.143	-.980	14	3
1227.00	.100696	.023110	24.080	.264	-1.275	14	3
1228.00	.106246	.017616	23.726	.174	-1.151	24	3
1229.00	.100037	.021575	23.778	.041	-1.077	14	3
1230.00	.105701	.020477	23.213	.053	-1.048	24	11
1231.00	.108009	.018011	22.480	-.105	-.865	24	11
1232.00	.109289	.015098	21.147	-.117	-.427	24	11
1233.00	.110864	.017992	21.206	-.162	-.561	24	11
1234.00	.111244	.014615	21.703	-.202	-.381	24	11
1235.00	.113717	.020143	20.867	-.193	-.542	24	11
1236.00	.113857	.019309	21.108	-.242	-.499	24	11
1237.00	.116140	.016279	22.449	-.305	-.648	24	11
1238.00	.120631	.019754	20.808	-.210	-.599	24	11
1239.00	.118753	.023119	20.957	-.248	-.703	24	11
1240.00	.126488	.022833	19.921	-.268	-.451	24	11
1241.00	.128929	.018862	21.135	-.320	-.508	24	11
1242.00	.138348	.025240	19.686	-.180	-.577	24	11
1243.00	.140629	.028790	20.172	-.164	-.753	24	11
1244.00	.146649	.028727	19.383	-.096	-.642	24	11
1245.00	.146281	.028877	20.200	-.196	-.727	24	11
1246.00	.153134	.036788	19.471	-.012	-.852	24	11
1247.00	.154751	.038693	19.970	-.083	-.929	24	11
1248.00	.161136	.040679	19.727	-.129	-.950	24	11
1249.00	.161504	.037130	20.769	-.066	-1.145	24	11
1250.00	.173505	.041896	20.427	-.050	-1.112	24	11
1251.00	.175774	.044277	20.462	-.031	-1.166	24	11
1252.00	.190361	.048375	20.515	-.006	-1.095	24	11
1253.00	.189152	.055560	20.989	.019	-1.256	13	11

FREQUENCY	MAX RESP	MIN RESP	STD	SKEW	KURT	BLR	BHR
1254.00	.198464	.052571	21.478	.015	-1.344	13	11
1255.00	.210052	.053923	21.832	.102	-1.348	13	11
1256.00	.225922	.052510	22.906	.134	-1.432	13	11
1257.00	.232884	.056501	23.244	.156	-1.483	13	11
1258.00	.247050	.055194	23.274	.129	-1.405	13	11
1259.00	.258823	.044507	24.499	.086	-1.367	13	11
1260.00	.291129	.055418	24.140	.233	-1.296	1	11
1261.00	.288455	.035184	25.905	.079	-1.309	13	15
1262.00	.332566	.036701	27.744	.144	-1.468	13	11
1263.00	.374522	.033182	28.244	.147	-1.419	13	11
1264.00	.420588	.006395	29.764	.102	-1.377	13	11
1265.00	.488475	.025979	32.204	.233	-1.343	17	11
1266.00	.596910	.014459	33.896	.177	-1.341	9	19
1267.00	.689919	.007615	33.053	.213	-1.353	9	15
1268.00	1.440111	.162804	28.628	.776	-.886	18	15
1269.00	7.098916	.732676	25.191	.895	-.175	18	11
1270.00	2.810873	.211526	30.159	.149	-1.368	8	9
1271.00	1.252844	.047038	29.421	.414	-.902	22	9
1272.00	2.187609	.027216	26.130	1.986	2.714	10	15
1273.00	2.271489	.020177	27.994	1.163	.345	22	8
1274.00	5.559202	.183570	23.115	1.606	1.900	22	24
1275.00	3.296157	.241797	28.442	.242	-1.296	5	20
1276.00	1.369063	.021921	28.155	.197	-1.306	13	12
1277.00	2.733591	.122583	19.997	3.183	10.048	15	12
1278.00	1.380233	.051997	21.993	1.382	2.205	3	12
1279.00	.753890	.051392	26.308	.625	-.604	4	17
1280.00	1.249625	.100553	21.615	1.175	1.348	19	9
1281.00	.785184	.014394	23.912	.479	-.180	19	17
1282.00	.836568	.008179	25.235	.306	-.588	23	17
1283.00	.920642	.033321	23.924	.328	-.222	8	17
1284.00	.988124	.094848	23.402	.298	-.386	24	17
1285.00	1.083749	.059504	22.856	.164	-.316	24	17
1286.00	1.353297	.042051	22.494	.164	-.098	8	17
1287.00	1.639761	.212582	22.210	.561	-.230	24	17
1288.00	2.056463	.205986	21.140	.445	.197	24	17
1289.00	2.798309	.377860	21.162	.537	.016	24	17
1290.00	4.910627	.584461	21.915	.528	-.156	8	17
1291.00	60.018681	1.374205	18.750	3.731	13.853	8	6
1292.00	15.731235	1.390814	21.524	1.294	1.233	8	11
1293.00	4.010046	.358630	21.269	.438	-.088	8	10
1294.00	2.455572	.190677	22.743	.320	-.439	8	17
1295.00	1.834423	.057152	26.058	.525	-.557	15	6
1296.00	1.620952	.099930	24.553	1.076	.414	12	6
1297.00	2.650859	.187578	24.017	1.097	.625	2	6
1298.00	1.569047	.158640	30.670	.077	-1.505	2	6
1299.00	1.770089	.104295	24.528	.332	-.679	4	6
1300.00	1.737794	.100185	20.574	1.373	1.831	22	1
1301.00	1.601588	.156217	25.171	1.361	.748	22	15
1302.00	.770402	.061946	27.552	.351	-1.106	22	21
1303.00	.845409	.030260	24.508	.630	-.395	22	24
1304.00	.808392	.043699	24.060	.795	.034	22	24
1305.00	.707167	.025315	25.465	.815	.039	16	24
1306.00	1.123838	.006088	21.174	2.408	5.973	8	24
1307.00	1.527942	.084769	21.417	2.045	4.192	12	24
1308.00	.555361	.021601	25.490	1.988	3.199	15	22
1309.00	1.607172	.029762	20.295	2.730	8.001	17	23
1310.00	3.495146	.084348	21.576	2.651	7.111	8	24
1311.00	7.624433	.048677	20.916	3.369	11.029	8	22

FREQUENCY	MAX. RESP	MIN RESP	STD	SKEW	KURT	BLR	BHR
1312.00	2.892298	.094109	21.188	2.503	6.369	8	6
1313.00	1.054321	.034181	24.425	1.524	1.841	7	15
1314.00	1.671582	.066022	23.556	.777	.073	13	15
1315.00	1.723602	.076755	19.804	2.204	5.622	13	12
1316.00	3.442150	.023039	19.462	3.386	11.843	13	12
1317.00	12.472944	.068398	22.465	2.871	7.649	13	9
1318.00	.890453	.062812	27.538	.491	-.942	10	17
1319.00	1.022036	.030385	22.204	1.335	2.112	10	17
1320.00	2.047249	.034867	23.050	.807	.603	3	17
1321.00	2.193520	.084754	24.796	.477	-.425	3	17
1322.00	1.458652	.072160	25.001	.804	-.302	3	4
1323.00	2.334932	.032454	25.473	.784	-.088	24	11
1324.00	3.060743	.183237	25.408	.669	-.313	14	4
1325.00	1.401954	.027011	25.884	.385	-.491	7	15
1326.00	.750998	.031516	28.479	.580	-.764	24	11
1327.00	.736644	.035370	23.884	1.224	.780	24	15
1328.00	.478001	.020003	29.638	.579	-.943	20	2
1329.00	1.112023	.029964	25.516	1.277	.882	19	2
1330.00	1.654649	.172594	22.384	1.015	.639	12	2
1331.00	.775149	.020878	27.373	.173	1.071	6	9
1332.00	.486493	.038026	22.980	.701	-.093	14	9
1333.00	.359693	.006421	25.037	.470	-.610	24	9
1334.00	.398505	.038973	22.135	.880	.648	3	9
1335.00	.468770	.015673	21.175	1.602	3.352	12	9
1336.00	.687685	.032934	27.642	.555	-.650	3	6
1337.00	1.164536	.045094	23.963	.647	-.171	23	9
1338.00	.626714	.043219	29.747	.498	-1.005	23	14
1339.00	2.629247	.037610	27.847	.922	-.204	4	1
1340.00	2.178368	.064885	28.066	1.533	1.209	15	1
1341.00	.515502	.025849	30.690	.587	-1.215	16	12
1342.00	.699504	.044226	26.665	.773	-.420	9	11
1343.00	.715895	.061900	23.866	.059	-.588	9	23
1344.00	.454748	.039794	25.728	-.196	-1.100	9	13
1345.00	.419535	.058042	27.427	.530	-1.099	9	13
1346.00	.950416	.067064	28.078	.512	-.953	21	1
1347.00	1.309709	.107716	26.509	-.040	-1.126	4	18
1348.00	.844856	.055152	23.642	.022	-.619	21	18
1349.00	.753654	.064789	25.921	1.003	-.147	21	11
1350.00	.471025	.027687	28.749	.640	-1.014	23	11
1351.00	.245060	.016181	27.332	-.043	-1.238	12	4
1352.00	.300953	.014036	29.877	.272	-1.360	8	2
1353.00	.241040	.007475	28.647	.528	-.981	24	20
1354.00	.581215	.039659	24.371	.440	-.451	18	2
1355.00	.593711	.033230	28.040	-.038	-1.033	7	19
1356.00	.677575	.052464	27.823	.040	-1.136	6	14
1357.00	.745030	.093542	23.460	.856	.019	11	19
1358.00	.655556	.022190	25.596	.999	.362	16	10
1359.00	.404712	.014713	27.753	.674	-.754	20	19
1360.00	.328335	.011130	30.996	.505	-1.248	16	19
1361.00	.571795	.035081	26.040	.514	-.864	12	7
1362.00	2.119219	.069212	25.035	1.093	.465	20	14
1363.00	.381671	.059906	24.492	.641	-.696	20	10
1364.00	.214640	.021878	25.926	.433	-.950	2	19
1365.00	.214499	.014850	25.926	.214	-1.020	2	19
1366.00	.246412	.033102	25.406	.241	-1.081	24	21
1367.00	.278362	.041527	26.133	-.291	-1.149	8	3
1368.00	.205667	.005409	24.664	.491	-.548	2	16
1369.00	.165408	.037207	23.617	.059	-1.260	24	19

FREQUENCY	MAX. RESP	MIN. RESP	STD	SKEW	KURT	BLR	BHR
1370.00	.155047	.032183	22.175	.128	-.937	2	19
1371.00	.153578	.034007	20.692	.306	-.619	23	18
1372.00	.146793	.031139	20.968	.277	-.616	23	18
1373.00	.142000	.037004	20.604	.264	-.669	23	18
1374.00	.139089	.036833	20.285	.289	-.660	23	18
1375.00	.133972	.037890	20.219	.226	-.737	23	18
1376.00	.136098	.037313	19.786	.352	-.546	23	18
1377.00	.134021	.039312	18.573	.310	-.594	23	18
1378.00	.129765	.037486	18.773	.259	-.661	23	18
1379.00	.128635	.037516	18.782	.327	-.596	23	18
1380.00	.126604	.036120	18.945	.233	-.634	23	18
1381.00	.125686	.037200	18.483	.330	-.614	23	18
1382.00	.124013	.036874	18.185	.326	-.556	23	18
1383.00	.120350	.036917	18.476	.297	-.628	23	18
1384.00	.120628	.036670	18.301	.300	-.604	23	18
1385.00	.120233	.035521	18.243	.316	-.578	23	18
1386.00	.118411	.035583	18.219	.274	-.588	23	18
1387.00	.116825	.035533	18.174	.298	-.552	23	18
1388.00	.115956	.034820	18.036	.327	-.442	23	18
1389.00	.113987	.033614	18.519	.257	-.581	23	18
1390.00	.115313	.033275	18.404	.234	-.581	23	18
1391.00	.113574	.033865	18.597	.198	-.647	23	18
1392.00	.113995	.032708	18.358	.266	-.437	23	18
1393.00	.111679	.031610	19.522	.130	-.747	23	18
1394.00	.112435	.030260	19.807	.169	-.739	23	18
1395.00	.117721	.031590	18.878	.281	-.474	23	18
1396.00	.109309	.030753	19.363	.094	-.759	23	18
1397.00	.109810	.029656	20.950	.180	-.780	23	18
1398.00	.113336	.029672	20.346	.153	-.784	23	18
1399.00	.115358	.029017	21.008	.291	-.774	13	18
1400.00	.115948	.027081	21.164	.072	-.867	13	18
1401.00	.114044	.024997	22.149	.027	-.999	13	18
1402.00	.116051	.021803	23.147	.127	-.940	13	18
1403.00	.115008	.018177	24.159	.073	-1.035	13	18
1404.00	.118230	.014763	24.996	.104	-1.021	13	18
1405.00	.120603	.010618	26.281	.109	-1.056	13	18
1406.00	.122354	.005558	27.813	.116	-1.081	13	18
1407.00	.125967	.000988	29.325	.164	-1.040	13	24
1408.00	.136903	.000567	29.242	.226	-1.096	12	24
1409.00	.149286	.008940	28.382	.371	-1.021	12	24
1410.00	.163350	.003311	28.396	.446	-.909	14	24
1411.00	.179834	.003457	28.006	.535	-.727	23	24
1412.00	.203152	.001864	26.653	.581	-.432	22	24
1413.00	.226069	.007418	26.093	.589	-.416	22	24
1414.00	.268238	.007585	26.719	.495	-.616	10	24
1415.00	.315259	.008030	29.768	.236	-1.209	4	24
1416.00	.649948	.058112	25.018	.823	-.176	4	12
1417.00	5.685543	.224839	26.436	1.458	.928	23	14
1418.00	.705743	.017710	28.118	.573	-.821	20	23
1419.00	.669933	.007709	22.842	1.511	2.442	5	24
1420.00	.601501	.014081	21.558	2.071	5.000	19	24
1421.00	.489444	.001591	22.098	1.984	4.569	1	24
1422.00	.397570	.002989	22.309	1.690	3.604	8	24
1423.00	.306875	.006001	22.952	1.401	2.153	7	24
1424.00	.259962	.001674	23.128	1.126	1.289	7	24
1425.00	.213001	.005313	23.463	.941	.546	7	24
1426.00	.170646	.008126	24.917	.682	-.364	7	24
1427.00	.149617	.012606	25.382	.553	-.675	7	24

FREQUENCY	MAX RESP	MIN RESP	STD	SKEW	KURT	BLR	BHR
1428.00	.131187	.014926	25.923	.417	-.928	7	24
1429.00	.120737	.017269	25.818	.416	-.906	7	11
1430.00	.116874	.018716	24.190	.362	-.859	7	12
1431.00	.113416	.020361	23.601	.360	-.847	7	12
1432.00	.116196	.021458	21.979	.432	-.655	7	11
1433.00	.107881	.022393	21.870	.335	-.724	7	11
1434.00	.106299	.024054	21.270	.400	-.576	7	11
1435.00	.103576	.023896	20.764	.376	-.544	7	11
1436.00	.100212	.024708	20.739	.359	-.546	7	11
1437.00	.099560	.025462	20.411	.413	-.500	7	11
1438.00	.098794	.026489	20.150	.411	-.506	7	11
1439.00	.098457	.027070	19.689	.468	-.447	7	11
1440.00	.096990	.027132	19.468	.426	-.483	7	11
1441.00	.093853	.027092	19.664	.418	-.567	7	11
1442.00	.094032	.027237	19.447	.427	-.574	7	11
1443.00	.092865	.026077	19.418	.409	-.578	1	11
1444.00	.091720	.027439	19.394	.368	-.664	7	11
1445.00	.090428	.028205	19.065	.398	-.657	1	11
1446.00	.089884	.027585	19.560	.352	-.723	1	11
1447.00	.088809	.027581	19.368	.347	-.725	1	11
1448.00	.087572	.027708	19.364	.309	-.764	1	11
1449.00	.089905	.027528	19.201	.342	-.683	1	11
1450.00	.086963	.027004	19.521	.275	-.756	1	11
1451.00	.085433	.026757	19.795	.235	-.857	1	11
1452.00	.085310	.025729	19.644	.189	-.870	24	11
1453.00	.086353	.023150	19.597	.208	-.822	24	11
1454.00	.083469	.025318	19.763	.150	-.879	24	11
1455.00	.084132	.023019	19.995	.152	-.845	24	11
1456.00	.083578	.020397	19.866	.050	-.771	24	11
1457.00	.082040	.019761	20.365	.054	-.861	24	11
1458.00	.083487	.019119	19.991	.090	-.762	24	11
1459.00	.081180	.018804	20.355	.019	-.823	24	11
1460.00	.080850	.018060	20.342	.006	-.800	24	11
1461.00	.081182	.016497	20.223	-.008	-.715	24	11
1462.00	.080401	.016963	20.725	-.009	-.814	24	11
1463.00	.079688	.015866	20.783	-.068	-.733	24	11
1464.00	.080191	.016413	20.492	-.005	-.748	24	11
1465.00	.078611	.013881	21.095	-.077	-.721	24	11
1466.00	.078655	.013622	21.197	-.084	-.713	24	11
1467.00	.078283	.013375	21.462	-.088	-.782	24	11
1468.00	.078609	.012879	21.354	-.080	-.750	24	11
1469.00	.078496	.012936	21.224	-.083	-.714	24	11
1470.00	.077943	.011724	21.568	-.125	-.688	24	11
1471.00	.077193	.011881	21.562	-.153	-.779	24	11
1472.00	.077200	.010062	21.835	-.194	-.737	24	11
1473.00	.077509	.010227	21.802	-.167	-.722	24	11
1474.00	.076122	.010605	22.149	-.149	-.697	24	11
1475.00	.076703	.007708	22.502	-.242	-.594	24	11
1476.00	.077240	.010357	22.001	-.187	-.791	24	11
1477.00	.076946	.009172	22.331	-.178	-.735	24	11
1478.00	.076097	.008808	22.298	-.201	-.737	24	11
1479.00	.076266	.007677	22.752	-.210	-.739	24	11
1480.00	.074796	.008536	22.641	-.232	-.755	24	11
1481.00	.075320	.007014	22.946	-.241	-.721	24	11
1482.00	.074730	.007846	23.056	-.209	-.792	24	11
1483.00	.074898	.004667	23.379	-.288	-.537	24	11
1484.00	.074396	.006074	23.368	-.263	-.629	24	12
1485.00	.075177	.003373	23.210	-.215	-.722	24	11

APPENDIX 3
List of Figures

Fig. 1.2.1 *Mathematical model of a bladed disc* Ellington & McCallion (1959)
Fig. 1.2.2 *Shrouded blades on a flexible disc* Belek (1977)
Fig. 1.2.3 *Mathemattical model of a packet of five blades*
Fig. 1.2.4 *Mistune patterns*
Fig. 1.2.5 *Bladed disc assembly modelled as beams on an elastic foundation* Wagner (1967)
Fig. 1.2.6 *Mathematical model of a mistuned assembly* Dye & Henry (1969)
Fig. 1.2.7 *Matthematical model of a mistuned assembly with friction damping* Muszynska *et al* (1980)

Fig. 2.1.1 *Mathematical model of a compressor rotor* adapted from Dye & Henry (1969)
Fig. 2.3.1 *Vibration excitation force induced by wakes*
Fig. 2.3.2 *Excitation force produced by partial admission*
Fig. 2.3.3a *Actual excitation force in some engines* Bellamy (1981)
Fig. 2.3.3b *Frequency response of auxilliary engine components*
Fig. 2.3.3c *Excitation force modulated by the vibration of other engine components*
Fig. 2.4.1 *Physical model of a turbine blade*
Fig. 2.4.2 *A scheme for deducing blade model parameters*
Fig. 2.4.3 *A lumped parameter model of a turbine blade*
Fig. 2.4.4 *Resonance diagrams showing the influence of disc stiffness on natural frequencies*
Fig. 2.4.5 *Natural frequency changes due to shrouding*
Fig. 2.4.6 *Natural frequencies of a tuned 30-bladed disc*
Fig. 2.5.1 *Scatter diagrams showing blade cantilever frequencies vs slot position*
Fig. 2.5.2 *Natural frequencies of Disc 10T*
Fig. 2.5.3 *Natural frequencies of Disc 30T*
Fig. 2.5.4 *Natural frequencies and mode-shapes of vibration for Disc 10T*
Fig. 2.5.5 *Natural frequencies and mode-shapes of vibration for Disc 10X*
Fig. 2.5.6 *Natural frequencies and mode-shapes of vibration for Disc 10Y*
Fig. 2.5.7 *Natural frequencies and mode-shapes of vibration for Disc 10A*
Fig. 2.5.8 *Natural frequencies and mode-shapes of vibration for Disc 30T*
Fig. 2.5.9 *Natural frequencies and mode-shapes of vibration for Disc 30A*
Fig. 2.5.10a *Critical and non-critical mode-shapes*
Fig. 2.5.10b *Relationship between critical blades and blades with extreme detune*
Fig. 2.5.11 *Frequency response of discs 30T and 30A to 3EO excitation*
Fig. 2.5.12 *Frequency response of Disc 10A to 1EO*
Fig. 2.5.13 *Frequency response of Disc 10A to 2EO*
Fig. 2.5.14 *Frequency response of Disc 10A to 3EO*
Fig. 2.5.15 *Frequency response of Disc 10A to 4EO*
Fig. 2.5.16 *Frequency response of Disc 10A to 5EO*
Fig. 2.5.17 *Stress amplitudes of blades on Disc 10A*
Fig. 2.5.18 *Response amplitudes of Disc 30A*
Fig. 2.5.19 *Response amplitudes of Disc 30B*
Fig. 2.2.20 *Resonant response patterns for Discs 30A and 30B*

Fig. 3.1.1 *Frequency response of a bladed disc showing upper and lower envelopes of blade response*

Fig. 3.1.2 *Similar mistune patterns with different scatter*
Fig. 3.2.1 *Statistical charateristics of blade response*
Fig. 3.3.1 *Frequency distribution histograms of a 10-bladed disc*
Fig. 3.3.2 *Response of Disc 10A to various EO excitations*
Fig. 3.3.3 *Response of Disc 30M to 3EO excitation*
Fig. 3.3.5 *Response of Disc 33R to 2EO excitation*
Fig. 4.2.1 *Typical convergence paths in inverse iteration for damped eigenvalues*
Fig. 4.3.1 *Eigensystems and characteristic motions of damped and undamped systems*
Fig. 4.3.2 *Variation of complex latent root with damping.*
Fig. 4.4.1 *Mathematical model of a bladed disc with aerodynamic damping*

Fig. 5.1.1 *Coordinates associated with the spatial motions of a beam*
Fig. 5.2.1 *Building blocks of a 4-bladed disc assembly*
Fig. 5.3.1 *Frequency scatter of Disc 24J*
Fig. 5.3.2 *Response of disc 24J to 1eo at selected frequencies*
Fig. 5.3.3 *Frequency response of Disc 24J (with damping)*

Fig. 6.2.1 *Schematic diagram of experimental set-up*
Fig. 6.3.1—6.3.24 *Frequency response of blades on Disc 24X*
Fig. 6.3.25 *Relative blade amplitudes at selected frequencies*

Fig. 7.2.1 *Mathematical model of a cantilever with restraining root springs*
Fig. 7.2.2 *Variation of dimensioless frequency with root resilence*
Fig. 7.3.1 *Physical model of a compressor rotor*
Fig. 7.3.2 *Physical model of the ith blade*
Fig. 7.3.3 *Frequency response of a flexibly mounted cantilever beam*
Fig. 7.4.1 *Frequency response of a stepped cantilever beam*
Fig. 7.4.2 *Frequency response of a stepped cantilever beam with stiffened joint*
Fig. 7.4.3 *Schematic illustration of experimetal layout*
Fig. 7.4.4 *Tip response of a steam turbine blade*
Fig. 7.4.5 *Root respose of a steam turbine blade*
Fig. 7.4.6 *Amplitude ratio of a steam turbine blade*

Fig. 8.2.1 *Mistune pattern for Disc 30A*
Fig. 8.2.2 *Mistune pattern for Disc 30B*
Fig. 8.3.1 *Natural frequencies and mode-shapes of vibration for Disc 10KB*
Fig. 8.3.2 *Natural frequencies and mode-shapes of vibration for Disc 10KM*
Fig. 8.3.3 *Natural frequencies and mode-shapes of vibration for Disc 10KY*
Fig. 8.3.4 *Parametric dependence of 'worst stress' on disc stiffnes*

Fig. 9.1.1a *Holographic mode-shapes of a bladed disc*
Fig. 9.1.1b *Measured modes of a 24-bladed disc*
Fig. 9.1.1c *Computed modes of a 24-bladed disc*
Fig. 9.1.1d *Frequency response of a 24-bladed disc*
Fig. 9.1.2a *Frequency scatter for a 72-bladed disc*
Fig. 9.1.2b *Variation of stress amplitude with blade slot position*

Fig. 9.1.2c *Variation of stress amplitude with blade frequency*
Fig. 9.1.2d *Regression of stress on blade frequency*
Fig. 9.1.3a *Frequency response of a 23-bladed disc*
Fig. 9.1.3b *Frequency scatter of a 23-bladed disc*
Fig. 9.1.4a *Mathematical model of a mistuned bladed disc*
Fig. 9.1.4b *Frequency scatter of an 11-bladed disc*
Fig. 9.1.4c *Frequency response of an 11-bladed disc*

List of Tables

Table 2.5.5 *Response characteristics of Disc 10A (3EO excitation)*
Table 3.3.1 *Response characteristics of Disc 10A to 1EO excitation*
Table 3.3.2 *Response characteristics of Disc 10A to 2EO excitation*
Table 3.3.3 *Response characteristics of Disc 10A to 3EO excitation*
Table 3.3.4 *Response characteristics of Disc 10A to 4EO excitation*
Table 3.3.5 *Response characteristics of Disc 10A to 5EO excitation*
Table 4.4.1 *Eigensolutions of a damped bladed disc*
Table 5.3.1 *Response characteristics of Disc 24J (tip displacement)*
Table 5.3.2 *Response characteristics of Disc 24J (root stress A)*
Table 5.3.3 *Response characteristics of Disc 24J (root stress B)*
Table 6.3.1 *Response characteristics of Disc 24X*
Table 7.2.1 *Variation of* λl *with* Z_R *and* Z_L *for a classical beam*
Table 7.2.2 *Variation of* λl *with* Z_R *and* Z_L *for a Timoshenko beam*
Table 7.2.3 *Natural frequencies of a cantilever with root flexibilty*

APPENDIX 5: Further details of assembly models

(see Figure 2.1.1, page 54, for mathematical model and notation.)

1. All units are in S.I.
2. For A5.1 to A5.6 inclusive, the disc stiffness parameters are as follows:

$$h = 1.500\ E{+}06$$
$$g = 2.1167E{+}01$$

A5.1 Disc 10A

i	m_i	M_i	W	k_i	K_i
1	.08948	.17896	.26774	2.08779596E+05	1.41841852E+07
2	.08948	.17896	.26774	2.18078159E+05	1.48159162E+07
3	.08948	.17896	.26774	2.13137060E+05	1.44802251E+07
4	.08948	.17896	.26774	2.06448412E+05	1.40258080E+07
5	.08948	.17896	.26774	2.04781221E+05	1.39125414E+07
6	.08948	.17896	.26774	2.03388321E+05	1.38179098E+07
7	.08948	.17896	.26774	2.07527843E+05	1.40991429E+07
8	.08948	.17896	.26774	2.07403165E+05	1.40906725E+07
9	.08948	.17896	.26774	2.00609239E+05	1.36291030E+07
10	.08948	.17896	.26774	2.06806009E+05	1.40501026E+07

Blade number	1F (Hz)
1	241.3
2	246.6
3	243.8
4	239.9
5	239.0
6	238.2
7	240.6
8	240.5
9	236.5
10	240.1

A5.2 Disc 10T

All the blades on this tuned model are identical

m_i = 0.08948

M_i = 0.17896

W = 0.26774

k_i = 2.0771E+05

K_i = 1.4112E+07

g = 2.1167E+01

h = 1.500E+05

blade 1F = 240.0 (Hz)

A5.3 Disc 30A

i	m_i	M_i	W	k_i	K_i
1	.08948	.17896	.26774	2.08779596E+05	1.41841852E+07
2	.08948	.17896	.26774	2.11933540E+05	1.43984596E+07
3	.08948	.17896	.26774	2.13137060E+05	1.44802251E+07
4	.08948	.17896	.26774	2.06448412E+05	1.40258080E+07
5	.08948	.17896	.26774	2.12871359E+05	1.44621737E+07
6	.08948	.17896	.26774	2.04781221E+05	1.39125414E+07
7	.08948	.17896	.26774	2.03388321E+05	1.38179098E+07
8	.08948	.17896	.26774	2.07527843E+05	1.40991429E+07
9	.08948	.17896	.26774	2.07403165E+05	1.40906725E+07
10	.08948	.17896	.26774	2.00609239E+05	1.36291030E+07
11	.08948	.17896	.26774	2.06806009E+05	1.40501026E+07
12	.08948	.17896	.26774	2.12997514E+05	1.44707445E+07
13	.08948	.17896	.26774	2.18078159E+05	1.48159162E+07
14	.08948	.17896	.26774	2.09070392E+05	1.42039415E+07
15	.08948	.17896	.26774	2.04130464E+05	1.38683299E+07
16	.08948	.17896	.26774	2.05902907E+05	1.39887472E+07
17	.08948	.17896	.26774	2.12364773E+05	1.44277570E+07
18	.08948	.17896	.26774	2.03015763E+05	1.37925987E+07
19	.08948	.17896	.26774	2.08246006E+05	1.41479339E+07
20	.08948	.17896	.26774	2.07922197E+05	1.41259348E+07
21	.08948	.17896	.26774	2.06927218E+05	1.40583373E+07
22	.08948	.17896	.26774	2.01795954E+05	1.37097266E+07
23	.08948	.17896	.26774	2.10984523E+05	1.43339848E+07
24	.08948	.17896	.26774	2.09156690E+05	1.42098045E+07
25	.08948	.17896	.26774	2.05199050E+05	1.39409281E+07
26	.08948	.17896	.26774	2.15591105E+05	1.46469493E+07
27	.08948	.17896	.26774	2.08135062E+05	1.41403965E+07
28	.08948	.17896	.26774	2.08284402E+05	1.41505425E+07
29	.08948	.17896	.26774	2.08551491E+05	1.41686881E+07
30	.08948	.17896	.26774	2.07703281E+05	1.41110619E+07

Blade no.	1F (Hz)
1	241.287
2	243.103
3	243.792
4	239.936
5	243.640
6	238.966
7	238.151
8	240.563
9	240.490
10	236.519
11	240.144
12	243.712
13	246.602
14	241.455
15	238.586
16	239.619
17	243.350
18	237.933
19	240.979
20	240.791
21	240.214
22	237.217
23	242.558
24	241.505
25	239.209
26	245.192
27	240.914
28	241.001
29	241.155
30	240.664

g = 2.1167E+01 h = 1.500E+06

A5.4 Disc 30B

i	m_i	M_i	W	k_i	K_i
1	8.9480E-02	1.7896E-01	2.6774E-01	2.0792E+05	1.4126E+07
2	8.9480E-02	1.7896E-01	2.6774E-01	2.1314E+05	1.4480E+07
3	8.9480E-02	1.7896E-01	2.6774E-01	2.0180E+05	1.3710E+07
4	8.9480E-02	1.7896E-01	2.6774E-01	2.0645E+05	1.4026E+07
5	8.9480E-02	1.7896E-01	2.6774E-01	2.0693E+05	1.4058E+07
6	8.9480E-02	1.7896E-01	2.6774E-01	2.0770E+05	1.4111E+07
7	8.9480E-02	1.7896E-01	2.6774E-01	2.0825E+05	1.4148E+07
8	8.9480E-02	1.7896E-01	2.6774E-01	2.1287E+05	1.4462E+07
9	8.9480E-02	1.7896E-01	2.6774E-01	2.0302E+05	1.3793E+07
10	8.9480E-02	1.7896E-01	2.6774E-01	2.1193E+05	1.4396E+07
11	8.9480E-02	1.7896E-01	2.6774E-01	2.0476E+05	1.3913E+07
12	8.9480E-02	1.7896E-01	2.6774E-01	2.0061E+05	1.3629E+07
13	8.9480E-02	1.7896E-01	2.6774E-01	2.1300E+05	1.4471E+07
14	8.9480E-02	1.7896E-01	2.6774E-01	2.0740E+05	1.4091E+07
15	8.9480E-02	1.7896E-01	2.6774E-01	2.0878E+05	1.4184E+07
16	8.9480E-02	1.7896E-01	2.6774E-01	2.0826E+05	1.4151E+07
17	8.9480E-02	1.7896E-01	2.6774E-01	2.0907E+05	1.4204E+07
18	8.9480E-02	1.7896E-01	2.6774E-01	2.0520E+05	1.3941E+07
19	8.9480E-02	1.7896E-01	2.6774E-01	2.1559E+05	1.4647E+07
20	8.9480E-02	1.7896E-01	2.6774E-01	2.0681E+05	1.4050E+07
21	8.9480E-02	1.7896E-01	2.6774E-01	2.0339E+05	1.3818E+07
22	8.9480E-02	1.7896E-01	2.6774E-01	2.0753E+05	1.4099E+07
23	8.9480E-02	1.7896E-01	2.6774E-01	2.0590E+05	1.3989E+07
24	8.9480E-02	1.7896E-01	2.6774E-01	2.0916E+05	1.4210E+07
25	8.9480E-02	1.7896E-01	2.6774E-01	2.0413E+05	1.3868E+07
26	8.9480E-02	1.7896E-01	2.6774E-01	2.0655E+05	1.4169E+07
27	8.9480E-02	1.7896E-01	2.6774E-01	2.1808E+05	1.4816E+07
28	8.9480E-02	1.7896E-01	2.6774E-01	2.1096E+05	1.4334E+07
29	8.9480E-02	1.7896E-01	2.6774E-01	2.1236E+05	1.4428E+07
30	8.9480E-02	1.7896E-01	2.6774E-01	2.0814E+05	1.4140E+07

Blade	(F(Hz)
1	240.8
2	243.8
3	237.2
4	239.9
5	240.2
6	240.7
7	241.0
8	243.6
9	237.9
10	243.1
11	239.0
12	236.5
13	243.7
14	240.5
15	241.3
16	241.0
17	241.4
18	239.2
19	245.2
20	240.1
21	238.2
22	240.6
23	239.6
24	241.5
25	238.6
26	241.2
27	246.6
28	242.6
29	243.4
30	240.9

g = 2.1167E+01 h = 1.500E+06

A5.5 Disc 30M

i	mi	Mi	W	ki	Ki
1	8.9480E-02	1.7896E-01	2.6774E-01	2.4113E+05	1.6382E+07
2	8.9480E-02	1.7896E-01	2.6774E-01	2.9444E+05	2.0004E+07
3	8.9480E-02	1.7896E-01	2.6774E-01	3.1607E+05	2.1473E+07
4	8.9480E-02	1.7896E-01	2.6774E-01	2.0492E+05	1.3922E+07
5	8.9480E-02	1.7896E-01	2.6774E-01	3.1124E+05	2.1145E+07
6	8.9480E-02	1.7896E-01	2.6774E-01	1.8071E+05	1.2277E+07
7	8.9480E-02	1.7896E-01	2.6774E-01	1.6158E+05	1.0978E+07
8	8.9480E-02	1.7896E-01	2.6774E-01	2.2134E+05	1.5038E+07
9	8.9480E-02	1.7896E-01	2.6774E-01	2.1942E+05	1.4907E+07
10	8.9480E-02	1.7896E-01	2.6774E-01	1.2645E+05	8.5909E+06
11	8.9480E-02	1.7896E-01	2.6774E-01	2.1029E+05	1.4287E+07
12	8.9480E-02	1.7896E-01	2.6774E-01	3.1353E+05	2.1301E+07
13	8.9480E-02	1.7896E-01	2.6774E-01	4.1218E+05	2.8003E+07
14	8.9480E-02	1.7896E-01	2.6774E-01	2.4584E+05	1.6702E+07
15	8.9480E-02	1.7896E-01	2.6774E-01	1.7165E+05	1.1662E+07
16	8.9480E-02	1.7896E-01	2.6774E-01	1.9684E+05	1.3373E+07
17	8.9480E-02	1.7896E-01	2.6774E-01	3.0211E+05	2.0525E+07
18	8.9480E-02	1.7896E-01	2.6774E-01	1.5664E+05	1.0642E+07
19	8.9480E-02	1.7896E-01	2.6774E-01	2.3260E+05	1.5802E+07
20	8.9480E-02	1.7896E-01	2.6774E-01	2.2749E+05	1.5455E+07
21	8.9480E-02	1.7896E-01	2.6774E-01	2.1213E+05	1.4412E+07
22	8.9480E-02	1.7896E-01	2.6774E-01	1.4096E+05	9.5764E+06
23	8.9480E-02	1.7896E-01	2.6774E-01	2.7788E+05	1.8879E+07
24	8.9480E-02	1.7896E-01	2.6774E-01	2.4724E+05	1.6797E+07
25	8.9480E-02	1.7896E-01	2.6774E-01	1.8664E+05	1.2680E+07
26	8.9480E-02	1.7896E-01	2.6774E-01	3.6235E+05	2.4618E+07
27	8.9480E-02	1.7896E-01	2.6774E-01	2.3084E+05	1.5683E+07
28	8.9480E-02	1.7896E-01	2.6774E-01	2.3321E+05	1.5844E+07
29	8.9480E-02	1.7896E-01	2.6774E-01	2.3746E+05	1.6133E+07
30	8.9480E-02	1.7896E-01	2.6774E-01	2.2407E+05	1.5223E+07

Blade	1F
1	259.3
2	286.5
3	296.9
4	239.0
5	294.6
6	224.5
7	212.3
8	248.4
9	247.4
10	187.8
11	242.2
12	295.7
13	339.0
14	261.8
15	218.8
16	234.3
17	290.3
18	209.0
19	254.7
20	251.9
21	243.2
22	198.3
24	262.6
25	228.1
26	317.9
27	253.7
28	255.0
29	257.3
30	250.0

g = 2.1167E+01 h = 1.500E+06

A5.6 Disc 30T

All the blades on this tuned model are identical

m_i = 0.08948

M_i = 0.17896

W = 0.26774

k_i = 2.0771E+05

K_i = 1.4112E+07

g = 2.1167E+01

h = 1.500 E+06

blade 1F = 240.0 (Hz)

A5.7 Disc 24X

Blade no.	no. of washers	approx. 1F
1	8	386.4
2	2	398.1
3	4	394.2
4	1	400.1
5	5	392.1
6	0	402.0
7	2	398.1
8	5	392.3
9	3	396.2
10	5	392.3
1	10	382.5
12	5	392.3
13	3	396.2
14	9	384.5
15	7	388.4
16	4	394.2
17	10	382.5
18	8	386.4
19	7	388.4
20	9	384.5
21	4	394.2
22	2	398.1
23	1	400.1
24	0	402.0